

Reg gene family and human diseases

Yu-Wei Zhang, Liu-Song Ding, Mao-De Lai

Yu-Wei Zhang, Department of Pathology, School of Medicine, Zhejiang University, Hangzhou 310006, Zhejiang Province, China and Department of Pathology, School of Basic Medical Sciences, Southeast University, Nanjing 210009, Jiangsu Province, China

Mao-De Lai, Department of Pathology, School of Medicine, Zhejiang University, Hangzhou 310006, Zhejiang Province, China

Liu-Song Ding, Zhejiang University Libraries, Hangzhou 310006, Zhejiang Province, China

Supported by National Natural Science Foundation of China, No. 30200333 and No.30371605

Correspondence to: Dr. Yu-Wei Zhang, Department of Pathology, School of Basic Medical Sciences, Southeast University, Nanjing 210009, Jiangsu Province, China. yuwei123@seu.edu.cn

Telephone: +86-571-87217134 **Fax:** +86-571-87951358

Received: 2003-05-10 **Accepted:** 2003-06-02

Abstract

Regenerating gene (Reg or REG) family, within the superfamily of C-type lectin, is mainly involved in the liver, pancreatic, gastric and intestinal cell proliferation or differentiation. Considerable attention has focused on Reg family and its structurally related molecules. Over the last 15 years, 17 members of the Reg family have been cloned and sequenced. They have been considered as members of a conserved protein family sharing structural and some functional properties being involved in injury, inflammation, diabetes and carcinogenesis. We previously identified Reg IV as a strong candidate for a gene that was highly expressed in colorectal adenoma when compared to normal mucosa based on suppression subtractive hybridization (SSH), reverse Northern blot, semi-quantitative reverse transcriptase PCR (RT-PCR) and Northern blot. *In situ* hybridization results further support that overexpression of Reg IV may be an early event in colorectal carcinogenesis. We suggest that detection of Reg IV overexpression might be useful in the early diagnosis of carcinomatous transformation of adenoma. This review summarizes the roles of Reg family in diseases in the literature as well as our recent results of Reg IV in colorectal cancer. The biological properties of Reg family and its possible roles in human diseases are discussed. We particularly focus on the roles of Reg family as sensitive reactants of tissue injury, prognostic indicators of tumor survival and early biomarkers of carcinogenesis. In addition to our current understanding of Reg gene functions, we postulate that there might be relationships between Reg family and microsatellite instability, apoptosis and cancer with a poor prognosis. Investigation of the correlation between tumor Reg expression and survival rate, and analysis of the Reg gene status in human malignancies, are required to elucidate the biologic consequences of Reg gene expression, the implications for Reg gene regulation of cell growth, tumorigenesis, and the progression of cancer. It needs to be further attested whether Reg gene family is applicable in early detection of cancer and whether Reg and Reg-related molecules can offer novel molecular targets for anticancer therapeutics. This has implications with regard to prognosis, such as in monitoring cancer initiation, progression and recurrence, as well as the design of chemotherapeutic drugs.

Zhang YW, Ding LS, Lai MD. Reg gene family and human diseases. *World J Gastroenterol* 2003; 9(12): 2635-2641

<http://www.wjgnet.com/1007-9327/9/2635.asp>

INTRODUCTION

Reg and Reg-related genes constitute a family belonging to calcium dependent lectin (C-type lectin) gene superfamily^[1-4]. It represents a group of small secretory proteins, which can function as acute phase reactants, lectins, antiapoptotic factors or growth factors for pancreatic β -cells, neural cells and epithelial cells in the digestive system^[5,6]. They play a wide range of roles in researching mammal physiology and human diseases. Ever since Reg (regenerating gene) I was discovered, special attentions have been paid to the regeneration of pancreatic β -cells and administration of Reg I protein and/or activation of the Reg I gene to be used as a potential therapeutic approach for diabetes^[7]. Successively, the potential role of Reg family in tumors especially in digestive tract has drawn more attention^[8-14]. We here focus on the members of Reg family, their functions and possible mechanisms.

REG FAMILY

Discovered members

In 1984, Yamanoto *et al.* found that administration of nicotinamide accelerated the regeneration of pancreatic islets in partially pancreatectomized rats. Subsequently, Terazono *et al.* screened a rat regenerating islet-derived cDNA library and isolated a novel gene encoding a 165 amino acid protein with a 21 amino acid signal peptide^[15,16], which was called Reg gene. It was not termed Reg I until 1997. They also cloned human Reg I cDNA encoding a 166 amino acid protein with a 22 amino acid signal peptide. Reg I has other synonyms such as PTP (pancreatic thread protein), PSP (pancreatic stone protein) and lithostathine^[17]. Human Reg I gene is a single copy gene spanning 3.0 kb, and is composed of six exons and five introns. The gene mRNA was detected predominantly in the pancreas, and at lower levels in gastric mucosa and kidneys^[18]. Later they isolated two genes, one of which was a mouse homologue to rat and human Reg gene, the other a novel type of Reg gene. The two genes were designated as Reg I and Reg II, respectively.

In 1999, Okamoto grouped the members of the family, Reg and Reg-related genes from human, rat and mouse, into three subclasses, types I, II, and III^[19]. Stephanova *et al.* determined that the three rat PAP genes and the related Reg gene (REGL, regenerating islet-derived-like/ pancreatic stone protein-like/ pancreatic thread protein-like) were all located at 4q33-q34^[20]. The mouse Reg family genes were mapped to a contiguous 75 kb region in chromosome 6, including Reg I, Reg II, Reg III alpha, Reg III beta, Reg III gamma, and Reg III delta^[21]. Reg III delta was expressed predominantly in exocrine pancreas, whereas both Reg I and Reg II were expressed in hyperplastic islets and Reg III alpha, Reg III beta and Reg III gamma were expressed strongly in the intestinal tract and weakly in pancreas.

Although Reg IV (1q12-q21), identified by Hartupée *et*

al., has not been found in the same chromosome as other members of human Reg gene and Reg-related gene (2p12), it shares some common features with other members such as: sequence homology, tissue expression profiles, and exon-intron junction genomic organization^[1]. Thus by 2001, four types of Reg gene family had been identified. Data of RT-PCR results in our laboratory were consistent with the hybridization result of Hartupee and colleagues, and Reg IV mRNAs level was higher in colon than in rectum. We compared the results with Reg I expression pattern. Kawanami *et al.* discovered that expression of Reg I mRNA was higher in the stomach than in any other region of the gastrointestinal tract^[22], which also suggested that Reg mRNA was higher in proximate gastrointestinal tract.

Table 1 Members of Reg family, length of amino acids and chromosome localization

Superfamily member	Species	Length of amino acid	Chromosome localization
Reg I	Mouse Reg I	165	6
	Rat Reg	165	4q33-q34
	Human Reg/PSP/PTP	166	2p12
Reg II	Mouse Reg II	173	6
Reg III	Rat PAP	175	4q33-q34
	Rat peptide 23	175	4q33-q34
	Human HIP	175	2p12
	Bovine PTP	175	
Reg IV	Human Reg IV	158	1q12-q21

So far, 17 members have been identified in mammals across human, pig, mouse, bovine and rat species. Table 1 lists some most important members of Reg family^[23,24]. Among the mammalian members of this family, there is only mouse Reg II in type II and human Reg IV in type IV. Hartupee *et al.* also reported that a mouse homologue of Reg IV was likely existed^[1], but up to now, there are no reports and also no investigations on mouse Reg IV.

Structure and function

Most members of Reg family have similar organization with respect to exon number and chromosome location. The most interesting characteristic is its common domain of lectin. Data have revealed a significant similarity of the sequences of Reg family with the C-type (Calcium-dependent) lectin superfamily. This domain of lectin could account for complex events such as human malignancy and other diseases^[25,26].

Studies on Reg I protein receptor (Reg-R) revealed that regenerating protein might act not only as a regulator of gastric epithelial cell proliferation but also as a modifier of many other multiple physiologic functions^[27,28]. Reg-R gene was isolated from a rat islet cDNA library^[27] encoding a cell surface 919-amino acid protein. Its expression was detected mainly in chief cells and parietal cells of the deep layers and faintly in surface epithelial cells and mucous neck cells of the proliferating zone^[29]. Reg I protein could induce β -cell proliferation via the Reg I receptor and ameliorate experimental diabetes^[30].

Under physiological conditions, Reg I protein is not expressed in pancreatic β -cells, although Reg-R is expressed. In the regenerative process of pancreatic islets, Reg I gene expression is induced. Therefore, activation of Reg I gene is thought to be one of the important events in β -cell regeneration.

REG FAMILY AND HUMAN DISEASES

Injury response and inflammation

Regenerating gene family members are expressed in tissue

injury. As tissue injury is concerned, pancreatitis is most frequently studied. Experimental induction of acute pancreatitis caused a coordinate increase both in PSP/reg (Reg I) and in PAP (Reg III). Since the regulation of this protein family was affected even under mild stress, they were defined as secretory stress proteins^[31-33]. Reg levels are sensitive markers for pancreatic injury and early stage of the disease, which might be useful prognostic indicators for disease severity^[34]. The expression level of PSP/Reg I protein varies with different degrees of injury. Mild to moderate injury to pancreatic tissue might stimulate the synthesis of PSP/reg-protein, whereas more severe injury tended to depress it^[32,34].

There are other evidences supporting Reg's roles in the healing of gastrointestinal mucosal lesions. Miyaara *et al.* measured Reg expression after implantation or resection of a solid insulinoma in rats and found that the diminution in pancreatic β -cell mass caused by subcutaneous implantation of insulinoma tissues was associated with reduced Reg I gene expression and increase of β -cell proliferation after resection of the tumor was preceded by return of Reg I gene expression toward normal^[35]. In an injured state following indomethacin treatment, Reg I gene expression was sharply increased, accompanied by an overexpression of c-fos and healing of mucosal lesions^[22]. In addition, Reg I mRNA was detected predominantly in the deepest mucosal layer. It was expressed almost exclusively in cells that were less than 11 μ m in diameter, which suggested a role of Reg I in the healing.

This also may be one of reasons why Reg genes have been frequently screened as differentially expressed genes^[8,10,36-38]. Shinozaki *et al.* isolated seven candidate genes that were presumed to be up-regulated in inflammatory colonic epithelia and Reg I was among them. Expression of Reg I alpha was confined to the crypt epithelia^[36] and its selective expression in the crypt epithelia of inflammatory colonic mucosa might suggest its important regulatory functions.

Another interesting change was the length of Reg mRNA. The elongated mRNA of PAP II/Reg III was strongly induced in the early phase after acute pancreatitis. The elongated mRNA might affect the function of PAP II/Reg III protein because the elongated mRNA with long 3' untranslated regions (3' UTR) was involved in the translation efficiency and thus played an important role in the progression of pancreatitis^[39].

Diabetes

Islet cells originate from the epithelial cells of primitive pancreatic ducts during embryogenesis, and can regenerate in response to the loss of islet cells even in adult pancreas. The ability of islet cells to regenerate could increase the possibility, which could restore the impaired and decreased islets of diabetic patients^[40]. On the other hand, aging may be associated with selective dysfunction of β -cells, which may involve the expression of Reg I gene. Reg I gene could play an important role in β -cell growth/regeneration^[41,42] and its expression could parallel to islet physiology, thus Reg I gene may become one of the targets of genetic engineering for diabetic β -cells.

In early 1980s, Takasawa *et al.* proposed a unifying model for β -cell damage (the okamoto model). In 1984, they demonstrated Reg I protein could induce β -cell proliferation and ameliorate experimental diabetes. Later, they showed that combined addition of IL-6 and dexamethasone could induce Reg I gene expression in β -cells and that inhibitors could enhance the expression^[43]. In 2002, they reported that PARP and its inhibitors had key roles in inducing β -cell regeneration, maintenance of insulin secretion, and prevention of β -cell death^[28].

The expression of Reg is a defense mechanism of the exocrine pancreas that is conserved in evolution. Sanchez *et al.* demonstrated that pancreatic Reg I and Reg II genes were overexpressed in non-obese diabetic (NOD) mice during active diabetogenesis^[44,45]. They suggested that overexpression of the Reg gene(s) might represent a defense of acinar cells against pancreatic aggression. Although some results were opposite to their hypothesis^[46,47], they further confirmed their previous findings by conducting the same protocol as Fu did.

Studies on differentially expressed genes have added proof to reveal Reg's potential application in treatment. As we know, genes overexpressed in pancreatic islets of patients with diabetes are potential candidates for novel disease-related autoantigens. Subtractive hybridization was used on islets from a patient who died at the onset of type I diabetes, and a type I diabetes-related cDNA encoding hepatocarcinoma-intestine-pancreas/pancreatic-associated protein (HIP/PAP, Reg III) was identified^[48]. In addition, treatment aimed at abrogation of autoimmunity combined with expansion of β -cell mass has become a potential therapeutic approach for the treatment of insulin-dependent diabetes^[49]. Therefore, diabetes might be ameliorated with Reg protein treatment.

Tumors

Watanabe *et al.* firstly studied the relationship between cancer and Reg^[16]. Reg I mRNA was detected at various levels in gastric cancer and colorectal cancer, but was not in esophageal cancers and nontumoral mucosae of the colon, rectum and esophagus. Reg gene family has been found to be up-regulated in human colorectal cancer cell lines during differentiation^[50], this was reflected at the protein level by Western blotting in a small series of human colorectal cancers^[14]. Macadam *et al.* later analyzed 142 cases of primary colorectal adenocarcinoma and demonstrated that 53 % tumors expressed Reg I mRNA, which was only detected in 16 out of 88 (18.1 %) paired normal mucosae^[12]. PAP was also over-expressed in colorectal cancer^[14]. Reg genes were expressed in a portion of cancers, whereas no expression was found in paired normal mucosae. The mechanisms altering the transcriptional control of Reg genes might be of interest from a therapeutic standpoint^[12].

Even though there is a long history of observations related to up-regulated Reg expression in cancer. Only in the last five years, there have been experimental evidences directly supporting a role of these proteins in neoplastic transformation and tumor progression. Bernard-Perrone *et al.* localized Reg I protein in Paneth cells and immature columnar cells of human small intestinal crypts^[50], which appeared to be associated with cell growth. Reg I protein may be down-regulated when growth is achieved and differentiation is induced.

Our study on Reg IV suggested that Reg IV might play an important role in initiating colorectal adenoma, and its detection might be useful in the early diagnosis of colorectal adenoma formation^[8]. Reg IV has been screened 13 times in a subtracted cDNA library of human colon adenoma/normal mucosa by using suppression subtractive hybridization (SSH) method^[8,38]. The overexpression of Reg IV in colorectal adenomas was testified by reverse Northern blot. Our recent results showed that Reg IV was up-regulated in colorectal adenoma and carcinoma. Violette *et al.* also found its overexpression in colorectal cancer^[10], and pointed out the potential role of Reg IV in colorectal tumors and its subsequent interest as a prognostic indicator.

Another interesting topic is involved in Reg I and gastric cancer. Reg I could be expressed in gastric enterochromaffin-like (ECL) cells^[51,52]. Mutations of Reg I that inhibit secretion are associated with ECL cell carcinoids, suggesting that Reg I functions as an autocrine or paracrine tumor suppressor. Chiba suggested that Reg I might normally function as a negative

regulator of ECL cell growth to restrain the stimulatory effect of gastrin in humans^[53]. Abolition of Reg I protein secretion might result in an enhanced proliferation of ECL cells, and eventually lead to the development of ECL carcinoid tumors.

In addition to the study on relationships between diseases of gastrointestinal tract and Reg expression, there are many reports dealing with Reg and other digestive organs. Harada *et al.* examined the expression of Reg I in intrahepatic cholangiocarcinoma (ICC) and its precursor lesion (biliary dysplasia) and showed that the expression of Reg I protein was significantly dependent on the histologic differentiation^[54]. HIP at a transcriptional level was elevated in liver tumors while it was not detected in nontumorous adjacent areas or in normal adult and fetal liver, suggesting that HIP could be involved in liver cell proliferation or differentiation. HIP mRNA expression is tissue specific, since it is expressed in the normal small intestine and pancreas, while it could not be evidenced in colon, brain, kidney, or lung^[37]. HIP gene shows several potential regulatory elements, which might account for the enhanced expression of the gene during pancreatic inflammation and liver carcinogenesis^[55]. Both Reg I mRNA and its product were localized in acinar cells of the pancreas, but neither was found in ductal or islet cells. Reg I protein has been considered as a useful marker for acinar cell differentiation^[56] and immunohistochemical application of reg I protein may help to show histogenesis and differential diagnosis of pancreatic tumors.

Few reports are available on the association of Reg and tumors outside the digestive system. Bartoli *et al.* showed a weak expression of PAP/HIP gene in the pituitary gland, Reg I expression was not observed in tested adenomas or in pituitary gland^[57], whereas REGL gene was observed in pituitary gland and in some subtypes of adenomas. Reg gene was expressed only in fetal pancreas and in some adult tissues. In contrast, REGL transcript was expressed not only in fetal pancreas but also in fetal colon and brain as well as in some adult tissues. In our results, we firstly reported Reg IV's potential role in prostate cancer^[8]. From the original results of bioinformatics analysis based on public databases (serial analysis of gene expression, SAGE), we could state that Reg IV was expressed in normal colon mucosa, colon adenocarcinoma, pancreatic cancer, gastric adenocarcinoma and prostate adenocarcinoma. Since Reg family was associated with different kinds of tumors in the digestive system, this was the report of Reg IV expression in prostate adenocarcinoma although its transcript level was rather low. On the other hand, if Reg is expressed in most cancers independent of their origins and is only expressed in limited normal tissues, it is of clinical significance that Reg expression is applied to early detection and treatment of cancer. But the most important point is to make sure whether its expression is tumor-specific.

ASPECTS TO BE FURTHER STUDIED

Reg family and microsatellite instability

Microsatellite instability (MSI) has been reported to be an important feature of solid malignancies^[58]. Inactivation of the mismatch repair system (MMR) would lead to MSI that can profoundly affect cellular behaviors, since many genes playing important roles in inducing signal transduction, apoptosis, DNA repair and cell cycle control could be altered in tumors with MSI^[59].

From the report of Akiyama *et al.*^[30], we can hypothesize the possible relationship between Reg and DNA repair. Although it cannot supply strong evidences for the relationship between Reg and microsatellite instability, but other reports may further reveal its potential relationship. Cancers with MSI have a unique histological appearance and an altered response

to chemotherapy and radiotherapy. It has been more frequently seen in mucoid cancer with poor differentiation^[60-64] and the subtype with MSI also has a characteristic of drug resistance. Interestingly, Violette *et al.* discovered that Reg IV mRNA-positive tumor cells displayed unique phenotypes such as: mucus-secreting, enterocyte-like or undifferentiated ones. What is more, it was overexpressed in HT-29 drug-resistant cells^[10].

Possible early biomarkers of carcinogenesis

Zenilman *et al.* observed a phenomenon of Reg I protein expression changed in colorectal cancer^[9] and postulated that colorectal production of Reg I might either be a marker for the presence of cancer or a risk of mucosa for development of neoplasia based on the fact that Reg I protein was ectopically expressed in colorectal mucosa at the transitional zone of colorectal cancer, and occasionally within the tumor itself^[9].

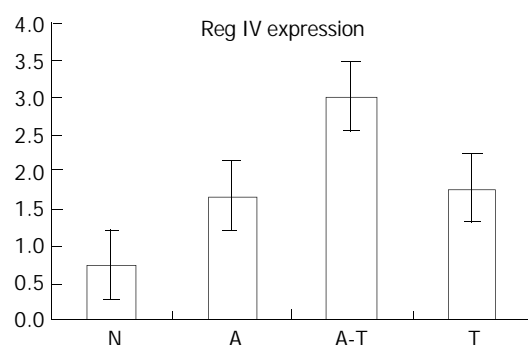


Figure 1 *In situ* hybridization results of 12 cases of colorectal adenoma with carcinomatous change. (N=normal mucosa, A=residual adenoma, A-T=adenoma with carcinomatous change, T=invasive cancer)^[13].

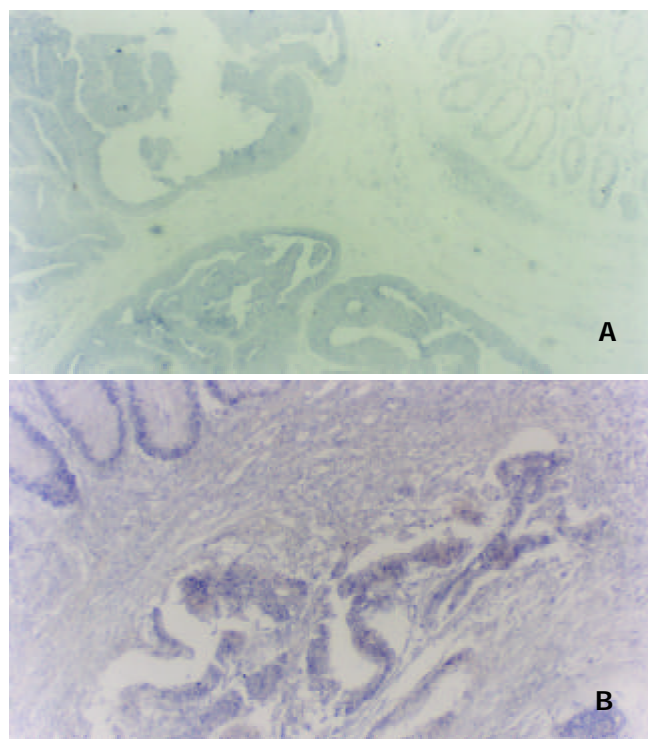


Figure 2 *In situ* hybridization of Reg IV. A: Reg IV is up-regulated in colorectal cancer, B: Reg IV is up-regulated in normal mucosa adjacent to adenoma and adenocarcinoma.

Other reports on Reg family can add some evidences to the confirmation of Reg family's role as a predictor of early cancer. Harada *et al.* suggested that expression of Reg I was a

good marker for biliary mucosa at risk for development of ICC, and that Reg I played a role in the early stages of biliary carcinogenesis, probably via a cell-proliferative effect^[54]. Our results of *in situ* hybridization showed that Reg IV was up-regulated in colorectal adenoma and carcinoma and the greatest Reg IV positivity was typically observed at regions with carcinomatous change (Figures 1, 2). Another interesting phenomenon was that at some regions near adenoma or adenocarcinoma (Figure 2b), Reg IV was also up-regulated as it was in colorectal adenoma and carcinoma, and the expression became weaker with increasing distance away from the tumor border in the direction of normal epithelia. Thus Reg IV may be thought as the biomarker of early transformations such as *in situ* carcinoma. This further presented evidences that overexpression of Reg IV might be an early event in colorectal adenoma-carcinoma sequence and carcinogenesis. Our present data also show that Reg IV is more frequently overexpressed in poorly differentiated colorectal carcinomas and carcinomas with metastasis.

The tumor-promoting activity of Reg protein should be considered for its possible clinical applications^[43]. Moreover, its sensitivity to carcinogenesis might be used for early diagnosis.

Antiapoptotic factors

Reg I might reduce epithelial apoptosis in inflammation^[65,66]. In addition, tumor necrosis factor (TNF) pathway also reflects Reg's potential role as an antiapoptotic factor. TNF-alpha contributes to the development of acute pancreatitis. Because TNF-alpha was involved in the control of apoptosis, Malka *et al.* studied its interaction with the pancreatic apoptotic pathway^[65,66]. The antiapoptotic pancreatitis-associated protein (PAP) I is a candidate for mediating TNF-alpha activity. Its expression is induced by TNF-alpha, and cells overexpressing PAP I show significantly less apoptosis on exposure to TNF-alpha. Therefore, PAP I is one of the effectors of apoptosis inhibition.

Reg gene product may regulate a series of regeneration. This regenerative response may switch off apoptotic signals. Thus, those cells, which exhibit both a regenerative response and genetic mutations in some growth promoting or metastasis inducing genes, would have a survival advantage^[12].

Up to now, we cannot confirm whether Reg I directly take part in apoptotic inhibition. But it is of interest to clarify the relationship between Reg I expression and inhibitors of apoptosis.

Predictions of poor prognosis

Expression of Reg might reflect the degree of tissue injury. Thus overexpression degree of Reg might be a useful marker to judge whether the tumor has a poor prognosis. The expression of Reg I alone and co-expression of Reg I with PAP have a significantly adverse effect on survival. Thus the expression of Reg I might provide a valuable selective indicator of adjuvant therapy in patients with early-stage colorectal cancer which would recur after curative surgery^[12].

Reports also revealed that a role of Reg gene in the healing of gastrointestinal mucosal lesions. Up-regulation of Reg I expression in ulcerative colitis might reflect the activation of mucosal injury followed by down-regulation when the injury was healed. Interestingly, a similar feature was also appeared in Reg IV. Our results showed that higher levels of Reg IV mRNA were consistently scored in regions with more severe dysplasia in the same adenoma sample displaying a varying degree of dysplasia. We postulate that Reg IV overexpression may reflect the degree of body injuries. However, when two tumors coexisted in a single case, Reg IV transcript was usually

higher in adenomas compared with paired carcinomas. The mechanism is not clear.

In addition to these mechanisms, Reg family has been found to be implicated in other physiological processes. Reg II has a distinctive role in injury response^[67] and its expression is a crucial step in ciliary neurotrophic factor (CNTF) survival pathway. Reg II has been found to be a neurotrophic factor and also an intermediate in the survival signalling pathway of CNTF-related cytokines^[68].

In conclusion, we have characterized the structure and expression of Reg genes. Their possible functions and mechanisms were also discussed. These studies have led to a better understanding of the essential functions of these Reg family genes in mammalian physiological processes and human diseases. In addition to its potential application in diabetes, future studies on Reg family and human malignancy will shed lights on Reg's unusual features on cancer. As we know, expression of Reg I inversely correlated with the level of cell differentiation, and it could be modulated via the glucocorticoid receptor, and has been found to be a potential marker of gastrointestinal epithelial differentiation^[69]. Rechreche *et al.* suggested that inhibition of PAP/reg expression in normal colon cells by silencing their gene promoters could be relieved during colon carcinogenesis, allowing their up-regulation by mediators such as cytokines. Reg's role in human malignancy especially in the digestive system should be further studied^[11,14]. More recently, Kamarainen *et al.* identified and characterized a gene encoding a regenerating protein (REG)-like protein called RELP^[70], and found there were several transcripts of RELP and the predicted protein product of the major transcript was annotated Reg IV.

All these encourage us to further study the potential roles of Reg family, especially Reg IV in human tumors. Are they sensitive reactants of tissue injury? Do they play oncogenic roles in colorectal cancers? Is there any potential if they are used as early biomarkers of carcinogenesis? Could they be used as prognostic indicators of tumor survival and disease severity? Before these conclusions can be drawn, further investigations are needed. Thus, detection of the expression level of Reg in cancers with different histological features and survival rates, and analysis of Reg gene status in human tumors at different stages or sites, are required to elucidate the pathophysiologic roles of Reg family.

REFERENCES

- Hartupée JC**, Zhang H, Bonaldo MF, Soares MB, Dieckgraefe BK. Isolation and characterization of a cDNA encoding a novel member of the human regenerating protein family: Reg IV. *Biochim Biophys Acta* 2001; **1518**: 287-293
- Lasserre C**, Simon MT, Ishikawa H, Diriong S, Nguyen VC, Christa L, Vernier P, Brechot C. Structural organization and chromosomal localization of a human gene (HIP/PAP) encoding a C-type lectin overexpressed in primary liver cancer. *Eur J Biochem* 1994; **224**: 29-38
- Chakraborty C**, Katsumata N, Myal Y, Schroedter IC, Brazeau P, Murphy LJ, Shiu RP, Friesen HG. Age-related changes in peptide-23/pancreatitis-associated protein and pancreatic stone protein/reg gene expression in the rat and regulation by growth hormone-releasing hormone. *Endocrinology* 1995; **136**: 1843-1849
- Katsumata N**, Chakraborty C, Myal Y, Schroedter IC, Murphy LJ, Shiu RP, Friesen HG. Molecular cloning and expression of peptide 23, a growth hormone-releasing hormone-inducible pituitary protein. *Endocrinology* 1995; **136**: 1332-1339
- Broekaert D**, Eyckerman S, Lavens D, Verhee A, Waelput W, Vandekerckhove J, Tavernier J. Comparison of leptin- and interleukin-6-regulated expression of the rPAP gene family: evidence for differential co-regulatory signals. *Eur Cytokine Netw* 2002; **13**: 78-85
- Duseti NJ**, Frigerio JM, Fox MF, Swallow DM, Dagorn JC, Iovanna JL. Molecular cloning, genomic organization, and chromosomal localization of the human pancreatitis-associated protein (PAP) gene. *Genomics* 1994; **19**: 108-114
- Okamoto H**. The Reg gene family and Reg proteins: with special attention to the regeneration of pancreatic β -cells. *J Hepatobiliary Pancreat Surg* 1999; **6**: 254-262
- Zhang YW**, Lai MD, Gu XM. Reg IV, a differentially expressed gene in colorectal adenoma. *Chinese Medical Journal* 2003; **116**: 918-922
- Zenilman ME**, Kim S, Levine BA, Lee C, Steinberg JJ. Ectopic Expression of reg Protein: A Marker of Colorectal Mucosa at Risk for Neoplasia. *J Gastrointest Surg* 1997; **1**: 194-202
- Violette S**, Festor E, Pandrea-Vasile I, Mitchell V, Adida C, Dussaulx E, Lacorte JM, Chambaz J, Lacasa M, Lesuffleur T. Reg IV, a new member of the regenerating gene family, is overexpressed in colorectal carcinomas. *Int J Cancer* 2003; **103**: 185-193
- Kadowaki Y**, Ishihara S, Miyaoka Y, Rumi MA, Sato H, Kazumori H, Adachi K, Takasawa S, Okamoto H, Chiba T, Kinoshita Y. Reg protein is overexpressed in gastric cancer cells, where it activates a signal transduction pathway that converges on ERK1/2 to stimulate growth. *FEBS Lett* 2002; **530**: 59-64
- Macadam RC**, Sarela AI, Farmery SM, Robinson PA, Markham AF, Guillou PJ. Death from early colorectal cancer is predicted by the presence of transcripts of the REG gene family. *Br J Cancer* 2000; **83**: 188-195
- Zhang Y**, Lai M, Lv B, Gu X, Wang H, Zhu Y, Shao L, Wang G. Overexpression of Reg IV in colorectal adenoma. *Cancer Letters* 2003; **200**: 69-76
- Rechreche H**, Montalto G, Mallo GV, Vasseur S, Marasa L, Soubeyran P, Dagorn JC, Iovanna JL. pap, reg Ialpha and reg Ibeta mRNAs are concomitantly up-regulated during human colorectal carcinogenesis. *Int J Cancer* 1999; **81**: 688-694
- Terazono K**, Yamamoto H, Takasawa S, Shiga K, Yonemura Y, Tochino Y, Okamoto H. A novel gene activated in regenerating islets. *J Biol Chem* 1988; **263**: 2111-2114
- Watanabe T**, Yonekura H, Terazono K, Yamamoto H, Okamoto H. Complete nucleotide sequence of human reg gene and its expression in normal and tumoral tissues. The reg protein, pancreatic stone protein, and pancreatic thread protein are one and the same product of the gene. *J Biol Chem* 1990; **265**: 7432-7439
- De Reggi M**, Gharib B. Protein-X, Pancreatic Stone-, Pancreatic thread-, reg-protein, P19, lithostathine, and now what? Characterization, structural analysis and putative function(s) of the major non-enzymatic protein of pancreatic secretions. *Curr Protein Pept Sci* 2001; **2**: 19-42
- Unno M**, Yonekura H, Nakagawara K, Watanabe T, Miyashita H, Moriizumi S, Okamoto H, Itoh T, Teraoka H. Structure, chromosomal localization, and expression of mouse reg genes, reg I and reg II. A novel type of reg gene, reg II, exists in the mouse genome. *J Biol Chem* 1993; **268**: 15974-15982
- Okamoto H**. The Reg gene family and Reg proteins: with special attention to the regeneration of pancreatic β -cells. *J Hepatobiliary Pancreat Surg* 1999; **6**: 254-262
- Stephanova E**, Tissir F, Duseti N, Iovanna J, Szpirer J, Szpirer C. The rat genes encoding the pancreatitis-associated proteins I, II and III (Pap1, Pap2, Pap3), and the lithostathin/pancreatic stone protein/regeneration protein (Reg) colocalize at 4q33→q34. *Cytogenet Cell Genet* 1996; **72**: 83-85
- Abe M**, Nata K, Akiyama T, Shervani NJ, Kobayashi S, Tomioka-Kumagai T, Ito S, Takasawa S, Okamoto H. Identification of a novel Reg family gene, Reg IIIdelta, and mapping of all three types of Reg family gene in a 75 kilobase mouse genomic region. *Gene* 2000; **246**: 111-122
- Kawanami C**, Fukui H, Kinoshita Y, Nakata H, Asahara M, Matsushima Y, Kishi K, Chiba T. Regenerating gene expression in normal gastric mucosa and indomethacin-induced mucosal lesions of the rat. *J Gastroenterol* 1997; **32**: 12-18
- Schiesser M**, Bimmler D, Frick TW, Graf R. Conformational changes of pancreatitis-associated protein (PAP) activated by trypsin lead to insoluble protein aggregates. *Pancreas* 2001; **22**: 186-192
- Zenilman ME**, Magnuson TH, Swinson K, Egan J, Perfetti R, Shuldiner AR. Pancreatic thread protein is mitogenic to pancre-

- atic-derived cells in culture. *Gastroenterology* 1996; **110**: 1208-1214
- 25 **Weis WI**, Kahn R, Fourme R, Drickamer K, Hendrickson WA. Structure of the calcium-dependent lectin domain from a rat mannose-binding protein determined by MAD phasing. *Science* 1991; **254**: 1608-1615
- 26 **Kishore U**, Eggleton P, Reid KB. Modular organization of carbohydrate recognition domains in animal lectins. *Matrix Biol* 1997; **15**: 583-592
- 27 **Kobayashi S**, Akiyama T, Nata K, Abe M, Tajima M, Shervani NJ, Unno M, Matsuno S, Sasaki H, Takasawa S, Okamoto H. Identification of a receptor for reg (regenerating gene) protein, a pancreatic β -cell regeneration factor. *J Biol Chem* 2000; **275**: 10723-10726
- 28 **Okamoto H**, Takasawa S. Recent advances in the Okamoto model: the CD38-cyclic ADP-ribose signal system and the regenerating gene protein (Reg)-Reg receptor system in β -cells. *Diabetes* 2002; **51** (Suppl 3): S462-473
- 29 **Kazumori H**, Ishihara S, Fukuda R, Kinoshita Y. Localization of Reg receptor in rat fundic mucosa. *J Lab Clin Med* 2002; **139**: 101-108
- 30 **Akiyama T**, Takasawa S, Nata K, Kobayashi S, Abe M, Shervani NJ, Ikeda T, Nakagawa K, Unno M, Matsuno S, Okamoto H. Activation of Reg gene, a gene for insulin-producing β -cell regeneration: poly(ADP-ribose) polymerase binds Reg promoter and regulates the transcription by autopoly(ADP-ribosyl)ation. *Proc Natl Acad Sci U S A* 2001; **98**: 48-53
- 31 **Graf R**, Schiesser M, Lussi A, Went P, Scheele GA, Bimmler D. Coordinate regulation of secretory stress proteins (PSP/reg, PAP I, PAP II, and PAP III) in the rat exocrine pancreas during experimental acute pancreatitis. *J Surg Res* 2002; **105**: 136-144
- 32 **Cavallini G**, Bovo P, Bianchini E, Carsana A, Costanzo C, Merola M, Sgarbi D, Frulloni L, Di Francesco V, Libonati M, Palmieri M. Lithostathine messenger RNA expression in different types of chronic pancreatitis. *Mol Cell Biochem* 1998; **185**: 147-152
- 33 **Meili S**, Graf R, Perren A, Schiesser M, Bimmler D. Secretory apparatus assessed by analysis of pancreatic secretory stress protein expression in a rat model of chronic pancreatitis. *Cell Tissue Res* 2003; **312**: 291-299
- 34 **Satomura Y**, Sawabu N, Ohta H, Watanabe H, Yamakawa O, Motoo Y, Okai T, Taya D, Makino H, Okamoto H. The immunohistochemical evaluation of PSP/reg-protein in normal and diseased human pancreatic tissues. *Int J Pancreatol* 1993; **13**: 59-67
- 35 **Miyaura C**, Chen L, Appel M, Alam T, Inman L, Hughes SD, Milburn JL, Unger RH, Newgard CB. Expression of reg/PSP, a pancreatic exocrine gene: relationship to changes in islet β -cell mass. *Mol Endocrinol* 1991; **5**: 226-234
- 36 **Shinozaki S**, Nakamura T, Iimura M, Kato Y, Iizuka B, Kobayashi M, Hayashi N. Upregulation of Reg 1alpha and GW112 in the epithelia of inflamed colonic mucosa. *Gut* 2001; **48**: 623-629
- 37 **Lasserre C**, Christa L, Simon MT, Vernier P, Brechot C. A novel gene (HIP) activated in human primary liver cancer. *Cancer Res* 1992; **52**: 5089-5095
- 38 **Luo MJ**, Lai MD. Identification of differentially expressed genes in normal mucosa, adenoma and adenocarcinoma of colon by SSH. *World J Gastroenterol* 2001; **7**: 726-731
- 39 **Honda H**, Nakamura H, Otsuki M. The elongated PAP II/Reg III mRNA is upregulated in rat pancreas during acute experimental pancreatitis. *Pancreas* 2002; **25**: 192-197
- 40 **Yamaoka T**, Itakura M. Development of pancreatic islets. *Int J Mol Med* 1999; **3**: 247-261
- 41 **Okamoto H**. Cyclic ADP-ribose-mediated insulin secretion and Reg, regenerating gene. *J Mol Med* 1999; **77**: 74-78
- 42 **Unno M**, Nata K, Noguchi N, Narushima Y, Akiyama T, Ikeda T, Nakagawa K, Takasawa S, Okamoto H. Production and characterization of Reg knockout mice: reduced proliferation of pancreatic β -cells in Reg knockout mice. *Diabetes* 2002; **51**(Suppl 3): S478-483
- 43 **Takasawa S**, Okamoto H. Pancreatic β -cell death, regeneration and insulin secretion: roles of poly(ADP-ribose) polymerase and cyclic ADP-ribose. *Int J Exp Diabetes Res* 2002; **3**: 79-96
- 44 **Sanchez D**, Baeza N, Blouin R, Devaux C, Grondin G, Mabrouk K, Guy-Crotte O, Figarella C. Overexpression of the reg gene in non-obese diabetic mouse pancreas during active diabetogenesis is restricted to exocrine tissue. *J Histochem Cytochem* 2000; **48**: 1401-1410
- 45 **Baeza N**, Sanchez D, Christa L, Guy-Crotte O, Guy-Crotte O, Vialettes B, Figarella C. Pancreatitis-associated protein (HIP/PAP) gene expression is upregulated in NOD mice pancreas and localized in exocrine tissue during diabetes. *Digestion* 2001; **64**: 233-239
- 46 **Ortiz EM**, Dusetti NJ, Vasseur S, Malka D, Bodeker H, Dagorn JC, Iovanna JL. The pancreatitis-associated protein is induced by free radicals in AR4-2 J cells and confers cell resistance to apoptosis. *Gastroenterology* 1998; **114**: 808-816
- 47 **Fu K**, Sarras MP Jr, De Lisle RC, Andrews GK. Regulation of mouse pancreatitis-associated protein-I gene expression during caerulein-induced acute pancreatitis. *Digestion* 1996; **57**: 333-340
- 48 **Gurr W**, Yavari R, Wen L, Shaw M, Mora C, Christa L, Sherwin RS. A Reg family protein is overexpressed in islets from a patient with new-onset type 1 diabetes and acts as T-cell autoantigen in NOD mice. *Diabetes* 2002; **51**: 339-346
- 49 **Gross DJ**, Weiss L, Reibstein I, van den Brand J, Okamoto H, Clark A, Slavin S. Amelioration of diabetes in nonobese diabetic mice with advanced disease by linomide-induced immunoregulation combined with Reg protein treatment. *Endocrinology* 1998; **139**: 2369-2374
- 50 **Bernard Perrone FR**, Renaud WP, Guy Crotte OM, Bernard P, Figarella CG, Okamoto H, Balas DC, Senegas-Balas FO. Expression of REG protein during cell growth and differentiation of two human colon carcinoma cell lines. *J Histochem Cytochem* 1999; **47**: 863-870
- 51 **Fukui H**, Kinoshita Y, Maekawa T, Okada A, Waki S, Hassan S, Okamoto H, Chiba T. Regenerating gene protein may mediate gastric mucosal proliferation induced by hypergastrinemia in rats. *Gastroenterology* 1998; **115**: 1483-1493
- 52 **Higham AD**, Bishop LA, Dimaline R. Mutations of RegIalpha are associated with enterochromaffin-like cell tumor development in patients with hypergastrinemia. *Gastroenterology* 1999; **116**: 1310-1318
- 53 **Chiba T**. Is reg gene mutation involved in the development of enterochromaffin-like cell carcinoid tumors? *Gastroenterology* 1999; **116**: 1489-1491
- 54 **Harada K**, Zen Y, Kanemori Y, Chen TC, Chen MF, Yeh TS, Jan YY, Masuda S, Nimura Y, Takasawa S, Okamoto H, Nakanuma Y. Human REG I gene is up-regulated in intrahepatic cholangiocarcinoma and its precursor lesions. *Hepatology* 2001; **33**: 1036-1042
- 55 **Lasserre C**, Simon MT, Ishikawa H, Diriong S, Nguyen VC, Christa L, Vernier P, Brechot C. Structural organization and chromosomal localization of a human gene (HIP/PAP) encoding a C-type lectin overexpressed in primary liver cancer. *Eur J Biochem* 1994; **224**: 29-38
- 56 **Kimura N**, Yonekura H, Okamoto H, Nagura H. Expression of human regenerating gene mRNA and its product in normal and neoplastic human pancreas. *Cancer* 1992; **70**: 1857-1863
- 57 **Bartoli C**, Baeza N, Figarella C, Pellegrini I, Figarella-Branger D. Expression of peptide-23/pancreatitis-associated protein and Reg genes in human pituitary and adenomas: comparison with other fetal and adult human tissues. *J Clin Endocrinol Metab* 1998; **83**: 4041-4046
- 58 **Mao L**, Lee DJ, Tockman MS, Erozan YS, Askin F, Sidransky D. Microsatellite alterations as clonal markers for the detection of human cancer. *Proc Natl Acad Sci U S A* 1994; **91**: 9871-9875
- 59 **Polato F**, Brogini M. Microsatellite instability and genetic alterations in ovarian cancer. *Minerva Ginecol* 2003; **55**: 129-138
- 60 **Zhang YW**, Lai MD. Microsatellite alterations on chromosome 9p21-22 in sporadic colorectal cancer. *Zhonghua Binglixue Zazhi* 1999; **28**: 418-421
- 61 **Chao A**, Gilliland F, Willman C, Joste N, Chen IM, Stone N, Ruschulte J, Viswanatha D, Duncan P, Ming R, Hoffman R, Foucar E, Key C. Patient and tumor characteristics of colon cancers with microsatellite instability: a population-based study. *Cancer Epidemiol Biomarkers Prev* 2000; **9**: 539-544
- 62 **Alexander J**, Watanabe T, Wu TT, Rashid A, Li S, Hamilton SR. Histopathological identification of colon cancer with microsatellite instability. *Am J Pathol* 2001; **158**: 527-535
- 63 **Samowitz WS**, Curtin K, Ma KN, Schaffer D, Coleman LW,

- Leppert M, Slattery ML. Microsatellite instability in sporadic colon cancer is associated with an improved prognosis at the population level. *Cancer Epidemiol Biomarkers Prev* 2001; **10**: 917-923
- 64 **Greenson JK**, Bonner JD, Ben-Yzhak O, Cohen HI, Miselevich I, Resnick MB, Trougouboff P, Tomsho LD, Kim E, Low M, Almog R, Rennert G, Gruber SB. Phenotype of microsatellite unstable colorectal carcinomas: Well-differentiated and focally mucinous tumors and the absence of dirty necrosis correlate with microsatellite instability. *Am J Surg Pathol* 2003; **27**: 563-570
- 65 **Malka D**, Vasseur S, Bodeker H, Ortiz EM, Dusetti NJ, Verrando P, Dagorn JC, Iovanna JL. Tumor necrosis factor alpha triggers antiapoptotic mechanisms in rat pancreatic cells through pancreatitis-associated protein I activation. *Gastroenterology* 2000; **119**: 816-828
- 66 **Dieckgraefe BK**, Crimmins DL, Landt V, Houchen C, Anant S, Porche-Sorbet R, Ladenson JH. Expression of the regenerating gene family in inflammatory bowel disease mucosa: Reg Ialpha upregulation, processing, and antiapoptotic activity. *J Investig Med* 2002; **50**: 421-434
- 67 **Averill S**, Davis DR, Shortland PJ, Priestley JV, Hunt SP. Dynamic pattern of reg-2 expression in rat sensory neurons after peripheral nerve injury. *J Neurosci* 2002; **22**: 7493-7501
- 68 **Nishimune H**, Vasseur S, Wiese S, Birling MC, Holtmann B, Sendtner M, Iovanna JL, Henderson CE. Reg-2 is a motoneuron neurotrophic factor and a signalling intermediate in the CNTF survival pathway. *Nat Cell Biol* 2000; **2**: 906-914
- 69 **Zenilman ME**, Magnuson TH, Perfetti R, Chen J, Shuldiner AR. Pancreatic reg gene expression is inhibited during cellular differentiation. *Ann Surg* 1997; **225**: 327-332
- 70 **Kamarainen M**, Heiskala K, Knuutila S, Heiskala M, Winqvist O, Andersson LC. RELP, a Novel Human Reg-Like Protein with Up-Regulated Expression in Inflammatory and Metaplastic Gastrointestinal Mucosa. *Am J Pathol* 2003; **163**: 11-20

Edited by Zhang JZ and Wang XL

Aberrant crypt foci as microscopic precursors of colorectal cancer

Lei Cheng, Mao-De Lai

Lei Cheng, Mao-De Lai, Department of pathology, School of Medical Sciences, Zhejiang University, Hangzhou, 310006, Zhejiang Province, China

Correspondence to: Mao-De Lai, M.D., Professor of pathology, Department of Pathology, School of Medical Sciences, Zhejiang University, Hangzhou, 310006, Zhejiang Province, China. lmd@sun.zju.edu.cn

Telephone: +86-571-87217134 **Fax:** +86-571-87951358

Received: 2003-05-12 **Accepted:** 2003-06-02

Abstract

Since the first detection of aberrant crypt foci (ACF) in carcinogen-treated mice, there have been numerous studies focusing on these microscopically visible lesions both in rodents and in humans. ACF have been generally accepted as precancerous lesions in regard to histopathological characteristics, biochemical and immunohistochemical alterations, and genetic and epigenetic alterations. ACF show variable histological features, ranging from hyperplasia to dysplasia. ACF in human colon are more frequently located in the distal parts than in the proximal parts, which is in accordance with those in colorectal cancer (CRC). The immunohistochemical expressions of carcinoembryonic antigen (CEA), β -catenin, placental cadherin (P-cadherin), epithelial cadherin (E-cadherin), inducible nitric oxide synthase (iNOS), cyclooxygenase (COX-2), and P16^{INK4a} are found to be altered. Genetic mutations of K-ras, APC and p53, and the epigenetic alterations of CpG island methylation of ACF have also been demonstrated. Genomic instabilities due to the defect of mismatch repair (MMR) system are detectable in ACF. Two hypotheses have been proposed. One is the "dysplasia ACF-adenoma-carcinoma sequence", the other is "heteroplastic ACF-adenoma-carcinoma sequence". The malignant potential of ACF, especially dysplastic ACF, makes it necessary to reveal the nature of these lesions, and to prevent CRC from the earliest possible stage. The technique of magnifying chromoscope makes it possible to detect "in vivo" ACF, which is beneficial to colon cancer research, identifying high-risk populations for CRC, and developing preventive procedures.

Cheng L, Lai MD. Aberrant crypt foci as microscopic precursors of colorectal cancer. *World J Gastroenterol* 2003; 9(12): 2642-2649
<http://www.wjgnet.com/1007-9327/9/2642.asp>

INTRODUCTION

Genetic changes in the malignant transformation process of colorectal mucosa include deletions, rearrangements, and mutations leading to either inactivation or activation of specific target genes^[1-3]. A number of biomarkers associated with genetic changes have been identified for early detection of CRC. Two major classes of genes, oncogenes and suppressor genes, are involved in addition to mismatch repair (MMR) genes^[4-6], which are associated with genomic instability. The major advances in understanding CRC include identification of the involvement of APC, p53, K-ras and MMR genes, as well as epigenetic alterations, such as CpG island methylation,

in the formation and progression of the disease. Identification of ACF as an early preinvasive lesion and its relationship to the development of cancer have aroused an increasing interest in recent years.

Since the first detection of ACF in carcinogen-treated mice by Bird in 1987 and the hypothesis of ACF as the earliest precursors of CRC, there have been numerous studies focusing on these microscopically visible lesions both in rodents and in humans. The following table (Table 1) shows some highlights of studies on human ACF.

Table 1 Highlights of human ACF in recent years (from NCBI)

Major fields	Magazines and authors	Year
Histopathology	Kristt D, <i>et al.</i> Hum Pathol.	1999
	Nascimbeni R, <i>et al.</i> Am J Surg Pathol.	1999
	Shipitz B, <i>et al.</i> Hum Pathol.	1998
	Siu IM, <i>et al.</i> Am J Pathol.	1997
	Di Gregorio C, <i>et al.</i> Histopathology.	
	Roncucci L, <i>et al.</i> Cancer Epidemiol Biomarkers Prev.	1997
	Roncucci L, <i>et al.</i> Hum Pathol.	1991
Gene mutations	Yuan P, <i>et al.</i> World J Gastroenterol.	2001
	Takayama T, <i>et al.</i> Gastroenterology.	2001
	Otori K, <i>et al.</i> Cancer.	1998
	Bjerknes M, <i>et al.</i> Am J Pathol.	1997
	Losi L, <i>et al.</i> J Pathol.	1996
	Zaidi NH, <i>et al.</i> Carcinogenesis.	1995
	Smith AJ, <i>et al.</i> Cancer Res.	1994
Epigenetic/phenotype alterations of genes		
CpG island methylation	Chan AO, <i>et al.</i> Am J Pathol.	2002
	Sakurazawa N, <i>et al.</i> Cancer Res.	2000
Microsatellite instability	Pedroni M, <i>et al.</i> Cancer Res.	2001
	Heinen CD, <i>et al.</i> Cancer Res.	1996
	Augenlicht LH, <i>et al.</i> Oncogene.	1996
Cell dynamics and proliferation	Roncucci L, <i>et al.</i> Cell Prolif.	2000
	Kristt D, <i>et al.</i> Pathol Oncol Res.	1999
	Otori K, <i>et al.</i> Cancer Res.	1995
	Roncucci L, <i>et al.</i> Cancer Res.	1993
	Dong M, <i>et al.</i> Carcinogenesis.	2003
Oncoproteins	Hao XP, <i>et al.</i> Cancer Res.	2001
	Shpitz B, <i>et al.</i> Anticancer Res.	1999
	Pretlow TP, <i>et al.</i> Gastroenterology.	1994
	Nascimbeni R, <i>et al.</i> Cancer Epidemiol Biomarkers Prev.	2002
	Johnson IT, <i>et al.</i> Food Chem Toxicol.	2002
Dietary agents	Alabaster O, <i>et al.</i> Mutat Res.	1996
	Hurlstone DP, <i>et al.</i> Br J Surg.	2002
	Matsumoto T, <i>et al.</i> Am J Gastroenterol. ^a	1999
	Takayama T, <i>et al.</i> N Engl J Med.	1998
	Yokota T, <i>et al.</i> Gastrointest Endosc.	1997
	Dolara P, <i>et al.</i> Cancer Detect Prev.	1997
	Murillo G, <i>et al.</i> Int J Cancer.	2003
Chemoprevention	Osawa E, <i>et al.</i> Gastroenterology.	2003
	Kassie F, <i>et al.</i> Carcinogenesis.	2003
	Osawa E, <i>et al.</i> Life Sci.	2002
	Mori H, <i>et al.</i> Biofactors.	2000
	Chung FL, <i>et al.</i> Carcinogenesis.	2000
Signal transduction pathways	Boon EM, <i>et al.</i> Cancer Res. ^b	2002

a: ileal microadenoma; b: in colorectal cell lines.

Identification of ACF both in carcinogen-treated rodents and in human colon makes the study of CRC at precancerous stages possible. The growth, morphological and molecular features of ACF support the contention that ACF are putative preneoplastic lesions. The traditional “adenoma-carcinoma” sequence of colorectal carcinogenesis has been extended to “ACF-adenoma-carcinoma” sequence. A better understanding of the underlying cellular and molecular events affected by cancer preventive or promoting agents will provide more insights into colorectal carcinogenesis and lead to the development of different cancer preventive strategies for high-risk individuals and the general population.

DEFINITION OF ACF

ACF was first reported by Bird in 1987^[7] in the colons of carcinogen-treated C57BL/6J or CF1 female mice, and the assumption of ACF as potential preneoplastic lesions in murine colon was put forward one year later, coming up with the methodological approach to detect ACF^[8]. Under microscope, aberrant crypts appeared larger and had a thicker epithelial lining compared to normal crypts, and usually gathered into a focus, consisting of aberrant crypts from one to hundreds^[9,10]. These aberrant crypts sometimes were slightly elevated from the surrounding normal mucosa and often had oval or slit-like lumens^[9,11-13]. It has been described as single or clusters of abnormally large crypts of the colon mucosal surface after stained with methylene blue. On colonoscopy, ACF were defined as being deeper with methylene blue staining than normal surrounding mucosa, and as a cluster of two or more crypts with dilated or slit-like openings rising above the surrounding mucosa^[14,15].

ACF with a single crypt met the following criteria by McLellan^[16]. The size of the crypt was at least twice that of the normal surrounding ones, the luminal opening was more elliptical than circular, and the epithelial lining was thicker than that of the normal surrounding crypts. ACF consisting of more than one crypt were defined as crypts to form a distinct focus. Individual crypts within the focus had a thicker epithelial lining and an elliptical luminal opening, and the total area occupied by the crypts of ACF was greater than that occupied by an equivalent number of surrounding morphologically normal crypts.

In humans, ACF were described and partially characterized for the first time in 1991^[9,11], and in 1994, Pretlow first detected altered enzymatic activity, crypt dynamics and proliferation. ACF in human colon closely resembled aberrant crypts seen in rodents treated with carcinogens^[7]. Some lines of evidences supported the view that ACF or at least some of them, might be precursors of CRC. In particular, ACF in human colon were more often located in the distal parts than in the proximal parts^[17], which was verified in animal model^[18]. Aberrant crypts had a hyperproliferative epithelium^[19-21]. The size of ACF could increase with time, and it was evident that the nuclear atypia noted in some ACF was similar to those seen in the crypts of adenocarcinomas in rat colons^[16]. In ACF, the immunohistochemical expressions of carcinoembryonic antigen^[22] and β -catenin^[23-25] were increased. K-ras, APC and P53 mutations, have been shown to be important genetic alterations in the development of CRC^[26,27], have been demonstrated in ACF^[28-33]. Identification of dysplasia and monoclonality in a putative precursor lesion would strongly link this lesion to neoplastic progression. ACF have been confirmed to arise from independent initiation events^[28-30,34], and when examined histologically, ACF showed variable features, ranging from mild hyperplasia to dysplasia^[12,22,35,36]

HISTOPATHOLOGICAL CHARACTERISTICS OF ACF

The final histological criteria for ACF are generally accepted

as “nondysplasia”, “dysplasia” and “mixed type”^[10,12,16,17,35-40].

ACF without dysplasia

ACF with normal mucosa: lacking significant modifications of the epithelium lining the crypts, enlarged crypts (at least 1.5 times larger than normal) with only slightly enlarged and elongated nuclei, but no crowding or stratification, and no mucin depletion. Crypt cells with positive staining of PCNA and Ki-67 remain at the lower part of the crypts.

ACF with hyperplasia: analogous to the manifestations of hyperplastic polyps of colon. The crypts are larger or longer than normal crypts sometimes showing apical branching. The luminal opening is serrated and slightly elevated from the surrounding normal mucosa, but without dysplasia. Goblet cells are mixed with absorbing cells, with partial mucin depletion. Nuclei are enlarged or sometimes crowded without stratification. Cells with positive staining of PCNA and Ki-67 remain at the lower and middle parts of the crypts.

ACF with dysplasia (microadenoma)

Both crypts and cells have different degree abnormalities, with enlarged, elongated and sometimes stratified and depolarized nuclei. The number of goblet cells is decreased obviously and mucin is depleted. The major site of positive staining cells of PCNA and Ki-67 is extended to the upper part of the crypts. Serrated adenomatous ACF^[41] could also be found to have similar histopathological manifestations of serrated adenomas^[42].

Dysplastic ACF were common in FAP patients, and also occurred in sporadic patients at a low frequency^[12,31,35]. Sporadic ACF had the characteristics similar to those of dysplastic ACF in FAP patients with less frequent APC mutations^[10,43] and more frequent methylation^[44].

Investigations showed the possibility of ACF transition from one pathological type to another. ACF have also been found to contain carcinoma *in situ*, or severe dysplasia in focal areas of human colon^[36,40,41], and invasive carcinoma in the rat model^[13], showing evidences of ACF as precancerous lesions^[10,21,30,38,43,45].

ACF with mixed type of hyperplasia and dysplasia

ACF with mixed hyperplastic and adenomatous components histologically showed the combination of various proportions of pure adenomatous pattern with dysplasia and pure hyperplastic pattern without dysplasia^[41].

The WHO classifications of ACF are simplified as hyperplastic ACF and dysplastic ACF.

ACF EVALUATION

The density of ACF is the number of ACF per square centimeter of mucosa surface, which was higher in diseases at a high risk of malignancy such as familial adenomatous polyposis (FAP) and in CRC, and was lower in patients with benign diseases of the colon such as diverticulosis^[11,37]. ACF density is also significantly and progressively higher from proximal colon toward distal, being the highest in sigmoid and rectum, which was in accordance with the location of CRC^[19,37]. It has been found that the density of FAP ACF was significantly higher than that of sporadic CRC and benign large bowel diseases^[9]. In a comparative research of sporadic CRC, Gardner's syndrome, and benign diseases such as diverticulosis, ACF density in Gardner's syndrome was more common and ACF occupied a larger area of mucosa as compared to sporadic CRC^[11]. All these findings showed that hereditary diseases prone to colon cancer had a higher density and crypt multiplicity of ACF than CRC, which shed lights on the differences between hereditary ACF and sporadic ACF, and helped to reveal the neoplastic nature of ACF.

The mechanism by which ACF increase in size seems to be a process of crypt division, which begins at the base of the crypt and proceeds upwards until two crypts are generated. Thus, the number of crypts per ACF, also termed "crypt multiplicity", would be an important parameter for evaluating ACF progression. It has been demonstrated that crypt multiplicity was significantly lower from proximal toward distal colon, which was opposite to that of ACF density, and was significantly larger when it was associated with carcinoma or adenoma than with nonneoplastic diseases^[39]. Also no gradient in ACF density and crypt multiplicity was observed according to the distance from the tumor^[11,37,39].

Increased mitotic activity, which has been proposed as a biomarker of colon cancer at early stages, was observed in a majority of ACF. Most of the crypts showed a mitotic pattern similar to that of normal adjacent crypts^[19,46]. In some of the dysplastic foci, mitotic activity was seen to distribute throughout the crypts, as reported in adenomas. The above findings may be consistent with the assumption that ACF were preneoplastic lesions^[47].

Protein kinase C (PKC) is a family of twelve distinct serine/threonine kinases that participate in signaling pathways involved in cell proliferation, differentiation, and apoptosis. Alterations in PKC isozyme levels also played a role in colon carcinogenesis^[48-50]. Elevated expression of PKC β_{II} was associated with neoplastic transformation both in rat and in human colonic epithelia^[48,50]. It has been demonstrated that overexpression of protein kinase C β_{II} (PKC β_{II}) made transgenic mice more susceptible to carcinogen-induced colonic hyperproliferation and ACF formation^[47], and the level of PKC β_{II} protein expression was strikingly increased in ACF compared with that in normal colonic epithelium^[51].

The study of ACF and their relationships to growth factors, such as TGF- α , TGF- β , EGFR, TGF β RII, phosphorylated cellular tyrosine (P-tyr) revealed a strong correlation between altered expression of TGFs in all ACF that have been examined and the degree of dysplasia and crypt multiplicity^[52]. TGF- α was undetectable in ACF^[52,53], which had a high incidence of apoptosis (AI). The result was similar to that both in adenomas and in carcinomas^[53]. Apoptosis provides a protective mechanism against neoplasia by moving genetically damaged stem cells from the epithelium before they can undergo clonal expansion. Manifestations are indicative of a high level of apoptosis in human ACF and carcinogen-treated animal ACF, in which apoptosis was said to eliminate cells damaged by carcinogen administration^[54].

DIFFERENCES OF FAP AND SPORADIC ACF

Most FAP ACF are histopathologically, phenotypically and genetically different from sporadic ACF. Apart from the differences in ACF density between FAP ACF and sporadic ACF, there are significant differences in regard to dysplasia. Most FAP ACF were dysplastic, whereas sporadic ACF had the histopathological features of hyperplastic polyps with little or no dysplasia^[38]. The degree of dysplasia in FAP ACF was severer than that of sporadic ACF^[9]. Most ACF from FAP patients have phenotypic characteristics of adenomas, which are vital to carcinogenesis, and lack ras gene mutations, while sporadic ACF and a subset of FAP ACF closely resemble hyperplastic polyps, which are benign, but usually have ras gene mutations. There are also evidences identified in the colon of Min/+ mice after azoxymethane (AOM) treatment. Germline mutations in murine Apc homologous to human APC, caused multiple intestinal neoplasia in mice (Min/+ mice)^[55]. ACF_{Min} resemble dysplastic ACF, which were described previously as potential precursors of adenomas in rodent and human colon carcinogenesis^[35,36,39,52], and more severe in FAP ACF than in

sporadic ACF. ACF_{Min} followed a continuous development from a single crypt to adenoma with fast crypt multiplication and altered expression of β -catenin, while classical ACF homologous to hyperplastic human ACF showed slow-growing crypts with normal β -catenin expression, and were probably not related to tumorigenesis^[56]. In carcinogen-treated rodents and patients with sporadic CRC, only a very small fraction of ACF progressed to tumor^[38]. This was consistent with the observation that a large fraction of ACF was hyperplastic whereas only a small fraction of ACF showed dysplasia, a hallmark of malignant potential^[38,55]. In contrast, most ACF in FAP patients were dysplastic, resembling that of adenomas^[38]. It has been proposed that only dysplastic ACF progressed to adenomas and carcinomas^[35]. In non-FAP cases, K-ras mutations were detected in 82 % (89/106) of nondysplastic ACF and 63 % (17/27) of dysplastic ACF. FAP patients showed K-ras mutations in only 13 % (1/8) of dysplastic ACF, which was the predominant form of ACF found in FAP. In FAP patients, somatic APC mutations were found in 100 % of dysplastic ACF, as they were in adenomas^[41]. A previous study showed an association between CpG island methylation in cancer and K-ras mutations^[55]. It was found that CpG island methylation was present in more ACF from sporadic cancer than in FAP ACF, implying that FAP ACF usually lacked methylation or K-ras mutations and were frequently dysplastic, while sporadic ACF usually had methylation and/or K-ras mutations and lacked dysplasia^[57].

BIOCHEMICAL AND IMMUNOHISTOCHEMICAL ALTERATIONS OF ACF

What we have discussed above is concerned about the determination of ACF under a microscope, and the histopathological characteristics of ACF. Yamada reported another kind of crypts with normal appearance harboring altered β -catenin expression, which was regarded as lesions different from ACF, and might occur earlier than ACF in rat models^[58-60]. Previous studies explored phenotype alterations of ACF by means of biochemical and immunohistochemical methods. Pretlow reported enzyme-altered foci with normal morphology in colon and decreased expression of hexosaminidase in these lesions for the first time^[61]. By using serial glycolmethacrylate-embedded sections of grossly normal colons from F344 rats treated with colon carcinogen, Pretlow's group was able to detect multiple lesions with altered enzyme activities in the distal colon and rectum of those rats, and found that histochemically decreased demonstrable hexosaminidase activity could be observed in more than 95 % of ACF in rats^[22,29,61], and was also able to demonstrate two groups of lesions with decreased hexosaminidase activity: one with aberrant morphology resembling ACF, the other with normal appearance^[29]. A decrease in hexosaminidase activity was also seen in colon tumors developed in those animals^[13]. Hexosaminidase provided a marker of colon epithelial cells throughout the carcinogenesis progression^[62]. Human ACF clearly resembled those seen in animals in morphology and histological appearance^[11,12,22,36,63], but hexosaminidase activity was not a useful marker of human ACF because human colonic neoplasia was accompanied by a number of phenotypic changes that frequently included increased expressions of a variety of tumor-associated glycoproteins^[64]. Carcinoembryonic antigen (CEA), a member of the immunoglobulin superfamily, was first isolated from human colon cancers, and seems to function as an intracellular adhesion molecule. The immunohistochemical expression of CEA was altered in as many as 93 % (39/42) of ACF in 15 patients, and was related to the size of the foci, but not to the presence or degree of dysplasia in Pretlow's study^[22]. The immunohistochemical localization of CEA in the

cytoplasm and on the basolateral membranes in ACF was similar to that of carcinomas. The finding that CEA appeared to be a marker of human ACF by means of immunohistochemistry should facilitate the identification and characterization of these lesions in human.

The other two members of the cadherin family of cell adhesion molecules were placental cadherin (P-cadherin) and epithelial cadherin (E-cadherin). It has been shown that striking membranous and/or cytoplasmic P-cadherin up-regulation and its co-expression with E-cadherin usually represented a pre-invasive dysplastic transformation^[65,66]. P-cadherin was expressed from ACF to hyperplastic and adenomatous polyps, and was prior to and independent of disturbance in E-cadherin and β -catenin expression in ACF. P-cadherin was aberrantly expressed at the earliest stage of aberrant crypt formation, before the disturbance in E-cadherin and β -catenin^[67].

β -catenin, which was originally discovered as a cadherin-binding protein, has been proved to function as a transcriptional activator^[68]. Inactivation of β -catenin with the product of adenomatous polyposis coli (APC) gene highlighted a role of catenins in epithelial tumorigenesis. Target genes of the β -catenin-Tcf pathway were determined to be growth-promoting genes, such as *c-myc* and *cyclin D1*^[69,70], suggesting β -catenin-Tcf pathway was oncogenic. Excessive β -catenin protein has been shown in colon cancers of rats and humans^[71,72], and the aberrant expression of β -catenin in ACF was also seen. It was reported that in most ACF, namely ACF with hyperplasia, β -catenin was localized at the cell membrane like normal colon epithelium^[25], and in ACF with dysplasia, reduced membranous expression of β -catenin was associated with increased nuclear and cytoplasmic expression. The membranous expression of β -catenin was reduced, and cytoplasmic and nuclear expression increased in ACF according to their degrees of dysplasia. Likewise, membranous expression of β -catenin was reduced, and the nuclear expression increased from ACF to adenoma and carcinoma^[24], strongly suggesting that ACF and their aberrant expression of β -catenin played an important role in colorectal carcinogenesis, and the immunohistochemical staining of ACF for β -catenin could evaluate the malignant potential of ACF^[25].

In carcinogen-treated animal carcinomas, it has been reported frequent mutation and altered cellular localization of β -catenin, and inducible nitric oxide synthase (iNOS) and cyclooxygenase (COX-2) were also found to be expressed in these carcinomas^[72]. In carcinogen-treated animal colon, an altered cellular localization of β -catenin in all dysplastic ACF, adenomas and adenocarcinomas was shown, and iNOS expression was also observed in all but one of the lesions in which β -catenin alterations were observed. Neither iNOS expression nor β -catenin alterations were observed in any hyperplastic ACF. Nitric oxide (NO) was known to cause DNA damage and nitrosylation of proteins^[73,74], and increased production in tumor cells would be expected to facilitate accumulation of sequential mutations. Since altered localization of β -catenin was apparent in all lesions expressing iNOS, it might be possible that β -catenin alteration was related to induction of iNOS expression. The positive expression of iNOS in dysplasia, but not hyperplastic ACF suggested that iNOS, like β -catenin, could be important at the early stages of tumor formation, and the cause of dysplastic changes^[68]. There was also an overexpression of COX-2 detected in ACF, adenomas and carcinomas^[68], which has been demonstrated to render tumor cells resistant to apoptosis^[75] and to enhance neovascularization^[76], thus conferring a survival advantage. The overexpression of COX-2 may contribute to ACF growth and sequential tumor growth.

P16^{INK4a} expression was seldom seen in epithelial cells at the base of normal colonic crypts. But at all the stages of tumor

progression, including ACF, a higher fraction of epithelial cells was seen to express p16^{INK4a}. The staining of p16^{INK4a} correlated inversely with that of Ki67, cyclin A, and the retinoblastoma protein in ACF, adenomas and carcinomas, suggesting that cell cycle progression was inhibited. Thus, p16^{INK4a} appeared to constrain the proliferation of subsets of cells throughout intestinal tumorigenesis, however, the exact mechanisms remain unclear^[77].

GENETIC AND EPIGENETIC ALTERATIONS OF ACF

Further development of ACF described by Gregorio had two pathways. One was headed for dysplastic ACF, which were to progress to adenomas, and the other was headed for hyperplastic polyps, which had little malignant potentials^[40]. The investigation of ACF by using 25 different genetic markers, such as microsatellite instabilities and mutations of APC, H-ras, k-ras, p53, DCC, and DNA repair genes hMLH1, hMSH2, showed no difference between hyperplastic ACF and normal mucosa^[78], which was in accordance with the latter hypothesis. Dysplastic ACF have been further identified to be precancerous lesions of CRC. However, an alternative pathway to the general adenoma-carcinoma sequence was also proposed as a hyperplastic polyp/serrated adenoma-carcinoma one^[79-83]. Nucci's study showed genetic differences between hyperplastic ACF and hyperplastic polyps in that the former had more frequent K-ras mutations. Therefore hyperplastic ACF should be named as "heteroplasia ACF" ("hetero" meaning "other", and "plasia" meaning "form") to avoid potential misleading as to their relationships^[38]. Though the role of heteroplastic ACF in colorectal carcinogenesis remains controversial because of the lack of dysplasia in spite of the high frequency of K-ras mutations, there have been still lines of evidences supporting heteroplastic ACF as a precursor to a subset of CRC. They were clonal^[84] and had genetic alterations of K-ras mutations^[10,29,35,38,41], chromosome 1p loss^[44], and CpG island methylation^[44], hence the heteroplastic ACF-adenoma-carcinoma sequence, in which K-ras mutations preceded APC mutations in rodents and humans^[41,85].

Stopera identified K-ras point mutation in carcinogen-induced colonic aberrant crypts in Sprague-Dawley rats in 1992 for the first time^[86], and numerous studies have proved K-ras mutation as one of the major events in ACF formation since then. The mutation rate of K-ras in ACF was similar to that of small adenomas^[28,29,35], and was found to be even significantly higher than that identified in CRC^[86]. K-ras 12 codon mutation was most frequently observed, and in Losi's study, different mutational types of GTT, TGT, GAT, *etc.*, occurred in ACF of the same patient^[31]. There were also different mutational types between carcinomas and ACF, the former had predominant GTT mutation, while the latter had GAT mutations almost as frequently as GTT in codon 12 of K-ras^[30]. Therefore each ACF might originate independently from different clones^[28-30,34]. Identification of monoclonality in a putative precursor lesion would strongly link this lesion to neoplastic progression. The monoclonality of various degrees of dysplastic ACF was determined by studying the differential methylation of a highly polymorphic site in the first exon of the androgen receptor gene to determine the pattern of X chromosome inactivation^[34]. Controversial results were produced also by using the same method of clonality analysis based on X chromosome inactivation of the polymorphically X-linked human androgen receptor (HUMARA) gene, in addition to K-ras mutation detection. It was observed that a significant fraction of individual aberrant crypts that made up an ACF to be polyclonal, although by K-ras mutation genotyping, all ACF appeared to be monoclonal^[84].

Other oncogenes as COX and *c-myc* were also found to

have an increased mRNA or protein expression in carcinogen-induced rats^[18,88]. The immunoreactivity of oncoproteins of c-fos, ras, bcl-2 and p53 was evaluated in ACF, and abnormal expression and coexpression of oncoproteins could be identified in colorectal tumorigenesis at the earliest stages^[89].

APC gene is considered to be “gatekeeper gene”, maintaining the stability of colon epithelium. In carcinogen-treated rats, a decreased mRNA expression of APC was observed^[18]. APC mutations could be detected in human ACF, but the mutation rates of APC in ACF were lower or undetectable compared to those in adenomas and carcinomas^[28,41,90], which were the same as in animal models^[85], suggesting that APC mutation was unlikely to initiate ACF. If a ras gene mutation occurred first, ACF would be nondysplasia, and if an APC mutation was the first to occur, it would result in a dysplastic ACF, whose progression was driven by subsequent K-ras and other gene mutations^[35]. It has been proposed that in sporadic colorectal carcinogenesis, assuming the biological potential of ACF as a precursor of adenomas, there was a route where K-ras mutations mainly occurred during the formation of ACF. Some ACF then became adenomas in which APC mutations occurred. In FAP, however, somatic mutations of APC predominantly occurred during ACF formation, followed by K-ras mutations^[35].

Apart from oncogene and tumor suppressor gene alterations in ACF, there is some other kind of genes concerning DNA repair. Inactivation of the mismatch repair (MMR) system can result in instability of the whole genome and an increased rate of spontaneous mutations of other vital genes to carcinogenesis. In addition to the cause of genomic instability, DNA mismatch repair proteins have several other functions that are highly relevant to cancer progression. Some MMR components have been found to be involved in cell-cycle regulation, and p53-dependent apoptotic response to a variety of DNA damages^[91-97]. Germline mutations of any of them, especially hMSH2 and hMLH1, gave rise to hereditary nonpolyposis of colorectal cancer (HNPCC)^[6,98]. There was also a link between hMSH6 mutations and a high incidence of endometrial cancer^[99], and prevalence of colon cancer with TGFβRII gene and Tcf-4 gene^[100,101]. hMSH2 deficiency resulted in the development of many ACF in mice colons, as well as reduced survival of the mice^[102].

Epigenetic alterations such as CpG island methylation, and genetic phenotype alterations such as microsatellite instability (MSI) as a result of MMR defect, also play important roles as in ACF. Inactivation of genes might occur not by mutation or loss, but through silencing mediated by CpG island methylation of the gene's promoter region. hMLH1 and MGMT are examples of DNA repair genes that were silenced by methylation. It has been demonstrated^[103-105] that hMLH1 gene promoter had aberrant methylation in sporadic CRC. A novel pathway characterized by methylation of multiple CpG islands in colorectal carcinomas and adenomas, including genes known to be vital in tumorigenesis, such as p16 tumor suppressor gene and hMLH1 mismatch repair gene, was proposed as a CpG island methylator phenotype (CIMP)^[57,106]. Ahuja questioned whether hMLH1 methylation preceded or was a consequence of the MSI phenotype^[107]. The answer was presented by Chan that methylation of hMLH1 mismatch repair gene in ACF was not associated with the development of MSI, suggesting that hMLH1 methylation preceded MSI^[44]. The frequency of CpG island methylation in ACF was related to the type of patients, as was concluded in Chan's research, that methylation was detected in 53 % of ACF from sporadic colorectal carcinomas but only in 11 % of ACF from FAP patients^[44], and methylation was more frequent in dysplastic sporadic ACF than in dysplastic FAP ACF. The epigenetic differences of CpG island methylation in ACF were similar to those in colorectal carcinomas.

Extensive genomic instabilities due to the defect of MMR

system could be detected as MSI both in animal model and in human ACF^[108,109]. MSI could occur either in dysplastic or hyperplastic (or “heteroplastic” as mentioned before) ACF from HNPCC patients, suggesting no association of MSI with histological features, being present even in small ACF. MSI in sporadic ACF also seemed to be independent of ACF size^[110]. Heinen *et al*^[45] detected MSI status in ACF, and found two ACFs from the same patient with different MSI status. One showed MSI-positive, while the other was MSI-negative, indicating independent initiation of individual ACF, as has been verified by sequential studies with different methods^[28-30,34,84]. The role of ACF as precursors of some CRCs was verified by the presence of MSI in ACF from HNPCC patients, in whom carcinoma with high levels of MSI was the hallmark, and in ACF from sporadic CRC as well^[44,108].

SUMMARY

The malignant potential of ACF, especially dysplastic ACF, makes it necessary to reveal the nature of these lesions. Many researches nowadays are focused on the mechanisms of ACF initiation, their genetic and environmental backgrounds, methods of early detection, dietary and chemoprevention. In spite of the increasing evidences of ACF as precancerous lesions of colorectal carcinomas, a lot remain to be clarified so as to reduce the incidence of CRC at the earliest stages.

First reported by Yokota in 1997^[14], the application of endoscopy, either magnifying or dye/chromoscopic colonoscopy, made it possible to detect “*in vivo*” ACF. It is of great advantage over the detection of surgical specimens from with CRC. It may offer much benefit to colon cancer researches and identify high-risk populations for colorectal tumors. Recent studies have proved the validity of chromoendoscopy, or dye colonoscopy, which allows easy detection of mucosal lesions in the colon and facilitates visualization of the margins of flat lesions^[111,112].

In summary, ACF, especially dysplastic ACF, are widely accepted as precursors of colon cancer morphologically, histologically, biologically, and genetically. They have an aberrant appearance of crypts, and display both hyperplasia and dysplasia. They are supposed to have alterations of enzymology and cell dynamics. They also harbor gene mutations that are vital to tumor formation and progression. By studying these lesions both grossly and genetically, it may be possible to learn more about the causes of colon carcinogenesis. By testing new compounds through ACF assay, it is possible to discover not only potentially new chemopreventive drugs, but also the mechanisms behind them. In addition, by developing available methods for “*in vivo*” ACF examination, it may be possible to evaluate high-risk individuals at the earliest possible stages, as well as the preventive procedures.

REFERENCES

- 1 **Fearon ER**, Vogelstein B. A genetic model for colorectal tumorigenesis. *Cell* 1990; **61**: 759-767
- 2 **Boland CR**. The biology of colorectal cancer. *Cancer Suppl* 1993; **71**: 4180-4186
- 3 **Kinzler KW**, Vogelstein B. Lessons from hereditary colorectal cancer. *Cell* 1996; **87**: 159-170
- 4 **Leach FS**, Nicolaides NC, Papadopoulos N, Liu B, Jen J, Parson R, Peltomaki P, Sistonen P. Mutation of a mutS homolog in hereditary nonpolyposis colorectal cancer. *Cell* 1993; **75**: 1215-1235
- 5 **Honchel R**, Halling KC, Schaid DJ, Pittelkow M, Thibodeau SN. Microsatellite instability in Muir-Torre syndrome. *Cancer Res* 1994; **54**: 1159-1163
- 6 **Jacob S**, Praz F. DNA mismatch repair defects: role in colorectal carcinogenesis. *Biochimie* 2002; **84**: 27-47
- 7 **Bird RP**. Observation and quantification of aberrant crypts in

- the murine colon treated with a colon carcinogen: preliminary findings. *Cancer Lett* 1987; **30**: 147-151
- 8 **McLellan EA**, Bird RP. Aberrant crypts: potential preneoplastic lesions in the murine colon. *Cancer Res* 1988; **48**: 6187-6192
 - 9 **Roncucci L**, Stamp D, Medline A, Cullen JB, Bruce WR. Identification and qualification of aberrant crypt foci and adenoma in the human colon. *Hum Pathol* 1991; **22**: 287-294
 - 10 **Otori K**, Sugiyama K, Hasebe T, Fukushima S, Esumi H. Emergence of adenomatous aberrant crypt foci (ACF) from hyperplastic ACF with concomitant increase in cell proliferation. *Cancer Res* 1995; **55**: 4743-4746
 - 11 **Pretlow TP**, Barrow BJ, Ashton WS, O' Riordan MA, Pretlow TG, Jurcisek JA, Stellato TA. Aberrant crypt foci: Putative preneoplastic foci in human colonic mucosa. *Cancer Res* 1991; **51**: 1564-1567
 - 12 **Roncucci L**, Medline A, Bruce WR. Classification of aberrant crypt foci and microadenomas in human colon. *Cancer Epidemiol Biomarkers Prev* 1991; **1**: 57-60
 - 13 **Pretlow TP**, O' Riordan MA, Pretlow TG, Stellato TA. Aberrant crypts in human colonic mucosa: putative preneoplastic lesions. *J Cell Biochem Suppl* 1992; **16G**: 55-62
 - 14 **Yokota T**, Sugano K, Kondo H, Saito D, Sugihara K, Fukayama N, Ohkura H, Ochiai M, Yoshida S. Detection of aberrant crypt foci by magnifying colonoscopy. *Gastrointest Endosc* 1997; **46**: 61-65
 - 15 **Adler DG**, Gostout CJ, Sorbi D, Burgart LJ, Wang L, Harmsen WS. Endoscopic identification and quantification of aberrant crypt foci in the human colon. *Gastrointest Endosc* 2002; **56**: 657-662
 - 16 **McLellan EA**, Medline A, Bird RP. Dose response and proliferative characteristics of aberrant crypt foci: putative preneoplastic lesions in rat colon. *Carcinogenesis* 1991; **12**: 2093-2098
 - 17 **Shpitz B**, Bomstein Y, Mekori Y, Cohen R, Kaufman Z, Neufeld D, Galkin M, Bernheim J. Aberrant crypt foci in human colons: distribution and histomorphologic characteristics. *Hum Pathol* 1998; **29**: 469-475
 - 18 **Furukawa F**, Nishikawa A, Kitahori Y, Tanakamaru Z, Hirose M. Spontaneous development of aberrant crypt foci in F344 rats. *J Exp Clin Cancer* 2002; **21**: 197-201
 - 19 **Roncucci L**, Pedroni M, Fante R, Di Gregorio C, Ponz de Leon M. Cell kinetic evaluation of human colonic aberrant crypts. *Cancer Res* 1993; **53**: 3726-3729
 - 20 **Dashwood RH**, Xu M, Orner GA, Horio DT. Colonic cell proliferation, apoptosis and aberrant crypt foci development in rats given 2-amino-3-methylimidaz. *Eur J Cancer Prev* 2001; **10**: 139-145
 - 21 **Nakagama H**, Ochiai M, Ubagai T, Tajima R, Fujiwara K, Sugimura T, Nagao M. A rat colon cancer model induced by 2-amino-1-methyl-6-phenylimidazo[4,5-b]pyridine, PhIP. *Mutat Res* 2002; **506-507**: 137-144
 - 22 **Pretlow TP**, Roukhadze EV, O' Riordan MA, Chan JC, Amini SB, Stellato TA. Carcinoembryonic antigen in human colonic aberrant crypt foci. *Gastroenterology* 1994; **107**: 1719-1725
 - 23 **Sparks AB**, Morin PJ, Vogelstein B, Kinzler KW. Mutational analysis of the APC/beta-catenin/Tcf pathway in colorectal cancer. *Cancer Res* 1998; **58**: 1130-1134
 - 24 **Hao XP**, Pretlow TG, Rao JS, Pretlow TP. β -catenin expression is altered in human colonic aberrant crypt foci. *Cancer Res* 2001; **61**: 8085-8088
 - 25 **Furihata T**, Kawamata H, Kubota K, Fujimori T. Evaluation of the malignant potential of aberrant crypt foci by immunohistochemical staining for beta-catenin in inflammation-induced rat colon carcinogenesis. *Int J Mol Med* 2002; **9**: 353-358
 - 26 **Vogelstein B**, Fearon ER, Hamilton SR, Kern SE, Preidinger AC, Leppert M, Nakamura Y, White R, Smits AMM, Bos JL. Genetic alterations during colorectal-tumor development. *N Engl J Med* 1988; **319**: 525-532
 - 27 **Powell SM**, Zilz N, Beazer-Barclay Y, Bryan TM, Hamilton SR, Thibodeau SN, Vogelstein B, Kinzler KW. APC mutations occur early during colorectal tumorigenesis. *Nature* 1992; **359**: 235-237
 - 28 **Smith AJ**, Stern HS, Penner M, Hay K, Mitri A, Bapat BV, Gallinger S. Somatic APC and K-ras codon 12 mutations in aberrant crypt foci from human colons. *Cancer Res* 1994; **54**: 5527-5530
 - 29 **Pretlow TP**, Brasitus TA, Fulton NC, Cheyer C, Kaplan EL. K-ras mutations in putative preneoplastic lesions in human colon. *J Natl Cancer Inst* 1993; **85**: 2004-2007
 - 30 **Minamoto T**, Yamashita N, Ochiai A, Mai M, Sugimura T, Ronai Z, Esumi H. Mutant K-ras in apparently normal mucosa of colorectal cancer patients. Its potential as a biomarker of colorectal tumorigenesis. *Cancer* 1995; **75**: 1520-1526
 - 31 **Losi L**, Roncucci L, di Gregorio C, de Leon MP, Benhattar J. K-ras and p53 mutations in human colorectal aberrant crypt foci. *J Pathol* 1996; **178**: 259-263
 - 32 **Shivapurkar N**, Huang L, Ruggeri B, Swalsky PA, Bakker A, Finkelstein S, Frost A, Silverberg S. K-ras and p53 mutations in aberrant crypt foci and colonic tumors from colon cancer patients. *Cancer Lett* 1997; **115**: 39-46
 - 33 **Janssen KP**, el-Marjou F, Pinto D, Sastre X, Rouillard D, Fouquet C, Soussi T, Louvard D, Robine S. Targeted expression of oncogenic K-ras in intestinal epithelium causes spontaneous tumorigenesis in mice. *Gastroenterology* 2002; **123**: 492-504
 - 34 **Siu IM**, Robinson DR, Schwartz S, Kung HJ, Pretlow TG, Petersen RB, Pretlow TP. The identification of monoclonality in human aberrant crypt foci. *Cancer Res* 1999; **59**: 63-66
 - 35 **Jen J**, Powell SM, Papadopoulos N, Smith KJ, Hamilton SR, Vogelstein B, Kinzler KW. Molecular determinants of dysplasia in colorectal lesions. *Cancer Res* 1994; **54**: 5523-5526
 - 36 **Siu IM**, Pretlow TG, Amini SB, Pretlow TP. Identification of dysplasia in human colonic aberrant crypt foci. *Am J Pathol* 1997; **150**: 1805-1813
 - 37 **Roncucci L**, Modica S, Pedroni M, Tamassia MG, Ghidoni M, Losi L, Fante R, Di Gregorio C, Manenti A, Gafa L, Ponz de Leon M. Aberrant crypt foci in patients with colorectal cancer. *Br J Cancer* 1998; **77**: 2343-2348
 - 38 **Nucci MR**, Robinson CR, Longo P, Campbell P, Hamilton SR. Phenotypic and genotypic characteristics of aberrant crypt foci in human colorectal mucosa. *Hum Pathol* 1997; **28**: 1396-1407
 - 39 **Bouzourene H**, Chaubert P, Seelentag W, Bosman FT, Saraga E. Aberrant crypt foci in patients with neoplastic and nonneoplastic colonic disease. *Hum Pathol* 1999; **30**: 66-71
 - 40 **Di Gregorio C**, Losi L, Fante R, Modica S, Ghidoni M, Pedroni M, Tamassia MG, Gafa L, Ponz de Leon M, Roncucci L. Histology of aberrant crypt foci in the human colon. *Histopathology* 1997; **30**: 328-334
 - 41 **Nascimbeni R**, Villanacci V, Mariani PP, Betta ED, Ghirardi M, Donato F, Salerni B. Aberrant crypt foci in the human colon: frequency and histologic patterns in patients with colorectal cancer or diverticular disease. *Am J Surg Pathol* 1999; **23**: 1256-1263
 - 42 **Longacre TA**, Fenoglio-Preiser CM. Mixed hyperplastic adenomatous polyps/serrated adenoma. A distinct form of colorectal neoplasia. *Am J Surg Pathol* 1990; **14**: 524-537
 - 43 **Takayama T**, Ohi M, Hayashi T, Miyanishi K, Nobuoka A, Nakajima T, Satoh T, Takimoto R, Kato J, Sakamaki S, Niitsu Y. Analysis of K-ras, APC, and beta-catenin in aberrant crypt foci in sporadic adenoma, cancer, and familial adenomatous polyposis. *Gastroenterology* 2001; **121**: 599-611
 - 44 **Chan AO**, Broadus RR, Houlihan PS, Issa JP, Hamilton SR, Rashid A. CpG island methylation in aberrant crypt foci of the colorectum. *Am J Pathol* 2002; **160**: 1823-1830
 - 45 **Heinen CD**, Shivapurkar N, Tang Z, Groden J, Alabaster O. Microsatellite instability in aberrant crypt foci from human colons. *Cancer Res* 1996; **56**: 5339-5341
 - 46 **Kishimoto Y**, Morisawa T, Hosoda A, Shiota G, Kawasaki H, Hasegawa J. Molecular changes in the early stage of colon carcinogenesis in rats treated with azoxymethane. *J Exp Clin Cancer Res* 2002; **21**: 203-211
 - 47 **Murray NR**, Davidson LA, Chapkin RS, Clay Gustafson W, Schattenberg DG, Fields AP. Overexpression of protein kinase C β talI induces colonic hyperproliferation and increased sensitivity to colon carcinogenesis. *J Cell Biol* 1999; **145**: 699-711
 - 48 **Craven PA**, DeRubertis FR. Alterations in protein kinase C in 1, 2-dimethylhydrazine induced colonic carcinogenesis. *Cancer Res* 1992; **52**: 2216-2221
 - 49 **Chapkin RS**, Gao J, Lee DY, Lupton JR. Dietary fibers and fats alter rat colon protein kinase C activity: correlation to cell proliferation. *J Nutr* 1993; **123**: 649-655
 - 50 **Kahl-Rainer P**, Karner-Hanusch J, Weiss W, Marian B. Five of six protein kinase C isoenzymes present in normal mucosa show reduced protein levels during tumor development in the human colon. *Carcinogenesis* 1994; **15**: 779-782
 - 51 **Gokmen-Polar Y**, Murray NR, Velasco MA, Gatalica Z, Fields AP. Elevated protein kinase C β talII is an early promotive event

- in colon carcinogenesis. *Cancer Res* 2001; **61**: 1375-1381
- 52 **Thorup I**. Histomorphological and immunohistochemical characterization of colonic aberrant crypt foci in rats: relationship to growth factor expression. *Carcinogenesis* 1997; **18**: 465-472
- 53 **Habel O**, Bertario L, Andreola S, Sirizzotti G, Marian B. Tissue localization of TGF α and apoptosis are inversely related in colorectal tumors. *Histochem Cell Biol* 2002; **117**: 235-241
- 54 **Pretlow TP**, Cheyer C, O' Riordan MA. Aberrant crypt foci and colon tumors in F344 rats have similar increases in proliferative activity. *Int J Cancer* 1994; **56**: 599-602
- 55 **Paulsen JE**. Modulation by dietary factors in murine FAP models. *Toxicol Lett* 2000; **112-113**: 403-409
- 56 **Paulsen JE**, Steffensen IL, Loberg EM, Husoy T, Namork E, Alexander J. Qualitative and quantitative relationship between dysplastic aberrant crypt foci and tumorigenesis in the Min/+ mouse colon. *Cancer Res* 2001; **61**: 5010-5015
- 57 **Toyota M**, Ohe-Toyota M, Ahuja N, Issa JP. Distinct genetic profiles in colorectal tumors with or without the CpG island methylator phenotype. *Proc Natl Acad Sci U S A* 2000; **97**: 710-715
- 58 **Yamada Y**, Yoshimi N, Hirose Y, Matsunaga K, Katayama M, Sakata K, Shimizu M, Kuno T, Mori H. Sequential analysis of morphological and biological properties of beta-catenin-accumulated crypts, provable premalignant lesions independent of aberrant crypt foci in rat colon carcinogenesis. *Cancer Res* 2001; **61**: 1874-1878
- 59 **Yamada Y**, Yoshimi N, Hirose Y, Kawabata K, Matsunaga K, Shimizu M, Hara A, Mori H. Frequent beta-catenin gene mutations and accumulations of the protein in the putative preneoplastic lesions lacking macroscopic aberrant crypt foci appearance, in rat colon carcinogenesis. *Cancer Res* 2000; **60**: 3323-3327
- 60 **Yamada Y**, Yoshimi N, Hirose Y, Hara A, Shimizu M, Kuno T, Katayama M, Qiao Z, Mori H. Suppression of occurrence and advancement of beta-catenin-accumulated crypts, possible premalignant lesions of colon cancer, by selective cyclooxygenase-2 inhibitor, celecoxib. *Jpn J Cancer Res* 2001; **92**: 617-623
- 61 **Pretlow TP**, O' Riordan MA, Kolman MF, Jurcisek JA. Colonic aberrant crypts in azoxymethane-treated F344 rats have decreased hexosaminidase activity. *Am J Pathol* 1990; **136**: 13-16
- 62 **Pretlow TP**, Pretlow TG. Putative preneoplastic changes identified by enzyme histochemical and immunohistochemical techniques. *J Histochem Cytochem* 1998; **46**: 577-583
- 63 **Konstantakos AK**, Siu IM, Pretlow TG, Stellato TA, Pretlow TP. Human aberrant crypt foci with carcinoma in situ from a patient with sporadic colon cancer. *Gastroenterology* 1996; **111**: 772-777
- 64 **Boland CR**, Martin MA, Goldstein JJ. Lectin reactivities as intermediate biomarkers in premalignant colorectal epithelium. *J Cell Biochem Suppl* 1992; **16G**: 103-109
- 65 **Williams HK**, Sanders DS, Jankowski JA, Landini G, Brown AM. Expression of cadherins and catenins in oral epithelial dysplasia and squamous cell carcinoma. *J Oral Pathol Med* 1998; **27**: 308-317
- 66 **Sanders DS**, Bruton R, Darnton SJ, Casson AG, Hanson I, Williams HK, Jankowski J. Sequential changes in cadherin-catenin expression associated with the progression and heterogeneity of primary oesophageal squamous carcinoma. *Int J Cancer* 1998; **79**: 573-579
- 67 **Hardy RG**, Tselepis C, Hoyland J, Wallis Y, Pretlow TP, Talbot I, Sanders DS, Matthews G, Morton D, Jankowski JA. Aberrant P-cadherin expression is an early event in hyperplastic and dysplastic transformation in the colon. *Gut* 2002; **50**: 513-519
- 68 **Takahashi M**, Mutoh M, Kawamori T, Sugimura T, Wakabayashi K. Altered expression of β -catenin, inducible nitric oxide synthase and cyclooxygenase-2 in azoxymethane-induced rat colon carcinogenesis. *Carcinogenesis* 2000; **21**: 1319-1327
- 69 **He TC**, Sparks AB, Rago C, Hermeking H, Zawel L, da Costa LT, Morin PJ, Vogelstein B, Kinzler KW. Identification of c-MYC as a target of the APC pathway. *Science* 1998; **281**: 1509-1512
- 70 **Tetsu O**, McCormick F. Beta-catenin regulates expression of cyclin D1 in colon carcinoma cells. *Nature* 1999; **398**: 422-426
- 71 **Morin PJ**, Sparks AB, Korinek V, Barker N, Clevers H, Vogelstein B, Kinzler KW. Activation of beta-catenin-Tcf signaling in colon cancer by mutations in beta-catenin or APC. *Science* 1997; **275**: 1787-1790
- 72 **Takahashi M**, Fukuda K, Sugimura T, Wakabayashi K. β -catenin is frequently mutated and demonstrates altered cellular location in azoxymethane-induced rat colon tumors. *Cancer Res* 1998; **58**: 42-46
- 73 **Wink DA**, Vodovotz Y, Laval J, Laval F, Dewhirst MW, Mitchell JB. The multifaceted roles of nitric oxide in cancer. *Carcinogenesis* 1998; **19**: 711-721
- 74 **Stamler JS**, Simon DI, Jaraki O, Osborne JA, Francis S, Mullins M, Singel D, Loscalzo J. S-nitrosylation of tissue-type plasminogen activator confers vasodilatory and antiplatelet properties on the enzyme. *Proc Natl Acad Sci U S A* 1992; **89**: 8087-8091
- 75 **Tsuji M**, DuBois RN. Alterations in cellular adhesion and apoptosis in epithelial cells overexpressing prostaglandin endoperoxide synthase 2. *Cell* 1995; **83**: 493-501
- 76 **Tsuji M**, Kawano S, Tsuji S, Sawaoka H, Hori M, DuBois RN. Cyclooxygenase regulates angiogenesis induced by colon cancer cells. *Cell* 1998; **93**: 705-716
- 77 **Dai CY**, Furth EE, Mick R, Koh J, Takayama T, Niitsu Y, Enders GH. p16 (INK4a) expression begins early in human colon neoplasia and correlates inversely with markers of cell proliferation. *Gastroenterology* 2000; **119**: 929-942
- 78 **Sedivy R**, Wolf B, Kalipciyan M, Steger GG, Karner-Hanusch J, Mader RM. Genetic analysis of multiple synchronous lesions of the colon adenoma-carcinoma sequence. *Br J Cancer* 2000; **82**: 1276-1282
- 79 **Jass JR**, Cottier DS, Pokos V, Parry S, Winship IM. Mixed epithelial polyps in association with hereditary non-polyposis colorectal cancer providing an alternative pathway of cancer histogenesis. *Pathology* 1997; **29**: 28-33
- 80 **Iino H**, Jass JR, Simms LA, Young J, Leggett B, Ajioka Y, Watanabe H. DNA microsatellite instability in hyperplastic polyps, serrated adenomas, and mixed polyps: a mild mutator pathway for colorectal cancer? *J Clin Pathol* 1999; **52**: 5-9
- 81 **Rashid A**, Houlihan PS, Booker S, Petersen GM, Giardiello FM, Hamilton SR. Phenotypic and molecular characteristics of hyperplastic polyposis. *Gastroenterology* 2000; **119**: 323-332
- 82 **Jass JR**, Iino H, Ruzsiewicz A, Painter D, Solomon MJ, Koorey DJ, Cohn D, Furlong KL, Walsh MD, Palazzo J, Edmonston TB, Fishel R, Young J, Leggett BA. Neoplastic progression occurs through mutator pathways in hyperplastic polyposis of the colorectum. *Gut* 2000; **47**: 43-49
- 83 **Jass JR**. Serrated route to colorectal cancer: back street or super highway? *J Pathol* 2001; **193**: 283-285
- 84 **Sakurazawa N**, Tanaka N, Onda M, Esumi H. Instability of X chromosome methylation in aberrant crypt foci of the human colon. *Cancer Res* 2000; **60**: 3165-3169
- 85 **De Filippo C**, Caderni G, Bazzicalupo M, Briani C, Giannini A, Fazi M, Dolara P. Mutations of the Apc gene in experimental colorectal carcinogenesis induced by azoxymethane in F344 rats. *Br J Cancer* 1998; **77**: 2148-2151
- 86 **Stopera SA**, Murphy LC, Bird RP. Evidence for a ras gene mutation in azoxymethane-induced colonic aberrant crypts in Sprague-Dawley rats: earliest recognizable precursor lesions of experimental colon cancer. *Carcinogenesis* 1992; **13**: 2081-2085
- 87 **Benhattar J**, Losi L, Chaubert P, Givel JC, Costa J. Prognostic significance of K-ras mutations in colorectal carcinoma. *Gastroenterology* 1993; **104**: 1044-1048
- 88 **Kitamura T**, Kawamori T, Uchiya N, Itoh M, Noda T, Matsuura M, Sugimura T, Wakabayashi K. Inhibitory effects of mofezolac, a cyclooxygenase-1 selective inhibitor, on intestinal carcinogenesis. *Carcinogenesis* 2002; **23**: 1463-1466
- 89 **Otori K**, Sugiyama K, Fukushima S, Esumi H. Expression of the cyclin D1 gene in rat colorectal aberrant crypt foci and tumors induced by azoxymethane. *Cancer Lett* 1999; **140**: 99-104
- 90 **Yuan P**, Sun MH, Zhang JS, Zhu XZ, Shi DR. APC and K-ras gene mutation in aberrant crypt foci of human colon. *World J Gastroenterol* 2001; **7**: 352-356
- 91 **Davis TW**, Wilson-Van Patten C, Meyers M, Kunugi KA, Cuthill S, Reznikoff C, Garces C, Boland CR, Kinsella TJ, Fishel R, Boothman DA. Defective expression of the DNA mismatch repair protein, MLH1, alters G2-M cell cycle checkpoint arrest following ionizing radiation. *Cancer Res* 1998; **58**: 767-778
- 92 **Duckett DR**, Bronstein SM, Taya Y, Modrich P. hMutS α - and hMutL α -dependent phosphorylation of p53 in response to DNA methylator damage. *Proc Natl Acad Sci U S A* 1999; **96**: 12384-12388
- 93 **Hickman MJ**, Samson LD. Role of DNA mismatch repair and p53 in signaling induction of apoptosis by alkylating agents. *Proc Natl Acad Sci U S A* 1999; **96**: 10764-10769

- 94 **Li GM.** The role of mismatch repair in DNA damage-induced apoptosis. *Oncol Res* 1999; **11**: 393-400
- 95 **Toft NJ,** Winton DJ, Kelly J, Howard LA, Dekker M, te Riele H, Arends MJ, Wyllie AH, Margison GP, Clarke AR. Msh2 status modulates both apoptosis and mutation frequency in the murine small intestine. *Proc Natl Acad Sci U S A* 1999; **96**: 3911-3915
- 96 **Wu J,** Gu L, Wang H, Geacintov NE, Li GM. Mismatch repair processing of carcinogen-DNA adducts triggers apoptosis. *Mol Cell Biol* 1999; **19**: 8292-8301
- 97 **Zhang H,** Richards B, Wilson T, Lloyd M, Cranston A, Thorburn A, Fishel R, Meuth M. Apoptosis induced by overexpression of hMSH2 or hMLH1. *Cancer Res* 1999; **59**: 3021-3027
- 98 **Peltomaki P.** DNA mismatch repair and cancer. *Mutat Re* 2001; **488**: 77-85
- 99 **Wijnen J,** de Leeuw W, Vasen H, van der Klift H, Moller P, Stormorken A, Meijers-Heijboer H, Lindhout D, Menko F, Vossen S, Moslein G, Tops C, Brocker-Vriends A, Wu Y, Hofstra R, Sijmons R, Cornelisse C, Morreau H, Fodde R. Familial endometrial cancer in female carriers of MSH6 germline mutations. *Nat Genet* 1999; **23**: 142-144
- 100 **Myeroff LL,** Parsons R, Kim SJ, Hedrick L, Cho KR, Orth K, Mathis M, Kinzler KW, Lutterbaugh J, Park K, Bang YJ, Lee HY, Park JG, Lynch HT, Roberts AB, Vogelstein B, Markowitz SD. A transforming growth factor beta receptor type II gene mutation common in colon and gastric but rare in endometrial cancers with microsatellite instability. *Cancer Res* 1995; **55**: 5545-5547
- 101 **Duval A,** Iacopetta B, Ranzani GN, Lothe RA, Thomas G, Hamelin R. Variable mutation frequencies in coding repeats of TCF-4 and other target genes in colon, gastric and endometrial carcinoma showing microsatellite instability. *Oncogene* 1999; **18**: 6806-6809
- 102 **Reitmair AH,** Cai JC, Bjerknes M, Redston M, Cheng H, Pind MT, Hay K, Mitri A, Bapat BV, Mak TW, Gallinger S. MSH2 deficiency contributes to accelerated APC-mediated intestinal tumorigenesis. *Cancer Res* 1996; **56**: 2922-2926
- 103 **Kane MF,** Loda M, Gaida GM, Lipman J, Mishra R, Goldman H, Jessup JM, Kolodner R. Methylation of the hMLH1 promoter correlates with lack of expression of hMLH1 in sporadic colon tumors and mismatch repair-defective human tumor cell lines. *Cancer Res* 1997; **57**: 808-811
- 104 **Veigl ML,** Kasturi L, Olechnowicz J, Ma AH, Lutterbaugh JD, Periyasamy S, Li GM, Drummond J, Modrich PL, Sedwick WD, Markowitz SD. Biallelic inactivation of hMLH1 by epigenetic gene silencing, a novel mechanism causing human MSI cancers. *Proc Natl Acad Sci U S A* 1998; **95**: 8698-8702
- 105 **Herman JG,** Umar A, Polyak K, Graff JR, Ahuja N, Issa JP, Markowitz S, Willson JK, Hamilton SR, Kinzler KW, Kane MF, Kolodner RD, Vogelstein B, Kunkel TA, Baylin SB. Incidence and functional consequences of hMLH1 promoter hypermethylation in colorectal carcinoma. *Proc Natl Acad Sci U S A* 1998; **95**: 6870-6875
- 106 **Rashid A,** Shen L, Morris JS, Issa JP, Hamilton SR. CpG island methylation in colorectal adenomas. *Am J Pathol* 2001; **159**: 1129-1135
- 107 **Ahuja N,** Mohan AL, Li Q, Stolker JM, Herman JG, Hamilton SR, Baylin SB, Issa JP. Association between CpG island methylation and microsatellite instability in colorectal cancer. *Cancer Res* 1997; **57**: 3370-3374
- 108 **Augenlicht LH,** Richards C, Corner G, Pretlow TP. Evidence for genomic instability in human colonic aberrant crypt foci. *Oncogene* 1996; **12**: 1767-1772
- 109 **Luceri C,** De Filippo C, Caderni G, Gambacciani L, Salvadori M, Giannini A, Dolara P. Detection of somatic DNA alterations in azoxymethane-induced F344 rat colon tumors by random amplified polymorphic DNA analysis. *Carcinogenesis* 2000; **21**: 1753-1756
- 110 **Pedroni M,** Sala E, Scarselli A, Borghi F, Menigatti M, Benatti P, Percepe A, Rossi G, Foroni M, Losi L, Di Gregorio C, De Pol A, Nascimbeni R, Di Betta E, Salerni B, de Leon MP, Roncucci L. Microsatellite instability and mismatch-repair protein expression in hereditary and sporadic colorectal carcinogenesis. *Cancer Res* 2001; **61**: 896-899
- 111 **Kiesslich R,** von Bergh M, Hahn M, Hermann G, Jung M. Chromoendoscopy with indigocarmine improves the detection of adenomatous and nonadenomatous lesions in the colon. *Endoscopy* 2001; **33**: 1001-1006
- 112 **Hurlstone DP,** Fujii T, Lobo AJ. Early detection of colorectal cancer using high-magnification chromoscopic colonoscopy. *Br J Surg* 2002; **89**: 272-282

Edited by Zhu LH and Wang XL

• ESOPHAGEAL CANCER •

Expression properties of recombinant pEgr-P16 plasmid in esophageal squamous cell carcinoma induced by ionizing irradiation

Cong-Mei Wu, Tian-Hua Huang, Qing-Dong Xie, De-Sheng Wu, Xiao-Hu Xu

Cong-Mei Wu, Tian-Hua Huang, Qing-Dong Xie, Research Center of Reproductive Medicine, Shantou University Medical College, Shantou 515041, Guangdong Province, China
Xiao-Hu Xu, Department of Forensic Medicine, Shantou University Medical College, Shantou 515041, Guangdong Province, China
De-Sheng Wu, Lanzhou Medical College, Lanzhou 730000, Gansu Province, China

Supported by the National Natural Science Foundation of China, No.30210103904 and the Science and Technology Program of Guangdong Province, No.2003C30304

Correspondence to: Dr. Tian-Hua Huang, Research Center of Reproductive Medicine, Shantou University Medical College, Shantou 515041, Guangdong Province, China. thhuang@stu.edu.cn
Telephone: +86-754-8900442 **Fax:** +86-754-8557562

Received: 2003-06-21 **Accepted:** 2003-07-24

Abstract

AIM: To construct the recombinant pEgr-P16 plasmid for the investigation of its expression properties in esophageal squamous cell carcinoma induced by ionizing irradiation and the feasibility of gene-radiotherapy for esophageal carcinoma.

METHODS: The recombinant pEgr-P16 plasmid was constructed and transfected into EC9706 cells with lipofectamine. Western blot, quantitative RT-PCR and flow cytometry were performed to study the expression of pEgr-P16 in EC9706 cells and the biological characteristics of EC9706 cell line after transfection induced by ionizing irradiation.

RESULTS: The eukaryotic expression vector pEgr-P16 was successfully constructed and transfected into EC9706 cells. The expression of P16 was significantly increased in the transfected cells after irradiation while the transfected cells were not induced by ionizing irradiation. The induction of apoptosis in transfection plus irradiation group was higher than that in plasmid alone or irradiation alone.

CONCLUSION: The combination of pEgr-P16 and irradiation could significantly enhance the P16 expression property and markedly induce apoptosis in EC9706 cells. These results may lay an important experimental basis for gene radiotherapy for esophageal carcinoma.

Wu CM, Huang TH, Xie QD, Wu DS, Xu XH. Expression properties of recombinant pEgr-P16 plasmid in esophageal squamous cell carcinoma induced by ionizing irradiation. *World J Gastroenterol* 2003; 9(12): 2650-2653

<http://www.wjgnet.com/1007-9327/9/2650.asp>

INTRODUCTION

Early growth response gene-1 (Egr-1), also known as zif/268, NGFI-A, Krox-24 and TIS-8, encodes a nuclear phosphoprotein with a cysteine/histidine zinc finger structure, which is partially homologous to the corresponding domain of the Wilm's tumor susceptibility gene^[1-4] Zinc fingers are a protein structural motif that serves as DNA-binding domains in several transcriptional

regulatory proteins. It was reported that Egr-1 was transcriptionally induced following exposure to irradiation. Promoter deletion analysis of Egr-1 promoter elements linked to the CAT reporter gene demonstrated that the first 5' CArG boxes (CC (A/T)₆GG elements) were of paramount importance for the induction of Egr-1 by irradiation or free radicals^[5-7].

In this study, the pEgr-P16 plasmid was constructed and transfected into the human esophageal cancer cell line EC9706. The expression of P16 in the transfected cells exposed to different doses of γ -ray irradiation and its bioactivities were detected to explore the feasibility of gene-radiotherapy for esophageal carcinoma.

MATERIALS AND METHODS

Cell line and vectors

The EC9706 was maintained in Dulbecco's modified Eagle's medium (DMEM), high glucose media (Life Technologies) and generously supplemented with 100 ml·L⁻¹ fetal bovine serum (Hyclone Laboratories), penicillin, streptomycin and nonessential amino acids (Life Technologies). The pcDNA3.1⁺ vector was purchased from Invitrogen and pGL3-enhancer vector from Promega-Biotec.

Construction of pEgr-P16 plasmid

The expression vector for P16 was constructed as shown in Figure 1.

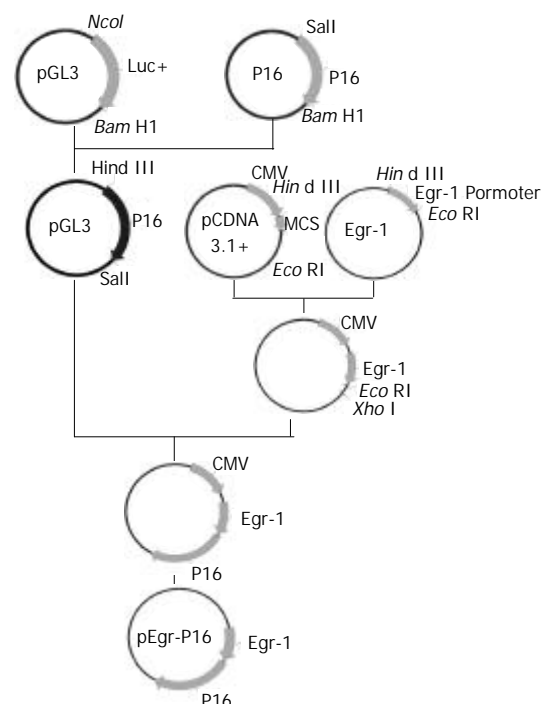


Figure 1 Diagram of the construction of the plasmid pEgr-P16.

Transfection

The transfection of EC9706 cells was carried out in a 6-well

plate. The transfection procedure began when the cells reached 70 % confluence on the surface of plate wells. Solution A was prepared by separate addition of 10 μ g of pEgr-P16 and pcDNA3.1⁺ to 100 μ l serum-free medium (SFM), and solution B by addition of 10 μ l Lipofectimine 2000 (Life Technologies) to 100 μ l SFM. The two solutions were combined for 30 min at room temperature, 0.8 ml SFM was added to the tube containing the above solutions, and the mixture was added to the rinsed cells. The medium was replaced with fresh and complete one after 18 h in transfection. The cells were exposed to irradiation after 36 h in transfection.

Ionizing irradiation

The dose rate was 0.784 Gy/min for 0, 2, 4, 8, 10 and 20 Gy Co⁶⁰ γ -ray irradiation, respectively.

Quantitative RT-PCR

Total RNAs of the transfection of EC9706 cells and control were obtained by extracting cells in Trizol (Invitrogen) and treated with heat-inactivated DNase I (Invitrogen). RNA quality and quantity were evaluated by UV spectrophotometry. Two μ g total RNA was used for cDNA synthesis (25 μ l) using M-MLV reverse transcriptase and random primers (Invitrogen).

A standard curve was constructed separately by the serial dilutions of PCR purified products of p16 and glyceraldehyde-3-phosphate-dehydrogenase (GAPDH). Template concentrations for reactions in the relative standard were 10⁸, 10⁷, 10⁶ and 10² copies/ μ l. The cDNA (1:5 dilution) from the sample was analyzed as unknown. Real-time PCR was performed containing SYBRgreen I (1:20 000 QIAGEN), forward and reverse primers (50 nmol each), sample cDNA (1 μ l) or standard sample (1 μ l) under the following condition: denaturation at 95 °C (3 min); 40 cycles at 95 °C (45 s), at 59 °C (45 s), at 72 °C (40 s), at 80 °C (5 s). GAPDH was used as an internal reference in each PCR reaction. Primers were as follows: GAPDH, forward primer 5'-TGCACCACCAACTGCTTAGC-3' and reverse one 5'-GGCATGGACTGTGGTCATGAG-3'. P16, forward primer: 5'-GAATAGTTACGGTTCGGAG-3' and reverse one 5'-CGGTGACTGATGATCTAA-3'. Amplification was followed by melting curve analysis using the program run at the step acquisition mode to verify the presence of a single amplification product in DNA contamination-free. For each set of primers, a non-cDNA template control was included to assess the overall specificity. Accumulation of PCR products was monitored and determined using the Icyler (Bio-Rad), and the crossing threshold (Ct) was determined using the Icyler software.

Flow cytometry analysis

Approximately 5 \times 10⁶ of centrifugally sedimented cells were immediately fixed in 700 ml L⁻¹ ethanol and stored at 4 °C in PBS in preparation for fluorescent-activated cell sorting. Flow cytometry analysis was performed on a FACStar flow cytometer (Becton Dickinson). Histograms of cell number logarithmic fluorescence intensity were recorded for 10 000 cells per sample. The apoptotic cell rate was calculated.

Statistical analysis

Student's *t* and correlation tests were used to determine the comparability of groups. Statistically significant *P* value was defined as <0.05.

RESULTS

Expression of P16 in EC9706 cells transfected with pEgr-P16 followed by different doses of γ -irradiation

EC9706 cells transfected with pEgr-P16 were irradiated by

different doses of γ -rays. The cells of control group were transfected with pcDNA3.1⁺. Eight hours after irradiation, the protein was extracted and the expression of P16 was detected by Western-blot. The results showed no P16 expression in the control and higher p16 expression in 2, 4, 8, 10 and 20 Gy groups than in 0Gy one.

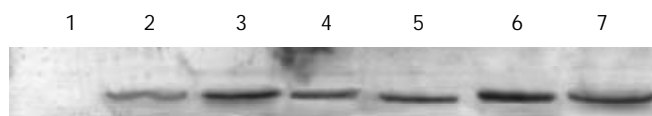


Figure 2 Expression of P16 in EC9706 cells after γ -irradiation. Lane 1: control; Lane 2: 0Gy; Lane 3: 2Gy; Lane 4: 4Gy; Lane 5: 8Gy; Lane 6: 10Gy; Lane 7: 20Gy.

P16 expression in EC9706 cells transfected with pEgr-P16 at different time points after 2Gy irradiation

EC9706 cells transfected with pEgr-P16 were irradiated by 2Gy irradiation. Total RNA was isolated at different time points after irradiation and the mRNA levels were detected by quantitative RT-PCR.

The results showed that P16 levels after 2Gy irradiation increased with time from 0 to 24 h. It reached the highest level at the 24th h and was about 4 times of that at the 2nd h (*P*<0.01).

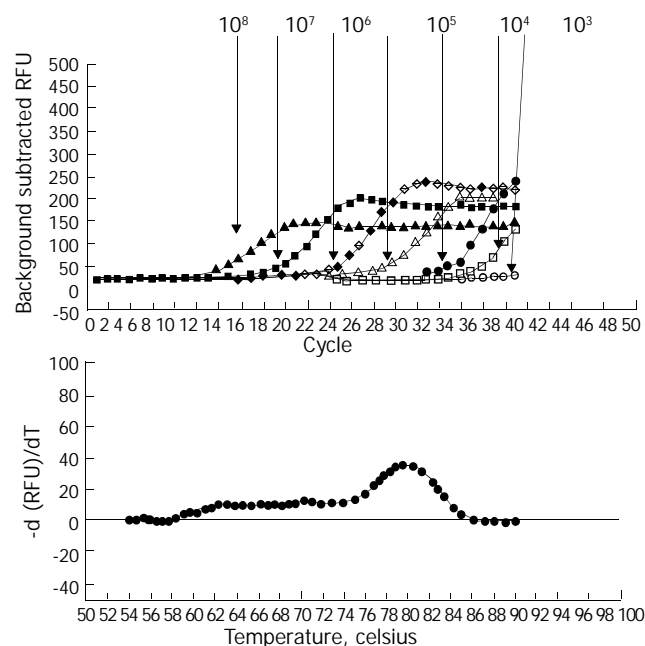


Figure 3 Amplification curves and post-amplification dissociation curves for P16 in EC9706 cells.

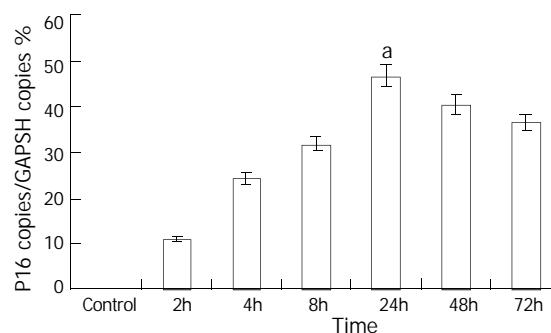


Figure 4 Expression of P16 in EC9706 cells at different time points after 2Gy γ -irradiation, ^a*P*<0.01 vs. 2 h group.

Apoptotic changes of transfected EC9706 cells after 2Gy γ -irradiation

In P16 transfected EC9706 cells the apoptosis rate was 25.00, being higher than that of pcDNA3.1+ group (18.03, $P < 0.05$). When exposed to 2Gy irradiation, the apoptosis rate was 33.23, higher than that in pcDNA3.1+ group (18.03, $P < 0.01$) and P16 group (25.00). The differences were not significant between P16 and P16 plus irradiation groups.

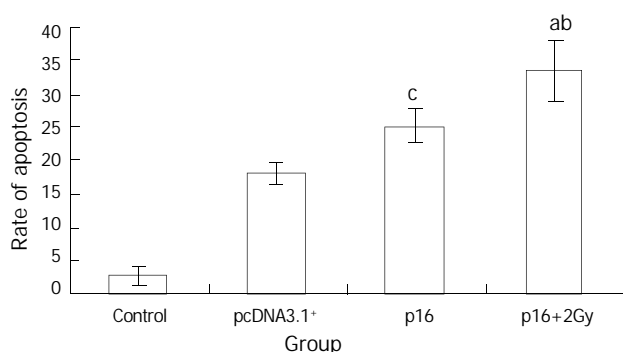


Figure 5 Apoptotic changes of transfected EC9706 cells. ^a $P < 0.01$ vs pcDNA3.1+ group, ^b $P < 0.001$ vs control group, ^c $P < 0.05$ vs pcDNA3.1+ group.

DISCUSSION

Radiotherapy is one of most important choices of the treatment for human tumors. Tumor destruction by radiation depends more on physical restriction of the radiation to a high-dose volume containing the tumor rather than a strict difference in radiosensitivity between tumor and normal cells. In fact, many tumor cells have lost the capacity for programmed cell death, resulting in radioresistance when compared with normal tissues. Vital structures are frequent within the radiotherapy volume restricting the amount of therapeutic radiation that can be safely delivered, thereby limiting tumor curability.

With the rapid development of molecular biology, gene radiotherapy has been considered as an effective way of cancer treatment. According to the mechanism that ionizing radiation could activate early Egr-1 gene promoter and induce the expression of downstream genes, Weichselbaum *et al* were the forerunners in tumor gene radiotherapy. They linked DNA sequences from the promoter region of Egr-1 with a cDNA sequence that encodes human tumor necrosis factor (TNF) α . The Egr-TNF construct was transfected into a human cell line of hematopoietic origin, HL525 (clone 2). The latter was injected into human xenografts of the radioresistant human squamous cell carcinoma cell line SQ-20B. Animals treated with radiation and clone 2 demonstrated an increase in tumor cures compared with animals treated with radiation alone or unirradiated animals given injections of clone 2 alone^[6]. Thereafter, a variety of downstream genes were introduced to Egr-1 promoter to treat different tumors, and similar results were obtained^[9-11].

The division cycle of eukaryotic cells is regulated by a family of protein kinases known as the cyclin-dependent kinases (CDKs). P16 is a tumor suppressor gene product. Serrano *et al* demonstrated that p16 could bind to CDK4 and inhibit the catalytic activity of the CDK4/cyclin D enzymes. P16 seemed to act in a regulatory feedback circuit with CDK4, D-type cyclins and retinoblastoma protein^[12]. Overexpression of P16 gene could block cell cycle progression through the G₁-to-S phase boundary in a pRB-dependent manner^[13-14]. Many P16 mutants identified from human tumors have been shown to have defects in this activity^[15-17]. These data suggest that the CDK4-inhibitory activity of p16 is involved in

regulating cell cycle progression through the G₁/S boundary.

On the basis of the antiangiogenic action of P16, we constructed pEgr-P16 plasmid and transfected EC9706 cells to study the expression properties of the plasmid induced by ionizing irradiation. The results revealed that no P16 expression in EC9706 cells transfected with pcDNA3.1+ was detected and that the P16 expression in cells transfected with pEgr-P16 induced by irradiation was higher than that of sham-irradiation group. Time-course studies revealed that the P16 expression reached its peak at the 24th h after 2Gy irradiation, and the highest level was 4 times of that at the 2nd h ($P < 0.01$). The combination of pEgr-P16 and radiation could induce markedly apoptosis of EC9706 cells although pEgr-P16 alone might induce transfected cells to undergo apoptosis. Our results suggested that pEgr-P16 could enhance expression property induced by radiation in EC9706 cells.

Esophageal carcinoma is still common in the world, especially in China^[18-24], and the treatment remains a big problem up to date^[25-31]. Gene radiotherapy may be of potential significance in the treatment of esophageal cancer. Our work will be a ground of further studies on esophageal cancer gene radiotherapy.

ACKNOWLEDGEMENT

We especially thank Prof. Ming Rong Wang for providing us the EC9706 cells line and Dr. Di Wu for providing the P16 gene.

REFERENCES

- Christy B, Nathans D. DNA binding site of the growth factor-inducible protein Zif268. *Proc Natl Acad Sci U S A* 1989; **86**: 8737-8741
- Seyfert VL, Sukhatme VP, Monroe JG. Differential expression of a zinc finger-encoding gene in response to positive versus negative signaling through receptor immunoglobulin in murine B-lymphocytes. *Mol Cell Biol* 1989; **9**: 2083-2088
- Joseph LJ, Le-Beau MM, Jamieson GA Jr, Acharya S, Shows TB, Rowley JD, Sukhatme VP. Molecular cloning, sequencing, and mapping of EGR2, a human early growth response gene encoding a protein with "zinc-binding finger" structure. *Proc Natl Acad Sci U S A* 1988; **85**: 7164-7168
- Sukhatme VP. Early transcriptional events in cell growth: The Egr family. *J Am Soc Nephro* 1990; **1**: 859-866
- Cao XM, Koski RA, Gashler A, McKiernan M, Morris CF, Gaffney R, Hay RV, Sukhatme VP. Identification and characterization of the Egr-1 gene product, a DNA-binding zinc finger protein induced by differentiation and growth signal. *Mol Cell Biol* 1990; **10**: 1931-1939
- Tsai-Morris CH, Cao XM, Sukhatme VP. 5' flanking sequence and genomic structure of Egr-1, a murine mitogen inducible zinc finger encoding gene. *Nucleic Acids Res* 1988; **16**: 8835-8846
- Datta R, Taneja N, Sukhatme VP, Qureshi SA, Weichselbaum R, Kufe DW. Reactive oxygen intermediates target CC(A/T)6GG sequences to mediate activation of the early growth response 1 transcription factor gene by ionizing radiation. *Proc Natl Acad Sci U S A* 1993; **90**: 2419-2422
- Weichselbaum RR, Hallahan DE, Beckett MA, Mauceri HJ, Lee H, Sukhatme VP, Kufe DW. Gene therapy targeted by radiation preferentially radiosensitizes tumor cells. *Cancer Res* 1994; **54**: 4266-4269
- Hanna NN, Seetharam S, Mauceri HJ, Beckett MA, Jaskowiak NT, Salloum RM, Hari D, Dahanabal M, Ramchandran R, Kalluri R, Sukhatme VP, Kufe DW, Weichselbaum RR. Antitumor interaction of short-course endostatin and ionizing radiation. *Cancer J* 2000; **6**: 287-293
- Takahashi T, Namiki Y, Ohno T. Induction of the suicide HSV-TK gene by activation of the Egr-1 promoter with radioisotopes. *Hum Gene Ther* 1997; **8**: 827-833
- Griscelli F, Li H, Cheong C, Opolon P, Bennaceur-Griscelli A, Vassal G, Soria J, Soria C, Lu H, Perricaudet M, Yeh P. Combined effects of radiotherapy and angiostatin gene therapy in glioma

- tumor model. *Proc Natl Acad Sci U S A* 2000; **97**: 6698-6703
- 12 **Serrano M**, Hannon GJ, Beach D. A new regulatory motif in cell-cycle control causing specific inhibition of cyclin D/CDK4. *Nature* 1993; **366**: 704-707
 - 13 **Koh J**, Enders GH, Dynlacht BD, Harlow E. Tumour-derived p16 alleles encoding proteins defective in cell-cycle inhibition. *Nature* 1995; **375**: 506-510
 - 14 **Lukas J**, Parry D, Aagaard L, Mann DJ, Bartkova J, Strauss M, Peters G, Bartek J. Retinoblastoma-protein-dependent cell-cycle inhibition by the tumour suppressor p16. *Nature* 1995; **375**: 503-506
 - 15 **Monzon J**, Liu L, Brill H, Goldstein AM, Tucker MA, From L, McLaughlin J, Hogg D, Lassam NJ. CDKN2A mutations in multiple primary melanomas. *N Engl J Med* 1998; **338**: 879-887
 - 16 **Nobori T**, Miura K, Wu DJ, Lois A, Takabayashi K, Carson DA. Deletions of the cyclin-dependent kinase-4 inhibitor gene in multiple human cancers. *Nature* 1994; **368**: 753-756
 - 17 **Soufir N**, Avril MF, Chompret A, Demenais F, Bombléd J, Spatz A, Stoppa-Lyonnet D, Benard J, Bressac-de-Paillerets B. Prevalence of p16 and CDK4 germline mutations in 48 melanoma-prone families in France. The French Familial Melanoma Study Group. *Hum Mol Genet* 1998; **7**: 209-216
 - 18 **Zhao XJ**, Li H, Chen H, Liu YX, Zhang LH, Liu SX, Feng QL. Expression of e-cadherin and beta-catenin in human esophageal squamous cell carcinoma: relationships with prognosis. *World J Gastroenterol* 2003; **9**: 225-232
 - 19 **Li X**, Lu JY, Zhao LQ, Wang XQ, Liu GL, Liu Z, Zhou CN, Wu M, Liu ZH. Overexpression of ETS2 in human esophageal squamous cell carcinoma. *World J Gastroenterol* 2003; **9**: 205-208
 - 20 **He YT**, Hou J, Qiao CY, Chen ZF, Song GH, Li SS, Meng FS, Jin HX, Chen C. An analysis of esophageal cancer incidence in Cixian county from 1974 to 1996. *World J Gastroenterol* 2003; **9**: 209-213
 - 21 **Zhou HB**, Yan Y, Sun YN, Zhu JR. Resveratrol induces apoptosis in human esophageal carcinoma cells. *World J Gastroenterol* 2003; **9**: 408-411
 - 22 **Song ZB**, Gao SS, Yi XN, Li YJ, Wang QM, Zhuang ZH, Wang LD. Expression of MUC1 in esophageal squamous-cell carcinoma and its relationship with prognosis of patients from Linzhou city, a high incidence area of northern China. *World J Gastroenterol* 2003; **9**: 404-407
 - 23 **Heidecke CD**, Weighardt H, Feith M, Fink U, Zimmermann F, Stein HJ, Siewert JR, Holzmann B. Neoadjuvant treatment of esophageal cancer: Immunosuppression following combined radiochemotherapy. *Surgery* 2002; **132**: 495-501
 - 24 **Tsunoo H**, Komura S, Ohishi N, Yajima H, Akiyama S, Kasai Y, Ito K, Nakao A, Yagi K. Effect of transfection with human interferon-beta gene entrapped in cationic multilamellar liposomes in combination with 5-fluorouracil on the growth of human esophageal cancer cells *in vitro*. *Anticancer Res* 2002; **22**: 1537-1543
 - 25 **Nemoto K**, Zhao HJ, Goto T, Ogawa Y, Takai Y, Matsushita H, Takeda K, Takahashi C, Saito H, Yamada S. Radiation therapy for limited-stage small-cell esophageal cancer. *Am J Clin Oncol* 2002; **25**: 404-407
 - 26 **Tachibana M**, Dhar DK, Kinugasa S, Yoshimura H, Fujii T, Shibakita M, Ohno S, Ueda S, Kohno H, Nagasue N. Esophageal cancer patients surviving 6 years after esophagectomy. *Langenbecks Arch Surg* 2002; **387**: 77-83
 - 27 **Wilson KS**, Wilson AG, Dewar GJ. Curative treatment for esophageal cancer: Vancouver Island Cancer Centre experience from 1993 to 1998. *Can J Gastroenterol* 2002; **16**: 361-368
 - 28 **Liu HH**, Yoshida M, Momma K, Oohashi K, Funada N. Detection and treatment of an asymptomatic case of early esophageal cancer using chromoendoscopy and endoscopic mucosal resection. *J Formos Med Assoc* 2002; **101**: 219-222
 - 29 **Hou J**, Lin PZ, Chen ZF, Ding ZW, Li SS, Men FS, Gou LP, He YI, Qiao CY, Gou CL, Duan JP, Wen DG. Field population-based blocking treatment of esophageal epithelia dysplasia. *World J Gastroenterol* 2002; **8**: 418-422
 - 30 **Wang AH**, Sun CS, Li LS, Huang JY, Chen QS. Relationship of tobacco smoking CYP1A1 GSTM1 gene polymorphism and esophageal cancer in Xi' an. *World J Gastroenterol* 2002; **8**: 49-53
 - 31 **Shen ZY**, Shen WY, Chen MH, Shen J, Cai WJ, Yi Z. Nitric oxide and calcium ions in apoptotic esophageal carcinoma cells induced by arsenite. *World J Gastroenterol* 2002; **8**: 40-43

Edited by Ma JY

Epoxide hydrolase *Tyr113His* polymorphism is not associated with susceptibility to esophageal squamous cell carcinoma in population of North China

Jian-Hui Zhang, Xia Jin, Yan Li, Rui Wang, Wei Guo, Na Wang, Deng-Gui Wen, Zhi-Feng Chen, Gang Kuang, Li-Zhen Wei, Shi-Jie Wang

Jian-Hui Zhang, Xia Jin, Yan Li, Wei Guo, Na Wang, Deng-Gui Wen, Zhi-Feng Chen, Gang Kuang, Li-Zhen Wei, Shi-Jie Wang, Hebei Cancer Institute, Hebei Medical University, Shijiazhuang 050011, Hebei Province, China

Rui Wang, Shi-Jie Wang, The Fourth Affiliated Hospital, Hebei Medical University, Shijiazhuang 050011, Hebei Province, China

Supported by the Scientific Grant of Educational Department of Hebei Province, China, No. 2001150

Correspondence to: Professor Shi-Jie Wang, The Fourth Affiliated Hospital, Hebei Medical University, Jiankanglu 12, Shijiazhuang 050011, China. wang.sj@hbmh.edu

Telephone: +86-311-6085231 **Fax:** +86-311-6077634

Received: 2003-06-16 **Accepted:** 2003-08-25

Abstract

AIM: To investigate the possible association of *microsomal epoxide hydrolase (mEH)* *Tyr113His* polymorphism with susceptibility to esophageal squamous cell carcinoma (ESCC) in a population of North China.

METHODS: The *mEH Tyr113His* genotypes were determined by polymerase-chain reaction (PCR)-restriction fragment length polymorphism (RFLP) analysis in 257 patients with esophageal squamous cell carcinoma (ESCC) and 252 healthy subjects as a control group.

RESULTS: The frequencies for *Tyr* and *His* alleles were 44.2 %, 55.8 % in ESCC patients, and 44.0 % and 56.0 % in healthy subjects, respectively. No statistic difference in allele distribution was observed between ESCC patients and controls ($\chi^2=0.008$, $P=0.929$). The overall genotype distribution difference was not observed between cancer cases and controls ($\chi^2=2.116$, $P=0.347$). Compared with *Tyr/Tyr* genotype, neither *His/His* genotype nor in combination with *Tyr/His* genotype significantly modified the risk of the development of ESCC, the adjusted odds ratio was 1.076 (95 % CI=0.850-1.361) and 0.756 (95 % CI=0.493-1.157), respectively. When stratified for sex, age, smoking status and family history of upper gastrointestinal cancer, *His/His* genotype alone or in combination with *Tyr/His* genotype also did not show any significant influence on the risk of developing ESCC.

CONCLUSION: *mEH Tyr113His* polymorphism may not be used as a stratification marker in screening individuals at a high risk of ESCC.

Zhang JH, Jin X, Li Y, Wang R, Guo W, Wang N, Wen DG, Chen ZF, Kuang G, Wei LZ, Wang SJ. Epoxide hydrolase *Tyr113His* polymorphism is not associated with susceptibility to esophageal squamous cell carcinoma in population of North China. *World J Gastroenterol* 2003; 9(12): 2654-2657

<http://www.wjgnet.com/1007-9327/9/2654.asp>

INTRODUCTION

China is one of the prevalent areas of esophageal squamous cell cancer (ESCC). Exposure to environmental carcinogens is considered as the main risk factors of ESCC^[1,2]. Among them, chemical carcinogens such as polycyclic aromatic hydrocarbons (PAHs) in consumed tobacco or ingested food may contribute to the high incidence of ESCC in China^[3,4]. Metabolization of PAHs involves a complex enzymatic mechanism. Microsomal epoxide hydrolase (mEH) is an enzyme that hydrolyzes epoxides such as PHA, yielding corresponding *trans*-dihydrodiols. Usually, this hydrolysis acts as a detoxifying step, although in some instances, *trans*-dihydrodiols generated from PAHs are highly toxic and mutagenic. Therefore, mEH plays a dual role in the detoxification and activation of procarcinogens, and its role in carcinogenesis may depend on exposures to different environmental substrates^[5].

There are two polymorphic sites that affect the enzyme activity in human *mEH* gene. One variant is characterized by substitution of histidine for tyrosine at the amino acid position 113, the other is characterized by substitution of arginine for histidine at the position 139. The proteins encoded by polymorphic alleles demonstrated different enzyme activities *in vitro*^[6]. *MEH* polymorphism has been associated with chemical carcinogen-induced cancers occurring in lung^[7,8], ovary^[9], colorectum^[10] and liver^[11]. The correlation of *mEH* polymorphism with susceptibility to ESCC has not been reported so far. Therefore, the current study investigated the *Tyr113His* polymorphism in *mEH* exon 3 in ESCC patients and healthy individuals from North China.

MATERIALS AND METHODS

Subjects

This study included 257 patients with histologically confirmed esophageal squamous cell carcinomas and 252 healthy individuals without overt cancer. The cancer patients were hospitalized for surgery in the Fourth Affiliated hospital, Hebei Medical University between 2001 and 2003. The healthy subjects were from the same hospital for physical examination in the same period. All of the patients and control subjects were from Shijiazhuang city or its surrounding regions. Information of sex, age, smoking habits and family history was obtained from cancer patients and healthy controls by interview following sampling. The smokers were defined as former or current smoking 5 cigarettes per day for at least two years. The individuals with at least one first-degree relative or at least two second-degree relatives having esophageal/cardiac/gastric cancer were defined as having family history of upper gastrointestinal cancers (UGIC). The smoking status and family history were available from some of the cases and controls. Informed consent was obtained from all the recruited subjects. The study was approved by the Ethics Committee of Hebei Cancer Institute.

DNA extraction

Five ml of venous blood from each subject was drawn in Vacutainer tubes containing EDTA and stored at 4 °C. Genomic DNA was extracted within one week after sampling by using proteinase K digestion followed by a salting out procedure.

mEH genotyping by PCR and restriction fragment analysis

The exon 3 T to C variant in *mEH* gene, changing tyrosine 113 to histidine, creates an *EcoR* restriction site (GATATC), which can be exploited for genotyping by PCR and subsequent RFLP analysis^[12]. PCR was performed in a 25 µl volume containing 100 ng of DNA template, 2.5 µl of 10×buffer, 1 U of *Taq*-DNA-polymerase (BioDev-Tech., Beijing, China), 200 µmol of dNTPs and 200 nmol of sense primer (5' - GATCGATAAGTTCCGTTTACC-3') and antisense primer (5' - ATCCTTAGTCTTGAAGTGAGGAT-3'). Initial denaturation at 94 °C for 5 min was followed by 35 cycles at 94 °C for 30 sec, at 56 °C for 30 sec and at 72 °C for 1 min. Subsequently, the PCR products were digested with 10 units of *EcoR* V (TakaRa Biotechnology Co., Ltd, Dalian, China) overnight at 37 °C and separated on a 3 % agarose gel. RFLP bands were visualized through ethidium bromide staining under UV light. *Tyr*113 wild-type homozygote was characterized by two bands at the position of 140 bp and 22 bp, while *His*113 homozygotes were identified by a single band (162 bp) and the heterozygotes by three bands (162 bp, 140 bp and 22 bp). For a negative control, each PCR reaction used distilled water instead of DNA in the reaction system. For 10 % of the samples, the reaction was repeated once.

Statistical analysis

Statistical analysis was performed using the SPSS10.0 software package (SPSS Company, Chicago, Illinois, USA). Comparison of *mEH* genotype distribution in the study groups was performed by means of two-sided contingency tables using Chi-square test. A probability level of 5 % was considered significant. The odds ratio (OR) and 95 % confidence interval (CI) were calculated using an unconditional logistic regression model and adjusted by age and sex accordingly.

RESULTS

The mean age of all ESCC cases was 58.5±9.39 years (range 32-85) and that of controls was 49.4±8.56 years (range 29-79 years). The gender distribution in ESCC patients (66.5 % men) was comparable to that in healthy controls (58.3 % men). Moreover, the proportion of smokers in ESCC patients (52.0 %) was also not significantly different from that in healthy controls (49.5 %) ($\chi^2=0.283$, $P=0.595$). In addition, the frequency of the positive family history of UGIC in ESCC patients (44.1 %) was significantly higher than that in healthy controls (14.0 %) ($\chi^2=49.87$, $P<0.0001$). Thus, the positive family history of UGIC significantly increased the relative risk to develop ESCC in this population, with an age and sex adjusted odds ratio of 4.06 (95 % CI=2.46-6.69). The demographic distribution of ESCC patients and healthy controls is shown in Table 1.

mEH Tyr113His genotyping was successfully performed in all study subjects. The *mEH* genotype distribution was not

Table 2 Influence of *mEH Tyr113His* polymorphism on ESCC development

	Tyr/Tyr	Tyr/His+His/His	His/His	aOR(95%CI) ^c	aOR (95%CI) ^d
Overall					
Normal	76 (30.2)	176 (69.8)	105 (41.7)		
ESCC	84 (32.7)	173 (67.3)	115 (44.7)	0.756 (0.493–1.157)	1.076 (0.850–1.361)
Male					
Normal	44 (30.6)	100 (69.4)	60 (41.7)		
ESCC	61 (35.7)	110 (64.3)	73 (42.7)	0.724 (0.427–1.225)	1.087 (0.811–1.458)
Female					
Normal	32 (29.6)	76 (70.4)	45 (41.7)		
ESCC	23 (26.8)	63 (73.2)	42 (48.8)	0.825 (0.398–1.710)	1.047 (0.704–1.558)
Age≤50					
Normal	46 (32.6)	95 (67.4)	60 (42.6)		
ESCC	19 (33.9)	37 (66.1)	22 (39.3)	0.867 (0.450–1.671)	1.064 (0.738–1.534)
Age>50					
Normal	30 (27.0)	81 (73.0)	45 (40.6)		
ESCC	65 (32.3)	136 (67.7)	93 (46.3)	0.790 (0.472–1.323)	1.018 (0.768–1.348)
Nonsmoker ^a					
Normal	31 (27.7)	81 (72.3)	49 (43.7)		
ESCC	34 (28.3)	86 (71.7)	60 (50.0)	0.659 (0.338–1.286)	1.135 (0.790–1.631)
Smoker					
Normal	35 (31.8)	75 (68.2)	41 (37.3)		
ESCC	46 (35.4)	84 (64.6)	52 (40.0)	0.901 (0.494–1.644)	1.022 (0.728–1.433)
Negative family history ^b					
Normal	59 (30.9)	132 (69.1)	80 (41.9)		
ESCC	49 (37.1)	83 (62.9)	51 (38.7)	0.660 (0.385–1.134)	1.237 (0.912–1.678)
Positive family history					
Normal	7 (22.6)	24 (77.4)	10 (32.2)		
ESCC	29 (27.9)	75 (72.1)	52 (50.0)	0.638 (0.241–1.689)	0.946 (0.546–1.639)

ESCC: esophageal squamous cell carcinoma. a,b. information of smoking status and family history was available from some of subjects. c,d. the age and sex adjusted odds ratio of Tyr/His+His/His (c) and His/His genotype (d) against Tyr/Tyr genotype.

correlated with gender, age and smoking status both in ESCC patients and in healthy controls (data not shown). The *Tyr* and *His* allele frequencies were 44.0 %, 56.0 % in ESCC patients and 44.2 %, 55.8 % in healthy controls, respectively. There was no statistic difference in allele distribution between ESCC patients and controls ($\chi^2=0.008$, $P=0.929$). The frequencies of *Tyr/Tyr*, *Tyr/His* and *His/His* genotype were 30.2 %, 28.2 % and 41.6 % in healthy controls, respectively. The overall *mEH* genotype distribution in ESCC patients was not significantly different from that in healthy controls ($\chi^2=2.116$, $P=0.347$) (Table 1).

Table 1 Demographic characteristics and *mEH Tyr113His* polymorphism in ESCC patients and healthy individuals

Groups	Control n (%)	ESCC n (%)
Sex		
Male	147 (58.3)	171 (66.5)
Female	105 (41.7)	86 (33.5)
Age (mean±SD)	49.4±8.56	58.5±9.39
Smoking status ^a		
Ex-or current smoker	110 (49.5)	130 (52.0)
Non-smoker	112 (50.5)	120 (48.0)
Family history of UGIC ^b		
Positive	31 (14.0)	104 (44.1)
Negative	191 (86.0)	132 (55.9)
Genotype		
<i>Tyr/Tyr</i>	76 (30.2)	49 (37.1)
<i>Tyr/His</i>	71 (28.2)	32 (24.2)
<i>His/His</i>	105 (41.6)	51 (38.7)
Allele type		
T	223 (44.2)	226 (44.0)
C	281 (55.8)	288 (56.0)

ESCC: esophageal squamous cell carcinoma, UGIC: upper gastrointestinal cancer. a. Information of smoking status was available from some of subjects, b. Positive family history of UGIC significantly increased the risk to develop ESCC. Age and sex adjusted OR=4.06 (95 % CI=2.46-6.69), $\chi^2=49.87$, $P<0.0001$.

By using *Tyr/Tyr* as the reference genotype, neither *His/His* genotype alone nor in combination with *Tyr/His* genotype significantly modified the risk of ESCC, the adjusted odds ratio was 1.076 (95 % CI=0.850-1.361) and 0.756 (95 % CI=0.493-1.157), respectively. When stratified for sex, age, smoking status and family history of upper gastrointestinal cancer, the frequency of *His/His* and *Tyr/His* genotype in ESCC patients was not significantly different from healthy controls. Consistently, *His/His* alone, or in combination with *Tyr/His* genotype, did not show any significant influence on the risk of ESCC (Table 2).

DISCUSSION

Chemical carcinogens in consumed alcohol and tobacco, polluted water, ingested food, are in general considered as the main risk factors of ESCC in China. However, not all individuals exposed to the above exogenous risk factors will develop ESCC, indicating that the host susceptibility factors may play an important role in cancer development. In recent years, many polymorphic carcinogen metabolic enzymes, such as aldehyde dehydrogenase-2 (ALDH2)^[13], cytochrome P450 (CYP)^[14,15], glutathione S-transferase (GST)^[15,16], methylenetetrahydrofolate reductase (MTHFR)^[17], NAD(P)H, quinone oxidoreductase 1 (NQO1)^[18,19] have been found to be able to modify the susceptibility to chemically induced cancers including esophageal and gastric cancer. Therefore, these

polymorphic genes, alone or in combination with each other or with other newly developed genetic markers, may be used as predictive parameters for screening individuals at a high risk of ESCC.

MEH is involved in the metabolism of environmental carcinogens. Polymorphisms in *mEH* gene might affect the enzyme expression and lead to different phenotypes, probably by the alteration of protein stability^[6]. *Tyr113His* substitution in exon 3 could reduce the enzyme expression by about 40 %, producing a slow phenotype with a low epoxide hydrolase activity. In contrast, *Arg139His* in exon 4 could increase the expression by about 25 %, producing a fast phenotype with an increased enzyme activity^[6]. The relationship between *mEH* gene polymorphisms and susceptibility to cancers studied had inconsistent conclusions due to different cancer types and populations. The *Tyr* allele in exon 3 was reported to increase the risk of several cancer types including ovarian cancer^[9], oropharyngeal cancer^[20] and acute leukaemia^[21], whereas the *His* allele was associated with increased susceptibility to cancers occurring in colon^[10], liver^[11] and cervix^[22]. In addition, gene-environment interaction was strongly suggested by some investigations, thus, cumulative cigarette smoking might play a pivotal role in association of *His* homozygous genotype with lung cancer development, altering the direction of risk from a risk factor in nonsmokers to a relatively protective factor in heavy smokers^[8].

Recently, a slight decrease in *mEH Tyr113* frequency was observed in esophageal adenocarcinoma (42 %) compared to controls (53 %, $P=0.05$)^[23]. In the present study, the frequencies of *Tyr/Tyr*, *Tyr/His* and *His/His* genotype in healthy controls were in consistent with a recent report from a Chinese group^[24]. The genotype distribution difference was not found in ESCC patients and healthy controls, as well as in stratification comparison according to the sex, age (>50 or ≤50), smoking status (never smoking or current and ever smoking), and family history of UGIC. The result suggests that although *mEH Tyr113His* polymorphism is correlated with some cancer types, this genetic alteration may not be associated with susceptibility to ESCC in population of North China.

ACKNOWLEDGEMENTS

We greatly acknowledge Mr. Baoshan Zhao and Mr. Fanshu Meng for their assistance in recruiting study subjects.

REFERENCES

- 1 Yokokawa Y, Ohta S, Hou J, Zhang XL, Li SS, Ping YM, Nakajima T. Ecological study on the risks of esophageal cancer in Ci-Xian, China: the importance of nutritional status and the use of well water. *Int J Cancer* 1999; **83**: 620-624
- 2 Launoy G, Milan CH, Faivre J, Pienkowski P, Milan CI, Gignoux M. Alcohol, tobacco and oesophageal cancer: effects of the duration of consumption, mean intake and current and former consumption. *Br J Cancer* 1997; **75**: 1389-1396
- 3 van Gijssel HE, Divi RL, Olivero OA, Roth MJ, Wang GQ, Dawsey SM, Albert PS, Qiao YL, Taylor PR, Dong ZW, Schrager JA, Kleiner DE, Poirier MC. Semiquantitation of polycyclic aromatic hydrocarbon-DNA adducts in human esophagus by immunohistochemistry and the automated cellular imaging system. *Cancer Epidemiol Biomarkers Prev* 2002; **11**: 1622-1629
- 4 Roth MJ, Dawsey SM, Wang G, Tangrea JA, Zhou B, Ratnasinghe D, Woodson KG, Olivero OA, Poirier MC, Frye BL, Taylor PR, Weston A. Association between GSTM1*0 and squamous dysplasia of the esophagus in the high risk region of Linxian, China. *Cancer Lett* 2000; **156**: 73-81
- 5 Omiecinski CJ, Aicher L, Swenson L. Developmental expression of human microsomal epoxide hydrolase. *J Pharmacol Exp Ther* 1994; **269**: 417-423
- 6 Hassett C, Aicher L, Sidhu JS, Omiecinski CJ. Human microso-

- mal epoxide hydrolase: genetic polymorphism and functional expression *in vitro* of amino acid variants. *Hum Mol Genet* 1994; **3**: 421-428
- 7 **Lee WJ**, Brennan P, Boffetta P, London SJ, Benhamou S, Rannug A, To-Figueras J, Ingelman-Sundberg M, Shields P, Gaspari L, Taioli E. Microsomal epoxide hydrolase polymorphisms and lung cancer risk: a quantitative review. *Biomarkers* 2002; **7**: 230-241
 - 8 **Zhou W**, Thurston SW, Liu G, Xu LL, Miller DP, Wain JC, Lynch TJ, Su L, Christiani DC. The interaction between microsomal epoxide hydrolase polymorphisms and cumulative cigarette smoking in different histological subtypes of lung cancer. *Cancer Epidemiol Biomarkers Prev* 2001; **10**: 461-466
 - 9 **Lancaster JM**, Brownlee HA, Bell DA, Futreal PA, Marks JR, Berchuck A, Wiseman RW, Taylor JA. Microsomal epoxide hydrolase polymorphism as a risk factor for ovarian cancer. *Mol Carcinog* 1996; **17**: 160-162
 - 10 **Harrison DJ**, Hubbard AL, MacMillan J, Wyllie AH, Smith CA. Microsomal epoxide hydrolase gene polymorphism and susceptibility to colon cancer. *Br J Cancer* 1999; **79**: 168-171
 - 11 **Tiemersma EW**, Omer RE, Bunschoten A, van't Veer P, Kok FJ, Idris MO, Kadaru AM, Fedail SS, Kampman E. Role of genetic polymorphism of glutathione-S-transferase T1 and microsomal epoxide hydrolase in aflatoxin-associated hepatocellular carcinoma. *Cancer Epidemiol Biomarkers Prev* 2001; **10**: 785-791
 - 12 **Cortessis V**, Siegmund K, Chen Q, Zhou N, Diep A, Frankl H, Lee E, Zhu QS, Haile R, Levy D. A case-control study of microsomal epoxide hydrolase, smoking, meat consumption, glutathione S-transferase M3, and risk of colorectal adenomas. *Cancer Res* 2001; **61**: 2381-2385
 - 13 **Matsuo K**, Hamajima N, Shinoda M, Hatooka S, Inoue M, Takezaki T, Tajima K. Gene-environment interaction between an aldehyde dehydrogenase-2 (ALDH2) polymorphism and alcohol consumption for the risk of esophageal cancer. *Carcinogenesis* 2001; **22**: 913-916
 - 14 **Tan W**, Song N, Wang GQ, Liu Q, Tang HJ, Kadlubar FF, Lin DX. Impact of genetic polymorphisms in cytochrome P450 2E1 and glutathione S-transferases M1, T1, and P1 on susceptibility to esophageal cancer among high-risk individuals in China. *Cancer Epidemiol Biomarkers Prev* 2000; **9**: 551-556
 - 15 **Cai L**, Yu SZ, Zhang ZF. Glutathione S-transferases M1, T1 genotypes and the risk of gastric cancer: a case-control study. *World J Gastroenterol* 2001; **7**: 506-509
 - 16 **Cai L**, Yu SZ, Zhang ZF. Cytochrome P450 2E1 genetic polymorphism and gastric cancer in Changle, Fujian Province. *World J Gastroenterol* 2001; **7**: 792-795
 - 17 **Song C**, Xing D, Tan W, Wei Q, Lin D. Methylenetetrahydrofolate reductase polymorphisms increase risk of esophageal squamous cell carcinoma in a Chinese population. *Cancer Res* 2001; **61**: 3272-3275
 - 18 **Zhang JH**, Li Y, Wang R, Gedder H, Guo W, Wen DG, Chen ZF, Wei LZ, Kuang G, He M, Zhang LW, Wu ML, Wang SJ. NQO1 C609T polymorphism associated with esophageal cancer and gastric cardiac carcinoma in North China. *World J Gastroenterol* 2003; **9**: 1390-1393
 - 19 **Zhang J**, Schulz WA, Li Y, Wang R, Zotz R, Wen D, Siegel D, Ross D, Gabbert HE, Sarbia M. Association of NAD(P)H: quinone oxidoreductase 1 (NQO1) C609T polymorphism with esophageal squamous cell carcinoma in a German Caucasian and a northern Chinese population. *Carcinogenesis* 2003; **24**: 905-909
 - 20 **Amador AG**, Righi PD, Radpour S, Everett ET, Weisberger E, Langer M, Eckert GJ, Christen AG, Campbell S Jr, Summerlin DJ, Reynolds N, Hartsfield JK Jr. Polymorphisms of xenobiotic metabolizing genes in oropharyngeal carcinoma. *Oral Surg Oral Med Oral Pathol Oral Radiol Endod* 2002; **93**: 440-445
 - 21 **Lebailly P**, Willett EV, Moorman AV, Roman E, Cartwright R, Morgan GJ, Wild CP. Genetic polymorphisms in microsomal epoxide hydrolase and susceptibility to adult acute myeloid leukaemia with defined cytogenetic abnormalities. *Br J Haematol* 2002; **116**: 587-594
 - 22 **Sierra-Torres CH**, Au WW, Arrastia CD, Cajas-Salazar N, Robazetti SC, Payne DA, Tyring SK. Polymorphisms for chemical metabolizing genes and risk for cervical neoplasia. *Environ Mol Mutagen* 2003; **41**: 69-76
 - 23 **Casson AG**, Zheng Z, Chiasson D, MacDonald K, Riddell DC, Guernsey JR, Guernsey DL, McLaughlin J. Associations between genetic polymorphisms of Phase I and II metabolizing enzymes, p53 and susceptibility to esophageal adenocarcinoma. *Cancer Detect Prev* 2003; **27**: 139-146
 - 24 **Yin L**, Pu Y, Liu TY, Tung YH, Chen KW, Lin P. Genetic polymorphisms of NAD(P)H quinone oxidoreductase, CYP1A1 and microsomal epoxide hydrolase and lung cancer risk in Nanjing, China. *Lung Cancer* 2001; **33**: 133-141

Edited by Su Q and Wang XL

Effect of body mass index on adenocarcinoma of gastric cardia

Ji Zhang, Xiang-Qian Su, Xiao-Jiang Wu, Ya-Hang Liu, Hua Wang, Xiang-Nong Zong, Yi Wang, Jia-Fu Ji

Ji Zhang, Xiang-Qian Su, Xiao-Jiang Wu, Xiang-Long Zong, Yi Wang, Jia-Fu Ji, Department of Surgery, Beijing Cancer Hospital, Beijing Institute of Cancer Research, School of Oncology, Peking University, Beijing 100036, China

Ya-Hang Liu, Hua Wang, Department of Surgery, 1st Teaching Hospital, Inner Mongolian Medical School, Hohhot 010005, Inner Mongolia Autonomous Region, China

Supported by the National High Technology Research and Development Program of China (863 Program), No.2001AA227101

Correspondence to: Professor Jia-Fu Ji, Department of Surgery, Beijing Cancer Hospital, Beijing Institute of Cancer Research, School of Oncology, Peking University, Beijing 100036, China. jiafuj@hotmail.com

Telephone: +86-10-88121122-2048 **Fax:** +86-10-88121122-2049

Received: 2003-07-12 **Accepted:** 2003-07-30

Abstract

AIM: Obesity has been proved as one of the main risk factors for gastric cardia adenocarcinoma (GCA) in the West. The objective of our research was to evaluate the relationship between obesity and the risk of GCA in people from North China.

METHODS: A total of 300 patients who had been diagnosed as GCA and had accepted surgical operation at Beijing Cancer Hospital from 1995 to 2002 were enrolled. Data were collected from pathology materials and hospital records. Two hundred and fifty-eight healthy people who had accepted health examination at the same hospital during the same period were enrolled as controls. Height, weight and gender of them at the time of examination were also collected. Obesity was estimated by body mass index (BMI), computed as weight in kilograms per square surface area (Kg/m^2). The degree of obesity was determined by using $\text{BMI} \leq 18.5$, $24-27.9$ and ≥ 28 (Kg/m^2) as the cut-off points for underweight/normal, overweight and obesity, respectively. Associations with obesity were estimated by odds ratios (ORs) and 95 % confidence intervals (CIs). All ORs were adjusted for age and sex.

RESULTS: The mean level of BMI was significantly lower in the patient group than that in the control group. The ORs for obesity in age groups 30-59 and 60-79 were 1.15 (95 % CI=0.37-3.65) and 0.16 (95 % CI=0.05-0.44) for males and 0.78 (95 % CI=0.26-2.36) and 0.28 (95 % CI=0.04-2.05) for females, respectively. The ORs for underweight were 2.42 (95 % CI=0.56-10.53) and 4.68 (95 % CI=1.13-19.40) for males in age subgroups 30-59 and 60-79 and 40.7 (95 % CI=9.32-177.92) for females older than 60 yrs. BMI was significantly associated with GCA ($P < 0.01$). Underweight people were at high risk for GCA.

CONCLUSION: BMI is an independent risk factor for GCA. Underweight is positively associated with GCA.

Zhang J, Su XQ, Wu XJ, Liu YH, Wang H, Zong XN, Wang Y, Ji JF. Effect of body mass index on adenocarcinoma of gastric cardia. *World J Gastroenterol* 2003; 9(12): 2658-2661
<http://www.wjgnet.com/1007-9327/9/2658.asp>

INTRODUCTION

The incidence of gastric cardia adenocarcinoma (GCA) has been rising steadily over the past two decades in the United States and Western Europe^[1-6]. Extensive studies have been conducted, trying to find its etiological reasons. Some studies showed that the risk for GCA was higher in obese people than that in normal counterparts. It has been generally accepted that obesity is one of the main risk factors for GCA^[7-9]. Of all the hypotheses explaining the association between obesity and GCA, reflux theory is the widely accepted one^[10-17]. Based on this theory, obesity can promote gastroesophageal reflux disease by increasing intra-abdominal pressure. Gastroesophageal reflux predisposes to Barrett's esophagus which is a metaplastic precursor state for GCA^[18-23]. But the reflux theory cannot explain every aspect of the manifestations of GCA. The real mechanism underlying the disease is still unclear.

We are still unaware if the incidence of GCA has the same pattern in China as in Western world. Based on previous studies, we know that GCA is not rare in China^[24]. Great differences exist in life styles and diet habits between Chinese and the Westerners. Elucidating the association between obesity and GCA among Chinese people will be very helpful for prevention and early diagnosis of the disease. The objectives of our study were to investigate whether obesity was more prevalent in patients with GCA than in healthy people, whether the risk for GCA was greater in obese people than in non-obese counterparts, and whether obesity was a dependent/independent risk factor for GCA.

We used body mass index (BMI) to evaluate the degree of obesity. In Western world, the cut-off points of BMI for overweight and obesity are $25 \text{ kg}/\text{m}^2$ and $30 \text{ kg}/\text{m}^2$. The Chinese people are relatively lean. It is not appropriate to use the same criteria. Recently, a population-based investigation was conducted^[25,26] by Zhou *et al* in China. Their results suggested that the cut-off points of BMI for underweight, overweight and obesity of the Chinese people were $18.5 \text{ kg}/\text{m}^2$, $24 \text{ kg}/\text{m}^2$ and $28 \text{ kg}/\text{m}^2$. We used the later criteria in our study.

MATERIALS AND METHODS

Materials

Three hundred patients were enrolled to receive radical operation for GCA in the Department of Surgery at Beijing Cancer Hospital from January 1, 1995 to December 31, 2002. All the hospital records and pathologic materials of these patients were reviewed. The inclusion criteria were listed as follows: The patients were 30 years old or older and the diagnosis of GCA was confirmed by pathologic examinations (reviewed by two independent pathologists). Classification was based on Dr. Siewert's criteria for gastric cardia carcinoma^[27].

The exclusion criteria were stipulated as follows: (1) The patients had a history of malignancies other than GCA; (2) The patients had a history of wasting disease before the diagnosis of the studied malignancy; (3) Adenocarcinoma was not diagnosed as the only histological type of the original malignancy; (4) The patients had a history of gastric cancer and received radical partial gastrectomy. The GCA arose from his/her gastric remnant.

Two hundred and fifty-eight residents who received health examination at Beijing Cancer Hospital from January 1, 2000 to December 31, 2002 were enrolled as healthy control subjects. All the healthy subjects were 30 years old or older, and had no history of any wasting disease. Pregnant women were not included in this study.

Methods

Data, including age, gender, height, weight of the patients and control subjects, were collected. For all patients who experienced weight loss during the disease, their usual height and weight before the disease were also collected. Patients whose hospital records could not provide all the information were not included in this study.

Obesity was measured by BMI, and computed as weight in kilograms per square surface area in square meters (kg/m^2). The height and weight before the disease were used to compute the BMI for patients who had experienced weight loss before the diagnosis was confirmed. The patients and control subjects of the same gender were compared with their mean values of BMI. The patients and control subjects were subdivided into five 10-year age subgroups (age 30-39, 40-49, 50-59, *etc.*). All the subjects were also divided into 2 age subgroups, age ≤ 60 yrs or age >60 yrs. Mean values of BMI were compared between patients and control subjects in the same age subgroup.

According to their value of BMI, all the subjects were subdivided into four subgroups (underweight, normal, overweight and obesity) using 18.5, 24 and 28 as the cut-off points of BMI for underweight, overweight and obesity. Relative risks of each group were estimated by odds ratios (ORs) and 95 % confidence intervals (CIs).

Statistic analysis of the data was performed using Chi-square test, with a level of significance at $P \leq 0.05$. Monte Carlo estimate was used to balance the differences in age and sex structure between the two groups. Lastly, we used logistic regression to evaluate whether obesity was an independent risk factor for GCA.

RESULTS

A total of 300 patients, including 51 women and 249 men, aged 34-80 yrs (median 61.9 yrs), and 258 healthy control subjects (144 women and 114 men) aged 31-78 yrs (median 53.57 yrs), were finally enrolled. The age and sex structure of the patient group differed significantly from those of the control group ($P < 0.01$).

The mean value of BMI was $22.90 \text{ kg}/\text{m}^2$ in the patient group and $24.85 \text{ kg}/\text{m}^2$ in the control group. In each coordinated sex or age subgroup, patients tended to have a low level of BMI than healthy control subjects (Table 1 and Table 2). After sex and age structures were balanced, the mean value of BMI was significantly lower in the patients group than that in the healthy control group ($P < 0.01$).

Table 1 Mean levels of BMI in each age group of patients and healthy control subjects

Age	Patient group		Control group	
	Number of cases	Median level of BMI	Number of cases	Median level of BMI
30-39	8	21.94	50	24.26
40-49	27	22.37	69	25.54
50-59	84	22.64	55	24.71
60-69	134	23.46	54	24.93
70-79	47	22.25	30	24.38
Total	300	22.90	258	24.85

Table 2 Mean levels of BMI in each sex group of patients and healthy control subjects

Gender	Patient group		Control group	
	Number of cases	Median level of BMI	Number of cases	Median level of BMI
Male	249	22.88	115	24.75
Female	51	23.02	143	24.94
Total	300	22.90	258	24.85

After all the subjects were labeled as underweight, normal, overweight or obesity based on their BMI, the odds ratios and 95 % confidence intervals in each BMI subgroup were calculated. We used Monte Carlo estimate to balance the differences in age and sex between the two groups, 60 yrs as the cut-off point for age subdivision. In each coordinated subgroup, high BMI people did not show any elevated risk for GCA compared with low BMI ones. On the contrary, the relative risk for GCA rose significantly when the BMI of the subject reached the underweight criteria, especially in women older than 60 yrs ($P < 0.05$ by Fisher's exact test). The risk did not show significant differences only in men of 60 yrs old and younger (Table 3 and Table 4).

Table 3 Odds ratios (ORs) and 95 % confidence intervals (CIs) with body mass index (BMI) by age and sex

Age	Sex	BMI group	Studied group		Total	ORs	95 %	CIs
			Control	Patient				
1 ^a	Male	UW ^c	2	16	18	2.42	0.56	10.53
		NM ^d	19	84	103	1.55	0.80	3.03
		OW ^e	20	42	62	0.45	0.23	0.89
		OB ^f	4	16	20	1.15	0.37	3.65
		TOTAL	45	158	203			
	Female	UW	0	5	5	-	-	-
		NM	18	12	30	1.01	0.40	2.55
		OW	18	8	26	0.56	0.21	1.49
		OB	11	6	17	0.78	0.26	2.36
		TOTAL	47	31	78			
2 ^b	Male	UW	2	11	13	4.68	1.13	19.40
		NM	26	45	71	1.66	0.88	3.13
		OW	26	31	57	0.87	0.46	1.68
		OB	16	4	20	0.16	0.05	0.44
		TOTAL	70	91	161			
	Female	UW	1	6	7	40.7	9.32	177.92
		NM	45	7	52	0.61	0.22	1.66
		OW	35	6	41	0.75	0.26	2.12
		OB	15	1	16	0.28	0.04	2.05
		TOTAL	96	20	116			

a. Age group 1: ≤ 60 yrs, b. Age group 2: >60 yrs, c. UW=underweight ($\text{BMI} < 18.5 \text{ kg}/\text{m}^2$), d. NM=Normal ($18.5 \leq \text{BMI} < 24 \text{ kg}/\text{m}^2$), e. OW=Overweight ($24 \leq \text{BMI} < 28 \text{ kg}/\text{m}^2$), f. OB=Obesity ($\text{BMI} \geq 28 \text{ kg}/\text{m}^2$).

Table 4 Fisher's exact test for evaluation of significance of association between underweight and high relative risk for GCA

Age	Sex	χ^2 value	P	Monte carlo sig. (2-sided)	
				99 % confidence interval	
				Lower bound	Upper bound
1 ^a	Male	5.357	0.136	0.127	0.144
	Female	8.161	0.036	0.031	0.041
2 ^b	Male	16.438	0.001	0.000	0.002
	Female	17.196	0.001	0.000	0.001

a. Age Group 1: ≤ 60 yrs, b. Age Group 2: >60 yrs.

Compared with age, sex, previous gastrointestinal disease history and family history of gastric cancer, MBI showed itself to be an independent risk factor for GCA (Table 5, Table 6) ($P < 0.01$).

Table 5 Logistic regression analysis of sex, BMI and age group 1

	B	SE ^a	P	OR	95%	CI _s
Sex	-1.714	0.210	<0.01	0.180	0.119	0.272
BMI	-0.152	0.028	<0.01	0.859	0.813	0.907
Age group1 ^b	1.082	0.198	<0.01	2.952	2.002	4.351
Constant	4.473	0.777	<0.01	87.589		

a. SE=standard error, b. Age group1: The subjects were divided into two age subgroup: age ≤ 60 yrs and age > 60 yrs.

Table 6 Logistic regression analysis of sex, BMI and age group 2

	B	SE ^a	P	OR	95%	CI _s
Sex	-1.668	0.214	<0.01	0.189	0.124	0.287
BMI	-0.156	0.029	<0.01	0.856	0.809	0.905
Age group2 ^b	0.609	0.090	<0.01	1.838	1.541	2.193
Constant	4.105	0.790	<0.01	60.662		

a. SE=standard error, b. Age group 2: The subjects were divided into 5 10-year age subgroups (30-39 yrs, 40-49 yrs, 50-59 yrs, 60-69 yrs, 70-79 yrs, etc.).

DISCUSSION

Firstly, we wanted to elucidate whether obesity was more prevalent in patients with GCA than in healthy people. After calculating BMI of all the subjects, using the height and weight before the disease for patients who had experienced weight loss before the diagnosis was confirmed, we found that obesity did not tend to be more prevalent in patients with GCA than in healthy control subjects. The mean value of BMI in each group was 22.90 kg/m² and 24.85 kg/m² ($P < 0.01$). Within each coordinated sex or age subgroup, the patients always had a lower level of BMI (Table 1 and Table 2). The trend did not show any change after sex and age were balanced between the two groups.

We divided all the subjects into four subgroups according to the criteria of BMI for underweight, overweight and obesity proposed by Zhou *et al*^[25,26]. After we calculated the relative risk in each group, we found that it did not rise with the elevation of BMI. The ORs for obesity in age groups of 30-59 and 60-79 years were 1.15 (95 % CI=0.37-3.65) and 0.16 (95 % CI=0.05-0.44) for males and 0.78 (95 % CI=0.26-2.36) and 0.28 (95 % CI=0.04-2.05) for females, respectively. On the contrary, underweight people had the greatest risk, ORs for underweight were 2.42 (95 % CI=0.56-10.53) and 4.68 (95 % CI=1.13-19.40) for males in age subgroup 30-59 and 60-79 and 40.7 (95 % CI=9.32-177.92) for females older than 60 yrs. No underweight subject was found in healthy female subjects of 60 yrs old or younger. So the ORs for underweight in this subgroup could not be calculated. After performing Fisher's exact test, we found that the underweight people were more likely to get GCA ($P < 0.05$) except for men under 60 yrs old (Table 4).

Sex and age might be the influence factors for BMI. Logistic regression was performed to investigate the relationship between BMI and GCA. As shown in Table 5 and Table 6, the association between risk of GCA and BMI was significant ($P < 0.01$). Underweight people showed a high possibility of GCA.

Our results differed greatly from not only those in the Western countries but also those of Chow *et al.* in Shanghai,

China^[7,8,9,28]. The reasons behind the difference might be the genetic background, life style and cut-off points for BMI. The genetic background of the Chinese people differs greatly from those of the Westerners. It even differs in different parts of China. It has been proved that life styles, including smoking, alcohol consumption, and dietary habits could influence the incidence and prognosis of GCA^[29]. Even in China, people in different areas have their particular life styles. For example, citizens of Shanghai take more fresh fruits and vegetables than residents of Beijing. Results of the correlative researches conducted in Shanghai were similar to those of the Westerners. The patients enrolled in our research were mainly from North China, which may cause the difference. Secondly, the cut-off points for underweight, overweight and obesity used in our study were different from those used in previous researches. Our study suggests that obesity should not be a risk factor for the North Chinese people.

According to Siewert's classification, GCA is classified into three types based on its anatomy location. Yasuhiro *et al* noticed a striking difference between the East and the West in the proportion of patients who fell into each type of GCA^[30]. Type I cancer, or adenocarcinoma of the lower esophagus was reported to be more prevalent in the Western countries^[31] while type III cancer, or adenocarcinoma of the proximal stomach was predominant in Japan. By reviewing pathologic materials of GCA patients, we found that the distribution of GCA types in our patient group was very similar to that of Japanese (data not shown). Obesity might be a risk factor for type I cancer. GCA might have a particular mechanism in the Eastern countries^[32].

GCA tended to be more prevalent in aged people^[33]. In our study, the median age of the patient group was significantly higher than that of the control group. Epidemiological evidences showed that the proportion of obese people rose with increase of age. It must be clarified that whether a high proportion of aged people can lead to a high prevalence of obesity in the patients group or obesity really predisposes to GCA. Evidences that were opposed to the reflux theory have been also available^[34,35]. Besides, one important precondition of the obesity-reflux-carcinogenesis theory is that reflux is the real risk factor. Our next research will be focused on how reflux influences cells at the gastric cardia.

REFERENCES

- 1 Blot WJ, Devesa SS, Kneller RW, Fraumeni JF Jr. Rising incidence of adenocarcinoma of the esophagus and gastric cardia. *JAMA* 1991; **265**: 1287-1289
- 2 Armstrong RW, Borman B. Trends in incidence rates of adenocarcinoma of the oesophagus and gastric cardia in New Zealand, 1978-1992. *Int J Epidemiol* 1996; **25**: 941-947
- 3 Zheng T, Mayne ST, Holford TR, Boyle P, Liu W, Chen Y, Mador M, Flannery J. The time trend and age-period-cohort effects on incidence of adenocarcinoma of the stomach in Connecticut from 1955-1989. *Cancer* 1993; **72**: 330-340
- 4 Pera M, Cameron AJ, Trastek VF, Carpenter HA, Zinsmeister AR. Increasing incidence of adenocarcinoma of the esophagus and esophagogastric junction. *Gastroenterology* 1993; **104**: 510-513
- 5 Walther C, Zilling T, Perfekt R, Moller T. Increasing prevalence of adenocarcinoma of the oesophagus and gastro-oesophageal junction: a study of the Swedish population between 1970 and 1997. *Eur J Surg* 2001; **167**: 748-757
- 6 Posner MC, Vokes EE, Weichselbaum RR. Cancer of the upper gastrointestinal tract. *Hamilton:BC Decker* 2002: 86-87
- 7 Chow WH, Blot WJ, Vaughan TL, Risch HA, Gammon MD, Stanford JL, Dubrow R, Schoenberg JB, Mayne ST, Farrow DC, Ahsan H, West AB, Rotterdam H, Niwa S, Fraumeni JF Jr. Body mass index and risk of adenocarcinomas of the esophagus and gastric cardia. *J Natl Cancer Inst* 1998; **90**: 150-155
- 8 Vaughan TL, Davis S, Kristal A, Thomas DB. Obesity, alcohol,

- and tobacco as risk factors for cancers of the esophagus and gastric cardia: adenocarcinoma versus squamous cell carcinoma. *Cancer Epidemiol Biomarkers Prev* 1995; **4**: 85-92
- 9 **Lagergren J**, Bergstrom R, Nyren O. Association between body mass and adenocarcinoma of the esophagus and gastric cardia. *Ann Intern Med* 1999; **130**: 883-890
 - 10 **Bremner CG**, Lynch VP, Ellis FH Jr. Barrett's esophagus: congenital or acquired? An experimental study of esophageal mucosal regeneration in the dog. *Surgery* 1970; **68**: 209-216
 - 11 **Fisher BL**, Pennathur A, Mutnick JL, Little AG. Obesity correlates with gastroesophageal reflux. *Dig Dis Sci* 1999; **44**: 2290-2294
 - 12 **Fraser-Moodie CA**, Norton B, Gornall C, Magnago S, Weale AR, Holmes GK. Weight loss has an independent beneficial effect on symptoms of gastro-oesophageal reflux in patients who are overweight. *Scand J Gastroenterol* 1999; **34**: 337-340
 - 13 **Terry P**, Lagergren J, Wolk A, Nyren O. Reflux-inducing dietary factors and risk of adenocarcinoma of the esophagus and gastric cardia. *Nutr Cancer* 2000; **38**: 186-191
 - 14 **Oberg S**, DeMeester TR, Peters JH, Hagen JA, Nigro JJ, DeMeester SR, Theisen J, Campos GM, Crookes PF. The extent of Barrett's esophagus depends on the status of the lower esophageal sphincter and the degree of esophageal acid exposure. *J Thorac Cardiovasc Surg* 1999; **117**: 572-580
 - 15 **Attwood SE**, DeMeester TR, Bremner CG, Barlow AP, Hinder RA. Alkaline gastroesophageal reflux: implications in the development of complications in Barrett's columnar-lined lower esophagus. *Surgery* 1989; **106**: 764-770
 - 16 **Ortiz-Hidalgo C**, De La Vega G, Aguirre-Garcia J. The histopathology and biologic prognostic factors of Barrett's esophagus: a review. *J Clin Gastroenterol* 1998; **26**: 324-333
 - 17 **Stein HJ**, Kauer WK, Feussner H, Siewert JR. Bile reflux in benign and malignant Barrett's esophagus: effect of medical acid suppression and nissen fundoplication. *J Gastrointest Surg* 1998; **2**: 333-341
 - 18 **Sampliner RE**. Practice guidelines on the diagnosis, surveillance, and therapy of Barrett's esophagus. The practice parameters committee of the American college of gastroenterology. *Am J Gastroenterol* 1998; **93**: 1028-1032
 - 19 **Cameron AJ**, Lomboy CT, Pera M, Carpenter HA. Adenocarcinoma of the esophagogastric junction and Barrett's esophagus. *Gastroenterology* 1995; **109**: 1541-1546
 - 20 **Spechler SJ**, Goyal RK. The columnar-lined esophagus, intestinal metaplasia, and Norman Barrett. *Gastroenterology* 1996; **110**: 614-621
 - 21 **DeMeester SR**, DeMeester TR. Columnar mucosa and intestinal metaplasia of the esophagus: fifty years of controversy. *Ann Surg* 2000; **231**: 303-321
 - 22 **Clark GW**, Smyrk TC, Burdiles P, Hoeft SF, Peters JH, Kiyabu M, Hinder RA, Bremner CG, DeMeester TR. Is Barrett's metaplasia the source of adenocarcinomas of the cardia? *Arch Surg* 1994; **129**: 609-614
 - 23 **Ishaq S**, Jankowski JA. Barrett's metaplasia: clinical implications. *World J Gastroenterol* 2001; **7**: 563-565
 - 24 **Wang LD**, Zheng S, Zheng ZY, Casson AG. Primary adenocarcinomas of lower esophagus, esophagogastric junction and gastric cardia: In special reference to China. *World J Gastroenterol* 2003; **9**: 1156-1164
 - 25 **Zhou BF**. Predictive values of body mass index and waist circumference for risk factors of certain related diseases in Chinese adults-study on optimal cut-off points of body mass index and waist circumference in Chinese adults. *Biomed Environ Sci* 2002; **15**: 83-96
 - 26 **Zhou BF**. Effect of body mass index on all-cause mortality and incidence of cardiovascular diseases-report for meta-analysis of prospective studies open optimal cut-off points of body mass index in Chinese adults. *Biomed Environ Sci* 2002; **15**: 245-252
 - 27 **Siewert JR**, Stein HJ. Classification of adenocarcinoma of the oesophagogastric junction. *Br J Surg* 1998; **85**: 1457-1479
 - 28 **Ji BT**, Chow WH, Yang G, McLaughlin JK, Gao RN, Zheng W, Shu XO, Jin F, Fraumeni JF Jr, Gao YT. Body mass index and the risk of cancers of the gastric cardia and distal stomach in Shanghai, China. *Cancer Epidemiol Biomarkers Prev* 1997; **6**: 481-485
 - 29 **Cai L**, Zheng ZL, Zhang ZF. Risk factors for the gastric cardia cancer: a case-control study in Fujian Province. *World J Gastroenterol* 2003; **9**: 214-218
 - 30 **Kodera Y**, Yamamura Y, Shimizu Y, Torii A, Hirai T, Yasui K, Morimoto T, Kato T. Adenocarcinoma of the gastroesophageal junction in Japan: relevance of Siewert's classification applied to 177 cases resected at a single institution. *J Am Coll Surg* 1999; **189**: 594-601
 - 31 **Wijnhoven BP**, Siersema PD, Hop WC, van Dekken H, Tilanus HW. Adenocarcinomas of the distal oesophagus and gastric cardia are one clinical entity. Rotterdam oesophageal tumour study group. *Br J Surg* 1999; **86**: 529-535
 - 32 **Gao SS**, Zhou Q, Li YX, Bai YM, Zheng ZY, Zou JX, Liu G, Fan ZM, Qi YJ, Zhao X, Wang LD. Comparative studies on epithelial lesions at gastric cardia and pyloric antrum in subjects from a high incidence area for esophageal cancer in Henan, China. *World J Gastroenterol* 1998; **4**: 332-333
 - 33 **Daly JM**, Karnell LH, Menck HR. National cancer Data Base report on esophageal carcinoma. *Cancer* 1996; **78**: 1820-1828
 - 34 **Lagergren J**, Bergstrom R, Lindgren A, Nyren O. Symptomatic gastroesophageal reflux as a risk factor for esophageal adenocarcinoma. *N Engl J Med* 1999; **340**: 825-831
 - 35 **Farrow DC**, Vaughan TL, Sweeney C, Gammon MD, Chow WH, Risch HA, Stanford JL, Hansten PD, Mayne ST, Schoenberg JB, Rotterdam H, Ahsan H, West AB, Dubrow R, Fraumeni JF Jr, Blot WJ. Gastroesophageal reflux disease, use of H2 receptor antagonists, and risk of esophageal and gastric cancer. *Cancer Causes Control* 2000; **11**: 231-238

Edited by Zhang JZ and Wang XL

Somatic mutation analysis of p53 and ST7 tumor suppressor genes in gastric carcinoma by DHPLC

Chong Lu, Hui-Mian Xu, Qun Ren, Yang Ao, Zhen-Ning Wang, Xue Ao, Li Jiang, Yang Luo, Xue Zhang

Chong Lu, Hui-Mian Xu, Zhen-Ning Wang, Laboratory of Medical Genomics, Oncology Department, the First Affiliated Clinical College, China Medical University, Shenyang, 110001, Liaoning Province, China

Qun Ren, Yang Ao, Xue Ao, Li Jiang, Yang Luo, Laboratory of Medical Genomics, China Medical University, Shenyang, 110001, Liaoning Province, China

Xue Zhang, Laboratory of Medical Genomics, China Medical University, Shenyang, 110001, Liaoning Province, China. Laboratory of Genetics, Peking Union Medical College, Chinese Academy of Medical Sciences, Beijing, 100021, China

Supported by National Science Fund for Distinguished Young Scholars, No. 30125017, and the Major State Basic Research Development Program of China (973 Program), No. G1998051203

Correspondence to: Xue Zhang, Laboratory of Medical Genomics, China Medical University, No. 92, Bei Er Road, Heping District, Shenyang, 110001, Liaoning Province, China. xzhang@mail.cmu.edu.cn

Telephone: +86-24-23256666-5532

Received: 2003-04-04 **Accepted:** 2003-06-07

Abstract

AIM: To verify the effectiveness of denaturing high-performance liquid chromatography (DHPLC) in detecting somatic mutation of p53 gene in gastric carcinoma tissues. The superiority of this method has been proved in the detection of germline mutations, but it was not very affirmative with respect to somatic mutations in tumor specimens. ST7 gene, a candidate tumor suppressor gene identified recently at human chromosome 7q31.1, was also detected because LOH at this site has also been widely reported in stomach cancer.

METHODS: DNA was extracted from 39 cases of surgical gastric carcinoma specimen and their correspondent normal mucosa. Seven fragments spanning the 11 exons were used to detect the mutation of p53 gene and the four exons reported to have mutations in ST7 gene were amplified by PCR and directly analyzed by DHPLC without mixing with wild-type allele.

RESULTS: In the analysis of p53 gene mutation, 9 aberrant DHPLC chromatographies were found in tumor tissues, while their normal-adjacent counterparts running in parallel showed a normal shape. Subsequent sequencing revealed nine sequence variations, 1 polymorphism and 8 mutations including 3 mutations not reported before. The mutation rate of p53 gene (21 %) was consistent with that previously reported. Furthermore, no additional aberrant chromatography was found when wild-type DNA was added into the DNA of other 30 tumor samples that showed normal shapes previously. The positivity of p53 mutations was significantly higher in intestinal-type carcinomas (40 %) than that in diffuse-type (8.33 %) carcinomas of the stomach. No mutation of ST7 gene was found.

CONCLUSION: DHPLC is a very convenient method for the detection of somatic mutations in gastric carcinoma. The amount of wild type alleles supplied by the non-tumorous

cells in gastric tumor specimens is enough to form heteroduplex with mutant alleles for DHPLC detection. ST7 gene may not be the target gene of inactivation at 7q31 site in gastric carcinoma.

Lu C, Xu HM, Ren Q, Ao Y, Wang ZN, Ao X, Jiang L, Luo Y, Zhang X. Somatic mutation analysis of p53 and ST7 tumor suppressor genes in gastric carcinoma by DHPLC. *World J Gastroenterol* 2003; 9(12): 2662-2665

<http://www.wjgnet.com/1007-9327/9/2662.asp>

INTRODUCTION

Denaturing high performance liquid chromatography (DHPLC) is a relatively new technique with a high degree of sensitivity in the analysis of germline mutations in various inherited diseases^[1-3]. It is known that equal amounts of wild-type and mutant DNA are required to form heteroduplexes for ideal DHPLC analysis. The pure mutant DNA could be available easily from germline mutations or tumor cell lines, but it is often not the case in actual tumor specimens because non-tumorous cells may be present in various amounts. Even using other methods, such as LCM, would not guarantee the gain of pure tumor DNA. So, there are few reports with respect to the analysis of somatic mutations in tumors. Fortunately, in more recent reports^[4-6], it was proved that DHPLC had the ability to detect the heteroduplexes formed by mixing wild type alleles with homogenous mutant alleles of cell lines over a broad range of mutant allele concentrations, differing from 5 % to 95 %, which suggested that DHPLC may be well suited for the analysis of somatic mutations in tumor tissue samples in which the proportion of mutant and wild-type alleles is variable.

In our investigation about the somatic mutation of 2 genes by DHPLC, PCR amplification of DNA extracted from surgical tumor specimen was directly conducted without mixing with wild-type DNA, only if the existence of both tumor and normal cells was confirmed by pathology in a certain proportion but not strictly in equal amount. One gene we detected was p53 gene, which was reported to have a relatively high frequency of mutation in gastric carcinoma^[7-10]. The other one was ST7 gene, which was cloned and mapped to chromosome 7q31.1-7q31.2, a region suspected of containing a tumor suppressor gene involved in a variety of human cancers^[11-13]. Strong evidences to support ST7 as the key TSG at this locus have recently been reported by Zenklusen *et al.*^[13]. LOH 7q31 in stomach cancer has also been widely reported^[14-16], so we detected four exons of ST7 gene that was reported^[13,17] to have mutations to clarify the role of ST7 gene in stomach cancer.

MATERIALS AND METHODS

Tissue samples and preparation of DNA

Thirty-nine cases of gastric cancer tissue and corresponding adjacent non-tumorous gastric tissue were obtained by surgical excision from patients at the Oncology Department of the First Affiliated Hospital of China Medical University, including 15

Table 1 Primer sequences used in PCR reactions (shown in the 5' to 3' direction)

Primer name		Forward sequence	Reverse sequence	Size (bp)	Annealing temp. (°C)
P53	Exon2+3	ccagggtgacccagggttg	gcaagggggactgtagatgg	402	62
	Exon4	acctgtctctgactgtc	gccaggcattgaagtctcat	363	60
	Exon5+6	ccgtgtccagttgctttat	ttaacccctctcccaga	488	58
	Exon7	tgttccacaggtctcc	ccggaatgtgatgagaggt	301	60
	Exon8+9	ttcttactgcctctgtt	agaaaacggcattttgagt	411	57
	Exon10	ctcaggtactgtgtatatac	ctatggctttccaacctagga	218	55
	Exon11	tcattctctctcctgcttc	ccacaacaaaacaccagtgc	300	60
ST7	Exon3	gtagtgtcactgaactacgc	gctctctgaaccagacca	154	55
	Exon4	aggtcttgcctttctctca	caaaaagccctccattcag	213	55
	Exon5	tgtcctctactgagtctacc	gtatcctatcaatggcaactg	223	55
	Exon12	gtgtagatgctccgggttg	taacgagttctgtggggat	187	55

Table 2 p53 mutations in sporadic gastric carcinomas

Specimen No.	Pathology	Exon	Codon	Mutation	Effect	DHPLC (temp)	DHPLC gradient (B% in 4.5 min)
H3	Poorly diff.	6	188	CTG>CCG	Leu188Pro	63	60-66
54	Tubular	7	246	Del 24bp ^a	8 amino acid deletion	57,59,61	54-63
57	Tubular	6	215	AGT>GGT	Ser215Gly	62	57-66
64	Tubular	5	167	Ins 3bp ^a	Gln insertion	60	57-66
77	Tubular	7	235	Del 1bp(C) ^a	Framshift (246stop)	61	53-62
79	Papillary	8	301	CCA>CTA	Pro301Leu	60	54-63
86	Poorly diff.	5	161	GCC>GGC	Ala161Gly	61	53-62
133	Papillary	5	135	TGC>TGG	Cys135Trp	62	57-66
36		Intron 7		C>T, T>G		57	54-63

^aMutation that hasn't been reported previously.

cases of intestinal type (4 cases of papillary type and 11 cases of tubular type) and 24 cases of diffuse type (18 cases of poorly differentiated type, 4 cases of mucinous type and 2 cases of signet-ring cell type). Their average age was 58.5 years (from 42 to 79 years), male/female was 27/12. A portion of tissue was frozen and stored at -80 °C for DNA extraction, and the remaining tissue was fixed in 10 % buffered formalin for histological examination. DNA was isolated by a standard proteinase K digestion and phenol-chloroform extraction procedure.

PCR conditions

Primer pairs for the amplification are listed in Table 1. Oligonucleotide primers for exons of p53 were published before^[18]. The underlying sequence was based on the NCBI database. The average fragment length ranged from 150 to 500 bp. Fragment amplification was accomplished with the UNO II PCR system (Biometra, Germany). PCR reactions were performed in a volume of 20-50 µl with 35 cycles consisting of a denaturation step at 94 °C for 45 s, primer annealing for 30 s and an elongation step at 72 °C for 1 min. The final step was extended at 72 °C for 5 min.

DHPLC analysis and DNA sequencing

Prior to DHPLC analysis, heteroduplex formation of the PCR products was carried out by heating for 5 min at 94 °C followed by cooling to 25 °C at a rate of 0.03 °C S⁻¹. DHPLC was performed using the transgenomic WAVE DNA fragment analysis system (transgenomic, Omaha, USA). Four µl of the PCR products was loaded on the DNasep column and DNA was eluted at a flow rate of 0.9 ml/min within a linear acetonitrile gradient consisting of buffer A (0.1 M triethylammonium acetate, TEAA) and buffer B (0.1 M TEAA, 25 % acetonitrile). Elution of DNA from column was detected by absorbing at 260 nm. The optimal melting temperature for

each fragment was selected by using WaveMaker 4.1 software (transgenomic) or by a software described before which is available freely at <http://insertion.Stanford.edu/melt.html>. PCR amplification of the DNA extracted from surgical tumor specimen was directly conducted without mixing with wild-type DNA. The original PCR products of any tumor sample showing an aberrant DHPLC elution profile and its corresponding normal tissue sample were purified using a PCR fragment purification kit (Takara, Dalian), then sequenced directly. Sequence analysis was conducted with the same primers as those used in the original PCR using an ABI 377 automated DNA sequencer. The PCR products of those tumor samples that showed normal DHPLC chromatography were mixed with wild-type at the ratio of 2:1 prior to the reannealing step, and run again.

PCR reaction and DHPLC analysis of all the samples with positive results were repeated at least 2 times and a double direction sequencing was used.

RESULTS

p53 mutations

The results of DHPLC analysis are summarized in Table 2. Mutations of the p53 gene were investigated in 39 surgical specimens of primary gastric cancer by DHPLC. Altogether, 9 aberrant DHPLC chromatographies were found and all of them were from tumor tissues, while their normal-adjacent counterparts running in parallel showed a normal shape. Subsequent sequencing revealed nine sequence variations of 8 mutations and 1 polymorphism. The 8 mutations were localized at exons 5, 6, 7 and 8, including 5 missense mutations, 1 frameshift deletion of 1 bp, 1 in frame insertion of 3 bp and 1 in frame deletion of 24 bp (one example is shown in Figure 1). The latter 3 base pairs changes were not reported previously. Through the European Bioinformatics Institute (EBI) available

at <ftp://ftp.ebi.ac.uk/pub/databases/p53/>, one polymorphism was localized in intron 7. The positivity for p53 mutations was significantly higher in intestinal-type carcinoma (40 %, 6/15) than that in diffuse-type (8.33 %, 2/24) carcinoma of the stomach ($P < 0.01$, χ^2 test).

ST7 mutations

All of the DHPLC chromatographies from 39 tumor tissues showed a normal single peak shape, just the same as with those from their corresponding normal adjacent tissues.

DISCUSSION

Some prescreening methods, such as single strand conformation polymorphism (SSCP) or denaturing gradient gel electrophoresis (DGGE), have been widely used for mutation analysis^[19-35], but they were characterized by their lower sensitivity and more labor intensity^[1,36,37]. A relatively new technique, DHPLC, is believed to be a superior method for its economic, automatic, time-saving features and higher sensitivities ranging from 95 % to 100 % for germline mutation detection^[2,3,38-40]. However, with respect to somatic mutation in actual tumor specimens, one potential drawback that should be considered was that heteroduplexes formed by normal and mutant alleles were necessary for DHPLC detection. Such heteroduplexes were usually got by mixing tumor DNA with an normal equal amount of wild-type DNA when germline mutation was detected. Excitingly, some more recent reports^[4-6] showed that heteroduplexes could still be detected by DHPLC when they changed the concentration of homogenous mutant alleles of cell lines from 5 % to 95 %. Their results indicated that DHPLC might also be well suitable for the analysis of somatic mutations in tumor tissue samples in which the proportion of mutants and wild-type alleles was variable. It has been demonstrated that many gastric cancers contained abundant non-neoplastic stromal cells^[9]. So when somatic mutations in gastric cancer tissues were detected, it might not only be unnecessary but also laborious to mix normal wild-type alleles with tumor alleles. Further more it might yield a pseudo-negative result if the tumor cell concentration was relatively low in specimens.

In our study, the PCR products, which were amplified from the extracted DNA of surgical tumor specimens without mixing with extra wild type alleles, were directly analyzed by DHPLC. In the analysis of p53 gene mutations, 9 aberrant DHPLC chromatographies were found and all of them were from tumor tissues, while their normal-adjacent counterparts running in parallel showed a normal shape. Subsequent sequencing revealed nine sequence variations of 8 mutations and 1 polymorphism. The mutation rate (21 %, 8/39) was similar to the previously reported frequency of 20 % to 50 %^[7-10]. Furthermore, no additional aberrant chromatography was found when wild-type DNA was added into the DNA of other 30 tumor samples that showed a normal shape previously. These results indicate that the amount of wild type alleles supplied by non-tumorous cells in actual gastric tumor specimens is enough to form heteroduplex with mutant alleles for the detection by DHPLC. So, DHPLC is a very convenient method for the detection of somatic mutations in gastric carcinomas.

In contrast to previous studies, p53 mutations did not follow a random distribution among different subtypes. The positivity for p53 mutations was significantly higher in intestinal-type carcinomas (40 %) than in diffuse-type carcinomas (8.33 %). This phenomenon was also observed in other reports^[9,41]. Two hot spots for p53 gene mutations in gastric cancer at codon 251 and codon 173^[42] were not observed in our study. Interestingly, we found three new mutations that have not been reported in the database of p53 mutations. Considering that all

the patients in our study were from the northeast area of China, the above differences might be due to the different etiologies of gastric cancer in different geographical areas.

Evidence of LOH 7q31 has been found in many kinds of malignant tumors and also in gastric carcinomas^[14-16], indicating that a putative tumor suppressor gene at this locus may be involved in the pathogenesis of many neoplasms. Strong evidences to support ST7 as the key TSG at this locus were recently reported by Zenklusen *et al.*^[13]. Using a prostate cancer-derived cell line they showed that ST7 could suppress *in vivo* tumorigenicity. In addition, they described protein-truncating mutations of ST7 in three out of seven breast cancer derived cell lines and in four out of 10 primary colon carcinomas. But in our investigation on 39 cases of gastric carcinoma, no mutation was found. This could be due to the fact that in the previous study all the tumors were pre-screened for LOH at 7q31, thus increasing the likelihood of detecting a mutation. Other mechanisms of inactivation such as promoter hypermethylation, homozygous deletion, or genomic rearrangement that were not explored in our study were the common mechanisms of ST7 inactivation in stomach cancer. Our results were coincident with a few other recent reports^[17,43-45] supporting the absence of ST7 alterations. In these studies, the researchers also failed to detect any further coding mutations in all exons of ST7 in a wide-range of carcinomas and cell lines, including that of ovarian, colon, breast, esophagus, head and neck, pancreatic and prostate. Our results extend the spectrum of malignant tumor types examined for ST7 somatic alterations, and suggest that one of the other tumor suppressor genes, or an undiscovered gene at 7q31 is the target involved in carcinogenesis of gastric carcinoma at this locus.

REFERENCES

- 1 **Gross E**, Arnold N, Goette J, Schwarz-Boeger U, Kiechle M. A comparison of BRCA1 mutation analysis by direct sequencing, SSCP and DHPLC. *Hum Genet* 1999; **105**: 72-78
- 2 **Holinski-Feder E**, Muller-Koch Y, Friedl W, Moeslein G, Keller G, Plaschke J, Ballhausen W, Gross M, Baldwin-Jedeke K, Jungck M, Mangold E, Vogelsang H, Schackert H, Lohse P, Murken J, Meitinger T. DHPLC mutation analysis of the hereditary nonpolyposis colon cancer (HNPCC) genes hMLH1 and hMSH2. *J Biochem Biophys Methods* 2001; **47**: 21-32
- 3 **O'Donovan MC**, Oefner PJ, Roberts SC, Austin J, Hoogendorn B, Guy C, Speight G, Upadhyaya M, Sommer SS, McGuffin P. Blind analysis of denaturing high-performance liquid chromatography as a tool for mutation detection. *Genomics* 1998; **52**: 44-49
- 4 **Wolford JK**, Blunt D, Ballecer C, Prochazka M. High-throughput SNP detection by using DNA pooling and denaturing high performance liquid chromatography (DHPLC). *Hum Genet* 2000; **107**: 483-487
- 5 **Keller G**, Hartmann A, Mueller J, Hofler H. Denaturing high pressure liquid chromatography (DHPLC) for the analysis of somatic p53 mutations. *Lab Invest* 2001; **81**: 1735-1737
- 6 **Liu MR**, Pan KF, Li ZF, Wang Y, Deng DJ, Zhang L, Lu YY. Rapid screening mitochondrial DNA mutation by using denaturing high-performance liquid chromatography. *World J Gastroenterol* 2002; **8**: 426-430
- 7 **Greenblatt MS**, Bennett WP, Hollstein M, Harris CC. Mutations in the p53 tumor suppressor gene: clues to cancer etiology and molecular pathogenesis. *Cancer Res* 1994; **54**: 4855-4878
- 8 **Hongyo T**, Buzard GS, Palli D, Weghorst CM, Amorosi A, Galli M, Caporaso NE, Fraumeni JF Jr, Rice JM. Mutations of the K-ras and p53 genes in gastric adenocarcinomas from a high-incidence region around Florence, Italy. *Cancer Res* 1995; **55**: 2665-2672
- 9 **Hsieh LL**, Hsieh JT, Wang LY, Fang CY, Chang SH, Chen TC. P53 mutations in gastric cancers from Taiwan. *Cancer Lett* 1996; **100**: 107-113
- 10 **Wu MS**, Lee CW, Shun CT, Wang HP, Lee WJ, Chang MC, Shen JC, Lin JT. Distinct clinicopathologic and genetic profiles in spo-

- radic gastric cancer with different mutator phenotypes. *Genes Chromosomes Cancer* 2000; **27**: 403-411
- 11 **Zenklusen JC**, Thompson JC, Klein-Szanto AJ, Conti CJ. Frequent loss of heterozygosity in human primary squamous cell and colon carcinomas at 7q31.1: evidence for a broad range tumor suppressor gene. *Cancer Res* 1995; **55**: 1347-1350
 - 12 **Matsuura K**, Shiga K, Yokoyama J, Saijo S, Miyagi T, Takasaka T. Loss of heterozygosity of chromosome 9p21 and 7q31 is correlated with high incidence of recurrent tumor in head and neck squamous cell carcinoma. *Anticancer Res* 1998; **18**: 453-458
 - 13 **Zenklusen JC**, Conti CJ, Green ED. Mutational and functional analyses reveal that ST7 is a highly conserved tumor-suppressor gene on human chromosome 7q31. *Nat Genet* 2001; **27**: 392-398
 - 14 **Kuniyasu H**, Yasui W, Yokozaki H, Akagi M, Akama Y, Kitahara K, Fujii K, Tahara E. Frequent loss of heterozygosity of the long arm of chromosome 7 is closely associated with progression of human gastric carcinomas. *Int J Cancer* 1994; **59**: 597-600
 - 15 **Nishizuka S**, Tamura G, Terashima M, Satodate R. Commonly deleted region on the long arm of chromosome 7 in differentiated adenocarcinoma of the stomach. *Br J Cancer* 1997; **76**: 1567-1571
 - 16 **Nishizuka S**, Tamura G, Terashima M, Satodate R. Loss of heterozygosity during the development and progression of differentiated adenocarcinoma of the stomach. *J Pathol* 1998; **185**: 38-43
 - 17 **Brown VL**, Proby CM, Barnes DM, Kelsell DP. Lack of mutations within ST7 gene in tumor-derived cell lines and primary epithelial tumours. *Br J Cancer* 2002; **87**: 208-211
 - 18 **Gross E**, Kiechle M, Arnold N. Mutation analysis of p53 in ovarian tumors by DHPLC. *J Biochem Biophys Methods* 2001; **47**: 73-81
 - 19 **Deng ZL**, Ma Y. Aflatoxin sufferer and p53 gene mutation in hepatocellular carcinoma. *World J Gastroenterol* 1998; **4**: 28-29
 - 20 **Luo D**, Liu QF, Gove C, Naomov NV, Su JJ, Williams R. Analysis of N-ras gene mutation and p53 gene expression in human hepatocellular carcinomas. *World J Gastroenterol* 1998; **4**: 97-99
 - 21 **Peng XM**, Peng WW, Yao JL. Codon 249 mutations of p53 gene in development of hepatocellular carcinoma. *World J Gastroenterol* 1998; **4**: 125-127
 - 22 **Berx G**, Nollet F, Strumane K, van Roy F. An efficient and reliable multiplex PCR-SSCP mutation analysis test applied to the human E-cadherin gene. *Hum Mutat* 1997; **9**: 567-574
 - 23 **Peng XM**, Yao CL, Chen XJ, Peng WW, Gao ZL. Codon 249 mutations of p53 gene in non-neoplastic liver tissues. *World J Gastroenterol* 1999; **5**: 324-326
 - 24 **Weng ML**, Li JG, Gao F, Zhang XY, Wang PS, Jiang XC. The mutation induced by space conditions in *Escherichia coli*. *World J Gastroenterol* 1999; **5**: 445-447
 - 25 **Elledge RM**, Fuqua SA, Clark GM, Pujol P, Allred DC, William L. McGuire Memorial Symposium. The role and prognostic significance of p53 gene alterations in breast cancer. *Breast Cancer Res Treat* 1993; **27**: 95-102
 - 26 **Yamada K**, Mori A, Seki M, Kimura J, Yuasa S, Matsuura Y, Miyamura T. Critical point mutations for hepatitis C virus NS3 proteinase. *Virology* 1998; **246**: 104-112
 - 27 **Qin Y**, Li B, Tan YS, Sun ZL, Zuo FQ, Sun ZF. Polymorphism of p16INK4a gene and rare mutation of p15INK4b gene exon2 in primary hepatocarcinoma. *World J Gastroenterol* 2000; **6**: 411-414
 - 28 **Wang Y**, Liu H, Zhou Q, Li X. Analysis of point mutation in site 1896 of HBV precore and its detection in the tissues and serum of HCC patients. *World J Gastroenterol* 2000; **6**: 395-397
 - 29 **Wang XJ**, Yuan SL, Li CP, Iida N, Oda H, Aiso S, Ishikawa T. Infrequent p53 gene mutation and expression of the cardia adenocarcinomas from a high-incidence area of Southwest China. *World J Gastroenterol* 2000; **6**: 750-753
 - 30 **He XS**, Su Q, Chen ZC, He XT, Long ZF, Ling H, Zhang LR. Expression, deletion and mutation of p16 gene in human gastric cancer. *World J Gastroenterol* 2001; **7**: 515-521
 - 31 **Yuan P**, Sun MH, Zhang JS, Zhu XZ, Shi DR. APC and K-ras gene mutation in aberrant crypt foci of human colon. *World J Gastroenterol* 2001; **7**: 352-356
 - 32 **Fang DC**, Luo YH, Yang SM, Li XA, Ling XL, Fang L. Mutation analysis of APC gene in gastric cancer with microsatellite instability. *World J Gastroenterol* 2002; **8**: 787-791
 - 33 **Liu H**, Wang Y, Zhou Q, Gui SY, Li X. The point mutation of p53 gene exon7 in hepatocellular carcinoma from Anhui Province, a non HCC prevalent area in China. *World J Gastroenterol* 2002; **8**: 480-482
 - 34 **Liao C**, Zhao MJ, Zhao J, Song H, Pineau P, Marchio A, Dejean A, Tiollais P, Wang HY, Li TP. Mutation analysis of novel human liver-related putative tumor suppressor gene in hepatocellular carcinoma. *World J Gastroenterol* 2003; **9**: 89-93
 - 35 **Zheng M**, Liu LX, Zhu AL, Qi SY, Jiang HC, Xiao ZY. K-ras gene mutation in the diagnosis of ultrasound guided fine-needle biopsy of pancreatic masses. *World J Gastroenterol* 2003; **9**: 188-191
 - 36 **Klein B**, Weirich G, Brauch H. DHPLC-based germline mutation screening in the analysis of the VHL tumor suppressor gene: usefulness and limitations. *Hum Genet* 2001; **108**: 376-384
 - 37 **Xiao W**, Oefner PJ. Denaturing high-performance liquid chromatography: A review. *Hum Mutat* 2001; **17**: 439-474
 - 38 **Arnold N**, Gross E, Schwarz-Boeger U, Pfisterer J, Jonat W, Kiechle M. A highly sensitive, fast, and economical technique for mutation analysis in hereditary breast and ovarian cancers. *Hum Mutat* 1999; **14**: 333-339
 - 39 **Jones AC**, Austin J, Hansen N, Hoogendorn B, Oefner PJ, Cheadle JP, O' Donovan MC. Optimal temperature selection for mutation detection by denaturing HPLC and comparison to single-stranded conformation polymorphism and heteroduplex analysis. *Clin Chem* 1999; **45**(8 Pt 1): 1133-1140
 - 40 **Roberts PS**, Jozwiak S, Kwiatkowski DJ, Dabora SL. Denaturing high-performance liquid chromatography (DHPLC) is a highly sensitive, semi-automated method for identifying mutations in the TSC1 gene. *J Biochem Biophys Methods* 2001; **47**: 33-37
 - 41 **Fukunaga M**, Monden T, Nakanishi H, Ohue M, Fukuda K, Tomita N, Shimano T, Mori T. Immunohistochemical study of p53 in gastric carcinoma. *Am J Clin Pathol* 1994; **101**: 177-180
 - 42 **Tamura G**, Kihana T, Nomura K, Terada M, Sugimura T, Hirohashi S. Detection of frequent p53 gene mutations in primary gastric cancer by cell sorting and polymerase chain single-strand conformation polymorphism analysis. *Cancer Res* 1991; **51**: 3056-3058
 - 43 **Dong SM**, Sidransky D. Absence of ST7 gene alterations in human cancer. *Clin Cancer Res* 2002; **8**: 2939-2941
 - 44 **Hughes KA**, Hurlstone AF, Tobias ES, McFarlane R, Black DM. Absence of ST7 mutations in tumor-derived cell lines and tumors. *Nat Genet* 2001; **29**: 380-381
 - 45 **Thomas NA**, Choong DY, Jokubaitis VJ, Neville PJ, Campbell IG. Mutation of the ST7 tumor suppressor gene on 7q31.1 is rare in breast, ovarian and colorectal cancers. *Nat Genet* 2001; **29**: 379-380

Edited by Xu JY and Wang XL

Hepatic arterial infusion chemotherapy for hepatocellular carcinoma with tumor thrombosis of the portal vein

Yung-Chih Lai, Cheng-Yen Shih, Chin-Ming Jeng, Sien-Sing Yang, Jui-Ting Hu, Yung-Chuan Sung, Han-Ting Liu, Shaw-Min Hou, Chi-Hwa Wu, Tzen-Kwan Chen

Yung-Chih Lai, Cheng-Yen Shih, Sien-Sing Yang, Jui-Ting Hu, Yung-Chuan Sung, Han-Ting Liu, Chi-Hwa Wu, Tzen-Kwan Chen, Department of Internal Medicine, Cathay General Hospital, Taipei, Taiwan, China

Chin-Ming Jeng, Department of Radiology, Cathay General Hospital, Taipei, Taiwan, China

Shaw-Min Hou, Department of Surgery, Cathay General Hospital, Taipei, Taiwan, China

Correspondence to: Dr. Yung-Chih Lai, Department of Internal Medicine, Cathay General Hospital, 280, Jen-Ai Road, Section 4, Taipei 106, Taiwan, China. yungchihlai@hotmail.com

Telephone: +86-2-27082121 Ext.3120 **Fax:** +86-2-27074949

Received: 2003-09-06 **Accepted:** 2003-10-12

Abstract

AIM: Hepatocellular carcinoma (HCC) with portal vein tumor thrombosis (PVTT) is associated with poor prognosis. The aim of this prospective study was to evaluate the efficacy of hepatic arterial infusion chemotherapy (HAIC) for patients with this disease.

METHODS: Eighteen HCC patients with PVTT were treated with HAIC via a subcutaneously implanted injection port. A course of chemotherapy consisted of daily cisplatin (10 mg for one hour) followed by 5-fluorouracil (250 mg for five hours) for five continuous days within a given week. The patients were scheduled to receive four consecutive courses of HAIC. Responders were defined in whom either a complete or partial response was achieved, while non-responders were defined based on stable or progressive disease status. The prognostic factors associated with survival after treatment were analyzed.

RESULTS: Six patients exhibited partial response to this form of HAIC (response rate = 33 %). The 3, 6, 9, 12 and 18-month cumulative survival rates for the 18 patients were 83 %, 72 %, 50 %, 28 %, and 7 %, respectively. Median survival times for the six responders and 12 non-responders were 15.0 (range, 11-18) and 7.5 (range, 1-13) months, respectively. It was demonstrated by both univariate and multivariate analyses that the therapeutic response and hepatic reserve function were significant prognostic factors.

CONCLUSION: HAIC using low-dose cisplatin and 5-fluorouracil may be a useful alternative for the treatment of patients with advanced HCC complicated with PVTT. There may also be survival-related benefits associated with HAIC.

Lai YC, Shih CY, Jeng CM, Yang SS, Hu JT, Sung YC, Lin HT, Hou SM, Wu CH, Chen TK. Hepatic arterial infusion chemotherapy for hepatocellular carcinoma with tumor thrombosis of the portal vein. *World J Gastroenterol* 2003; 9(12): 2666-2670

<http://www.wjgnet.com/1007-9327/9/2666.asp>

INTRODUCTION

Hepatocellular carcinoma (HCC) is one of the most common

malignancies worldwide, especially in Asia and South Africa^[1]. The incidence of HCC has increased over the past decade, and it has become the leading cause of death among patients with cirrhosis^[2]. Despite the marked progress in diagnostic techniques and therapeutic procedures, the prognosis for HCC patients remains discouraging. Surgical resection or liver transplantation for these individuals is frequently not feasible due to poor hepatic reserve function, advanced HCC stage, and/or lack of suitable donor livers^[3,4]. In past studies, the median survival period for unresectable HCC cases has been only a few months. The survival rate for patients with advanced HCC with portal vein tumor thrombosis (PVTT) was even worse^[5-8]. It has been reported that patients with diffuse HCC complicated with PVTT survived only 1-2 months if effective treatment could not be delivered^[9]. Transcatheter arterial embolization (TAE), microwave coagulation therapy (MCT), radiofrequency ablation (RFA), and percutaneous ethanol injection (PEI) were all of limited value for such patients^[10,11]. Systemic chemotherapy has also been trialed in cases of this type, but without any appreciable survival benefit^[12].

Recent advances in implantable drug delivery systems have made it possible to administer repeated arterial infusion of chemotherapy agents^[13,14]. Hepatic arterial infusion chemotherapy (HAIC) has the advantages of increased local drug concentrations and a reduction in systemic side effects, making it appropriate, therefore, as a palliative treatment for patients with advanced, unresectable HCC complicated with PVTT. Several authors in this field have reported the efficacy of HAIC^[15], with favorable results achieved by a regimen consisting of cisplatin and 5-fluorouracil (5-FU)^[16-18]. Based on these considerations, the aim of our prospective study was to evaluate the efficacy of low-dose cisplatin and 5-FU chemotherapy for cases of advanced HCC with PVTT, and analyze the clinical results.

MATERIALS AND METHODS

Patients

From June 1, 2000 to May 31, 2003, twenty patients with unresectable HCC complicated with PVTT received HAIC at the Department of Internal Medicine, Cathay General Hospital. The treatment consisted of low-dose cisplatin and 5-FU delivered via a subcutaneously implanted injection port. Given the severity of HCC or coexisting liver cirrhosis, these patients were not suitable for either surgical resection^[4] or nonsurgical treatments such as MCT^[19], RFA^[20], PEI^[21], or TAE^[22]. Of the initial 20 subjects, two withdrew due to technical difficulties associated with the indwelling catheter. These were related to the excessive size of the tumor, which hindered insertion of the catheter in one case; and stenosis of the hepatic artery in the other. In total, 18 patients were enrolled in the current study. Informed consent was obtained from all the subjects before the start of the investigation. The diagnosis of HCC was made by histopathology and/or imaging study. Of the 18 diagnoses, six were proven by histopathology and 12 were confirmed clinically using imaging studies, including ultrasonography

(US), computed tomography (CT), angiography, and magnetic resonance imaging, and/or based on a high plasma level of α -fetoprotein (AFP). There were no distant metastases at the time of commencement of the interventional therapy. Patients with any evidence of cardiac disease (congestive heart failure or history of myocardial infarction within the previous three months), severe vascular disease or uncontrolled concomitant infection were excluded. The exclusion criteria also included hepatic encephalopathy, hepatorenal syndrome, gastrointestinal bleeding, refractory ascites, serum bilirubin >5 mg/dl, serum creatinine >1.8 mg/dl, WBC count $<3\,000/\text{mm}^3$, and platelet count $<30\,000/\text{mm}^3$. The presence of PVTT was confirmed in all the cases by demonstration of one of the following: an intraluminal mass in the portal vein or portal branch from US or enhanced CT scan^[23]; the “thread-and streaks” sign or arteriportal shunts on hepatic angiography^[24]; or filling defects in the portal vein or in the portal branch as noted in an indirect portogram obtained from a venous phase angiogram of the superior mesenteric artery.

The clinical characteristics for the 18 HAIC-treated HCC patients with PVTT are shown in Table 1. The average age of the 16 male and two female patients was 56.9 (range, 43–75) years. Thirteen individuals were infected with hepatitis B virus (HBV) and five with hepatitis C virus (HCV). The Child-Pugh’s staging classification was used to estimate the degree of hepatic reserve function^[25]. Ten patients had a past history of HCC treatment using surgery and/or TAE. The PVTT grading and tumor-extent rating were evaluated using the criteria of the Liver Cancer Study Group of Japan^[26]. The PVTT grading was based on the location of the tumor thrombus in the portal vein as follows: Vp1, tumor thrombus in a third or more of the peripheral branch of the portal vein; Vp2, tumor thrombus in a second branch of the portal vein; and, Vp3, tumor thrombus in the first branch or trunk of the portal vein. Tumor-extent rating was estimated from imaging study. The rating system was based on the tumor-extent percentage (E): E1, less than 20 % of the whole liver; E2, 20–40 % of the whole liver; E3, 40–60 % of the whole liver; and, E4, greater than 60 % of the whole liver.

Catheter-implantation technique

The hepatic artery was catheterized using a femoral approach. The tip of the catheter was placed in the proper hepatic artery after HCC localization. The other end of the catheter was connected to the injection port which was implanted in a subcutaneous pocket in the right lower abdominal quadrant^[16]. The gastroduodenal artery was occluded using steel coils to prevent injury to the gastrointestinal tract from exposure to the chemotherapy agents^[15,16]. Heparin solution was infused regularly via the injection port to keep the catheter from occluding.

Chemotherapeutic regimen

After the set up of drug delivery system, the patients began to receive repeated arterial infusions of chemotherapy agents via the injection port. One course of chemotherapy consisted of cisplatin (10 mg per day) followed by 5-FU (250 mg per day) for five continuous days, with the patients resting on days 6 and 7. Both the cisplatin and 5-FU were administered by a mechanical infusion pump set at a rate of 10 mg for 1 hour and 250 mg for 5 hours, respectively^[16]. Basically, the patients were expected to undergo four consecutive courses of chemotherapy, and then they were deemed to have completed HAIC. HAIC was considered incomplete for patients whose chemotherapy was suspended before the completion of the four consecutive courses because of adverse reactions or complications. Maintenance therapy based on the above regimen (cisplatin 10 mg and 5-FU 250 mg for one day) was continued every two weeks after the completion of

the initial four courses of the HAIC, with duration depending on tumor response, hepatic function, adverse reactions, and complications.

Assessment of therapeutic response

Abdominal US and CT were performed regularly (every 2–3 and 4–6 months, respectively) to measure the size of the tumor. Local response to treatment was classified according to World Health Organization criteria^[27]. Complete response (CR) was defined as the complete disappearance of all known disease, and no new lesions, as determined from two observations no less than four weeks apart. Partial response (PR) was deemed to have occurred where there was a greater than 50 % reduction in total tumor load for all measurable lesions, as determined by two observations no less than four weeks apart. Stable disease (ST) did not qualify for CR/PR or progressive disease (PD) status, with the latter defined as a greater than 25 % increase in the size of one or more measurable lesions or the appearance of new lesions.

Statistical analysis

The Kaplan and Meier method was used to plot the estimated survival curves from the first day of treatment to the last day of follow-up. The results of the univariate analysis were compared to those from the log-rank test to identify predictors of survival. The results of the multivariate analysis were then investigated using Cox’s proportional hazards model. A *P* value less than 0.05 was considered to be statistically significant.

RESULTS

Therapeutic response and patient survival

The salient clinical characteristics for the patients are presented in Table 1. Fifteen patients completed HAIC, while three did not complete the initial four courses series because of deteriorating liver function, sepsis, and gastric ulcer bleeding, respectively. Overall the CR, PR, ST, and PD in response to chemotherapy were zero (0 %), six (33 %), seven (39 %), and five (28 %) in the 18 patients respectively. The response rate (CR and PR/all patients) was 33 %.

Table 1 Clinical characteristics of the 18 patients with hepatocellular carcinoma

Characteristics	<i>n</i>
Gender (male/female)	16/2
Age (younger than 60 yrs/60 yrs and older)	9/9
HBV/HCV	13/5
Child-Pugh’s stage (A/B/C)	7/7/4
Previous treatment (yes/no)	10/8
Serum AFP ($<1\,000$ ng.ml ⁻¹ / $\geq 1\,000$ ng.ml ⁻¹)	6/12
Tumor location (unilobe/bilobe)	10/8
Tumor type (nodular/massive/diffuse)	7/6/5
Maximum tumor size (<5 cm/ ≥ 5 cm)	13/5
Tumor extent (E1/E2/E3/E4) ^a	1/6/7/4
Grade of portal vein invasion (Vp1 / Vp2 / Vp3) ^{bc}	0/5/13
Completion of protocol (yes/no)	15/3
Therapeutic response (CR/PR/ST/PD)	0/6/7/5

HBV: hepatitis B virus; HCV: hepatitis C virus; AFP: α -fetoprotein; Vp: portal vein tumor thrombosis; CR: complete response; PR: partial response; ST: stable disease; PD: progressive disease. ^aTumor extent. Tumor replacement of liver parenchyma: E1, <20 %; E2, 20–40 %; E3, 40–60 %; E4, >60 %. ^{bc}Portal vein invasion. Vp1: in a third or more of the peripheral branch; Vp2: in the second branch; Vp3: in the first branch or trunk.

The cumulative survival for the 18 patients is shown in Figure 1. The 3, 6, 9, 12, 15 and 18-month cumulative survival rates for all the 18 patients were 83 %, 72 %, 50 %, 28 %, 14 %, and 7 %, respectively. While for the six responders (CR and PR), the 3, 6, 9, 12, 15 and 18-month cumulative survival rates were 100 %, 100 %, 100 %, 67 %, 44 %, and 22 %, respectively. The median survival time for the 18 HAIC-treated patients was 9.5 (range, 1-18) months.

The median survival times for the six responders (CR and PR) and the 12 non-responders (ST and PD) were 15.0 (range, 11-18) and 7.5 (range, 1-13) months, respectively. Based on hepatic reserve function, the median survival times for Child-Pugh's stages A, B, and C were 13.0 (range, 11-18), 8.0 (range, 2-15), and 3.5 (range, 1-9) months, respectively.

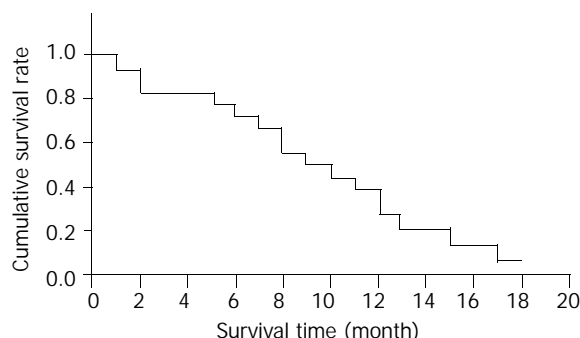


Figure 1 Cumulative survival for 18 hepatocellular carcinoma patients with portal vein tumor thrombosis undergoing hepatic arterial infusion chemotherapy. The 3, 6, 9, 12, 15 and 18-month cumulative survival rates for the 18 patients were 83 %, 72 %, 50 %, 28 %, 14 %, and 7 %, respectively.

Prognostic factors related to survival

Two of the 13 factors was demonstrated to have prognostic significance using univariate analysis: Child-Pugh's stage ($P=0.001$) and therapeutic response ($P<0.001$; Table 2). Multivariate analysis also confirmed these two variables as independent predictors of survival ($P=0.005$ and 0.001 , respectively). None of the other factors were significantly related to patient survival.

Serial computed tomography (CT) revealed progressive improvement in a 55-year-old male patient with HCC complicated with PVT who presented with a good partial response to HAIC (Figure 2). The huge tumor was decreased markedly from $14\times 10\times 9$ cm initially to $5\times 5\times 3$ cm after four months of HAIC.

Table 2 Factors associated with cumulative survival of patients by univariate analysis (log-rank test)

	<i>P</i> value*
Gender (male/female)	0.950
Age (younger than 60 yrs/60 yrs and older)	0.948
HBV/HCV	0.825
Child-Pugh's stage (A/B/C)	0.001
Previous treatment (yes/no)	0.753
Serum AFP ($<1\ 000\ \text{ng}\cdot\text{ml}^{-1}$ / $\geq 1\ 000\ \text{ng}\cdot\text{ml}^{-1}$)	0.994
Tumor location (unilobe/bilobe)	0.938
Tumor type (nodular/massive/diffuse)	0.541
Maximum tumor size ($<5\ \text{cm}$ / $\geq 5\ \text{cm}$)	0.761
Tumor extent (E1/E2/E3/E4) ^{ac}	0.429
Grade of portal vein invasion (Vp1/Vp2/Vp3) ^{bd}	0.309
Completion of protocol (yes/no)	0.155
Therapeutic response (CR/ PR/ ST/PD)	<0.001

HBV: hepatitis B virus; HCV: hepatitis C virus; AFP: α -

fetoprotein; Vp: portal vein tumor thrombosis; CR: complete response; PR: partial response; ST: stable disease; PD: progressive disease. ^{ac}Tumor extent. Tumor replacement of liver parenchyma: E1, $<20\%$; E2, $20\text{--}40\%$; E3, $40\text{--}60\%$; E4, $>60\%$. ^{bd}Portal vein invasion. Vp1: in a third or more of the peripheral branch; Vp2: in the second branch; Vp3: in the first branch or trunk.

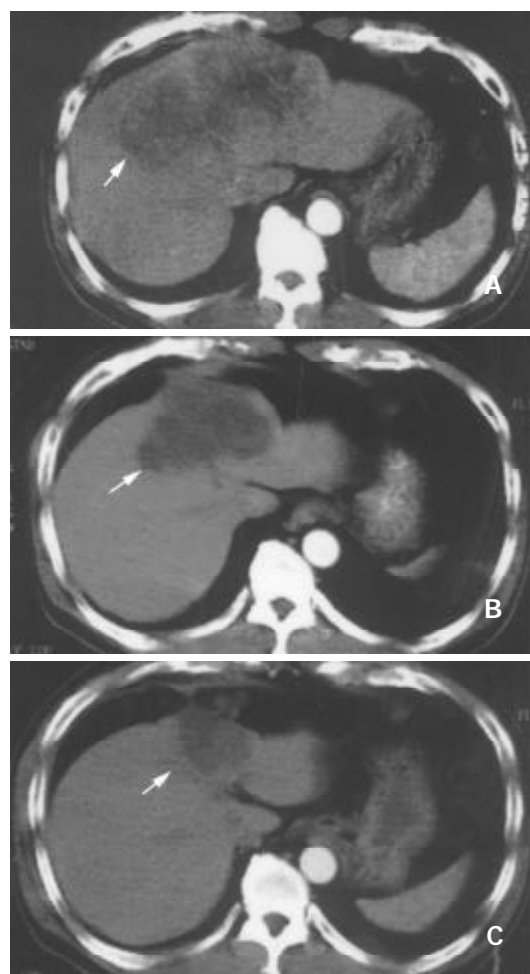


Figure 2 Image study using abdominal computed tomography (hepatic artery phase) of an HCC patient with good partial response to hepatic arterial infusion chemotherapy (HAIC) shows a marked decrease in tumor size from $14\times 10\times 9$ cm (A: before HAIC) to $9\times 8\times 7$ cm (B: 1.5 months after initiation of HAIC) and $5\times 5\times 3$ cm (C: 4 months after initiation of HAIC).

Side effects and complications

The most common adverse reactions to HAIC were nausea and loss of appetite (five cases, 28 %). Two patients (11 %) experienced leukopenia and thrombocytopenia, with one of them unable to continue the chemotherapy due to severe leukopenia. Peptic ulcer was a complication in one case and renal damage in another. Deterioration of liver function occurred in two individuals, causing one of them to quit therapy. Most of these side effects were managed using medical treatment and were not considered serious.

Complications associated with the indwelling catheter were obstruction ($n=2$), infection ($n=2$), dislocation of the catheter tip ($n=1$), and hematoma around the injection port ($n=1$). All these technical problems were overcome by medical treatment, infusion of heparin solution, or implantation of a new catheter.

Causes of death

Two patients survived the follow-up period. The remaining 16 patients expired, ten (63 %) due to cancer-related causes.

Of these, seven were as a result of tumor extension and three due to tumor rupture. Three individuals (19 %) died of gastrointestinal bleeding; of the rest, three (19 %) died of sepsis related to pneumonia ($n=2$) or urinary tract infection ($n=1$).

DISCUSSION

A standard optimal therapy for advanced unresectable HCC is still lacking^[28]. HCC has a high predilection for portal vein invasion, which has been shown to be a poor prognostic factor^[5-8]. Although surgery may be considered for some HCC patients with PVTT^[6], most are not suitable for this invasive treatment because of dissemination of the tumor throughout the liver, or the coexistence of cirrhotic change. The presence of tumoral portal invasion precludes most potential curative interventions such as TAE, PEI, MCT, and RFA^[7]. Further, liver transplantation is not indicated for such patients. Additionally, systemic chemotherapy, hormonal therapy, and IFN therapy are all reported to be of limited value^[11,11].

Most of the blood supply to HCC is derived from the hepatic artery, whereas the portal vein supplies the normal liver parenchyma. It is reasonable to assume, therefore, that intra-arterial administration of cytotoxic agents may facilitate delivery of a higher therapeutic concentration to the tumor tissue^[29]. Both cisplatin and 5-FU have an anti-tumor effect^[30]. In addition, cisplatin plays a synergistic role as a modulator of 5-FU, inhibiting the transport of neutral amino acids, including L-methionine, into tumor cells, and resulting in enhancement of its antitumor effects^[31]. Additionally, the combination of cisplatin and 5-FU allows low-dose administration with an associated reduction in adverse reactions. Hepatic extraction of chemotherapeutic agents can result in minimal systemic concentrations of these agents and, thus, minimize systemic toxicity^[32].

In comparison to analogous research, more patients were enrolled in the study of Ando *et al.*, (2002), with an HAIC response rate and median survival duration of 48 % and 10.2 (range, 1.7-76.9) months, respectively for their 48 patients with PVTT^[18]. By comparison, our response rate and median survival time was 33.3 % and 9.5 (range, 1-18) months, respectively. Moreover, the median survival time for our six responders and 12 non-responders were 15.0 (range, 11-18) and 7.5 (range, 1-13) months, respectively. In the above larger study, the median survival times for the 23 responders and 25 non-responders were 31.6 (range, 9.3-76.9) and 5.4 (range, 1.9-29.0) months, respectively^[18]. The longest follow-up for a survivor in their study was 76.9 months, whereas it was only 18 months in our investigation. This variation in the follow-up period may account for the difference in the results outlined above. More cases are needed to continue this study and deliver a more comprehensive and accurate result. Even in our non-responder group, however, the median survival time was 7.5 months, which is still longer than analogous reports^[5,7]. The reason that some tumors responded to HAIC, and others not, was not determined in the current study, however. This critical piece of information awaits further investigations, including immunological and/or molecular biological study of tumor cells, to reveal the underlying causes.

In an evaluation of HCC prognosis conducted by the Liver Cancer Study Group of Japan, the severity of any associated cirrhosis, and the size and number of lesions were independent predictive factors^[33]. In our study, however, only hepatic reserve function and the patient's therapeutic response were associated with survival. This difference may result from variations in the patient-enrollment criteria. Our subjects were confined to cases of unresectable HCC with PVTT. In such advanced-stage patients, the influence of lesion size and number on survival is no longer significant. Cirrhosis-related

complications (e.g. hepatic failure, variceal bleeding, and spontaneous bacterial peritonitis) were known to play key roles in HCC mortality^[34]. The patients with more-favorable Child-Pugh's classifications have fewer complications and may thus have better and more-favorable outcomes.

Kupffer cells and polymorphonuclear cell function are depressed in liver cirrhosis. The serum also shows a reduction in factors such as fibronectin, opsonins and chemo-attractants, including members of the complement system^[35,36]. The hepatic cellular-immune responses, which involve natural killer cells, cytotoxic T lymphocytes and macrophages (Kupffer cells), and their cytotoxic reactions against tumor cells are important as a defense mechanism against hepatocarcinogenesis^[37]. In cases of poor residual liver function, the complex molecular and cellular mechanisms, which prevent tumor formation and further development and spread of established tumors, are impaired^[38]. Therefore, the prognosis for advanced HCC occurring in such patients is inevitably bleak and dismal.

Chemotherapeutic toxicity was infrequent in our study. Myelosuppression was noted in two cases, and deterioration of liver function also diagnosed in two individuals. The most common adverse reaction, nausea or loss of appetite, was related to the gastrointestinal tract.

Although the survival of HCC patients with PVTT can be improved using HAIC, the results remain unsatisfactory. Further research and investigation is still necessary. Combined therapy, consisting of an intra-arterial infusion of a cytotoxic agent and systemic administration of interferon- α was reportedly useful as a palliative treatment for HCC patients with major vascular involvement^[1]. Additional therapy following HAIC, including surgery, MCT, PEI, and extra chemotherapy, might be another option for the prolongation of survival in advanced HCC patients^[18,39]. Moreover, the identification of tumors which are more sensitive to cytotoxic agents, and the reason for this are also important areas for future research.

In conclusion, the use of HAIC improves the survival of HCC patients with PVTT. Further, most of the side effects are transient and well tolerated. Hepatic reserve function and therapeutic response are the most important survival-related prognostic factors. Based on our findings, therefore, it seems reasonable to suggest that HAIC is a safe and effective alternative for the treatment of advanced HCC.

REFERENCES

- 1 **Chung YH**, Song H, Song BC, Lee GC, Koh MS, Yoon HK, Lee YS, Sung KB, Suh DJ. Combined therapy consisting of intraarterial cisplatin infusion and systemic interferon- α for hepatocellular carcinoma patients with major portal vein thrombosis or distant metastasis. *Cancer* 2000; **88**: 1986-1991
- 2 **El-Serag HB**, Mason AC. Rising incidence of hepatocellular carcinoma in United States. *N Engl J Med* 1999; **340**: 745-750
- 3 **Bismuth H**, Chiche L, Adam R, Castaing D, Diamond T, Dennison A. Liver resection versus transplantation for hepatocellular carcinoma in cirrhotic patients. *Ann Surg* 1993; **218**: 145-151
- 4 **Nagasue N**, Uchida M, Makino Y, Takemoto Y, Yamanoi A, Hayashi T, Chang YC, Kohno H, Nakamura T, Yukaya H. Incidence and factors associated with intrahepatic recurrence following resection of hepatocellular carcinoma. *Gastroenterology* 1993; **105**: 488-494
- 5 **Okuda K**, Ohtsuki T, Obata H, Tomimatsu M, Okazaki N, Hasegawa H, Nakajima Y, Ohnishi K. Natural history of hepatocellular carcinoma and prognosis in relation to treatment. Study of 850 patients. *Cancer* 1985; **56**: 918-928
- 6 **Fujii T**, Takayasu K, Muramatsu Y, Moriyama N, Wakao F, Kosuge T, Takayama T, Makuuchi M, Yamasaki S, Okazaki N. Hepatocellular carcinoma with portal tumor thrombus: analysis of factors determining prognosis. *Jpn J Clin Oncol* 1993; **23**: 105-109

- 7 **Llovet JM**, Bustamante J, Castells A, Vilana R, Ayuso Mde J, Sala M, Bru C, Rodes J, Bruix J. Natural history of untreated non-surgical hepatocellular carcinoma: rationale for the design and evaluation of therapeutic trials. *Hepatology* 1999; **29**: 62-67
- 8 **Fan J**, Wu ZQ, Tang ZY, Zhou J, Qiu SJ, Ma ZC, Zhou XD, Ye SL. Multimodality treatment in hepatocellular carcinoma patients with tumor thrombi in portal vein. *World J Gastroenterol* 2001; **7**: 28-32
- 9 **Cady B**. Natural history of primary and secondary tumors of the liver. *Semin Oncol* 1983; **10**: 127-134
- 10 **Sakurai M**, Okamura J, Kuroda C. Transcatheter chemo-embolization effective for treating hepatocellular carcinoma: A histopathologic study. *Cancer* 1984; **54**: 387-392
- 11 **Bruix J**. Treatment of hepatocellular carcinoma. *Hepatology* 1997; **25**: 259-262
- 12 **Friedman M**. Primary hepatocellular cancer-present results and future prospects. *Int J Radiat Oncol Biol Phys* 1983; **9**: 1841-1850
- 13 **Iwamiya T**, Sawada S, Ohta Y. Repeated arterial infusion chemotherapy for inoperable hepatocellular carcinoma using an implantable drug delivery system. *Cancer Chemother Pharmacol* 1994; **33**(Suppl): S134-138
- 14 **Une Y**, Uchino J, Yasuhara M, Misawa K, Kamiyama T, Shimamura T, Sato N, Nakajima Y, Hata Y. Intra-arterial infusion chemotherapy on unresectable hepatocellular carcinoma under occlusion of hepatic arterial flow. *Clin Ther* 1993; **15**: 347-354
- 15 **Toyoda H**, Nakano S, Kumada T, Takeda I, Sugiyama K, Osada T, Kiriya S, Suga T, Takahashi M. The efficacy of continuous local arterial infusion of 5-fluorouracil and cisplatin through an implanted reservoir for severe advanced hepatocellular carcinoma. *Oncology* 1995; **52**: 295-299
- 16 **Ando E**, Yamashita F, Tanaka M, Tanigawa K. A novel chemotherapy for advanced hepatocellular carcinoma with tumor thrombosis of the main trunk of the portal vein. *Cancer* 1997; **79**: 1890-1896
- 17 **Itamoto T**, Nakahara H, Tashiro H, Haruta N, Asahara T, Naito A, Ito K. Hepatic arterial infusion of 5-fluorouracil and cisplatin for unresectable or recurrent hepatocellular carcinoma with tumor thrombosis of the portal vein. *J Surg Oncol* 2002; **80**: 143-148
- 18 **Ando E**, Tanaka M, Yamashita F, Kuromatsu R, Yatani S, Fukumori K, Sumie S, Yano Y, Okuda K, Sata M. Hepatic arterial infusion chemotherapy for advanced hepatocellular carcinoma with portal vein tumor thrombosis: analysis of 18 cases. *Cancer* 2002; **95**: 588-595
- 19 **Sato M**, Watanabe Y, Ueda S, Iseki S, Abe Y, Sato N, Kimura S, Okubo K, Onji M. Microwave coagulation therapy for hepatocellular carcinoma. *Gastroenterology* 1996; **110**: 1507-1514
- 20 **Livraghi T**, Goldberg SN, Lazzaroni S, Meloni F, Solbiati L, Gazelle GS. Small hepatocellular carcinoma: treatment with radio-frequency ablation versus ethanol injection. *Radiology* 1999; **210**: 655-661
- 21 **Shiina S**, Tagawa K, Unuma T, Terano A. Percutaneous ethanol injection therapy for treatment of the hepatocellular carcinoma. *Am J Roentgenol* 1990; **154**: 947-951
- 22 **Nakamura H**, Hashimoto T, Oi H, Sawada S. Transcatheter oily chemoembolization of hepatocellular carcinoma. *Radiology* 1989; **170**(3 Pt1): 783-786
- 23 **Mathieu D**, Grenier P, Larde D, Vasile N. Portal vein involvement in hepatocellular carcinoma: dynamic CT features. *Radiology* 1984; **152**: 127-132
- 24 **Okuda K**, Musha H, Yamasaki T, Jinnouchi S, Nakasaki Y, Kubo Y, Shimokawa Y, Nakayama T, Kojiro M, Sakamoto K, Nakashima T. Angiographic demonstration of intrahepatic arterio-portal anastomoses in hepatocellular carcinoma. *Radiology* 1977; **122**: 53-58
- 25 **Pugh RN**, Murray-Lyon IM, Dawson JL, Pietroni MC, Williams R. Transection of the oesophagus for bleeding oesophageal varices. *Br J Surg* 1973; **60**: 646-649
- 26 **The Liver Cancer Study Group of Japan**. Classification of primary liver cancer. 1st Engl edi Tokyo: Kanehara Shuppan Co 1997: 14
- 27 **Tang ZY**, Uy YQ, Zhou XD, Ma ZC, Lu JZ, Lin ZY, Liu KD, Ye SL, Yang BH, Wang HW. Cytoreduction and sequential resection for surgically verified unresectable hepatocellular carcinoma: evaluation with analysis of 72 patients. *World J Surg* 1995; **19**: 784-789
- 28 **Llovet JM**, Beaugrand M. Hepatocellular carcinoma: present status and future prospects. *J Hepatol* 2003; **38**: S136-149
- 29 **Sangro B**, Rios R, Bilbao I, Belouqui O, Herrero JI, Quiroga J, Prieto J. Efficacy and toxicity of intra-arterial cisplatin and etoposide for advanced hepatocellular carcinoma. *Oncology* 2002; **62**: 293-298
- 30 **Scanlon KJ**, Newman EW, Lu Y, Priest DG. Biochemical basis for cisplatin and 5-fluorouracil synergism in human ovarian carcinoma cells. *Proc Natl Acad Sci U S A* 1986; **83**(Suppl): 8923-8925
- 31 **Shirasaki T**, Shimamoto Y, Ohshimo H, Saito H, Fukushima M. Metabolic basis of the synergistic antitumor activities of 5-fluorouracil and cisplatin in rodent tumor models *in vivo*. *Cancer Chemother Pharmacol* 1993; **32**: 167-172
- 32 **Ensminger WD**, Gyves JW. Clinical pharmacology of hepatic artery chemotherapy. *Semin Oncol* 1983; **10**: 176-182
- 33 **The Liver Cancer Study Group of Japan**. Predictive factors for longterm prognosis after partial hepatectomy for patients with hepatocellular carcinoma. *Cancer* 1994; **74**: 2772-2780
- 34 **Li YH**, Wang CS, Liao LY, Wang CK, Shih LS, Chen RC, Chen PH. Long-term survival of Taiwanese patients with hepatocellular carcinoma after combination therapy with transcatheter arterial chemoembolization and percutaneous ethanol injection. *J Formos Med Assoc* 2003; **102**: 141-146
- 35 **Imawari M**, Hughes RD, Gove CD, Williams R. Fibronectin and Kupffer cell function in fulminant hepatic failure. *Dig Dis Sci* 1985; **30**: 1028-1033
- 36 **Rajkovic IA**, Williams R. Abnormalities of neutrophil phagocytosis, intracellular killing, and metabolic activity in alcoholic cirrhosis and hepatitis. *Hepatology* 1986; **6**: 252-262
- 37 **Wisse E**, Luo D, Vermijlen D, Kanellopoulou C, De Zanger R, Braet F. On the function of pit cells, the liver-specific natural killer cells. *Semin Liver Dis* 1997; **17**: 265-286
- 38 **Tabor E**. Liver tumors and host defense. *Semin Liver Dis* 1997; **17**: 351-355
- 39 **Meric F**, Patt YZ, Curley SA, Chase J, Roh MS, Vanthey JN, Ellis LM. Surgery after downstaging of unresectable hepatic tumors with intra-arterial chemotherapy. *Ann Surg Oncol* 2000; **7**: 490-495

Edited by Zhu LH

Overexpression of HBxAg in hepatocellular carcinoma and its relationship with Fas/FasL system

Xiao-Zhong Wang, Xiao-Chun Chen, Yun-Xin Chen, Li-Juan Zhang, Dan Li, Feng-Lin Chen, Zhi-Xin Chen, Hong-Ying Chen, Qi-Ming Tao

Xiao-Zhong Wang, Xiao-Chun Chen, Yun-Xin Chen, Li-Juan Zhang, Dan Li, Feng-Lin Chen, Zhi-Xin Chen, Hong-Ying Chen, Department of Gastroenterology, Affiliated Union Hospital, Fujian Medical University, Fuzhou 350001, Fujian Province, China
Qi-Ming Tao, Research Institute of Hepatology, Beijing University, Beijing 100044, China

Supported by the Science Foundation of Fujian Province, No.99-Z-162

Correspondence to: Xiao-Zhong Wang, Department of Gastroenterology, Affiliated Union Hospital, Fujian Medical University, Fuzhou 350001, Fujian Province, China. drwangxz@pub6.fz.fj.cn

Telephone: +86-591-3322384

Received: 2003-06-04 **Accepted:** 2003-09-28

Abstract

AIM: To study the expression and serum level of HBxAg, Fas and FasL in tissues of HCC patients, and to assess the relationship between HBxAg and Fas/FasL system.

METHODS: Tissues from 50 patients with HCC were tested for the expression of HBxAg, Fas and FasL by S-P immunohistochemistry. Serum levels of sFas/sFasL and HBsAg/HBeAg were measured by ELISA assay. HBV X gene was detected by PCR in serum and confirmed by automatic sequencing. Fifty cases of liver cirrhosis and 30 normal controls were involved in serum analysis.

RESULTS: The expression of HBxAg, Fas and FasL in carcinoma tissues was 96 %, 84 % and 98 %, respectively. Staining of HBxAg, Fas and FasL was observed predominately in cytoplasm, no significant difference was found in intensity between HBxAg, Fas and FasL ($P>0.05$). HBxAg, Fas and FasL might express in the same area of carcinoma tissues and this co-expression could be found in most patients with HCC. The mean levels of sFas in serum from HCC, cirrhosis and normal controls were $762.29\pm391.56\text{ }\mu\text{g}\cdot\text{L}^{-1}$, $835.36\pm407.33\text{ }\mu\text{g}\cdot\text{L}^{-1}$ and $238.27\pm135.29\text{ }\mu\text{g}\cdot\text{L}^{-1}$. The mean levels of sFasL in serum from HCC, cirrhosis and normal controls were $156.36\pm9.61\text{ }\mu\text{g}\cdot\text{L}^{-1}$, $173.63\pm18.74\text{ }\mu\text{g}\cdot\text{L}^{-1}$ and $121.96\pm7.83\text{ }\mu\text{g}\cdot\text{L}^{-1}$. Statistical analysis showed that both sFas and sFasL in HCC and cirrhosis patients were significantly higher than those in normal controls ($P<0.01$). Serum HBV X gene was found in 32 % of HCC patients and 46 % of cirrhotic patients. There was no significant relationship between serum level of sFas/sFasL and serum X gene detection ($P>0.05$). Eight percent of HCC patients with negative HBsAg and HBeAg in serum might have X gene in serum and HBxAg expression in carcinoma tissues.

CONCLUSION: Our data suggest that HBxAg and Fas/FasL system plays an important role in the development of human HCC. Expression of HBxAg can lead to expression of Fas/FasL system which and reverse apoptosis of hepatocellular carcinoma induced by FasL.

Wang XZ, Chen XC, Chen YX, Zhang LJ, Li D, Chen FL, Chen ZX, Chen HY, Tao QM. Overexpression of HBxAg in hepatocellular

carcinoma and its relationship with Fas/FasL system. *World J Gastroenterol* 2003; 9(12): 2671-2675

<http://www.wjgnet.com/1007-9327/9/2671.asp>

INTRODUCTION

Chronic infection with hepatitis B virus (HBV) is a major risk factor for the development of hepatocellular carcinoma (HCC). The pathogenesis of HBV-induced malignant transformation is incompletely understood^[1-3]. HBV X gene encodes a 154 amino acid protein called HBV X protein (HBxAg)^[4]. This protein is suspected as an oncogenic molecule responsible for hepatocarcinogenesis because of its multifunctional activities affecting gene transcription, intracellular signal transmission, cell proliferation and apoptotic cell death^[5-7]. Of these activities, the best known is its promiscuous transactivation activity^[8], which is subjected to complex mechanisms such as protein-protein interaction, regulation of phosphorylation, mRNA stabilization and alteration of nucleocytoplasmic translocation^[9-11]. Several transgenic mice experiments indicate that mice harboring HBV X gene either develop liver cancer or have accelerated development of neoplasms when they are exposed to other carcinogens^[12,13]. HBxAg inhibits the function of tumor suppressor protein P⁵³, which is thought to be an early event in hepatocyte transformation before the later accumulation of inactivating P⁵³ point mutations^[14]. HBxAg inhibits apoptosis but also exerts pro-apoptotic effects^[15,16]. In addition, HBxAg activates cell signaling cascades involving mitogen-activated protein kinase (MAPK) and Janus family tyrosine kinase (JAK) signal transducer and activators of transcription (STAT) pathways^[17,18].

The signaling pathway mediated by “death factors” including TNFR1, Fas and TRAILR1 and their cognate ligands is an important mechanism to regulate apoptosis^[19]. Fas is the first identified member of “death receptors” and the crosslinking of Fas by its ligand FasL binding leads to conformational changes of Fas, which result in formation of DISC (death induced signaling complex) followed by activation of Caspase-8 and finally induce apoptosis by cleaving their substrates. The Fas/FasL system is likely to play an important role in the regulation of apoptosis including apoptosis of tumor cells^[20]. Up-regulation of Fas in the liver has been demonstrated in active viral hepatitis^[21]. Human HCC cell lines have been shown to be resistant to Fas-mediated apoptosis^[22], but very limited data are available on FasL expression in HCC tissue and its relationship with HBxAg. We investigated the immunohistochemical expression of HBxAg, Fas and FasL in specimens of HCC. The serum level of sFas, sFasL and HBV X gene was also determined.

MATERIALS AND METHODS

Tissue and blood samples

Tumor samples were randomly collected from 50 patients undergoing hepatic resection at the Affiliated Union Hospital

of Fujian Medical University from 1999-2001. Formalin-fixed and paraffin embedded tissues from these samples were used for immunohistochemical analysis. The diagnosis of each tumor was confirmed by pathologists. Blood samples of the tumor patients were taken from the cubital vein on day 3 of hospital admission before the tumor resection. Serum was separated within 30 minutes in a refrigerated centrifuge at 4 °C, centrifuged at 1 000 g for 5 minutes and stored at -70 °C until analysis of sFas/sFasL and HBsAg/HBeAg. Anti- HCV analysis was also performed in order to exclude HCV-positive HCC. The sera of 50 patients with hepatic cirrhosis and 30 normal controls from the blood donors were enrolled in this study. Diagnosis of cirrhotic patients was made on the basis of clinical history, clinical examinations, laboratory findings, gastroscopy and ultrasonography. All the patients had decompensated cirrhosis complicated with ascites, variceal bleeding, or hepatic encephalopathy without infection. All the cirrhotic patients had no HCV infection and alcoholic cirrhosis.

Immunohistochemical analysis

Immunohistochemical staining of HBxAg, Fas and FasL was performed by S-P method. Paraffin embedded sections of 4 µm thickness were cut from the resected tumor samples and transferred onto glass slides. The slides were dewaxed and re-hydrated through a graded descending alcohol series (100 %, 90 %, and 70 %). The slides' endogenous peroxidase activity was blocked by covering the sections with freshly prepared 0.5 % H₂O₂ in methanol, the slides were incubated with horse serum (Vector Laboratories) to block non-specific binding of antibodies. Then, the slides were incubated with a 1:100 dilution of mouse anti-HBx monoclonal antibody, a 1:100 dilution of rabbit polyclonal anti-Fas and anti-FasL antibodies (Maixin-Bio) respectively, washed and incubated with secondary antibody. The slides were subsequently incubated with a freshly prepared 0.1 % v/v diaminobenzidine/TBS solution and counter-stained with haematoxylin. Stained slides were differentiated in acid alcohol prior to blueing in Scott's solution (Sigma), followed by a wash in running tap water. Finally, the sections were dehydrated through a graded ascending (70 %, 90 %, and 100 %) alcohol series and mixed xylenes on the resulting slides, the sites of immunoperoxidase activity were stained brown and nuclei were blue. As a negative control for HBxAg immunohistochemistry, we used nonimmune mouse serum instead of HBxAg antibody. As negative controls of Fas and FasL, we used nonimmune sera of rabbits. The reaction for immunohistochemistry was evaluated as strong (3+), moderate (2+), weak (+) or negative (-).

DNA extraction and PCR amplification

DNA was extracted from the serum by using phenol-chloroform extracting method. In brief, the serum was mixed with phenol-chloroform-iso-pentanol (volume fraction 25:24:1). After centrifugation at 10 000 g for 10 minutes at 4 °C. The supernatant was stored in 0.1 M sodium citrate and 100 % ethanol for 30 minutes at -20 °C. The resulting pellet was dissolved in sterilized water. The sequences of oligonucleotide primers optimized to X region were 5' -ACGGAATTCATGGCTGCTAGGCTGTG-3', 3' -ATCCTGCAGAGGTGAAAAAGTTGCAT-5', respectively. PCR was carried in a final volume of 50 µl containing 5 µl of DNA solution, 20 pmol of each primer, 50 mM of each dNTP, PCR buffer (10 mmol·L⁻¹ Tris-HCl, 50 mmol·L⁻¹ KCl, 1.5 mmol·L⁻¹ MgCl₂, 0.001 % gelatin), and 2.5 units of Taq DNA polymerase. Each PCR was as follows: 35 cycles of at 93 °C for 30 seconds, at 55 °C for 1 minute and at 72 °C for 1 minute. The resulting PCR products were separated in a 1 % agarose gel. Assessment of the positive results of PCR was essentially performed on ethidium bromide-stained

gel. To confirm the results, PCR products of a positive sample were analyzed by automatic sequencing (Shanghai Shengsong).

Enzyme-linked immunosorbent assay

Serum level of sFas, sFasL, HBsAg and HBeAg was measured using a sandwich enzyme-linked immunosorbent assay (ELISA). Commercially available ELISA kits of sFas, sFasL, HBsAg and HBeAg (MBL) were used. ELISA was performed according to the manufacturer's instructions. Briefly, diluted serum samples were added in duplicate to 96-well plates coated with antibody and incubated at 37 °C for 2 hours. After each well was washed five times with washing buffer (saline containing 0.05 % Tween20), peroxidase-labeled secondary antibody was added to each well and the plate was incubated at 37 °C for 1 hour. After each well was washed in a similar manner, the plate was incubated with tetramethylbenzidine at room temperature for 20 minutes. The reaction was stopped by adding 1 N sulfuric acid. Optical density was measured at 450 nm using a spectrophotometric microtiter plate reader. The concentration of sample was determined from a standard curve.

Statistical analysis

The expression of HBxAg, Fas and FasL was analyzed using Redit analysis. The sFas and sFasL levels were expressed as mean ±SD, and analyzed using *t*-test. *P* value less than 0.05 was regarded as significant.

RESULTS

Expression of HBxAg and Fas/FasL system

HBxAg, Fas and FasL were detected in the majority of specimens from HCC patients. The results are summarized in Table 1. In most specimens HBxAg, Fas and FasL were detectable in a large number of carcinoma cells (Figures 1-3). No significant differences were found in the expression degrees of HBxAg whether the HCC patients were sero-positive in HBsAg/HBeAg or not (*P*>0.05). Staining of HBxAg, Fas and FasL was observed predominantly in cytoplasm, but no significant difference was found in intensity between HBxAg and Fas/FasL system (*P*>0.05). HBxAg could also express in membrane of carcinoma cells. Surprisingly, we found that HBxAg, Fas and FasL might express in the same area of HCC tissues and this co-expression could be found in most patients with HCC.

Table 1 Expression of HBxAg, Fas and FasL in HCC (n=50)

Expression	HBxAg (%)	Fas(%)	FasL(%)
-	2 (4)	8 (16)	1 (2)
+	5 (10)	9 (18)	4 (8)
++	11 (22)	9 (18)	12 (24)
+++	32 (64)	24 (48)	33 (66)

Table 2 Serum levels of sFas and sFasL in patients with HCC and Cirrhosis (µg·L⁻¹)

Group	n	sFas	sFasL
HCC	50	762.29±391.56 ^a	158.36±9.67 ^a
Cirrhosis	50	835.63±407.33 ^a	173.63±18.74 ^a
Control	30	238.27±135.29	121.96±7.83

^a*P*<0.01, vs control.

Serum level of sFas and sFasL

Concentrations of sFas and sFasL in HCC, cirrhotic patients and normal controls are shown in Table 2. The serum levels of

sFas and sFasL in both HCC and cirrhotic patients were significantly higher than those of normal controls ($P < 0.01$), but there was no significant difference between cirrhosis and HCC patients in serum level of sFas and sFasL ($P > 0.05$). In addition, we did not find a correlation between sFas/sFasL concentrations and serum HBV X gene detection ($P > 0.05$).

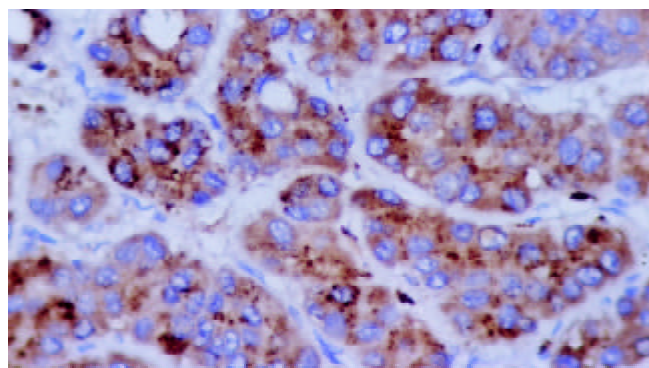


Figure 1 Positive expression of HBxAg in plasma of hepatocellular carcinoma (S-P stain, $\times 400$).

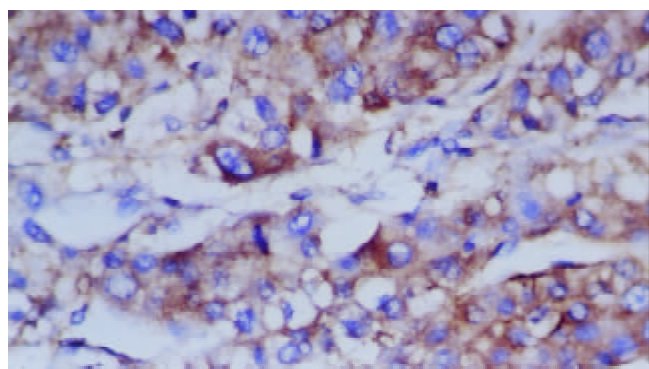


Figure 2 Positive expression of Fas in plasma of hepatocellular carcinoma (S-P stain, $\times 400$).

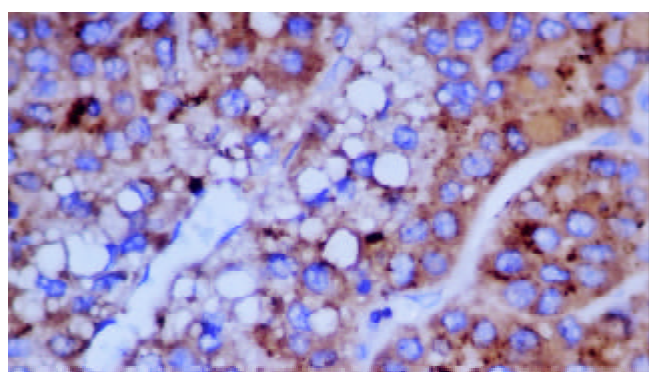


Figure 3 Positive expression of FasL in plasma of hepatocellular carcinoma (S-P stain, $\times 400$).

Table 3 Positive rates of HBV X gene, HBsAg and HBeAg in HCC and cirrhotic patients (%)

Group	HBV X gene	HBsAg	HBeAg
HCC	32	86	34
Cirrhosis	46	82	38

Determination of X gene and HBsAg/HBeAg

The positive rates of HBV X gene, HBsAg and HBeAg in HCC and cirrhotic patients are shown in Table 3. Serum HBV

X gene was found in 32 % of HCC patients and 46 % of cirrhotic patients. Eight percent of HCC patients with negative HBsAg and HBeAg in serum might have X gene in serum and HBxAg expression in carcinoma tissues.

The PCR products of X gene positive samples were analyzed by automatic sequencing and the resulting sequence was proved by Genebank.

DISCUSSION

HBV is one of the several agents causing infectious hepatitis, such as acute and chronic viral hepatitis. A strong association was found between chronic HBV infection and the development of HCC in our study. Multiple factors including damage caused by inflammatory cytokines, integration of viral DNA into host cell genomes, host genomic instability, activation of cellular oncogenes, and induction of cell survival pathways have been implicated as causes leading to HCC. However, HBV X gene and HBxAg play a major role in viral infection and carcinogenesis. X gene was the most frequently integrated protein of HBV DNA found in hepatocyte chromosomes during the development of HCC^[23]. HBxAg was expressed in these integrated fragments, although no other viral proteins were present in most tumor cells. Recent studies using cDNA microarray analysis revealed that HBxAg expression in HepG2 cells could up- or down-regulate the expression of 39 genes^[24]. These genes have a variety of cellular functions including oncogenesis, cell cycle regulation and cell adhesion. Our results demonstrated high levels of HBxAg expression in cirrhotic and HCC cells. Intracellular localization showed that HBxAg was predominant in cytoplasm. Serum levels of sFas and sFasL in both HCC and cirrhotic patients were significantly higher than those in controls. This could be explained by previous observations that X gene was greatly correlated with the development of cirrhosis and integrated into host chromosomes during chronic infection. It seems likely that HBxAg contributes to the initiation of tumor formation in the liver during the process of chronic active hepatitis and cirrhosis. However, whether this process is induced by Fas/FasL system remains to be elucidated.

With PCR detection, we found that some HBsAg and HBeAg negative HCC patients were X gene positive. These results were consistent with a previous report that circulating HBV X gene was detectable in a high proportion of Japanese HCC patients without HBsAg^[25]. It could be explained as follows: First, a low level of viremia might exist and hardly result in expression^[26]. Second, variant HBV clones might predominantly emerge, the variant HBV might have lost its common "A" determinant of HBsAg and result in loss of HBsAg^[27]. Third, disrupted form of HBV was integrated into cellular chromosomes, resulting in failure to produce viral protein translated from deleted DNA^[23]. Our results suggested that negative HBsAg and HBeAg HCC patients were required to examine HBV DNA in serum or in liver tissues in order to better understand HBV involvement in the etiology.

Our results indicated that HCC cells could strongly express both Fas and FasL in the same area of carcinoma. What is the target of this ligand? There are some hypotheses. First, because HCC cells can co-express Fas and FasL, they may undergo apoptosis induced not only by activated FasL-positive lymphocytes but also by their own FasL in an autocrine or paracrine manner. Such a fratricide mechanism may be involved in chemotherapeutic drug-induced death of HCC cells, as evidenced by the observations that bleomycin upregulated the expression of Fas and FasL in HepG₂ cells, and that apoptosis induced by this drug was almost completely inhibited by antibodies that interfere with Fas/FasL interaction^[28]. Second, FasL expressed on HCC cells might be important in their

infiltration as well as dissemination into the liver^[29], as has been demonstrated in the hepatic metastasis of colon cancer cells^[30]. The third possibility is the so-called “counterattack” hypothesis. FasL expressed on tumor cells may be engaged with Fas receptors expressed on the surfaces of antitumor immune cells, causing them to undergo apoptosis. Strand *et al*^[31] reported that HepG2 cells, expressing FasL after treatment with cytostatic drugs, could kill Fas-positive Jurkat lymphocytes, providing the first evidence that FasL is functional on HCC. Although the idea that tumor cells counterattack immune cells and escape from antitumor immunity has attracted popular attention, several investigators reported that the presence of surface FasL might be only an inflammatory response. The presence and function of FasL on HCC cells have become the subject of hot debate^[32,33]. But why this happened only in HCC? Ito *et al*^[34] examined the expression of Fas/FasL system in human HCC tissues and found that FasL expressing HCCs were moderately or poorly differentiated carcinomas. But FasL expression was not a critical factor in determining intrahepatic tumor spread. Fukuzawa *et al*^[35] reported some conflicting results. They examined the expression of Fas and FasL in human HCC tissues, and found that Fas/FasL expression decreased in proportion to the malignancy of tumor cells. According to the concept that tumor cells become resistant to apoptosis during disease progression, their observation implies that FasL expressed on HCC may be involved in a self-regulatory mechanism of apoptosis, rather than being involved in a counterattack against immune cells or infiltration into the liver. Indeed, so far, HCC cells have often been found to be resistant to Fas-mediated apoptosis, despite their expression of Fas receptors^[36]. Thus, there is no clinical evidence to directly support the idea that FasL expressed on HCCs was involved in their immune escape or infiltration into the liver. Because the mitochondrial death pathway was predominantly involved in Fas-mediated apoptosis in liver cells^[37], overexpression of HBxAg might contribute to FasL-resistance in HCC. We found that Fas, FasL and HBxAg might express in the same area of HCC tissues. The precise mechanism of the co-expression of HBxAg and Fas/FasL system remains to be established. Recently Terradillos *et al*^[38] reported that the proapoptotic activity of HBxAg could overcome or bypass the inhibitory effect of Bcl-2 against Fas cytotoxicity. The inability of Bcl-2 to protect HBxAg-expressing hepatocytes against Fas cytotoxicity might be resulted either from inactivation of Bcl-2 or from execution of a Bcl-2-independent death pathway. These indicate that the dominant function of HBxAg upon Bcl-2-regulated apoptosis might play an important role in carcinogenesis. It is known that HBxAg could activate various cellular transcription factors such as AP-1 and NF- κ B^[39]. In addition, HBxAg may induce FasL expression through activation of cellular transcription factors. Although there is no confirmative report of transcription factors regulating FasL expression, it has been found that the enhancer region of FasL gene has a putative binding site of NF- κ B^[40] and the important role of NF- κ B has been reported in FasL gene activation. Because HBxAg could activate NF- κ B, it is possible that HBxAg might induce FasL expression through NF- κ B activation^[41,42]. Our results also suggest that the expression of HBxAg can lead to expression of Fas/FasL system, which might not reflex apoptosis of hepatocellular carcinoma induced by FasL. This implies that Fas/FasL expression by itself, cannot be used as a reliable marker of apoptosis in HCC.

REFERENCES

- Koike K**, Tsutsumi T, Fujie H, Shintani Y, Moriya K. Molecular mechanism of viral hepatocarcinogenesis. *Oncology* 2002; **62** (Suppl 1): 29-37
- Tang ZY**. Hepatocellular carcinoma-cause, treatment and metastasis. *World J Gastroenterol* 2001; **7**: 445-454
- Wang WL**, Gu GY, Hu M. Expression and significance of HBV genes and their antigens in human primary intrahepatic cholangiocarcinoma. *World J Gastroenterol* 1998; **4**: 392-396
- Yeh CT**. Hepatitis B virus X protein: searching for a role in hepatocarcinogenesis. *J Gastroenterol Hepatol* 2000; **15**: 339-341
- Lian ZR**, Liu J, Pan JB, Tufan NLS, Zhu MH, Arbuthnot P, Kew M, Clayton MM, Feitelson MA. A cellular gene up-regulated by hepatitis B virus-encoded X antigen promotes hepatocellular growth and survival. *Hepatology* 2001; **34**: 146-157
- Qin LX**, Tang ZY. The prognostic molecular markers in hepatocellular carcinoma. *World J Gastroenterol* 2002; **8**: 385-392
- Qin LL**, Su JJ, Li Y, Yang C, Ban KC, Yian RQ. Expression of IGF-II, p53, p21 and HBxAg in precancerous events of hepatocarcinogenesis induced by AFB1 and/or HBV in tree shrews. *World J Gastroenterol* 2000; **6**: 138-139
- Murakami S**. Hepatitis B virus X protein: a multifunctional viral regulator. *J Gastroenterol* 2001; **36**: 651-660
- Diao J**, Garces R, Richardson CD. X protein of hepatitis B virus modulates cytokine and growth factor related signal transduction pathways during the course of viral infections and hepatocarcinogenesis. *Cytokine Growth Factor Rev* 2001; **12**: 189-205
- Wang XZ**, Jiang XR, Chen XC, Chen ZX, Li D, Lin JY, Tao QM. Seek protein which can interact with hepatitis B virus X protein from human liver cDNA library by yeast two-hybrid system. *World J Gastroenterol* 2002; **8**: 95-98
- Kong HJ**, Hong SH, Lee MY, Kim HD, Lee JW, Cheong JH. Direct binding of hepatitis B virus X protein and retinoid X receptor contributes to phosphoenolpyruvate carboxykinase gene transactivation. *FEBS Lett* 2000; **483**: 114-118
- Kim CM**, Koike K, Saito I, Miyamura T, Jay G. HBx gene of hepatitis B virus induces liver cancer in transgenic mice. *Nature* 1991; **351**: 317-320
- Slagle BL**, Lee TH, Medina D, Finegold MJ, Butel JS. Increased sensitivity to the hepatocarcinogen diethylnitrosamine in transgenic mice carrying the hepatitis B virus X gene. *Mol Carcinog* 1996; **15**: 261-269
- Staib F**, Perwez Hussain S, Hofseth LJ, Wang XW, Harris CC. TP53 and liver carcinogenesis. *Hum Mutat* 2003; **21**: 201-216
- Pollicino T**, Terradillos O, Lecoecur H, Gougeon ML, Buendia MA. Pro-apoptotic effect of the hepatitis B virus X gene. *Biomed Pharmacother* 1998; **52**: 363-368
- Xu ZH**, Zhao MJ, Li TP. P73 beta inhibits transcriptional activities of enhancer I and X promoter in hepatitis B virus more efficiently than p73alpha. *World J Gastroenterol* 2002; **8**: 1094-1097
- Kang-Park S**, Lee JH, Shin JH, Lee YI. Activation of the IGFII gene by HBV-X protein requires PKC and p44/p42 map kinase signalings. *Biochem Biophys Res Commun* 2001; **283**: 303-307
- Arbuthnot P**, Capovilla A, Kew M. Putative role of hepatitis B virus X protein in hepatocarcinogenesis: effects on apoptosis, DNA repair, mitogen-activated protein kinase and JAK/STAT pathways. *J Gastroenterol Hepatol* 2000; **15**: 357-368
- Nagata S**. Apoptosis by death factor. *Cell* 1997; **88**: 355-365
- Takehara T**, Hayashi N. Fas and Fas ligand in human hepatocellular carcinoma. *J Gastroenterol* 2001; **36**: 727-728
- Ibuki N**, Yamamoto K, Yabushita K, Okano N, Okamoto R, Shimada N, Hakoda T, Mizuno M, Higashi T, Tsuji T. *In situ* expression of Granzyme B and Fas-ligand in the liver of viral hepatitis. *Liver* 2002; **22**: 198-204
- Natoli G**, Ianni A, Costanzo A, De Petrillo G, Ilari I, Chirillo P, Balsano C, Levvero M. Resistance to Fas-mediated apoptosis in human hepatoma cells. *Oncogene* 1995; **11**: 1157-1164
- Paterlini P**, Poussin K, Kew M, Franco D, Brechot C. Selective accumulation of the X transcript of hepatitis B virus in patients negative for hepatitis B surface antigen with hepatocellular carcinoma. *Hepatology* 1995; **21**: 313-321
- Han J**, Yoo HY, Choi BH, Rho HM. Selective transcriptional regulations in the human liver cell by hepatitis B viral X protein. *Biochem Biophys Res Commun* 2000; **272**: 525-530
- Shiota G**, Oyama K, Udagawa A, Tanaka K, Nomi T, Kitamura A, Tsutsumi A, Noguchi N, Takano Y, Yashima K, Kishimoto Y, Suou T, Kawasaki H. Occult hepatitis B virus infection in HBs antigen-negative hepatocellular carcinoma in a Japanese

- population: involvement of HBx and p53. *J Med Virol* 2000; **62**: 151-158
- 26 **Niitsuma H**, Ishii M, Miura M, Kobayashi K, Toyota T. Low level hepatitis B viremia detected by polymerase chain reaction accompanies the absence of the HBe antigenemia and hepatitis in hepatitis B virus carriers. *Am J Gastroenterol* 1997; **92**: 119-123
 - 27 **Carman WF**. S gene variation of HBV. *Acta Gastroenterol Belg* 2000; **63**: 182-184
 - 28 **Muller M**, Strand S, Hug H, Heinemann EM, Walczak H, Hofmann WJ, Stremmel W, Krammer PH, Galle PR. Drug-induced apoptosis in hepatoma cells is mediated by the CD95 (APO-1/Fas) receptor/ligand system and involves activation of wild-type p53. *J Clin Invest* 1997; **99**: 403-413
 - 29 **Roskams T**, Libbrecht L, Damme BV, Desmet V. Fas and Fas ligand: strong co-expression in human hepatocellular carcinoma; can cancer induce suicide in peritumoural cells? *J Pathol* 2000; **191**: 150-153
 - 30 **Shiraki K**, Tsuji N, Shioda T, Isselbacher KJ, Takahashi H. Expression of Fas ligand in liver metastases of human colonic adenocarcinoma. *Proc Natl Acad Sci U S A* 1997; **94**: 6420-6425
 - 31 **Strand S**, Hofmann WJ, Hug H, Muller M, Otto G, Strand D, Mariani SM, Stremmel W, Krammer PH, Galle PR. Lymphocyte apoptosis induced by CD95(APO-1/Fas) ligand-expressing tumor cells-a mechanism of immune evasion? *Nat Med* 1996; **2**: 1361-1366
 - 32 **O'Connell J**, Houston A, Bennett MW, O'Sullivan GC, Shanahan F. Immune privilege or inflammation? Insights into the Fas ligand enigma. *Nat Med* 2001; **7**: 271-274
 - 33 **Restifo NP**. Countering the 'counterattack' hypothesis. *Nat Med* 2001; **7**: 259
 - 34 **Ito Y**, Monden M, Takeda T, Eguchi H, Umeshita K, Nagano H, Nakamori S, Dono K, Sakon M, Nakamura M, Tsujimoto M, Nakahara M, Nakao K, Yokosaki Y, Matsuura N. The status of Fas and Fas ligand expression can predict recurrence of hepatocellular carcinoma. *Br J Cancer* 2000; **82**: 1211-1217
 - 35 **Fukuzawa K**, Takahashi K, Furuta K, Tagaya T, Ishikawa T, Wada K, Omoto Y, Koji T, Kakumu S. Expression of fas/fas ligand(fasL) and its involvement in infiltrating lymphocytes in hepatocellular carcinoma (HCC). *J Gastroenterol* 2001; **36**: 727-728
 - 36 **Shin EC**, Shin JS, Park JH, Kim H, Kim SJ. Expression of Fas ligand in human hepatoma cell lines: role of hepatitis-B virus X (HBX) in induction of Fas ligand. *Int J Cancer* 1999; **82**: 587-591
 - 37 **Yin XM**, Wang K, Cross A, Zhao Y, Zinkel S, Klocke B, Roth KA, Korsmeyer SJ. Bid-deficient mice are resistant to Fas-induced hepatocellular apoptosis. *Nature* 1999; **400**: 886-891
 - 38 **Terradillos O**, Coste ADL, Pollicino T, Neuveut C, Sitterlin D, Lecoecur H, Gougeon ML, Kahn A, Buendia MA. The hepatitis B virus X protein abrogates Bcl-2-mediated protection against Fas apoptosis in the liver. *Oncogene* 2002; **21**: 377-386
 - 39 **Li J**, Xu ZM, Zheng YY, Johnson DL, Ou JH. Regulation of hepatocyte nuclear factor 1 activity by wild-type and mutant hepatitis B virus X proteins. *J Virol* 2002; **76**: 5875-5881
 - 40 **Lu B**, Wang L, Medan D, Toledo D, Huang C, Chen F, Shi X, Rojanasakul Y. Regulation of Fas (CD95)-induced apoptosis by nuclear factor-kappaB and tumor necrosis factor-alpha in macrophages. *Am J Physiol Cell Physiol* 2002; **283**: C831-838
 - 41 **Kasibhatla S**, Genestier L, Green DR. Regulation of fas-ligand expression during activation-induced cell death in T lymphocytes via nuclear factor kappaB. *J Biol Chem* 1999; **274**: 987-992
 - 42 **Guo SP**, Wang WL, Zhai YQ, Zhao YL. Expression of nuclear factor-kappa B in hepatocellular carcinoma and its relation with the X protein of hepatitis B virus. *World J Gastroenterol* 2001; **7**: 340-344

Edited by Wang XL

Combined transarterial chemoembolization and arterial administration of *Bletilla striata* in treatment of liver tumor in rats

Jun Qian, Daryusch Vossoughi, Dirk Woitaschek, Elsie Oppermann, Wolf O. Bechstein, Wei-Yong Li, Gan-Sheng Feng, Thomas Vogl

Jun Qian, Gan-Sheng Feng, Department of Radiology, Xiehe Hospital, Tongji Medical College, Huazhong University of Science and Technology, Wuhan 430022, China

Wei-Yong Li, Department of Pharmacology, Xiehe Hospital, Tongji Medical College, Huazhong University of Science and Technology, Wuhan 430022, China

Daryusch Vossoughi, Dirk Woitaschek, Thomas Vogl, Department of Diagnostic and Interventional Radiology, University Hospital Frankfurt, J. W. Goethe University of Frankfurt, Theodor-Stern-Kai 7, 60590 Frankfurt, Germany

Elsie Oppermann, Wolf O. Bechstein, Department of Surgery, University Hospital Frankfurt, J. W. Goethe University of Frankfurt, Theodor-Stern-Kai 7, 60590 Frankfurt, Germany

Correspondence to: Professor Dr. Thomas Vogl, Department of Diagnostic and Interventional Radiology, University Hospital Frankfurt, Johann Wolfgang Goethe-University, Theodor-Stern-Kai 7, D-60590 Frankfurt/Main, Germany. t.vogl@em.uni-frankfurt.de

Telephone: +49-69-63017277 **Fax:** +49-69-63017258

Received: 2003-08-23 **Accepted:** 2003-09-25

Abstract

AIM: To evaluate and compare the effect of combined transarterial chemoembolization (TACE) and arterial administration of *Bletilla striata* (a Chinese traditional medicine against liver tumor) versus TACE alone for the treatment of hepatocellular carcinoma (HCC) in ACI rats.

METHODS: Subcapsular implantation of a solid Morris hepatoma 3 924A (2 mm³) in the liver was carried out in 30 male ACI rats. Tumor volume (V1) was measured by magnetic resonance imaging (MRI) on day 13 after implantation. The following different agents of interventional treatment were injected after retrograde catheterization via gastroduodenal artery (on day 14), namely, (A) TACE (0.1 mg mitomycin + 0.1 ml Lipiodol) + *Bletilla striata* (1.0 mg) (*n*=10); (B) TACE + *Bletilla striata* (1.0 mg) + ligation of hepatic artery (*n*=10), (C) TACE alone (control group, *n*=10). Tumor volume (V2) was assessed by MRI (on day 13 after treatment) and the tumor growth ratio (V2/V1) was calculated.

RESULTS: The mean tumor volume before (V1) and after (V2) treatment was 0.0355 cm³ and 0.2248 cm³ in group A, 0.0374 cm³ and 0.0573 cm³ in group B, 0.0380 cm³ and 0.3674 cm³ in group C, respectively. The mean ratio (V2/V1) was 6.2791 in group A, 1.5324 in group B and 9.1382 in group C. Compared with the control group (group C), group B showed significant inhibition of tumor growth (*P*<0.01), while group A did not (*P*>0.05). None of the animals died during implantation or in the postoperative period.

CONCLUSION: Combination of TACE and arterial administration of *Bletilla striata* plus ligation of hepatic artery is more effective than TACE alone in the treatment of HCC in rats.

Qian J, Vossoughi D, Woitaschek D, Oppermann E, Bechstein WO,

Li WY, Feng GS, Vogl T. Combined transarterial chemoembolization and arterial administration of *Bletilla striata* in treatment of liver tumor in rats. *World J Gastroenterol* 2003; 9(12): 2676-2680
<http://www.wjgnet.com/1007-9327/9/2676.asp>

INTRODUCTION

HCC is a highly malignant tumor with a very high morbidity and mortality rate worldwide, carrying a poor prognosis due to its rapid infiltrating growth and complicating liver cirrhosis^[1,2].

Surgical resection, liver transplantation and cryosurgery are regarded as potentially curative treatment for HCC^[3-5], but most patients are not suitable candidates^[6-9]. Thus, the local interventional therapy of liver tumor has been rapidly evolving currently, which includes transarterial chemoembolization (TACE), percutaneous ethanol injection (PEI), radiofrequency ablation (RFA), laser-induced thermotherapy (LITT) and microwave coagulation therapy (MCT)^[10-19]. TACE is one of the most common forms of interventional therapies and seems most effective against encapsulated small HCCs without extracapsular invasion, whereas in large HCCs, viable residual tumor cells remain and the tumor frequently recurs^[20-22]. Moreover, in patients with large lesions, multiple TACE sessions are necessary to control tumor growth but may increase the risk of worsening hepatic function through damage to noncancerous liver parenchyma^[8,21,23].

In the past years, locoregional Chinese medicinal therapy for treating unresectable HCC has been reported with encouraging results, especially for inhibiting arterial collaterals of liver tumor and recurrence of HCC^[24,25]. Such an adjuvant treatment in conjunction with TACE has the potential to enhance the therapeutic effect of TACE alone in experimental and clinical studies. However, no experimental study to assess the value and efficacy of this combined therapy in an animal model of HCC has been performed.

The current prospective randomized study was designed to compare the effect of combined TACE and arterial administration of *Bletilla striata* (a Chinese traditional medicine against liver tumor) versus TACE alone for the treatment of HCC in ACI rats.

MATERIALS AND METHODS

Tumor

The hepatoma cell line (Morris hepatoma 3924A), a rapidly growing, poorly differentiated hepatocellular carcinoma^[26], was used in ACI rats in this study. The hepatoma specimens were obtained from the German Cancer Research Center (DKFZ; Heidelberg, Germany).

Animal

Thirty inbred male ACI-rats (Harlan Winkelmann; Borcheln, Germany) weighing 220-260 g were used. The animals were kept under conventional conditions with a temperature of 22±2 °C, a relative humidity of 55±10 %, a dark-light rhythm

of 12 hr, and had free access to laboratory chow and tap water. All of the experiments on animals were approved by the German government.

Agents

The original material of *Bletilla striata* microspheres is the stem tubers of *Bletilla striata*. *Bletilla striata* microspheres were kindly provided by Tongji Medical College (Wuhan, China). A dose of 1.0 mg *Bletilla striata* microspheres (50 μ m) was suspended in 0.5 ml 0.9 % NaCl for 10 minutes before administration.

Anesthesia

The animals were anesthetized with intraperitoneal injection of ketamine hydrochloride (Ketanest, Parke-Davis, Germany; 100 mg/kg), Xylazinehydrochloride (Rompun, Bayer, Germany; 15 mg/kg) and atropine sulfate (Atropinsulfat Braun, Braun, Germany; 0.1 mg/kg) in all interventional and imaging procedures.

Tumor implantation (on day 1)

The technique for tumor implantation was basically similar to that described by Yang *et al.*^[26] with minor modifications^[27-29]. The Morris hepatoma 3924A tumor tissue, recovered from the passaged animals 2 weeks after subcutaneous implantation (corresponding to 5×10^6 tumor cells), was cut into small cubes about 2 mm³.

A small subcapsular incision on the left lateral lobe of the liver was made in the recipient ACI-rats under anesthesia. The tumor fragment was gently placed into the pocket with a small cotton swab on the liver surface and the abdominal wall was then closed.

Interventional therapy (on day 14)

For interventional studies a second laparotomy was performed. By using a binocular operative microscope (M651, Leica; Wetzler, Germany), a PE-10 polyethylene microcatheter (inner diameter 0.28 mm, outer diameter 0.61 mm; Wenzel; Heidelberg, Germany) was retrogradely inserted into the gastroduodenal artery. Different agents were then injected (20 minutes a duration time) through the microcatheter via hepatic artery using sandwich technique. Administration was as follows:

Group A ($n=10$): Mitomycin (0.1 mg) + Lipiodol (0.1 ml) + *Bletilla striata* (1.0 mg)

Group B ($n=10$): Mitomycin (0.1 mg) + Lipiodol (0.1 ml) + *Bletilla striata* (1.0 mg) + ligation of A. hepatica propria

Group C ($n=10$): Mitomycin (0.1 mg) + Lipiodol (0.1 ml) (control group).

MR imaging and analysis (on day 13 and 27)

A 1.5 Tesla Sonata (Siemens; Erlangen, Germany) supplemented by a wrist coil (Small field of view) was used for MRI before and after therapy (on day 13 and 27). T1-weighted (SE: TR/TE, 460/15 ms) and T2-weighted (TSE: TR/TE, 3170/99 ms) transverse images with a section thickness of 2 mm and 184×256 matrix were acquired. There was no gap between sections and no contrast medium was administered. The tumor volume was determined and evaluated in T2-weighted image according to the formula^[30]:

$$\text{Tumor volume (mm}^3\text{)} = \frac{\text{Largest diameter (mm)} \times [\text{smallest diameter (mm)}]^2}{2}$$

The mean tumor growth ratio (V2/V1) was analyzed by using *t* test for comparing the effect of each therapeutic group with control group respectively. A *P*-value less than 0.05 was considered to indicate a significant difference.

RESULTS

The rate of tumor implantation reached 100 % in all the rats receiving tumor implantation with Morris hepatoma 3924A. None of the animals died during implantation or interventional therapy. A total of 30 individual HCC tumors were seen with unenhanced MR imaging in the livers of 30 rats (100 %) before treatment. The tumors showed homogeneously hypointense on the T1-weighted images and hyperintense on the T2-weighted images. T2-weighted sequences provided significantly higher tumor-liver contrast than T1-weighted sequences, and improved the detectability of intrahepatic metastasis. Intrahepatic metastasis occurred in two of 10 rats (20 %) in group C.

The mean tumor volume before (V1) and after (V2) therapy was 0.0355 cm³ and 0.2248 cm³ in group A, 0.0374 cm³ and 0.0573 cm³ in group B, 0.0380 cm³ and 0.3674 cm³ in group C, respectively. The mean ratio of V2/V1 was 6.2791 in group A, 1.5324 in group B and 9.1382 in group C. Compared with the control group (group C, TACE alone), group B (TACE + *Bletilla striata* + ligation of hepatic artery) showed significant inhibition of tumor growth ($P < 0.01$), while group A (TACE + *Bletilla striata*) did not ($P > 0.05$).

The tumor volume ratio (V2/V1) in different groups ($n=30$) is shown in Table 1.

Table 1 Tumor volume rate (V2/V1) in different groups ($n=30$)

Rat No.	Group A (BS)	Group B (BS+Lig.)	Group C (control)
1	6.4810	0.8556	5.6284
2	5.7038	1.4565	9.5091
3	6.2490	1.6469	10.5063
4	7.8920	1.3920	7.7416
5	7.8023	1.6577	8.6378
6	7.4781	1.6911	8.2029
7	5.5685	0.9025	8.3670
8	6.8346	1.9530	8.5399*
9	5.5800	1.9636	11.5310
10	3.2015	1.8054	12.7182*

BS: *Bletilla striata*. Lig.: Ligation of hepatic artery; *: tumor with intrahepatic metastasis.

In group B (TACE + *Bletilla striata* + ligation), relative small tumors with the size of 0.52×0.37 mm² and 0.44×0.38 mm² in diameter were shown in two treated rats, respectively, indicating a minimal response but no tumor growth after therapy compared with that before therapy (Figure 1).

In group C (control group), the tumor volume was generally markedly increased in treated rats compared to untreated. Two rats appeared to be accompanied with intrahepatic metastasis (Figure 2).

DISCUSSION

Since TACE was introduced as a palliative treatment in patients with unresectable HCC, it has become one of the most common forms of interventional therapies^[11,31]. TACE with iodized oil has been shown to result in regression of HCC and reduction of systemic toxicity, thus improving the therapeutic effects^[21,32,33]. However, prolongation of the overall survival of patients remains questionable^[34]. TACE might ablate a significant portion of the tumor but had a high rate of recurrence^[35]. In patients with focal HCC, TACE was well tolerated and provided a survival benefit. However, no apparent benefit of it has been found for patients with diffuse HCC^[36,37]. TACE using various embolizers has been well documented to include

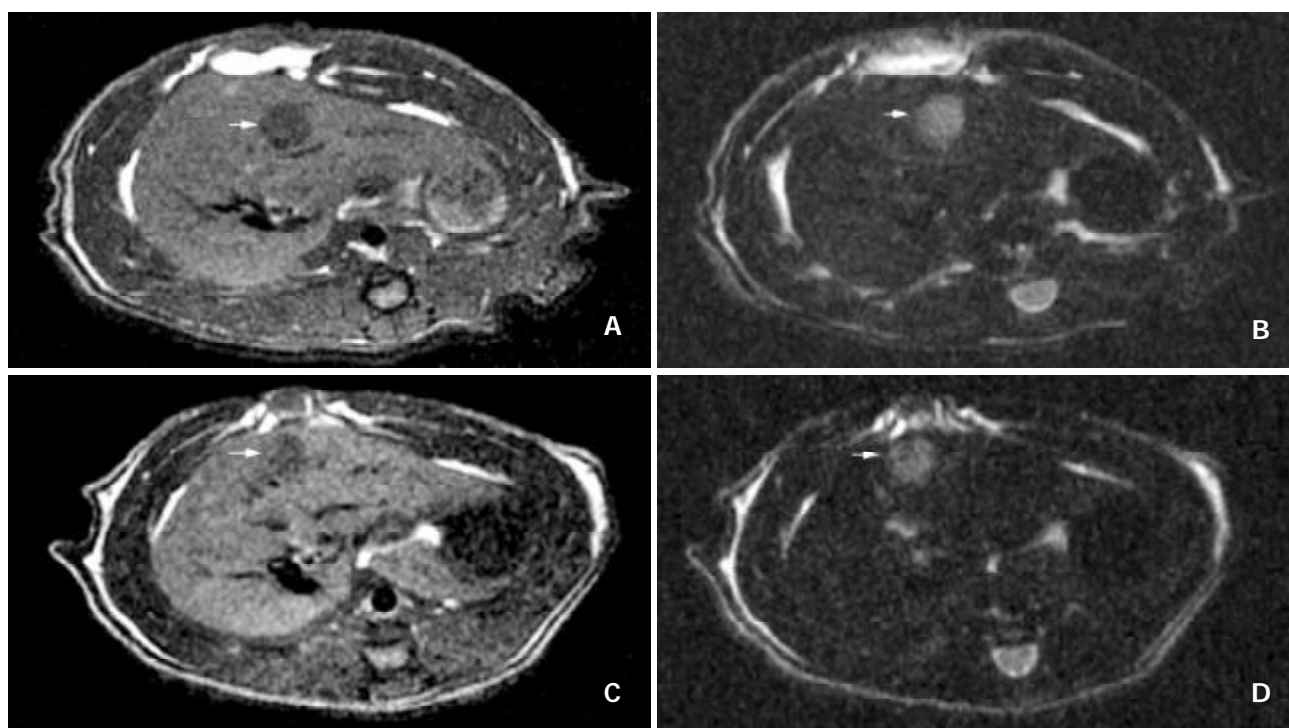


Figure 1 A: Images in a ACI rat with a solid HCC in group B. (a) Pretherapy did not enhance T1-weighted MR imaging with SE sequence (460/15). It shows a small hypointense tumor (arrow) in the left lateral lobe of liver; B: Pretherapeutic unenhanced T2-weighted MR imaging with TSE sequence (3170/99). The hyperintense lesion with a size of $0.44 \times 0.40 \text{ mm}^2$ (arrow) is well discernible from the surrounding liver tissue. C: Images in a ACI rat with a solid HCC in group B. (a) Posttherapy did not enhance T1-weighted MR imaging with SE sequence (460/15). It shows a small hypointense tumor (arrow) in the left lateral lobe of liver. D: Unenhanced T2-weighted MR imaging with TSE sequence (3170/99) after therapy. It shows the inhomogeneous hyperintense lesion with a size of $0.44 \times 0.38 \text{ mm}^2$ (arrow) and demonstrates that there is no difference between the tumor volume before and after therapy.

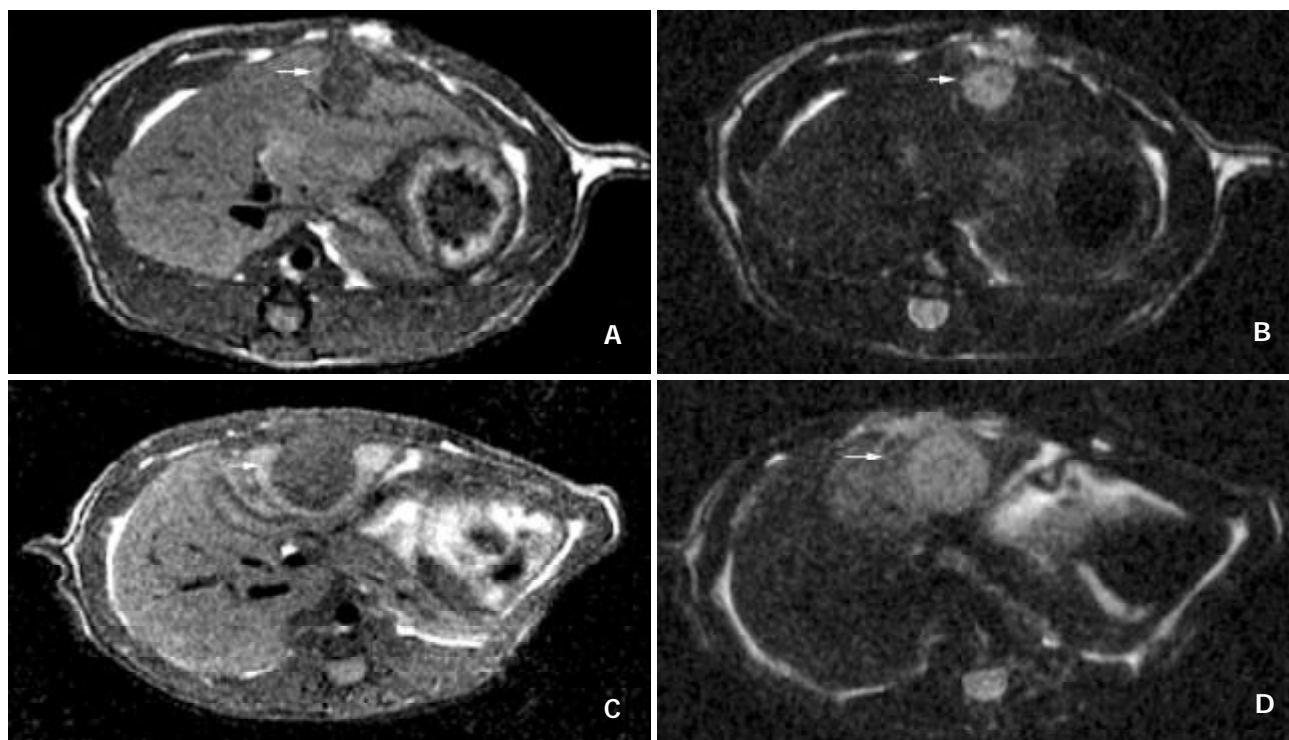


Figure 2 A: Images in a ACI rat with a solid HCC in group C. (a) Pretherapy did not enhance T1-weighted MR imaging with SE sequence (460/15). It shows a small hypointense tumor (arrow) in the left lateral lobe of liver. B: Unenhanced T2-weighted MR imaging with TSE sequence (3170/99) after therapy. The hyperintense lesion with a size of $0.49 \times 0.46 \text{ mm}^2$ (arrow) is well discernible from the surrounding liver tissues. C: Images in a ACI rat with a solid HCC in group C. (a) Posttherapy did not enhance T1-weighted MR imaging with SE sequence (460/15). It shows a large hypointense tumor (arrow) in the left lateral lobe of liver. The lesion is surrounded by an irregular hypointense area. D: Unenhanced T2-weighted MR imaging with TSE sequence (3170/99) after therapy. The tumor with a size of $0.96 \times 0.96 \text{ mm}^2$ had a rapid growth compared with that before therapy. It also shows the unhomogeneous hyperintense area (arrow) corresponding to the intrahepatic metastasis.

controlled studies. However, it is not indicated for patients with thrombosed main portal veins. Its therapeutic effect was also doubtful when the tumor was infiltrative in nature or hypovascular, too large or too small^[38,39]. The rapid development of arterial collaterals after these treatments might reduce this therapeutic effect and thus, inhibition of the development of arterial collaterals might be important in enhancing the therapeutic efficacy of these treatments^[40]. In addition, in patients with large lesions, multiple TACE sessions were necessary to control tumor growth but might increase the risk of worsening hepatic function through damage to noncancerous liver parenchyma^[23]. Moreover, the types and doses of embolic agents have been extremely variable in several reported studies. The major problem with embolic agents were twofold^[41]. First, they could often completely obstruct the hepatic artery, leading to difficulties in administration of subsequent courses of hepatic artery chemotherapy. With a relative short half-life of embolic agents, the effectiveness of TACE was not significantly improved. Second, it was easy to aggravate the liver cirrhosis and lead to hepatic failure after repeated TACE. The optimal treatment modality of TACE is still unknown^[42].

Today, it is well known that improvement of the overall therapeutic effect of liver malignancies depends on the combined therapies. In the past years, locoregional Chinese medicinal therapy has gained wide acceptance as a safe, palliative and effective treatment even in patients with large HCC and liver cirrhosis in China. *Bletilla striata* (BS) is a common Chinese traditional medicinal herb and is usually used as an embolic material in TACE for HCC. Its compositions are mucilage, starch, and a little volatile oil. In a previous study, Zheng *et al*^[24] used BS to embolize the hepatic artery in order to induce ischemic necrosis and shrinkage of tumor. It mainly blocked the trunk of the blood-supplying artery of tumor with a "vascular cast-like appearance". The embolization was extensive and lasted longer, hence a better therapeutic effect^[24]. The mechanisms of embolization by BS are attributable to the following factors: non-absorbent property, total mechanical obstruction, no influence on coagulative and anticoagulative systems and secondary obstruction due to injury of the wall of blood vessels^[43,44]. Zheng *et al*^[25] have confirmed that BS has an adherent function and can expand slowly in blood flow, leading to mechanical blockade of vessels. It was also hypothesized that BS could slowly diffuse into the liver parenchyma around the tumor as a colloidal form, leading to prolonged anticancer effect and inhibition of collateralisation and metastasis of tumor^[25]. Compared with gelfoam embolus, BS had the following characteristics. It could produce extensive and permanent vascular embolization, while it could not be absorbed by body tissue. After embolization, tumor necrosis and shrinkage were significant with less collateral circulation that formed later. The mucilage component of BS is a wide-spectrum anticancer element that might inhibit tumor occurrence and development^[45]. The 1, 2 and 3 year survival rates were 44.9 %, 33.6 % and 33.6 % in BS group while the rates were 48.9 %, 31.1 % and 16.0 % in gelfoam group, suggesting that BS is superior to gelfoam as an embolic agent, and transarterial administration of BS might provide a beneficial therapeutic modality for HCC^[45]. In our experimental study, the best therapeutic effect was the combined therapy of BS+TACE+ligation of hepatic artery. There was almost no significant difference between the tumor volume before and after therapy (Figure 1). No intrahepatic metastasis was observed in this group. This approach of central- and peripheral chemoembolization is able to increase the inhibition of tumor growth more completely, resulting in local control of tumor growth in rats and has a promising prospect for treating patients with HCC in the future.

In summary, by combining TACE and arterial administration

of *Bletilla striata* plus ligation of hepatic artery for treating HCC in ACI rats, an encouraging result can be obtained compared with TACE alone. However, the detailed therapeutic mechanisms, therapeutic indications, optimal strategy for the use, monitoring, and validation of these combined therapies remain unclear and more randomized experimental and clinical studies are required.

REFERENCES

- 1 **Cha C**, DeMatteo RP, Blumgart LH. Surgery and ablative therapy for hepatocellular carcinoma. *J Clin Gastroenterol* 2002; **35**(5 Suppl 2): S130-S137
- 2 **Yuen MF**, Cheng CC, Laufer JJ, Lam SK, Ooi CG, Lai CL. Early detection of hepatocellular carcinoma increases the chance of treatment: Hong Kong experience. *Hepatology* 2000; **31**: 330-335
- 3 **Tang ZY**. Treatment of hepatocellular carcinoma. *Digestion* 1998; **59**: 556-562
- 4 **Franco D**, Usatoff V. Resection of hepatocellular carcinoma. *Hepatogastroenterology* 2001; **48**: 33-36
- 5 **Durand F**, Belghiti J. Liver transplantation for hepatocellular carcinoma. *Hepatogastroenterology* 2002; **49**: 47-52
- 6 **Alsowmely AM**, Hodgson HJ. Non-surgical treatment of hepatocellular carcinoma. *Aliment Pharmacol Ther* 2002; **16**: 1-15
- 7 **Durand F**, Belghiti J. Liver transplantation for hepatocellular carcinoma. *Hepatogastroenterology* 2002; **49**: 47-52
- 8 **Poon RT**, Fan ST, Tsang FH, Wong J. Locoregional therapies for hepatocellular carcinoma: a critical review from the surgeon's perspective. *Ann Surg* 2002; **235**: 466-486
- 9 **Sturm JW**, Keese MA, Bonninghoff RG, Wustner M, Post S. Locally ablative therapies of hepatocellular carcinoma. *Onkologie* 2001; **24**(Suppl 5): 35-45
- 10 **Chen MS**, Li JQ, Zhang YQ, Lu LX, Zhang WZ, Yuan YF, Guo YP, Lin XJ, Li GH. High-dose iodized oil transcatheter arterial chemoembolization for patients with large hepatocellular carcinoma. *World J Gastroenterol* 2002; **8**: 74-78
- 11 **Li L**, Wu PH, Li JQ, Zhang WZ, Lin HG, Zhang YQ. Segmental transcatheter arterial embolization for primary hepatocellular carcinoma. *World J Gastroenterol* 1998; **4**: 511-512
- 12 **Huo TI**, Huang YH, Wu JC, Lee PC, Chang FY, Lee SD. Survival benefit of cirrhotic patients with hepatocellular carcinoma treated by percutaneous ethanol injection as a salvage therapy. *Scand J Gastroenterol* 2002; **37**: 350-355
- 13 **Teratani T**, Ishikawa T, Shiratori Y, Shiina S, Yoshida H, Imamura M, Obi S, Sato S, Hamamura K, Omata M. Hepatocellular carcinoma in elderly patients: beneficial therapeutic efficacy using percutaneous ethanol injection therapy. *Cancer* 2002; **95**: 816-823
- 14 **Jiang HC**, Liu LX, Piao DX, Xu J, Zheng M, Zhu AL, Qi SY, Zhang WH, Wu LF. Clinical short-term results of radiofrequency ablation in liver cancers. *World J Gastroenterol* 2002; **8**: 624-630
- 15 **Allgaier HP**, Galandi D, Zuber I, Blum HE. Radiofrequency thermal ablation of hepatocellular carcinoma. *Dig Dis* 2001; **19**: 301-310
- 16 **Vogl TJ**, Mack MG, Roggan A, Straub R, Eichler KC, Muller PK, Knappe V, Felix R. Internally cooled power laser for MR-guided interstitial laser-induced thermotherapy of liver lesions: initial clinical results. *Radiology* 1998; **209**: 381-385
- 17 **Pacella CM**, Bizzarri G, Ceconi P, Caspani B, Magnolfi F, Bianchini A, Anelli V, Pacella S, Rossi Z. Hepatocellular carcinoma: long-term results of combined treatment with laser thermal ablation and transcatheter arterial chemoembolization. *Radiology* 2001; **219**: 669-678
- 18 **Itamoto T**, Katayama K, Fukuda S, Fukuda T, Yano M, Nakahara H, Okamoto Y, Sugino K, Marubayashi S, Asahara T. Percutaneous microwave coagulation therapy for primary or recurrent hepatocellular carcinoma: long-term results. *Hepatogastroenterology* 2001; **48**: 1401-1405
- 19 **Seki T**, Tamai T, Nakagawa T, Imamura M, Nishimura A, Yamashiki N, Ikeda K, Inoue K. Combination therapy with transcatheter arterial chemoembolization and percutaneous microwave coagulation therapy for hepatocellular carcinoma. *Cancer* 2000; **89**: 1245-1251
- 20 **Liad inverted question marko L**, Virgili J, Figueras J, Valls C, Dominguez J, Rafecas A, Torras J, Fabregat J, Guardiola J, Jaurrieta

- E. A prognostic index of the survival of patients with unresectable hepatocellular carcinoma after transcatheter arterial chemoembolization. *Cancer* 2000; **88**: 50-57
- 21 **Llovet JM**, Real MI, Montana X, Planas R, Coll S, Aponte J, Ayuso C, Sala M, Muchart J, Sola R, Rodes J, Bruix J. Arterial embolisation or chemoembolisation versus symptomatic treatment in patients with unresectable hepatocellular carcinoma: a randomised controlled trial. *Lancet* 2002; **359**: 1734-1739
- 22 **Vogl TJ**, Trapp M, Schroeder H, Mack M, Schuster A, Schmitt J, Neuhaus P, Felix R. Transarterial chemoembolization for hepatocellular carcinoma: volumetric and morphologic CT criteria for assessment of prognosis and therapeutic success-results from a liver transplantation center. *Radiology* 2000; **214**: 349-357
- 23 **Bartolozzi C**, Lencioni R, Caramella D, Vignali C, Cioni R, Mazzeo S, Carrai M, Maltinti G, Capria A, Conte PF. Treatment of large HCC: transcatheter arterial chemoembolization combined with percutaneous ethanol injection versus repeated transcatheter arterial chemoembolization. *Radiology* 1995; **197**: 812-818
- 24 **Zheng C**, Feng G, Liang H. *Bletilla striata* as a vascular embolizing agent in interventional treatment of primary hepatic carcinoma. *Chin Med J* 1998; **111**: 1060-1063
- 25 **Zheng C**, Feng G, Zhou R. New use of *Bletilla striata* as embolizing agent in the intervention treatment of hepatic carcinoma. *Zhonghua Zhongliu Zazhi* 1996; **18**: 305-307
- 26 **Yang R**, Rescorla FJ, Reilly CR, Faught PR, Sanghvi NT, Lumeng L, Franklin TD Jr, Grosfeld JL. A reproducible rat liver cancer model for experimental therapy: introducing a technique of intrahepatic tumor implantation. *J Surg Res* 1992; **52**: 193-198
- 27 **Qian J**, Trubenbach J, Graepler F, Pereira P, Huppert P, Eul T, Wiemann G, Claussen C. Application of poly-lactide-co-glycolide-microspheres in the transarterial chemoembolization in an animal model of hepatocellular carcinoma. *World J Gastroenterol* 2003; **9**: 94-98
- 28 **Trubenbach J**, Pereira PL, Graepler F, Huppert PE, Eul T, Konig CW, Duda SH, Claussen CD. Animal experiment studies on the effectiveness of permanent occlusion of the hepatic artery in transarterial chemoembolization. *Rofo Fortschr Geb Rontgenstr Neuen Bildgeb Verfahr* 2000; **172**: 274-277
- 29 **Trubenbach J**, Graepler F, Pereira PL, Ruck P, Lauer U, Gregor M, Claussen CD, Huppert PE. Growth characteristics and imaging properties of the morris hepatoma 3924A in ACI rats: a suitable model for transarterial chemoembolization. *Cardiovasc Intervent Radiol* 2000; **23**: 211-217
- 30 **Carlsson G**, Gullberg B, Hafstrom L. Estimation of liver tumor volume using different formulas-an experimental study in rats. *J Cancer Res Clin Oncol* 1983; **105**: 20-23
- 31 **Achenbach T**, Seifert JK, Pitton MB, Schunk K, Junginger T. Chemoembolization for primary liver cancer. *Eur J Surg Oncol* 2002; **28**: 37-41
- 32 **Yan FH**, Zhou KR, Cheng JM, Wang JH, Yan ZP, Da RR, Fan J, Ji Y. Role and limitation of FMPSGR dynamic contrast scanning in the follow-up of patients with hepatocellular carcinoma treated by TACE. *World J Gastroenterol* 2002; **8**: 658-662
- 33 **Fan J**, Ten GJ, He SC, Guo JH, Yang DP, Weng GY. Arterial chemoembolization for hepatocellular carcinoma. *World J Gastroenterol* 1998; **4**: 33-37
- 34 **Choi BI**, Kim HC, Han JK, Park JH, Kim YI, Kim ST, Lee HS, Kim CY, Han MC. Therapeutic effect of transcatheter oily chemoembolization therapy for encapsulated nodular hepatocellular carcinoma: CT and pathologic findings. *Radiology* 1992; **182**: 709-713
- 35 **Clavien PA**, Kang KJ, Selzner N, Morse MA, Suhocki PV. Cryosurgery after chemoembolization for hepatocellular carcinoma in patients with cirrhosis. *J Gastrointest Surg* 2002; **6**: 95-101
- 36 **Lee HS**, Kim JS, Choi IJ, Chung JW, Park JH, Kim CY. The safety and efficacy of transcatheter arterial chemoembolization in the treatment of patients with hepatocellular carcinoma and main portal vein obstruction. A prospective controlled study. *Cancer* 1997; **79**: 2087-2094
- 37 **Lopez RR Jr**, Pan SH, Hoffman AL, Ramirez C, Rojter SE, Ramos H, McMonigle M, Lois J. Comparison of transarterial chemoembolization in patients with unresectable, diffuse vs focal hepatocellular carcinoma. *Arch Surg* 2002; **137**: 653-657
- 38 **Lin DY**, Lin SM, Liaw YF. Non-surgical treatment of hepatocellular carcinoma. *J Gastroenterol Hepatol* 1997; **12**: S319-S328
- 39 **Raoul JL**. Is chemoembolisation of value in inoperable primary hepatocellular carcinoma. *HPB Surg* 1998; **10**: 406-408
- 40 **Qian J**, Feng GS, Vogl TJ. Combined interventional therapies of hepatocellular carcinoma. *World J Gastroenterol* 2003; **9**:
- 41 **Iwai K**, Maeda H, Konno T. Use of oily contrast medium for selective drug targeting to tumor: Enhanced therapeutic effect and X-ray image. *Cancer Res* 1984; **44**: 2115-2121
- 42 **Camma C**, Schepis F, Orlando A, Albanese M, Shahied L, Trevisani F, Andreone P, Craxi A, Cottone M. Transarterial chemoembolization for unresectable hepatocellular carcinoma: meta-analysis of randomized controlled trials. *Radiology* 2002; **224**: 47-54
- 43 **Feng XS**, Qiu FZ, Xu Z. Experimental studies of embolization of different hepatotropic blood vessels using *Bletilla striata* in dogs. *J Tongji Med Univ* 1995; **15**: 454-459
- 44 **Qian J**, Feng G, Liang H. Action of DDPH in the interventional treatment of portal hypertension induced by liver cirrhosis in rabbits. *J Tongji Med Univ* 1998; **18**: 108-112
- 45 **Feng G**, Kramann B, Zheng C, Zhou R. Comparative study on the long-term effect of permanent embolization of hepatic artery with *Bletilla striata* in patients with primary liver cancer. *J Tongji Med Univ* 1996; **16**: 111-116

Edited by Wang XL

Side effects of budesonide in liver cirrhosis due to chronic autoimmune hepatitis: effect of hepatic metabolism versus portosystemic shunts on a patient complicated with HCC

Andreas Geier, Carsten Gartung, Christoph G. Dietrich, Hermann E. Wasmuth, Patrick Reinartz, Siegfried Matern

Andreas Geier, Carsten Gartung, Christoph G. Dietrich, Hermann E. Wasmuth, Siegfried Matern, Department of Internal Medicine III, University of Technology (RWTH) Aachen, Aachen, Germany
Patrick Reinartz, Nuclear Medicine, University of Technology (RWTH) Aachen, Aachen, Germany
Supported by Falk Pharma, Freiburg, Br., Germany
Correspondence to: Andreas Geier, MD, Department of Internal Medicine III, University of Technology Aachen, Pauwelsstrasse 30, D-52074 Aachen, Germany. ageier@ukaachen.de
Telephone: +49-241-8088634 **Fax:** +49-241-8082455
Received: 2003-07-12 **Accepted:** 2003-09-13

Abstract

AIM: To investigate the systemic availability of budesonide in a patient with Child A cirrhosis due to autoimmune hepatitis (AIH) and primary hepatocellular carcinoma, who developed serious side effects.

METHODS: Serum levels of budesonide, 6 β -OH-budesonide and 16 α -OH-prednisolone were measured by HPLC/MS/MS; portosystemic shunt-index (SI) was determined by 99mTc nuclear imaging. All values were compared with a matched control patient without side effects.

RESULTS: Serum levels of budesonide were 13-fold increased in the index patient. The ratio between serum levels of the metabolites 6 β -OH-budesonide and 16 α -OH-prednisolone, respectively, and serum levels of budesonide was diminished (1.0 vs. 4.0 for 6 β -OH-budesonide, 4.2 vs. 10.7 for 16 α -OH-prednisolone). Both patients had portosystemic SI (5.7 % and 3.1 %) within the range of healthy subjects.

CONCLUSION: Serum levels of budesonide vary up to 13-fold in AIH patients with Child A cirrhosis in the absence of relevant portosystemic shunting. Reduced hepatic metabolism, as indicated by reduced metabolite-to-drug ratio, rather than portosystemic shunting may explain systemic side effects of this drug in cirrhosis.

Geier A, Gartung C, Dietrich CG, Wasmuth HE, Reinartz P, Matern S. Side effects of budesonide in liver cirrhosis due to chronic autoimmune hepatitis: effect of hepatic metabolism versus portosystemic shunts on a patient complicated with HCC. *World J Gastroenterol* 2003; 9(12): 2681-2685
<http://www.wjgnet.com/1007-9327/9/2681.asp>

INTRODUCTION

Autoimmune hepatitis is a chronic necroinflammatory liver disorder of unknown etiology associated with interface hepatitis, hypergammaglobulinemia and circulating autoantibodies, which was first described by Waldenström in 1950^[1] and termed “autoimmune hepatitis” by the International

Autoimmune Hepatitis Group in 1992^[2]. The identification and characterization of serum autoantibodies led to differentiation of three different types characterized by antinuclear antibodies (type I), liver-kidney microsomal antibodies (type II) and soluble liver antigen (type III)^[3,4]. The distinction between autoimmune hepatitis and other autoimmune liver diseases like primary biliary cirrhosis (PBC) and primary sclerosing cholangitis (PSC) is based on characteristic clinical, histological, biochemical and immunological features but overlap and variant syndromes may occur^[5].

Primary hepatocellular carcinoma (HCC) is thought to be a consequence of the progression from chronic hepatitis to cirrhosis, although this sequence appears to be rare in autoimmune hepatitis^[6]. In many patients who develop HCC hepatitis C virus infection has been found to be a complicating condition^[7]. However, HCC also occurs in the absence of risk factors like hepatitis C infection and corticosteroid therapy^[8].

Autoimmune hepatitis is generally responsive to corticosteroid therapy despite its striking heterogeneity^[1]. Corticosteroids alone or in combination with azathioprine are the treatment of choice and result in remission induction in over 80 % of patients^[9,10]. Early clinical trials with prednisolone documented improvement of liver function tests, amelioration of symptoms and prolonged survival, thereby establishing corticosteroids as the “standard therapy”^[11-13]. Azathioprine has no role in inducing remission but may be used for maintenance of remission induced by initial corticosteroid therapy or their dose reduction in combination therapy^[9]. The potential usefulness of other immunosuppressives like cyclosporine and tacrolimus has been shown but has not yet been clinically established^[9]. Since about 70 % of patients with AIH require lifelong immunosuppressive therapy, long-term use of corticosteroids is often accompanied by numerous systemic side effects, such as osteoporosis, diabetes mellitus, systemic hypertension, psychiatric disorders and altered steroid metabolism^[14].

The search for new corticosteroids with a more favourable risk-to-benefit ratio led to the discovery of a new class of corticosteroids with high receptor affinity and particularly high first-pass effect in the liver resulting in lower systemic side effects. Budesonide, a nonhalogenated glucocorticoid derivative of the second generation exhibits a receptor affinity 15-20 times that of prednisolone and a 90 % first-pass metabolism in healthy liver^[9]. Two major metabolites, 6 β -OH-budesonide and 16 α -OH-prednisolone, have been identified which lack glucocorticoid activity making the original compound virtually devoid of systemic side effects^[15]. Budesonide has been evaluated in patients with primary biliary cirrhosis (PBC) and primary sclerosing cholangitis (PSC) at a dose of 9 mg/day with contradicting results concerning additional benefit to the standard therapy with ursodeoxycholic acid (UDCA)^[16-19]. In autoimmune hepatitis only two small uncontrolled trials with a limited number of patients and rather disappointing results have been published^[20,21]. In one study including 10 patients who were dependent on continuous

treatment to prevent exacerbation budesonide failed to induce clinical and biochemical remission in 7 patients who either deteriorated or became drug intolerant^[21]. In a second study with 13 patients budesonide has been found to lower transaminase levels significantly while causing a low frequency of systemic side effects and only a marginal reduction in plasma cortisol in noncirrhotic patients^[20]. However, the majority of patients did not reach full biochemical remission defined as normal ALT values. Patients with cirrhosis experienced higher serum cortisol levels and a partial suppression of the hypothalamic-pituitary-adrenal (HPA) axis suggestive for at least a latent systemic activity of budesonide^[20].

An explanation for a variable and so far unpredictable extent of systemic side effects in patients with early liver disease treated with budesonide may be either a reduced metabolic function or the presence of latent portosystemic shunts bypassing the liver. However, no data are presently available on the metabolism of budesonide in cirrhotic livers and the incidence of side effects in these patients. Thus, there are no recommendations for therapy with budesonide in cirrhotic patients with AIH to date.

To our knowledge, treatment of patients with coexisting HCC or other malignancies has so far not been reported in literature. Systemic immunosuppression exposes such patients to an increased risk of tumor recurrence after curative surgical treatment of the malignant disorder. A risk stratification for systemic effects of budesonide by assessment of the portosystemic shunt-index (SI) and the metabolic activity of the cirrhotic liver is of major importance in these patients. We report the first case of successful treatment of a patient with AIH after resection of a HCC and show a predominance of hepatic metabolism over portosystemic shunting on systemic availability and side effects of budesonide in this patient with Child A cirrhosis.

MATERIALS AND METHODS

Clinical data

A 65-year-old caucasian woman (patient 1) with a 27-year history of unclassified chronic hepatitis was referred to our liver unit with a newly diagnosed liver mass during regular ultrasound screening. She experienced icteric episodes 27 and 14 years ago and a known asymptomatic cholecystolithiasis. Physical examination of the anicteric patient was unremarkable despite liver enlargement without a palpable mass. Clinical chemistry on admission showed mild signs of hepatic inflammation (AST 24 U/L, GGT 53 U/L) without elevation of further liver function tests or pancreatic enzymes. Biochemical tests revealed type I autoimmune hepatitis with antinuclear (titer 1:320), anticytoplasmatic (titer 1:320) and anti-smooth muscle antibodies (titer 1:640) as well as elevated gamma-globulins (29 % of total proteins, IgG 25.7 g/L). Quantification of alpha-1-antitrypsin, ceruloplasmin, serum iron, ferritin, transferrin saturation, serum copper and urinary copper excretion were within normal limits, and serologic tests for anti-HAV, anti-HBs, anti-HBc, HBs-antigen and anti-HCV were all negative. On ultrasound the liver appeared cirrhotic with a 4.5×3.9 cm mass in the right lobe. Computed tomography (CT) depicted a 4 cm mass in segment VI of the right lobe of the liver with contrast enhancement. Alpha-1-fetoprotein (AFP) was not elevated. A CT-guided Tru-cut biopsy confirmed the diagnosis of a primary HCC in a cirrhotic liver. Tumor staging revealed no signs of metastasis in thoracic CT, ¹⁸F-fluor deoxyglucose positron emission tomography. Preoperative staging of the liver disease led to a grade A cirrhosis according to the Child-Pugh classification. Endoscopy

of the upper GI tract did not detect obvious varices of the esophagus and gastric fundus.

The patient underwent atypical resection of segment VI liver without further complications. Follow-up in our liver outpatient clinic showed functional liver tests at the preoperative level with mild AST and GGT elevation. Three months after resection of the HCC, transaminase levels sharply increased over a period of 4 months with peak transaminases of ALT 247 U/L and AST 312 U/L. No signs of tumor recurrence were detectable by abdominal CT and AFP levels. In order to prevent further progression of the Child A cirrhosis, we initiated a therapy with budesonide which was favoured over systemic immunosuppressive treatment with respect to the anticipated lower risk of tumor recurrence. Transaminase levels dropped rapidly to the normal range during a daily dose of 9 mg budesonide. Remission was achieved within two months after starting budesonide, but systemic side effects such as facial swelling, leg edemas and weight gain occurred. To minimize these adverse effects and systemic immunosuppression, we tapered the dose to 6 mg/day for maintenance therapy. Follow-up for potential tumor recurrence with corticosteroid therapy revealed normal CT-scans and AFP levels so far. Almost four years after tumor resection, the patient is still in remission in regard to AIH at a daily dose of 6 mg budesonide. In this index patient we assessed the determinants of systemic effects of budesonide in comparison with another AIH patient matched for age, sex and functional Child-Pugh stage (patient 2, caucasian female, 67 years of age, Child A cirrhosis diagnosed by liver biopsy) with steroid dependency, no apparent varices) and historic healthy controls.

Budesonide and its metabolites

Levels of budesonide, 6 β -OH-budesonide and 16 α -OH-prednisolone were determined in serum 3 hours (allowance \pm 60 minutes) after intake by a validated HPLC/MS/MS assay. Serum was extracted by solid phase extraction and the reconstituted extract was analyzed by HPLC/MS/MS on a Micromass Quattro LC using reversed phase chromatography and the negative electrospray ionization mode. The limit of detection was defined as 100 pg/ml for all analytes. All determinations have been performed by H.W. Moellmann (Medical Clinic Bergmannsheil, Bochum, Germany) and funded by Falk Pharma (Freiburg i.B., Germany). Falk Pharma had no involvement in analysis, interpretation and publication of the data.

Cortisol levels

Basal cortisol levels and cortisol levels in response to 100 μ g corticotropine releasing hormone (CRH) were measured with routine clinical chemistry. Both tests were performed at 8 A. M. and stimulated cortisol levels were determined over 90 minutes after intravenous application of CRH.

Portosystemic shunt-index (SI)

Portosystemic SI was determined by nuclear imaging after rectal application of ^{99m}Tc-technetium pertechnetate (Tc) as described^[22]. Briefly, the rectum was emptied by administration of a laxative and a polyethylene tube was inserted. After positioning of a large-field scintillation camera over the patient 340 MBq of ^{99m}Tc pertechnetate was given over the tube and time-activity curves for the areas of the liver and heart were obtained. After normalization portosystemic SI was calculated from the activity of the liver and heart.

Cortisol and portosystemic shunt-index was measured at the time of the first serum analysis on budesonide and metabolites. All measurements were determined with informed consent by both patients.

RESULTS

Serum levels of budesonide and its metabolites

Serum budesonide levels were determined 3 h after intake of 6 mg at 4 different time points during five months (Figure 1). At all time points serum budesonide levels were markedly elevated in the index case (mean 1.9 ng/ml) when compared with the control patient (mean budesonide level 0.15 ng/ml) and historic healthy controls without liver disease (0.4–0.7 ng/ml)^[23]. Systemic availability in patient 2 was remarkably lower even with a higher dose of 9 mg budesonide. However, serum levels of this control patient was in close comparison with the historic healthy controls, further supporting a potential clinical relevance of the elevated serum budesonide levels in the index patient. To determine whether elevated serum budesonide levels resulted from impaired hepatic metabolism, 6 β -OH-budesonide and 16 α -OH-prednisolone as its major inactive metabolites were measured in both patients (Figure 2). Although both metabolites were detectable in both the index and control patient, the mean ratio of metabolites to drug serum levels were significantly lower for both 6 β -OH-budesonide (1.0- vs. 4.0-fold) and 16 α -OH-prednisolone (4.2- vs. 10.7-fold) in the index compared with the control patient (Figure 2).

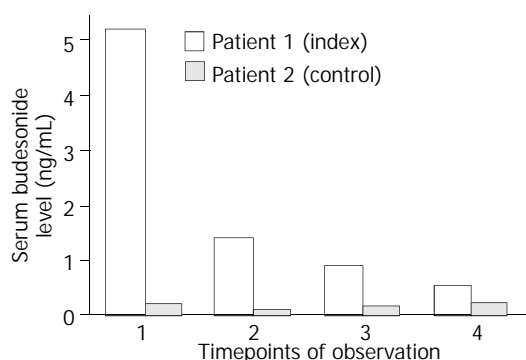


Figure 1 Serum concentration of budesonide. Serum levels of budesonide were analyzed 3 hours after intake of 6 mg 4 times during a 5-month period of follow-up. Budesonide levels were largely elevated in the index case compared to the control patient 2 with average drug levels of 1.9 \pm 2.1 ng/mL and 0.15 \pm 0.07 ng/mL, respectively. The dashed line indicates serum levels of healthy controls.

Effect of budesonide on cortisol levels

To further determine the potential systemic effects of budesonide, serum cortisol levels were measured at baseline and after stimulation by 100 μ g corticotropine releasing hormone (CRH). Whereas basal and stimulated serum cortisol levels were within the normal range in the control patient, the

index patient showed marked suppression of serum cortisol [<6 nmol/L (normal range 119–618 nmol/L)] and no significant stimulation by CRH within 90 min after application (maximum level 63 nmol/L at 60 min).

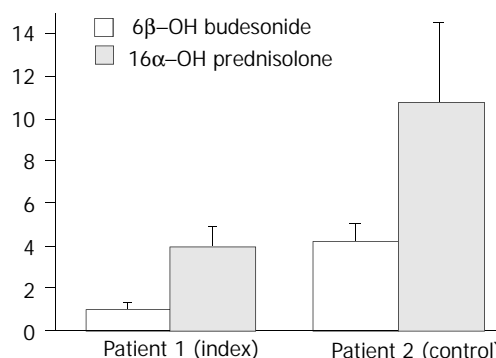


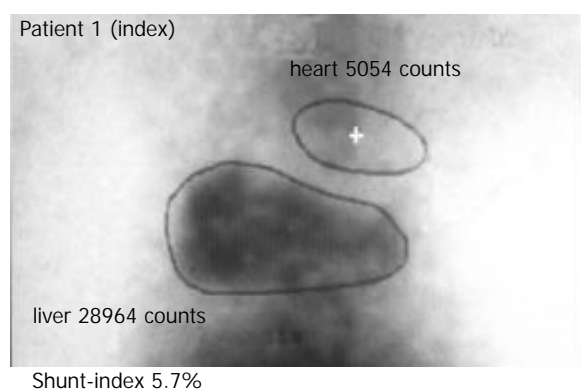
Figure 2 Ratio of metabolites to budesonide. 6 β -OH-budesonide and 16 α -OH-prednisolone serum levels were determined at the same time points as given in Figure 1. Metabolite-to-drug ratios were calculated and data are given as average \pm SEM.

Portosystemic shunt index

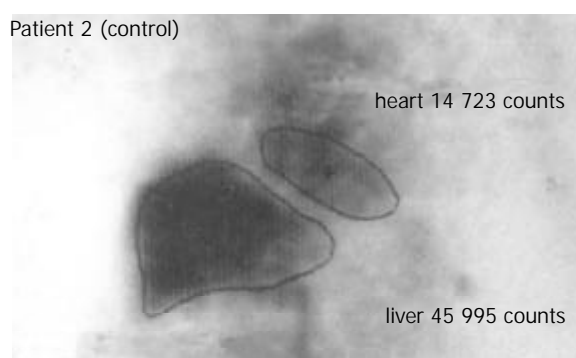
To differentiate whether elevated serum budesonide levels were caused by increased portosystemic shunting due to liver cirrhosis, portal hemodynamics were assessed by per-rectal portal scintigraphy with ^{99m}Tc pertechnetate in both patients. In both the index and the control patient measurement of the portosystemic shunt index was 5.7 % and 3.1 %, respectively, which was in the range of healthy subjects (median 4.1 %; 25th percentile 2.8; 75th percentile 6.3 %)^[22]. Thus, these data confirmed that no significant portosystemic shunting occurred in both patients (Figure 3).

DISCUSSION

Autoimmune hepatitis is currently treated with systemic administration of prednisolone, which has been shown to improve liver function tests and prolong survival^[11–13]. These first-generation glucocorticoids may cause marked side effects in long-term therapy. In order to minimize the systemic bioavailability, a new class of corticosteroids with greater topical anti-inflammatory activity and particularly high first-pass effect in healthy liver was synthesized^[24]. Budesonide, a member of this second generation, has a 90 % first pass metabolism in the healthy liver and its metabolites are virtually devoid of systemic side effects^[9]. Therefore, it does not reduce peripheral cortisol levels as a measure of systemic effect on adrenal function to the same extent as prednisolone in



Shunt-index 5.7%



Shunt-index 3.1%

Figure 3 Portosystemic shunt index. Summed images with regions of interest over heart and liver of patients 1 (A) and 2 (B) after per rectal scintigraphy using 340MBq Tc-99m pertechnetate.

noncirrhotic patients^[24]. However, in a double-blind crossover study in healthy volunteers ileal release budesonide had a greater effect on plasma cortisol levels compared with placebo^[25]. In patients with Crohn's disease budesonide reduced the median plasma cortisol concentrations at doses of 9-15 mg/day, whereas median cortisol values in the group given 3 mg/day were not different from placebo^[26].

In patients with liver disease, systemic side effects are variable. In patients with primary biliary cirrhosis treated with 9 mg budesonide per day (in addition to UDCA) changes in bone mineral density were not significantly different as compared with pretreatment data and placebo over 2 years in the study by Leuschner *et al.*^[16], whereas Angulo and coworkers found a significant loss of bone mass with the same treatment regimen over one year^[17]. This difference may be related to the number of patients with PBC stage IV of disease who experienced a significantly greater loss of bone mass in the Angulo study compared with non-cirrhotic patients. Leuschner and coworkers enrolled only patients of PBC stages I to III in this study. Similar findings were obtained in patients with primary sclerosing cholangitis in whom budesonide appears to be of minimal if any benefit and is associated with a significant worsening of osteoporosis^[18,19]. Although the drug is considered to be a promising candidate for treatment, only two small uncontrolled studies on budesonide in patients with autoimmune hepatitis have been published to date^[20,21]. In parallel with findings in PBC and PSC therapeutic efficacy of budesonide on AIH appeared to be limited and systemic side effects shown as decreased plasma cortisol levels were noted predominantly in those patients with cirrhosis^[15,20]. Although there are no published data on a possible decrease in first pass hepatic metabolism in patients with cirrhosis and consecutive higher incidence of systemic adverse effects, indirect findings such as increased osteoporosis in budesonide-treated patients with more advanced liver disease support this hypothesis^[17]. This could be due to reduced hepatic metabolism in the cirrhotic liver or, alternatively, due to increased spontaneous portosystemic shunting in these patients who may have a substantial bypass of the liver.

Portosystemic collaterals develop as chronic hepatitis and cirrhosis progress. Several methods for measurement of portosystemic shunting have been established, of which radioisotopic imaging after per-rectal ^{99m}Tc administration with determination of the heart-liver ratio (shunt index) is most common^[22,27-30]. A cross sectional study using this method has shown an increasing portal shunt index (SI) with progression of various liver diseases^[22]. In this study, healthy controls and patients with chronic hepatitis showed shunt indices with medians between 5.9 % and 10 %, respectively. Patients with cirrhosis without esophageal varices had only moderately increased portosystemic shunt indices with a median of 15 % (25th percentile 9 %, 75th percentile 28 %) whereas those cirrhotics with varices appeared to have dramatically increased shunting with a median SI of 70 % (25th percentile 52 %, 75th percentile 82 %).

Hepatic metabolism and the extent of the portosystemic shunting largely affects the bioavailability of drugs with high first-pass metabolism such as budesonide. To date, there are no data about systemic availability of the drug and its determinants in patients with advanced liver disease. To address this question and to distinguish between reduced hepatic metabolism and portosystemic shunting as the cause of higher bioavailability, we determined the serum levels of budesonide, its two major metabolites and the portal shunt index in two patients. The index patient 1 was compared with an age and sex matched AIH-patient with the same stage of cirrhosis but absent systemic effects as control. Serum levels of budesonide were largely elevated in the index case (1.9±2.1 ng/mL, *n*=4)

compared with the control patient 2 (0.15±0.07 ng/mL, *n*=4) and historically healthy controls without liver disease (0.4-0.7 ng/mL)^[23] (Figure 1). Although 6β-OH-budesonide and 16α-OH-prednisolone serum levels were also elevated 3-fold and 4.4-fold in the index patient as against patient 2, we detected 4-fold decreased metabolite-to-drug ratios for both 6β-OH-budesonide and 16α-OH-prednisolone in the index patient 1 compared with the control patient 2 (Figure 2). Both patients had similar shunt indices which were in the range of healthy subjects (Figure 3). These data demonstrate that an increased systemic bioavailability of budesonide may be rather due to a reduced hepatic metabolizing capacity in patients with early stages of liver disease than portosystemic shunting of an undetectable volume.

In these patients with coexisting malignancies, there is major concern about corticosteroid-related systemic immunosuppression which imposes a substantial risk of recurrence or progression of malignancy on these patients. To our knowledge, there is no report available on steroid therapy in a patient with autoimmune hepatitis and coexisting hepatic malignancy. The present case is the first reported patient with successful treatment of AIH complicated by HCC. The substantial inflammatory activity in this patient, who had already developed liver cirrhosis, made an anti-inflammatory therapy inevitable to halt progression. In this complex situation between progression to end stage cirrhosis and recurrence of the carcinoma, budesonide seems to be the only therapeutic alternative to minimize both risks. Although low bioavailability and high first pass metabolism of budesonide are observed in healthy volunteers, systemic availability in patients with liver cirrhosis seems to be associated with decreased hepatic metabolism after exclusion of significant portosystemic shunting (Figure 3). In order to minimize systemic immunosuppression with a concomitant risk of recurrent malignancy, we tapered the daily dose from 9 mg to 6 mg per day after systemic side effects appeared. Our present study identified increased systemic budesonide levels due to reduced hepatic metabolism as a risk factor of tumor recurrence in this patient. Therefore, we closely monitored the recurrence of the HCC in short intervals by ultrasound, computed tomography and AFP levels without any signs of recurrent malignancy under budesonide for 36 months.

Whether budesonide becomes standard therapy in autoimmune hepatitis remains to be determined in larger clinical trials. In patients with concomitant malignant disorders, this drug may have the best benefit-to-risk ratio of all immunosuppressants and may be helpful even in patients with reduced hepatic metabolism due to liver cirrhosis. However, these patients have a substantial risk of systemic side effects even in the absence of detectable portosystemic shunting and need to be monitored carefully.

REFERENCES

- 1 Krawitt EL. Autoimmune hepatitis. *N Engl J Med* 1996; **334**: 897-903
- 2 Johnson PJ, McFarlane IG. Meeting report: International Autoimmune Hepatitis Group. *Hepatology* 1993; **18**: 998-1005
- 3 Manns MP, Strassburg CP. Autoimmune hepatitis: clinical challenges. *Gastroenterology* 2001; **120**: 1502-1517
- 4 Strassburg CP, Manns MP. Autoantibodies and autoantigens in autoimmune hepatitis. *Semin Liver Dis* 2002; **22**: 339-352
- 5 Alvarez F, Berg PA, Bianchi FB, Bianchi L, Burroughs AK, Cancado EL, Chapman RW, Cooksley WG, Czaja AJ, Desmet VJ, Donaldson PT, Eddleston AL, Fainboim L, Heathcote J, Homberg JC, Hoofnagle JH, Kakumu S, Krawitt EL, Mackay IR, MacSween RN, Maddrey WC, Manns MP, McFarlane IG, Meyer ZBK, Zeniya M. International Autoimmune Hepatitis Group Report: review of criteria for diagnosis of autoimmune hepatitis. *J Hepatol* 1999; **31**: 929-938

- 6 **Wang KK**, Czaja AJ. Hepatocellular carcinoma in corticosteroid-treated severe autoimmune chronic active hepatitis. *Hepatology* 1988; **8**: 1679-1683
- 7 **Ryder SD**, Koskinas J, Rizzi PM, McFarlane IG, Portmann BC, Naoumov NV, Williams R. Hepatocellular carcinoma complicating autoimmune hepatitis: role of hepatitis C virus. *Hepatology* 1995; **22**: 718-722
- 8 **Watanabe M**, Moritani M, Hamamoto S, Uchida Y, Ishihara S, Adachi K, Kinoshita Y. Hepatocellular carcinoma complicating HCV-negative autoimmune hepatitis without corticosteroid therapy. *J Clin Gastroenterol* 2000; **30**: 445-446
- 9 **Heneghan MA**, McFarlane IG. Current and novel immunosuppressive therapy for autoimmune hepatitis. *Hepatology* 2002; **35**: 7-13
- 10 **Czaja AJ**. Treatment of autoimmune hepatitis. *Semin Liver Dis* 2002; **22**: 365-378
- 11 **Soloway RD**, Summerskill WH, Baggenstoss AH, Geall MG, Gitnick GL, Elveback IR, Schoenfield LJ. Clinical, biochemical, and histological remission of severe chronic active liver disease: a controlled study of treatments and early prognosis. *Gastroenterology* 1972; **63**: 820-833
- 12 **Cook GC**, Mulligan R, Sherlock S. Controlled prospective trial of corticosteroid therapy in active chronic hepatitis. *Q J Med* 1971; **40**: 159-185
- 13 **Murray-Lyon IM**, Stern RB, Williams R. Controlled trial of prednisone and azathioprine in active chronic hepatitis. *Lancet* 1973; **1**: 735-737
- 14 **Obermayer-Straub P**, Strassburg CP, Manns MP. Autoimmune hepatitis. *J Hepatol* 2000; **32** (1 Suppl): 181-197
- 15 **Ryrfeldt A**, Andersson P, Edsbacker S, Tonnesson M, Davies D, Pauwels R. Pharmacokinetics and metabolism of budesonide, a selective glucocorticoid. *Eur J Respir Dis Suppl* 1982; **122**: 86-95
- 16 **Leuschner M**, Maier KP, Schlichting J, Strahl S, Herrmann G, Dahm HH, Ackermann H, Happ J, Leuschner U. Oral budesonide and ursodeoxycholic acid for treatment of primary biliary cirrhosis: results of a prospective double-blind trial. *Gastroenterology* 1999; **117**: 918-925
- 17 **Angulo P**, Jorgensen RA, Keach JC, Dickson ER, Smith C, Lindor KD. Oral budesonide in the treatment of patients with primary biliary cirrhosis with a suboptimal response to ursodeoxycholic acid. *Hepatology* 2000; **31**: 318-323
- 18 **Van Hoogstraten HJ**, Vleggaar FP, Boland GJ, van Steenberghe W, Griffioen P, Hop WC, van Hattum J, van Berge H, Schalm SW, van Buuren HR. Budesonide or prednisone in combination with ursodeoxycholic acid in primary sclerosing cholangitis: a randomized double-blind pilot study. Belgian-Dutch PSC Study Group. *Am J Gastroenterol* 2000; **95**: 2015-2022
- 19 **Angulo P**, Batts KP, Jorgensen RA, LaRusso NA, Lindor KD. Oral budesonide in the treatment of primary sclerosing cholangitis. *Am J Gastroenterol* 2000; **95**: 2333-2337
- 20 **Danielsson A**, Prytz H. Oral budesonide for treatment of autoimmune chronic active hepatitis. *Aliment Pharmacol Ther* 1994; **8**: 585-590
- 21 **Czaja AJ**. Drug therapy in the management of type 1 autoimmune hepatitis. *Drugs* 1999; **57**: 49-68
- 22 **Shiomi S**, Sasaki N, Habu D, Takeda T, Nishiguchi S, Kuroki T, Tanaka T, Ochi H. Natural course of portal hemodynamics in patients with chronic liver diseases, evaluated by per-rectal portal scintigraphy with Tc-99m pertechnetate. *J Gastroenterol* 1998; **33**: 517-522
- 23 **Mollmann HW**, Hochhaus G, Tromm A, Froehlich P, Mollmann AC, Krieg M, Weiser H, Derendorf H, Barth J. Pharmacokinetics and pharmacodynamics of budesonide pH-modified release capsules. In: Mollmann HW, May B, eds. Glucocorticoid therapy in chronic inflammatory bowel disease - from basic principles to rational therapy. Dordrecht, Boston, London: *Kluwer Academic Publishers* 1996: 107-120
- 24 **Spencer CM**, McTavish D. Budesonide. A review of its pharmacological properties and therapeutic efficacy in inflammatory bowel disease. *Drugs* 1995; **50**: 854-872
- 25 **Edsbacker S**, Nilsson M, Larsson P. A cortisol suppression dose-response comparison of budesonide in controlled ileal release capsules with prednisolone. *Aliment Pharmacol Ther* 1999; **13**: 219-224
- 26 **Greenberg GR**, Feagan BG, Martin F, Sutherland LR, Thomson AB, Williams CN, Nilsson LG, Persson T. Oral budesonide for active Crohn's disease. Canadian Inflammatory Bowel Disease Study Group. *N Engl J Med* 1994; **331**: 836-841
- 27 **Shiomi S**, Kuroki T, Kurai O, Kobayashi K, Ikeoka N, Monna T, Ochi H. Portal circulation by technetium-99m pertechnetate per-rectal portal scintigraphy. *J Nucl Med* 1988; **29**: 460-465
- 28 **Shiomi S**, Kuroki T, Ueda T, Takeda T, Ikeoka N, Nishiguchi S, Nakajima S, Kobayashi K, Ochi H. Clinical usefulness of evaluation of portal circulation by per rectal portal scintigraphy with technetium-99m pertechnetate. *Am J Gastroenterol* 1995; **90**: 460-465
- 29 **D'Arienzo A**, Celentano L, Cimino L, Panarese A, Lancia C, Vergara E, Castaldo G, Oriani G, Squame G, Budillon G. Per-rectal portal scintigraphy with technetium-99m pertechnetate for the early diagnosis of cirrhosis in patients with chronic hepatitis. *J Hepatol* 1992; **14**: 188-193
- 30 **Wang JY**, Chen SL, Chen FZ, Xu WG, Hu DC, Chen XF, Jin G, Liu HY. A non-invasive method for evaluating cirrhotic portal hypertension by administration of 99mTc-MIBI per rectum. *J Gastroenterol Hepatol* 1995; **10**: 169-173

Percutaneous cryoablation in combination with ethanol injection for unresectable hepatocellular carcinoma

Ke-Cheng Xu, Li-Zhi Niu, Wei-Bin He, Zi-Qian Guo, Yi-Ze Hu, Jian-Sheng Zuo

Ke-Cheng Xu, Li-Zhi Niu, Wei-bin He, Zi-Qian Guo, Yi-Ze Hu, Jian-Sheng Zuo, Fuda Cancer Hospital of Guangzhou, Guangzhou 510300, Guangdong Province, China

Correspondence to: Dr. Ke-Cheng Xu, Fuda Cancer Hospital of Guangzhou, Guangzhou 510300, Guangdong Province, China. xukc1818@sina.com

Telephone: +86-20-84196175 **Fax:** +86-20-84195515

Received: 2003-03-10 **Accepted:** 2003-05-16

Abstract

AIM: To evaluate the effectiveness and safety of percutaneous hepatic cryoablation in combination with percutaneous ethanol injection (PEI) in patients with unresectable hepatocellular carcinoma (HCC).

METHODS: A total of 105 masses in 65 HCC patients underwent percutaneous hepatic cryoablation. The cryoablation was performed with the Cryocare system (Endocare, Irvine, CA, USA) using argon gas as a cryogen. Two freeze-thaw cycles were performed, each reaching a temperature of -180 °C at the tip of the probe. PEI was given in 36 patients with tumor masses larger than 6 cm in diameter 1-2 weeks after cryoablation and then once per week for 4 to 6 sessions. The efficacy was evaluated with survival, change of tumor size and alpha-fetoprotein (AFP) levels.

RESULTS: During a follow-up duration of 14 months in average with a range of 5 to 21 months, 33 patients (50.8 %) were free of tumors, 22 patients (33.8 %) alive with tumor recurrence: two had bone metastases, three were found to have lung metastases, and the remaining 17 recurrences occurred in the liver, of whom only 3 developed a cryosite recurrence. Among the 41 patients who were followed up for more than one year, 32 (78 %) were alive despite of tumor recurrence. Seven patients (10.8 %) died due to disease recurrence. Three patients (4.6 %) died due to some noncancer-related causes. Among the 43 patients who had a CT scan available for review, 38 (88.4 %) had a shrinkage of tumor mass. Among the 22 patients who received biopsies of cryoablated tumor mass, all biopsies except one, showed only dead or scar tissues. Of the patients who had an increased AFP preablatively, 91.3 % had a decrease of AFP to normal or nearly normal levels during postablation 3-6 months. Complications of cryoablation included liver capsular cracking in one patient, transient thrombocytopenia in 4 patients and asymptomatic right-sided pleural effusions in 2 patients. Two patients developed liver abscess at the previous cryoablation site at 2 and 4 months, respectively, following cryoablation, and was recovered after treated with antibiotics and drainage.

CONCLUSION: Percutaneous cryoablation offers a safe and possibly curative treatment option for patients with HCC that cannot be surgically removed, and its integration with PEI, may serve as an alternative to partial liver resection in selective patients.

Xu KC, Niu LZ, He WB, Guo ZQ, Hu YZ, Zuo JS. Percutaneous cryoablation in combination with ethanol injection for unresectable hepatocellular carcinoma. *World J Gastroenterol* 2003; 9(12): 2686-2689

<http://www.wjgnet.com/1007-9327/9/2686.asp>

INTRODUCTION

Hepatocellular carcinoma (HCC) is one of the most common and lethal cancers. Curative surgical resection of HCC is considered to be the optimal treatment. Unfortunately, only about 10 % of newly diagnosed HCC patients are eligible candidates for resection^[1]. Therefore, alternative treatment modalities have been developed, including localized ablative techniques involving either freezing (cryoablation) or chemical desiccation (ethanol ablation)^[2].

Cryoablation uses extremely low temperature to destroy tumor tissues, and has been shown to be as effective as surgical resection for treatment of primary or metastatic liver cancer^[3]. Percutaneous ethanol injection (PEI) has been reported to be effective against small HCC, but is not eligible for advanced HCC^[4]. We employed percutaneous cryoablation in combination with ethanol injection following cryoablation for treatment of unresectable HCC and yielded better results. This paper reports our experience using the combined therapy in 65 HCC patients and evaluates the effectiveness and safety.

MATERIALS AND METHODS

Subjects

Between March 2001 and January 2003, 65 HCC patients underwent combined treatment of percutaneous hepatic cryoablation and PEI. There were 47 men and 18 women. Their ages ranged from 32 to 78 years, with a mean age of 51 years. Sixty patients had histories of hepatitis B infection, and 4 had hepatitis C infection. Informed consents were obtained from all patients undergoing combined therapy.

The diagnosis of HCC in 43 patients was proven by liver pathology, and the remaining cases had HCC diagnosed by classical imagings, including computed tomography (CT), magnetic resonance and ultrasonography, and biochemical markers, such as increased alpha-fetoprotein (AFP). Forty-four patients had only one mass in the liver, being 4.8 cm to 15 cm in diameter with an average of 7.3 cm. Twenty-one patients had 2-4 masses from 6 cm to 14 cm in diameter. There were a total of 105 masses in 65 patients and the average number of masses per patient was 2.6. No patient had evidence of extrahepatic metastases.

All except 2 cases had cirrhosis. Using Child-Pugh's score in assessing the severity of cirrhosis, 39 patients were classified as class A, and 25 as class B.

Cryoablation procedure

The cryoablation was performed with the Cryocare system (Endocare, Irvine, CA, USA) using argon gas as a cryogen.

Cryoprobes (3, 5 or 8 mm) were inserted into the center of tumor mass under ultrasonographic guidance, and two freeze-thaw cycles were performed, each reaching a temperature of -180°C at the tip of the probe. The time of freezing was dependent on the achievement of an “ice ball”, visible as a hypoechoic region by ultrasonography. Generally, the tumor was frozen at a maximum flow rate for about 15 minutes, thawed for 5 minutes and then refrozen for another 15 minutes. A margin of at least 1 cm normal hepatic tissue was frozen circumferentially around the tumor. For the mass larger than 5 cm in diameter, two or three cryoprobes were placed within the center and periphery of tumor respectively, to insure freezing of the entire tumor. Finally, the cryoprobe was removed when the tip temperature reached above 0°C , and the tract formed was sealed off with fibrin glue immediately after removal of the cryoprobe to ensure haemostasis.

Alcohol ablation

PEI was administered in 36 patients with tumor masses larger than 6 cm in diameter and was given 1-2 weeks after cryoablation and then once a week for up to 4-6 sessions. Absolute alcohol (100 %) was slowly injected into the peripheral zone of cancerous tissues in liver through a 20-gauge needle under ultrasonographic guidance. The goal of this procedure was to achieve a “black stain” shown by ultrasonography in the tumor tissues. A maximum of 5 ml alcohol was injected per site, with a maximum of 20 ml per session.

Postoperative follow-up

All patients were followed up at monthly intervals. The serum α -fetoprotein (AFP) levels were assayed during each visit. The first CT scanning was performed within one month after cryoablation to detect residual tumor, and then CT scan study was done every 3 months in the initial six months and every 6 months subsequently to detect recurrence.

RESULTS

Disease status and survival

All patients were followed up for a median duration of 14 months with a range of 5-21 months. The disease status of the patients is shown in Table 1. Thirty-three patients (50.8 %) were currently free of tumor with an average follow-up of 13.8 months. Twenty-two patients (33.8 %) were alive with disease recurrence: two had bone metastases, three were found to have lung metastases, and the remaining 17 had recurrences in the liver, of whom only 3 developed a cryosite recurrence. Among the 41 patients who were followed up for more than one year, 32 (78 %) were alive despite of tumor recurrence. Seven patients (10.8 %) died from their tumors, and had recurrence of tumor in the liver remnant at a mean of 7.8 months with an overall survival of 13.2 months. Three patients (4.6 %) died of noncancer-related causes. One died of myocardial infarction, 1 died of pneumonia, and 1 died of liver failure, respectively.

Table 1 Disease status

	Number of patients	Percent of patients	Follow-up (months)
Alive free of tumor	33	50.8	16.8
Alive with tumor recurrence	22	33.8	17.2
Died of tumor recurrence	7	10.8	13
Died of noncancer-related diseases	3	4.6	4

Tumor size

Among the forty-three patients who had a CT scan available

for review, 38 (88.4 %) had a shrinkage of tumor mass, with an average size of the dominant tumor changing from a preablative size of 7.9 cm (3.7-13.2 cm) to a 3-month postablative size of 5.6 cm (2.1-8 cm). Twenty-two received biopsies of their cryoablated tumor mass under ultrasonography guidance. All biopsies except one, showed only dead or scar tissues.

Serum AFP levels

An increased serum AFP, with a median level of 367 ng/L, ranging from 68 to 1 210 ng/L, was detected in 46 patients preablative. The AFP levels were lowered to normal or nearly normal range in 42 patients (91.3%) during postablative 3-6 months, and the median AFP level was 59 ng/L with a range of 12-365 ng/L.

Complications

Complications of cryoablation included liver capsular cracking in one patient and recovered after blood transfusion. Transient thrombocytopenia occurred in 4 patients within 1 week following cryoablation, 2 of whom received platelet transfusion. Two patients developed asymptomatic right-sided pleural effusions, both had cancer in the right lobe which was close to the dome of the diaphragm. The pleural effusions disappeared spontaneously within 2-3 weeks. Two patients developed liver abscess at the previous cryoablation site 2 and 4 months respectively following cryoablation, and were recovered after antibiotics and drainage treatment.

The majority of patients receiving PEI had pain at injection site, fever and a feeling of alcohol intoxication, which were transient and subsided with conservative management. No patient experienced an appreciable risk.

DISCUSSION

Prognosis of unresectable HCC is very poor. In Japan, the median survival for 229 patients receiving no specific treatment was 1.6 months^[5]. Although chemoembolization is associated with good objective responses in the tumor, a recent controlled trial showed that by itself, chemoembolization offered no improvement in survival compared with supportive therapy alone^[6]. During the past years, great efforts have been made to improve the survival of patients with this disease^[7]. In this trial, percutaneous cryoablation in combination with PEI showed more satisfactory therapeutic efficacy. Among the 65 HCC patients receiving this combined therapy and followed up for a median duration of 14 months, 50.8 % of the patients are currently free of tumor and 33.8 % are alive with tumor recurrences. Among the 41 patients who were followed up for more than one year, 78 % are alive despite of tumor recurrence. Only 10.8 % died from tumor recurrence with an overall survival for 13.2 months. Of the patients who had CT scan available for review, 88.4 % had a shrinkage of tumor masses. Of the 22 patients who received biopsies of their cryoablated tumor masses, all but one showed only dead tumor cells or scar. Of the patients who had an increased AFP preablative, 91.3 % had a decrease of AFP to normal or nearly normal levels during postablative 3-6 months.

The present result is comparable with those by other authors. Crews *et al*^[8] reported that forty patients with hepatic malignancy underwent cryoablation and the estimated 18-month survival was 60 % and 30 % for patients with HCC and with colorectal metastasis, respectively. Lam *et al*^[9] treated 4 patients with recurrent HCC after previous curative hepatectomy with cryoablation. All their patients are still alive with a survival after cryoablation ranging from 12 to 23 months. Sheen *et al*^[10] have demonstrated that the median survival for HCC patients after cryoablation was 36 months. Zhou *et al*^[11,12]

reported 1-, 3- and 5-year survival rates of 78 %, 54 % and 40 %, respectively in 235 HCC patients who received cryoablation. It should be noted that the cryoablation reported by these authors was mainly performed through intraoperative approach with a large invasion, while in the present trial, cryoablation was performed percutaneously, being minimally invasive and allowing for a rapid recovery.

Cryoablation is a method of *in situ* tumor ablation. A circulated cryogen is used to target tumors to induce irreversible tissue destruction at a temperature below 40 °C. Tumor cell death is caused by both direct and indirect mechanisms. The direct cellular damage is a result of intra- and extra-cellular ice crystal formation and solute-solvent shifts, which induce cell dehydration and rupture. The indirect effect was found to be resulted from the vessel obliteration which would result in ischemic hypoxia^[13,14].

As a local therapy, cryoablation has been found to carry certain advantages over other forms of HCC treatment^[15]. First, it is able to destroy only the tumor tissue in liver sparing more noninvolved tissues, which is of important significance to HCC patients, because the majority of these patients would be found to have cirrhosis and decreased reserve of liver function^[16]. Second, because of the warming effect of flowing blood, large blood vessels, such as inferior vena cava and portal vein, are somewhat imperious to the effect of freezing. Therefore, tumors close to these venous systems could safely undergo cryoablation, whereas resection of tumors close to large vascular structures would be very difficult^[17]. Third, it is known that liver cirrhosis is a basis of HCC development, if the entire liver is cirrhotic, any part of the liver can develop new tumors. Liver cryoablation has been found to be more effective than surgical resection in treating multiple new tumors^[13]. Fourth, in contrast with other local ablations, such as radiofrequency, which are difficult to reliably destroy tumors greater than 5 cm in diameter, cryoablation would be a promising means for the treatment of this larger form of tumor^[2]. Lastly, the rapid freeze-thaw process could enhance necrosis and help induce an immune response against the surviving tumor cells^[18].

During cryoablation, freezing would occur in three main areas: (1) The center of iceball near the cryoprobe, where freezing would be rapid and the temperature would be lowest. (2) The middle of the iceball, where the tissue experienced intermediate cooling rate. (3) The periphery of the iceball, where slow rates of cooling would occur^[18]. The cytotoxic effect from rapid cooling was the greatest in the center of the iceball, while cells at the periphery of the iceball might survive, particularly if the tumor abutted a large intrahepatic blood vessel that abrogated the effects of tissue cooling. The surviving tumor cells would result in recurrence of the disease. PEI has been used extensively for treatment of HCC. Ethanol could diffuse into the tumor cells and cause nonselective protein denaturation and cellular dehydration, leading to coagulated necrosis. Subsequent fibrosis and small vessel thrombosis would also contribute to cellular death. Therefore, after cryoablation which could destroy the majority of tumors, PEI used at periphery of tumor could destroy residue tumor tissues. It is obvious that cryoablation in combination with PEI had a complementary effects on preventing recurrence^[18]. In this series, PEI was given to 36 patients with tumor masses larger than 6 cm in diameter 1-2 weeks after cryoablation, that might be contributory to a better outcome. Moreover, among the 17 patients who had recurrent tumors, only 3 had recurrence at the original cryosite, suggesting that the effectiveness of this combined therapy was good.

Cryoablation has been considered as a safe modality^[10]. Transient intra-ablative hypothermia is the most common side effects. The use of warming blankets and fluid warmers has

been proven beneficial. Transient thrombocytopenia and hypoglycemia have been observed. Patients should be observed for possible coagulopathy when large tumor (greater than 5 cm) has been frozen. Pleural effusions may occur in tumor mass treated close to the dome of the diaphragm. Cracking of the hepatic capsule might occur during the thawing process^[13,17,19], which was seen in one patient in this series. It is one of the most serious complications of hepatic cryoablation, and could be controlled with conservative therapies for most of the cases. Cryoshock manifested as varying degrees of acute renal failure, disseminated intravascular coagulation and adult respiratory distress syndrome, was reported^[15]. It has been shown that cryoshock occurred in greater than 40 % of the volume of tissue treated, and lesions over 6 cm were associated with a greater risk^[17]. However, lesions up to 10 cm in size were treated safely in the present series. This complication might be related more to the total duration of cryoablation than to the volume of tumor tissue treated^[10]. Nevertheless, it is necessary to prevent the disastrous complication. Diuresis with mannitol and alkalization of urine should be used in all patients to avoid myoglobinuria and subsequent renal damage^[8]. PEI has been proven safe, and no significant complication was associated with this modality in the present series.

In conclusion, this technique offers the curative treatment option for HCC that cannot be surgically removed due to the anatomic location of the tumor, and the presence of other comorbid conditions that would otherwise preclude a major liver resection. Percutaneous approach has the advantage of a minimal invasion and allows for a rapid recovery and does not produce appreciable complications. The integration of this technique with other adjuvant regional modalities, especially PEI, may be used as an alternative to resection, so as to improve a long-term disease-free survival in selected patients.

REFERENCES

- 1 **Staley CA.** Surgical therapy of hepatic tumors. In: Zakim D and Boyer TD, eds. *Hepatology. A Textbook of Liver Disease.* Philadelphia: Saunders 2003: 1371-1381
- 2 **Adam R,** Hagopian EJ, Linhares M, Krissat J, Savier E, Azoulay D, Kunstlinger F, Castaing D, Bismuth H. A comparison of percutaneous cryosurgery and percutaneous radiofrequency for unresectable hepatic malignancies. *Arch Surg* 2002; **137**: 1332-1339
- 3 **Onik GM,** Atkinson D, Zemel R, Weaver ML. Cryosurgery of liver cancer. *Semin Surg Oncol* 1993; **9**: 309-317
- 4 **Gournay J,** Tchuente J, Richou C, Masliah C, Lerat F, Dupas B, Martin T, Nouel JF, Schnee M, Montigny P, D'Alincourt A, Hamy A, Paineau J, Le Neel JC, Le Borgne J, Galmiche JP. Percutaneous ethanol injection vs. resection in patients with small single hepatocellular carcinoma: a retrospective case-control study with cost analysis. *Aliment Pharmacol Ther* 2002; **16**: 1529-1538
- 5 **Okuda K,** Ohtsuki T, Obata H, Tomimatsu M, Okazaki N, Hasegawa H, Nakajima Y, Ohnishi K. Natural history of hepatocellular carcinoma and prognosis in relation to treatment. Study of 850 patients. *Cancer* 1985; **56**: 918-928
- 6 **Groupe d' Etude et de Traitement du Carcinome Hepatocellulaire.** A comparison of lipiodol, chemoembolization and conservative treatment for unresectable hepatocellular carcinoma. *N Engl J Med* 1995; **332**: 1256-1261
- 7 **Lau WY,** Leung TW, Yu SC, Ho SK. Percutaneous local ablative therapy for hepatocellular carcinoma: a review and look into the future. *Ann Surg* 2003; **237**: 171-179
- 8 **Crews KA,** Kuhn JA, McCarty TM, Fisher TL, Goldstein RM, Preskitt JT. Cryosurgical ablation of hepatic tumors. *Am J Surg* 1997; **174**: 614-618
- 9 **Lam CM,** Yuen WK, Fan ST. Hepatic cryoablation for recurrent hepatocellular carcinoma after hepatectomy: a preliminary report.

- J Surg Oncol* 1998; **68**: 104-106
- 10 **Sheen AJ**, Poston GJ, Sherlock DJ. Cryotherapeutic ablation of liver tumours. *Br J Surg* 2002; **89**: 1396-1401
 - 11 **Zhou XD**, Tang ZY, Yu YQ, Ma ZC. Clinical evaluation of cryosurgery in the treatment of primary liver cancer. Report of 60 cases. *Cancer* 1988; **61**: 1889-1892
 - 12 **Zhou XD**, Tang ZY, Yu YQ, Weng JW, Ma ZC, Zhang BH, Zheng YX. The role of cryosurgery in the treatment of hepatic cancer: areport of 113 cases. *J Cancer Res Clin Oncol* 1993; **120**: 100-102
 - 13 **Ross WB**, Horton M, Bertolino P, Morris DL. Cryotherapy of liver tumours-a practical guide. *HPB Surg* 1995; **8**: 167-173
 - 14 **Erce C**, Parks RW. Interstitial ablative techniques for hepatic tumours. *Br J Surg* 2003; **90**: 272-289
 - 15 **Shafir M**, Shapiro R, Sung M, Warner R, Sicular A, Klipfel A. Cryoablation of unresectable malignant liver tumors. *Am J Surg* 1996; **171**: 27-31
 - 16 **Bilchik AJ**, Sarantou T, Wardlaw JC, Ramming KP. Cryosurgery causes a profound reduction in tumor markers in hepatoma and noncolorectal hepatic metastases. *Am Surg* 1997; **63**: 796-800
 - 17 **Seifert JK**, Morris DL. Indicators of recurrence following cryotherapy for hepatic metastases from colorectal cancer. *Br J Surg* 1999; **86**: 234-240
 - 18 **Wong WS**, Patel SC, Cruz FS, Gala KV, Turner AF. Cryosurgery as a treatment for advanced stage hepatocellular carcinoma: results, complication, and alcohol ablation. *Cancer* 1998; **82**: 1268-1278
 - 19 **Dwerryhouse SJ**, Seifert JK, McCall JL, Iqbal J, Ross WB, Morris DL. Hepatic resection with cryotherapy to involved or inadequate resection margin (edge freeze) for metastases from colorectal cancer. *Br J Surg* 1998; **85**: 185-187

Edited by Ma JY and Wang XL

• COLORECTAL CANCER •

Comparative evaluation of immune response after laparoscopic and open total mesorectal excisions with anal sphincter preservation in patients with rectal cancer

Jian-Kun Hu, Zong-Guang Zhou, Zhi-Xin Chen, Lan-Lan Wang, Yong-Yang Yu, Jin Liu, Bo Zhang, Li Li, Ye Shu, Jia-Ping Chen

Jian-Kun Hu, Zong-Guang Zhou, Zhi-Xin Chen, Yong-Yang Yu, Bo Zhang, Li Li, Ye Shu, Jia-Ping Chen, Department of General Surgery and Institute of Digestive Surgery, West China Hospital, Sichuan University, Chengdu 610041, Sichuan Province, China
Lan-Lan Wang, Jin Liu, Laboratory of Clinical Immunology, West China Hospital, Sichuan University, Chengdu 610041, Sichuan Province, China

Supported by the Key Project of National Outstanding Youth Foundation of China, No. 39925032

Correspondence to: Zong-Guang Zhou, Department of General Surgery and Institute of Digestive Surgery, West China Hospital, Sichuan University, Chengdu 610041, Sichuan Province, China. zhou767@21cn.com

Telephone: +86-28-85422479 **Fax:** +86-28-85422484

Received: 2003-05-12 **Accepted:** 2003-06-02

Abstract

AIM: The study of immune response of open *versus* laparoscopic total mesorectal excision with anal sphincter preservation in patients with rectal cancer has not been reported yet. The dissected retroperitoneal area that contacts directly with carbon dioxide is extensive in laparoscopic total mesorectal excision with anal sphincter preservation surgery. It is important to clarify whether the immune response of laparoscopic total mesorectal excision with anal sphincter preservation (LTME with ASP) in patients with rectal cancer is suppressed more severely than that of open surgery (OTME with ASP). This study was designed to compare the immune functions after laparoscopic and open total mesorectal excision with anal sphincter preservation for rectal cancer.

METHODS: This study involved 45 patients undergoing laparoscopic ($n=20$) and open ($n=25$) total mesorectal excisions with anal sphincter preservation for rectal cancer. Serum interleukin-2 (IL-2), interleukin-6 (IL-6), tumor necrosis factor α (TNF α) were assayed preoperatively and on days 1 and 5 postoperatively. CD3 $^{+}$ and CD56 $^{+}$ T lymphocyte count, CD3 $^{-}$ and CD56 $^{+}$ natural killer cell (NK) count and immunoglobulin (IgG/IgM/IgA) were assayed preoperatively and on day 5 postoperatively. The numbers of CD3 $^{+}$ and CD56 $^{+}$ T lymphocytes and CD3 $^{-}$ and CD56 $^{+}$ NK cells were counted using flow cytometry. An enzyme-linked immunosorbent assay (ELISA) was used for IL-2, IL-6 and TNF α determination. And IgG, IgM, and IgA were assayed using immunonephelometry.

RESULTS: The demographic data of the two groups had no difference. The preoperative levels of CD3 $^{+}$ and CD56 $^{+}$ T lymphocyte count, CD3 $^{-}$ and CD56 $^{+}$ NK count, serum IgG, IgM, IgA, IL-2, IL-6 and TNF α also had no significant difference in the two groups ($P>0.05$). The CD3 $^{+}$ and CD56 $^{+}$ T lymphocyte counts had no obvious changes after surgery in laparoscopic ($d=-0.79\pm3.83\%$) and open ($d=0.42\pm2.09\%$) groups. The CD3 $^{-}$ and CD56 $^{+}$ NK counts were decreased

postoperatively in both laparoscopic ($d=-7.23\pm11.33\%$) and open ($d=-9.21\pm13.93\%$) groups. The differences of the determined values of serum IgG, IgM and IgA on the fifth day after operation subtracted those before operation were -2.56 ± 2.14 g/L, -252.35 ± 392.94 mg/L, -506.15 ± 912.24 mg/L in laparoscopic group, and -1.81 ± 2.10 g/L, -282.72 ± 356.75 mg/L, -252.20 ± 396.28 mg/L in open group, respectively. The levels of IL-2 were decreased after operation in both groups. However, the levels of IL-6 were decreased after laparoscopic surgery ($d_1=-23.14\pm263.97$ ng/L and $d_5=-40.08\pm272.03$ ng/L), and increased after open surgery ($d_1=27.38\pm129.14$ ng/L and $d_5=21.67\pm234.31$ ng/L). The TNF α levels were not elevated after surgery in both groups. There were no significant differences in the numbers of CD3 $^{+}$ and CD56 $^{+}$ T lymphocytes and CD3 $^{-}$ and CD56 $^{+}$ NK cells, the levels of IgG, IgM, IgA, IL-2, IL-6 and TNF α between the two groups ($P>0.05$).

CONCLUSION: There are no differences in immune responses between the patients having laparoscopic total mesorectal excision with anal sphincter preservation and those undergone open surgery for rectal cancer.

Hu JK, Zhou ZG, Chen ZX, Wang LL, Yu YY, Liu J, Zhang B, Li L, Shu Y, Chen JP. Comparative evaluation of immune response after laparoscopic and open total mesorectal excisions with anal sphincter preservation in patients with rectal cancer. *World J Gastroenterol* 2003; 9(12): 2690-2694

<http://www.wjgnet.com/1007-9327/9/2690.asp>

INTRODUCTION

General anesthesia, major surgery, and severe trauma are all known to cause significant inhibition of the immune response^[1]. The immunosuppression associated with major surgery is believed to contribute to the increased risk of metastasis and sepsis in the postoperative period^[1]. In order to improve the immune response of postoperative patients, minimally invasive surgery has been performed. Reduced hospital stay, less wound pain, earlier resumption of diet and recovery of bowel function are recognized as benefits of laparoscopic cholecystectomy or colectomy^[2]. The effects of laparoscopic colorectal surgery on the immune system varied from study to study. Meanwhile, study on immune response of open *versus* laparoscopic total mesorectal excision with anal sphincter preservation in patients with rectal cancer has not been reported yet. The dissected retroperitoneal area that contacts directly with carbon dioxide is extensive in laparoscopic total mesorectal excision with anal sphincter preservation surgery. It is important to clarify whether the immune response of laparoscopic total mesorectal excision with anal sphincter preservation (LTME with ASP) in patients with rectal cancer is suppressed more severely than that of open surgery (OTME with ASP). The aim of this nonrandomized prospective study was to compare the effects of LTME and OTME on immune response.

MATERIALS AND METHODS

Patients selection

From October 2001 to July 2002, 49 patients admitted to the General Surgery Department of West China Hospital with the diagnosis of rectal cancer confirmed by pathology were prospectively evaluated. The criterion for inclusion in the study was patients diagnosed with biopsy as adenocarcinoma of the rectum localized below 15 cm from the anal margin. The criteria for exclusion included age older than 80 years and younger than 18 years, presence of a fixed palpable mass or cancer infiltrating adjacent organs, evidence of metastatic disease, neoadjuvant chemoradiotherapy, severe cardiovascular (New York Heart Association class 3 or more) or respiratory dysfunction, patients with previous abdominal operation, acute intestinal obstruction or perforation, any malignancy within the recent 5 years, synchronous multiple adenocarcinomas and pregnancy, any contraindication to pneumoperitoneum, and patients with unresectable tumor.

Preoperative examinations including flexible endoscopy as well as biopsy, ultrasonography, computed tomography scan, radiography of the chest, etc. were routinely performed. All patients underwent preoperative bowel preparation (1L 10 % mannite electrolyte solution). Prophylactic antibiotics of ciprofloxacin and metronidazole were routinely given orally for three days before operation. A urinary catheter and a nasogastric tube were routinely used.

Data collection

The parameters measured were demographic data, operating time, distance of the tumor from the anal margin, time of first passing flatus, time removing urinary catheter, duration of hospital stay, postoperative complications and death. Demographic data included age, sex, serum total protein (TP), albumin (Alb), hemoglobin (Hb), weight, and underlying diseases.

Operation techniques

All patients were administrated general anesthesia and operations were carried out in lithotomy position with 15° head-down tilt. Premedication and anesthetic techniques were standardized. Induction was made by intravenous injection of 3-5 mg/kg thiopentone together with fentanyl. Anesthesia was maintained by ventilation with an O₂/N₂O mixture and isoflurane. Operations were performed by surgeons experienced in both laparoscopic and conventional surgeries. The rectal surgery was performed according to the principle of total mesorectal excision (TME)^[3,4]. Our laparoscopic techniques were reported previously^[5].

Pneumoperitoneum was introduced through subumbilical incision to maintain the pressure at 12-14 mmHg (1 mmHg=0.133 kPa). Camera port with subumbilical trocar was first created, then one operative port in the right midclavicular line at the level of umbilicus, and other two operative ports in the left and right McBurney point were also created respectively under the guidance of laparoscopic view to facilitate dissection. A laparoscope with 25 or 30 curvy degree was inserted into the abdominal cavity via a subumbilical trocar, following the no-touch technique. Routine exploration was performed to ascertain whether the tumor metastasized to the organs in the abdominal cavity and infiltrated the serosa or implanted in the abdominal cavity. With the operation proceeding of total mesorectal excision, division was moved downward into the pelvis along the anatomic space between visceral and parietal endopelvic fascia. In order to extract the bowel loop of the tumor, the port at the left McBurney's point was extended to about 3.5 cm long, the tumor was routinely isolated by inserting it into a sheath-shaped bacteria-free plastic bag through the

incision, and the tumor as well as the proximal colon were extracted through the bag, and then the bowel was transected at the level of 10-15 cm above upper margin of the tumor. After the anvil of a 29 mm-sized circular stapler was inserted into the end of the proximal bowel and secured with 2/0 prolene purse-string suture, the proximal bowel was internalized and the extended incision was closed. Pneumoperitoneum was then induced again, and laparoscopic colo-anal or colo-rectal anastomosis was performed using a CDH 29 circular stapler.

Immunological studies

Seven milliliters of venous blood were taken by peripheral venipuncture before surgery and on days 1 and 5 after surgery into one plain vacutainer and one heparin vacutainer. The specimens were centrifuged and the collected serum was stored at -20 °C for the assay of interleukin-2 (IL-2), interleukin-6 (IL-6) and tumor necrosis factor α (TNF α). IL-2, IL-6 and TNF α were assayed preoperatively and on days 1 and 5 postoperatively. CD3⁺ and CD56⁺ T lymphocyte count, CD3⁺ and CD56⁺ natural killer cell (NK) count and immunoglobulin (IgG/IgM/IgA) were determined preoperatively and on day 5 postoperatively. The numbers of CD3⁺ and CD56⁺ T lymphocytes and CD3⁺ and CD56⁺ NK cells were counted using flow cytometry (Elite-Esp, Beckman-Coulter, USA). An enzyme-linked immunosorbent assay (ELISA) was used for IL-2, IL-6 and TNF α determination (Bio-Rad system, Immune Company, France), and immunoglobulin (Ig) G, IgM, and IgA were assayed using immunonephelometry (Image analyzer, Beckman-Coulter, USA).

Statistics analysis

All the data were collected on designed forms, and analyzed with SPSS version 10.0 software. The differences of the determined values on fifth or first postoperative day subtracted those before operation were compared between laparoscopic and open groups. Student's *t* test was used for quantitative variables and chi-square test for qualitative variables. All *P* values were two sided. Statistical significance was established as *P*<0.05. The data were expressed as mean \pm standard deviation (SD).

RESULTS

A total of 49 patients were entered into the study. Four patients did not meet the eligibility criteria for the trial (three in laparoscopic group and one in open). Three were found to have hepatic metastasis and one did not receive resection because the cancer infiltrated several adjacent organs.

Patient characteristics

The demographic features of the patients are shown in Table 1. The two groups had no differences with respect to age, gender, TP, Alb, Hb, weight and Duke's classification (*P*>0.05).

Surgical treatment

Table 2 shows the results of the two treatments. All the 45 patients received the curative anterior resection with total mesorectal excision, and the low/ultralow/colo-anal anastomosis was performed by laparoscopic or open surgery. In laparoscopic group, no one required conversion to open surgery.

There was no surgical death in both groups. Operation time was significantly longer in the laparoscopic group than that in the open group (226.75 \pm 46.15 min *versus* 146.40 \pm 38.09 min, *P*<0.05). The time of first passing flatus in laparoscopic group was significantly shorter than that in the open group (3.15 \pm 1.14 min *versus* 4.36 \pm 1.19 min, *P*<0.05). There were

no differences in time of removing urinary catheter, duration of hospital stay and distance of tumor from anal margin between the two groups ($P>0.05$).

The two groups of patients had comparable preoperative underlying diseases. As for the postoperative complications, one patient in the open group had anastomotic leakage and one in the same group experienced wound infection, both of them were successfully treated conservatively. There was no postoperative complication in the laparoscopic group. There were no local recurrence, port site recurrence, and mortality in any patients observed during follow-up ranged from 8 to 17 months.

Table 1 Demographic and clinical characteristics of patients (mean \pm SD)

	LTME $n=20$	OTME $n=25$	P value
Age (year)	61.60 \pm 8.44	57.96 \pm 10.70	0.213
Sex (n)			>0.05
M	9	16	
F	11	9	
TP (g/L)	69.36 \pm 5.14	71.55 \pm 8.23	0.298
Alb (g/L)	41.70 \pm 4.16	43.36 \pm 4.49	0.199
Hb (g/L)	123.05 \pm 14.43	125.18 \pm 15.14	0.627
Weight (kg)	58.45 \pm 7.86	59.88 \pm 10.85	0.619
Duke's classification (n)			>0.05
A	10	6	
B	4	7	
C ₁	3	7	
C ₂	3	5	
Underlying diseases (n)			>0.05
Diabetes mellitus	1	0	
Hypertension	1	1	
Anemia	0	2	

Table 2 Surgical treatment of patients

	LTME $n=20$	OTME $n=25$	P value
Operating time (min)	226.75 \pm 46.15	146.40 \pm 38.09	0.000 ^b
Time of first passing flatus (day)	3.15 \pm 1.14	4.36 \pm 1.19	0.001 ^b
Time of removing urinary catheter (day)	7.35 \pm 2.18	6.28 \pm 1.59	0.065
Duration of hospital stay (day)	18.30 \pm 4.28	18.04 \pm 5.47	0.863
Distance of tumor from anal margin (cm)	8.35 \pm 3.72	7.00 \pm 3.93	0.247

^b $P<0.01$ vs open group.

Immune response

As expected, the preoperative levels of CD3⁺ and CD56⁺ T lymphocyte count, CD3⁺ and CD56⁺ NK count, serum IgG, IgM, IgA, IL-2, IL-6 and TNF α had no difference in the two groups (Table 3, $P>0.05$).

Table 3 Preoperative immune indicators of two groups (mean \pm SD)

	LTME $n=20$	OTME $n=25$	P value
CD3 ⁺ CD56 ⁺ T (%)	4.56 \pm 5.08	3.74 \pm 4.19	0.556
CD3 ⁺ CD56 ⁺ NK (%)	20.87 \pm 13.76	25.41 \pm 16.79	0.335
IgG (g/L)	11.50 \pm 2.41	12.61 \pm 2.90	0.178
IgM (mg/L)	1 407.40 \pm 420.27	1 582.40 \pm 735.41	0.350
IgA (mg/L)	2 726.40 \pm 2 048.28	2 380.16 \pm 928.99	0.454
IL-2 (ng/L)	85.20 \pm 303.81	128.30 \pm 387.12	0.686
IL-6 (ng/L)	88.70 \pm 231.52	49.06 \pm 81.63	0.429
TNF α (ng/L)	7.69 \pm 5.71	12.99 \pm 26.61	0.387

Table 4 shows the differences of the values of IL-2, IL-6 and TNF α on the fifth or first postoperative day subtracted those before operation, respectively. The TNF α levels were not elevated after surgery, and there were no significant differences between the two groups ($P>0.05$). However, the levels of IL-6 were decreased after laparoscopic surgery ($d_1=-23.14\pm263.97$ ng/L and $d_5=-40.08\pm272.03$ ng/L), but there were no significant differences between the laparoscopic and open groups ($P>0.05$). The levels of IL-2 were decreased after operation in both groups, the differences were no significant in postoperative days between the two groups ($P>0.05$).

Table 4 Changes of IL-2, IL-6 and TNF α after surgery in two groups (mean \pm SD)

		LTME $n=20$	OTME $n=25$	P value
IL-2(ng/L)	d_1	-80.54 \pm 304.30	-98.82 \pm 412.38	0.869
	d_5	-27.55 \pm 344.29	-33.59 \pm 560.20	0.967
IL-6(ng/L)	d_1	-23.14 \pm 263.97	27.38 \pm 129.14	0.405
	d_5	-40.08 \pm 272.03	21.67 \pm 234.31	0.418
TNF α (ng/L)	d_1	2.23 \pm 12.78	-1.01 \pm 7.82	0.301
	d_5	1.84 \pm 12.84	0.56 \pm 9.86	0.705

(d_1 =the differences of the values of IL-2, IL-6 and TNF α on the first postoperative day subtracted those before operation, respectively. d_5 = the differences of the values of IL-2, IL-6 and TNF α on the fifth postoperative day subtracted those before operation, respectively).

Table 5 shows the differences of the values of CD3⁺ and CD56⁺ T lymphocyte count, CD3⁺ and CD56⁺ NK count, and serum IgG, IgM, and IgA on the fifth postoperative day from those before operation, respectively. There were no significant differences of CD3⁺ and CD56⁺ T lymphocyte count, CD3⁺ and CD56⁺ NK count, and serum IgG, IgM, and IgA levels after surgery between the two groups ($P>0.05$).

Table 5 Changes of CD3⁺ CD56⁺ T lymphocyte count, CD3⁺ CD56⁺ NK count, and serum immunoglobulin after surgery in two groups (mean \pm SD)

	LTME $n=20$	OTME $n=25$	P value
CD3 ⁺ CD56 ⁺ T lymphocyte (%)	-0.79 \pm 3.83	0.42 \pm 2.09	0.214
CD3 ⁺ CD56 ⁺ NK (%)	-7.23 \pm 11.33	-9.21 \pm 13.93	0.609
IgG (g/L)	-2.56 \pm 2.14	-1.81 \pm 2.10	0.248
IgM (mg/L)	-252.35 \pm 392.94	-282.72 \pm 356.75	0.787
IgA (mg/L)	-506.15 \pm 912.24	-252.20 \pm 396.28	0.216

Numbers listed were the differences of the values of CD3⁺ CD56⁺ T lymphocyte count, CD3⁺ CD56⁺ NK count, and serum IgG, IgM, IgA on the fifth postoperative day subtracted those before operation, respectively.

DISCUSSION

Rectal cancer is the common malignance in our country. Studies on rectal cancer have made great progresses both in clinical practice^[6-15] and in theoretical basis^[16-26] during the latest years. Multiple clinical studies have demonstrated the correlation of high pelvic recurrence with the degree of mesorectal excision^[27]. Residual mesorectum, especially inadequate excision of distal mesorectum (DMR), contributed to poor oncologic outcomes. In order to reduce the rate of local recurrence in the pelvis of rectal carcinoma, total mesorectal excision (TME) has been performed in many colorectal surgery centers. TME has been applied in clinical practice, and the local recurrence rate has decreased dramatically to 5-7.1 %^[28,29],

while the mean local recurrence rate of conventional operative procedure for treatment of rectal cancer remained 18.5 %. TME has been claimed to improve not only local recurrence rate, but also long term survival^[30-34]. With the improvement of laparoscopic technique, laparoscopic colorectal surgery has been attempted in many countries^[4,35-39]. The laparoscopic colorectal surgery has been proposed to be less traumatic than open surgery. It has been demonstrated that laparoscopic-assisted colectomy has many advantages during immediate postoperative period over the open colectomy with regard to the disappearance of postoperative ileus, fewer analgesia, early ambulation, less postoperative complications, and shorter hospital stay^[4,35-39]. In this study, the time of first flatus in the laparoscopic group was significantly shorter than that in the open group.

Some randomised clinical trials of open versus laparoscopically assisted colectomy on systematic immunity in patients with colorectal cancer have been performed. Delgado *et al*^[40] found that the plasma levels of cortisol and prolactin were higher in postoperative period, but no significant differences were observed between both groups of the patients. The level of interleukin-6 was higher with significant differences at 4, 12 and 24 hours in the patients undergone open colectomy than that in laparoscopic group. The plasma level of C-reactive protein (CRP) was significantly lower at 72 hours in patients receiving laparoscopic-assisted colectomy than that in patients receiving open one. They suggested that acute phase systematic response was attenuated in patients undergone laparoscopic-assisted colectomy in comparison with those undergone open colectomy. Leung *et al*^[41] clarified tissue trauma as reflected by systematic cytokine response, such as interleukin-1 β , interleukin-6 and CRP, was less after laparoscopic resection than after open resection of rectosigmoid carcinoma. Nishiguchi *et al*^[42] showed that interleukin-6 and CRP levels were significantly higher in the open group than those in the laparoscopic group one day and two days after surgery, respectively. Lymphocyte counts were significantly higher in the laparoscopic group than those in the open group two days after surgery. They concluded that laparoscopic surgery for colorectal carcinoma led to less postoperative stress than conventional open surgery. Some researchers verified that the levels of serum IL-2, CRP, and TNF α were significantly lower after surgery in the laparoscopic group than those in the open group^[43-45]. Braga *et al*^[46] also found that laparoscopic colorectal surgery was associated with less pronounced immunosuppression and inflammatory response and lower consumption of analgesic drugs than open surgery. But Tang *et al*^[47] and Mehigan *et al*^[48] showed that there was no difference in the systematic immune response in patients having laparoscopically assisted colectomy compared with those undergone conventional open surgery for colorectal cancer. Sandoval *et al*^[49] also revealed that the laparoscopic surgery did not affect natural antitumoral cellular immunity in an animal model. Moreover, Fukushima *et al*^[50] found that serum IL-6 after surgery was significantly higher in laparoscopic sigmoid colectomy than in the open group. They proposed that early IL-6 response after surgery be associated with operation time.

Previous immune response studies were only performed in colorectal surgery. However, the study on immune response of open *versus* laparoscopic total mesorectal excision with anal sphincter preservation in patients with rectal cancer has not been reported yet. The dissected retroperitoneal area that contacted directly with carbon dioxide was extensive in laparoscopic total mesorectal excision with anal sphincter preservation surgery. It is important to clarify whether the immune response of laparoscopic total mesorectal excision with anal sphincter preservation in patients with rectal cancer is

suppressed more severely than that of open surgery or not. In this study, TNF α levels were not elevated after surgery, and there were no significant differences between the two groups ($P>0.05$). However, the levels of IL-6 were decreased after laparoscopic surgery ($d_1=-23.14\pm263.97$ ng/L and $d_5=-40.08\pm272.03$ ng/L), but there were no significant differences between the laparoscopic and open groups ($P>0.05$). The levels of IL-2 were decreased after operation in both groups, and the differences were not significant in postoperative days between the two groups ($P>0.05$). There were no significant differences in CD3⁺ and CD56⁺ T lymphocyte count, CD3⁻ and CD56⁺ NK count, and serum IgG, IgM, and IgA levels after surgery between the two groups ($P>0.05$). Based on the results of our study, it is concluded that there is difference in immune responses in patients having laparoscopic total mesorectal excision with anal sphincter preservation compared with those undergone open surgery for rectal cancer.

REFERENCES

- 1 Walker CB, Bruce DM, Heys SD, Gough DB, Binnie NR, Eremin O. Minimal modulation of lymphocyte and natural killer cell subsets following minimal access surgery. *Am J Surg* 1999; **177**: 48-54
- 2 Vittimberga FJ Jr, Foley DP, Meyers WC, Callery MP. Laparoscopic surgery and the systemic immune response. *Ann Surg* 1998; **227**: 326-334
- 3 Heald RJ, Husband EM, Ryall RD. The mesorectum in rectal cancer surgery -the clue to pelvic recurrence? *Br J Surg* 1982; **69**: 613-616
- 4 Hartley JE, Mehigan BJ, Qureshi AE, Duthie GS, Lee PW, Monson JR. Total mesorectal excision: assessment of the laparoscopic approach. *Dis Colon Rectum* 2001; **44**: 315-321
- 5 Zhou ZG, Wang Z, Yu YY, Shu Y, Cheng Z, Li L, Lei WZ, Wang TC. Laparoscopic total mesorectal excision of low rectal cancer with preservation of anal sphincter: A report of 82 cases. *World J Gastroenterol* 2003; **9**: 1477-1481
- 6 Sun XN, Yang QC, Hu JB. Pre-operative radiochemotherapy of locally advanced rectal cancer. *World J Gastroenterol* 2003; **9**: 717-720
- 7 Gu J, Ma ZL, Li Y, Li M, Xu GW. Angiography for diagnosis and treatment of colorectal cancer. *World J Gastroenterol* 2003; **9**: 288-290
- 8 Cai SJ, Xu Y, Cai GX, Lian P, Guan ZQ, Mo SJ, Sun MH, Cai Q, Shi DR. Clinical characteristics and diagnosis of patients with hereditary nonpolyposis colorectal cancer. *World J Gastroenterol* 2003; **9**: 284-287
- 9 Liu LX, Zhang WH, Jiang HC. Current treatment for liver metastases from colorectal cancer. *World J Gastroenterol* 2003; **9**: 193-200
- 10 Chen K, Cai J, Liu XY, Ma XY, Yao KY, Zheng S. Nested case-control study on the risk factors of colorectal cancer. *World J Gastroenterol* 2003; **9**: 99-103
- 11 Liu LX, Zhang WH, Jiang HC, Zhu AL, Wu LF, Qi SY, Piao DX. Arterial chemotherapy of 5-fluorouracil and mitomycin C in the treatment of liver metastases of colorectal cancer. *World J Gastroenterol* 2002; **8**: 663-667
- 12 Zheng S, Liu XY, Ding KF, Wang LB, Qiu PL, Ding XF, Shen YZ, Shen GF, Sun QR, Li WD, Dong Q, Zhang SZ. Reduction of the incidence and mortality of rectal cancer by polypectomy: a prospective cohort study in Haining County. *World J Gastroenterol* 2002; **8**: 488-492
- 13 Wan J, Zhang ZQ, Zhu C, Wang MW, Zhao DH, Fu YH, Zhang JP, Wang YH, Wu BY. Colonoscopic screening and follow-up for colorectal cancer in the elderly. *World J Gastroenterol* 2002; **8**: 267-269
- 14 Zhang YL, Zhang ZS, Wu BP, Zhou DY. Early diagnosis for colorectal cancer in China. *World J Gastroenterol* 2002; **8**: 21-25
- 15 Qing SH, Rao KY, Jiang HY, Wexner SD. Racial differences in the anatomical distribution of colorectal cancer: a study of differences between American and Chinese patients. *World J Gastroenterol* 2003; **9**: 721-725
- 16 Fang J, Jin HB, Song JD. Construction, expression and tumor tar-

- geting of a single-chain Fv against human colorectal carcinoma. *World J Gastroenterol* 2003; **9**: 726-730
- 17 **Hu HY**, Liu XX, Jiang CY, Zhang Y, Bian JF, Lu Y, Geng Z, Liu SL, Liu CH, Wang XM, Wang W. Cloning and expression of ornithine decarboxylase gene from human colorectal carcinoma. *World J Gastroenterol* 2003; **9**: 714-716
- 18 **Jiang YA**, Fan LF, Jiang CQ, Zhang YY, Luo HS, Tang ZJ, Xia D, Wang M. Expression and significance of PTEN, hypoxia-inducible factor-1 alpha in colorectal adenoma and adenocarcinoma. *World J Gastroenterol* 2003; **9**: 491-494
- 19 **Ma L**, Tai H, Li C, Zhang Y, Wang ZH, Ji WZ. Photodynamic inhibitory effects of three perylenequinones on human colorectal carcinoma cell line and primate embryonic stem cell line. *World J Gastroenterol* 2003; **9**: 485-490
- 20 **Huang ZH**, Fan YF, Xia H, Feng HM, Tang FX. Effects of TNP-470 on proliferation and apoptosis in human colon cancer xenografts in nude mice. *World J Gastroenterol* 2003; **9**: 281-283
- 21 **Chen XX**, Lai MD, Zhang YL, Huang Q. Less cytotoxicity to combination therapy of 5-fluorouracil and cisplatin than 5-fluorouracil alone in human colon cancer cell lines. *World J Gastroenterol* 2002; **8**: 841-846
- 22 **Xiong B**, Yuan HY, Hu MB, Zhang F, Wei ZZ, Gong LL, Yang GL. Transforming growth factor-beta1 in invasion and metastasis in colorectal cancer. *World J Gastroenterol* 2002; **8**: 674-678
- 23 **Zhou CZ**, Peng ZH, Zhang F, Qiu GQ, He L. Loss of heterozygosity on long arm of chromosome 22 in sporadic colorectal carcinoma. *World J Gastroenterol* 2002; **8**: 668-673
- 24 **Xiong B**, Gong LL, Zhang F, Hu MB, Yuan HY. TGF beta1 expression and angiogenesis in colorectal cancer tissue. *World J Gastroenterol* 2002; **8**: 496-498
- 25 **Li J**, Guo WJ, Yang QY. Effects of ursolic acid and oleanolic acid on human colon carcinoma cell line HCT15. *World J Gastroenterol* 2002; **8**: 493-495
- 26 **Wang X**, Lan M, Wu HP, Shi YQ, Lu J, Ding J, Wu KC, Jin JP, Fan DM. Direct effect of croton oil on intestinal epithelial cells and colonic smooth muscle cells. *World J Gastroenterol* 2002; **8**: 103-107
- 27 **Wexner SD**, Rotholtz NA. Surgeon influenced variables in resectional rectal cancer surgery. *Dis Colon Rectum* 2000; **43**: 1606-1627
- 28 **Killingback M**, Barron P, Dent OF. Local recurrence after curative resection of cancer of the rectum without total mesorectal excision. *Dis Colon Rectum* 2001; **44**: 473-483
- 29 **McCall JL**, Cox MR, Wattchow DA. Analysis of local recurrence rates after surgery alone for rectal cancer. *Int J Colorectal Dis* 1995; **10**: 126-132
- 30 **Law WL**, Chu KW. Impact of total mesorectal excision on the results of surgery of distal rectal cancer. *Br J Surg* 2001; **88**: 1607-1612
- 31 **Dahlberg M**, Pahlman L, Bergstrom R, Glimelius B. Improved survival in patients with rectal cancer: a population-based register study. *Br J Surg* 1998; **85**: 515-520
- 32 **Dahlberg M**, Glimelius B, Pahlman L. Changing strategy for rectal cancer is associated with improved outcome. *Br J Surg* 1999; **86**: 379-384
- 33 **Arenas RB**, Fichera A, Mhoon D, Michelassi F. Total mesenteric excision in the surgical treatment of rectal cancer: a prospective study. *Arch Surg* 1998; **133**: 608-612
- 34 **Heald RJ**, Moran BJ, Ryall RD, Sexton R, MacFarlane JK. Rectal cancer: the Basingstoke experience of total mesorectal excision, 1978-1997. *Arch Surg* 1998; **133**: 894-899
- 35 **Chapman AE**, Levitt MD, Hewett P, Woods R, Sheiner H, Maddern GJ. Laparoscopic-assisted resection of colorectal malignancies: a systematic review. *Ann Surg* 2001; **234**: 590-606
- 36 **Feliciotti F**, Paganini AM, Guerrieri M, Sanctis A, Campagnacci R, Lezoche E. Results of laparoscopic vs open resections for colon cancer in patients with a minimum follow-up of 3 years. *Surg Endosc* 2002; **16**: 1158-1161
- 37 **Hong D**, Tabet J, Anvari M. Laparoscopic vs open resection for colorectal adenocarcinoma. *Dis Colon Rectum* 2001; **44**: 10-18
- 38 **Lezoche E**, Feliciotti F, Paganini AM, Guerrieri M, De Sanctis A, Minervini S, Campagnacci R. Laparoscopic vs open hemicolectomy for colon cancer. *Surg Endosc* 2002; **16**: 596-602
- 39 **Maxwell-Armstrong CA**, Robinson MH, Scholefield JH. Laparoscopic colorectal cancer surgery. *Am J Surg* 2000; **179**: 500-507
- 40 **Delgado S**, Lacy AM, Filella X, Castells A, Garcia-Valdecasas JC, Pique JM, Momblan D, Visa J. Acute phase response in laparoscopic and open colectomy in colon cancer: randomized study. *Dis Colon Rectum* 2001; **44**: 638-646
- 41 **Leung KL**, Lai PB, Ho RL, Meng WC, Yiu RY, Lee JF, Lau WY. Systemic cytokine response after laparoscopic-assisted resection of rectosigmoid carcinoma: A prospective randomized trial. *Ann Surg* 2000; **231**: 506-511
- 42 **Nishiguchi K**, Okuda J, Toyoda M, Tanaka K, Tanigawa N. Comparative evaluation of surgical stress of laparoscopic and open surgeries for colorectal carcinoma. *Dis Colon Rectum* 2001; **44**: 223-230
- 43 **Ordemann J**, Jacobi CA, Schwenk W, Stosslein R, Muller JM. Cellular and humoral inflammatory response after laparoscopic and conventional colorectal resections. *Surg Endosc* 2001; **15**: 600-608
- 44 **Schwenk W**, Jacobi C, Mansmann U, Bohm B, Muller JM. Inflammatory response after laparoscopic and conventional colorectal resections-results of a prospective randomized trial. *Langenbecks Arch Surg* 2000; **385**: 2-9
- 45 **Kuntz C**, Wunsch A, Bay F, Windeler J, Glaser F, Herfarth C. Prospective randomized study of stress and immune response after laparoscopic vs conventional colonic resection. *Surg Endosc* 1998; **12**: 963-967
- 46 **Braga M**, Vignali A, Zuliani W, Radaelli G, Gianotti L, Martani C, Toussoun G, Di Carlo V. Metabolic and functional results after laparoscopic colorectal surgery: a randomized, controlled trial. *Dis Colon Rectum* 2002; **45**: 1070-1077
- 47 **Tang CL**, Eu KW, Tai BC, Soh JG, Machin D, Seow-Choen F. Randomized clinical trial of the effect of open versus laparoscopically assisted colectomy on systemic immunity in patients with colorectal cancer. *Br J Surg* 2001; **88**: 801-807
- 48 **Mehigan BJ**, Hartley JE, Drew PJ, Saleh A, Dore PC, Lee PW, Monson JR. Changes in T cell subsets, interleukin-6 and C-reactive protein after laparoscopic and open colorectal resection for malignancy. *Surg Endosc* 2001; **15**: 1289-1293
- 49 **Sandoval BA**, Robinson AV, Sulaiman TT, Shenk RR, Stellato TA. Open versus laparoscopic surgery: a comparison of natural antitumoral cellular immunity in a small animal model. *Am Surg* 1996; **62**: 625-630
- 50 **Fukushima R**, Kawamura YJ, Saito H, Saito Y, Hashiguchi Y, Sawada T, Muto T. Interleukin-6 and stress hormone responses after uncomplicated gasless laparoscopic-assisted and open sigmoid colectomy. *Dis Colon Rectum* 1996; **39**(10 Suppl): S29-S34

Edited by Zhang JZ and Wang XL

Hepatitis B virus genotype has no impact on hepatitis B e antigen seroconversion after lamivudine treatment

Henry Lik-Yuen Chan, May-Ling Wong, Alex Yui Hui, Angel Mei-Ling Chim, Ada Mei-Ling Tse, Lawrence Cheung-Tsui Hung, Francis Ka-Leung Chan, Joseph Jao-Yiu Sung

Henry Lik-Yuen Chan, May-Ling Wong, Alex Yui Hui, Angel Mei-Ling Chim, Ada Mei-Ling Tse, Lawrence Cheung-Tsui Hung, Francis Ka-Leung Chan, Joseph Jao-Yiu Sung, Department of Medicine and Therapeutics, Chinese University of Hong Kong, Hong Kong

Correspondence to: Dr. Henry Lik-Yuen Chan, Department of Medicine and Therapeutics, 9/F Prince of Wales Hospital, Shatin, Hong Kong. hlychan@cuhk.edu.hk

Telephone: +852-26323594 **Fax:** +852-26373852

Received: 2003-07-04 **Accepted:** 2003-10-08

Abstract

AIM: To investigate the association of hepatitis B virus (HBV) genotype and HBeAg seroconversion after nucleotide analogue treatment.

METHODS: Chronic hepatitis B patients receiving lamivudine followed up for at least 6 months post-treatment were studied. Consecutive treatment-naïve patients who were prospectively followed up in the clinic for at least 18 months were studied as controls. HBeAg seroconversion was defined as loss of HBeAg, appearance of anti-HBe and normalization of alanine aminotransferase for at least 6 months.

RESULTS: Thirty-five patients on lamivudine and 96 control patients followed up for 39 (18-49) months were studied. Lamivudine was given for 12 (10-18) months, and patients were followed up for 15 (6-34) months after drug cessation. Genotype B and C HBV were found in 43 and 88 patients and HBeAg seroconversion occurred in 12 (28 %) and 16 (18 %) patients, respectively ($P=0.30$). There was no difference in HBeAg seroconversion between patients infected by genotype B and C HBV in the control (35 % vs 21 %, $P=0.25$) and lamivudine-treated (14 % vs 10 %, $P=1.00$) groups.

CONCLUSION: HBeAg seroconversion after treatment by lamivudine was not influenced by the HBV genotype.

Chan HLY, Wong ML, Hui AY, Chim AML, Tse AML, Hung LCT, Chan FKL, Sung JY. Hepatitis B virus genotype has no impact on hepatitis B e antigen seroconversion after lamivudine treatment. *World J Gastroenterol* 2003; 9(12): 2695-2697
<http://www.wjgnet.com/1007-9327/9/2695.asp>

INTRODUCTION

Hepatitis B virus (HBV) has 7 different genotypes (A-G) according to the homogeneity of the viral sequence^[1,2]. In Southeast Asia including Hong Kong, genotype B and C HBV are the predominant species^[3-6]. There are increasing evidences showing that genotype C HBV is associated with a more aggressive disease as compared with genotype B HBV^[3,7-10]. A recent Japanese study suggests that HBV genotype is not associated with the development of lamivudine resistance after

a median of 1.8 years of treatment^[11]. However, data on the association of HBV genotype and HBeAg seroconversion response to anti-viral treatment is scanty. This information is potentially important in the selection of patients for anti-viral treatment and development of future therapeutic regimens as in the case of chronic hepatitis C.

Previous studies suggest that genotype B HBV is associated with a higher rate of HBeAg seroconversion versus genotype C HBV among patients receiving interferon treatment^[12,13]. This finding, however, cannot be extrapolated to nucleos(t)ide analogues which have completely different mechanisms of action as compared with interferon. A study including 31 Taiwanese HBeAg-positive chronic hepatitis B patients treated by lamivudine does not show any difference in HBeAg seroconversion between patients infected by genotype B and C HBV^[14]. This study is limited by the small number of patients and the absence of control group. Phase III, multi-centered studies on adefovir dipivoxil reveal no difference in viral load reduction among patients infected by different HBV genotypes, but both HBeAg-positive and HBeAg-negative patients are included and HBeAg seroconversion has not been studied^[15]. In this study, we aimed to investigate the association of HBV genotype and HBeAg seroconversion after treatment by lamivudine, and a control group of untreated HBeAg-positive chronic hepatitis B patients was included for comparison.

MATERIALS AND METHODS

Patients on anti-viral treatment

Clinical data and stored serum samples of patients on lamivudine treated in Prince of Wales Hospital from 1998 to 2000 were included for analysis. These patients had positive hepatitis B surface antigen (HBsAg) for at least 6 months and positive hepatitis B e antigen (HBeAg), HBV DNA >1 000 000 copies/ml by DNA cross-linking assay (NAXCOR XLnt™, NAXCOR, Menlo Park, CA) or branched DNA assay (bDNA, Chiron Diagnostic, Emeryville, CA) before treatment^[16]. None of these patients had evidence of liver cirrhosis complications, hepatocellular carcinoma (HCC) or co-infection by hepatitis C or human immunodeficiency viruses. All patients received lamivudine 100 mg daily. HBeAg seroconversion was defined as loss of HBeAg, appearance of antibodies to HBeAg (anti-HBe) and normalization of ALT at the end of anti-viral treatment and the response sustained for at least 6 months after cessation of treatment till the last follow-up visit.

Control patients

Consecutive chronic hepatitis B patients with positive HBeAg at the initial clinic visit recruited since 1997 in our hospital were studied as controls^[3,17]. Patients who had previously received interferon or anti-viral treatment, liver cirrhosis complications and HCC were excluded from the study. To match the follow-up duration of patients treated by nucleoside analogues, patients who were followed up for less than 18 months were also excluded. All patients were followed up every 6 months, or more frequently as clinically indicated, with monitoring of HBeAg status and liver biochemistry. HBeAg

seroconversion was defined as sustained loss of HBeAg, appearance of anti-HBe and normalization of ALT during the follow-up period lasting for at least 6 months till the last visit.

HBV genotyping

The baseline samples of patients in clinical trial before starting anti-viral treatment and the serum samples at the first clinic visits of control patients were studied for HBV genotyping by restriction fragment length polymorphism as described previously^[7,18]. In short, extracted HBV DNA was amplified by polymerase chain reaction (PCR) using primers flanking the HBV genome between nucleotide 256 to 796 (sense primer 5'-GTGGTGGACTTCTCTCAATTTTC and anti-sense primer 5'-CGGTA(A/T)AAAGGGACTCA(A/C)GAT). PCR product was then mixed and incubated with restriction enzymes *Tsp* 5091 (New England Biolabs, Beverly, MA) and *Hinf*I (Boehringer Mannheim, Mannheim, Germany) respectively. The samples were run on agarose gel and DNA was visualized by ethidium bromide staining. The restriction pattern was read accordingly.

Statistical analysis

Results were expressed as median (range). Data were analyzed using SPSS version 11.0 software package. Categorical variables were compared by Chi-square test and continuous variables were compared by Mann-Whitney U test. Proportion of patients developing HBeAg seroconversion in different HBV genotypes were also compared after adjustment of potential confounding variables with *P* value <0.1 by logistic regression analysis. All tests were two-tailed. Statistical significance was taken as *P*<0.05.

RESULTS

Thirty-five patients on lamivudine and 96 control patients were identified. The clinical data and viral genotype of the studied patients of two groups of patients are shown in Table 1. Lamivudine was given for 12 (10-18) months and the treated patients were followed up for 15 (6-34) months after the cessation of lamivudine. Only 1 of 35 lamivudine-treated patients had been treated for 10 months whereas the remaining patients had treatment for at least 12 months. All patients who did not achieve HBeAg seroconversion after lamivudine treatment developed biochemical relapse with ALT elevation after cessation of lamivudine. The 24 control patients who achieved sustained HBeAg seroconversion were followed up for 24.5 (8-40) months after the development of HBeAg seroconversion. Patients on lamivudine were significantly older with higher initial ALT levels and shorter follow-up duration as compared with the controls. There was no difference in the distribution of HBV genotypes and the percentage of HBeAg seroconversion between the treated and control patients.

Table 1 Clinical characteristics of patients on anti-viral treatments and controls

	Overall (n=131)	Controls (n=96)	Lamivudine (n=35)	<i>P</i> value
Age	30 (12-68)	29 (12-68)	38 (22-47)	0.007
Male gender (n, %)	75 (57 %)	50 (52 %)	25 (71 %)	0.074
Initial ALT (IU/l)	73 (17-1122)	57.5 (17-753)	135 (36-1122)	<0.001
Follow-up (months)	39 (18-49)	39 (19-49)	27 (18-46)	0.009
Genotype				0.40
B (n, %)	43 (33 %)	29 (30 %)	14 (40 %)	
C (n, %)	88 (67 %)	67 (70 %)	21 (60 %)	
HBeAg seroconversion (n, %)	28 (21 %)	24 (25 %)	4 (11 %)	0.15

Forty-three (33 %) and 88 (67 %) patients were infected by genotype B and C respectively. The clinical characteristics of patients infected by genotype B and C HBV are shown in Table 2. There was no difference in the age, gender ratio, initial ALT levels, follow-up duration and drug treatment between patients infected by the two HBV genotypes. There was no difference in HBeAg seroconversion among patients infected by the 2 HBV genotypes, and the overall trend was confirmed after adjusted for age, gender ratio, initial ALT level and the follow-up duration (Table 3).

Table 2 Clinical characteristics of patients infected by genotype B and C HBV

	Genotype B (n=43)	Genotype C (n=88)	<i>P</i> value
Age	34 (13-67)	29 (12-68)	0.14
Male gender (n, %)	28 (65 %)	47 (53 %)	0.28
Initial ALT (IU/l)	70 (17-1094)	77 (18-1122)	0.60
Follow-up (months)	38 (18-49)	39 (18-49)	0.49
Treatment (n, %)			0.40
Nil	29 (67 %)	67 (76 %)	
Lamivudine	14 (33 %)	21 (24 %)	

Table 3 Comparison of HBeAg seroconversion among patients infected by genotype B and C HBV

HBeAg seroconversion	Genotype B	Genotype C	<i>P</i> value 1	<i>P</i> value 2
Control	10/29 (35 %)	14/67 (21 %)	0.25	0.41
Lamivudine	2/14 (14 %)	2/21 (10 %)	1.00	0.51

P value 1: unadjusted comparison of genotype B versus genotype C; *P* value 2: comparison of genotype B versus genotype C after adjustment for age, gender, initial ALT levels and follow-up duration.

DISCUSSION

The results of this study concurred with previous data that HBV genotype could not predict HBeAg seroconversion after 1 year treatment of lamivudine. The percentages of patients infected by genotype B and C HBV undergoing HBeAg seroconversion were similar among the treatment and control groups.

In the previous study in Taiwan, the proportion of patients achieving HBeAg seroconversion after lamivudine treatment was similar between genotype B and C HBV^[14]. However, genotype B HBV was reported to associate with earlier spontaneous HBeAg seroconversion by several series^[9,10]. It was therefore uncertain whether there was really no difference in lamivudine response between the 2 HBV genotypes or the improved response of genotype C HBV has closed up the existing difference. In this study, a control group of untreated patients was included in the analysis. As the control group was not recruited together with the treated patients in a randomized manner, it was not surprising that untreated patients were generally younger and had lower ALT levels than the treated ones. In this study, the absence of association between HBV genotypes and HBeAg seroconversion among patients treated by nucleotide analogues was confirmed as there was no difference in HBeAg seroconversion between the 2 HBV genotypes in both the treated groups and the control group after adjustment for all the differences between the two groups.

The earlier age of spontaneous HBeAg seroconversion associated with genotype B HBV reported by recent longitudinal studies was not shown in this study^[9,10]. Patient recruitment in the previous studies may be biased as one of them was a retrospective study and the other included only

patients who have consented for liver biopsy. The consecutive patient recruitment and prospective follow-up in our series has minimized the bias of sampling. Although the age of spontaneous HBeAg seroconversion did not differ between the 2 HBV genotypes, our previous studies agreed with others that genotype C HBV is associated with a more aggressive disease course than genotype B HBV^[3,7].

In this study, the rate of HBeAg seroconversion was comparable between the treated and untreated patients. The rate of HBeAg seroconversion after 1 year of lamivudine treatment was comparable to that reported in the previous multicenter Asian lamivudine trial^[19]. The rate of spontaneous HBeAg seroconversion (25 % in 3 years) was also comparable to previous reported Asian series after taken into consideration the young age and relatively lower ALT level of the control patients in this study^[20,21]. As patients in the control group were followed up for longer duration and some of these patients might have milder disease as compared with the treated patients, the effect of treatment could not be concluded by the results of this study. This study was also not designed to assess the predictive factor of treatment response to the nucleoside analogues.

In conclusion, the results of this study did not support a role of HBV genotype in response to lamivudine among HBeAg-positive patients. Further studies are required to probe into the association of HBV genotypes and treatment response in other geographical locations where other HBV genotypes prevail.

REFERENCES

- Norder H**, Courouce AM, Magnius LO. Complete genomes, phylogenetic relatedness, and structural proteins of six strains of the hepatitis B virus, four of which represent two new genotypes. *Virology* 1994; **198**: 489-503
- Stuyver L**, De Gendt S, Van Geyt C, Zoulim F, Fried M, Schinazi RF, Rossau R. A new genotype of hepatitis B virus: complete genome and phylogenetic relatedness. *J Gen Virol* 2000; **81**: 67-74
- Chan HLY**, Wong ML, Hui AY, Hung LCT, Chan FKL, Sung JY. Hepatitis B virus genotype C takes a more aggressive disease course than hepatitis B virus genotype B in hepatitis B e antigen-positive patients. *J Clin Microbiol* 2003; **41**: 1277-1279
- Sung JY**, Chan HLY, Wong ML, Tse CH, Yuen SCH, Tam JSL, Leung NWY. Relationship of clinical and virological factors with hepatitis activity in hepatitis B e antigen-negative chronic hepatitis B virus-infected patients. *J Viral Hepat* 2002; **9**: 229-223
- Orito E**, Ichida T, Sakugawa H, Sata M, Horiike N, Hino K, Okita K, Okanoue T, Iino S, Tanada E, Suzuki K, Watanabe H, Hige S, Mizokami M. Geographic distribution of hepatitis B virus (HBV) genotype in patients with chronic HBV infection in Japan. *Hepatology* 2001; **34**: 590-594
- Kao JH**, Chen PJ, Lai MY, Chen DS. Hepatitis B genotypes correlate with clinical outcome in patients with chronic hepatitis B. *Gastroenterology* 2000; **118**: 554-559
- Chan HLY**, Tsang SWC, Liew CT, Tse CH, Wong ML, Ching JYL, Leung NWY, Tam JSL, Sung JY. Viral genotype and hepatitis B virus DNA levels are correlated with histological liver damage in HBeAg-negative chronic hepatitis B virus infection. *Am J Gastroenterol* 2002; **97**: 406-412
- Kao JH**, Chen PJ, Lai MY, Chen DS. Genotypes and clinical phenotypes of hepatitis B virus in patients with chronic hepatitis B virus infection. *J Clin Microbiol* 2002; **40**: 1207-1209
- Chu CJ**, Hussain M, Lok ASF. Hepatitis B virus genotype B is associated with earlier HBeAg seroconversion compared with hepatitis B virus genotype C. *Gastroenterology* 2002; **122**: 1756-1762
- Sumi H**, Yokosuka O, Seki N, Arai M, Imazeki F, Kurihara T, Kanda T, Fukai K, Kato M, Saisho H. Influence of hepatitis B virus genotypes on the progression of chronic type B liver disease. *Hepatology* 2003; **37**: 19-26
- Akuta N**, Suzuki F, Kobayashi M, Tsubota A, Suzuki Y, Hosaka T, Someya T, Kobayashi M, Saitoh S, Arase Y, Ikeda K, Kumada H. The influence of hepatitis B virus genotype on the development of lamivudine resistance during long-term treatment. *J Hepatol* 2003; **38**: 315-321
- Kao JH**, Wu NH, Chen PJ, Lai MY, Chen DS. Hepatitis B genotypes and the response to interferon therapy. *J Hepatol* 2000; **33**: 998-1002
- Wai CT**, Chu CJ, Hussain M, Lok ASF. HBV genotype B is associated with better response in interferon therapy in HBeAg(+) chronic hepatitis than genotype C. *Hepatology* 2002; **36**: 1425-1430
- Kao JH**, Liu CJ, Chen DS. Hepatitis B viral genotypes and lamivudine resistance. *J Hepatol* 2002; **36**: 303-305
- Westland C**, Delaney W, Yang HL, Fry J, Brosgart C, Gibbs C, Miller M, Xiong S. Distribution and clinical response of HBV genotypes in phase III studies of adefovir dipivoxil. *J Hepatol* 2002; **36**(Suppl 1): 105
- Chan HLY**, Leung NWY, Lau TCM, Wong ML, Sung JY. Comparison of three different sensitive assays for hepatitis B virus DNA in monitoring of responses to anti-viral therapy. *J Clin Microbiol* 2000; **38**: 3205-3208
- Chan HLY**, Leung NWY, Hussain M, Wong ML, Lok ASF. Hepatitis B e antigen negative chronic hepatitis B in Hong Kong. *Hepatology* 2000; **31**: 763-768
- Lindh M**, Andersson AS, Gusdal A. Genotypes, nt 1858 variants, and geographical origin of hepatitis B virus – large-scaled analysis using a new genotyping method. *J Infect Dis* 1997; **175**: 1285-1293
- Lai CL**, Chien RN, Leung NW, Chang TT, Guan R, Tai DI, Ng KY, Wu PC, Dent JC, Barber J, Stephenson SL, Gray DF. A one-year trial of lamivudine for chronic hepatitis B. *N Engl J Med* 1998; **339**: 61-68
- Lok ASF**, Lai CL. Acute exacerbation in Chinese patients with chronic hepatitis B virus (HBV) infection. *J Hepatol* 1990; **10**: 29-34
- Yuen MF**, Yuan HJ, Hui CK, Wong DK, Wong WM, Chan AO, Wong BC, Lai CL. A large population study of spontaneous HBeAg seroconversion and acute exacerbation of chronic hepatitis B infection: implications for antiviral therapy. *Gut* 2003; **52**: 416-419

Edited by Ma JY

N-acetyl cysteine therapy in acute viral hepatitis

Huseyin Gunduz, Oguz Karabay, Ali Tamer, Resat Özaras, Ali Mert, Ömer Fehmi Tabak

Huseyin Gunduz, Department of Internal Medicine and Gastroenterology, Izzet Baysal Medical Faculty, Izzet Baysal University/Bolu, Turkey
Oguz Karabay, Department of Infectious Diseases and Clinical Microbiology, Izzet Baysal Medical Faculty, Izzet Baysal University/Bolu, Turkey

Ali Tamer, Department of Internal Medicine, Izzet Baysal Medical Faculty, Izzet Baysal University/Bolu, Turkey

Resat Özaras, Ali Mert, Ömer Fehmi Tabak, Department of Infectious Diseases and Clinical Microbiology, Cerrahpasa Medical Faculty, Istanbul University, Findikzade/İstanbul, Turkey

Correspondence to: Huseyin Gunduz, (MD, assistant professor) Department of Internal Medicine and Gastroenterology, Izzet Baysal Medical Faculty, Izzet Baysal University/Bolu, 14100 Turkey. drhuseyngunduz@yahoo.com

Telephone: +903742534656 **Fax:** +903742534559

Received: 2003-07-17 **Accepted:** 2003-09-02

Abstract

AIM: To investigate the effect of N-acetyl cysteine (NAC) on acute viral hepatitis (AVH).

METHODS: We administered 200 mg oral NAC three times daily (600 mg/day) to the study group and placebo capsules to the control group. All patients were hospitalized and diagnosed as AVH. Blood total and direct bilirubin, ALT, AST, alkaline phosphatase, albumin and globulin levels of each patient were measured twice weekly until total bilirubin level dropped under 2 mg/dl, ALT level under 100 U/L, follow up was continued and then the patients were discharged.

RESULTS: A total of 41 (13 female and 28 male) AVH patients were included in our study. The period for normalization of ALT and total bilirubin in the study group was 19.7 ± 6.9 days and 13.7 ± 8.5 days respectively. In the control group it was 20.4 ± 6.5 days and 16.9 ± 7.8 days respectively ($P > 0.05$).

CONCLUSION: NAC administration effected neither the time necessary for normalization of ALT and total bilirubin values nor duration of hospitalization, so we could not suggest NAC for the treatment of icteric AVH cases. However, our results have shown that this drug is not harmful to patients with AVH.

Gunduz H, Karabay O, Tamer A, Özaras R, Mert A, Tabak ÖF. N-acetyl cysteine therapy in acute viral hepatitis. *World J Gastroenterol* 2003; 9(12): 2698-2700

<http://www.wjgnet.com/1007-9327/9/2698.asp>

INTRODUCTION

Acute viral hepatitis (AVH) is an infectious disease that occurs as liver cell necrosis and inflammation as a result of the infection of liver cells by various viruses^[1,2]. Its significant symptoms and alterations occur in the liver and its functions^[3,4]. It is accepted that AVH is a liver disease with the highest incidence in the world and that it is a major cause of jaundice^[5]. It is a public health problem in developing countries which include our country as well. Moreover, hepatitis B and C may lead to chronic hepatitis, cirrhosis and cancer, and also constitute an endemic health problem for the society and is a cause of

serious economic loss^[6,7]. Various medications have been tried in the treatment of acute viral hepatitis, but no superiorities to placebo was demonstrated in most of these medications and they were not recommended for routine use^[8-9].

NAC (N-acetyl cysteine) is frequently used as a mucolytic and as an antidote in paracetamol intoxication^[10-11]. NAC may maintain cell integrity by increasing the amount of glutathione within the cell or coming into direct reaction with spontaneous conjugation and/or reduction^[12]. Recently, some studies have shown good results and absence of side effects in patients treated with interferon and NAS in chronic hepatitis C patients^[13-15]. In addition, treatment of HBV-producing cell lines with NAC resulted in an at least 50-fold reduction of viral DNA in the tissue culture supernatant within 48 hours^[16]. The need for a treatment to shorten duration of AVH is obvious, but it has not been found yet. We thought this problem might be solved with NAC which protects the cellular architecture by increasing the amount of intracellular glutathione that reacts with toxic free oxygen radicals^[17].

We could not find any study that focused on the effects of NAC on acute viral hepatitis. For this reason, we aimed to determine the effect of NAC on acute hepatitis in this study.

MATERIALS AND METHODS

In this study, 41 acute viral hepatitis A or B cases were included. These cases were hospitalized and monitored in the Infectious Diseases Department Cerrahpasa Faculty of Medicine, Istanbul University.

Those aged 14-60 years, with transaminase values more than 10 times of the upper limit of the normal value (>400 U/L), total bilirubin values above 3 mg/dl and positive antiHBc-IgM or antiHAV-IgM detected in serological examinations and negative serologic tests for hepatitis C virus, hepatitis D virus and HIV were included. Serological tests were done for HBsAg, HBcIgM, antibody to Hepatitis C virus (Abbott Lab.) and antibody to hepatitis delta virus (Anti-HDV, Wellcozyme, Wellcome Diagnostic, England) using the EIA method.

The cases who were hospitalized and monitored in the clinic were randomized into study group (20 patients) and control group (21 patients). Randomization was carried out according to age, gender and etiological agents. In the study group, 200 mg NAC was given orally 3 times a day (600 mg/day). In the control group, placebo was given orally 3 times a day.

The study protocol was approved by the local ethics committee. All patients were informed to participate in by an inscription form in the study.

Levels of the biochemical parameters [total and direct bilirubin, alanine aminotransferase (ALT), aspartate aminotransferase (AST), alkaline phosphatase, albumin and globulin levels and prothrombine activities] were monitored in both drug and control groups. This monitoring process continued until the level of total serum bilirubin reached 2 mg/dl and the ALT level fell below 100 U/L. Then the patients were discharged from the hospital. All patients were followed up for six months after discharge.

In evaluating the results of the study, Student's *t* test was used for average age, gender, values concerning the etiologic agents and covariate analysis tests were used for biochemical

parameters, averages of hyperbilirubinemia, ALT, and time needed before they reached normal values.

RESULTS

A total of 41 patients (28 female /13 male) were included in the study. The median age was 24 (range: 15-52). The median age of hepatitis A patients was 17 (range: 16-28) and that of hepatitis B patients was 26 (range: 15-52).

The median age was 23 (range: 15-48) in the study group and was 24 (range: 16-52) in the control group ($P>0.05$). Patients with HAV infection were younger than those with HBV infection. In the serological distinction of the cases, type A was detected in 9 (22 %) and type B in 32 (78 %). In study group type A was detected in 4, type B was detected in 16. In control group type A was detected in 5 (23 %) and B in 16 (76 %).

In our study, the most important finding was the time needed for ALT and total bilirubin to reach normal. The criteria used to include a case in our study was ALT value that was ten times higher than the normal and the criteria used to end the surveillance of a case was its falling below 100 U/L. Jaundice was defined as the situation in which the serum total bilirubin level was higher than 3 mg/dl. Period of jaundice was defined as the duration that ended when the increasing bilirubin decreased to 2 mg/dl.

The period for normalization of ALT in study group was 19.7 ± 6.9 days (type A 11.2 ± 6.1 days, type B 21.8 ± 6.1 days), while in the control group it was 20.4 ± 6.5 days (type A 16 ± 7.4 days, type B 21.8 ± 6.7 days). The period for normalization of total bilirubin in the study group was 13.7 ± 8.5 days (type A 7.9 ± 4.9 days, type B 15.2 ± 8.6 days), in control group was 16.9 ± 7.8 days (type A 7.9 ± 4.9 days, type B 18.4 ± 8.1 days). No significant difference could be found between the two groups ($P>0.05$). These data are summarized in Table 1.

As a conclusion, the hospitalization duration and time to normalization of ALT and total bilirubin of the patients did not get shorter or longer (as an adverse effect) with the use of NAC.

Table 1 Comparison of study and control groups

	Study group	Control group
Case number	20	21
Median Age (min -max) (year)	23 (15-48)	24 (16-52)
Genus (M/F)	12/8	16/5
ALT (U/L)	1730 ± 628	2129 ± 1278
AST (U/L)	987 ± 545	1397 ± 1002
ALP (U/L)	488 ± 201	410 ± 149
Total bilirubin (mg/dL)	7.75 ± 4.36	10.1 ± 3.04
Direct bilirubin (mg/dL)	5.29 ± 3.14	7.17 ± 3.26
Activity of prothrombin (%)	72.6 ± 22.7	74.1 ± 18.9
Albumin (g/dL)	3.95 ± 0.54	3.98 ± 0.40
Type of hepatitis (A/B)	4/16	5/16
Time consumption for ALT <100 U/L	19.7 ± 6.9	20.4 ± 6.5
Time consumption for total bilirubin <2 mg/dl	13.7 ± 8.5	16.9 ± 7.8

DISCUSSION

Virus hepatitis is an important health problem in the world. Hepatitis A is a common infection in our country, so is in the world and 50 % of the population aged up to 15 and 90 % of the adults are exposed to this disease^[18]. Annual disease reporting was approximately 25 000 according to the data of the Ministry of Health in Turkey^[19]. However it was believed that the real number of the cases was at least 250 000-500 000

per year, when the unreported cases and anicteric and subclinical cases were added^[20,21].

When AVH displays a symptomatic presentation, it is generally cured at the end but after a long course. It is a public health problem in developing countries which include our country as well. Hepatitis B, C, D viruses causing AVH may lead to cirrhosis and cancer, and also constitute an endemic health problem for the society and are the cause for serious economic losses^[22,23]. Various medications including steroids, interferon, vidarabine, levamisol, ursodeoxycolic acids, *ribavarine* have been tried in the treatment of acute viral hepatitis, but advantages over placebo offered by most of these medications were not found to be good enough to be recommended for routine use^[24,25]. Thus the gap in the treatment of AVH has not been filled yet. We thought that this gap could be filled by NAC.

NAC is frequently used as mucolytic and as an antidote for paracetamol intoxication. It was used in paracetamol intoxication as it could fill the mitochondrial and cytosolic glutathione stocks consumed by N acetyl benzoquinoneimine, which is a paracetamol metabolite, by stimulating glutathione synthesis^[26]. Under physiological conditions, there is basal glutathione outflow from the liver into the blood. It has been observed that intracellular glutathione participated in some critical physiological activities such as provision of membrane and cell skeleton unity, arrangement of enzyme activities and biosynthesis of protein and nucleic acids^[8,13]. It might also lead to serious decreases in the intracellular and tissue glutathione and heavy pathological transformations in this tissue^[9,10].

Recently, some studies have shown good results and absence of side effects in patients treated with NAC in hepatitis B and chronic hepatitis C patients^[13]. Addition of NAC which is a glutathione precursor, to 14 patients with chronic hepatitis C and high ALT level, caused a regular decrease of ALT in all patients and after a combined treatment it helped 41 % of the cases to heal completely after 5- 6 months. Consequently, it was reported that NAC increased interferon response in patients with hepatitis C^[14]. Recently Neri *et al.* reported the presence of oxidative stress in patients with chronic hepatitis C, earlier relapse in patients treated with interferon alone. They obtained significant results in patients treated with interferon plus NAC compared to those with interferon alone^[13]. Weiss *et al.* showed that NAC was able to inhibit hepatitis B virus (HBV) replication, by a mechanism independent of the intracellular level of reactive oxygen intermediates. Treatment of HBV-producing cell lines with NAC resulted in an at least 50-fold reduction of viral DNA in the tissue culture supernatant within 48 h. This decrease of viral DNA and thus of virions in the tissue culture supernatant was caused by a disturbance of the virus assembly, rather than by a reduction of viral transcripts. Their data strongly suggested a potential use of this well-established, non-toxic drug for the treatment of HBV infection. They found that NAC, in contrast to interferon, exerted its anti-HBV activity at a posttranscriptional level, a combination of NAC with the established interferon therapy could also be suggested.

We conducted a comparative study to examine the effects of NAC on the functions of liver in AVH. Taking the disease period as the period in which the ALT value came back to normal, we measured the duration of this period in the study group and control group. We also examined the effect of NAC on the period of jaundice. AST, ALT and serum bilirubin measurements were among the tests that were not specific in the diagnosis of AVH, and these were parameters in harmony with the hepatocellular injury. In AVHs, transaminases had diagnostic value, rather than prognostic value. It was accepted that in AVH, these enzymes increased 10 times, ALT maintained to be higher than AST and then it decreased in an evident way in the first week, then it came back to normal in 2- 4 weeks.

In AVH infections, the value of total serum bilirubin increased up to 3-20 mg/dl in 1-2 weeks under normal conditions and although serum aminotransferases levels started to fall, bilirubin levels might continue to increase, then they gradually decreased. In the study and control groups, total bilirubin levels were 7.75 ± 4.36 mg/dl and 10.1 ± 3.04 mg/dl respectively. The average period of jaundice was 13.7 ± 8.5 days in the study group, and 16.9 ± 7.8 days in the control group ($P > 0.05$).

During ALT, AST, bilirubin values came back to normal in the study and control groups, the patients with hepatitis A and B infection were evaluated separately, the difference was not statistically meaningful. The curves of AST and ALT in the study and control groups were not statistically different (Figures 1 and 2). Thus it became obvious that NAC did not change the liver enzyme activities in the patients with AVH.

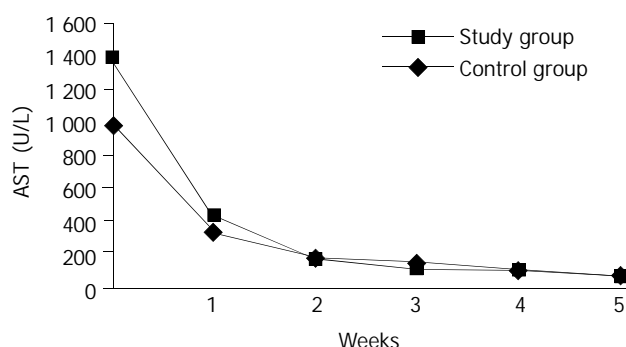


Figure 1 Changes in averages of ALT values in the study and control groups in time.

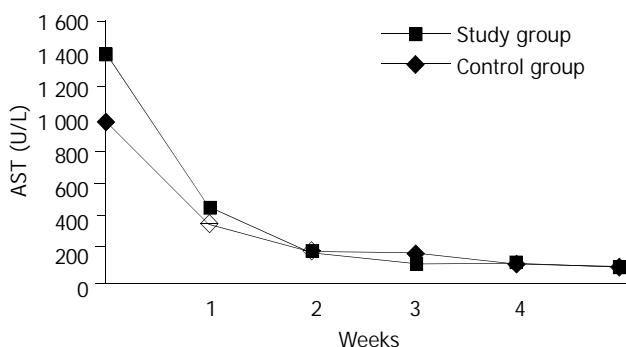


Figure 2 Changes in averages of AST values in the study and control groups in time.

This was the first study investigating the effect of NAC on AVH. In this study, it was determined that NAC had no effect on the jaundice duration in AVH infection and the period in which the ALT value came back to normal and accordingly hospitalization duration of AVH patients and the prognosis of biochemical parameters.

In conclusion, the use of NAC in acute viral hepatitis complicated by jaundice is no more effective than placebo. However, the use of NAC in AVH cases is not harmful.

REFERENCES

- Banker DD. Viral hepatitis. *Indian J Med Sci* 2003; **57**: 363-368
- Mathur P, Arora NK. Considerations for HAV vaccine in India. *Indian J Pediatr* 2001; **68**(Suppl 1): 23-30
- Batra Y, Bhatkal B, Ojha B, Kaur K, Saraya A, Panda SK, Acharya SK. Vaccination against hepatitis A virus may not be required for schoolchildren in northern India: results of a seroepidemiological survey. *Bull World Health Organ* 2002; **80**: 728-731
- Alter MJ, Mast EE. The epidemiology of viral hepatitis in the United States. *Gastroenterol Clin North Am* 1994; **23**: 437-455
- Ertekin V, Selimoglu MA, Altinkaynak S. Sero-epidemiology of hepatitis B infection in an urban paediatric population in Turkey. *Public Health* 2003; **117**: 49-53
- Khan WI, Sultana R, Rahman M, Akhter H, Haq JA, Ali L, Mohsin MA, Khan AK. Viral hepatitis: recent experiences from serological studies in Bangladesh. *Asian Pac J Allergy Immunol* 2000; **18**: 99-103
- Centers for Disease Control and Prevention (CDC). Transmission of hepatitis B and C viruses in outpatient settings—New York, Oklahoma, and Nebraska, 2000-2002. *MMWR Morb Mortal Wkly Rep* 2003; **52**: 901-906
- Gregory PB, Knauer CM, Kempson RL, Miller R. Steroid therapy in severe viral hepatitis, a double blind, randomized trial of methylprednisolone versus placebo. *N Eng J Med* 1976; **294**: 681-687
- Mackenzie AR, Molyneaux PJ, Cadwgan AM, Laing RB, Douglas JG, Smith CC. Increasing incidence of acute hepatitis B virus infection referrals to the Aberdeen Infection Unit: a matter for concern. *Scott Med J* 2003; **48**: 73-75
- Kucukardali Y, Cinan U, Acar HV, Ozkan S, Top C, Nalbant S, Cermik H, Cankir Z, Danaci M. Comparison of the therapeutic efficacy of 4-methylpyrazole and N-acetylcysteine on acetaminophen (paracetamol) hepatotoxicity in rats. *Curr Med Res Opin* 2002; **18**: 78-81
- Zhao C, Sheryl D, Zhou YX. Effects of combined use of diallyl disulfide and Nacetyl-cysteine on acetaminophen hepatotoxicity in β -naphthoflavone-pretreated mice. *World J Gastroenterol* 1998; **4**: 112-116
- Flanagan RJ, Meredith TJ. Use of N-acetylcysteine in clinical toxicology. *Am J Med* 1991; **91**(Suppl 3C): 131-139
- Neri S, Ierna D, Antoci S, Campanile E, D'Amico RA, Noto R. Association of alpha-interferon and acetyl cysteine in patients with chronic C hepatitis. *Panminerva Med* 2000; **423**: 187-192
- Beloqui O, Prieto J, Suarez M, Gil B, Qian CH, Garcia N, Civeira MP. N-acetyl cysteine enhances the response to interferon-alpha in chronic hepatitis C: a pilot study. *J Interferon Res* 1993; **13**: 279-282
- Grand PR, Black A, Garcia N, Prieto J, Garson JA. Combination therapy with interferon-alpha plus N-acetyl cysteine for chronic hepatitis C: a placebo controlled double-blind multicentre study. *J Med Virol* 2000; **61**: 439-442
- Weiss L, Hildt E, Hofschneider PH. Anti hepatitis B virus activity of N acetylcysteine, new aspect a well established drug. *Antiviral Res* 1996; **32**: 43-53
- Mandal AK, Sinha J, Mandal S, Mukhopadhyay S, Das N. Targeting of liposomal flavonoid to liver in combating hepatocellular oxidative damage. *Drug Deliv* 2002; **9**: 181-185
- Wie J, Wang YQ, Lu ZM, Li GD, Wang Y, Zhang ZC. Detection of anti-preS1 antibodies for recovery of hepatitis B patients by immunoassay. *World J Gastroenterol* 2002; **8**: 276-281
- T.C Government Statistically Instutuy. *Statistical annual of Turkey Republic* 1993: 151-154
- Ozturk R. Laboratuary Diagnosis of Viral Hepatitis. Yucel A, Tabak F (Eds): *Currently Viral Hepatitis. Istanbul Infectious Diseases Association's publications* 1998; **11**: 53-54
- Ozdemir O, Arda K, Soylu M, Alyan O, Demir AD, Kutuk E. Seroprevalence of hepatitis B and C in subjects admitted to a cardiology clinics in Turkey. *Eur J Epidemiol* 2003; **18**: 255-258
- Shiell A, Law MG. The cost of hepatitis C and the cost-effectiveness of its prevention. *Health Policy* 2001; **58**: 121-131
- Jacobs RJ, Saab S, Meyerhoff AS, Koff RS. An economic assessment of pre-vaccination screening for hepatitis A and B. *Public Health Rep* 2003; **118**: 550-558
- Maier I, Wu GY. Hepatitis C and HIV co-infection: a review. *World J Gastroenterol* 2002; **8**: 577-579
- Ryder SD, Beckingham IJ. ABC of diseases of liver, pancreas, and biliary system: Acute hepatitis. *BMJ* 2001; **322**: 151-153
- MacNee W, Bridgeman MME, Marsden M. Effects of N-acetylcysteine and glutathione on smoke induced changes in lung phagocytes and epithelial cells. *Am J Med* 1991; **91**(Suppl 3C): 60-71
- Taylor ER, Hurrell F, Shannon RJ, Lin TK, Hirst J, Murphy MP. Reversible glutathionylation of complex I increases mitochondrial superoxide formation. *J Biol Chem* 2003; **278**: 19603-19610

• *H pylori* •

Expression of mucosal addressin cell adhesion molecule 1 on vessel endothelium of gastric mucosa in patients with nodular gastritis

Hiroshi Ohara, Hajime Isomoto, Chun-Yang Wen, Chieko Ejima, Masahiro Murata, Masanobu Miyazaki, Fuminao Takeshima, Yohei Mizuta, Ikuo Murata, Takehiko Koji, Hiroshi Nagura, Shigeru Kohno

Hiroshi Ohara, Hajime Isomoto, Masanobu Miyazaki, Fuminao Takeshima, Yohei Mizuta, Ikuo Murata, Shigeru Kohno, Second Department of Internal Medicine, 1-7-1 Sakamoto, Nagasaki, Japan
Chun-Yang Wen, Department of Molecular Pathology, Atomic Bomb Disease Institute, 1-12-4 Sakamoto, Nagasaki, Japan
Takehiko Koji, Department of Histology and Cell Biology, Nagasaki University School of Medicine, Nagasaki, 1-12-4 Sakamoto, Nagasaki, Japan

Chieko Ejima, Masahiro Murata, Hiroshi Nagura, Department of Pathology, Tohoku University School of Medicine, Aobaku, Sendai, Japan

Correspondence to: Dr. Hajime Isomoto, Second Department of Internal Medicine, Nagasaki University School of Medicine, 1-7-1 Sakamoto, Nagasaki, Japan. hajime2002@yahoo.co.jp

Telephone: +81-95-849-7567 **Fax:** +81-95-849-7568

Received: 2003-09-06 **Accepted:** 2003-10-23

Abstract

AIM: The interaction of mucosal addressin cell adhesion molecule 1 (MAdCAM-1) with integrin $\alpha 4\beta 7$ mediates lymphocyte recruitment into mucosa-associated lymphoid tissue (MALT). Nodular gastritis is characterized by a unique military pattern on endoscopy representing increased numbers of lymphoid follicles with germinal center, strongly associated with *H pylori* infection. The purpose of this study was to address the implication of the MAdCAM-1/integrin $\beta 7$ pathway in NG.

METHODS: We studied 17 patients with NG and *H pylori* infection and 19 *H pylori*-positive and 14 *H pylori*-negative controls. A biopsy sample was taken from the antrum and snap-frozen for immunohistochemical analysis of MAdCAM-1 and integrin $\beta 7$. In simultaneous viewing of serial sections, the percentage of MAdCAM-1-positive to von Willebrand factor-positive vessels was calculated. We also performed immunostaining with anti-CD20, CD4, CD8 and CD68 antibodies to determine the lymphocyte subsets co-expressing integrin $\beta 7$.

RESULTS: Vascular endothelial MAdCAM-1 expression was more enhanced in gastric mucosa with than without *H pylori* infection. Of note, the percentages of MAdCAM-1-positive vessels were significantly higher in the lamina propria of NG patients than in *H pylori*-positive controls. Strong expression of MAdCAM-1 was identified adjacent to lymphoid follicles and dense lymphoid aggregates. Integrin $\beta 7$ -expressing mononuclear cells, mainly composed of CD20 and CD4 lymphocytes, were associated with vessels lined with MAdCAM-1-expressing endothelium.

CONCLUSION: Our results suggest that the MAdCAM-1/integrin $\alpha 4\beta 7$ homing system may participate in gastric inflammation in response to *H pylori*-infection and contributes to MALT formation, typically leading to the development of NG.

Ohara H, Isomoto H, Wen CY, Ejima C, Murata M, Miyazaki M, Takeshima F, Mizuta Y, Murata I, Koji T, Nagura H, Kohno S. Expression of mucosal addressin cell adhesion molecule 1 on vessel endothelium of gastric mucosa in patients with nodular gastritis. *World J Gastroenterol* 2003; 9(12): 2701-2705
<http://www.wjgnet.com/1007-9327/9/2701.asp>

INTRODUCTION

Lymphocyte recruitment to inflammatory sites is regulated by differential expression of cell surface homing receptors and their interactions with relevant vascular adhesion molecules^[1]. An immunoglobulin super family, single-chain 60-kDa glycoprotein, mucosal addressin cell adhesion molecule 1 (MAdCAM-1) is selectively expressed on the endothelium of high endothelial venules in gut-associated lymphoid tissues and vascular endothelial cells in the lamina propria of the small and large intestine^[2]. Engagement of MAdCAM-1 to its exclusive ligand, integrin $\alpha 4\beta 7$, on lymphocytes represents a tissue-specific homing mechanism for the intestine and gut-associated lymphoid tissue^[2].

Helicobacter pylori causes one of the most common chronic infections in humans^[3]. Although *H pylori* is a noninvasive pathogen^[4], persistent infection causes chronic gastritis, which predisposes the mucosa to peptic ulceration, and is thought to be eventually linked to gastric cancer and primary gastric lymphoma, especially the lymphoma of mucosa-associated lymphoid tissue (MALT) type^[5,6]. The histopathological features of *H pylori*-associated gastritis include intense infiltration of granulocytes and lymphocytes^[7] and the formation of organized lymphoid follicles^[8]. In this regard, nodular gastritis (NG), which is a unique military pattern resembling "goose flesh" on endoscopy^[9], is characterized by increased numbers of lymphoid follicles with germinal center^[10], in close association with *H pylori* infection^[9, 10]. Although NG frequently occurs in children, there are ample evidences at present suggesting that NG is not so uncommon in adults, especially in pre-menopausal women^[9,10].

Recently, Hatanaka *et al*^[11] reported that expression of vascular endothelial MAdCAM-1 was enhanced in murine chronic gastritis induced by *H pylori*. Furthermore, Dogan *et al*^[12] demonstrated strong expression of MAdCAM-1 protein on the vasculature in patients with *H pylori*-associated MALT type lymphoma. However, little is known about the implication of such adhesion molecules in the pathogenesis of NG. In this study, we investigated MAdCAM-1 expression on vessel endothelium in gastric mucosa of patients with NG by immunohistochemistry, along with the interaction with integrin $\alpha 4\beta 7$. This could shed light on the mechanism of MALT organization in gastric mucosa in response to *H pylori* infection.

MATERIALS AND METHODS

Subjects and samples

We studied 17 patients who underwent upper gastrointestinal

endoscopy for dyspepsia and were diagnosed as having NG between April 1999 and March 2002. They included 2 men and 15 women, ranging 24 to 58 years old (mean, 43 years). As a control, age- and sex- matched 33 subjects with non-ulcer dyspepsia during the same period were recruited in the study. They consisted of 19 *H pylori*-infected patients without nodular gastritis (*H pylori*-positive controls) and 14 *H pylori*-negative ones. None of the control subjects had been treated with non-steroidal anti-inflammatory drugs, proton pump inhibitors, antibiotics, or bismuth compounds during the 4-week period prior to the present study. There were no differences in baseline characteristics such as alcohol intake, current tobacco use and body mass index among the three groups.

At endoscopy, one biopsy specimen was obtained from the antrum within 2 cm of the pyloric ring along the greater curvature. The sample was snap-frozen in OCT compound (Tissue-tek; Miles Inc., Elkhart, IN) in ethanol-dry ice bath and stored at -80 °C until use.

Detection of *Helicobacter pylori* infection

H pylori status was assessed by serology (anti-*H pylori* immunoglobulin G antibody, HEL-p TEST, AMRAD Co., Melbourne, Australia), rapid urease test (CLO test; Delta West Co., Bentley, Australia) using additional biopsy specimens obtained during endoscopy from the antrum within 2 cm of the pyloric ring and the corpus along the greater curvature. Patients were considered positive for *H pylori* infection when at least one examination yielded positive results. On the other hand, patients were defined as *H pylori*-negative if all test results were negative.

Immunohistochemical analysis

MAdCAM-1 protein expression on vascular endothelial cells was studied *in situ* by immunohistochemistry with the streptavidin-biotin-peroxidase-complex method (Histofine SAB-PO kit, Nichirei Co., Tokyo), as described previously^[13]. In brief, frozen tissues were cut into 4-μm thick sections and placed on glass slides coated with 3-aminopropyltriethoxysilane (Dako Co., Glostrup, Denmark). The following steps were performed at room temperature unless otherwise specified. Sections were fixed in 4 % paraformaldehyde (Merck Co., Darmstadt, Germany) in phosphate-buffered saline (PBS, pH 7.4) for 20 minutes. After a brief washing in PBS, endogenous peroxidase activity was inhibited for 30 min with methanol containing 0.3 % H₂O₂. Sections were reacted for 20 min with 10 % normal rabbit serum (Nichirei Co.) to prevent non-specific binding, and incubated with anti-MAdCAM-1 mouse monoclonal antibody (clone 1G2)^[14] at a concentration of 1:100 in PBS overnight at 4 °C. On the next day, the sections were washed three times (10 min each) in PBS and incubated for 20 min with 10 mg/ml biotinylated rabbit anti-mouse immunoglobulins (Nichirei). After washed three times (10 min each) in PBS, the sections were re-incubated for 20 min with 100 μg/ml HRP-conjugated streptavidin (Nichirei). After washed three times (10 min each) in PBS, a color reaction was performed with 0.05 M Tris-HCl (pH 7.6) containing 3, 3'-diaminobenzidine tetrahydrochloride (Dojin Chemical Co., Kumamoto, Japan) and H₂O₂. Sections were counterstained with Mayer's hematoxylin and then dehydrated, cleared and mounted by standard procedures.

In each serial section of the same tissue specimen, vessels were immunostained with anti-von Willebrand factor monoclonal antibody (Dako Co.) in the same fashion described above, in order to assess quantitatively the difference in the extent of expression of endothelial adhesion molecules, based on the method reported by Hatz *et al*^[15]. Briefly, two independent observers who were blind to the diagnosis and experimental results, counted the number of von Willebrand factor-positive vessels and then the number of MAdCAM-1-

positive vessels on the section serial to that stained for von Willebrand factor. Percentage of the ratio of MAdCAM-1-positive to von Willebrand factor-positive vessels was calculated. As a negative control, each non-specific isotype antibody was used instead of the primary antibodies, or the primary antibodies were omitted. When the interobserver variability exceeded 10 %, the areas were simultaneously re-evaluated by the two investigators to reach a consensus.

Furthermore, immunoreactivity for integrin β7 on inflammatory cells infiltrating the gastric mucosa was similarly analyzed using a specific monoclonal antibody (Pharmingen Co., San Diego, CA) at a concentration of 1:10. On the section serial to that stained for β7, we also performed immunohistochemistry using anti-CD20, -CD4, -CD8 and -CD68 monoclonal antibodies (purchased from Dako Co.).

Reverse transcriptase polymerase chain reaction (RT-PCR)

Total RNA from biopsy samples that were also collected from the same location was extracted using a commercial kit according to the instructions provided by the supplier (ISOGEN, Nippon Gene Co., Toyama, Japan). Equivalent amounts of RNA were monitored by absorption at 260 nm and by monitoring the density of 28S and 18S RNA detected after electrophoresis. After 1 μg of total RNA was reverse transcribed to complementary DNA, the target sequence of MAdCAM-1 was amplified in 35 cycles, each consisting of 1 min at 94 °C for denaturation, 1 min at 60 °C for annealing and 1 min at 72 °C for extension, followed by a final extension for 5 min at 72 °C with specific primers^[16], using a RT-PCR kit (Takara Shuzo Co., Otsu, Japan). Two primers designed to nucleotide positions 978-999 (TGC GGT GCT GGG ACT GCT GCT C, sense) and 1 344-1 364 (TCA GGG AGG GGC TTC AGG TCA, antisense) of human MAdCAM-1 cDNA sequence were used for amplification of a 387 bp product^[16]. A 10 μl aliquot of each PCR product was analyzed by electrophoresis on 2 % agarose gel containing ethidium bromide, and the bands were examined under ultraviolet light for the presence of amplified DNA. Glyceraldehyde-3-phosphate dehydrogenase (G3PDH) gene transcript was routinely amplified as described previously^[17] and used as an internal control of the processed RNA for each preparation.

All samples were obtained with informed consent in accordance with the Helsinki Declaration.

Statistical analysis

Statistical analyses were performed using Fisher's exact, χ^2 , Student's *t*, and Mann-Whitney *U* tests, whichever appropriate. A *P* value less than 0.05 was accepted as statistically significant. Data were expressed as mean ± standard deviation (SD).

RESULTS

Clinicopathological features of NG

All 17 patients with NG were *H pylori*-positive. Among the 17 patients, no less than 9 (52.9 %) had endoscopic evidence of peptic ulcer (duodenal ulcer in 7 and gastric ulcer in 2). All except one specimen from the NG patients showed lymphoid follicle formation and/or dense lymphoid aggregates.

MAdCAM-1 expression on vessel endothelium

The MAdCAM-1 antigen, recognized by the 1G2 antibody, was seen on vascular endothelial cells in gastric mucosa. In *H pylori*-negative group, MAdCAM-1 was rarely or occasionally localized in vascular endothelial cells in the lamina propria (Figure 1A). However, the relative endothelial area expressing MAdCAM-1 increased in inflammatory settings induced by *H pylori* infection (Figure 1B), particularly in association with

dense lymphocytic infiltration (Figure 1C). High endothelial venule-like vessels adjacent to the lymphoid follicle were intensely immunoreactive (Figure 1D). There was a significant difference in the percentages of MAdCAM-1-positive vessels between *H. pylori*-positive and -negative controls ($P<0.001$, Figure 2). In addition, the expression of vascular MAdCAM-1 was more enhanced in patients with NG than that in *H. pylori*-negative controls ($P<0.0001$, Figure 2). Of note, MAdCAM-1-positive vessels were more abundant in the antral mucosa of patients with NG, compared with *H. pylori*-positive controls ($P<0.05$, Figure 2). The percentages of MAdCAM-1-positive vessels detected by the two observers were almost identical. When each non-specific isotype serum was used or primary antibodies were omitted, the specimens showed no immunoreactivity.

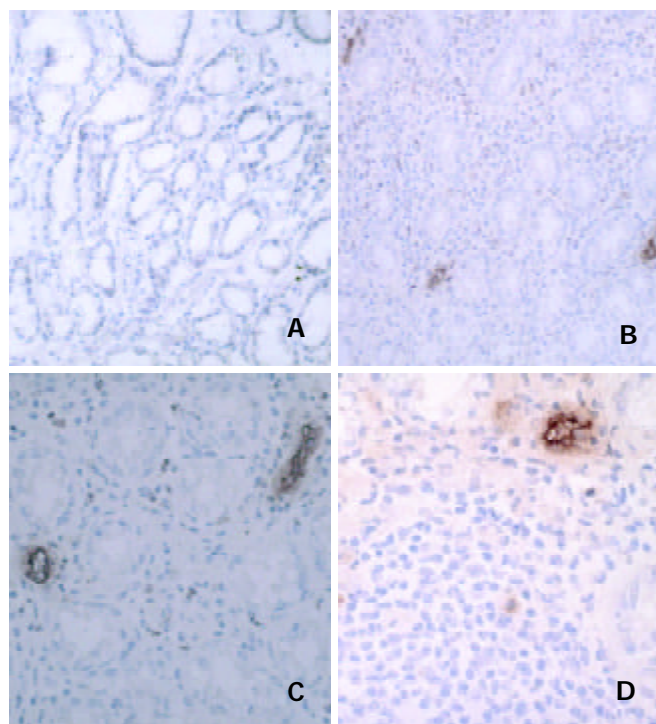


Figure 1 (A): *H. pylori*-negative gastric mucosa showed little immunoreactivity for mucosal addressin cell adhesion molecule 1 (MAdCAM-1). MAdCAM-1 was expressed on the endothelium of numerous vessels within the lamina propria with *H. pylori* infection (B), particularly in association with dense mononuclear infiltration (C). Strong endothelial expression of MAdCAM-1 was localized on high endothelial venule-like vessels adjacent to the lymphoid follicles D.

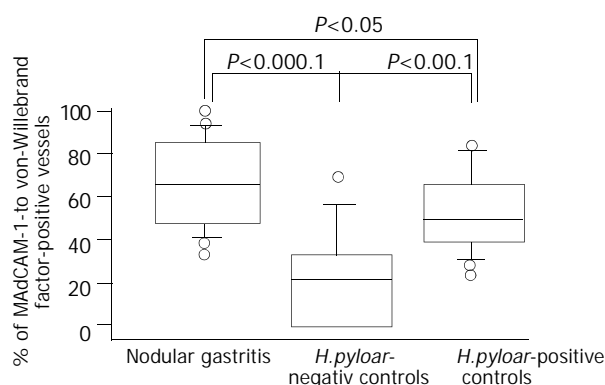


Figure 2 MAdCAM-1 immunoreactivity on mucosal vasculature of antral biopsy specimens from patients with nodular gastritis and *H. pylori*-positive and -negative controls. Results were expressed as the percentage of von-Willebrand factor-positive vessels immunoreactive for MAdCAM-1 in serial sections.

Integrin $\beta 7$ was expressed on increased number of mononuclear cells in the lamina propria of patients with *H. pylori* infection, whereas there were few integrin $\beta 7$ -positive cells in the mucosa of *H. pylori*-negative controls. Analysis of serial sections showed lymphocytes co-expressing anti-CD4 antibody and integrin $\beta 7$ (Figure 3). Also, some CD20-positive cells also expressed integrin $\beta 7$. However, the integrin $\beta 7$ -positive infiltrating cells showed little immunoreactivity for CD8 and CD68. The vessels lined with endothelial cells positive for MAdCAM-1 correlated well with the infiltration of integrin $\beta 7$ -expressing lymphocytes (Figure 4).

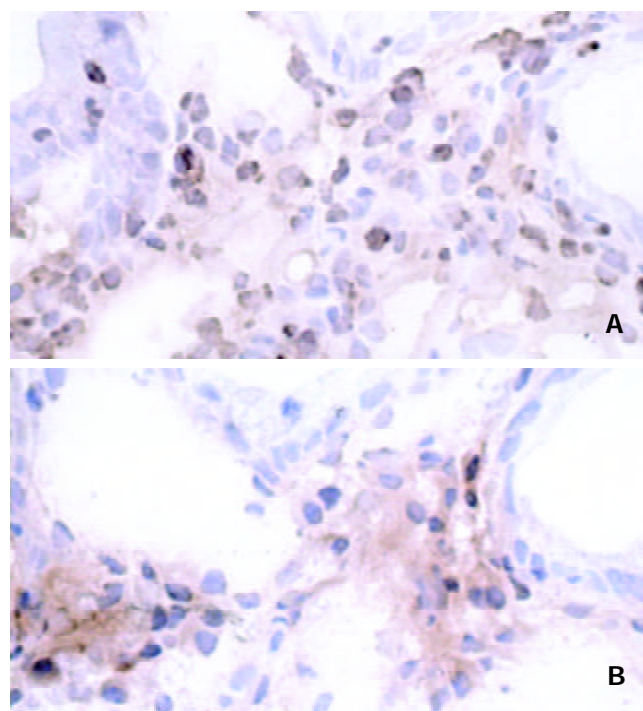


Figure 3 In simultaneous viewing of serial sections, integrin $\beta 7$ -expressing cells (A) consisted of CD-4-positive T lymphocytes (B).

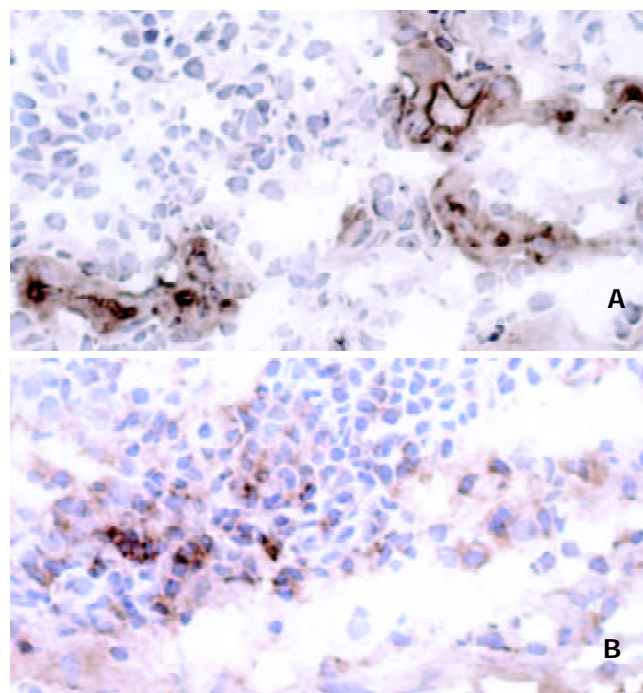


Figure 4 Vessels lined with MAdCAM-1-positive endothelium (A) were associated with infiltration of lymphocytes immunoreactive for integrin $\beta 7$ (B).

Expression of MadCAM-1 gene in antral biopsy specimens

We identified the *MadCAM-1* gene-specific product as a 387-bp band by RT-PCR both in patients with NG and in *H pylori*-positive controls, but not in *H pylori*-negative controls despite the constitutive *G3PDH* housekeeping gene expression (Figure 5).

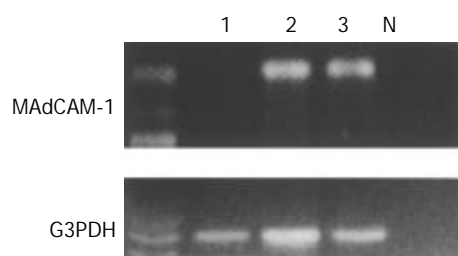


Figure 5 MADCAM-1 and glyceraldehyde-3-phosphate dehydrogenase (G3PDH) mRNA transcripts were detected as 387 and 983 base pair-bands with reverse transcriptase-polymerase chain reaction, respectively. Lane N: negative control, lane 1: *H pylori*-negative control, lane 2: *H pylori*-positive control, lane 3: patients with nodular gastritis.

DISCUSSION

In the present study, vascular expression of MADCAM-1 protein assessed by immunohistochemistry was more enhanced in gastric mucosa of *H pylori*-positive than in *H pylori*-negative subjects. On RT-PCR analysis, the mRNA for MADCAM-1 was detected only in *H pylori*-infected gastric mucosa, but not in the mucosa negative for the organism. In the previous *in vitro* study, MADCAM-1 was induced on a murine endothelial cell line, by proinflammatory cytokines including interleukin 1 and tumor necrosis factor α ^[18], which were much more increased in human gastric mucosa with than without *H pylori* infection^[19]. Considered together, these results indicate that MADCAM-1 is selectively upregulated in the infected gastric mucosa. Integrin β 7-expressing mononuclear cells were found surrounding blood vessels lined with MadCAM-1-positive endothelium, suggesting that the MADCAM-1/integrin α 4 β 7 pathway directs lymphocytes to the inflamed sites of *H pylori* infection, as shown in the murine model^[11]. Together with other endothelially expressed adhesion molecules such as intercellular cell adhesion molecule 1 and vascular cell adhesion molecule 1^[15], though more specifically, MADCAM-1 could play a role in chronic inflammation induced by *H pylori*.

The striking finding of this study was that the percentages of MADCAM-1-positive to von Willebrand factor-positive vessels in the lamina propria was significantly higher in patients with NG than in *H pylori*-positive controls. In addition to the prominent development of lymphoid follicles, intense mucosal inflammatory cell infiltration consisting mainly of lymphocytes was characteristic of NG^[10]. The recruitment and emigration of circulating lymphocytes, on which integrin α 4 β 7 is certainly expressed^[20], may be accelerated in the gastric mucosa of NG, through, in part, the substantially enhanced expression of this vascular addressin.

MADCAM-1 protein was strongly expressed on high endothelial venule-like vessels adjacent to lymphoid follicles and dense lymphoid aggregates within gastric mucosa. In the gut-associated lymphoid tissues such as Peyer's patches and mesenteric lymph nodes, the homing of their constituent lymphocytes has been found to be largely dependent on the interaction of MADCAM-1 on high endothelial venules with integrin α 4 β 7^[2]. Similarly, the vascular MADCAM-1 localized near the lymphoid follicles may be a principal ligand for circulating lymphocytes to the specialized lymphoid sites and

may contribute to the formation of MALT in *H pylori*-induced gastric inflammation, typically leading to the development of NG. This is a topic that warrants further studies, with special attention to the relationship between NG and MALT lymphoma^[21], as a recent report documented the strong expression of MADCAM-1 on the vasculature of patients with this type of lymphoma^[12].

In the present study, simultaneous viewing of serial sections revealed the presence of integrin β 7-expressing mononuclear cells in the infected gastric mucosa. These cells were mainly CD4-positive T and CD20-positive B cell populations, as described previously^[12,20,22]. Several *in vitro* studies showed that *H pylori* antigen could induce the expression of integrin α 4 β 7 on the surface of these cells^[20,22]. In addition, employing immunomagnetic cell sorting, *H pylori* reactive circulating T lymphocytes were mainly found in the α 4 β 7-positive cell fraction^[20]. Accordingly, we believe that mucosally activated lymphocytes in response to *H pylori* infection can migrate from the inductive sites via circulation to their effector sites in the gastric mucosa, using this exclusive homing receptor as a ligand for MADCAM-1.

In conclusion, our study demonstrated enhanced expression of MADCAM-1 on the vascular endothelium and increased number of integrin β 7-expressing T and B cells in *H pylori*-positive gastric mucosa. In NG, the proportion of MADCAM-1-positive vessels was higher than that even in *H pylori*-positive controls. The selective MADCAM-1/integrin α 4 β 7 homing system is thought to play a significant role in gastric mucosal immunity in response to *H pylori* infection, especially in lymphoid follicle formation.

REFERENCES

- 1 **Springer TA**. Traffic signals for lymphocyte recirculation and leukocyte emigration: the multistep paradigm. *Cell* 1994; **76**: 301-314
- 2 **Briskin M**, Winsor-Hines D, Shyjan A, Cochran N, Bloom S, Wilson J, McEvoy LM, Butcher EC, Kassam N, Mackay CR, Newman W, Rindler DJ. Human mucosal addressin cell adhesion molecule-1 is preferentially expressed in intestinal tract and associated lymphoid tissue. *Am J Pathol* 1997; **151**: 97-110
- 3 **Dytoc M**, Gold B, Louie M, Huesca M, Fedorko L, Crowe S, Lingwood C, Brunton J, Sherman P. Comparison of *Helicobacter pylori* and attaching-effacing *Escherichia coli* adhesion to eukaryotic cells. *Infect Immun* 1993; **61**: 448-456
- 4 **Kuipers EJ**. *Helicobacter pylori* and the risk and management of associated diseases: gastritis, ulcer disease, atrophic gastritis and gastric cancer. *Aliment Pharmacol Ther* 1997; **11** (Suppl 1): 71-88
- 5 **Weber DM**, Dimopoulos MA, Anandu DP, Pugh WC, Steinbach G. Regression of gastric lymphoma of mucosa-associated lymphoid tissue with antibiotic therapy for *Helicobacter pylori*. *Gastroenterology* 1994; **107**: 1835-1838
- 6 **Blaser MJ**. *Helicobacter pylori* and the pathogenesis of gastro-duodenal inflammation. *J Infect Dis* 1990; **161**: 626-633
- 7 **Meining A**, Stolte M, Hatz R, Lehn N, Miehle S, Morgner A, Bayerdorffer E. Differing degree and distribution of gastritis in *Helicobacter pylori*-associated diseases. *Virchows Arch* 1997; **431**: 11-15
- 8 **Genta RM**, Hamner HW, Graham DY. Gastric lymphoid follicles in *Helicobacter pylori* infection: frequency, distribution, and response to triple therapy. *Hum Pathol* 1993; **24**: 577-583
- 9 **Miyamoto M**, Haruma K, Yoshihara M, Hiyama T, Sumioka M, Nishisaka T, Tanaka S, Chayama K. Nodular gastritis in adults is caused by *Helicobacter pylori* infection. *Dig Dis Sci* 2003; **48**: 968-975
- 10 **De Giacomo C**, Fiocca R, Villani L, Lisato L, Licardi G, Diegoli N, Donadini A, Maggiore G. *Helicobacter pylori* infection and chronic gastritis: clinical, serological, and histologic correlations in children treated with amoxicillin and colloidal bismuth subcitrate. *J Pediatr Gastroenterol Nutr* 1990; **11**: 310-316
- 11 **Hatanaka K**, Hokari R, Matsuzaki K, Kato S, Kawaguchi A, Nagao S, Suzuki H, Miyazaki K, Sekizuka E, Nagata H, Ishii H,

- Miura S. Increased expression of mucosal addressin cell adhesion molecule-1 (MAdCAM-1) and lymphocyte recruitment in murine gastritis induced by *Helicobacter pylori*. *Clin Exp Immunol* 2002; **130**: 183-189
- 12 **Dogan A**, Du M, Koulis A, Briskin MJ, Isaacson PG. Expression of lymphocyte homing receptors and vascular addressins in low-grade gastric B-cell lymphomas of mucosa-associated lymphoid tissue. *Am J Pathol* 1997; **151**: 1361-1369
- 13 **Isomoto H**, Furusu H, Shin M, Ohnita K, Miyazaki M, Omagari K, Mizuta Y, Murase K, Inoue K, Murata I, Koji T, Kohno S. Enhanced expression of transcription factor E2F in *Helicobacter pylori*-infected gastric mucosa. *Helicobacter* 2002; **7**: 152-162
- 14 **Arihiro S**, Ohtani H, Suzuki M, Murata M, Ejima C, Oki M, Kinouchi Y, Fukushima K, Sasaki I, Nakamura S, Matsumoto T, Torii A, Toda G, Nagura H. Differential expression of mucosal addressin cell adhesion molecule-1 (MAdCAM-1) in ulcerative colitis and Crohn's disease. *Pathol Int* 2002; **52**: 367-374
- 15 **Hatz RA**, Rieder G, Stolte M, Bayerdorffer E, Meimarakis G, Schildberg FW, Enders G. Pattern of adhesion molecule expression on vascular endothelium in *Helicobacter pylori*-associated antral gastritis. *Gastroenterology* 1997; **112**: 1908-1919
- 16 **Leung E**, Berg RW, Langley R, Greene J, Raymond LA, Augustus M, Ni J, Carter KC, Spurr N, Choo KH, Krissansen GW. Genomic organization, chromosomal mapping, and analysis of the 5' promoter region of the human MAdCAM-1 gene. *Immunogenetics* 1997; **46**: 111-119
- 17 **Ikeda K**, Oka M, Yamada Y, Soda H, Fukuda M, Kinoshita A, Tsukamoto K, Noguchi Y, Isomoto H, Takeshima F, Murase K, Kamihira S, Tomonaga M, Kohno S. Adult T-cell leukemia cells over-express the multidrug-resistance-protein (MRP) and lung-resistance-protein (LRP) genes. *Int J Cancer* 1999; **82**: 599-604
- 18 **Takeuchi M**, Baichwal VR. Induction of the gene encoding mucosal vascular addressin cell adhesion molecule 1 by tumor necrosis factor alpha is mediated by NF-kappa B proteins. *Proc Natl Acad Sci U S A* 1995; **92**: 3561-3565
- 19 **Yamaoka Y**, Kita M, Kodama T, Sawai N, Kashima K, Imanishi J. Induction of various cytokines and development of severe mucosal inflammation by cagA gene positive *Helicobacter pylori* strains. *Gut* 1995; **41**: 442-451
- 20 **Quiding-Jarbrink M**, Ahlstedt I, Lindholm C, Johansson EL, Lonroth H. Homing commitment of lymphocytes activated in the human gastric and intestinal mucosa. *Gut* 2001; **49**: 519-525
- 21 **Miyamoto M**, Haruma K, Hiyama T, Kamada T, Masuda H, Shimamoto F, Inoue K, Chayama K. High incidence of B-cell monoclonality in follicular gastritis: a possible association between follicular gastritis and MALT lymphoma. *Virchows Arch* 2002; **440**: 376-380
- 22 **Barrett SP**, Riordon A, Toh BH, Gleeson PA, van Driel IR. Homing and adhesion molecules in autoimmune gastritis. *J Leukoc Biol* 2000; **67**: 169-178

Edited by Wang XL

• *H pylori* •

Epithelial cell proliferation and glandular atrophy in lymphocytic gastritis: Effect of *H pylori* treatment

Johanna M. Mäkinen, Seppo Niemelä, Tuomo Kerola, Juhani Lehtola, Tuomo J. Karttunen

Johanna M. Mäkinen, Tuomo J. Karttunen, Department of Pathology, University of Oulu, Oulu, Finland

Seppo Niemelä, Juhani Lehtola, Department of Internal Medicine, Oulu University Hospital, Oulu, Finland

Tuomo Kerola, Department of Pathology, Länsi-Pohja Central Hospital, Kemi, Finland

Correspondence to: Tuomo J. Karttunen, Department of Pathology, P.O. Box 5000 (Aapistie 5), FIN-90014 University of Oulu, Finland. tuomo.karttunen@oulu.fi

Telephone: +358-8-537-5951 **Fax:** +358-8-537-5953

Received: 2003-08-11 **Accepted:** 2003-10-12

Abstract

AIM: Lymphocytic gastritis is commonly associated with *Helicobacter pylori* infection. The presence of glandular atrophy and foveolar hyperplasia in lymphocytic gastritis suggests abnormalities in cell proliferation and differentiation, forming a potential link with the suspected association with gastric cancer. Our aim was to compare epithelial proliferation and morphology in *H pylori* associated lymphocytic gastritis and *H pylori* gastritis without features of lymphocytic gastritis, and to evaluate the effect of *H pylori* treatment.

METHODS: We studied 14 lymphocytic gastritis patients with *H pylori* infection. For controls, we selected 14 matched dyspeptic patients participating in another treatment trial whose *H pylori* infection had successfully been eradicated. Both groups were treated with a triple therapy and followed up with biopsies for 6-18 months (patients) or 3 months (controls). Blinded evaluation for histopathological features was carried out. To determine the cell proliferation index, the sections were labeled with Ki-67 antibody.

RESULTS: Before treatment, lymphocytic gastritis was characterized by foveolar hyperplasia ($P=0.001$) and glandular atrophy in the body ($P=0.008$), and increased proliferation in both the body ($P=0.001$) and antrum ($P=0.002$). Proliferation correlated with foveolar hyperplasia and inflammation activity. After eradication, the number of intraepithelial lymphocytes decreased in the body ($P=0.004$) and antrum ($P=0.065$), remaining higher than in controls ($P<0.001$). Simultaneously, the proliferation index decreased in the body from 0.38 to 0.15 ($P=0.043$), and in the antrum from 0.34 to 0.20 ($P=0.069$), the antral index still being higher in lymphocytic gastritis than in controls ($P=0.010$). Foveolar hyperplasia and glandular atrophy in the body improved ($P=0.021$), reaching the non-LG level.

CONCLUSION: In lymphocytic gastritis, excessive epithelial proliferation is predominantly present in the body, where it associates with foveolar hyperplasia and glandular atrophy. These characteristic changes of lymphocytic gastritis are largely related to *H pylori* infection, as shown by their improvement after eradication. However, some residual deviation was still seen in lymphocytic gastritis, indicating either an abnormally slow improvement or the presence of some persistent abnormality.

Mäkinen JM, Niemelä S, Kerola T, Lehtola J, Karttunen TJ. Epithelial cell proliferation and glandular atrophy in lymphocytic gastritis: Effect of *H pylori* treatment. *World J Gastroenterol* 2003; 9(12): 2706-2710

<http://www.wjgnet.com/1007-9327/9/2706.asp>

INTRODUCTION

Lymphocytic gastritis (LG) is an inflammatory disorder first described by Haot and his group in 1985^[1]. This histopathological entity is characterized by a marked increase in the number of intraepithelial lymphocytes (IELs), most being CD8+ or CD3+ cytotoxic T-cells^[2]. The amount of 25 IELs per 100 epithelial cells is usually considered diagnostic^[3]. The reported prevalence of LG among patients with dyspepsia varies between 1-8 %^[4,5]. Most dyspeptic patients with LG are seropositive for *Helicobacter pylori*, indicating that LG may represent an atypical host immune response to the infection^[6]. Cases associated with *H pylori* infection have been reported to respond to *H pylori* eradication treatment^[7-9]. Gluten is one of the other suspected trigger factors in particular cases, and the prevalence of LG is high in patients with celiac disease, reaching levels up to 45 % in some series^[10,11].

LG is common in patients with gastric carcinoma and gastric MALT lymphoma, suggesting that it may be pathogenetically related to gastric malignancies^[12,13]. However, mechanisms linking LG with malignancy are not known. Atrophic changes and foveolar hyperplasia in the body mucosa are common in LG, suggesting that abnormal epithelial proliferation and differentiation may be present. Without treatment these abnormalities are usually considered to be persistent^[5]. Furthermore, our previous follow-up study has shown that LG is linked to a tendency of more severe progression of intestinal metaplasia than in *H pylori* gastritis without LG^[5].

Since foveolar hyperplasia is a characteristic of lymphocytic gastritis, we hypothesized that this might be associated with abnormal proliferation rate. In addition to testing this hypothesis by comparing the proliferation rate with non-LG *H pylori* gastritis, we evaluated the effect of *H pylori* treatment on epithelial cell proliferation and other histopathological features of LG, including glandular atrophy, to find out whether the abnormalities are related to *H pylori* infection and whether they are irreversible.

MATERIALS AND METHODS

Subjects

Two separate series of patients were studied with some differences in the treatment and follow-up protocol. Patients with LG were collected from among the out-patients referred to one endoscopist (SN) for upper abdominal complaints. Patients with histologically proven LG and either histologically or serologically confirmed *H pylori* infection were subsequently included in the open study, in which their *H pylori* infection was treated and they were invited to take part in the post-treatment examinations to document the effects of *H pylori* eradication. An informed consent was obtained from all the

patients according to the usual clinical practice. A total of 14 patients (six men, eight women; mean age 55.2 years, range 41–70 years) who fulfilled the criteria were included. Originally all of them were seropositive for *H pylori*, while only three patients (21 %) could be confirmed as positive on histology. All of the patients had normal findings in duodenal biopsy; no subjects with celiac disease were included. Follow-up gastroscopies with gastric biopsies were performed on all the patients after the eradication. The mean follow-up time was 12 months, ranging from six to 18 months. The effect of treatment on intraepithelial lymphocyte counts in a subset of these patients has been previously reported^[9].

For the control group, a series of age and gender matched *H pylori* positive subjects were selected from another treatment trial: Prospective Phase IV clinical multicenter study aiming at testing the effects of sucralfate as an adjuvant to *H pylori* eradication therapy in non-ulcer dyspepsia (F-SUC-CL-0191-FIN; Orion Corporation, Orion Pharma, Finland). Inclusion criteria included the following: age over 18 years, dyspeptic symptoms not explained by any other disease, normal upper abdominal ultrasound, no active peptic ulcer or a history of ulcer, no endoscopic esophagitis, no other severe illness, no need for continuous use of NSAID or steroids. The patients were not allowed to use any anti-ulcer drugs including antacids or H₂-antagonists during the two weeks before the trial. The study was approved by the ethical committees in the participating hospitals in Northern Finland. Only subjects with a successful eradication result based on histology were selected. The control group consisted of 14 patients (seven men, seven women, mean age 53.8 years, range 38–67 years) all presenting with *H pylori* positive gastritis without either LG, celiac disease or malignancy. Biopsies taken before the treatment and three months after the eradication therapy were studied.

Histopathology

A minimum of two biopsies was taken from both the antrum and the body at the initial and follow-up gastroscopy. In addition, routine biopsies from the descending part of the duodenum were taken during the primary endoscopy. The biopsies were fixed in formalin, embedded in paraffin and stained with hematoxylin and eosin. During the collection of the patient series one pathologist (TKa) made a preliminary diagnosis of LG. The diagnosis was based on the presence of intraepithelial lymphocytes at a ratio of 30 per 100 epithelial cells, or greater, in the areas of their maximal density.

After the follow-up of the whole series was completed, the slides were coded and evaluated for IEL counts by a second pathologist (TKe), blinded for any clinical data including treatment status and the results of preliminary histopathological evaluation. The IEL number was counted at three randomly selected fields of surface and foveolar epithelium separately in the antral and body mucosa. In addition, IEL number was counted in the area of the maximal IEL density in antral and body mucosa. Around 100 to 150 cells in epithelium were counted in each field. The grade of gastritis, quantity of different types of inflammatory cells, grade of atrophy, foveolar hyperplasia and intestinal metaplasia were similarly analyzed by a blinded investigator (TKa) according to the histological criteria of the updated Sydney system. The presence and quantity of *H pylori* was evaluated from sections stained with a modified Giemsa stain.

Immunohistochemistry and determination of the Ki-67 labeling index

Sections from each gastric biopsy specimen were treated with 10 mM citrate buffer, pH 6.0, for 2 x 5 minutes for antigen retrieval. The sections were incubated with Ki-67 monoclonal

antibody (clone 7B11, Zymed, South San Francisco, CA, USA; 1:50 dilution) for 60 minutes at 37 °C. Bound antigen was detected with labeled streptavidin-biotin method using AEC as a chromogen (Histostain™-plus, Zymed, South San Francisco, CA, USA). Hematoxylin was used as a counterstain.

Labeled and unlabeled epithelial cells were counted under a high-power microscope (×100) in the optimal, longitudinally orientated and complete foveolae. The proportion of positive cells among foveolar epithelial cells indicated the proliferation (labeling) index (LI %). The mean LI % for each biopsy was calculated as an average from several foveolae. The counting was performed by a single person (JM) blinded for all previous clinical and histopathological data.

Serology

The serological diagnosis of *H pylori* was made by testing the specific IgG antibodies with an enzyme linked immunosorbent assay (ELISA, Pyloriset®, Orion Diagnostica, Finland). Titers of 1:500 or higher were considered positive.

Eradication treatment

In the LG group, *H pylori* eradication therapy consisted of a ten day course of bismuth subsalicylate (240 mg twice daily) and metronidazole (400 mg three times daily) or amoxicillin (1 g twice daily). The controls were treated for two weeks with metronidazole (400 mg three times daily) and tetracycline (500 mg three times daily). In addition they got sucralfate (2 g twice daily for 6 weeks followed by 1 g once daily for 6 weeks). No proton inhibitors were allowed in the control group.

Statistics

LG patients and controls were compared by using the nonparametric Mann-Whitney test. Temporal changes in the results were evaluated by using the Wilcoxon signed ranks test. Spearman's two-tailed rank correlation test was used to assess the correlations between the variables. A probability of *P* less than 0.05 in two-tailed tests was considered statistically significant. Analyses were made with the Statistical Package for Social Sciences (SPSS 10.0, Chicago, IL, USA).

RESULTS

Histopathological features and cell proliferation in *H pylori* related lymphocytic gastritis and controls before eradication

In all the patients with LG the maximal number IELs was 30 IEL/100 epithelia in either the body or antral mucosa. The histopathological features including the IEL density (per 100 epithelial cells) in random fields. (Table 1; Figure 1) and epithelial cell proliferation (Figure 2) before eradication treatment were compared between LG and non-LG *H pylori* gastritis. The density of *H pylori* organisms was higher in the control group in the body (*P*=0.009) and antral mucosa (*P*=0.001), and showed a significant negative correlation with age in LG (body mucosa; *c*=−0.633, *P*=0.002). The pre-treatment levels of specific IgG antibody titers were lower in the control group (median 1:1 575, range 1:140–1:5 600) than in LG (1:6 000, range 1:1 000–1:17 000; *P*=0.011).

In the antral mucosa the degree of atrophy did not show any significant differences between LG and non-LG *H pylori* gastritis, but the body mucosa showed significantly more severe atrophy in LG (Table 1; *P*=0.008). Of LG subjects 50 % (*n*=7) showed mild and 14 % (*n*=2) moderate atrophy of the body mucosa (Figure 1), while 36 % (*n*=5) showed no sign of atrophy. No cases with severe atrophy were found. The severity of atrophy in the body showed a trend towards a positive association with IEL count (*c*=0.542, *P*=0.069). In the control group, only 17 % (*n*=2) of the cases showed atrophy of the body

mucosa prior to eradication. In the antrum, gastritis was more active in the controls ($P=0.034$), but no significant difference was seen in the body. The eosinophilic leukocytes score in the body mucosa was higher in LG (Table 1; $P=0.001$), while in the antral mucosa the score tended to be higher in the control group ($P=0.062$). The extent of intestinal metaplasia in the body mucosa tended to be greater in LG (Table 1; $P=0.095$). Elongation of the foveolae was more often seen in LG (Table 1; Figure 1; body mucosa $P=0.001$; antral mucosa $P=0.074$).

Due to tangential sectioning, the proliferation index based on the number of cells with nuclear expression of Ki-67 could be determined in only about 80 % of the specimen slides. The pre-treatment epithelial cell proliferation rate was higher in LG in both the body ($P=0.001$) and antral mucosa ($P=0.002$) compared to the controls (Figure 1). In LG, the proliferation index of the body mucosa showed correlation with the degree of foveolar hyperplasia ($c=0.798$, $P=0.010$), but did not correlate with atrophy or any other histologic feature, except for a trend towards correlation with the activity of gastritis ($c=0.655$, $P=0.078$). In the antral mucosa the proliferation index correlated negatively with the patient's age ($c=-0.707$, $P=0.050$). In the controls, proliferation showed no significant correlation with any of the histological markers or age.

Table 1 Antrum and body gastritis in subjects with lymphocytic gastritis (LG) and controls (non-LG) before and after *H. pylori* eradication

Antrum	LG	Non-LG
<i>H. pylori</i> score	0 (0-2) ^f	2 (0-3) ^{bf}
After treatment	0 (0-0)	0 (0-0) ^b
Atrophy	2 (1-2)	2 (0-3)
After treatment	1 (1-2)	2 (0-3)
Metaplasia	0 (0-2)	0 (0-1)
After treatment	0 (0-1)	0 (0-1)
Foveolar length (μm)	340 (290-650) ^a	300 (260-370)
After treatment	300 (250-330) ^a	320 (220-480)
IEL count (mean)	9.5 (1.0-30.7) ^f	1.7 (1.0-4.0) ^f
After treatment	5.7 (0.7-11.0)	1.3 (0.3-3.7)
Activity	1 (0-2) ^{ad}	2 (0-3) ^{ad}
After treatment	0 (0-0) ^{ad}	0 (0-2) ^{ad}
Eosinophils	1 (0-2)	1 (0-2)
After treatment	0 (0-1) ^d	1.5 (0-3) ^d
Body	LG	Non-LG
<i>H. pylori</i> score	0 (0-3) ^d	2 (0-3) ^{bd}
After treatment	0 (0-0)	0 (0-0) ^b
Atrophy	2 (1-3) ^{ad}	1 (0-2) ^d
After treatment	1 (1-2) ^a	1 (0-2)
Metaplasia	0 (0-2) ^d	0 (0-0) ^d
After treatment	0 (0-1)	0 (0-0)
Foveolar length (μm)	310 (250-800) ^{bf}	170 (130-210)
After treatment	210 (140-290) ^b	200 (150-320)
IEL count (mean)	26.3 (3.7-56.7) ^{bf}	1.7 (0.3-2.7) ^f
After treatment	5.7 (1.0-41.7) ^{bf}	2.0 (0.3-3.7) ^f
Activity	1 (0-2) ^a	0.5 (0-2) ^a
After treatment	0 (0-2) ^a	0 (0-1) ^a
Eosinophils	1 (1-2) ^{af}	1 (0-1) ^f
After treatment	1 (0-2) ^{ad}	0 (0-1) ^d

Note: Median score and range are indicated except for IEL count, where mean is used. The significance of temporal changes was evaluated by Wilcoxon signed ranks test (a). LG patients and controls were compared with the Mann-Whitney test (d). c, f: $P<0.001$; b, e: $P<0.005$; a, d: $P<0.05$ (two-tailed significance).

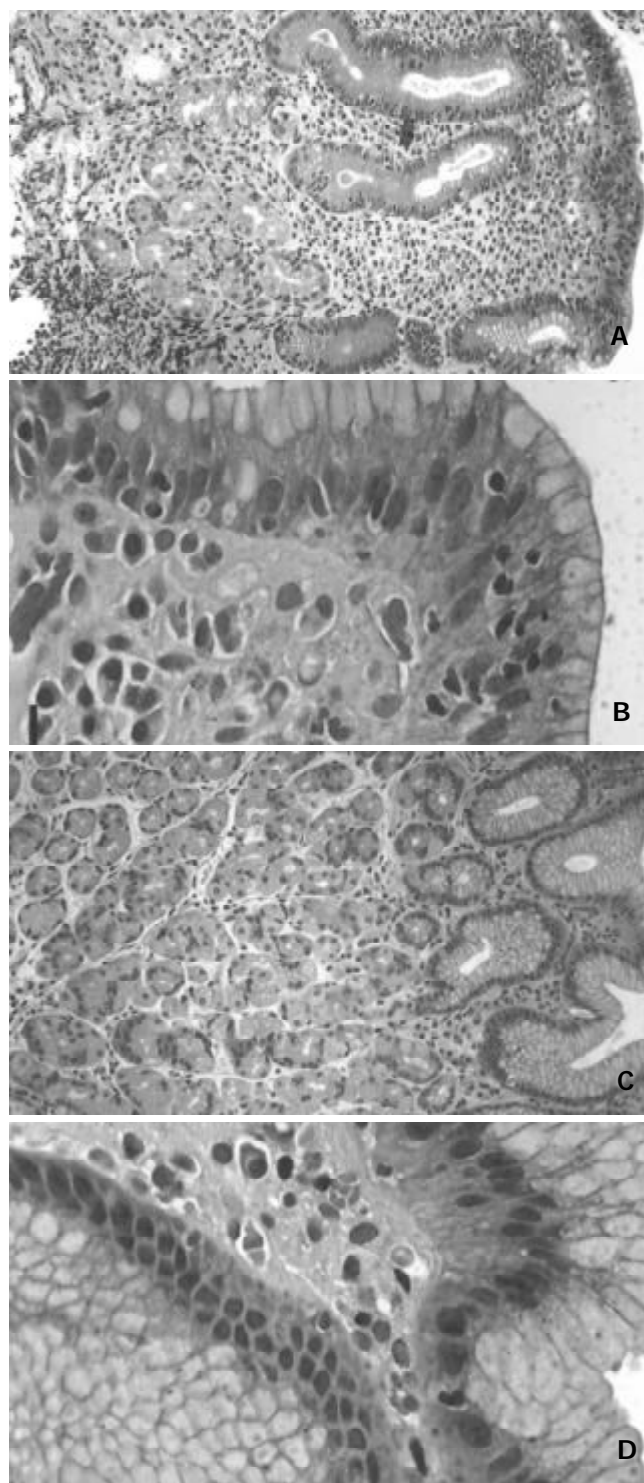


Figure 1 A,B,C,D. Hematoxylin-Eosin stained sections from gastric body mucosa in a case of lymphocytic gastritis before and after eradication treatment. Before treatment (A,B) there was a sharp increase of intraepithelial lymphocytes, moderate glandular atrophy and foveolar hyperplasia. After treatment (C,D) there were only occasional intraepithelial lymphocytes and no signs of glandular atrophy or foveolar hyperplasia. A,C, Bar=25 μm. B,D, Bar=10 μm.

Effect of eradication treatment

We then analyzed what kind of impact the eradication treatment had on cell proliferation and gastritis in LG patients and controls. In LG, successful eradication could be verified in 12 out of 14 patients. All the three patients initially positive on histology were now found to be *H. pylori* negative, and showed a decrease of 50 % or more in titer of specific IgG antibodies. Nine cases initially negative on histology showed a similar

decrease in their antibody titers, thus indicating a successful eradication. In two patients, both negative on histology, the decrease in the IgG titers did not quite reach 50 %. However, on histological evaluation of the inflammation, these two patients showed a similar shift towards normal mucosal morphology as the other LG patients. In the control group, all cases were successfully eradicated and turned histologically negative. Yet on serology, only five non-LG patients showed a decrease of the IgG titer of 50 % or more.

In LG, the proliferation index decreased significantly after the eradication in the body mucosa (Figure 2; median from 0.38 to 0.15, $P=0.043$), and showed a similar trend in the antrum (from 0.34 to 0.20, $P=0.069$). In controls, no significant changes were seen (Figure 2). The post-eradication proliferation index in the antrum was nonetheless significantly higher in LG patients ($P=0.010$).

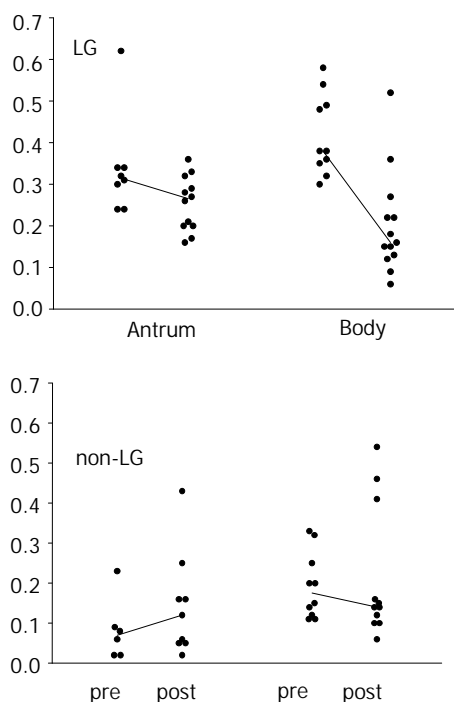


Figure 2 A scatterplot showing epithelial cell proliferation indexes in antral and body mucosa in patients with LG and non-LG *H pylori* gastritis before (pre) and after (post) treatment. The median is indicated with a solid line.

The IEL number decreased significantly in LG (Figure 1) both in areas of maximal density (data not shown) and in random fields (Table 1; body, $P=0.004$), but no change was seen among controls. The post-eradication IEL counts were still significantly higher in LG compared to the controls (Table 1; $P<0.001$). The overall score of inflammatory cells in the lamina propria decreased significantly in both groups (Table 1). In LG, glandular atrophy of the body mucosa improved significantly ($P=0.021$; Figure 1), and after the treatment most subjects (83 %) showed no atrophy at all. Two cases had mild atrophic changes at this stage. However, such a change could not be observed in the antrum. In the control group, eradication did not have any effect on the degree of atrophy in the body (Table 1; $P=0.564$) or in the antrum ($P=0.783$). In LG, a significant shallowing of the gastric pits was seen, as evidence of reduction in the foveolar hyperplasia (body, $P=0.005$; antrum, $P=0.050$). No significant changes were observed in controls.

Since both the IEL counts and proliferation remained significantly increased in LG, we searched for any correlation with inflammatory cell scores to see whether these features were related to residual inflammation, or possibly inherently

abnormal. No significant correlations were seen in either antral or body mucosa between neutrophil, eosinophil or mononuclear inflammatory cell scores, but in the body the proliferation index showed a significant correlation with the IEL count ($c=0.779$, $P=0.005$). In controls, the proliferation index correlated similarly with the IEL number in the body mucosa ($c=0.654$, $P=0.040$).

DISCUSSION

In the present study we have shown that gastric epithelial cell proliferation rate, as measured by the Ki-67 labeling index, was increased in LG associated with *H pylori* infection as compared to *H pylori* gastritis without significant increase of intraepithelial lymphocytes. Increased proliferation was predominantly present in the body mucosa, where it was correlated with foveolar hyperplasia and inflammation activity. In addition, our results suggest that in LG, the characteristic increase of IELs, abnormal proliferation, and atrophic changes of the body mucosa are all largely related to *H pylori* infection, as shown by their improvement after eradication therapy.

Increased proliferation induced by the chronic inflammation has been observed in *H pylori* associated gastritis, and the proliferation rate seems in principal to normalize after eradication therapy^[14], although the antral mucosa may retain a somewhat abnormal proliferation pattern^[15]. In LG, according to our findings, neither the IEL counts nor cell proliferation fell to the level observed in controls after successful treatment, even though the follow-up time was longer in LG patients (minimum six months, mean 12 months) than in controls (three months). This slow rate of normalization is likely to be related to the more pronounced initial abnormality in LG, possibly necessitating a longer period of time for full recovery. A more extended follow-up might be needed to see if these subjects show any permanent abnormality in the proliferation rate. Some intrinsic malfunction causing either a constant abnormal epithelial lymphocyte response or proliferation, or both, is also possible, but no such defects have been reported in LG. A further possible explanation is that there is some other environmental factor in addition to *H pylori* inducing these changes, the effect of which continues after eradication. In some cases, LG is associated with celiac disease^[10,11]. The present study included no patients with this disorder. Other nutritional factors could be involved, as in the duodenal mucosa where an increase of IELs has been described in food allergy^[16]. No such antigen related changes in the gastric mucosa are yet known.

The controversy between the negative histology and positive serology for *H pylori* in LG in the present and previous studies^[5,6,13] might be explained by the fact that the bacteria are present in very small numbers, which could make them impossible to detect. In the present study, even the patients histologically positive for *H pylori* showed only a small amount of bacteria. This is likely to be related to decreased acid secretion associated with the atrophic changes in the body mucosa, which have been shown to associate with a low number of bacteria and a shift of bacteria to the body mucosa^[17] in a way similar to the effect of proton pump inhibitors^[18]. A significant decrease of the specific antibodies after treatment, along with the improvement of the inflammatory changes, indicates that even the cases negative on histology represent a true *H pylori* infection. It is of interest that the levels of *H pylori* specific IgG antibodies were significantly higher in LG than in non-LG *H pylori* positive gastritis. This has been noted previously^[5]. Whether the intensive serological response is related to a certain bacterial strain, amount of antigen, or a matter of a genetically determined pattern of immune response, is not known.

The mechanisms behind the processes of body glandular atrophy and foveolar hyperplasia in LG are unknown. The question of whether atrophy is based on an autoimmune reaction, metaplasia, fibrosis, or on a disturbance in cell regeneration or differentiation in connection with foveolar hyperplasia, needs further study, but the last alternative is most likely the correct one. We could not see any significant change in the extent of intestinal metaplasia after eradication. No auto-antibodies targeted against the gastric parietal cells have been found in LG patients (Niemelä *et al*, unpublished observation), suggesting that autoimmune mechanisms are not important in the pathogenesis of body atrophy in LG. The gastric epithelial stem cells situated in the proliferation zone are capable of differentiating into the direction of either gastric glandular cells or foveolar epithelial cells^[19]. It is unknown which mechanisms are involved in the actual regulation of the direction of differentiation. We speculate that in untreated LG, the cells in the foveolar border area have a greater stimulus for differentiation towards foveolar epithelial cells than towards glandular cells, this pressure eventually leading to glandular atrophy and foveolar hyperplasia. Thus LG might provide a model for studying the mechanisms of selection of epithelial cell differentiation.

A longstanding *H pylori* infection has been shown to be associated with an increased risk of gastric malignancies^[20,21], and successful eradication of this pathogen resulted in the disappearance of histologically malignant lymphomatous proliferation^[22]. Mechanisms of the suggested increased risk of malignancy in LG^[12,13] are unknown. The increased epithelial cell proliferation rate, as detected in the present study, might play an important part by increasing the potential for the accumulation of genetic changes. Glandular atrophy as seen in the present study, and reported previously^[5,13], forms another potential link for gastric cancer, since an increased cancer risk has been documented with body atrophy^[23]. Without any treatment, atrophy and foveolar hyperplasia seen in LG are generally considered to be persistent, and even to progress at a faster rate than in subjects with a non-LG *H pylori* gastritis^[5], supporting the idea that LG has pre-malignant potential. However, more studies are required to find out whether patients with LG are indeed at an increased risk of a gastric malignancy, and whether *H pylori* eradication reduces the risk of gastric neoplasia in these patients.

In conclusion, we have shown that the highly increased epithelial cell proliferation, predominantly in the body mucosa, is a characteristic feature of LG. Abnormal proliferation together with atrophic changes in the body mucosa in LG provide a potential mechanism for the observed association with gastric malignancy. Furthermore, these changes in LG are largely caused by *H pylori* infection as shown by their normalization by eradication therapy.

REFERENCES

- 1 **Haot J**, Hamichi L, Wallez L, Mainguet P. Lymphocytic gastritis: a newly described entity: a retrospective endoscopic and histological study. *Gut* 1988; **29**: 1258-1264
- 2 **Oberhuber G**, Bodingbauer M, Mosberger I, Stolte M, Vogelsang H. High proportion of granzyme B-positive (activated) intraepithelial and lamina propria lymphocytes in lymphocytic gastritis. *Am J Surg Pathol* 1998; **22**: 450-458
- 3 **Lynch DA**, Dixon MF, Axon AT. Diagnostic criteria in lymphocytic gastritis. *Gastroenterology* 1997; **112**: 1426-1429
- 4 **Lynch DA**, Sobala GM, Dixon MF, Gledhill A, Jackson P, Crabtree JE. Lymphocytic gastritis and associated small bowel disease: a diffuse lymphocytic gastroenteropathy? *J Clin Pathol* 1995; **48**: 939-945
- 5 **Niemelä S**, Karttunen T, Kerola T, Karttunen R. Ten year follow up study of lymphocytic gastritis: further evidence on *Helicobacter pylori* as a cause of lymphocytic gastritis and corpus gastritis. *J Clin Pathol* 1995; **48**: 1111-1116
- 6 **Dixon MF**, Wyatt JJ, Burke DA, Rathbone BJ. Lymphocytic gastritis: relationship to *Campylobacter pylori* infection. *J Pathol* 1988; **154**: 125-132
- 7 **Hayat M**, Arora DS, Dixon MF, Clark B, O' Mahony S. Effects of *Helicobacter pylori* eradication on the natural history of lymphocytic gastritis. *Gut* 1999; **45**: 495-498
- 8 **Müller H**, Volkholz H, Stolte M. Healing of lymphocytic gastritis by eradication of *Helicobacter pylori*. *Digestion* 2001; **63**: 14-19
- 9 **Niemelä S**, Karttunen TJ, Kerola T. Treatment of *Helicobacter pylori* in patients with lymphocytic gastritis. *Hepatogastroenterology* 2001; **48**: 1176-1178
- 10 **Karttunen TJ**, Niemelä S. Lymphocytic gastritis and coeliac disease. *J Clin Pathol* 1990; **43**: 436-437
- 11 **Wolber R**, Owen D, DelBuono L, Appelman H, Freeman H. Lymphocytic gastritis in patients with celiac sprue or spruelike intestinal disease. *Gastroenterology* 1990; **98**: 310-315
- 12 **Griffiths AP**, Wyatt J, Jack AS, Dixon MF. Lymphocytic gastritis, gastric adenocarcinoma, and primary gastric lymphoma. *J Clin Pathol* 1994; **47**: 1123-1124
- 13 **Miettinen A**, Karttunen T, Alavaikko M. Lymphocytic gastritis and *Helicobacter pylori* infection in gastric lymphoma. *Gut* 1995; **37**: 471-476
- 14 **Brenes F**, Ruiz B, Correa P, Hunter F, Rhamakrishnan T, Fonthan E. *Helicobacter pylori* causes hyperproliferation of the gastric epithelium: pre- and post-eradication indices of proliferating cell nuclear antigen. *Am J Gastroenterol* 1993; **88**: 1870-1875
- 15 **El-Zimaity HM**, Graham DY, Genta RM, Lechago J. Sustained increase in gastric antral epithelial cell proliferation despite cure of *Helicobacter pylori* infection. *Am J Gastroenterol* 2000; **95**: 930-935
- 16 **Augustin M**, Karttunen TJ, Kokkonen J. TIA1 and mast cell tryptase in food allergy of children: increase of intraepithelial lymphocytes expressing TIA1 associates with allergy. *J Pediatr Gastroenterol Nutr* 2001; **32**: 11-18
- 17 **Karttunen T**, Niemelä S, Lehtola J. *Helicobacter pylori* in dyspeptic patients. Quantitative association with severity of gastritis, intragastric pH, and serum gastrin concentration. *Scand J Gastroenterol Suppl* 1991; **186**: 124
- 18 **Kuipers EJ**, Lundell L, Klinkenberg-Knol EC, Havu N, Festen HP, Liedman B. Atrophic gastritis and *Helicobacter pylori* infection in patients with reflux esophagitis treated with omeprazole or fundoplication. *N Engl J Med* 1996; **334**: 1018-1022
- 19 **Brittan M**, Wright NA. Gastrointestinal stem cells. *J Pathol* 2002; **197**: 492-509
- 20 **Nomura A**, Stemmermann GN, Chyou PH, Kato I, Perez-Perez GI, Blaser MJ. *Helicobacter pylori* infection and gastric carcinoma among Japanese Americans in Hawaii. *N Engl J Med* 1991; **325**: 1132-1136
- 21 **Parsonnet J**, Friedman GD, Vandersteen DP, Chang Y, Vogelstein JH, Orentreich N. *Helicobacter pylori* infection and the risk of gastric carcinoma. *N Engl J Med* 1991; **325**: 1127-1131
- 22 **Wotherspoon AC**, Doglioni C, Diss TC, Pan L, Moschini A, de Boni M. Regression of primary low-grade B-cell gastric lymphoma of mucosa-associated lymphoid tissue type after eradication of *Helicobacter pylori*. *Lancet* 1993; **342**: 575-577
- 23 **Sipponen P**, Kekki M, Haapakoski J, Ihmäki T, Siurala M. 1985. Gastric cancer risk in chronic atrophic gastritis: statistical calculations of cross-sectional data. *Int J Cancer* 1985; **35**: 173-177

• *H pylori* •

Expression of *Helicobacter pylori* Hsp60 protein and its immunogenicity

Yang Bai, Liang-Ren Li, Ji-De Wang, Ye Chen, Jian-Feng Jin, Zhao-Shan Zhang, Dian-Yuan Zhou, Ya-Li Zhang

Yang Bai, Liang-Ren Li, Ji-De Wang, Ye Chen, Dian-Yuan Zhou, Ya-Li Zhang, PLA Institute for Digestive Medicine, Nanfang Hospital, First Military Medical University, Guangzhou 510515, Guangdong Province, China

Jian-Feng Jin, Chemistry University of Beijing, Beijing 100071, China

Zhao-Shan Zhang, Institute of Biotechnology, Academy of Military Medical Science, Beijing 100071, China

Supported by the National Natural Science Foundation of China, No.30270078

Correspondence to: Dr. Ya-Li Zhang, PLA Institute for Digestive Medicine, Nanfang Hospital, First Military Medical University, Guangzhou 510515, Guangdong Province, China. baiyang1030@hotmail.com

Telephone: +86-20-61641532

Received: 2003-03-12 **Accepted:** 2003-05-16

Abstract

AIM: To express Hsp60 protein of *H pylori* by a constructed vector and to evaluate its immunogenicity.

METHODS: Hsp60 DNA was amplified by PCR and inserted into the prokaryotic expression vector pET-22b (+), which was transformed into BL21 (DE3) *E.coli* strain to express recombinant protein. Immunogenicity of expressed Hsp60 protein was evaluated with animal experiments.

RESULTS: DNA sequence analysis showed Hsp60 DNA was the same as GenBank's research. Hsp60 recombinant protein accounted for 27.2 % of the total bacterial protein, and could be recognized by the serum from *H pylori* infected patients and Balb/c mice immunized with Hsp60 itself.

CONCLUSION: Hsp60 recombinant protein might become a potential vaccine for controlling and treating *H pylori* infection.

Bai Y, Li LR, Wang JD, Chen Y, Jin JF, Zhang ZS, Zhou DY, Zhang YL. Expression of *Helicobacter pylori* Hsp60 protein and its immunogenicity. *World J Gastroenterol* 2003; 9(12): 2711-2714
<http://www.wjgnet.com/1007-9327/9/2711.asp>

INTRODUCTION

Helicobacter pylori (*H pylori*) infection is the major cause of chronic active gastritis and most peptic ulcer diseases^[1-11], and is also closely related with gastric cancers such as adenocarcinoma, mucosa-associated lymphoid tissue (MALT) lymphoma and primary gastric non-Hodgkin's lymphoma^[12-18]. This organism has been categorized as a class I carcinoma by the World Health Organization, and direct evidences of its carcinogenesis was recently demonstrated both in an animal model and in retrospective cohort and nested case-control studies in China^[19-21]. In addition, seroprevalence studies indicated that *H pylori* infection was also associated with cardiovascular, respiratory, extra-gastrointestinal digestive, autoimmune diseases^[22-24]. Successful eradication of *H pylori* is thus an important goal. Currently, its treatment involves

antibiotic therapy, but this has some associated problems such as low patient compliance and increase of resistant strains^[25-27]. An alternative approach is to develop a vaccine, which would not only clear the organism, but also prevent its reinfection^[28-31].

Selection of antigenic targets and adjuvants is critical in developing *H pylori* vaccine. So far this area has achieved only a limited success. With most studies focusing on urease enzyme combined with cholera toxin (CT) or heat-labile toxin of *Escherichia coli* (LT), this antigen/adjuvant combination has been proved to be effective in many animal models, but some problems still exist such as toxicity of LT or CT and inadequate protection of urease enzyme, so new antigens and adjuvants should be looked for^[32]. Some studies have proved that heat shock protein 60 (Hsp60) of mycobacteria was a kind of adjuvants, and could cause immune responses of priority in mouse and mankind models, so some researchers suspected *H pylori* Hsp60 might be an excellent antigen candidate^[33,34]. In this study, recombinant plasmid of *H pylori* Hsp60 gene was constructed and expressed for the development of *H pylori* vaccine.

MATERIALS AND METHODS

Materials

Bacterial strain BL21(DE3) and plasmid pET-22b(+) were provided by the Institute of Biotechnology, Academy of Military Medical Sciences. *H pylori* SS1 was preserved in this research institute. Restriction enzyme Not I, Nco I and T4 DNA ligase, Vent DNA polymerase, isopropyl-β-D-thiogalactopyranoside (IPTG) were purchased from New England Biolabs Company. Goat anti-mouse and goat anti-human IgG-HRP were purchased from Huamei Bioengineering Company, China and His-Tag precolumn from Invitrogen Company. Specific-pathogen-free, female BALB/c mice were housed according to Health Research Council of China guidelines with free access to food and water. Eight *H pylori* positive sera (which were positive by urease test, pathological dying and germ culture) and three *H pylori* negative sera (which were detected negative by the above-mentioned three examinations) were from patients treated in the Endoscopy Center of this institute. Other reagents were analytically pure reagents produced in China.

Recombinant DNA techniques

All restriction enzyme digestions, ligations and other common DNA manipulations, unless otherwise stated, were performed by standard procedures^[31,35]. The genome of *H pylori* was prepared from cells collected from colonies on a agar plate. The gene of *H pylori* Hsp60 was amplified from the genome of *H pylori* by PCR (Technique PROGENE) using the primers Hsp601 (5'-TG GCC ATG GAT GGG CCA AGA GGC AGG AAT-3') as upstream primer and Hsp602 (5'-AG TGC GGC CGC CAT CAT GCC GCC CAT G-3') as downstream primer as described in the literature^[36]. Hsp601 and Hsp602 contained *Nco* I and *Not* I sites, respectively. PCR was performed with the hot start method. PCR condition was that after initial denaturing at 95 °C for 30 s, each cycle of amplification consisted of denaturing at 95 °C for 30 s, annealing at 55 °C for

30 s and polymerization at 72 °C for 60 sec and further polymerization for 10 min after 35 PCR cycles. PCR product was harvested from agarose gel, digested with *Nco* I and *Not* I, and inserted into *Nco* I and *Not* I restriction fragments of the expression vector pET-22b(+) using T4 DNA ligase. The resulting plasmid pET- Hsp60 was transformed into competent *E.coli* BL21 (DE3) cells using ampicillin resistance for selection. The alkaline lysis method was chosen for large-scale preparations of recombinant plasmid and the plasmids were identified by restriction enzymes. DNA sequence was performed with a DNA automatic sequencer.

Induced expression, purification and SDS-polyacrylamide gel electrophoresis

The recombinant strains were incubated overnight at 37 °C while shaking in 5 ml LB with 100 µg/mL ampicillin, 50 mL LB were inoculated and the cells grew until the optical density at 600 nm reached 0.4-0.6. Isopropyl-β-D-thiogalactopyranoside (IPTG) was added to a final concentration of 0.1, 0.2, 0.4, 0.6, 0.8, 1.0 mM, respectively. *E.coli* cells growing in 50 mL LB 3 h or 5 h after induction were harvested by centrifugation at 12 000 g for 10 min and the pellet was resuspended in 1 ml 30 mM Tris buffer (pH8.0) containing 1 mmol/L EDTA (pH8.0), 20 % sucrose. The suspension was put on ice for 10 min, and then centrifuged for 10 min at 12 000 g, and the resulting supernatant contained proteins from periplasms. The resulting pellet was resuspended in 5 mL 50 mM Tris buffer (pH8.0) containing 2 mM EDTA, 0.1 mg/mL lysozyme and 1 % Triton X-100. The suspension was incubated at 30 °C for 20 min and then sonicated on ice until it became clarified. The lysate was centrifuged at 12 000 g for 15 min at 4 °C, and then the resulting supernatant containing proteins from cytoplasm was purified with Ni-NTA column. Whole-cell lysates, sonicated supernatant, osmotic shock liquid of recombinant strains expressing *H pylori* Hsp60 genes and the purified rHsp60 were analyzed by electrophoretic analysis in a 10 % polyacrylamide gel.

Immunization of mice

Six to eight week old mice were immunized four times by hypodermic injection in the back of mice at weekly intervals. Each dose consisted of 20 µg of *H pylori* rHsp60 protein and 200 µg of adjuvant aluminum hydroxide gel. Age-matched control mice were not immunized. Four weeks after the last immunization, blood samples were taken from the retro-orbital sinus to measure anti Hsp60 systemic immune responses and stored at -20 °C until assay.

Serum antibody responses

Indirect ELISA as described evaluated serum samples from mice and patients for Hsp60-specific IgG previously^[35]. Purified *H pylori* rHsp60 was used as the coating antigen in ELISA immunoassays.

RESULTS

PCR amplification of *H pylori* Hsp60 gene

According to the literature, the gene encoding Hsp60 protein was amplified by PCR with chromosomal DNA of *H pylori* Sydney strain (ss1) as templates. The cloning products were electrophoresed and visualized on 8 g·L⁻¹ agarose gel (Figure 1). It revealed that Hsp60 DNA fragment amplified by PCR contained a gene with approximately 1 548 nucleotides, which was compatible with previous reports^[36].

Construction of recombinant plasmid and restriction enzyme confirmation

After PCR products and pET-22b(+) plasmid were cut by *Not*

I and *Nco* I, directional cloning was performed, resulting in a recombinant plasmid named pET-22b(+)/Hsp60. The recombinant plasmids pET-22b(+)/Hsp60 were all digested by *Not* I or *Nco* I, and by *Not* I and *Nco* I simultaneously, then digestive products were visualized on 8 g·L⁻¹ agarose gel electrophoreses (Figure 2). It demonstrated that recombinant plasmid contained the objective gene.

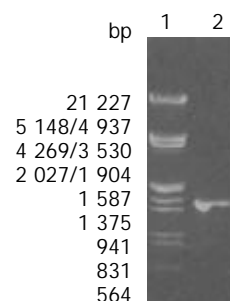


Figure 1 Eight g·L⁻¹ agarose gels electrophoreses of Hsp60 DNA fragment amplified by PCR from *H pylori*. Lane1: Nucleotide marker, Lane2: PCR products.

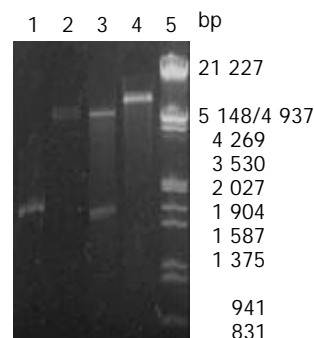


Figure 2 Identification of recombinant plasmid by restriction enzyme digestion. Lane1: PCR products, Lane2: pET22b (+)/*Not* I, Lane3: Recombinant plasmid/*Not* I and *Nco* I, Lane4: Recombinant plasmid/*Not* I, Lane5: Nucleotide marker.

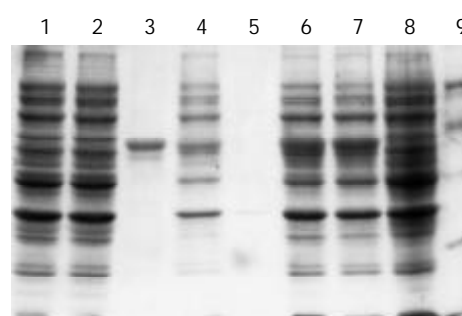


Figure 3 100 g·L⁻¹ SDS-PAGE analysis of the fusion protein expressed in BL21(DE3). Lane1: control strain BL21(pET) before induction, Lane2: control strain BL21(pET) after 3 h induction with IPTG, Lane3: purified recombinant protein Hsp60, Lane4: sonicated supernatant of BL21(pET-Hsp60) cells after 3 h induction with IPTG, Lane5: BL21(pET-Hsp60) cell periplasm protein after 3 h induction with IPTG, Lane6: BL21(pET-Hsp60) cells after 5 h induction with IPTG, Lane7: BL21(pET-Hsp60) cells after 3 h induction with IPTG, Lane8: BL21(pET-Hsp60) cells before induction, Lane9: molecular weight marker (20,30,43,67,94)×10³.

Sequence analysis of cloned Hsp60 nucleotide

The nucleotide sequence of cloned genes inserted in pET22b (+) was analyzed by automatic sequencing across the cloning

junction, using the universal primer T7. The results were as follows the cloned genes contained 1 548 nucleotides with a promoter and a start codon coding a putative protein of 516 amino acid residues with a calculated molecular mass of Hsp60. As compared with previous reports, the homogeneity was 100 % between them^[36].

Expression and purification of Hsp60 gene in *Escherichia coli*

Whole-cell lysates, sonicated supernatant, osmotic shock liquid of recombinant strains expressing *H pylori* Hsp60 genes and the purified rHsp60 were analyzed by electrophoretical analysis in a 10 % polyacrylamide gel for detection of fusion proteins (Figure 3). The results showed that the clearly identifiable band was 60 000 Dalton highly expressed fusion proteins, which was similar to that predicted. Gel automatic scan analysis showed that it was 0.6 at D value and the final concentration of IPTG was 0.1 mmol/L and induction for 5 hours, the expression of Hsp60 rose remarkably, which accounted for 27.2 % of total bacterial proteins. Among them, soluble substance accounted for 14.7 % of supernatant. Hsp60 was further purified with Ni-NTA column; its final purity was 80 %.

Antigenicity study of recombinant fusion protein

The positive results by ELISA had colors, but the negative results had no colors, or weak colors. The results showed that the eight mice sera immunized with rHsp60 showed positive results. In contrast, the eight mice sera in control group showed negative results. At the same time, sera from patients also showed the same results. Eight *H pylori* positive sera from patients showed positive results and three *H pylori* negative sera from patients showed negative results, it showed that anti-Hsp60 antibody existed in sera of infected patients, indicating that rHsp60 could enable the organism to generate specific humoral immunity.

DISCUSSION

Hsps exists widely in nature and is one of the most conservative proteins of biosphere. For a long time, people have researched low Hsps as a molecular partner took part in physiological activities of cells. However, their results indicate that Hsps from microorganisms are the most important protective antigens when people and animals are infected with microorganisms. The protective immune response to 20 kinds of infectious diseases, such as tuberculosis and lepra was directly aimed at Hsps as far as reported^[33,34]. Especially in the model of mice infected with tubercle bacillus, specific anti-Hsp60 only produced immunoreaction with Hsp60 of tubercle bacillus, not with mice Hsp60 themselves^[37]. This resolved the autoimmune problems because of high conservation, which was perplexed. Furthermore, in models of mice and monkeys infected with plasmodium, immunoreactions did not depend on adjuvants when polypeptides were combined with Hsp60^[38]. It showed that Hsp60 had similar functions of adjuvants. So under the uncertainty of *H pylori* urease preventing *H pylori* infection, *H pylori* Hsp60 as a *H pylori* vaccine component is not only used to combine urease to constitute multivalence vaccine, but also used as adjuvants to resolve the disadvantages of CT or LT.

In fact, *H pylori* Hsp60 immune protection function has been confirmed by experiments *in vitro* and *in vivo*. Yamaguchi *et al* reported *H pylori* Hsp60 monoclonal antibody could significantly inhibit adhesion of *H pylori* to human gastric epithelial MKN45 cells and gastric cancer cells^[39]. Yamaguchi *et al* also evaluated the protective effect of immunization with amino acids 189 to 203 (VEGMQFDRGYLSPYF) on *H pylori* Hsp60 molecules^[40]. The results suggested that the immune response to the epitope (VEGMQFDRGYLSPYF) was unique

and could prevent *H pylori* infection in animal models. In this study, specific antibody to Hsp60 was detected in sera from the mice immunized with purified recombinant protein Hsp60, but not in sera from the mice in control group. Sera from patients also showed the same results. These results suggest that Hsp60 of *H pylori* may be a good candidate for a vaccine. However, whether it can be used as an adjuvant and antigen needs to be further researched.

REFERENCES

- 1 **Bai Y**, Zhang YL, Wang JD, Lin HJ, Zhang ZS, Zhou DY. Conservative region of the genes encoding four adhesins of *Helicobacter pylori*: cloning, sequence analysis and biological information analysis. *Di Yi Jun Yi Daxue Xuebao* 2002; **22**: 869-871
- 2 **Vandenplas Y**. *Helicobacter pylori* infection. *World J Gastroenterol* 2000; **6**: 20-31
- 3 **Bai Y**, Chang SH, Wang JD, Chen Y, Zhang ZS, Zhang YL. Construction of the *E. coli* clone expressing adhesin BabA of *Helicobacter pylori* and evaluation of the adherence activity of BabA. *Di Yi Jun Yi Daxue Xuebao* 2003; **23**: 293-295
- 4 **Hobsley M**, Tovey FI. *Helicobacter pylori*: the primary cause of duodenal ulceration or a secondary infection? *World J Gastroenterol* 2001; **7**: 149-151
- 5 **Huang XQ**. *Helicobacter pylori* infection and gastrointestinal hormones: a review. *World J Gastroenterol* 2000; **6**: 783-788
- 6 **Olbe L**, Fandriks L, Hamlet A, Svennerholm AM, Thoreson AC. Mechanisms involved in *Helicobacter pylori* induced duodenal ulcer disease: an overview. *World J Gastroenterol* 2000; **6**: 619-623
- 7 **Hou P**, Tu ZX, Xu GM, Gong YF, Ji XH, Li ZS. *Helicobacter pylori* vacA genotypes and cagA status and their relationship to associated diseases. *World J Gastroenterol* 2000; **6**: 605-607
- 8 **Bai Y**, Dan HL, Wang JD, Zhang ZS, Odenbreit S, Zhou DY, Zhang YL. Cloning, expression, purification and identification of conservative region of four *Helicobacter pylori* adhesin genes in AlpA gene. *Prog Biochem Biophys* 2002; **29**: 922-926
- 9 **Bai Y**, Zhany YL, Chen Y, Wang JD, Zhou DY. Study of Immunogenicity and safety and adherence of conservative region of four *Helicobacter pylori* adhesin *in vitro*. *Prog Biochem Biophys* 2003; **30**: 422-426
- 10 **Chi J**, Lu M, Fu BY, Nakajima S, Hattori T. The effect of mast cell on the induction of *Helicobacter pylori* infection in Mongolian gerbils. *World J Gastroenterol* 2000; **6**: 440-441
- 11 **Pena A**. Genetic factors determining the host response to *Helicobacter pylori*. *World J Gastroenterol* 2000; **6**: 624-625
- 12 **Morgner A**, Miehke S, Stolte M, Neubauer A, Alpen B, Thiede C, Klann H, Hierlmeier FX, Ell C, Ehninger G, Bayerdorffer E. Development of early gastric cancer 4 and 5 years after complete remission of *Helicobacter pylori* associated gastric low grade marginal zone B cell lymphoma of MALT type. *World J Gastroenterol* 2001; **7**: 248-253
- 13 **Miehke S**, Kirsch C, Dragosics B, Gschwandler M, Oberhuber G, Antos D, Dite P, Lauter J, Labenz J, Leodolter A, Malfertheiner P, Neubauer A, Ehninger G, Stolte M, Bayerdorffer E. *Helicobacter pylori* and gastric cancer: current status of the Austrian Czech German gastric cancer prevention trial (PRISMA Study). *World J Gastroenterol* 2001; **7**: 243-247
- 14 **Gao H**, Wang JY, Shen XZ, Liu JJ. Effect of *Helicobacter pylori* infection on gastric epithelial cell proliferation. *World J Gastroenterol* 2000; **6**: 442-444
- 15 **Zhuang XQ**, Lin SR. Research of *Helicobacter pylori* infection in precancerous gastric lesions. *World J Gastroenterol* 2000; **6**: 428-429
- 16 **Cai L**, Yu SZ, Zhang ZF. *Helicobacter pylori* infection and risk of gastric cancer in Changle County, Fujian Province, China. *World J Gastroenterol* 2000; **6**: 374-376
- 17 **Liu WZ**, Zheng X, Shi Y, Dong QJ, Xiao SD. Effect of *Helicobacter pylori* infection on gastric epithelial proliferation in progression from normal mucosa to gastric carcinoma. *World J Gastroenterol* 1998; **4**: 246-248
- 18 **Harry XH**. Association between *Helicobacter pylori* and gastric cancer: current knowledge and future research. *World J Gastroenterol* 1998; **4**: 93-96
- 19 **Lan J**, Xiong YY, Lin YX, Wang BC, Gong LL, Xu HS, Guo GS. *Helicobacter pylori* infection generated gastric cancer through p53-

- Rb tumor-suppressor system mutation and telomerase reactivation. *World J Gastroenterol* 2003; **9**: 54-58
- 20 **Wang RT**, Wang T, Chen K, Wang JY, Zhang JP, Lin SR, Zhu YM, Zhang WM, Cao YX, Zhu CW, Yu H, Cong YJ, Zheng S, Wu BQ. *Helicobacter pylori* infection and gastric cancer: evidence from a retrospective cohort study and nested case-control study in China. *World J Gastroenterol* 2002; **8**: 1103-1107
- 21 **Yao YL**, Xu B, Song YG, Zhang WD. Overexpression of cyclin E in Mongolian gerbil with *Helicobacter pylori*-induced gastric precancerosis. *World J Gastroenterol* 2002; **8**: 60-63
- 22 **Bulajic M**, Stimec B, Milicevic M, Loehr M, Mueller P, Boricic I, Kovacevic N, Bulajic M. Modalities of testing *Helicobacter pylori* in patients with nonmalignant bile duct diseases. *World J Gastroenterol* 2002; **8**: 301-304
- 23 **Xu CD**, Chen SN, Jiang SH, Xu JY. Seroepidemiology of *Helicobacter pylori* infection among asymptomatic Chinese children. *World J Gastroenterol* 2000; **6**: 759-761
- 24 **Pace F**, Porro GB. Gastroesophageal reflux and *Helicobacter pylori*: a review. *World J Gastroenterol* 2000; **6**: 311-314
- 25 **Harris A**. Treatment of *Helicobacter pylori*. *World J Gastroenterol* 2001; **7**: 303-307
- 26 **She FF**, Su DH, Lin JY, Zhou LY. Virulence and potential pathogenicity of coccoid *Helicobacter pylori* induced by antibiotics. *World J Gastroenterol* 2001; **7**: 254-258
- 27 **Hua JS**, Bow H, Zheng PY, Khay-Guan Y. Prevalence of primary *Helicobacter pylori* resistance to metronidazole and clarithromycin in Singapore. *World J Gastroenterol* 2000; **6**: 119-121
- 28 **Bai Y**, Wang JD, Zhang ZS, Zhang YL. Construction of the Attenuated Salmonella typhimurium Strain Expressing *Helicobacter pylori* Conservative Region of Adhesin Antigen. *Chin J Biotech* 2003; **19**: 77-82
- 29 **Bai Y**, Zhang YL, Wang JD, Zhang ZS, Zhou DY. Cloning and immunogenicity of conservative region of adhesin gene of *Helicobacter pylori* [Article in Chinese]. *Zhonghua Yixue Zazhi* 2003; **83**: 736-739
- 30 **Bai Y**, Zhang YL, Wang JD, Zhang ZS, Zhou DY. Construction of the non-resistant attenuated Salmonella typhimurium strain expressing *Helicobacter pylori* catalase. *Di Yi Junyi Daxue Xuebao* 2003; **23**: 101-105
- 31 **Bai Y**, Zhang YL, Jin JF, Wang JD, Zhang ZS, Zhou DY. Recombinant *Helicobacter pylori* catalase. *World J Gastroenterol* 2003; **9**: 1119-1122
- 32 **Solnick JV**, Canfield DR, Hansen LM, Torabian SZ. Immunization with recombinant *Helicobacter pylori* urease in specific-pathogen-free rhesus monkeys (*Macaca mulatta*). *Infect Immun* 2000; **68**: 2560-2565
- 33 **Zugel U**, Schoel B, Yamamoto S, Hengel H, Morein B, Kaufmann SH. Crossrecognition by CD8 T cell receptor alpha beta cytotoxic T lymphocytes of peptides in the self and the mycobacterial hsp60 which share intermediate sequence homology. *Eur J Immunol* 1995; **25**: 451-458
- 34 **Zugel U**, Kaufmann SH. Activation of CD8 T cells with specificity for mycobacterial heat shock protein 60 in Mycobacterium bovis bacillus Calmette-Guerin-vaccinated mice. *Infect Immun* 1997; **65**: 3947-3950
- 35 **Sambrook J**, Fritsch EF, Maniatis T. Molecular cloning: a laboratory manual. 2nd ed. New York: Cold Spring Harbor Laboratory Press 1989: 35-400
- 36 **Macchia G**, Massone A, Burroni D, Covacci A, Censini S, Rappuoli R. The Hsp60 protein of *Helicobacter pylori*: structure and immune response in patients with gastroduodenal diseases. *Mol Microbiol* 1993; **9**: 645-652
- 37 **Lowrie DB**, Silva CL, Colston MJ, Ragno S, Tascon RE. Protection against tuberculosis by a plasmid DNA vaccine. *Vaccine* 1997; **15**: 834-838
- 38 **Del Giudice G**. Stress proteins in medicine. New York: Marcel Dekker Inc 1996: 533-545
- 39 **Yamaguchi H**, Osaki T, Kurihara N, Taguchi H, Hanawa T, Yamamoto T, Kamiya S. Heat-shock protein 60 homologue of *Helicobacter pylori* is associated with adhesion of *H. pylori* to human gastric epithelial cells. *J Med Microbiol* 1997; **46**: 825-831
- 40 **Yamaguchi H**, Osaki T, Kai M, Taguchi H, Kamiya S. Immune response against a cross-reactive epitope on the heat shock protein 60 homologue of *Helicobacter pylori*. *Infect Immun* 2000; **68**: 3448-3454

Edited by Xia HHX and Wang XL

Distribution and expression of non-muscle myosin light chain kinase in rabbit livers

Hua-Qing Zhu, Yuan Wang, Ruo-Lei Hu, Bin Ren, Qing Zhou, Zhi-Kui Jiang, Shu-Yu Gui

Hua-Qing Zhu, Yuan Wang, Ruo-Lei Hu, Qing Zhou, Laboratory of Molecular Biology and Department of Biochemistry, Anhui Medical University, Hefei 230032, Anhui Province, China

Hua-Qing Zhu, Yuan Wang, Ruo-Lei Hu, Qing Zhou, Shu-Yu Gui, Anhui Province Key Laboratory of Genomic Research, Hefei 230032, Anhui Province, China

Bin Ren, Department of Pathology, BIDMC and Harvard Medical School, 99 Brookline, MA 02215, Boston, U S A

Shu-yu Gui, Department of Respiratory Disease, the First Affiliated Hospital of Anhui Medical University, Hefei 230032, Anhui Province, China

Zhi-Kui Jiang, 105 Hospital of PLA, Hefei 230031, Anhui Province, China

Supported by National Natural Science Foundation of China, No. 39870324, Grant for Excellent Young Teachers of Ministry of education of China, No.39870324, National Science Foundation of Anhui Province, No.9904312

Correspondence to: Professor Yuan Wang, Laboratory of Molecular Biology and Department of Biochemistry, Anhui Medical University, Hefei 230032, Anhui Province, China. wangyuan@mail.hf.ah.cn

Telephone: +86-551-5161140

Received: 2003-05-10 **Accepted:** 2003-06-02

Abstract

AIM: To study the distribution and expression of non-muscle myosin light chain kinase (nmMLCK) in rabbit livers.

METHODS: Human nmMLCK N-terminal cDNA was amplified by polymerase chain reaction (PCR) and was inserted into pBKcmv to construct expression vectors. The recombinant plasmid was transformed into XL1-blue. Expression protein was induced by IPTG and then purified by SDS-PAGE and electroelution, which was used to prepare the polyclonal antibody to detect the distribution and expression of nmMLCK in rabbit livers with immunofluorescence techniques.

RESULTS: The polyclonal antibody was prepared, by which nmMLCK expression was detected and distributed mainly in peripheral hepatocytes.

CONCLUSION: nmMLCK can express in hepatocytes peripherally, and may play certain roles in the regulation of hepatic functions.

Zhu HQ, Wang Y, Hu RL, Ren B, Zhou Q, Jiang ZK, Gui SY. Distribution and expression of non-muscle myosin light chain kinase in rabbit livers. *World J Gastroenterol* 2003; 9(12): 2715-2719
<http://www.wjgnet.com/1007-9327/9/2715.asp>

INTRODUCTION

Protein kinase plays an important regulatory role in response to both intracellular and extracellular signals^[1]. Specific protein kinase is thought to control various cellular functions including glycogen metabolism, muscle contraction and growth, etc. Myosin light chain kinase (MLCK) is a Ca^{2+} /calmodulin activated enzyme in the kinase family which catalyses the

phosphorylation of the 20-ku myosin light chain (MLC-20)^[2]. In skeletal muscle, the phosphorylation of MLC-20 correlates with potentiated twitch tension after repetitive stimulation. In smooth muscle cells, this phosphorylation leads to an increase in actomyosin ATPase activity and contraction which appears to be required for initiation of contraction. Phosphorylation of MLC-20 by smooth muscle MLCK is a key event initiating smooth muscle contraction. Although the roles of MLCK in non-muscle cells have not been well defined, a variety of morphological changes such as cellular motility and organelle movement occur concurrently with the increased cytoplasmic Ca^{2+} levels, light chain phosphorylation and activation of MLCK. Intracellular localization studies performed in mammalian fibroblast cells have colocalized MLCK to the spindle apparatus and midbody of mitotic cells. These observations have led to the suggestion that the phosphorylation of MLC-20 by MLCK in non-muscle cells might have a role in cell division and cell motility^[3]. There are at least two different stress fiber systems in fibroblasts including central stress fiber system and periphery stress fiber system and the latter system depends on MLCK^[4]. And at least two distinct classes of MLCK (short and long) phosphorylate the MLC-20 of myosin in thick filaments but bind with high affinity to actin in thin filaments^[5]. But which form of MLCK exists in hepatocytes? How is MLCK involved in cellular functions in hepatocytes? In order to investigate the roles of MLCK in the maintenance of liver functions and its association with some liver diseases in the future study, we prepared polyclonal antibody through expressed MLCK protein in *E. Coli* system, and the antibody was used to detect the distribution and expression of MLCK in hepatocytes with immunofluorescence microscopy. Our research provides the basis for further investigation MLCK functions of in the liver and its relation with the pathology of some hepatic diseases such as hepatocellular carcinoma and hyperlipoproteinemia.

MATERIALS AND METHODS

Reagents and instruments

Plasmid pBKcmv and *E. coli* XL1-blue were from STRATAGENE (La Jolla, CA, USA). The human-non-muscle-MLCK cDNA was a gift from Dr. Stull at University of Texas Southwestern Medical Center, USA. Concept rapid PCR purification system kit was purchased from Life Technology, GibcoBRL. pGEM-T vector system I was purchased from Promega (Madison WI, USA). Restriction endoenzyme, T_4 DNA ligase, dNTPs, amplitaq DNA polymerase, mounting media were obtained from Sigma Chemical Company. PCR primers were synthesized by BioAsia Biotechnology Co., Ltd (Shanghai, China). Other reagents were made in China and were of analytical purity. DYY-III type-2 electrophoresis and transfer system were made by Beijing Instrument Factory. UV-754 spectrophotometer was made by The Third Factory of Analytical Instrument of Shanghai. Nikon eclipse E800 microscope was from Japan.

PCR of hnmMLCK DNA

The primers were designed according to human MLCK cDNA,

prime 1: 5' TGG AAT TCC ATG GGG GAC GTG AA3' containing *EcoRI* restriction site and prime 2: 5' CCA CTG CTG AAG AAG CTT AAA ATC3' containing *HindIII* restriction site. The PCR parameters were pre-denaturation at 94 °C for 5 min before amplification was done for 35 cycles at 94 °C for 1 min, annealing at 55 °C for 1 min and extension at 72 °C for 1 min, and final extension for 10 min at 72 °C after the last cycle. The PCR products were examined by 20 g.L⁻¹ agarose gel electrophoresis with TAE buffer at 80V for 40 min, visualized with ethidium bromide, and photographed under UV light.

Ligation, transformation and sequence of hnmMLCK DNA^[6]

The PCR products were purified by concept rapid PCR purification system kit and inserted into the T-vector, the resulting ligation products were transferred into XL1-blue *E. coli* competent cells. The positive clone was picked up and the plasmids were prepared. The plasmid and pBKcmv vector were digested with *EcoRI* and *HindIII* and ligated before transferred into XL1-blue *E. coli* competent cells. Individual recombinant white clones were picked up and recombinant DNA was prepared before digested with restrictive endonuclease. The recombinant plasmid sequence was detected with ABI377 auto analytical instrument.

Expression and purification of hnmMLCK in *E. coli*^[7]

The positive recombinant plasmids were transformed into XL-1blue *E. coli*, the single clone was picked up and cultured overnight at 37 °C with shaking at 250 rpm. The media were diluted (1:100) with Luria-bertani liquid medium and isopropyl- β -D-thiogalactoside (IPTG) was added into the medium to induce protein expression when OD₆₀₀=0.6-0.8, and cultured for 4 h. The bacteria were harvested by centrifugation at 5 000 rpm for 10 min and the expressed protein was analyzed by SDS-PAGE. The expressed band was cut from SDS-PAGE gel and electroeluted in transfer buffer for isolation and purification.

Anti-myosin light chain kinase polyclonal antibody preparation

Polyclonal antibody to human MLCK was prepared according to the previously described method^[8].

Immunofluorescence detection of MLCK in rabbit livers

The New Zealand rabbit liver tissues were embedded with O.C.T and frozen sections were prepared. The slices were incubated in 100 % acetone for 10 min at -20 °C and dried in air, then blocked in 5 % non-fat milk in PBS (pH7.4) overnight. The blocking solution was removed and anti-MLCK polyclonal antibody was added, and then incubated in a wet box for 2-3 h. The reactions were incubated with FITC-labeled secondary antibody for 1 h. Finally, the reactions were covered with mounting media before observation with a Nikon fluorescent microscope^[9,10].

RESULTS

Amplification of human MLCK cDNA

The PCR products were detected by 20 g·L⁻¹ agarose gel. The results showed that there was a 450 bp band in the gel (Figure 1), corresponding to the fragment of human MLCK cDNA N-terminate.

Enzymatic and sequence analysis of recombinant plasmid and cloned DNA

The recombinant plasmid was digested with *EcoRI* and *HindIII* and then run in 20 g·L⁻¹ agarose gel, which showed that the PCR products were inserted into the pBKcmv vector (Figure

2). The DNA sequences of pBK-hnmMLCK were detected by ABI377 auto analytical instrument (Figure 3), and compared with Genbank (Figure 4).

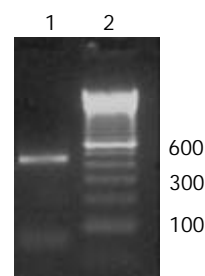


Figure 1 Amplification of hnmMLCK cDNA by PCR. 1. products of PCR amplification, 2. the 100 bp ladder.

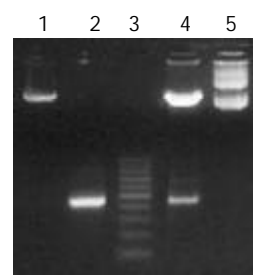


Figure 2 Analysis of human MLCK recombinant plasmids with restriction endonucleases mapping. 1. pBKcmv/*EcoRI-HindIII*, 2. PCR products/*EcoRI-HindIII*, 3. the 100 bp DNA ladder, 4. pBK-hnmMLCK/*EcoRI-HindIII*, 5. pBK-hnmMLCK.

Protein expression and purification

The expressed protein hnmMLCK in *E. coli* was induced with IPTG and bacteria were centrifuged at 5 000 rpm for 10 min. The pellet was resuspended with PBS, and an equal volume of 2×protein loading buffer was added, boiled at 100 °C for 5 min and analyzed by SDS-PAGE. The percentage of the expressed protein was about 21 % by scanning analysis (Figure 5).

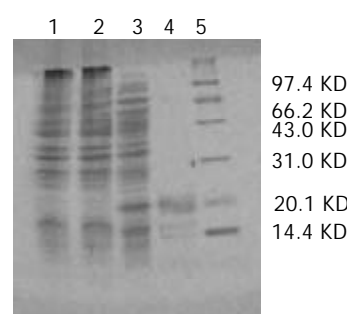


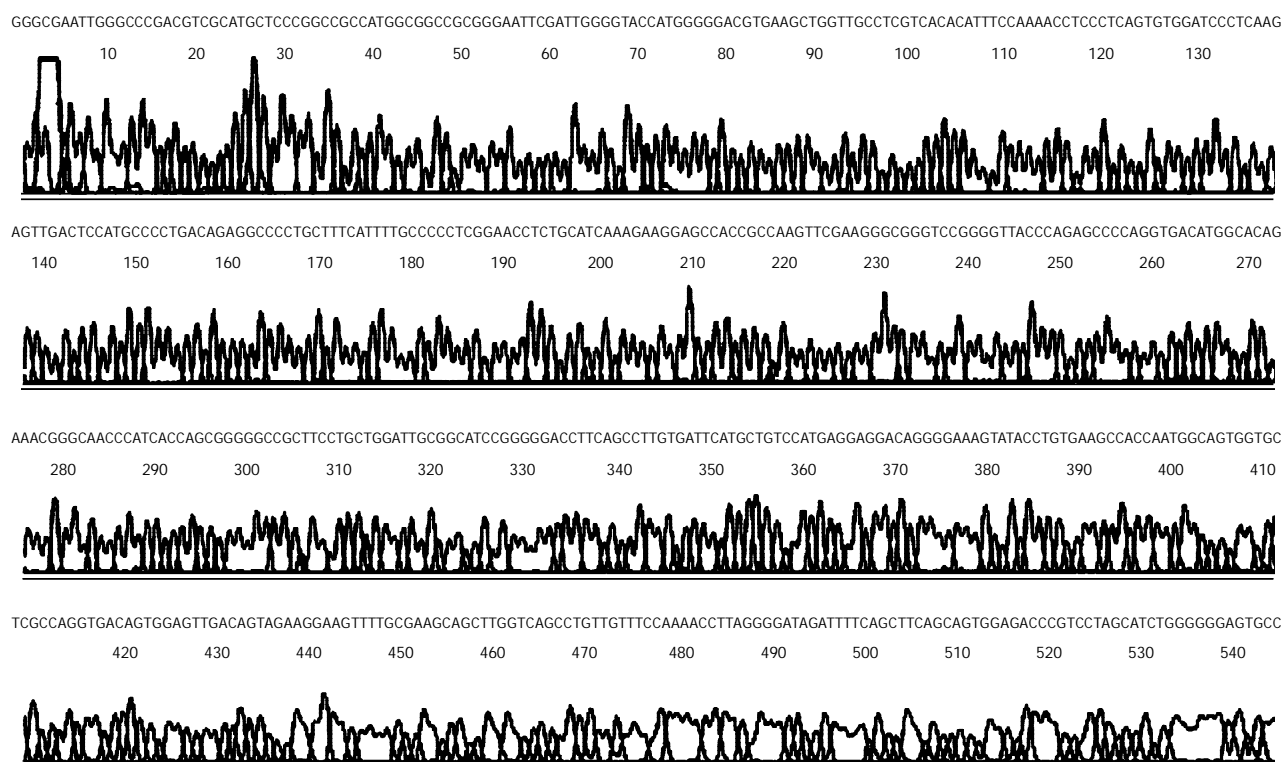
Figure 5 Analysis of pBK-hnmMLCK with SDS-PAGE. 1. pBKcmv in XL1-blue, 2. pBK-hnmMLCK in XL1-blue before induced, 3. pBK-hnmMLCK in XL1-blue after induced, 4. purified expression protein, 5. protein markers.

Antiserum detection by immune double-diffusion

The ratio of antigen to antibody was at least 1:16 (Figure 6), suggesting that the polyclonal antibody could be used for immunofluorescence analysis.

Distribution of MLCK in rabbit livers

MLCK was mainly distributed peripherally in hepatocytes (Figure 7), and was hardly detected cytoplasm by immunofluorescence.



>gi|7239697|gb|AF069601.2|AF069601 pBKcmv-hMLCK85-144

Homo sapiens myosin light chain kinase isoform 2 (MLCK) mRNA, complete cds
Length = 5719 Score = 852 bits (430), Expect = 0.0
Identities = 439/442 (99%) Strand = Plus / Plus

Query: 39 ccattgggggacgtgaagctggttgccctgcacacatttccaaacctcccctcagtgtgg 98
||||||| ||||||| ||||||| ||||||| |||||||
Sbjct:118 ccattgggggatgtgaagctggttgccctgcacacatttccaaacctcccctcagtgtgg 177
Query: 99 atcccccaaggatgtactcatgccctgacagaggccccctgttttcattttgccccctc 158
||||||| ||||||| ||||||| ||||||| |||||||
Sbjct:178 atcccccaaggatgtactcatgccctgacagaggccccctgttttcattttgccccctc 237
Query:159 ggaacctctgcatcaaagaaggagccaccgccaagttcgaggggcggttcgggggttac 218
||||||| ||||||| ||||||| ||||||| |||||||
Sbjct:238 ggaacctctgcatcaaagaaggagccaccgccaagttcgaggggcggttcgggggttac 297
Query:219 cagagccccaggtgacatggcacagaaacgggcaaccatcaccagcggggggccgttcc 278
||||||| ||||||| ||||||| ||||||| |||||||
Sbjct:298 cagagccccaggtgacatggcacagaaacgggcaaccatcaccagcggggggccgttcc 357
Query:279 tgctgattgcggcatccgggggaccttcagccttgtgattcatgctgtccatgaggagg 338
||||||| ||||||| ||||||| ||||||| |||||||
Sbjct:358 tgctgattgcggcatccgggggaccttcagccttgtgattcatgctgtccatgaggagg 417
Query:339 acaggggaaaagtatacctgtgaagccaccaaatggcagtggtgctcgccaggtgacagtgg 398
||||||| ||||||| ||||||| ||||||| |||||||
Sbjct:418 acaggggaaaagtatacctgtgaagccaccaaatggcagtggtgctcgccaggtgacagtgg 477
Query:399 agttgacagtagaagggaagttttgcgaagcagcttggtcagcctgtgtttccaaaacct 458
||||||| ||||||| ||||||| ||||||| |||||||
Sbjct:478 agttgacagtagaagggaagttttgcgaagcagcttggtcagcctgtgtttccaaaacct 537
Query:459 taggggatagattttaagcttc 480
||||||| |||||
Sbjct:538 taggggatagattttaagcttc 559

Figure 4 Comparison between sequencing results of hnmMLCK DNA and those published by Genbank.

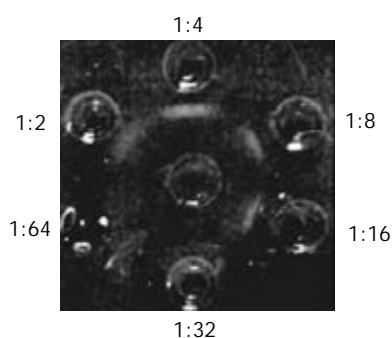


Figure 6 Antiserum titer detected by immuno-double-diffusion.

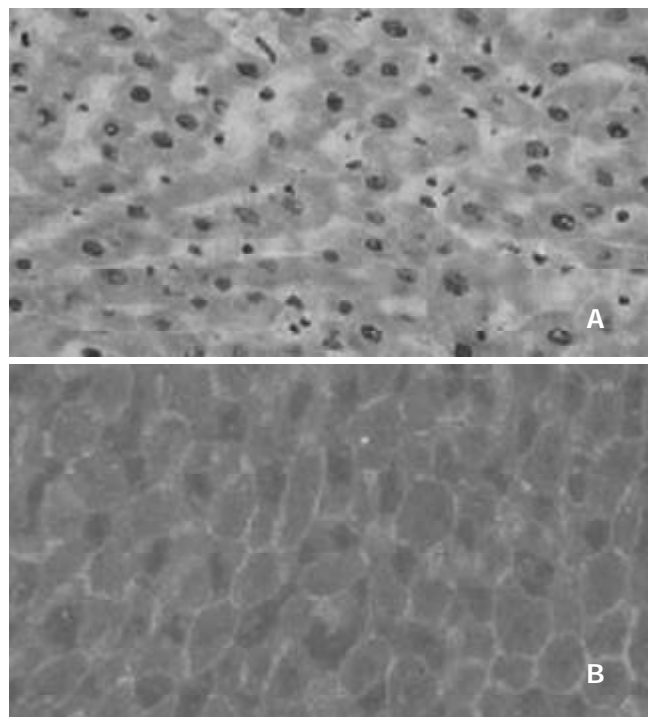


Figure 7 MLCK distribution in hepatocytes of New Zealand rabbits. A: H and E staining; B: MLCK distribution.

DISCUSSION

MLCK is the key regulator of cell motility and smooth muscle contraction in higher vertebrates^[11-13]. MLCK expression shows a complex pattern. In undifferentiated myoblasts, 220-ku long or non-muscle form of MLCK is expressed during differentiation of skeletal muscle. During myoblast differentiation, the expression of 220-ku MLCK declines and expression of this long-term is replaced by 103-ku smooth muscle MLCK and a skeletal muscle-specific MLCK. The two isoforms are products of a single gene^[14], and both short and long MLCKs are expressed in embryonic and adult non-muscle as well as smooth muscle cells^[15,16]. Recently, some study showed the existence of a 208-ku protein, named embryonic MLCK because its expression could be detected in early embryonic tissue stem cells and in proliferating culture cells^[17]. MLCK has several well characterized domains, and they are comprised of an amino-terminal "tail" of unknown function and a central catalytic core that is homologous to the catalytic core of other protein kinases, carboxy-terminal to the catalytic core and calmodulin binding domains, which are involved in the activation of the kinase in responses to increased Ca^{2+} ^[18]. In this study we constructed the expression vector which could express N-terminal MLCK, and used this protein to prepare polyclonal antibody. The results showed that the antibody could

react with hepatic cells and MLCK was distributed in the peripheral region of hepatic cells. In rabbit portal vein myocytes, MLCK could mediate noradrenaline-evoked non-selective cation current^[19]. In the liver, agents that elevated intercellular free Ca^{2+} concentration could increase tight junctional permeability and stimulate bile canaliculi contraction. Myosin phosphorylation might be responsible for the tight junctional permeability caused by elevation of intercellular Ca^{2+} in hepatocytes. Moreover, the integrity of the phosphorylation systems of myosin is essential for normal bile flow. In addition, hepatic sinusoidal Ito cells play a regulatory role on hepatic blood flow through their contraction, while the integrity of MLCK is essential for Ito cell contractions and normal sinusoidal blood flow. However, the role of myosin phosphorylation by MLCK in non-muscle tissues has not been well characterized but correlated with important activities such as cell division, receptor capping^[20,21], etc. It has been found that MLCK was closely associated with non-muscle cells^[16,19,20]. Phosphorylation of myosin light chain by MLCK in non-muscle cells and tissues demonstrated an important physiological function^[22]. For example, myosin light chain phosphorylation has been implicated in secretory vesicle movement, cellular locomotion and changes in cellular morphology^[23]. MLCK activation was a critical step in cytoskeletal changes causing pseudopod formation during polymorphonuclear leukocyte phagocytosis^[24]. MLCK was also associated with the gap formations and endothelial hyperpermeability of coronary venular endothelial cell monolayers^[25]. The preliminary studies showed that the light chain was obviously phosphorylated when CaM was added into the reaction buffer at a suitable concentration of Ca^{2+} . The activity of MLCK in rabbit livers increased markedly when CaM was added, and the activity changed with a substrate concentration or the concentration of light chain kinase^[26]. MLCK immunoreactivity was found to be colocalized with the insulin granules, suggesting that it increased insulin granules in the ready-releasable pool by acting on different steps in the secretory cascade^[27]. In this study, the expressed vector was successfully constructed and MLCK was expressed in *E. coli* system, which lays a good basis for the manufacture and clinical application of the enzyme. The anti-MLCK polyclonal antibody was prepared and used to detect the distribution of MLCK in the cells of rabbit liver. MLCK may play an important role in maintaining the normal functions of tissues. But in the liver, which form of MLCK was expressed, long or short? If there are both forms, which form expresses more? What are their roles in the liver? What roles will it play in liver regeneration, injury or hepatic carcinoma? And what is the mechanism of MLCK activity in the liver? All these remain to be investigated and elucidated in future studies.

REFERENCES

- 1 **Kishi H**, Mikawa T, Seto M, Sasaki Y, Kanayasu-Toyoda T, Yamaguchi T, Imamura M, Ito M, Karaki H, Bao J, Nakamura A, Ishikawa R, Kohama K. Stable transfectants of smooth muscle cell line lacking the expression of myosin light chain kinase and their characterization with respect to the actomyosin system. *J Biol Chem* 2000; **275**: 1414-1420
- 2 **Deng JT**, Van Lierop JE, Sutherland C, Walsh MP. Ca^{2+} -independent smooth muscle contraction: a novel function for integrin-linked kinase. *J Biol Chem* 2001; **276**: 16365-16373
- 3 **Goekeler ZM**, Masaracchia RA, Zeng Q, Chew TL, Gallagher P, Wysolmerski RB. Phosphorylation of myosin light chain kinase by p21-activated kinase PAK2. *J Biol Chem* 2000; **275**: 18366-18374
- 4 **Katoh K**, Kano Y, Amano M, Kaibuchi K, Fujiwara K. Stress fiber organization regulated by MLCK and Rho-kinase in cultured human fibroblasts. *Am J Physiol Cell Physiol* 2001; **280**: C1669-1679

- 5 **Smith L**, Parizi-Robinson M, Zhu MS, Zhi G, Fukui R, Kamm KE, Stull JT. Properties of long myosin light chain kinase binding to F-actin *in vitro* and *in vivo*. *J Biol Chem* 2002; **277**: 35597-35604
- 6 **Xu CS**, Li YC, Lin JT, Zhang HY, Zhang YH. Cloning and analysing the up-regulated expression of transthyretin-related gene (LR1) in rat liver regeneration following short interval successive partial hepatectomy. *World J Gastroenterol* 2003; **9**: 148-151
- 7 **Hu RL**, Zhu HQ, Zhou Q, Gui SY, Wang Y. Construction of pBK-human non-muscle MLCK N-terminal and its expression in *E. coli* XL1-blue. *Anhui Yike Daxue Xuebao* 2002; **37**: 11-13
- 8 **Nunnally MH**, Stull JT. Mammalian skeletal muscle myosin light chain kinases. A comparison by antiserum cross-reactivity. *J Biol Chem* 1984; **259**: 1776-1780
- 9 **Huang ZS**, Wang ZW, Liu MP, Zhong SQ, Li QM, Rong XL. Protective effects of polydatin against CCl(4)-induced injury to primarily cultured rat hepatocytes. *World J Gastroenterol* 1999; **5**: 41-44
- 10 **Chen YM**, Qian ZM, Zhang J, Chang YZ, Duan XL. Distribution of constitutive nitric oxide synthase in the jejunum of adult rat. *World J Gastroenterol* 2002; **8**: 537-539
- 11 **Jin Y**, Atkinson SJ, Marrs JA, Gallagher PJ. Myosin ii light chain phosphorylation regulates membrane localization and apoptotic signaling of tumor necrosis factor receptor-1. *J Biol Chem* 2001; **276**: 30342-30349
- 12 **Schmidt JT**, Morgan P, Dowell N, Leu B. Myosin light chain phosphorylation and growth cone motility. *J Neurobiol* 2002; **52**: 175-188
- 13 **Dudek SM**, Birukov KG, Zhan X, Garcia JG. Novel interaction of cortactin with endothelial cell myosin light chain kinase. *Biochem Biophys Res Commun* 2002; **298**: 511-519
- 14 **Birukov KG**, Schavocky JP, Shirinsky VP, Chibalina MV, Van Eldik LJ, Watterson DM. Organization of the genetic locus for chicken myosin light chain kinase is complex: multiple proteins are encoded and exhibit differential expression and localization. *J Cell Biochem* 1998; **70**: 402-413
- 15 **Blue EK**, Goekeler ZM, Jin Y, Hou L, Dixon SA, Herring BP, Wysolmerski RB, Gallagher PJ. 220- and 130-kDa MLCKs have distinct tissue distributions and intracellular localization patterns. *Am J Physiol Cell Physiol* 2002; **282**: C451-460
- 16 **Davis JS**, Hassanzadeh S, Winitzky S, Lin H, Satorius C, Vemuri R, Aletras AH, Wen H, Epstein ND. The overall pattern of cardiac contraction depends on a spatial gradient of myosin regulatory light chain phosphorylation. *Cell* 2001; **107**: 631-641
- 17 **Murata-Hori M**, Suizu F, Iwasaki T, Kikuchi A, Hosoya H. ZIP kinase identified as a novel myosin regulatory light chain kinase in HeLa cells. *FEBS Lett* 1999; **451**: 81-84
- 18 **Gallagher PJ**, Herring BP. The carboxyl terminus of the smooth muscle myosin light chain kinase is expressed as an independent protein, telokin. *J Biol Chem* 1991; **266**: 23945-23952
- 19 **Aromolaran AS**, Albert AP, Large WA. Evidence for myosin light chain kinase mediating noradrenaline-evoked cation current in rabbit portal vein myocytes. *J Physiol* 2000; **524**(Pt 3): 853-863
- 20 **Watanabe H**, Tran QK, Takeuchi K, Fukao M, Liu MY, Kanno M, Hayashi T, Iguchi A, Seto M, Ohashi K. Myosin light-chain kinase regulates endothelial calcium entry and endothelium-dependent vasodilation. *FASEB J* 2001; **15**: 282-284
- 21 **Tran QK**, Watanabe H, Le HY, Pan L, Seto M, Takeuchi K, Ohashi K. Myosin light chain kinase regulates capacitative Ca²⁺ entry in human monocytes/macrophages. *Arterioscler Thromb Vasc Biol* 2001; **21**: 509-515
- 22 **Wadgaonkar R**, Nurmukhambetova S, Zaiman AL, Garcia JG. Mutation analysis of the non-muscle myosin light chain kinase (MLCK) deletion constructs on CV1 fibroblast contractile activity and proliferation. *J Cell Biochem* 2003; **88**: 623-634
- 23 **Iida Y**, Senda T, Matsukawa Y, Onoda K, Miyazaki JI, Sakaguchi H, Nimura Y, Hidaka H, Niki I. Myosin light-chain phosphorylation controls insulin secretion at a proximal step in the secretory cascade. *Am J Physiol* 1997; **273**(4 Pt 1): E782-789
- 24 **Mansfield PJ**, Shayman JA, Boxer LA. Regulation of polymorphonuclear leukocyte phagocytosis by myosin light chain kinase after activation of mitogen-activated protein kinase. *Blood* 2000; **95**: 2407-2412
- 25 **Tinsley JH**, De Lanerolle P, Wilson E, Ma W, Yuan SY. Myosin light chain kinase transference induces myosin light chain activation and endothelial hyperpermeability. *Am J Physiol Cell Physiol* 2000; **279**: C1285-1289
- 26 **Ren B**, Zhu HQ, Lou ZF, Zhou Q, Wang Y, Wang YZ. Preliminary research on myosin light chain kinase in rabbit liver. *World J Gastroenterol* 2001; **7**: 868-871
- 27 **Yu W**, Niwa T, Fukasawa T, Hidaka H, Senda T, Sasaki Y, Niki I. Synergism of protein kinase A, protein kinase C, and myosin light-chain kinase in the secretory cascade of the pancreatic beta-cell. *Diabetes* 2000; **49**: 945-952

Edited by Zhang JZ and Wang XL

Identification of *alkA* gene related to virulence of *Shigella flexneri* 2a by mutational analysis

Zhao-Xing Shi, Heng-Liang Wang, Kun Hu, Er-Ling Feng, Xiao Yao, Guo-Fu Su, Pei-Tang Huang, Liu-Yu Huang

Zhao-Xing Shi, Heng-Liang Wang, Kun Hu, Er-Ling Feng, Guo-Fu Su, Pei-Tang Huang, Liu-Yu Huang, Beijing Institute of Biotechnology, Beijing 100071, China

Xiao Yao, College of Environmental and Chemical Engineering, Xi'an Jiaotong University, Xi'an 710049, Shaanxi Province, China

Supported by the Major State Basic Research Development Program of China (973 Program), No. G1999054103; National High-technology Research and Development Program of China (863 Program), No. 2001AA215211; and Capital "248" Key Innovation Program of China, No. H010210360119

Correspondence to: Liu-Yu Huang, Beijing Institute of Biotechnology, 20 East Fengtai Street, Beijing 100071, China. huangly@nic.bmi.ac.cn

Telephone: +86-10-66948805 **Fax:** +86-10-63833521

Received: 2003-07-17 **Accepted:** 2003-07-30

Abstract

AIM: *In vivo* induced genes are thought to play an important role during infection of host. *AlkA* was identified as an *in vivo*-induced gene by *in vivo* expression technology (IVET), but its virulence in *Shigella flexneri* was not reported. The purpose of this study was to identify the role of *alkA* gene in the pathogenesis of *S. flexneri*.

METHODS: PCR was used to amplify *alkA* gene of *S. flexneri* 2a and fragment 028pKm. The fragment was then transformed into 2457T05 strain, a *S. flexneri* 2a strain containing Red recombination system, which was constructed with a recombinant suicide plasmid pXLkd46. By *in vivo* homologous recombination, *alkA* mutants were obtained and verified by PCR and sequencing. Intracellular survival assay and virulence assay were used to test the intracellular survival ability in HeLa cell model and the virulence in mice lung infection model respectively.

RESULTS: Deletion mutant of *S. flexneri* 2a *alkA* was successfully constructed by λ Red recombination system. The mutant exhibited significant survival defects and much significant virulence defects in mice infection assay.

CONCLUSION: *AlkA* gene plays an important role in the infection of epithelial cells and is a virulent gene of *Shigella* spp.

Shi ZX, Wang HL, Hu K, Feng EL, Yao X, Su GF, Huang PT, Huang LY. Identification of *alkA* gene related to virulence of *Shigella flexneri* 2a by mutational analysis. *World J Gastroenterol* 2003; 9(12): 2720-2725

<http://www.wjgnet.com/1007-9327/9/2720.asp>

INTRODUCTION

Shigella spp. is a Gram-negative facultative pathogen, which causes bacillary dysentery, a world endemic bloody diarrhea, particularly in developing countries. The disease is caused by invasion of the colorectal mucosa by *Shigella* spp., replicating within epithelial cells and moving between cells. The interaction between epithelial cells and *Shigella* spp. plays an

important role in the pathogenicity of *Shigella* spp.^[1-3]. During infection of epithelial cells, genes with inducible expression are important for *Shigella* spp. to replicate and survive in the cells. Hereby, these genes are generally thought to be related to the virulence of *Shigella* spp.. Many methods could be used to isolate *in vivo* expressed genes^[4]. Using *in vivo* expression technology (IVET) to identify the virulence-related genes of pathogens is a flourishing field in the world^[5-11]. We have employed *in vivo* expression technology with *asd* gene as a reporter to screen *S. flexneri* 2a fusion gene library. The result indicated that *alkA* gene is an *in vivo*-induced gene for *Shigella flexneri* 2a.

AlkA gene or its homologous genes have been cloned from many organisms, such as *Escherichia coli*, *Helicobacter pylori*, *Bacillus subtilis*, *Saccharomyces cerevisiae*, human, etc^[12-14]. They encode 3-methyladenine DNA glycosylase, whose function is excising hypoxanthine, demethylating, and mainly taking part in the repair of damaged DNA^[15,16]. Up to now researches on *alkA* have mainly focused on regulation of its expression and its role in inducing repair after DNA alkylation damage. As for its relation to bacterial pathogenesis, it is a noteworthy issue. In this experiment, based on the sequence of *E. coli alkA*, *alkA* gene of *S. flexneri* 2a 2457T was cloned. Its mutant was constructed, and its role in pathogenesis was analyzed by a HeLa cell model and a mice infection model. This study perhaps would provide insights into the pathogenicity of this pathogen.

MATERIALS AND METHODS

Materials

The strains and plasmids used in this study are listed in Table 1.

HeLa cell line was maintained in our laboratory. BALB/c mice were bought from the Laboratory Animal Center in the Academy of Military Medical Sciences, Beijing. All mice used in this study were female, specific pathogen free animals, with an age of 7-8 weeks and weight of 18-22 g. DNA endonucleases, DNA marker, T4 DNA ligase, T4 DNA polymerase, Ex *Taq* DNA polymerase, and CIAP were purchased from Takara Company. Newborn calf sera and RPMI1640 media were from HyClone, and deoxycholate sodium from Sigma. Primers (P1, P2, P3, and P4) were synthesized in our laboratory.

Methods

Culture and maintenance of strains and HeLa cells Luria-Bertani (LB) broth and agar plate were used for the growth of *S. flexneri* and *Escherichia coli* strains at 37 °C. SOC culture medium was applied to the restoration of bacteria after electroporation. When appropriate, antibiotics were added in media as follows: 100 µg ampicillin (Ap), 100 µg streptomycin (Sm), 50 µg kanamycin (Km), 25 µg chloramphenicol (Cm), and 25 µg naladixic acid (Nal) per ml. HeLa cells were maintained in the RPMI-1640 medium supplemented with 10 % fetal bovine serum, 200 mM L-glutamine, 2 mg sodium hydrogen carbonate per ml and 100 µg penicillin-streptomycin per ml. The cells were cultured in 37.5 cm² or 10 cm² flasks at 37 °C in a humidified atmosphere of 5% CO₂. Confluent monolayers were split by treatment with sterile phosphate-buffered saline (PBS) and trypsin-EDTA.

Table 1 Strains and plasmids

Strains and plasmids	Characteristics	Source (reference)
Strains		
DH5 α	endA1 hsdR17(r _k ⁻ m _k ⁻) supE44 thi-1 recA1 gyrA(Nal ^r) RelA1 Δ lacIZYA-argF) U169 deoR (ϕ 80dlac Δ (lacZ)M15)	Our lab
S ₁₇ - λ pir	thi-1 thr leu tonA lacY supE recA::RP4-2-Tc::Mu, Sm ^r , λ pir	Guzman CA
MC1061	hsdR2 mcrB araD139 Δ (ara ABC-leu)7679 Δ lacX74 galU galK rpsL thi, Sm ^r	Our lab
2457T	<i>S. flexneri</i> 2a wild type, Nal ^r	Maurelli AT
2457T05	a derivative strain of 2457T, contained araBp-gam-bet-exo, Nal ^r	This study
2457T028D	Δ alkA, derivative strain of 2457T, Nal ^r , Km ^r	This study
Plasmids		
pMD18-T	a derivative constructed from pUC18, Ap ^r	TaKaRa
pXL275	a mobile and suicide plasmid, ori R6K, mob RK2, sacBR, Cm ^r	Rui <i>et al.</i> ^[17]
pKD46	oriR101, repA101(ts), araBp-gam-bet-exo, Ap ^r	CGSC ^a
pXLkd46	pXL275 derivative, inserted a fragment containing araBp-gam-bet-exo, Cm ^r	This study
pMDKm05	pMD18-T derivative, inserted Km ^r gene, Km ^r , Ap ^r	Our lab
pMD028	pMD18-T derivative, inserted <i>alkA</i> gene, Ap ^r	This study
pMD028pKm	pMD18-T derivative, inserted a cassette (5' <i>alkA</i> end-Km ^r -3' <i>alkA</i> end), Km ^r , Ap ^r	This study

^aCGSC: *E. coli* Genetic Stock Center.

Genetic techniques Plasmid DNA extraction was carried out using a Qiagen plasmid kit. Digestion, ligation, transformation, and other conventional methods of molecular biology were performed as previously described^[18].

DNA amplifications For the amplification of *S. flexneri* 2a *alkA* gene, PCR was performed in a standard 100 μ l reaction volume containing 2.5 mM Mg Cl₂, 0.25 mM of each dNTP, 100 pmol of P1 and P2 primers, 10 μ l boiled *S. flexneri* 2a 2457T, and 5 U Taq DNA polymerase. Reactions were allowed to proceed in a Perkin-Elmer 2400 thermal cycler programmed for 10 min at 94 °C, 30 cycles (for 45 s at 94 °C, for 40 s at 55 °C, for 3 min at 72 °C) and an additional extension reaction for 10 min at 72 °C. For the amplification of fragment 028pKm, PCR was carried out in 100 μ l reaction volume containing 2.5 mM MgCl₂, 0.25 mM of each dNTP, 100 pmol of P3 and P4 primers, 2 μ l plasmid pMD028pKm (about 10 ng), and 5 U Taq DNA polymerase. The program of this PCR was at 94 °C for 10 min, 30 cycles (for 30 s at 94 °C, for 40 s at 58 °C, for 1.5 min at 72 °C) and for 10 min at 72 °C.

Bacterial mating The donor and recipient strains were grown in LB medium containing appropriate antibiotics overnight. The liquid cultures were then washed in PBS, mixed at 1:1 ratio, and spreaded on LB agar plates. The plates were incubated at 37 °C for 6-8 h. After incubation, the conjugation mixture was washed in PBS and spread onto LB agar plates containing chloramphenicol (25 μ g \cdot mL⁻¹) and naladixic acid (25 μ g \cdot mL⁻¹). The plates were incubated at 37 °C until transconjugants were visible.

Disruption of *S. flexneri* 2a *alkA* gene *S. flexneri* 2a 2457T05 was grown in 5 ml LB cultures with chloramphenicol, naladixic acid and L-arabinose to an OD₆₀₀=0.45 and then made electrocompetent by concentrating 100-fold and washing three times with ice-cold 10 % glycerol. The gel-purified 028pKm PCR products were digested with *DpnI*, repurified, and suspended in elution buffer (10 mM Tris, pH 8.0). Electroporation was done using a gene pulser[®] II with a pulse controller plus and 0.1 cm chambers according to the manufacturer's instructions (Bio-RAD) using 40 μ l of competent cells and 100 ng of 028pKm fragments. The parameters for electro- transformation were resistance 200 Ω , capacitance 25 μ F, and voltage 2 500 V. Shocked cells were added to 1 ml SOC culture, incubated for 1 h at 37 °C, and then one-half was spread onto agar to select Km^r and Nal^r transformants. If none grew within 24 h, the remainder was spread after standing overnight at room temperature.

Intracellular survival assay HeLa cell infection assay was

routinely used to detect the intracellular replication or survival ability of the mutant^[19-21]. *S. flexneri* 2a 2457T, 2457T05, mutant strain and *E. coli* MC1061 (noninvasive control) were grown in an appropriate medium overnight. The liquid cultures were then washed in PBS and resuspended in antibiotic-free medium. Approximately 10⁶ HeLa cells were cultured in a 10 cm² flask. HeLa cells were washed three times in PBS prior to incubation with about 10⁸ CFU bacteria at 37 °C for 3 h. The medium was removed from infected cells after 2.5 h, and the cells were washed three times in PBS. Fresh medium containing gentamicin (20 μ g \cdot mL⁻¹) was added and the flasks were incubated for 5 h to eliminate extracellular bacteria. After that, the medium was replaced by RPMI1640 containing gentamicin (20 μ g \cdot mL⁻¹) and the infected cells were cultured for another 40 h. The supernatants of culture were tested for extracellular surviving bacteria by plating them on LB agar plates. The monolayers were then washed three times in PBS and lysed by addition of 0.1 % deoxycholate sodium to liberate the intracellular bacteria. Dilutions of the lysates of HeLa cells infected with bacteria were plated on LB agar plates and cultured at 37 °C overnight. The CFU of the bacteria was then counted.

Competition assay To test the mutant strains for alterations in virulence relative to the wild type, a competition assay was carried out by using a murine intranasal infection model^[22-24] with some modifications. The mutant or MC1061 (negative control) or 2457T (positive control) and 2457T05 grown overnight were mixed at 1:1 (v/v) ratio and washed in PBS. After concentration of the mixture was adjusted by dilutions, 20 μ l mixtures containing about 10⁶ CFU in PBS was used to introduce droplets into the nares of BALB/c mice that was anesthetized. The number of bacteria in each inoculum was determined by plating serial dilutions of the inoculum. After 24 h, the recovered bacteria from the lungs of mice were counted, and then the number of mutant strains and 2457T was counted. According to the method of Camilli *et al.*^[25], the competitive index of each mutant was obtained.

Bioinformatics analysis The sequence of *S. flexneri* 2a *alkA* gene was analyzed by BLAST (<http://www.ncbi.nlm.nih.gov/BLAST/>). The identity and gene function were also analyzed by NCBI.

Statistical analysis

Data from the intracellular survival assay were analyzed by Dunnett *t* test, and *P* value less than 0.05 was considered as statistically significant. Data from the competition assay were analyzed by the sign test, and *P* value less than 0.0078 was

considered as statistically significant. The Dunnet *t* test and the sign test were performed using the SAS (Statistical Analysis Systems Inc., USA) program.

RESULTS

Cloning and homologous analysis of *S. flexneri* 2a *alkA* gene

In our previous work, we identified *S. flexneri* 2a *alkA* as an *in vivo*-induced gene, and obtained the partial sequence of *S. flexneri* 2a *alkA* gene which had an alignment with other bacteria. Based on the sequence of *E. coli alkA*, the primers, P1 (CGAGGAACGATTTTGGTGAT) and P2 (CTCGCT-GAAAGCGAATATGG) (Figure 3 B) were designed. Using *S. flexneri* 2a 2457T chromosome DNA as a template, PCR was performed and the PCR products were purified by agarose gel electrophoresis, and ligated into plasmid pMD18-T to produce plasmid pMD028 after the confirmation of *EcoRV* and *HindIII* digestion analysis. The recombinant plasmid pMD028 was subjected to DNA sequencing to obtain the whole length DNA sequence of *alkA*. Its open read frame was 849 bp. In the upstream there was a promoter sequence (AGCAAAGCGTAACGTCTGAATAACGTTTATGCT) and the binding site (AAAGCAAA) of Ada protein which was a regulator of *alkA* gene expression in *E. coli*. Based on the sequence of *S. flexneri* 2a *alkA*, homologous analysis was carried out on the NCBI website. The results are listed in Table 2. Interestingly, the sequence alignment revealed a Helix-

hairpin-Helix (HhH) motif common to DNA glycosylases. *E. coli alkA* was identified as the helix-hairpin-helix DNA glycosylase^[26]. Very possibly, *alkA* protein from *S. flexneri* 2a belonged to an HhH-GPD super family. Its hallmark was Helix-hairpin-Helix and Gly/Pro rich loop followed by a conserved aspartate and its function was presumably involved in DNA replication and repair.

Construction of *S. flexneri* 2a engineering strain

To delete *alkA* gene of *S. flexneri* 2a, construction of *S. flexneri* 2a engineering strain expressing *gam*, *bet*, and *exo* genes, was required. The fragment (about 4 kb) containing *gam*, *bet*, and *exo* genes was obtained by digestion of pKD46 plasmid with *PvuI* and *BstxI* and ligated into the *SalI* site of suicide plasmid pXL275. Then the ligation products were then transformed into *S*₁₇₋₁λpir. The recombinant plasmid was confirmed by *BamHI* digestion and known as pXLkd46. After bacterial mating of the donor (*S*₁₇₋₁λpir/pXLkd46) and recipient (2457T), pXLkd46 plasmid was integrated into chromosome of *S. flexneri* 2a by homologous recombination. The process of pXLkd46 plasmid construction and chromosomal integration is showed in Figure 1. The resulting strain was verified with antibiotic selection and serum agglutination and designated as 2457T05.

Construction of deletion mutant of *S. flexneri alkA* gene

After 2457T05 was successfully constructed, the linear targeting DNA, 028p*Km*, was required for disruption of *S.*

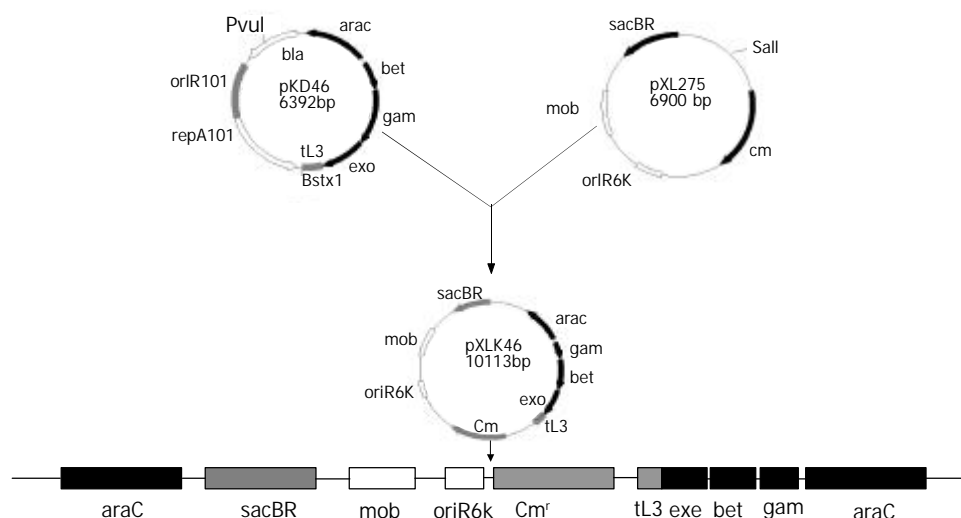


Figure 1 Construction and chromosomal integration of pXLkd46 plasmid.

Table 2 BLAST analysis of *S. flexneri* 2a *alkA* gene

Bacteria	Gene product	Gene function	Identities (%)
Escherichia coli K12	3-methyl-adenine DNA glycosylase II	DNA - replication, repair, restriction/modification	97 %
Escherichia coli O157:H7	3-methyl-adenine DNA glycosylase II	Macromolecule synthesis, modification: DNA-replication, repair, restriction/modification	97 %
Salmonella typhimurium	3-methyl-adenine DNA glycosylase II	Unknown	74 %
Ralstonia solanacearum	putative transcription regulator protein	Miscellaneous; not classified regulator	38 %
Pseudomonas aeruginosa	DNA-3-methyladenine glycosidase II	Unknown	37 %
Xanthomonas axonopodis	DNA methylation and regulatory protein	Unknown	35 %
Mycobacterium bovis	Methylated-DNA-protein-cysteine methyltransferase	Adaptative response	34 %
Mycobacterium tuberculosis	<i>alkA</i> protein	Unknown	34 %
Vibrio cholerae	<i>ada</i> regulatory protein	Unknown	32 %
Bacillus anthracis	DNA-3-methyladenine glycosidase	Unknown	32 %
Archaeoglobus fulgidus	3-methyladenine DNA glycosylase	DNA repair at suboptimal and maybe even mesophilic temperatures	30 %

flexneri 2a *alkA* gene with λ Red recombination system. To obtain the fragment *028pKm*, recombinant plasmid pMD028pKm was firstly to be constructed. Km^r gene fragment was obtained from plasmid pMDKm05 digested by *Hinc*I and *Sma*I and inserted into the *alkA* gene of plasmid pMD028 digested by *Eco*RV and *Stu*I and dephosphorized by CIAP. The ligation products were then transformed into *E. coli* DH5 α . The recombinant plasmids were isolated from the transformants, confirmed by *Eco*RI digestion, and designated as pMD028pKm (Figure 2). Using pMD028pKm as a PCR template, P3 (TGTGCCAGTGAGGAAAGACC) and P4 (GAGAGAGCGT TTGCCATTG) (Figure 3A) as primers, PCR was carried out. In order to reduce the interference of plasmid pMD028pKm, the second PCR was carried out at the same experimental condition except that the template was the first PCR products diluted by 1 000 times. The second PCR products (*028pKm*) did not contain the template plasmid pMD028pKm that would lead to false positive colonies in the latter electroporation experiment. The *028pKm* fragment was a cassette, 5' *alkA* end-Km^r-3' *alkA* end (Figure 3A). The concentrated *028pKm* was electroporated into *S. flexneri* 2a engineering strain 2457T05. The *alkA* gene was then replaced by kanamycin resistance gene through homologous recombination mediated by λ Red system. The positive transformants were selected on LB agar plates containing Km and Nal.

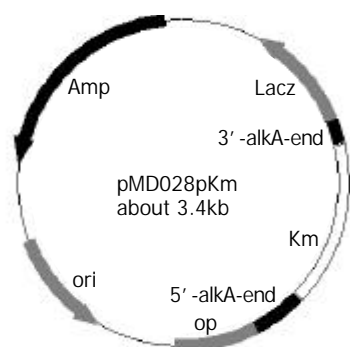


Figure 2 Construction of recombinant plasmid pMD028pkm.

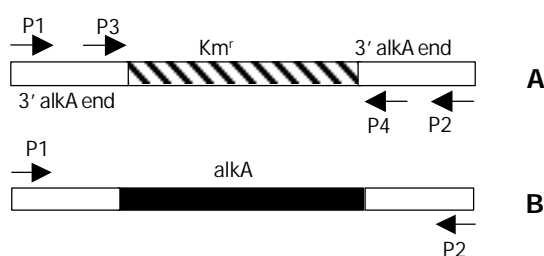


Figure 3 Location of primers P1, P2, P3 and P4 in PCR products of *alkA* and *028pKm*. A: *028pKm* (about 1.4 kb); B: *alkA* (about 1.7 kb).

To verify the replacement of *S. flexneri* 2a *alkA* gene, PCR and sequencing were used. PCR was performed in which 2457T05 (negative control), the transformant and pMD028pKm plasmid (positive control) were used as templates. The reaction conditions were the same as the amplification of *S. flexneri* *alkA* gene, and the primers were also P1 and P2. The PCR products from the transformant and pMD028pKm plasmid were about 1.4 kb and 1.7 kb from 2457T05 respectively (Figure 3, 4). Then the PCR products were sequenced and analyzed by BLAST (data not shown). The result indicated that *alkA* gene of *S. flexneri* 2a was replaced by Km^r gene. Hereby, the deletion mutant of *alkA* gene was successfully constructed and designated as 2457T028D.

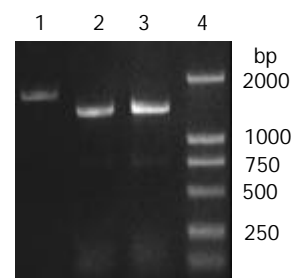


Figure 4 Verification of *alkA* gene deletion of 2457T028D mutant by PCR. 1: *alkA* PCR product (amplified from 2457T05), 2: *028pKm* PCR product (amplified from 2457T028D), 3: *028Kkm* PCR product (amplified from pMD028pKm), 4: DL2000 Marker.

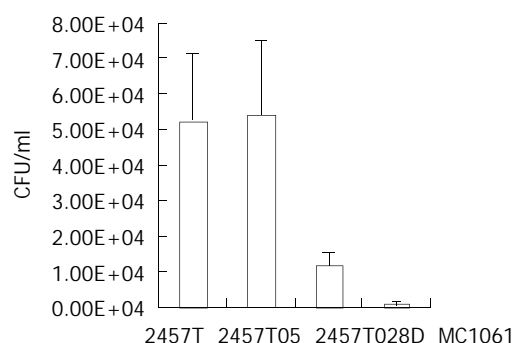


Figure 5 Comparison of HeLa cells infected by 2457T, 2457T05, 2457T028D and MC1061.

Functional analysis of deletion mutant of *S. flexneri* 2a *alkA* gene

In order to detect the role of *alkA* in the pathogenesis of *S. flexneri*, intracellular survival assay and virulence assay were respectively carried out in HeLa cells and BALB/c mice.

Mutant 2457T028D was tested for its survival ability in HeLa cells relative to the wild-type strain. Equal volume of each strain (2457T, 2457T05, 2457T028D and MC1061) was respectively used to infect the HeLa cell monolayer. Within 48 h, the integrity of the infected HeLa cell monolayer was good and the configuration of HeLa cells had no significant alterations relative to normal cells. But the growth rate of the infected cells became slow. After 48 h, CFU of bacteria recovered from HeLa cells was counted. The results of the infection assay are summarized in Figure 5. Noticeably, CFU levels of the mutant recovered from HeLa cells were five-fold lower than that of the wild type ($P < 0.01$), indicating that the mutant had a lower capability of survival or replication. The survival probability of 2457T and 2457T05 showed no significant difference (Figure 5). In order to further confirm the survival probability of the mutant, competition assay was carried out with the HeLa cell infection model. A 1:1 (v/v) mixture of *S. flexneri* 2a 2457T05 and the mutant or 2457T or MC1061 was used to infect HeLa cells. The number of bacteria in each inoculum was determined by plating serial dilutions of the inoculum. After 48 h, recovered bacteria from HeLa cells were counted, and the number of bacteria was counted respectively. The experiment was separately repeated 3 times. Therefore, the competitive index of each strain obtained is shown in Table 3. The mutant 2457T028D whose survival probability was significantly lower in the infection assay, exhibited significant survival defects in this experiment ($P < 0.0078$). The data strongly indicated that the mutant was much less able to survive in HeLa cells.

The mutant was also tested in a mice lung infection model for alterations in virulence relative to the wild-type parental strain. Mice that were challenged only with *S. flexneri* 2457T

showed early acute bronchiolitis at 24 h, followed by severe pneumonia at 48 h. Five mice were used for each group in the murine lung infection model. After 24 h, recovered bacteria from the lungs of mice were counted, and the number of each strain was counted. Then the competitive index of each strain obtained is summarized in Table 3. The mutant also exhibited significant colonization defects ($P < 0.0078$). The data further indicated that *alkA* gene was potentially related to the virulence of *S. flexneri* 2a 2457T.

Table 3 Competitive analysis of different strains of *S. flexneri* 2a

Strains	Competitive index (CI) ^a	
	BALB/c mouse infection	HeLa cells infection
2457T05	0.96±0.27	1.07±0.35
2457T028D	0.21±0.09 ^b	0.25±0.11 ^b
MC1061	0.03±0.02 ^b	0.02±0.01 ^b

^aCompetitive index (CI) is the ratio of mutant CFU to wild-type CFU after correcting the ratios for deviations of the inoculum ratio from a value of 1. ^b $P < 0.0078$.

DISCUSSION

It has been reported that *in vivo*-induced gene played an important role in the process of interaction between pathogen and host^[27]. *In vivo*-induced genes are those whose expression is induced when pathogens infect their hosts. Their inducible expression is a molecular-level genetic adaptive response to special environments of host. Many virulent genes have been identified by mutational analysis of *in vivo*-induced genes. Heithoff *et al.*^[28] used *purA-lacZY* as a reporter to identify *in vivo*-induced genes of *Salmonella typhimurium* utilizing macrophages or BALB/c mice as a model. They discovered some *in vivo*-induced genes, including regulatory genes (*phoP*, *pmrB*, *cadC*, etc.) and metabolic genes (*recD*, *hemA*, *mgtA*, *entF*, etc.). Furthermore, insertion mutants of these genes were constructed, and their virulence was detected. Seven of them exhibited significant virulence defects. In another research on *Pseudomonas aeruginosa*, 22 genes were *in vivo*-induced during infecting BALB/c mice, including *np20*, which has been proved to be a virulence gene, and known as virulent factor FptA^[29]. In our previous study, we identified *alkA* as an *in vivo*-induced gene. However, it is unknown if *alkA* gene is related to the virulence of *S. flexneri*.

In order to detect the role of *alkA* gene in the virulence of *S. flexneri* 2a, it is required to construct the deletion mutant of *alkA* gene. The mutant is conventionally constructed by twice homologous recombination mediated by suicide plasmid. Although the *asd* gene of *S. flexneri* 2a was successfully disrupted in our previous study^[30], the efficiency of this method is very low and the experimental period is quite long. Recently, a new method, which depends on Red recombination system of λ phage, has been successfully established and used to speed up the knockout of genes^[31,32]. However, its application was limited to *E. coli*^[33-35]. It was not reported in other bacteria except that the *asd* gene was deleted with λ Red system in our laboratory^[36]. In this study, the deletion mutant of *S. flexneri* 2a *alkA* gene was successfully constructed also with λ Red system. Importantly, an engineering strain 2457T05 of *S. flexneri* 2a was constructed, and it was confirmed that the strain could be used to study the function of *S. flexneri* 2a genes.

After the mutant of *S. flexneri* 2a *alkA* gene was constructed, intracellular survival and competition assays were carried out. The results showed that *alkA* mutant of *S. flexneri* could exhibit a low intracellular survival ability and a significant virulence defect, indicating that *alkA* was a virulence-related gene in *S. flexneri* 2a. However, it has not been reported before whether

alkA was associated with the virulence of pathogens. *AlkA* is an expression-induced gene and its product, 3-methyladenine DNA glycosylase II, is involved in the SOS-dependent adaptive response. Expression of *alkA* is regulated by Ada protein. When alkylation damages bacterial DNA, *ada* gene would be induced by alkyl-DNA. The produced Ada finishes directly-repairing damage of alkyl-DNA by transferring the methyl group from alkyl-DNA to its cysteine residues. At the same time Ada loses its activity. The methyl-Ada turns into a positive regulator of *alkA*, *aidB*, *alkB*, and itself as well. Methyl-Ada could recognize and bind onto the special region (AAAGCAAA) of *alkA* promoter, start transcription of *alkA*, and further complete repairing damage of other type alkylation, avoiding bacterial death due to damage of DNA alkylation^[37-40]. The base excision repair could protect against the deleterious effects of DNA alkyl lesions. However, the activities of *alkA* gene must be balanced for optimal protection against the biological consequences of damaged DNA bases because inappropriate expression of this activity might have a detrimental consequence^[41]. During infection of host, *Shigella spp.* probably suffers strong damage of alkyl in host. But alkylated DNA activates the adaptive response of *Shigella spp.* to host. Expression of *alkA* effectively repairs damage of DNA alkylation so that the killing-effect resulted from DNA damage could not carry out. Therefore, from this point of view, *in vivo*-induced-expression of *alkA* provides a significant safeguard for infection of *Shigella spp.* and is an essential gene for exhibiting *Shigella spp.* virulence.

Although there has been no report about the relationship between *alkA* and virulence of pathogens, it is known that a close relation lies between DNA methylation and bacterial virulence. Heithoff *et al.*^[42] discovered that DNA adenine methylase (Dam) could regulate expression of at least 20 *in vivo*-induced genes and that Dam⁺ *S. typhimurium* as a live vaccine had a protective role with no side-effect. *S. typhimurium* with over-expressing Dam also exhibited a significant virulence defect and a protective effect as an oral vaccine^[43]. Similar results have also been obtained in *Yersinia pseudotuberculosis* and *Vibrio cholerae*^[44]. Hereby, during infection expression of Dam could induce the expression of *in vivo*-induced genes, but its over-expression could also lead to damage of methylation and attenuation of pathogens. Thus a suitable level of DNA methylation might play a key role for pathogens to keep the virulence. From this point of view, *alkA* may be a virulence-related gene of pathogens. The hypothesis illustrating the relationship between DNA methylation damage and *alkA* gene is shown in Figure 6. Whether a regulatory relation exists between *alkA* and *dam* remains to be further confirmed. However, we believe that *alkA* is a new target for studying on molecular pathogenesis mechanism of *Shigella spp.* and construction of attenuated live vaccines.

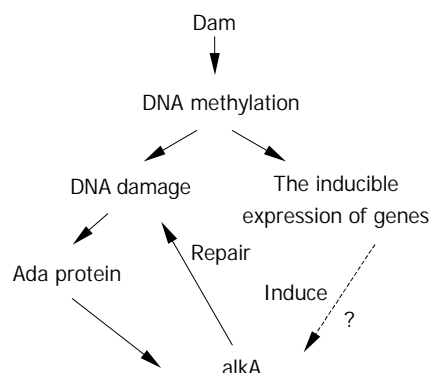


Figure 6 Hypothesis illustrating the relationship between *alkA* and damage of DNA methylation.

ACKNOWLEDGEMENTS

We thank Prof. Qi-Nong Ye and Dr Bao-Chang Fan for critical review of this manuscript. We also thank Miss Run-Yan Liu and Miss Hui-Ping Zhang for their help with experiments.

REFERENCES

- Sansonetti PJ.** Rupture, invasion and inflammatory destruction of the intestinal barrier by *Shigella*, making sense of prokaryote-eukaryote cross-talks. *FEMS Microbiol Rev* 2001; **25**: 3-14
- Fernandez MI, Sansonetti PJ.** *Shigella* interaction with intestinal epithelial cells determines the innate immune response in shigellosis. *Int J Med Microbiol* 2003; **293**: 55-67
- Yao X, Wang HL, Shi ZX, Yan XY, Feng E, Yang BL, Huang LY.** Identification of RanBMP interacting with *Shigella flexneri* IpaC invasion by two-hybrid system of yeast. *World J Gastroenterol* 2003; **9**: 1347-1351
- Handfield M, Levesque RC.** Strategies for isolation of *in vivo* expressed genes from bacteria. *FEMS Microbiol Rev* 1999; **23**: 69-91
- Mahan MJ, Slauch JM, Mekalanos JJ.** Selection of bacterial virulence genes that are specifically induced in host tissues. *Science* 1993; **259**: 686-688
- Young GM, Miller VL.** Identification of novel chromosomal loci affecting *Yersinia enterocolitica* pathogenesis. *Mol Microbiol* 1997; **25**: 319-328
- Staib P, Kretschmar M, Nichterlein T, Kohler G, Michel S, Hof H, Hacker J, Morschhauser J.** Host-induced, stage-specific virulence gene activation in *Candida albicans* during infection. *Mol Microbiol* 1999; **32**: 533-546
- Gahan CG, Hill C.** The use of listeriolysin to identify *in vivo* induced genes in the gram-positive intracellular pathogen *Listeria monocytogenes*. *Mol Microbiol* 2000; **36**: 498-507
- Lai YC, Peng HL, Chang HY.** Identification of genes induced *in vivo* during *Klebsiella pneumoniae* CG43 infection. *Infect Immun* 2001; **69**: 7140-7145
- Wu Y, Lee SW, Hillman JD, Progulsk-Fox A.** Identification and testing of *Porphyromonas gingivalis* virulence genes with a pPGIVET system. *Infect Immun* 2002; **70**: 928-937
- Bartoleschi C, Pardini MC, Scaringi C, Martino MC, Pazzani C, Bernardini ML.** Selection of *Shigella flexneri* candidate virulence genes specifically induced in bacteria resident in host cell cytoplasm. *Cell Microbiol* 2002; **4**: 613-626
- Morohoshi F, Hayashi K, Munkata N.** *Bacillus subtilis alkA* gene encoding inducible 3-methyladenine DNA glycosylase is adjacent to the *ada* operon. *J Bacteriol* 1993; **175**: 6010-6017
- O'Rourke EJ, Chevalier C, Boiteux S, Labigne A, Ielpi L, Radicella JP.** A novel 3-methyladenine DNA glycosylase from *Helicobacter pylori* defines a new class within the endonuclease III family of base excision repair glycosylases. *J Biol Chem* 2000; **275**: 20077-20083
- Saparbaev M, Mani JC, Laval J.** Interactions of the human, rat, *Saccharomyces cerevisiae* and *Escherichia coli* 3-methyladenine-DNA glycosylases with DNA containing dIMP residues. *Nucleic Acids Res* 2000; **28**: 1332-1339
- Privezentzev CV, Saparbaev M, Sambandam A, Greenberg MM, Laval J.** AlkA protein is the third *Escherichia coli* DNA repair protein excising a ring fragmentation product of thymine. *Biochemistry* 2000; **39**: 14263-14268
- Mansfield C, Kerins SM, McCarthy TV.** Characterisation of *Archaeoglobus fulgidus* Aika hypoxanthine DNA glycosylase activity. *FEBS Lett* 2003; **540**: 171-175
- Rui X, Xu Y, Wan H, Su G, Huang C.** Construction of a stable and non-resistant bivalent vaccine candidate strain against *Shigella flexneri* 2a and *Shigella sonnei*. *Chin J Biotechnol* 1996; **12**: 89-97
- Sambrook J, Fritton EF, Maniatis T.** Molecular Cloning: a Laboratory Manual. The 2nd edition. New York: Cold Spring Harbor Laboratory Press 1989: 34-56, 237-261
- Roy S, Biswas T.** Murine splenocyte proliferation by porin of *Shigella dysenteriae* type 1 and inhibition of bacterial invasion of HeLa cell by anti-porin antibody. *FEMS Microbiol Lett* 1996; **141**: 25-29
- Niesel DW, Chambers CE, Stockman SL.** Quantitation of HeLa cell monolayer invasion by *Shigella* and *Salmonella* species. *J Clin Microbiol* 1985; **22**: 897-902
- Zhong QP.** Pathogenic effects of Opolysaccharide from *Shigella flexneri* strain. *World J Gastroenterol* 1999; **5**: 245-248
- Mallett CP, VanDeVerg L, Collins HH, Hale TL.** Evaluation of *Shigella* vaccine safety and efficacy in an intranasally challenged mouse model. *Vaccine* 1993; **11**: 190-196
- Van de Verg LL, Mallett CP, Collins HH, Larsen T, Hammack C, Hale TL.** Antibody and cytokine responses in a mouse pulmonary model of *Shigella flexneri* serotype 2a infection. *Infect Immun* 1995; **63**: 1947-1954
- Way SS, Borczuk AC, Dominitz R, Goldberg MB.** An essential role for gamma interferon in innate resistance to *Shigella flexneri* infection. *Infect Immun* 1998; **66**: 1342-1348
- Camilli A, Mekalanos JJ.** Use of recombinase gene fusions to identify *Vibrio cholerae* genes induced during infection. *Mol Microbiol* 1995; **18**: 671-683
- Hollis T, Ichikawa Y, Ellenberger T.** DNA bending and a flip-out mechanism for base excision by the helix-hairpin-helix DNA glycosylase, *Escherichia coli* AlkA. *EMBO J* 2000; **19**: 758-766
- Chiang SL, Mekalanos JJ, Holden DW.** *In vivo* genetic analysis of bacterial virulence. *Annu Rev Microbiol* 1999; **53**: 129-154
- Heithoff DM, Conner CP, Hanna PC, Julio SM, Hentschel U, Mahan MJ.** Bacterial infection as assessed by *in vivo* gene expression. *Proc Natl Acad Sci U S A* 1997; **94**: 934-939
- Wang J, Mushegian A, Lory S, Jin S.** Large-scale isolation of candidate virulence genes of *Pseudomonas aeruginosa* by *in vivo* selection. *Proc Natl Acad Sci U S A* 1996; **93**: 10434-10439
- Wang HL, Feng EL, Lin Y, Liao X, Su GF.** Construction of Δ asd mutant of *Shigella flexneri* 2a strain T32. *Bull Acad Mil Med Sci* 2000; **24**: 81-87
- Murphy KC.** Use of bacteriophage lambda recombination functions to promote gene replacement in *Escherichia coli*. *J Bacteriol* 1998; **180**: 2063-2071
- Yu D, Ellis HM, Lee EC, Jenkins NA, Copeland NG, Court DL.** An efficient recombination system for chromosome engineering in *Escherichia coli*. *Proc Natl Acad Sci U S A* 2000; **97**: 5978-5983
- Hou S, Chen X, Wang H, Tao M, Hu Z.** Efficient method to generate homologous recombinant baculovirus genomes in *E. coli*. *Biotechniques* 2002; **32**: 783-784, 786, 788
- Murphy KC, Campellone KG, Poteete AR.** PCR-mediated gene replacement in *Escherichia coli*. *Gene* 2000; **246**: 321-330
- Loh T, Murphy KC, Marinus MG.** Mutational analysis of the MutH Protein from *Escherichia coli*. *J Biol Chem* 2001; **276**: 12113-12119
- Wang HL, Feng EL, Shi ZX, Yao X, Su GF, Huang LY.** Quick knockout of *Shigella flexneri* *asd* gene with Red system. *Bull Acad Mil Med Sci* 2002; **26**: 172-175
- Furuichi M, Yu CG, Anai M, Sakumi K, Sekiguchi M.** Regulatory elements for expression of the *alkA* gene in response to alkylating agents. *Mol Gen Genet* 1992; **236**: 25-32
- Landini P, Busby SJ.** Expression of the *Escherichia coli* *ada* regulon in stationary phase: evidence for *rpoS*-dependent negative regulation of *alkA* transcription. *J Bacteriol* 1999; **181**: 6836-6839
- Landini P, Busby SJ.** The *Escherichia coli* Ada protein can interact with two distinct determinants in the sigma70 subunit of RNA polymerase according to promoter architecture: identification of the target of Ada activation at the *alkA* promoter. *J Bacteriol* 1999; **181**: 1524-1529
- Saget BM, Walker GC.** The Ada protein acts as both a positive and a negative modulator of *Escherichia coli*'s response to methylating agents. *Proc Natl Acad Sci U S A* 1994; **91**: 9730-9734
- Wyatt MD, Allan JM, Lau AY, Ellenberger TE, Samson LD.** 3-methyladenine DNA glycosylases: structure, function, and biological importance. *BioEssays* 1999; **21**: 668-676
- Heithoff DM, Sinsheimer RL, Low DA, Mahan MJ.** An essential role for DNA adenine methylation in bacterial virulence. *Science* 1999; **284**: 967-970
- Dueger EL, House JK, Heithoff DM, Mahan MJ.** *Salmonella* DNA adenine methylase mutants elicit protective immune responses to homologous and heterologous serovars in chickens. *Infect Immun* 2001; **69**: 7950-7954
- Julio SM, Heithoff DM, Provenzano D, Klose KE, Sinsheimer RL, Low DA, Mahan MJ.** DNA adenine methylase is essential for virulence and plays a role in the pathogenesis of *Yersinia pseudotuberculosis* and *Vibrio cholerae*. *Infect Immun* 2001; **69**: 7610-7615

Differentially expressed proteins of gamma-ray irradiated mouse intestinal epithelial cells by two-dimensional electrophoresis and MALDI-TOF mass spectrometry

Bo Zhang, Yong-Ping Su, Guo-Ping Ai, Xiao-Hong Liu, Feng-Chao Wang, Tian-Min Cheng

Bo Zhang, Yong-Ping Su, Guo-Ping Ai, Xiao-Hong Liu, Feng-Chao Wang, Tian-Min Cheng, Institute of Combined Injury of PLA, Third Military Medical University, Chongqing 400038, China
Supported by the National Natural Science Foundation of China, No.30230360

Correspondence to: Professor Yong-Ping Su, Institute of Combined Injury of PLA, Third Military Medical University, Gaotanyan Street 30, Chongqing 400038, China. mouse@mail.tmmu.com.cn
Telephone: +86-23-68752355 **Fax:** +86-23-68752279
Received: 2003-05-13 **Accepted:** 2003-06-12

Abstract

AIM: To identify the differentially expressed proteins involved in ionizing radiation in mice and to explore new ways for studying radiation-related proteins.

METHODS: Bal B/c mice grouped as sham-irradiation, 3 h and 72 h irradiation were exposed to 9.0Gy single dose of γ -irradiation. Intestinal epithelia were isolated from mice, and total proteins were extracted with urea containing solution. A series of methods were used, including two-dimensional electrophoresis, PDQuest 2-DE software analysis, peptide mass fingerprinting based on matrix-assisted laser desorption/ionization time of flight mass spectrometry (MALDI-TOF-MS) and SWISS-PROT database searching, to separate and identify the differential proteins. Western blotting and RT-PCR were used to validate the differentially expressed proteins.

RESULTS: Mouse intestine was severely damaged by 9.0 Gy γ -irradiation. Image analysis of two-dimensional gels revealed that averages of 638 ± 39 , 566 ± 32 and 591 ± 29 protein spots were detected in 3 groups, respectively, and the majority of these protein spots were matched. About 360 protein spots were matched between normal group and 3 h irradiation group, and the correlation coefficient was 0.78 by correlation analysis of gels. Also 312 protein spots matched between normal group and 72 h irradiation group, and 282 protein spots between 3 h and 72 h irradiation groups. Twenty-eight differential protein spots were isolated from gels, digested with trypsin, and measured with MALDI-TOF-MS. A total of 25 spots yielded good spectra, and 19 spots matched known proteins after database searching. These proteins were mainly involved in anti-oxidation, metabolism, signal transduction, and protein post-translational processes. Western-blotting confirmed that enolase was up-regulated by γ -irradiation. Up-regulation of peroxiredoxin I was verified by applying RT-PCR technique, but no change occurred in Q8VC72.

CONCLUSION: These differentially expressed proteins might play important roles when mouse intestine was severely injured by γ -irradiation. It is suggested that differential proteomic analysis may be a useful tool to study the proteins involved in radiation damage of mouse intestinal epithelia.

Zhang B, Su YP, Ai GP, Liu XH, Wang FC, Cheng TM. Differentially expressed proteins of gamma-ray irradiated mouse intestinal epithelial cells by two-dimensional electrophoresis and MALDI-TOF mass spectrometry. *World J Gastroenterol* 2003; 9(12): 2726-2731

<http://www.wjgnet.com/1007-9327/9/2726.asp>

INTRODUCTION

Since Wilkins and Williams first proposed the concept of "Proteome" in 1994^[1], advances in the studies on proteome have made it possible to compare the total proteins of cells under different conditions on large scale. The proteomic strategy based on two-dimensional electrophoresis (2-DE) and mass spectrometry has been applied in a variety of studies^[2,3].

Ionizing radiation is one of the main treatment modalities used in the management of pelvic cancer. Selective internal radiation therapy is a new method that can be used for patients given other routine therapies but without effects, and preoperative radiotherapy is effective and safe^[4,5]. Although great success has been documented in cancer patients, certain side effects and complications have limited its applications in cancer radiotherapy. One of the major side effects of ionizing radiation is the depletion of normal cells along with cancer cells. For patients with pelvic cancer, a serious complication of radiotherapy is the radiation injury to small intestinal epithelium^[6].

Small intestinal epithelium contains four major cell types: columnar cells, goblet cells, stem cells, and Paneth cells^[7]. Intestinal stem cells, which are most sensitive to ionizing radiation, are located in the crypt portion of the intestine. The impact of ionizing radiation on intestinal stem cells can be detected at a dose as low as 0.05 Gy^[8]. One of the early morphological changes that occur in mouse crypt cells upon treatment with ionizing radiation is the occurrence of apoptosis within 2-3 h after administration of the treatment. This apoptotic death can be visualized under both light and electron microscopy. Because of the emigration of crypt cells from the villi and the decreased proliferation of intestinal stem cells, the crypts become noticeably smaller 14-15 h after radiation^[9]. The villous epithelial cells begin to decline from about the second day post radiation, and the villi become shorter. If a crypt contains viable clonogenic cells, the crypt begins to replenish its cellular population in the next few days.

Ionizing radiation can generate a series of biochemical events inside the cell. Free radicals produced from intercellular water interact with DNA and proteins, thus inducing inactivation of these macromolecules. It has been demonstrated that ionizing radiation can induce gene expression of intestinal epithelia^[10,11]. As genes encode proteins, we can deduce that proteins of intestinal epithelia can be induced by ionizing radiation^[12]. These proteins are associated with many important cellular processes including DNA repair, apoptosis, cell cycle control, and oxidative stress response^[13,14]. With accumulating evidences in the literature that new proteins are implicated in

radiation response, the molecular mechanism underlying radiation response of the small intestine remains unknown. Our aim was to identify these proteins in the early stage of radiation injury. To achieve this purpose, we adopted comparative proteome approach to identify the mouse proteins whose expression was regulated by ionizing radiation. The proteomes of sham-irradiated mice were compared with those of irradiated mice 3 h and 72 h post-irradiation. The differentially displayed proteins were subjected to MALDI-TOF-MS to establish the identity. We also confirmed some differential proteins by Western blot and RT-PCR technique.

MATERIALS AND METHODS

Animal model and irradiation

A total of 15 male Bal b/c mice, 58–62 days of age, weighing 20–24 g, at the time of irradiation, were housed in conventional cages with free access to drinking water and standard chow. A pathogen-free environment with controlled humidity and temperature was maintained. These mice were randomly divided into 3 groups: one group received sham-irradiation ($n=5$), the other two groups received single dose of 9.0 Gy ($n=5$). The dose was chosen based on the data from our previous experiments. Whole-body irradiation was performed with a ^{60}Co -source at a dose rate of 0.78 Gy/min. The irradiated mice were killed 3 h and 72 h post-radiation, and intestines were removed and histological sections were made according to reference^[15].

Isolation of mouse intestinal epithelia

Mouse intestinal epithelial cells were isolated according to the method described by Bjerknes^[16] with slight modifications. In brief, animals were sacrificed, and the small intestine was removed and perfused with 30 ml of cold PBS. Then it was gently everted using a glass rod and flushed by PBS with its two ends enveloped. The swollen intestine was transferred to a flask, and immersed into warm PBSE solution (PBS containing EDTA 1 mmol/L), and shaken at 150 cycles per min. After shaken for 5 min, the intestine was transferred to another clean flask with warm PBSE solution, and vibrated for another 5 min. The shed intestinal epithelial cells were centrifuged at $500\times g$ for 10 min, and prepared for protein extraction.

Protein extraction

The cell pellet harvested as described above was then washed in ice-cold PBS 3 times. Cells were resuspended in cold PBS, and counted. Total proteins were extracted from 10^7 cells with an appropriate volume (200 μl) of lysis buffer containing 7 mol/L urea, 2 mol/L thiourea, 65 mmol/L DTT, 2 % CHAPS, 2 mmol/L PMSF, 0.5 % IPG buffer, and protease inhibitor mixture. The extraction mixture was sonicated using a MSE 100 ultrasonic probe, and then centrifuged at $12\,000\times g$ for 20 min. After transferred to a clean tube, the supernatant was stored at -70°C as aliquots. The protein concentration was determined using Bradford dye-binding assay with bovine serum albumin as the standard.

Two-dimensional electrophoresis

Two-dimensional electrophoresis was carried out by using the Mini-PROTEIN 2-D apparatus (Bio-Rad). For isoelectric focusing (IEF), precast IPG strips (Immobiline DryStrips, Amersham Pharmacia Biotech, Uppsala, Sweden) were used. Samples were applied via rehydration of IPG strips in sample solution for more than 12 h. Before application, the samples were diluted to a total volume of 350 μl with rehydration buffer (8 mol/L urea, 2 % CHAPS, 0.5 % IPG buffer, 0.3 % DTT,

and a trace of bromophenol blue). Protein sample (1 000 μg) was loaded onto an 18 cm IPG strip (pH3–10, linear), and isoelectric focusing was run for 45 KVh at 20°C . To improve the sample entry, low voltage (100V) was applied for 2 h at the beginning. After IEF separation, the IPG strips were immediately equilibrated for 2×15 min with buffer (50 mmol/L Tris-HCl, pH6.8, 6 mol/L urea, 30 % glycerol, 2 % SDS, and a trace of bromophenol blue). DTT (2 %) was added in the first step, and iodoacetamide in the second step. For the second dimensional separation, the concentration of homogeneous SDS-polyacrylamide gels was 13 %. The proteins in the equilibrated strips were run at a current of 30 mA/strip for about 5 h until the bromophenol dye reached the bottom of the gels. Molecular mass marker was run on the same gel to determine the relative molecular masses of the proteins.

Image processing and analysis

After electrophoresis, the resolved proteins in 2-DE gels were fixed in ethanol/acetic acid/water (4/1/5) for at least 1 h, and then visualized by Coomassie blue R-250. The gels were scanned (Gel Doc 2000, Bio-Rad), and the images were processed with PDQuest software (Ver 7.0, Bio-Rad). To determine the variation, three gels were prepared for each sample. The computer analysis allowed automatic detection and quantification of protein spots, as well as matching between control gel and treatment. Protein spots that were new, absent, up- and down-regulated, were simultaneously displayed on the same image using the gels of sham-irradiated sample as the reference.

Protein identification by MALDI-TOF-MS

The differential protein spots were exactly excised from the gels. Gel pieces were destained with 50 % acetonitrile for several times until Coomassie blue was invisible. Then gel pieces were dried in a vacuum centrifuge. The shrinking gel pieces were re-swollen with 5 μl of protease solution (trypsin at 0.05 $\mu\text{g}/\mu\text{l}$ in digestion buffer of 25 mmol/L NH_4HCO_3). Additional 50 μl of digestion buffer was added into the gel piece. Digestion was performed overnight at 37°C . Next, 50 μl of 5 % TFA solution was added to the gel piece, followed by incubation for 60 min at 42°C . The supernatant was collected and concentrated using ZipTip pipette tips (Millipore) according to the manufacturer's instructions. The samples were mixed on the MALDI target with matrix DBA solution. Peptide mass maps were generated by applying Biosystems Voyager 6192 MALDI-TOF-Mass Spectrometry (ABI, USA). Database searching was performed using monoisotopic peptide masses obtained from MALDI-TOF-MS. The SWISS-PROT and TrEMBL database was searched with PeptIdent software (<http://www.expasy.org/tools/pep-tident.html>). Peptide masses were assumed to be monoisotopic masses and cystines were assumed to be iodoacetamidated. The peptide mass tolerance was set to 0.2Da, and the maximum of missed cleavage site was set to 1. Species was set as mouse.

Immunoblotting

Total proteins were separated on 12 % SDS-polyacrylamide gel, and then transferred to nitrocellulose membranes. After blocked for 1 h in the Tris/NaCl (50 mmol/L Tris-HCl, 200 mmol/L NaCl, 0.05 % Tween-20, pH7.4) containing 2 % BSA, membranes were probed with the goat anti-mouse Enolase polyclonal antibody (Santa Cruz, USA). Immunoreactive bands were visualized with a solution containing 1 mg/ml DAB and 0.01 % H_2O_2 .

Semi-quantitative RT-PCR

Total RNAs were isolated from mouse intestinal epithelia with

TriPure isolation reagent (Roche, USA) according to the manufacturer's descriptions. Peroxiredoxin I, Q72VC8, and GAPDH transcripts were determined by reverse transcriptase-polymerase chain reaction (RT-PCR) with RNA PCR kit (Takara, China). The primers for peroxiredoxin I are 5' GTTCTCACGGCTCTTTCTGTTT-3' and 5' CTTCTGGCTGCTCAATGCTG-3', Q8VC72 5' TGGACAAAGCCTTCATAGCA-3' and 5' CCTGGCAGAAACCACAGTAGA-3', GAPDH 5' ACCACAGTCCATGCCATCAC-3' and 5' TCCACCACCTGTTGCTGTA-3'. The amplification was performed with one denaturing cycle at 94 °C for 5 min, then 25-27 cycles at 94 °C for 40 s, at 55 °C for 40 s, at 72 °C for 40 s, and one final extension at 72 °C for 5 min. RT-PCR products were run on 1.2 % agarose gel.

RESULTS

Histological changes of mouse intestine after radiation

Mice after 9.0 Gy irradiation died within 4-6 days post-radiation, with the intestines severely injured. As shown in Figure 1, the histological changes after irradiation were in agreement with our previous experiments. Though the height of villi and crypts remained unchanged 3 h post-radiation, cell division of intestinal epithelia ceased, and the intestines were severely injured morphologically. Moreover, the height of intestinal crypts was obviously increased 72 h post-radiation, with villi decreased. This indicated that many survival epithelial cells proliferated.

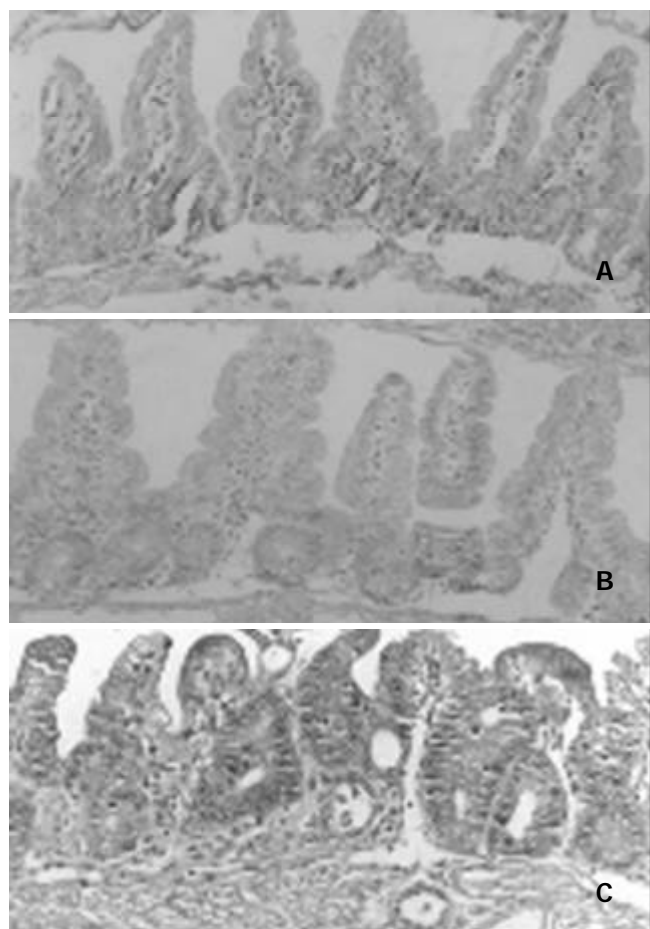


Figure 1 Histological changes in crypts following irradiation. A: Unirradiated controls ($\times 100$). B: 3 hours after a single dose of 9.0 Gy ($\times 100$). Villi and crypts remained unchanged, but cell division of intestinal epithelia ceased. C: 3 days after a single dose of 9.0 Gy ($\times 100$).

Two-dimensional electrophoresis and image analysis of mouse intestinal epithelia

To study the different proteins involved in ionizing radiation, we applied 2-DE to analyze the proteomic alteration of mouse intestinal epithelia. The 2-D patterns were highly reproducible since each experiment was performed in triplicate and produced similar results. Figure 2 showed the representative 2-D maps of the mouse intestinal epithelia. Image analysis of 2-D gels revealed that averages of 638 ± 39 , 566 ± 32 and 591 ± 29 protein spots were detected in 3 groups respectively, and the majority of these protein spots were matched. About 360 protein spots were matched between normal group and 3 h irradiation group, and the correlation coefficient was 0.78 by correlation analysis of gels. Three hundred and twelve protein spots were matched between normal group and 72 h irradiation group, and 282 protein spots between 3 h and 72 h irradiation groups. The unmatched spots represented those induced by irradiation as new or absent proteins, which were the main alteration of proteome.

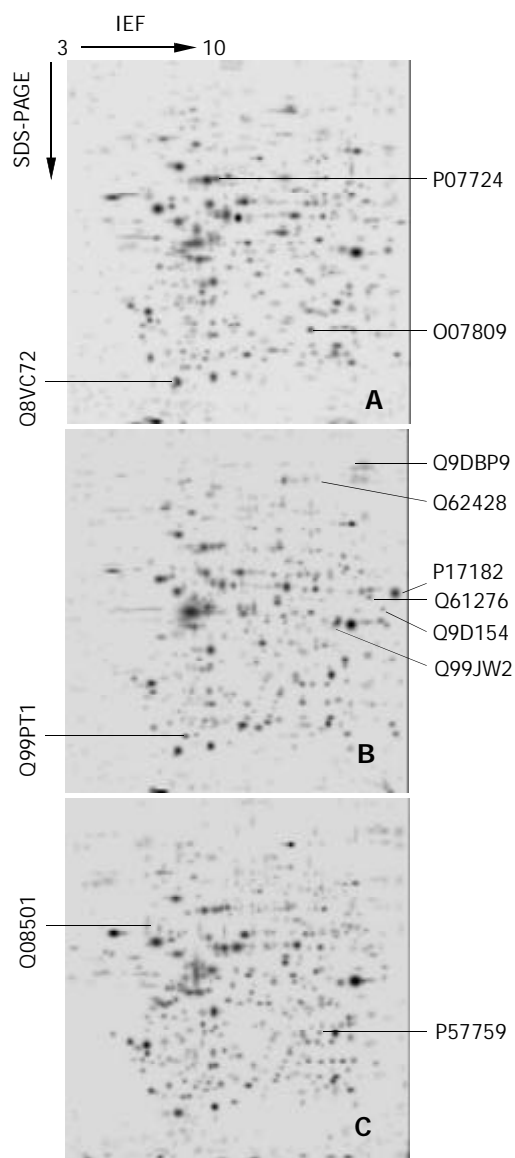


Figure 2 Two-dimensional electrophoresis maps. A: normal intestinal epithelial cells, B: 3 h irradiated epithelial cells, C: 72 h post-radiation. Number indicated proteins were summarized in Table 2.

Identification of proteins from 2-D gel spots

Out of a total of 28 spots excised from the gels, 25 spots yielded

nearly perfect MALDI spectra. A total of 19 spots were preliminarily identified by peptide mass fingerprinting. Figure 3 showed the typical peptide mass fingerprinting of Spot No. 11, whose peptides matched the mouse peroxiredoxin I. This spot was up-regulated by ionizing radiation. The identified proteins were summarized in Table 1. These proteins were involved in cellular process of anti-oxidation, metabolism, and protein post-translational processes. Other proteins, such as

cellular structural proteins and hypothetic proteins derived from nucleic acid sequences, were also altered after irradiation. We also found, 6 spots with good MALDI spectra were returned with inconclusive match results, suggesting that they might be unknown proteins.

Induction of enolase by radiation

A protein spot was preliminarily identified as Enolase by

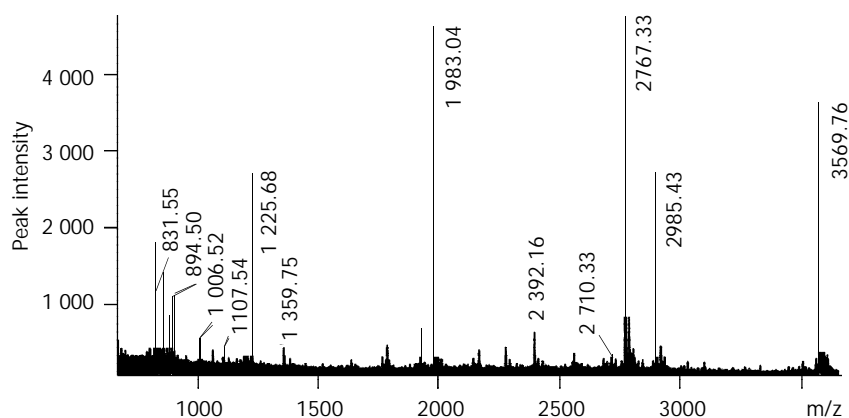


Figure 3 MALDI-TOF-MS spectrum of spot P35700 in 2-DE map. MS spectrum of peptide mixture was obtained from a typical in-gel digestion of the 2-DE separated protein.

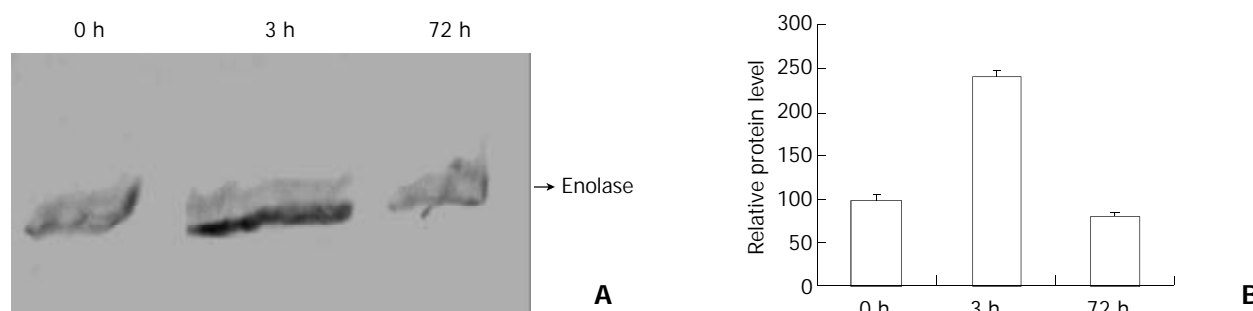


Figure 4 Western blot analysis of Enolase after radiation. A: Protein samples, obtained at indicated time after radiation, were separated by SDS-PAGE, and immunoblotted with corresponding antibody. Equal amounts of total proteins were applied to each lane. B: Relative protein level of Enolase was determined by quantitating the intensity of Enolase bands with a densitometer.

Table 1 Result of Peptident search of differential protein spots derived from BALB/c mice

Spot No.	Swiss-prot accession	Match rate	Theoretical pI/Mw	Sequence covered(%)	Protein name
N1	O08709	7/23	5.70/24871	28	Antioxidant protein 2
N2	P07724	17/39	5.53/65892	37.2	Serum albumin.
N3	Q8VC72	8/13	5.19/18573	58.9	Hypothetical 18.6 kDa protein
R1	Q9D154	8/28	5.85/42574	24.8	Serine protease inhibitor EIA
R2	Q99PT1	6/26	5.12/23391	27.0	Rho GDP-dissociation inhibitor 1
R3	Q61276	6/29	6.0/41693	26.0	A-X actin
R4	Q99JW2	9/31	5.9/45781	25.0	RIKEN cDNA 1110014J22 gene
R5	Q62428	15/27	5.72/92669	29.2	Villin 1
R6	Q9DBP9	12/38	6.2/105834	15.0	homolog to LON protease
R7	P17182	12/52	6.36/47009	36.7	Alpha enolase
R8	Q08501	5/20	5.00/68241	15.0	Prolactin receptor precursor
R9	P57759	5/17	5.74/25721	27.6	ERP29
R10	P19157	9/22	7.70/23609	48.8	Glutathione S-transferase P2
R11	Q9R0V2	6/40	4.86/21927	32.7	Truncated annexin IV.
R12	P35700	13/26	8.3/22177	33.0	Peroxiredoxin I
R13	P09041	5/33	6.6/44912	27.0	Phosphoglycerate kinase, testis specific
R14	P14701	5/15	4.80/19462	25.6	Translationally controlled tumor protein (TCTP)
R15	12847100 ^a	8/14	6.9/28869	33.0	Aldo-keto reductase family 1, member A4
R16	P17182	13/35	6.36/47009	50.4	Alpha enolase

a: This protein was recorded in NCBI database.

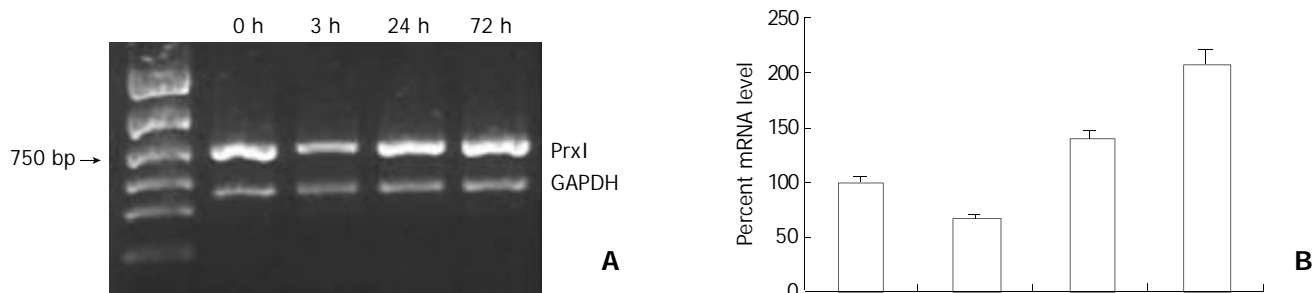


Figure 5 Semi-quantitative RT-PCR analysis of peroxiredoxin I. A: PCR product run on an agarose gel. The upper band represented peroxiredoxin I (750 bp), and the lower band represented GAPDH (450 bp). B: Relative abundance of the mRNA of peroxiredoxin I was normalized by GAPDH.

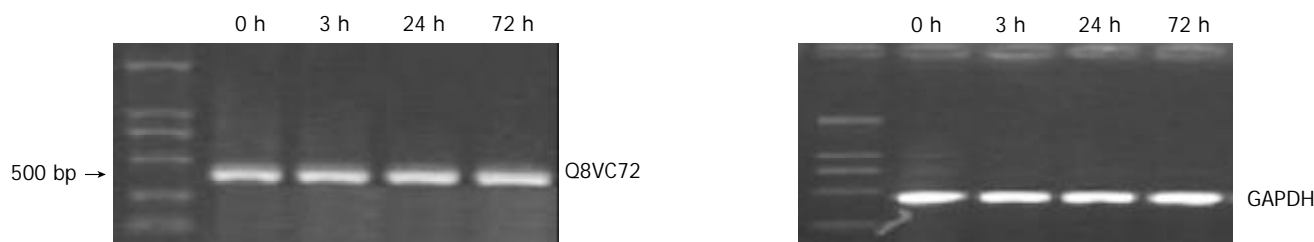


Figure 6 Semi-quantitative RT-PCR analysis of Q8VC72. RNA samples were prepared from mouse intestinal epithelia at indicated time. Left: The band represents Q8VC72 (461 bp). Right: The band represents GAPDH (450 bp). The expression of Q8VC72 remained unchanged after radiation.

MALDI-TOF-MS (Table 1), which was significantly increased in 3 h radiation group. Immunoblotting showed that Enolase was significantly up-regulated (2.1 fold more than the normal control, $P < 0.01$, Figure 4). This confirmed our data of 2-D electrophoresis.

Induction of peroxiredoxin I and Q8VC72 by radiation

Semi-quantitative RT-PCR was used to detect the gene expression of peroxiredoxin I and Q8VC72. Total RNAs were isolated from normal and irradiated mouse intestine. The expression of peroxiredoxin I was markedly induced by radiation (Figure 5), using GAPDH as standard. However, the expression of Q8VC72 remained unchanged after radiation (Figure 6). This indicated that Q8VC72 might be a false-positive result.

DISCUSSION

A variety of techniques, including differential hybridization, differential display PCR, serial analysis of gene expression (SAGE), and gene array, have been used to identify the genes whose expression is selectively altered after radiation^[17-19]. Recently, a new method termed gene trap strategy has also been used to predict radiation responsive genes^[20]. All these methods are used to analyze the mRNA expression levels of radiation responsive genes. As mRNAs are easy to be degraded after transcription, and some are selectively translated, the quality and quantity of proteins do not correlate with that of mRNAs. Here, we applied 2-D electrophoresis to analyze the proteins involved in radiation response at protein level. As a large-scale screening of proteins, proteomics has been driven forward by the advent of the genome era^[21], and it has become advantageous in analyzing total proteins of cells or tissues.

Many proteins have been demonstrated to be involved in radiation response among mammals^[22,23]. These proteins are associated with many important cellular processes such as DNA repair, apoptosis, signal transduction, and oxidative stress. Among the 19 preliminarily identified proteins, three spots belong to oxidative stress response proteins, i.e., peroxiredoxin

I, glutathione S-transferase P2, and antioxidant protein 2. Radiation injuries are manifested as a result of increased production of reactive oxygen species (ROS), such as O_2 , OH , and H_2O_2 . These substances can induce the cellular antioxidant defense enzymes such as superoxide dismutase and glutathione peroxidase. In this study, peroxiredoxin I and glutathione S-transferase P2 were up-regulated by ionizing radiation, while antioxidant protein 2 was down-regulated. These proteins have been demonstrated to be involved in radiation^[24-26]. Peroxiredoxin I is involved in the redox regulation of cells, such as reducing peroxides with reducing equivalents through the thioredoxin system but not from glutaredoxin. The function of glutathione S-transferase P2 has been found in conjugation of reduced glutathione to a large number of exogenous and endogenous hydrophobic electrophiles^[27]. Antioxidant protein 2, also named 1-Cys peroxiredoxin, reduces H_2O_2 and phospholipid hydroperoxides. Our data confirmed the alteration of oxidative stress proteins with the exception of antioxidant protein 2. However, further studies will be performed to determine the mechanism as to why antioxidant protein 2 does not play a critical role in ionizing radiation of small intestinal epithelial cells.

Using the proteomic strategy, we detected an interesting protein of ERP29 involved in ionizing radiation. ERP29 was first cloned from rat enamel cells, which had limited homology with protein disulfide isomerase and its cognate^[28]. In this work, it was upregulated with ionizing radiation *in vivo*. ERP29 played an important role in the process of secretory proteins in the ER. Some researchers found that it played a role as a chaperone in protein folding^[29,30]. The relationship between ERP29 and ionizing radiation has not yet been clarified, so it is worthy of further studying. In addition, some metabolic enzymes and hypothetical proteins, which were derived from nucleic acid sequences, were also found in this differential system. Their roles in ionizing radiation are unclear. Further researches are needed to draw precise conclusions. These data of hypothetical proteins suggest that these hypothetical proteins are expressed in intestinal epithelium indeed.

In brief, we compared the proteomics of mouse intestinal

epithelial cells with its irradiated counterparts *in vivo*. This strategy provides an efficient resolution to analyze radiation related proteins directly at protein level. The preliminarily identified proteins will be further studied in order to determine the cell signaling and molecular mechanisms of gene expression in radiation responses. This proteomic technique may contribute to the elucidation of the molecular mechanism of radiation damage, and can be applied in other research work as a useful tool.

REFERENCES

- Swinbanks D.** Government backs proteome proposal. *Nature* 1995; **378**: 653
- Xiong XD,** Xu LY, Shen ZY, Cai WJ, Luo JM, Han YL, Li EM. Identification of differentially expressed proteins between human esophageal immortalized and carcinomatous cell lines by two-dimensional electrophoresis and MALDI-TOF-mass spectrometry. *World J Gastroenterol* 2002; **8**: 777-781
- Fang DC,** Wang RQ, Yang SM, Yang JM, Liu HF, Peng GY, Xiao TL, Luo YH. Mutation and methylation of hMLH1 in gastric carcinomas with microsatellite instability. *World J Gastroenterol* 2003; **9**: 655-659
- Liu LX,** Zhang WH, Jiang HC. Current treatment for liver metastases from colorectal cancer. *World J Gastroenterol* 2003; **9**: 193-200
- Sun XN,** Yang QC, Hu JB. Pre-operative radiochemotherapy of locally advanced rectal cancer. *World J Gastroenterol* 2003; **9**: 717-720
- Smith DH,** DeCosse JJ. Radiation damage to the small intestine. *World J Surg* 1986; **10**: 189-194
- MacNaughton WK.** Review article: new insights into the pathogenesis of radiation-induced intestinal dysfunction. *Aliment Pharmacol Ther* 2000; **14**: 523-528
- Potten CS,** Owen G, Roberts SA. The temporal and spatial changes in cell proliferation within the irradiated crypts of the murine small intestine. *Int J Radiat Biol* 1990; **57**: 185-199
- Potten CS.** A comprehensive study of the radiobiological response of the murine (BDF1) small intestine. *Int J Radiat Biol* 1990; **58**: 925-973
- Somosy Z,** Horvath G, Telbisz A, Rez G, Palfia Z. Morphological aspects of ionizing radiation response of small intestine. *Micron* 2002; **33**: 167-178
- Hauer-Jensen M,** Richter KK, Wang J, Abe E, Sung CC, Hardin JW. Changes in transforming growth factor beta1 gene expression and immunoreactivity levels during development of chronic radiation enteropathy. *Radiat Res* 1998; **150**: 673-680
- Subramanian V,** Meyer B, Evans GS. The murine Cdx1 gene product localises to the proliferative compartment in the developing and regenerating intestinal epithelium. *Differentiation* 1998; **64**: 11-18
- Picard C,** Wysocki J, Fioramonti J, Griffiths NM. Intestinal and colonic motor alterations associated with irradiation-induced diarrhoea in rats. *Neurogastroenterol Motil* 2001; **13**: 19-26
- Dorr W,** Hendry JH. Consequential late effects in normal tissues. *Radiother Oncol* 2001; **61**: 223-231
- Jensen MH,** Sauer T, Devik F, Nygaard K. Late changes following single dose roentgen irradiation of rat small intestine. *Acta Radiol Oncol* 1983; **22**: 299-303
- Bjerknes M,** Cheng H. Methods for the isolation of intact epithelium from the mouse intestine. *Anat Rec* 1981; **199**: 565-574
- Hartmann KA,** Modlich O, Prisack HB, Gerlach B, Bojar H. Gene expression profiling of advanced head and neck squamous cell carcinomas and two squamous cell carcinoma cell lines under radio/chemotherapy using cDNA arrays. *Radiother Oncol* 2002; **63**: 309-320
- Amundson SA,** Bittner M, Meltzer P, Trent J, Fornace AJ Jr. Induction of gene expression as a monitor of exposure to ionizing radiation. *Radiat Res* 2001; **156**(5 Pt 2): 657-661
- Liu LX,** Jiang HC, Liu ZH, Zhou J, Zhang WH, Zhu AL, Wang XQ, Wu M. Integrin gene expression profiles of human hepatocellular carcinoma. *World J Gastroenterol* 2002; **8**: 631-637
- Vallis KA,** Chen Z, Stanford WL, Yu M, Hill RP, Bernstein A. Identification of radiation-responsive genes *in vitro* using a gene trap strategy predicts for modulation of expression by radiation *in vivo*. *Radiat Res* 2002; **157**: 8-18
- Yanagida M.** Functional proteomics; current achievements. *J Chromatogr B Analyt Technol Biomed Life Sci* 2002; **771**: 89-106
- Potten CS,** Booth C. The role of radiation-induced and spontaneous apoptosis in the homeostasis of the gastrointestinal epithelium: a brief review. *Comp Biochem Physiol B Biochem Mol Biol* 1997; **118**: 473-478
- Johnston MJ,** Robertson GM, Frizelle FA. Management of late complications of pelvic radiation in the rectum and anus: a review. *Dis Colon Rectum* 2003; **46**: 247-259
- Lee K,** Park JS, Kim YJ, Soo Lee YS, Sook Hwang TS, Kim DJ, Park EM, Park YM. Differential expression of Prx I and II in mouse testis and their up-regulation by radiation. *Biochem Biophys Res Commun* 2002; **296**: 337-342
- Mittal A,** Pathania V, Agrawala PK, Prasad J, Singh S, Goel HC. Influence of Podophyllum hexandrum on endogenous antioxidant defence system in mice: possible role in radioprotection. *J Ethnopharmacol* 2001; **76**: 253-262
- Lee YS,** Lee MJ, Lee M, Jang J. Susceptibility to the induction of glutathione S-transferase positive hepatic foci in offspring rats after gamma-ray exposure during gestation. *Oncol Rep* 2000; **7**: 387-390
- Strange RC,** Spiteri MA, Ramachandran S, Fryer AA. Glutathione-S-transferase family of enzymes. *Mutat Res* 2001; **482**: 21-26
- Hubbard MJ,** McHugh NJ, Carne DL. Isolation of ERp29, a novel endoplasmic reticulum protein, from rat enamel cells evidence for a unique role in secretory-protein synthesis. *Eur J Biochem* 2000; **267**: 1945-1957
- Sargsyan E,** Baryshev M, Szekely L, Sharipo A, Mkrtchian S. Identification of ERp29, an endoplasmic reticulum luminal protein, as a new member of the thyroglobulin folding complex. *J Biol Chem* 2002; **277**: 17009-17015
- Kwon OY,** Park S, Lee W, You KH, Kim H, Shong M. TSH regulates a gene expression encoding ERp29, an endoplasmic reticulum stress protein, in the thyrocytes of FRTL-5 cells. *FEBS Lett* 2000; **475**: 27-30

Edited by Ma JY

Heterologous expression of human cytochrome P450 2E1 in HepG2 cell line

Jian Zhuge, Ye Luo, Ying-Nian Yu

Jian Zhuge, Ye Luo, Ying-Nian Yu, Department of Pathophysiology, School of Medicine, Zhejiang University, Hangzhou 310031, Zhejiang Province, China

Supported by National Natural Science Foundation of China, No. 39670801 and Natural Science Foundation of Zhejiang Province, No. 396467

Correspondence to: Professor Ying-Nian Yu, Department of Pathophysiology, School of Medicine, Zhejiang University, Hangzhou 310031, Zhejiang Province, China. ynyu@mail.hz.zj.cn

Telephone: +86-571-87217149 **Fax:** +86-571-87217149

Received: 2003-06-05 **Accepted:** 2003-07-24

Abstract

AIM: Human cytochrome P-450 2E1 (CYP2E1) takes part in the biotransformation of ethanol, acetone, many small-molecule substrates and volatile anesthetics. CYP2E1 is involved in chemical activation of many carcinogens, procarcinogens, and toxicants. To assess the metabolic and toxicological characteristics of CYP2E1, we cloned *CYP2E1* cDNA and established a HepG2 cell line stably expressing recombinant CYP 2E1.

METHODS: Human *CYP2E1* cDNA was amplified with reverse transcription-polymerase chain reaction (RT-PCR) from total RNAs extracted from human liver and cloned into pGEM-T vector. The cDNA segment was identified by DNA sequencing and subcloned into a mammalian expression vector pREP9. A transgenic cell line was established by transfecting the recombinant plasmid of pREP9-CYP2E1 to HepG2 cells. The expression of CYP2E1 mRNA was validated by RT-PCR. The enzyme activity of CYP2E1 catalyzing oxidation of 4-nitrophenol in postmitochondrial supernate (S9) fraction of the cells was determined by spectrophotometry. The metabolic activation of HepG2-CYP2E1 cells was assayed by *N*-nitrosodiethylamine (NDEA) cytotoxicity and micronucleus test.

RESULTS: The cloned *CYP2E1* cDNA segment was identical to that reported by Umeno *et al* (GenBank access No. J02843). HepG2-CYP2E1 cells expressed CYP2E1 mRNA and had 4-nitrophenol hydroxylase activity (0.162 ± 0.025 nmol·min⁻¹·mg⁻¹ S9 protein), which were undetectable in parent HepG2 cells. HepG2-CYP2E1 cells increased the cytotoxicity and micronucleus rate of NDEA in comparison with those of HepG2 cells.

CONCLUSION: The cDNA of human *CYP2E1* can be successfully cloned, and a cell line, HepG2-CYP2E1, which can efficiently express mRNA and has CYP2E1 activity, is established. The cell line is useful for testing the cytotoxicity, mutagenicity and metabolism of xenobiotics, which may possibly be activated or metabolized by CYP2E1.

Zhuge J, Luo Y, Yu YN. Heterologous expression of human cytochrome P450 2E1 in HepG2 cell line. *World J Gastroenterol* 2003; 9(12): 2732-2736

<http://www.wjgnet.com/1007-9327/9/2732.asp>

INTRODUCTION

Cytochrome P450 2E1 (CYP2E1) is the only member of the CYP2E subfamily in humans. Approximately 7 % of the liver CYP content consists of CYP2E1, although individual variation of the level of hepatic CYP2E1 expression can be existed by an order of magnitude. CYP2E1 is also expressed in a number of extrahepatic tissues including the lungs^[1] and brain^[2]. CYP2E1 takes part in the biotransformation of ethanol, acetone, and many small-molecule substrates such as halogenated hydrocarbons (1,1,1-trichloroethane, 1,2-dichloropropane, carbon tetrachloride, chloroform, ethylene dibromide, ethylene dichloride, halothane, methylchloride, methylene dichloride, vinylchloride and trichloroethylene, most of which are hepatotoxic), acetaldehyde, benzene, and styrene. It is known for its ability to metabolize volatile anesthetics such as halothane, enflurane, isoflurane, and sevoflurane, acetaminophen, phenacetin and chlorzoxazone. Another group of CYP2E1 substrates are nitrosamines. CYP2E1 is involved in chemical activation of many carcinogens, procarcinogens, and toxicants^[3-5].

Genetically engineered mammalian cells expressing CYP subtypes have provided new tools for investigations of the metabolism and CYP-mediated metabolic activation of chemicals. The stable expression system of CYP in cells has made it possible to evaluate the relative risk of a chemical in toxicological testing *in vitro*^[6,7]. Human CYP1A1^[8], CYP2B6^[8], CYP2A6^[9], CYP3A4^[10], CYP2C9^[11], CYP2C18^[12] and a phase II metabolism enzyme UDP-glucuronosyltransferase, UGT1A9^[13] have been stably expressed in Chinese hamster lung CHL cells in our laboratory. Among the human hepatic cell lines, HepG2 derived from a human liver tumor has been characterized to retain many xenobiotic-metabolizing activities as compared to fibroblasts. Therefore, HepG2 cell is useful in prediction of the metabolism and cytotoxicity of chemicals in human liver^[14]. But it does not produce significant amounts of CYP^[15,16]. Yoshitomi *et al*^[17] have established in HepG2 cells stable expression of a series of human CYP subtypes, such as CYP1A1, CYP1A2, CYP2A6, CYP2B6, CYP2C8, CYP2C9, CYP2C19, CYP2D6, CYP2E1 and CYP3A4.

In this study, human *CYP2E1* cDNA was amplified by reverse transcription-polymerase chain reaction (RT-PCR), and a transgenic cell line HepG2-CYP2E1 stably expressing CYP2E1 was established to assess the metabolic and toxicological characteristics of CYP2E1.

MATERIALS AND METHODS

Materials

Restriction endonucleases, Moloney murine leukemia virus (M-MuLV) reverse transcriptase were supplied by MBI Fermentas AB, Lithuania. PCR primers, DNA sequence primers, random hexamer primers, and dNTPs were synthesized or supplied by Shanghai Sangon Biotechnology Corp. Expand fidelity PCR system and NADPH were from Roche Molecular Biochemicals. DNA sequencing kit was purchased from Perkin-Elmer Co. The TRIzol reagent, G418, Dulbecco's modified Eagle's medium (DMEM) and newborn

bovine calf sera were from Gibco. Diethyl pyrocarbonate (DEPC), MTT, and *N*-nitrosodiethylamine (NDEA) were purchased from Sigma Chemical Co. T4 DNA ligase and pGEM-T vector system were from Promega. 4-nitrophenol and *p*-nitrocatechol were from Tokyo Kasei Kogyo Co. Ltd, Japan. Other chemical reagents used were of analytical purity from the commercial sources.

Methods

Cloning of human CYP2E1 cDNA from human liver Total RNA was extracted from a surgical specimen of human liver with TRIzol reagent according to the manufacture's instructions. RT-PCR amplifications were described before, using Expand fidelity PCR system^[11]. Two specific 27 mer oligonucleotide PCR primers were designed according to the mRNA sequence of CYP2E1 reported by Song *et al.*^[18] (GenBank access No. J02625). The sense primer corresponding to base position -8 to 19 was 5'-AGGGTACCATGTCTGCCCTCGGAGTGA-3', with a restriction site of *Kpn* I (underlined). The anti-sense primer, corresponding to the base position from 1 507 to 1 534, was 5'-ACAATTGAAAGCTTGTTTGAAGCGG-3', with a restriction site of *Hind* III (underlined). The anticipated PCR product was 1 542 bp in length. PCR was performed at 94 °C for 2 min, then 35 cycles at 94 °C for 60 s, at 62 °C for 60 s, at 72 °C for 2 min, and extension at 72 °C for 10 min. An aliquot (10 µL) from PCR was subjected to electrophoresis in a 1 % agarose gel stained with ethidium bromide.

Construction of recombinant pGEM-CYP2E1 and sequencing of CYP2E1 cDNA The PCR products were ligated with a pGEM-T vector, and transformed to *E. coli* DH5α. CYP2E1 cDNA cloned in pGEM-T was sequenced by Perkin-Elmer-ABI Prism 310 automated DNA sequencer with primers of T7 and SP6 promoters and two specific primers of 2E1 m1 5'-GCATCTCTTGCCCTATCCTT-3' (1 042-1 024), and 2E1 m2 5'-ATGGACCTACCTGGAAGGACAT-3' (353-374).

Construction of pREP9 based expression plasmid for CYP2E1 *Kpn* I/*Hind* III fragment having the total span of human CYP2E1 cDNA and correctly deduced amino acids sequence in pGEM-CYP2E1 were subcloned to a mammalian expression vector pREP9 (Invitrogen). The recombinant was transformed to *E. coli* Top 10, screened by ampicillin resistant, and identified by restriction mapping.

Transfection and selection^[11, 19] HepG2 cells grown in DMEM containing 10 % (V/V) new born calf sera were transfected with the resultant recombinant plasmid, pREP9-CYP2E1, using a modified calcium phosphate method. The culture was split and then selected in the culture medium containing the neomycin analogue G418 (400 mg·L⁻¹). A transgenic cell line named HepG2-CYP2E1 was established.

Detection of CYP2E1 mRNA expression by RT-PCR Total RNA was prepared from G-418-resistant clones by TRIzol reagent. RT-PCR was performed as described before^[11], using two primers 2E1 m1 and 2E1 m2 (200 nmol·L⁻¹), their sequence was described in above, with 20 nmol·L⁻¹ primers of beta-actin as an internal control. The sense and anti-sense primers used for PCR amplification of beta-actin (GenBank access No. NM_001101) were 5'-TCCCTGGAGAAGAGCTACGA-3' (776-795) and 5'-CAAGAAAGGGTGTAACGCAAC-3' (1 217-1 237), respectively. PCR was performed at 94 °C for 2 min, then 35 cycles at 94 °C for 30 s, at 62 °C for 30 s, at 72 °C for 30 s, and extension at 72 °C for 7 min. The anticipated beta-actin PCR product was 462 bp in length and that of CYP2E1 was 690 bp in length. An aliquot (10 µL) from PCR was subjected to electrophoresis in a 1.5 % agarose gel stained with ethidium bromide.

Preparation of postmitochondrial supernate (S9) of HepG2-CYP2E1 The procedure of preparation of S9 fraction was described before^[11]. The protein in S9 was determined by the

Lowry's method, with bovine serum albumin as standard.

4-nitrophenol hydroxylase assays^[20-22] CYP2E1 4-nitrophenol hydroxylase activity of S9 was determined by spectrophotometry, 0.5 mL incubations contained 0.25 mg S9 protein, 0.2 mmol·L⁻¹ 4-nitrophenol in 0.1 mmol·L⁻¹ potassium phosphate buffer (pH 6.8), reactions were initiated with 1 mmol·L⁻¹ NADPH and carried out in air at 37 °C for 60 min. Reactions were terminated by adding 0.25 mL of 0.6 mmol·L⁻¹ perchloric acid and centrifuged at 10 000×g for 5 min to remove protein. The supernatant was mixed with 1/10 volume of 10 mol·L⁻¹ NaOH. The absorbance of clarified supernatants was measured at 510 nm, and the amount of product was quantitated using a standard curve generated by adding known amounts of *p*-nitrocatechol to incubations without NADPH.

Cytotoxicity assay^[23, 24] HepG2 and HepG2-CYP2E1 cells were seeded in 96 well cell culture plates at a density of 1×10⁴ cells each well and incubated overnight. The medium was discarded, and a new medium containing NDEA 0, 1, 10, 100 mmol·L⁻¹ was added to respective wells, with 6 duplications at each concentration. 72 h later, the medium was discarded and 20 µL of 50 g·L⁻¹ MTT in PBS was added to each well. The MTT was discarded 4 h later and 100 µL dimethylsulfoxide was added. After formazan was dissolved, the absorbance was read at 570 nm with 630 nm as reference on the microtiter plate reader. Relative survival was represented as the relative toxicity to the control culture without NDEA. The significance of difference of relative survival between HepG2-CYP2E1 and HepG2 cells was analyzed by Student's *t* test.

Micronucleus test^[25-28] 1×10⁵ HepG2 and HepG2-CYP2E1 cells were seeded in each 100 mL culture bottle and cultured overnight. The medium was discarded and 0, 5, 10, 20 mol·L⁻¹ NDEA in 4 mL serum-free medium was applied to respective bottles and incubated for 4 h. Subsequently the cells were washed twice in PBS and incubated for 20 h with 4 mL completed medium containing 3 mg·L⁻¹ of cytochalasin B. Then the cells were washed twice in PBS and harvested in 2 mL PBS and fixed with 0.4 mL fixed solution (methanol: acetic acid 3:1) for 30 min. The cells were centrifugated, the PBS was discarded and pelleted cells were refixed with 2 mL of fixed solution for 30 min. The cells were centrifugated, refixed and centrifugated again, and then dropped onto slides, dried in the air and stained with 10 % Giemsa solution. The scoring criteria for binucleated cells and micronucleus (MN) were based on a report of Human Micronucleus project^[27]. The frequency of MN formation was expressed as per thousand of binucleated cells with MN. The significance of difference of MN rate between HepG2-CYP2E1 and HepG2 cells was analyzed by checking the tables for determining the statistical significance of mutation frequencies^[28].

RESULTS

Construction of recombinants of pGEM-CYP2E1

The recombinant of pGEM-CYP2E1 was constructed with the human CYP2E1 cDNA inserted into the cloning site of pGEM-T vector. Selection and identification of the recombinant were carried out by *Kpn* I/*Hind* III endonuclease digestion and agarose gel electrophoresis (Figure 1). The cloned cDNA segment was sequenced completely. In comparison with the cDNA sequence reported by Song *et al.* (GenBank access No. J02625), there was only one base difference in cloned cDNA, 105 T→C, while the encoding amino acid was 35G. But there was no sequence difference as compared with that reported by Umeno *et al.*^[29] (GenBank access No. J02843).

Construction of recombinants of pREP9-CYP2E1

The *Kpn* I/*Hind* III fragment (1.54 kb) containing complete CYP2E1 cDNA was subcloned into the *Kpn* I/*Hind* III site

of mammalian expression vector pREP9. Selection and identification of the recombinant were carried out by *Kpn* I/*Hind* III endonuclease digestion and agarose gel electrophoresis (Figure 2). The resulting plasmid was designated as pREP9-CYP2E1 and contained the entire coding region, along with 8 bp of the 5' and 52 bp of the 3' untranslated region of *CYP2E1* cDNA, respectively.

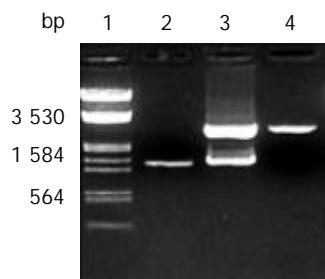


Figure 1 Electrophoretic identification of recombinant of pGEM-CYP2E1. Lane 1: Markers (λ /EcoR I and *Hind* III), 2: PCR products of *CYP2E1* (1.54 kb), 3: Recombinant of pGEM-CYP2E1 digested by *Kpn* I and *Hind* III, 4: pGEM-T vector.

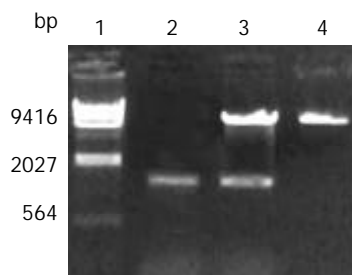


Figure 2 Electrophoretic identification of recombinant of pREP9-CYP2E1. Lane 1: λ DNA/*Hind* III Markers, 2: PCR products of *CYP2E1* (1.54 kb), 3: Recombinant of pREP9-CYP2E1 digested by *Kpn* I and *Hind* III, 4: pREP9 vector.

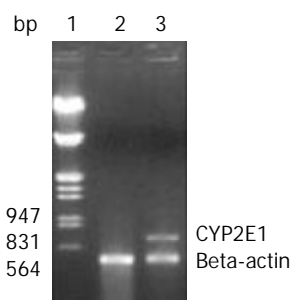


Figure 3 Identification of *CYP2E1* mRNA expression in HepG2-CYP2E1 and HepG2 cells by RT-PCR with beta-actin as internal control. Lane 1: Markers (λ /EcoR I and *Hind* III), 2: RT-PCR products of HepG2 cells showing only beta-actin 462 bp, 3: RT-PCR products of HepG2-CYP2E1 cells showing 462 bp of beta-actin and 690 bp of *CYP2E1*.

Establishment of transgenic cell line with *CYP2E1* mRNA expression and 4-nitrophenol hydroxylase activity

HepG2 cells were transfected with pREP9-CYP2E1, and selected with G418. The surviving clones were propagated and a cell line termed HepG2-CYP2E1 was established. The expression of *CYP2E1* mRNA could be detected in HepG2-CYP2E1 cells but not in HepG2 cells by RT-PCR (Figure 3). The 4-nitrophenol hydroxylase activity in S9 of HepG2-CYP2E1 cells was found 0.162 ± 0.025 nmol \cdot min $^{-1}$ \cdot mg $^{-1}$ S9 protein ($n=3$), but not detectable in parent HepG2 cells.

HepG2-CYP2E1 cells increased cytotoxicity and MN rate by NDEA

Cells were exposed to various concentrations of NDEA. The relative survival rate of HepG2-CYP2E1 cells was lower than that of HepG2 cells in 10 and 100 mmol \cdot L $^{-1}$ NDEA ($P<0.05$ and $P<0.01$, respectively), as shown in Figure 4. The MN rate of HepG2-CYP2E1 was higher than that of HepG2 cells in 10 and 20 mmol \cdot L $^{-1}$ NDEA ($P<0.05$ and $P<0.01$ respectively) as shown in Figure 5.

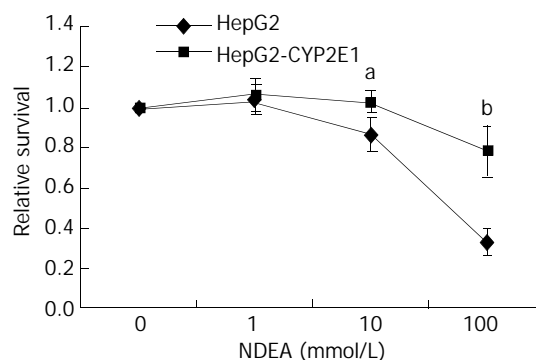


Figure 4 Cytotoxicity of NDEA against HepG2-CYP2E1 and HepG2 cells. Cells were exposed to various concentrations of NDEA. Relative survival rate was represented as the relative toxicity to the control culture without NDEA. The results presented were the average of six duplications ($\bar{x} \pm s$). ^a $P<0.05$, ^b $P<0.01$ vs HepG2 cells.

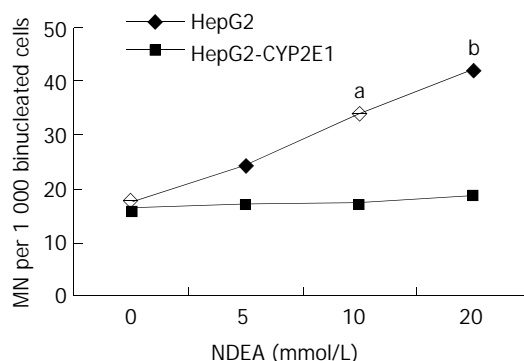


Figure 5 MN rates in HepG2-CYP2E1 and HepG2 cells induced by NDEA. Cells were exposed to various concentrations of NDEA. The data were expressed as per thousand of binucleated cells with MN. ^a $P<0.05$, ^b $P<0.01$ vs HepG2 cells.

DISCUSSION

Human *CYP2E1* gene is located on the chromosome 10q24.3-pter. Up to date, seven *CYP2E1* alleles have been identified (see: *CYP2E1* alleles nomenclature at: <http://www.imm.ki.se/CYPalleles/cyp2e1.htm>). Only 3 alleles have nucleotide substitute, resulting in amino acid change. *CYP2E1**1 is the wild type of human *CYP2E1*. *CYP2E1**2 has a 1 168 G \rightarrow A point mutation in exon 2 causing an R76H amino acid substitution, and *CYP2E1**3 has a 10 059 G \rightarrow A base substitution in exon 8 yielding a V389I amino acid exchange. The corresponding *CYP2E1* cDNAs were expressed in COS-1 cells by Hu *et al*^[30]. The cellular levels of *CYP2E1* mRNA, protein, and the rate of chlorzoxazone hydroxylation were monitored. *CYP2E1**3 cDNA variant was indistinguishable from the wild type cDNA on all variables investigated, whereas *CYP2E1**2 cDNA, although yielding similar amounts of mRNA, only caused 37 % of the protein expression and 36 % of the catalytic activity compared with the wild type cDNA. Complete screening by single-stranded conformation polymorphism of the three

populations revealed that these variant alleles were rare. Human *CYP2E1* gene was functionally well conserved compared with other CYP enzymes active in drug metabolism, which suggested an important endogenous function in humans^[30]. *CYP2E1**4 has a 4 804 G→A point mutation in exon 4, resulting in V179I amino acid exchange. No significant difference in kinetic constants for chlorzoxazone hydroxylation between mutant and wild type was observed by expression of the wild type and mutated full length cDNAs in lymphoblastoid cells^[31]. Our laboratory has once cloned a *CYP2E1* cDNA (GenBank access No. AF182276), which has two point mutations, i.e. 105 T→C, no amino change 35G, and 704G→T, and can result in V235A amino acid exchange. This cDNA was expressed in Chinese hamster lung CHL cells. We could not detect the *N*-nitrosodimethylamine demethylase activity in transgenic cells (data not shown). According to the homology modelling of human CYP2E1 based on the CYP2C5 crystal structure, the substrate recognition site (SRS) 1 was located at codon 100-118, SRS 2 at 200-211, SRS3 at 236-241, SRS4 at 291-305, SRS5 at 361-370, SRS6 at 470-480. The point mutations of *CYP2E1**2, *3, *4 were not located on the SRS. The V235A amino acid exchange in our formerly cloned *CYP2E1* was just at the front of SRS3. This might influence SRS3 and reduce the enzyme activity. Fortunately, this time we cloned a wild type *CYP2E1*.

It has been found that polymorphism of *CYP2E1* gene is significant for inter-individual differences in toxicity of its substrates^[33], and has some effect on the development of gastric cancer^[34] and colorectal cancer^[35].

The expression of *CYP2E1* mRNA in HepG2 cells was validated by RT-PCR. The commonly used *CYP2E1* probe substrates were chlorzoxazone^[36, 37] and 4-nitrophenol^[38]. In this research, we used 4-nitrophenol 2-hydroxylase activity to evaluate the expression of *CYP2E1*, and the 4-nitrophenol hydroxylase activity of HepG2-*CYP2E1* cells was found to be 0.162 ± 0.025 nmol·min⁻¹·mg⁻¹ S9 protein, a little lower than those of HepG2-*CYP2E1* E43 and E47 cells (0.19 and 0.34 nmol·min⁻¹·mg⁻¹ of microsome, respectively)^[39], much lower than that of human liver (1.91 ± 0.28 nmol·min⁻¹·mg⁻¹ of microsome)^[40].

The most frequently used genotoxicity test in mammals is the micronucleus test, which provides a simple and rapid indirect measure of induced structural and numerical chromosome aberrations and is a scientific and regulatory assay accepted by supranational authorities such as the Organization for Economic Cooperation and Development (OECD), International Conference on Harmonization (ICH) and European Union (EU). NDEA could induce early experimental hepatocellular carcinomas^[41] and esophageal neoplasms^[42]. The metabolic activation of NDEA was mediated mainly by CYP2A6 and CYP2E1^[43]. This study has shown that NDEA can decrease the relative survival rate of HepG2-*CYP2E1* cells and increase the MN rate in binucleated cells as compared with HepG2 cells.

cDNA of human *CYP2E1* was successfully cloned and a cell line, HepG2-*CYP2E1*, efficiently expressing mRNA and having the *CYP2E1* enzymatic activities, was established. The cell line is useful for testing the cytotoxicity, mutagenicity and metabolism of xenobiotics and drugs, which may possibly be activated by *CYP2E1*.

REFERENCES

- Hukkanen J, Pelkonen O, Hakkola J, Raunio H. Expression and regulation of xenobiotic-metabolizing cytochrome P450 (CYP) enzymes in human lung. *Crit Rev Toxicol* 2002; **32**: 391-411
- Upadhyay SC, Tirumalai PS, Boyd MR, Mori T, Ravindranath V. Cytochrome P4502E (CYP2E) in brain: constitutive expression, induction by ethanol and localization by fluorescence *in situ* hybridization. *Arch Biochem Biophys* 2000; **373**: 23-34
- Lieber CS. Cytochrome P-4502E1: its physiological and pathological role. *Physiol Rev* 1997; **77**: 517-544
- Tanaka E, Terada M, Misawa S. Cytochrome P450 2E1: its clinical and toxicological role. *J Clin Pharm Ther* 2000; **25**: 165-175
- Anzenbacher P, Anzenbacherova E. Cytochromes P450 and metabolism of xenobiotics. *Cell Mol Life Sci* 2001; **58**: 737-747
- Sawada M, Kamataki T. Genetically engineered cells stably expressing cytochrome P450 and their application to mutagen assays. *Mutat Res* 1998; **411**: 19-43
- Crespi CL, Miller VP. The use of heterologously expressed drug metabolizing enzymes--state of the art and prospects for the future. *Pharmacol Ther* 1999; **84**: 121-131
- Wu J, Dong H, Cai Z, Yu Y. Stable expression of human cytochrome CYP2B6 and CYP1A1 in Chinese hamster CHL cells: their use in micronucleus assays. *Chin Med Sci J* 1997; **12**: 148-155
- Yan LQ, Yu YN, Zhuge J, Xie HY. Cloning of human cytochrome P450 2A6 cDNA and its expression in mammalian cells. *Zhongguo Yaolixue Yu Dulixue Zazhi* 2000; **14**: 31-35
- Chen Q, Wu J, Yu Y. Establishment of transgenic cell line CHL-3A4 and its metabolic activation. *Zhonghua Yufang Yixue Zazhi* 1998; **32**: 281-284
- Zhugue J, Yu YN, Li X, Qian YL. Cloning of cytochrome P-450 2C9 cDNA from human liver and its expression in CHL cells. *World J Gastroenterol* 2002; **8**: 318-322
- Zhugue J, Yu YN, Qian YL, Li X. Establishment of a transgenic cell line stably expressing human cytochrome P450 2C18 and identification of a CYP2C18 clone with exon 5 missing. *World J Gastroenterol* 2002; **8**: 888-892
- Li X, Yu YN, Zhu GJ, Qian YL. Cloning of UGT1A9 cDNA from liver tissues and its expression in CHL cells. *World J Gastroenterol* 2001; **7**: 841-845
- Rueff J, Chiapella C, Chipman JK, Darroudi F, Silva ID, Duverger-van Bogaert M, Fonti E, Glatt HR, Isern P, Laires A, Leonard A, Lagostera M, Mossesso P, Natarajan AT, Palitti F, Rodrigues AS, Schinoppi A, Turchi G, Werle-Schneider G. Development and validation of alternative metabolic systems for mutagenicity testing in short-term assays. *Mutat Res* 1996; **353**: 151-176
- Rodriguez-Antona C, Donato MT, Boobis A, Edwards RJ, Watts PS, Castell JV, Gomez-Lechon MJ. Cytochrome P450 expression in human hepatocytes and hepatoma cell lines: molecular mechanisms that determine lower expression in cultured cells. *Xenobiotica* 2002; **32**: 505-520
- Jover R, Bort R, Gomez-Lechon MJ, Castell JV. Cytochrome P450 regulation by hepatocyte nuclear factor 4 in human hepatocytes: a study using adenovirus-mediated antisense targeting. *Hepatology* 2001; **33**: 668-675
- Yoshitomi S, Ikemoto K, Takahashi J, Miki H, Namba M, Asahi S. Establishment of the transformants expressing human cytochrome P450 subtypes in HepG2, and their applications on drug metabolism and toxicology. *Toxicol In Vitro* 2001; **15**: 245-256
- Song BJ, Gelboin HV, Park SS, Yang CS, Gonzalez FJ. Complementary DNA and protein sequences of ethanol-inducible rat and human cytochrome P-450s. Transcriptional and post-transcriptional regulation of the rat enzyme. *J Biol Chem* 1986; **261**: 16689-16697
- Sambrook J, Fritsch EF, Maniatis T. Molecular Cloning, A Laboratory Manual. 2nd ed. New York: Cold Spring Harbor Laboratory Press 1989: 6.28-6.29
- Lin HL, Roberts ES, Hollenberg PF. Heterologous expression of rat P450 2E1 in a mammalian cell line: in situ metabolism and cytotoxicity of *N*-nitrosodimethylamine. *Carcinogenesis* 1998; **19**: 321-329
- Koop DR. Hydroxylation of *p*-nitrophenol by rabbit ethanol-inducible cytochrome P-450 isozyme 3a. *Mol Pharmacol* 1986; **29**: 399-404
- Tassaneeyakul W, Veronese ME, Birkett DJ, Gonzalez FJ, Miners JO. Validation of 4-nitrophenol as an *in vitro* substrate probe for human liver CYP2E1 using cDNA expression and microsomal kinetic techniques. *Biochem Pharmacol* 1993; **46**: 1975-1981
- Zhugue J, Wang LR, Bi AH, Liu GH. Investigation of the role of Interleukin-2 and soluble Interleukin-2 receptor in the pathogenesis of asthma. *Mianyixue Zazhi* 1994; **10**: 242-244

- 24 **Moskatelo D**, Benjak A, Laketa V, Polanc S, Kosmrlj J, Osmak M. Cytotoxic effects of diazenes on tumor cells *in vitro*. *Chemotherapy* 2002; **48**: 36-41
- 25 **Garriott ML**, Phelps JB, Hoffman WP. A protocol for the *in vitro* micronucleus test. I. Contributions to the development of a protocol suitable for regulatory submissions from an examination of 16 chemicals with different mechanisms of action and different levels of activity. *Mutat Res* 2002; **517**: 123-134
- 26 **Erexson GL**, Periago MV, Spicer CS. Differential sensitivity of Chinese hamster V79 and Chinese hamster ovary (CHO) cells in the *in vitro* micronucleus screening assay. *Mutat Res* 2001; **495**: 75-80
- 27 **Fenech M**, Chang WP, Kirsch-Volders M, Holland N, Bonassi S, Zeiger E. HUMN project: detailed description of the scoring criteria for the cytokinesis-block micronucleus assay using isolated human lymphocyte cultures. *Mutat Res* 2003; **534**: 65-75
- 28 **Kastenbaum MA**, Bowman KO. Tables for determining the statistical significance of mutation frequencies. *Mutat Res* 1970; **9**: 527-549
- 29 **Umeno M**, McBride OW, Yang CS, Gelboin HV, Gonzalez FJ. Human ethanol-inducible P450IIE1: complete gene sequence, promoter characterization, chromosome mapping, and cDNA-directed expression. *Biochemistry* 1988; **27**: 9006-9013
- 30 **Hu Y**, Oscarson M, Johansson I, Yue QY, Dahl ML, Tabone M, Arinco S, Albano E, Ingelman-Sundberg M. Genetic polymorphism of human CYP2E1: characterization of two variant alleles. *Mol Pharmacol* 1997; **51**: 370-376
- 31 **Fairbrother KS**, Grove J, de Waziers I, Steimel DT, Day CP, Crespi CL, Daly AK. Detection and characterization of novel polymorphisms in the CYP2E1 gene. *Pharmacogenetics* 1998; **8**: 543-552
- 32 **Lewis DF**, Lake BG, Bird MG, Loizou GD, Dickins M, Goldfarb PS. Homology modelling of human CYP2E1 based on the CYP2C5 crystal structure: investigation of enzyme-substrate and enzyme-inhibitor interactions. *Toxicol In Vitro* 2003; **17**: 93-105
- 33 **Bolt HM**, Roos PH, Thier R. The cytochrome P-450 isoenzyme CYP2E1 in the biological processing of industrial chemicals: consequences for occupational and environmental medicine. *Int Arch Occup Environ Health* 2003; **76**: 174-185
- 34 **Cai L**, Yu SZ, Zhan ZF. Cytochrome P450 2E1 genetic polymorphism and gastric cancer in Changle, Fujian Province. *World J Gastroenterol* 2001; **7**: 792-795
- 35 **Le Marchand L**, Donlon T, Seifried A, Wilkens LR. Red meat intake, CYP2E1 genetic polymorphisms, and colorectal cancer risk. *Cancer Epidemiol Biomarkers Prev* 2002; **11**(10 Pt 1): 1019-1024
- 36 **Lucas D**, Ferrara R, Gonzalez E, Bodenez P, Albores A, Manno M, Berthou F. Chlorzoxazone, a selective probe for phenotyping CYP2E1 in humans. *Pharmacogenetics* 1999; **9**: 377-388
- 37 **Yuan R**, Madani S, Wei XX, Reynolds K, Huang SM. Evaluation of cytochrome p450 probe substrates commonly used by the pharmaceutical industry to study *in vitro* drug interactions. *Drug Metab Dispos* 2002; **30**: 1311-1319
- 38 **Spatzenegger M**, Liu H, Wang Q, Debarber A, Koop DR, Halpert JR. Analysis of differential substrate selectivities of CYP2B6 and CYP2E1 by site-directed mutagenesis and molecular modeling. *J Pharmacol Exp Ther* 2003; **304**: 477-487
- 39 **Chen Q**, Cederbaum AI. Cytotoxicity and apoptosis produced by cytochrome P450 2E1 in Hep G2 cells. *Mol Pharmacol* 1998; **53**: 638-648
- 40 **Adas F**, Berthou F, Salaun JP, Dreano Y, Amet Y. Interspecies variations in fatty acid hydroxylations involving cytochromes P450 2E1 and 4A. *Toxicol Lett* 1999; **110**: 43-55
- 41 **Wang Z**, Ruan YB, Guan Y, Liu SH. Expression of IGF-II in early experimental hepatocellular carcinomas and its significance in early diagnosis. *World J Gastroenterol* 2003; **9**: 267-270
- 42 **Waddell WJ**. Threshold for carcinogenicity of *N*-nitrosodiethylamine for esophageal tumors in rats. *Food Chem Toxicol* 2003; **41**: 739-741
- 43 **Fujita K**, Kamataki T. Predicting the mutagenicity of tobacco-related *N*-nitrosamines in humans using 11 strains of *Salmonella typhimurium* YG7108, each coexpressing a form of human cytochrome P450 along with NADPH-cytochrome P450 reductase. *Environ Mol Mutagen* 2001; **38**: 339-346

Edited by Zhang JZ and Wang XL

Hepatocellular apoptosis after hepatectomy in obstructive jaundice in rats

De-Sheng Wang, Ke-Feng Dou, Kai-Zong Li, Zhi-Qing Gao, Zhen-Shun Song, Zheng-Cai Liu

De-Sheng Wang, Ke-Feng Dou, Kai-Zong Li, Zhi-Qing Gao, Zhen-Shun Song, Zheng-Cai Liu, Department of Hepatobiliary Surgery, Xijing Hospital, the Fourth Military Medical University, Xi'an 710032, Shannxi Province, China

Supported in part by a Grant-in-aid for Cancer Research and Scientific Research From the Osaka University of Japan

Correspondence to: De-Sheng Wang, MD, Department of Hepatobiliary Surgery, Xijing Hospital, the Fourth Military Medical University, Xi'an 710032, Shannxi Province, China. wangdesh@163.com

Telephone: +86-29-3375259 **Fax:** +86-29-3375255

Received: 2003-05-11 **Accepted:** 2003-06-04

Abstract

AIM: To investigate the hepatocellular apoptosis after hepatectomy in obstructive jaundice and biliary decompression rats.

METHODS: After bile duct ligation for 7 days, rats were randomly divided into OB group in which the rats underwent 70 % hepatectomy, OB-CD group in which the rats underwent hepatectomy accompanied by choledochoduodenostomy, CD-Hx group in which the rats underwent choledochoduodenostomy and then received 70 % hepatectomy on the fifth day after biliary decompression. The control group (Hx group) only underwent hepatectomy.

RESULTS: The level of total serum bilirubin and serum enzymes was significantly lower in CD-Hx group than in OB-CD and OB groups on day 1, 3 and 5 after hepatectomy. The apoptotic index was significantly lower in CD-Hx group than in OB-CD and OB groups on day 3 and 5. The oligonucleosomal DNA fragments and Caspase-3 activity were also lower in CD-Hx group than in OB-CD and OB groups 3 days after hepatectomy, without differences between CD-Hx and Hx groups.

CONCLUSION: Hepatocellular apoptosis plays vital roles in jaundice rats, and biliary decompression is more effective in treatment of patients with severe jaundice before operation.

Wang DS, Dou KF, Li KZ, Gao ZQ, Song ZS, Liu ZC. Hepatocellular apoptosis after hepatectomy in obstructive jaundice in rats. *World J Gastroenterol* 2003; 9(12): 2737-2741
<http://www.wjgnet.com/1007-9327/9/2737.asp>

INTRODUCTION

Obstructive jaundice is often a clinical manifestation of the disease of extrahepatic biliary system or pancreas. In jaundiced patients with hilar bile duct carcinoma or gallbladder carcinoma, hepatectomy is one of the surgical regimens, but surgical procedures are associated with increases of morbidity and mortality rates, mainly due to postoperative complications such as hepatic failure, sepsis, bleeding and renal failure^[1,2]. The significance of biliary drainage before surgery is controversial. Preoperative biliary drainage decreased the mortality and morbidity rates in patients with obstructive

jaundice in some studies but not in others^[3-5]. Experimental and clinical studies have identified several etiological factors including hypotension, impaired nutritional status, depressed immune function, hepatic dysfunction and the presence of toxic bile salts in circulation^[6-8]. A high serum bilirubin concentration in jaundiced patients undergoing operation has been recognized as a predictor of mortality^[3].

Hepatocyte injury and progression of liver disease are due to direct chemical damage to hepatocytes by toxic hydrophobic bile salts^[9]. Although toxic bile salts are known to cause hepatocyte toxicity by inducing apoptosis, the precise mechanisms responsible for bile salt-mediated apoptosis remain to be established. This information is important because it could help provide rational strategies for the treatment of cholestatic liver disorders and decreasing postoperative complications. The aim of this study was to investigate the hepatocellular apoptosis after hepatectomy in obstructive jaundice and biliary decompression rats.

MATERIALS AND METHODS

Animals and experimental design

Male Wistar rats (Shionogi Aburabi Laboratory, Shiga, Japan) weighing 190-240 g were used for this study. Animals were housed in a controlled environment with a 12 h light/dark cycle. Rats had free access to normal rat chow and water before surgery. The care and handling of the animals were made in accordance with the National Institutes of Health Guidelines for the Care and Use of Laboratory Animals. The rats were divided into four groups each containing 6 animals. Hx group in which normal rats underwent 70 % hepatectomy, OB group in which the rats underwent 70 % hepatectomy after bile duct ligation for 7 days, OB-CD group in which the rats underwent 70 % hepatectomy accompanied by choledochoduodenostomy after bile duct ligation for 7 days, CD-Hx group in which the rats underwent choledochoduodenostomy after bile duct ligation for 7 days and then received 70 % hepatectomy on the fifth day after biliary decompression, as described below.

Surgical procedures

All surgical procedures were carried out under ether anesthesia. All rats were weighed before surgery and at the end of the study.

Laparotomy was performed through an upper midline incision. After ligation of the proximal and distal bile ducts, the common bile duct was divided to prevent recanalization^[10]. The ligatures were placed in the same position in all rats. The 70 % hepatectomy was done according to the method of Higgins and Anderson^[11] on the seventh day after biliary obstruction in OB and OB-CD groups and on the fifth days after the biliary decompression in CD-Hx group.

Choledochoduodenostomy was performed according to the method of Ryan *et al* with minor modifications^[12]. After biliary obstruction for 7 days, the abdomen was reopened through the previous incision. The dilated common hepatic bile duct was freed from its surrounding tissues and the contents were aspirated. A small incision was made in the bile duct and a silicone tube with an outer diameter of 0.9 mm was inserted and secured in position with a 7-0 silk suture. The free end of

the tube was inserted into duodenum approximately 1.5 cm from the pylorus, and then tied in position with a 6-0 PDS purse-string suture. Then the suture was carried out between the bile duct and the duodenal wall to protect the separation of the anastomosis.

Measurement of bilirubin and enzymes in blood

Blood samples were collected from the tail vein with a 27-gauge needle. Serum total bilirubin, activities of alkaline phosphatase (ALP) and aspartate aminotransferase (AST) levels were measured enzymatically using a commercial kit (Spotchem Co., Kyoto, Japan).

Quantification of oligonucleosomal (histone-associated) DNA fragments

An aliquot from the liver homogenate was centrifuged at $13\,000\times g$. The supernatant was diluted 1 000-fold and subjected to a sandwich ELISA designed to detect DNA/histone fragments using a test kit from Boehringer Mannheim, according to the manufacturer's instructions. Briefly, a 96-well microtiter plate was coated with antibody against histones. Diluted samples were then applied to the wells for 90 min, followed by incubation with peroxidase-conjugated anti-DNA antibody for 90 min. Color substrate was added and absorbance was measured at 405 nm at 5, 10, and 15 min using a 96-well microtiter plate reader.

In situ TdT-UTP nick-end labeling (TUNEL staining)

On the third and fifth day after hepatectomy, a section of liver tissue measuring approximately 5 mm in thickness was cut from the right lateral lobe and fixed in 10 % buffered formalin, processed by standard techniques and embedded in paraffin. Apoptotic change in the liver was analyzed by *in situ* TUNEL method using an apoptosis detection kit (ApopTag, Oncor S7100, Gaithersburg, MD) according to the manufacturer's instructions. Briefly, after deparaffinization and rehydration, 4 μ m thick tissue sections were incubated in PBS, and then preincubated with equilibration buffer for 15 min, and digoxigenin-labelled dUTP and dATP in TdT buffer were added to cover the section, which was then incubated in a humidified chamber at 37 °C for 60 min. The reaction was stopped by immersing the slides in a stop/wash buffer. Following washing in PBS, the sections were incubated in anti-digoxigenin-peroxidase for 30 min at room temperature. The slides were incubated with DAB and hydrogen peroxide and counterstained with hematoxylin. Apoptotic cells were counted from at least 10 randomly chosen high-power fields at $\times 400$ magnification. Cells with clear brown nuclear labelling were defined as TUNEL-positive. Apoptotic index was defined as the total number of apoptotic cells seen in every ten high-power field sections.

Caspase-3-like protease activity assay

Liver tissues were immediately frozen by liquid nitrogen and stored at -80 °C on the third and fifth days after hepatectomy. The Caspase 3-like activity was measured using a commercially available kit (Clontech Laboratories, Palo Alto, CA) according to the manufacturer's instructions. Caspase enzymatically cleaved the substrate and released free 7-amino-4-trifluoromethyl coumarin (AFC) that produced a blue-green fluorescence, which was measured fluorometrically. Liver samples were homogenized in 500 μ l of lysis buffer. Samples were centrifuged at $16\,000\times g$ in a microfuge for 10 min at 4 °C and normalized to protein using the Bradford assay (Bio-Rad). Fluorescent substrate, DEVD-AFC was incubated with 50 μ l supernatants for liver extracts at 37 °C for 60 min. The fluorescence of cleaved substrates was measured using a

fluorometer (Molecular Dynamics Inc.) at an excitation wavelength of 400 nm and an emission wavelength of 505 nm. An AFC calibration curve was established by serial dilution of a pure AFC solution provided in the kit.

Statistical analysis

All data were expressed as mean \pm SEM. Statistical analysis was done by statistical package of SPSS for Window release 9.0. Differences between mean were tested with the Mann-Whitney test. A probability value less than 0.05 was considered statistically significant.

RESULTS

Bilirubin and enzymes in blood

The level of total serum bilirubin reached more than 7 mg/dl after 7 days' biliary obstruction, and the high bilirubin level rapidly decreased to 0.8 mg/dl only on day 1 after biliary decompression. We therefore thought that our models functioned well for biliary decompression. The total serum bilirubin concentration on the first day after hepatectomy in OB-CD group was 1.6 mg/dl, which was higher than that in CD-Hx group. The level of bilirubin in OB group was increased, while there was no statistically significant differences among other three groups on day 5 after hepatectomy (Figure 1).

The ALP concentration of OB group was significantly higher than that of other groups, but no differences of serum ALP level were found among the other groups after hepatectomy (Figure 2).

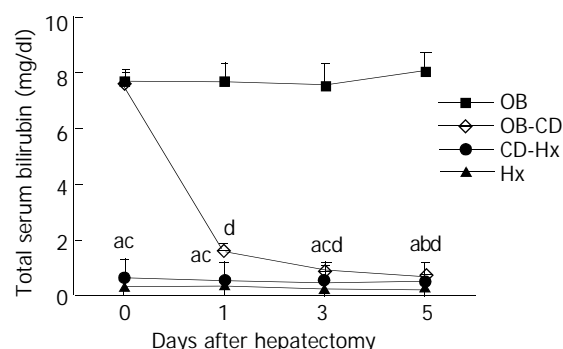


Figure 1 Changes of total serum bilirubin after hepatectomy. Blood was withdrawn from the tail vein while each rat was under ether anesthesia, and serum was obtained by means of centrifugation. Each point represents the mean \pm SEM for six animals. ^a $P < 0.01$ CD-Hx group vs OB group, ^b $P < 0.05$ CD-Hx group vs OB-CD group, ^c $P < 0.01$ CD-Hx group vs OB-CD group, ^d $P < 0.01$ OB-CD group vs OB group.

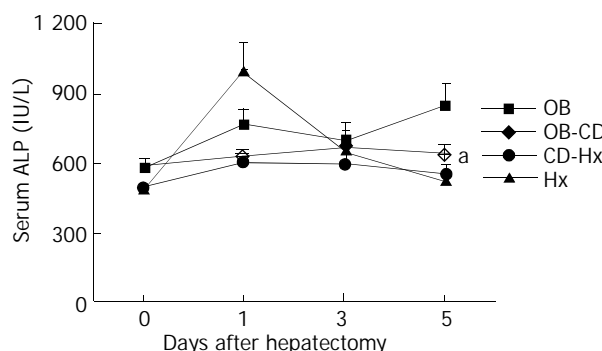


Figure 2 Changes of serum ALP after hepatectomy. Six rats were used for each group. Results were the mean \pm SEM. ^a $P < 0.05$ CD-Hx group vs OB group.

The level of serum AST peaked on the first day after hepatectomy and decreased gradually (Figure 3). There was no difference of AST concentration between CD-Hx and Hx groups on the third and fifth days after hepatectomy. The serum AST concentration in OB group on the fifth day was nearly 6 times that of the concentration in CD-Hx group.

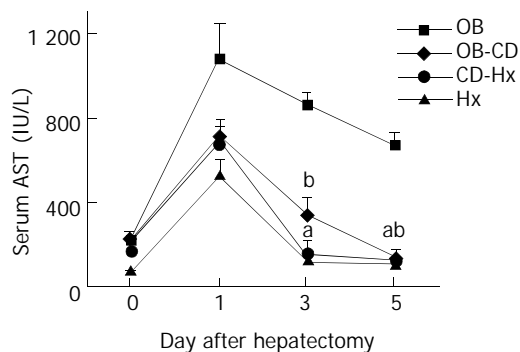


Figure 3 Changes of serum AST after hepatectomy. Six rats were used for each group. Results were the mean \pm SEM. ^a $P < 0.01$ CD-Hx group vs OB group, ^b $P < 0.01$ OB-CD group vs OB group.

Accumulation of oligonucleosomal fragments

The cytoplasmic levels of DNA (histone-associated) oligonucleosomal fragments in hepatocytes after hepatectomy were determined. The presence of these fragments in the cytoplasm reflected the extent of DNA fragmentation and nuclear disruption that are characteristic of apoptosis. The level of DNA fragments in CD-Hx group was significantly lower than that in OB and OB-CD groups on the third day after hepatectomy (Figure 4). There was no significant difference between CD-Hx and OB groups.

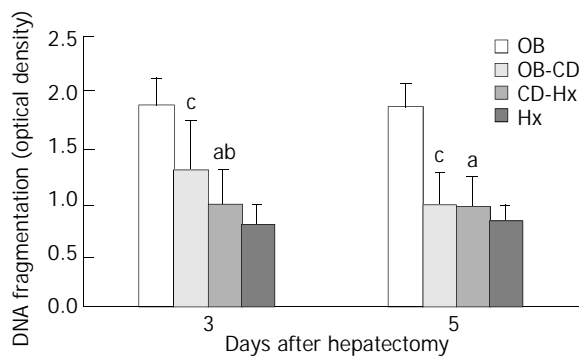


Figure 4 Quantification of oligonucleosomal DNA fragments. The supernatant from the liver homogenate was subjected to a sandwich ELISA designed to detect DNA/histone fragments. Each group consisted of 6 rats. Values were expressed as mean \pm SEM. ^a $P < 0.01$ CD-Hx group vs OB group, ^b $P < 0.05$ CD-Hx group vs OB-CD group, ^c $P < 0.01$ OB-CD group vs OB group.

Hepatocellular apoptosis index

TUNEL signal was defined by distinct nuclear staining. The number of hepatocellular apoptosis was high on day 3 and decreased on day 5 when the liver was harvested on days 3 and 5 from rats after hepatectomy. The data shown in Figure 5 indicate that apoptosis positive cells were significantly higher in OB group than in other groups. A very low rate of apoptosis was found in CD-Hx group, with no difference between CD-Hx and Hx groups.

Caspase-3-like protease activity

Cleavage of peptide substrate DEVD-AFC was used as an indicator of Caspase-3-like protease activity. The level of

Caspase-3 activity in CD-Hx group was significantly lower than that in OB and OB-CD groups on the third day after hepatectomy. But on day 5, the level of Caspase-3 activity in OB-CD group decreased rapidly, without differences between OB-CD and CD-Hx groups (Figure 6).

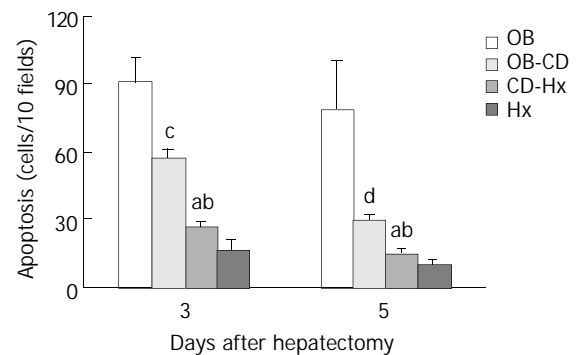


Figure 5 Changes of hepatocellular apoptotic index after hepatectomy. Morphometric analysis of the positive cells in tissue stained by TUNEL method was performed under high power magnification ($\times 400$) in a blinded fashion. Each group consisted of 6 rats. The number of positive cells was counted and expressed as the total number of apoptotic cells seen in every ten high-power fields sections. Values were expressed as mean \pm SEM. ^a $P < 0.01$ CD-Hx group vs OB group, ^b $P < 0.01$ CD-Hx group vs OB-CD group, ^c $P < 0.05$ OB-CD group vs OB group, ^d $P < 0.01$ OB-CD group vs OB group.

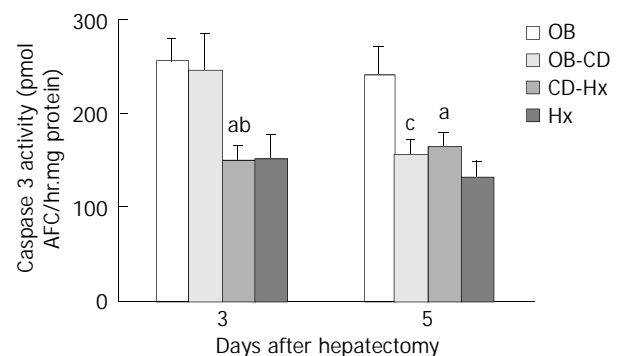


Figure 6 Changes of Caspase-3-like protease activity after hepatectomy. 50 μ M DEVD-AFC was added to whole cell lysates (50 μ g of total protein) for 1 h. The activity of Caspase-3-like protease was measured by determining the cleaved fluorogenic substrates using a spectrofluorometer at 400/505 nm. Each group consisted of 6 rats. Values shown represented mean \pm SEM. ^a $P < 0.05$ CD-Hx group vs OB group, ^b $P < 0.05$ CD-Hx group vs OB-CD group, ^c $P < 0.05$ OB-CD group vs OB group.

DISCUSSION

The perioperative mortality rate in patients with obstructive jaundice was reported to be 8 % to 28 %^[13]. Perioperative complications in patients with obstructive jaundice included infections, endotoxemia, renal failure, stress ulceration, disseminated intravascular coagulation, and wound dehiscence^[14,15]. Numerous reports suggested that in obstructive jaundice there was not only impairment of hepatocellular function but also depression of Kupffer cell activity and ultimately hepatic structural damage, leading to the development of portal hypertension^[16,17]. In addition, it could result in depressed wound healing, significant portal and systemic endotoxaemia, decreased reticuloendothelial cell function, reduced T cell responses, depressed non-specific cell-mediated immunity, decreased bacterial clearance and increased bacterial translocation^[18,19].

This animal model was designed to simulate the clinical treatment procedures used for patients with obstructive jaundice undergoing hepatectomy. Choledochoduodenal drainage was performed before or at the same time as 70 % hepatectomy. Obstruction at the choledochoduodenostomy occurred in about 2 % rats. These rats were excluded from further studies. The mortality rate was about 20 % following choledochoduodenostomy or hepatectomy in jaundice rats. No rats died during the procedure and all deaths occurred in the first 3 days postoperatively, usually secondary to bleeding.

During obstructive jaundice, the retention of biliary constituents and high biliary pressure caused hepatocellular injury^[20]. This is supported by the fact that serum AST and ALP levels increased during obstructive jaundice and decreased after choledochoduodenostomy (data not shown). Kanno^[21] reported that biliary obstruction for even 5 days suppressed rat liver function, as assessed with aminopyrine breath test and galactose tolerance test. These results suggested that obstructive jaundice could cause serious impairment of pivotal liver functions, consequently resulting in poor prognosis after partial hepatectomy. The present study clearly showed that biliary drainage before hepatectomy significantly improved liver functions and decreased hepatocellular apoptosis. Serum liver function tests showed that choledochoduodenal drainage was effective in both OB-CD and CD-Hx groups. Furthermore, serum enzyme levels, apoptotic index, DNA fragments and Caspase-3 activity were significantly lower in CD-Hx group than in other groups. These data suggested that biliary drainage before hepatectomy had beneficial effects in severe jaundice patients.

Accumulation of these toxic bile salts within hepatocytes has been thought to play a key role in liver injury during obstructive jaundice. Indeed, hepatic levels of toxic bile salts chenodeoxycholate and deoxycholate correlated with the degree of liver damage^[22]. Because widespread necrosis was not prominent in most cholestatic liver diseases, it has become apparent that the occurrence of hepatocyte death during cholestasis was rather due to apoptosis than due to necrosis^[23]. The mechanisms of apoptosis by toxic bile salts could be partially elucidated in recent years. Toxic bile salts could directly cause apoptosis in cultured rodent hepatocytes^[24]. Bile acid-induced toxicity is typically characterized by hepatocyte swelling, disruption of plasma membrane integrity, and release of intracellular constituents. The apoptotic pathway in hepatocytes could be initiated by a ligand-independent activation of Fas by bile salt^[25]. Apoptosis was triggered by the Fas pathway, at least in part, by the activation of intracellular enzymes called Caspases. Caspases have been found to be cysteine-containing, aspartic acid-specific proteases which exist as zymogens in the soluble cytoplasm, mitochondrial intermembrane space, and nuclear matrix of virtually all cells^[26]. Upon activation of the apoptotic pathway, initiator Caspases (i.e., Caspases 8 and 9) were converted to their active forms, which in turn activated downstream Caspase 3, which could activate other Caspases and ultimately cleave various substrates^[27]. One of these substrates has been found to be a Caspase-dependent endonuclease that is freed from its inhibitor by Caspase-3 in the cytoplasm, and subsequently enters the nucleus, where it cuts DNA into oligonucleosomal (180 bp) fragments^[28]. Additionally, Bid, a protein responsible for the release of mitochondrial cytochrome C and amplification of the apoptotic cascade, could also be activated by Caspases^[29]. Ultimately, this pathway would ensure the self-destruction of cells with the characteristic morphological features of apoptosis, including nuclear fragmentation, cellular shrinkage, and acidophilic staining of the cytoplasm^[30]. Bile acid induced apoptosis also appeared to require an activation and translocation of protein kinase C, which then could lead to an increase of

intracellular magnesium^[31,32]. This would cause an activation of Mg²⁺-dependent endonucleases, leading to DNA cleavage.

In conclusion, hepatocellular apoptosis plays a vital role in jaundice rats. Biliary drainage is preferable, as evidenced in rats by significantly better liver function and decrease of hepatocellular apoptosis. Biliary decompression is an effective preoperative treatment for patients with severe jaundice.

ACKNOWLEDGEMENTS

We would express our sincere thanks to Prof. Monden and Dr. Umeshita for their technical and financial support.

REFERENCES

- 1 **Su CH**, Tsay SH, Wu CC, Shyr YM, King KL, Lee CH, Lui WY, Liu TJ, P'eng FK. Factors influencing postoperative morbidity, mortality, and survival after resection for hilar cholangiocarcinoma. *Ann Surg* 1996; **223**: 384-394
- 2 **Qin LX**, Tang ZY. Hepatocellular carcinoma with obstructive jaundice: diagnosis, treatment and prognosis. *World J Gastroenterol* 2003; **9**: 385-391
- 3 **Dixon JM**, Armstrong CP, Duffy SW, Davies GC. Factors affecting morbidity and mortality after surgery for obstructive jaundice: a review of 373 patients. *Gut* 1983; **24**: 845-852
- 4 **Cherqui D**, Benoist S, Malassagne B, Humeres R, Rodriguez V, Fagniez PL. Major liver resection for carcinoma in jaundiced patients without preoperative biliary drainage. *Arch Surg* 2000; **135**: 302-308
- 5 **McPherson GA**, Benjamin IS, Hodgson HJ, Bowley NB, Allison DJ, Blumgart LH. Pre-operative percutaneous transhepatic biliary drainage: the results of a controlled trial. *Br J Surg* 1984; **71**: 371-375
- 6 **Greve JW**, Gouma DJ, Soeters PB, Buurman WA. Suppression of cellular immunity in obstructive jaundice is caused by endotoxins: a study with germ-free rats. *Gastroenterology* 1990; **98**: 478-485
- 7 **Ito Y**, Machen NW, Urbaschek R, McCuskey RS. Biliary obstruction exacerbates the hepatic microvascular inflammatory response to endotoxin. *Shock* 2000; **14**: 599-604
- 8 **Yerushalmi B**, Dahl R, Devereaux MW, Gumprich E, Sokol RJ. Bile acid-induced rat hepatocyte apoptosis is inhibited by antioxidants and blockers of the mitochondrial permeability transition. *Hepatology* 2001; **33**: 616-626
- 9 **Rodrigues CM**, Steer CJ. Mitochondrial membrane perturbations in cholestasis. *J Hepatol* 2000; **32**: 135-141
- 10 **Lee E**. The effect of obstructive jaundice on the migration of reticulo-endothelial cells and fibroblasts into early experimental granulomata. *Br J Surg* 1972; **59**: 875-877
- 11 **Fukuhara Y**, Hirasawa A, Li XK, Kawasaki M, Fujino M, Funeshima N, Katsuma S, Shiojima S, Yamada M, Okuyama T, Suzuki S, Tsujimoto G. Gene expression profile in the regenerating rat liver after partial hepatectomy. *J Hepatol* 2003; **38**: 784-792
- 12 **Ryan CJ**, Than T, Blumgart LH. Choledochoduodenostomy in the rat with obstructive jaundice. *J Surg Res* 1977; **23**: 321-331
- 13 **Friedman LS**. The risk of surgery in patients with liver disease. *Hepatology* 1999; **29**: 1617-1623
- 14 **Gong JP**, Wu CX, Liu CA, Li SW, Shi YJ, Li XH, Peng Y. Liver sinusoidal endothelial cell injury by neutrophils in rats with acute obstructive cholangitis. *World J Gastroenterol* 2002; **8**: 342-345
- 15 **Plusa S**, Webster N, Primrose J. Obstructive jaundice causes reduced expression of polymorphonuclear leucocyte adhesion molecules and a depressed response to bacterial wall products *in vitro*. *Gut* 1996; **38**: 784-787
- 16 **Daglar GO**, Kama NA, Atli M, Yuksek YN, Reis E, Doganay M, Dolapci M, Kologlu M. Effect of 5-lipoxygenase inhibition on Kupffer cell clearance capacity in obstructive jaundiced rats. *J Surg Res* 2001; **96**: 158-162
- 17 **Zimmermann H**, Reichen J, Zimmermann A, Sagesser H, Thenisch B, Hoflin F. Reversibility of secondary biliary fibrosis by biliodigestive anastomosis in the rat. *Gastroenterology* 1992; **103**: 579-589
- 18 **Kimings AN**, van Deventer SJ, Obertop H, Rauws EA, Huibregtse K, Gouma DJ. Endotoxin, cytokines, and endotoxin

- binding proteins in obstructive jaundice and after preoperative biliary drainage. *Gut* 2000; **46**: 725-731
- 19 **Megison SM**, Dunn CW, Horton JW, Chao H. Effects of relief of biliary obstruction on mononuclear phagocyte system function and cell mediated immunity. *Br J Surg* 1991; **78**: 568-571
- 20 **Trauner M**, Meier PJ, Boyer JL. Molecular regulation of hepatocellular transport systems in cholestasis. *J Hepatol* 1999; **31**: 165-178
- 21 **Kanno Y**, Miyazaki M, Udagawa I, Koshikawa H, Ito H, Teramoto O, Okui K. Relation of hepatic protein synthesis and hepatic functional mass in obstructive jaundiced rats. *Nippon Geka Gakkai Zasshi* 1991; **92**: 160-166
- 22 **Schmucker DL**, Ohta M, Kanai S, Sato Y, Kitani K. Hepatic injury induced by bile salts: correlation between biochemical and morphological events. *Hepatology* 1990; **12**: 1216-1221
- 23 **Patel T**, Gores GJ. Apoptosis and hepatobiliary disease. *Hepatology* 1995; **21**: 1725-1741
- 24 **Takikawa Y**, Miyoshi H, Rust C, Roberts P, Siegel R, Mandal PK, Millikan RE, Gores GJ. The bile acid-activated phosphatidylinositol 3-kinase pathway inhibits fas apoptosis upstream of bid in rodent hepatocytes. *Gastroenterology* 2001; **120**: 1810-1817
- 25 **Faubion WA**, Guicciardi ME, Miyoshi H, Bronk SF, Roberts PJ, Svingen PA, Kaufmann SH, Gores GJ. Toxic bile salts induce rodent hepatocyte apoptosis via direct activation of Fas. *J Clin Invest* 1999; **103**: 137-145
- 26 **Hatano E**, Bennett BL, Manning AM, Qian T, Lemasters JJ, Brenner DA. NF-kappaB stimulates inducible nitric oxide synthase to protect mouse hepatocytes from TNF-alpha- and Fas-mediated apoptosis. *Gastroenterology* 2001; **120**: 1251-1262
- 27 **Cong B**, Li SJ, Yao YX, Zhu GJ, Ling YL. Effect of cholecystokinin octapeptide on tumor necrosis factor alpha transcription and nuclear factor-kappaB activity induced by lipopolysaccharide in rat pulmonary interstitial macrophages. *World J Gastroenterol* 2002; **8**: 718-723
- 28 **Sakahira H**, Enari M, Nagata S. Cleavage of CAD inhibitor in CAD activation and DNA degradation during apoptosis. *Nature* 1998; **391**: 96-99
- 29 **Luo X**, Budihardjo I, Zou H, Slaughter C, Wang X. Bid, a Bcl2 interacting protein, mediates cytochrome c release from mitochondria in response to activation of cell surface death receptors. *Cell* 1998; **94**: 481-490
- 30 **Hoglen NC**, Hirakawa BP, Fisher CD, Weeks S, Srinivasan A, Wong AM, Valentino KL, Tomaselli KJ, Bai X, Karanewsky DS, Contreras PC. Characterization of the caspase inhibitor IDN-1965 in a model of apoptosis-associated liver injury. *J Pharmacol Exp Ther* 2001; **297**: 811-818
- 31 **Liu XJ**, Yang L, Wu HB, Qiang O, Huang MH, Wang YP. Apoptosis of rat hepatic stellate cells induced by anti-focal adhesion kinase antibody. *World J Gastroenterol* 2002; **8**: 734-738
- 32 **Jones BA**, Rao YP, Stravitz RT, Gores GJ. Bile salt-induced apoptosis of hepatocytes involves activation of protein kinase C. *Am J Physiol* 1997; **272**: G1109-G1115

Edited by Ma JY and Wang XL

Effects of long-term tea polyphenols consumption on hepatic microsomal drug-metabolizing enzymes and liver function in Wistar rats

Tao-Tao Liu, Ning-Sheng Liang, Yan Li, Fan Yang, Yi Lu, Zi-Qing Meng, Li-Sheng Zhang

Tao-Tao Liu, Department of Pharmacy, First Affiliated Hospital, Guangxi Medical University, Nanning 530021, Guangxi Zhuang Autonomous Region, China

Ning-Sheng Liang, Yan Li, Fan Yang, Yi Lu, Zi-Qing Meng, Li-Sheng Zhang, Department of Pharmacology, Guangxi Cancer Institute, Nanning 530021, Guangxi Zhuang Autonomous Region, China

Supported by the National Natural Science Foundation of China, No. 39869001 and Guangxi Natural Science Foundation, No.9912038

Correspondence to: Professor Ning-Sheng Liang, Department of Pharmacology, Guangxi Cancer Institute, Nanning 530021, Guangxi Zhuang Autonomous Region, China. liangn01@163.net

Telephone: +86-771-5310576

Received: 2002-07-26 **Accepted:** 2002-09-25

Abstract

AIM: To investigate the effects of long-term tea polyphenols (TPs) consumption on hepatic microsomal drug-metabolizing enzymes and liver function in rats.

METHODS: TPs were administered intragastrically to rats at the doses of 833 mg·kg⁻¹·d⁻¹ (n=20) and 83.3 mg·kg⁻¹·d⁻¹ (n=20) respectively for six months. Controlled group (n=20) was given same volume of saline solution. Then the contents of cytochrome P450, b₅, enzyme activities of aminopyrine N-demethylase (ADM), glutathione S-transferase (GST) and the biochemical liver function of serum were determined.

RESULTS: The contents of cytochrome P450 and b₅ in the livers of male rats in high dose groups (respectively 2.66±0.55, 10.43±2.78 nmol·mg MS pro⁻¹) were significantly increased compared with the control group (1.08±1.04, 5.51±2.98 nmol·mg MS pro⁻¹; P<0.01, respectively). The enzymatic activities of ADM in the livers of female rats in high dose groups (0.91±0.08 mmol·mg MS pro⁻¹min⁻¹) were increased compared with the control group (0.82±0.08 mmol·mg MS pro⁻¹·min⁻¹; P<0.05). The GST activity was unchanged in all treated groups, and the function of liver was not obviously changed.

CONCLUSION: The antidotal capability of rats' livers can be significantly improved after long-term consumption of TPs. There are differences in changes of drug-metabolizing enzymes between the sexes induced by TPs and normal condition.

Liu TT, Liang NS, Li Y, Yang F, Lu Y, Meng ZQ, Zhang LS. Effects of long-term tea polyphenols consumption on hepatic microsomal drug-metabolizing enzymes and liver function in Wistar rats. *World J Gastroenterol* 2003; 9(12): 2742-2744
<http://www.wjgnet.com/1007-9327/9/2742.asp>

INTRODUCTION

Tea polyphenols (TPs) are a large and diverse class of compounds extracted from tea. These polyphenolic

compounds, specifically catechins epigallocatechin-3-gallate (EGCG), epigallocatechin (EGC), and epicatechin-3-gallate (ECG), account for 30-40 % of the extractable solids in green tea leaves^[1]. Many health benefits are associated with consumption of tea and such effects are mainly attributed to the polyphenolic constituents of tea^[2-8]. We are more concerned about the beneficial effect of TPs on cancer^[9-13].

Primary liver cancer (PLC) is a very prevalent form of cancer in the world. The incidence of PLC in China is high. Guangxi Zhuang Autonomous Region is a high mortality and morbidity region of PLC. Unfortunately, its curative effect is disappointed no matter what therapy is used. How to improve the prevention and treatment of PLC is a long-term goal of our research work. There are some evidences indicating that TPs may play a positive role in PLC prevention and treatment^[14-16]. However, the mechanism of the action is not fully understood. It is known that the risk factors of PLC are intake of AFB₁, pollution of drinking water and HBV infection^[17-20]. The factors are closely related to the activity of hepatic microsomal drug metabolizing enzymes and function of the liver. Because bioactivation of precarcinogens and detoxification of ultimate carcinogens are mainly carried out by drug metabolizing enzymes in the liver, to explore the effects of TPs on these enzymes and the liver function will be helpful to understanding the mechanism of TPs in prevention and treatment of PLC, and the safety of TPs. Further more, this work will provide some useful information for the application of TPs in PLC chemoprevention and chemotherapy.

MATERIALS AND METHODS

Chemicals and reagents

TPs were purchased from Shili Natural Food Co. Ltd (Guilin, China), NADPH from Lizhudongfang Biological Technology Co. (Shanghai, China), aminopyrine from Shanghai Chemical Co., glutathione S-transferase (GST) and protein assay kits from Jiancheng Biological Technology Institute (Nanjing, China), serum biochemical tests of liver function kits from Shenneng Co. (Shanghai, China).

Animals

Five-week-old Wistar rats weighing from 80 to 130 g provided by Experimental Animal Center of Guangxi Medical University were used in the study. The rats were randomly divided into high dose, low dose, and control groups, 20 each group. The animals in high dose and low dose groups were administered intragastrically with TPs at doses of 833 mg·kg⁻¹·d⁻¹ and 83.3 mg·kg⁻¹·d⁻¹ respectively six times each week for six months. Same procedures were also performed in the control rats except feeding equal amount of normal saline (1.0 ml·100 g⁻¹·day⁻¹) instead of TPs. The animals were housed in a temperature-controlled room at 22 °C-24 °C and fed with standard rat chow. At the end of six months experimental period, all the rats were anesthetized with intramuscular injection of sodium pentobarbital (30 mg/kg) before sacrificed. Blood was collected

from the heart and serum obtained through centrifugation to measure liver function. The livers were removed immediately, perfused with cold 0.15M KCl and homogenized in 4 volumes of 0.15M KCl solution containing 10 mM EDTA using a Potter-type Teflon glass homogenizer. The homogenate was centrifuged, 10 000×g for 15 min at 4 °C in a refrigerated centrifuge (OM 3593 IEC Co. Ltd.USA). The supernatant was then centrifuged 105 000×g for 60 min at 4 °C in a preparative ultracentrifuge (20PR-52D; Hitachi, Tokyo). The pellet of microsomes was suspended in the homogenization solution in the homogenizer and centrifuged again as described above. The resulting pellet was suspended in 20 mM potassium phosphate buffer (PH7.4) containing 15 % glycerol until analysis.

Microsomal enzyme assays

The content of cytochrome P450 was determined by the method of Omura and Sato^[21,22]. The content of cytochrome b5 was assayed as described by Omura and Takesue^[23]. The activities of ADM were determined as described by Imai *et al*^[24]. The content of liver microsomal protein and the activities of GST were measured as described in the booklet of kits. All the microsomal enzymes were assayed by using a spectrophotometer (DU-64; Beckman, Fullerton, CA, USA).

Biochemical liver function tests

Biochemical liver function tests (ALT, AST, TP, and ALB) were performed by using an automatic biochemical analyzer (7170A, Hitachi, Tokyo).

Statistical analyses

Data were counted separately in male and female rats and expressed as $\bar{x} \pm s$. Statistical significances were analyzed by *t*-test. The difference was considered significant in case of a two-tailed *P* value less than 0.05, and *P*<0.01 as very significant.

RESULTS

Effects of TPs on contents of P450, b5 and activities of ADM and GST

In high dose group, the contents of P450 and b5 were significantly increased in male rats (respectively 2.66 ± 0.55 , 10.43 ± 2.78 nmol·mg MS pro⁻¹) compared with those in the control group (1.08 ± 1.04 , 5.51 ± 2.98 nmol·mg MS pro⁻¹; *P*<0.01, respectively). The enzymatic activities of ADM in female rats (0.91 ± 0.08 mmol·mg MS pro⁻¹min⁻¹) were higher

than those in the control group (0.82 ± 0.08 mmol·mg MS pro⁻¹·min⁻¹; *P*<0.05). But the activities of GST were unchanged in all treated groups. In control group, the contents of b5 and the activities of ADM in male and female rats were significantly different (5.51 ± 2.98 , 13.42 ± 1.85 nmol·mg MS pro⁻¹; 0.92 ± 0.11 , 0.82 ± 0.08 mmol·mg MS pro⁻¹min⁻¹, respectively, *P*<0.05). The results indicated that there was a difference of hepatic microsomal drug-metabolizing enzymes under normal conditions in different sex rats (Table 1).

Effects of TPs on biochemical liver functions

TPs did not damage rat liver function after used for a long-term, and it indicated that TPs were a quite safe agent, even at a high dose of 833.3 mg·kg⁻¹·d⁻¹, for six months (Table 2).

DISCUSSION

Hepatic drug metabolizing enzyme is called mixed-function oxidase or monooxygenase containing many enzymes including phase I enzymes such as cytochrome P450, cytochrome b5 and NADPH-cytochrome P450 reductase and phase II enzymes such as GST, sulfatase and UDP-glucuronyl transferase^[25]. AFB1, one of the risk factors of PLC, damages DNA after conversion to the reactive compound AFB1-epoxide, by the action of cytochrome P450-dependent enzymes^[26]. Sufficient evidences have shown that tea and TPs possessed anticarcinogenic effects^[27-32]. Some works have been done in the field of TPs modulated or interacted with drug metabolizing enzymes. Maliakal *et al* reported that treating with green tea from different sources could markedly increase cytochrome P450 1A2 activity in rats, and green tea from certain sources could increase cytochrome P450 1A1 and cytosolic GST activities^[33]. However, *in vitro* experiment, Mukhtar *et al* and Wang *et al* reported that TPs had an inhibitory effect on microsomal cytochrome P450 enzyme system^[34,35]. Until now, no one could give a clear explanation of the different results. We tried to make clear what would happen in these enzyme activities in rats treated with TPs. Considering PLC chemopreventive and chemotherapeutic effects could not be achieved in a short term of TPs administration, and a long-term experiment has not been carried out in this aspect, so the rats were treated for 6 months. At the end of treatment, we determined the contents of cytochrome P450 and b5, the activities of ADM and GST, and the liver function in the rats. The results showed that the contents and activities

Table 1 Effects of long-term TPs consumption on microsomal enzymes

	Group	P450 nmol/mg MS pro	b5 nmol/mg MS pro	ADM mmol/mg MS pro/min	GST U/mgpro
♂	High dose (n=10)	2.66 ± 0.55^a	10.43 ± 2.78^a	0.90 ± 0.12	24.66 ± 4.06
	Low dose (n=10)	1.94 ± 0.90	7.82 ± 1.66	0.94 ± 0.11	27.05 ± 4.59
	Control (n=10)	1.08 ± 1.04	5.51 ± 2.98^c	0.92 ± 0.11^c	25.88 ± 4.02
♀	High dose (n=10)	0.66 ± 0.42	11.74 ± 2.31	0.91 ± 0.08^b	29.48 ± 4.16
	Low dose (n=10)	0.66 ± 0.38	11.34 ± 3.17	0.73 ± 0.09	26.44 ± 4.54
	Control (n=10)	0.36 ± 0.18	13.42 ± 1.85	0.82 ± 0.08	29.40 ± 4.19

^a*P*<0.01 vs ♂ control, ^b*P*<0.05 vs ♀ control, ^c*P*<0.05 vs ♀ control.

Table 2 Effects of long-term TPs consumption on major biochemical parameters of rat liver

	Group	ALT U/L	AST U/L	TP g/L	ALB g/L
♂	High dose (n=10)	76.31 ± 32.0	294.69 ± 68.8	75.26 ± 3.44	32.96 ± 1.39
	Low dose (n=10)	74.75 ± 11.62	285.4 ± 54.95	78.75 ± 1.83	32.71 ± 1.34
	Control (n=10)	65.5 ± 9.89	271.5 ± 37.32	80.97 ± 3.43	32.42 ± 1.90
♀	High dose (n=10)	59.15 ± 9.14	247.3 ± 61.03	81.43 ± 3.87	34.64 ± 1.11
	Low dose (n=10)	50.31 ± 22.32	213.15 ± 75.92	78.76 ± 5.31	34.86 ± 2.30
	Control (n=10)	56.92 ± 7.62	236.08 ± 51.94	79.56 ± 2.35	35.63 ± 1.06

ALT: serum alanine transaminase, AST: serum aspartate transaminase, TP: total protein, ALB: albumin.

of drug metabolizing enzymes and the antidotal capability of liver were significantly improved in the high dose group. It shortened the time of carcinogen staying in the body and reduced DNA damages. Therefore, TPs could protect human against the risk of chemically induced PLC and other cancers.

Gender differences in drug metabolism in rats have been known for more than 60 years since it was reported that the much shorter duration of drug action in the male was due to the effects of testicular androgens^[36]. The activities of hepatic drug-metabolizing enzymes, especially cytochrome P450 and sulfotransferase, were regulated through the sex-related secretion pattern of growth hormone^[37]. Some studies reported the sex-related effect on drug -metabolizing enzymes^[38,39]. In our study, a marked sex difference in the effects of long-term treatment with TPs on hepatic drug-metabolizing enzymes in rats was observed. In control groups, there were differences between male and female rats. The results indicated that there was a sex difference in activities of hepatic drug-metabolizing enzymes and ability of liver detoxification in normal rats. Epidemiological studies of PLC showed that there was a sex difference in human (male>female). But it is not known whether this difference is related to the difference of hepatic drug-metabolizing enzymes.

ACKNOWLEDGMENTS

We appreciate the assistance of Drs Ren-Bin Huang, Xiao-Qun Duan and Yang Jiao from Gunagxi Medical University.

REFERENCES

- Brown MD**. Green tea (*Camellia sinensis*) extract and its possible role in the prevention of cancer. *Altern Med Rev* 1999; **4**: 360-370
- Ho CT**, Chen Q, Shi H, Zhang KQ, Rosen RT. Antioxidative effect of polyphenol extract prepared from various Chinese teas. *Prev Med* 1992; **21**: 520-525
- Wang ZY**, Cheng SJ, Zhou ZC, Athar M, Khan WA, Bickers DR, Mukhtar H. Antimutagenic activity of green tea polyphenols. *Mutat Res* 1989; **223**: 273-285
- Mukhtar H**, Wang ZY, Katiyar SK, Agarwal R. Tea components: antimutagenic and anticarcinogenic effects. *Prev Med* 1992; **21**: 351-360
- Zhang G**, Miura Y, Yagasaki K. Suppression of adhesion and invasion of hepatoma cells in culture by tea compounds through antioxidative activity. *Cancer Lett* 2000; **159**: 169-173
- Mcs KS**, Kuttan R. Anti-diabetic activity of green tea polyphenols and their role in reducing oxidative stress in experimental diabetes. *J Ethnopharmacol* 2002; **83**: 109-116
- Nie G**, Cao Y, Zhao B. Protective effects of green tea polyphenols and their major component, (-)-epigallocatechin-3-gallate (EGCG), on 6-hydroxydopamine-induced apoptosis in PC12 cells. *Rebox Ren* 2002; **7**: 171-177
- Shi S**, Zheng S, Jia C, Zhu Y, Xie H. The effect of an antioxidant tea polyphenols on cell apoptosis in rat model of cyclosporine-induced chronic nephrotoxicity. *Zhonghua Waike Zazhi* 2002; **40**: 709-712
- Yang CS**, Wang ZY. Tea and cancer. *J Natl Cancer Inst* 1993; **85**: 1038-1049
- Bushman JL**. Green tea and cancer in humans: a review of the literature. *Nutr Cancer* 1998; **31**: 151-159
- Gong Y**, Han C, Chen J. Effect of tea polyphenols and tea pigments on the inhibition of precancerous liver lesions in rats. *Nutr Cancer* 2000; **38**: 81-86
- Hammons GJ**, Fletcher JV, Stepps KR, Smith EA, Balentine DA, Harbowy ME, Kadlubar FF. Effects of chemoprotective agents on the metabolic activation of the carcinogenic arylamines PhIP and 4-aminobiphenyl in human and rat liver microsomes. *Nutr Cancer* 1999; **33**: 46-52
- Jung YD**, Ellis LM. Inhibition of tumour invasion and angiogenesis by epigallocatechin gallate (EGCG), a major component of green tea. *Int J Exp Pathol* 2001; **82**: 309-316
- Lambert JD**, Yang CS. Cancer chemopreventive activity and bioavailability of tea and tea polyphenols. *Mutat Res* 2003; **523-524**: 201-208
- Hsu S**, Lewis J, Singh B, Schoenlein P, Osaki T, Athar M, Porter AG, Schuster G. Green tea polyphenol targets the mitochondria in tumor cells inducing caspase 3-dependent apoptosis. *Anticancer Res* 2003; **23**: 1533-1539
- Roy M**, Siddiqi M, Bhattacharya RK. Cancer chemoprevention: tea polyphenol induced cellular and molecular responses. *Asian Pac J Cancer Prev* 2001; **2**: 109-116
- Wogan GN**. Aflatoxins as risk factors for hepatocellular carcinoma in humans. *Cancer Res* 1992; **52**(7 Suppl): 2114s-2118s
- Lu P**, Kuang S, Wang J. Hepatitis B virus infection and aflatoxin exposure in the development of primary liver cancer. *Zhonghua Yixue Zazhi* 1998; **78**: 340-342
- Yen FS**, Shen KN. Epidemiology and early diagnosis of primary liver cancer in China. *Adv Cancer Res* 1986; **47**: 297-329
- Yu SZ**. Primary prevention of hepatocellular carcinoma. *J Gastroenterol Hepatol* 1995; **10**: 674-682
- Heffernan LM**, Winston GW. Distribution of microsomal CO-binding chromophores and EROD activity in sea anemone tissues. *Mar Environ Res* 2000; **50**: 23-27
- Bhamre S**, Anandatheerthavarada HK, Shankar SK, Ravindranath V. Microsomal cytochrome P450 in human brain regions. *Biochem Pharmacol* 1992; **44**: 1223-1225
- Omura T**, Takesue S. A new method for simultaneous purification of cytochrome b5 and NADPH-cytochrome c reductase from rat liver microsomes. *J Biochem* 1970; **67**: 249-257
- Imai Y**, Ito A, Sato R. Evidence for biochemically different types of vesicles in the hepatic microsomal fraction. *J Biochem* 1966; **60**: 417-428
- Sheweita SA**. Drug-metabolizing enzymes: mechanisms and functions. *Curr Drug Metab* 2000; **1**: 107-132
- De Oliveira CA**, Germano PM. Aflatoxins: current concepts on mechanisms of toxicity and their involvement in the etiology of hepatocellular carcinoma. *Rev Saude Publica* 1997; **31**: 417-424
- Ferguson LR**. Role of plant polyphenols in genomic stability. *Mutat Res* 2001; **475**: 89-111
- Suganuma M**, Okabe S, Kai Y, Sueoka N, Sueoka E, Fujiki H. Synergistic effects of (-)-epigallocatechin gallate with (-)-epicatechin, sulindac, or tamoxifen on cancer-preventive activity in the human lung cancer cell line PC-9. *Cancer Res* 1999; **59**: 44-47
- Isemura M**, Saeki K, Kimura T, Hayakawa S, Minami T, Sazuka M. Tea catechins and related polyphenols as anti-cancer agents. *Biofactors* 2000; **13**: 81-85
- Qi L**, Han C. Induction of NAD(P)H: quinone reductase by anticarcinogenic ingredients of tea. *Weisheng Yanjiu* 1998; **27**: 323-326
- Wei D**, Mei Y, Liu J. Quantification of doxorubicin and validation of reversal effect of tea polyphenols on multidrug resistance in human carcinoma cells. *Biotechnol Lett* 2003; **25**: 291-294
- Mei Y**, Wei D, Liu J. Reversal of cancer multidrug resistance by tea polyphenol in KB cells. *J Chemother* 2003; **15**: 260-265
- Maliakal PP**, Coville PF, Wanwimolruk S. Tea consumption modulates hepatic drug metabolizing enzymes in Wistar rats. *J Pharm Pharmacol* 2001; **53**: 569-577
- Mukhtar H**, Wang ZY, Katiyar SK, Agarwal R. Tea components: antimutagenic and anticarcinogenic effects. *Prev Med* 1992; **21**: 351-360
- Wang ZY**, Das M, Bickers DR, Mukhtar H. Interaction of epicatechins derived from green tea with rat hepatic cytochrome P-450. *Drug Metab Dispos* 1988; **16**: 98-103
- Shapiro BH**, Agrawal AK, Pampori NA. Gender differences in drug metabolism regulated by growth hormone. *Int J Biochem Cell Biol* 1995; **27**: 9-20
- Kato R**. Molecular pharmacological and toxicological studies of drug-metabolizing enzymes. *Yakugaku Zasshi* 1995; **115**: 661-680
- Finnen MJ**, Hassall KA. Effects of hypophysectomy on sex differences in the induction and depression of hepatic drug-metabolizing enzymes in the rat. *J Pharmacol Exp Ther* 1984; **229**: 250-254
- Kobayashi Y**, Ohshiro N, Suzuki M, Sasaki T, Tokuyama S, Yoshida T, Yamamoto T. Sex-related effect of hemin on cytochrome P450 and drug-metabolizing enzymes in rat liver. *J Toxicol Sci* 2000; **25**: 213-222

Oil A induces apoptosis of pancreatic cancer cells via caspase activation, redistribution of cell cycle and GADD expression

Mi-Lian Dong, Yue-Chun Zhu, John V. Hopkins

Mi-Lian Dong, Affiliated Taizhou Hospital, Wenzhou Medical College, Linhai 317000, Zhejiang, Province China

Yue-Chun Zhu, John V. Hopkins, Northwestern University Medical School, Chicago, IL60611-3008, U.S.A

Supported by the National Cancer Institute of USA, No. CA72712, and Special Funds for Zhejiang 151 Talent Project of China, No. 98-2095

Correspondence to: Dr Mi-Lian Dong, Taizhou Hospital of Wenzhou Medical College, 150 Ximen Street, Linhai 317000, Zhejiang, Province China. mdong2@hotmail.com

Telephone: +86-576-5315829 **Fax:** +86-576-5315829

Received: 2003-08-23 **Accepted:** 2003-09-10

Abstract

AIM: To explore the mechanisms of effects of oil A on apoptosis of human pancreatic cancer cells.

METHODS: Cellular DNA content was analyzed by flow cytometry. Western blotting was used for caspase-3 and PARP, caspase-7, caspase-9, cytochrome c, Bcl-2, Bax, Mcl-1, cyclinA, cyclin B1, cyclin D1, cyclin E, CDK2, CDK4, CDK6, P21, P27, GADD45, GADD153.

RESULTS: The caspase-3, caspase-7, and caspase-9 activities were significantly increased as well as the cleavage of caspase-3, downstream substrate poly-ADP ribose polymerase (PARP) was induced. The amount of cytochrome c in the cytosolic fraction was increased, while the amount of cytochrome c in the mitochondrial fraction was decreased after oil A treatment. The anti-apoptosis proteins Bcl-2 and Mcl-1 were decreased in parallel and Bax increased, indicating that Bcl-2 family proteins-mitochondria-caspase cascade was responsible for oil-induced apoptosis. The proportion of cells in the G0/G1 decreased in MiaPaCa-2 and AsPC-1 cells after the treatment of oil A for 24 hours. The number of cells in S phase was increased in two cancer cell lines at 24 hours. Therefore, cells were significantly accumulated in G2/M phase. The cells with a sub-G0/G1 DNA content, a hallmark of apoptosis, were seen at 24 hours both in MiaPaCa-2 and AsPC-1 cells following exposure to oil A. The expression of cyclin A and cyclin B1 was slightly decreased and cyclin D1 levels were markedly lowered in MiaPaCa-2 cells. The expression of cyclin A and cyclin B1 was markedly decreased and cyclin D1 levels were slightly lowered in AsPC-1 cells, while cyclin E was not affected and the levels of CDK2, CDK4, and CDK6 were unchanged in MiaPaCa-2 and AsPC-1 cells. In response to oil A, P21 expression was increased, but P27 expression was not affected. The expression of both GADD45 and GADD153 was increased in two cell lines following oil A treatment.

CONCLUSION: Oil A induces apoptosis of pancreatic cancer cells via activating caspase cascade, modifying cell cycle progress and changing cell cycle-regulating proteins and GADD expression.

Dong ML, Zhu YC, Hopkins JV. Oil A induces apoptosis of pancreatic cancer cells via caspase activation, redistribution of

cell cycle and GADD expression. *World J Gastroenterol* 2003; 9 (12): 2745-2750

<http://www.wjgnet.com/1007-9327/9/2745.asp>

INTRODUCTION

It is reported that oil A appears to exert anti-cancer effect by activating apoptosis. It should be speculated that oil A may be broadly active against pancreatic cancer cells. However, whether the use of oil A can be extended to pancreatic tumors is still uncertain. The alternative mechanisms of oil A effect need to be further studied. Our previous experiments showed the inhibition of proliferation and the induction of apoptotic effect by treatment of oil A in pancreatic cancer cells^[1]. However, to date, no further information is available regarding the mechanism of effects of oil A on pancreatic cancer cells. In the present study, the mechanism of oil A effect on induction of apoptosis was investigated through activating caspase cascade, inducing cytochrome c release from the mitochondria, Bax, Bcl-2, and Mcl-1 expression, the distribution of cell cycle, changes of cycle-regulating proteins, P21 and P27 expression, and GADD expression in pancreatic cancer cells.

MATERIALS AND METHODS

Reagents

The human pancreatic cancer cell lines, MiaPaCa-2 and AsPC-1 were purchased from the American Type Culture Collection (Rockville, MD, USA). Oil A (Coastside Research Chemical Co., USA) was dissolved in 1:2 DMEM as a stock solution. The stock solution was diluted to appropriate concentrations in serum-free medium prior to experiments. Mitochondria/Cytosol Fractionation Kit was purchased from BioVision (Mountain View, CA, USA). Enhanced chemiluminescence system (ECL) was obtained from Santa Cruz Biotechnology, Inc. (Santa Cruz, CA, USA). Mouse monoclonal antibodies against PARP, Bcl-2, Bax, Mcl-1, cyclin B1, cyclin D1, cyclin E, CDK2, CDK4, CDK6, P21, P27, GADD45, GADD153 and rabbit polyclonal antibodies against caspase-3, caspase-7, caspase-9, cytochrome c and cyclin A were purchased from Santa Cruz Biotechnology, Inc. (Santa Cruz, CA, USA). All other chemicals were purchased from Sigma (St Louis, MO, USA).

Cell culture

Cells were cultured in DMEM medium supplemented with penicillin G (100 U/mL), streptomycin (100 U/mL) and 10 % FBS at 37 °C in humidified air with 5 % CO₂. The cells were harvested by incubation in trypsin-EDTA solution for 10-15 minutes. Then cells were centrifuged at 300×g for 5 minutes and cell pellets suspended in fresh culture medium prior to seeding into culture flasks or plates^[1].

Analysis of cellular DNA content by flow cytometry

The cells were grown to 50-60 % confluence in T75 flasks, serum-starved for 24 hours and then treated with or without 1:32 000 oil A for 24 hours. At the end of treatment, the cells were harvested with trypsin-EDTA solution to produce a single

cell suspension. The cells were then pelleted by centrifugation and washed twice with PBS. Cell pellets were then suspended in 0.5 ml PBS and fixed in 5 mL ice-cold 70 % ethanol at 4 °C. The fixed cells were centrifuged at 300×g for 10 minutes and the pellets were washed with PBS. After resuspension with 1 ml PBS, the cells were incubated with 10 µL of RNase I (10 g/L) and 100 µL of propidium iodide (400 mg/L; Sigma) and shaken for 1 hour at 37 °C in the dark. Samples were analyzed by flow cytometry. The red fluorescence of the single events was recorded using a laser beam at 488 nm excitation λ with 610 nm as emission λ to measure the DNA index.

Preparation of cytosolic and mitochondrial extract

Collect cells (5×10^7) were centrifuged at 600×g for 5 minutes at 4 °C from control and oil A-treated MiaPaCa-2 and AsPC-1 cells. Wash cells with ice-cold PBS twice, and centrifuge at 600×g for 5 minutes at 4 °C. Remove supernatant. Resuspend cells with 1.0 mL of 1×cytosol extraction buffer mix containing DTT and protease inhibitors. Incubate on ice for 10 minutes. Homogenize cells in an ice-cold dounce tissue grinder (45 strokes) until 70-80 % of the nuclei did not have the shiny ring. Transfer homogenate to a 1.5 mL microcentrifuge tube, and centrifuge at 700×g for 10 minutes at 4 °C. Transfer the supernatant to a fresh 1.5 mL tube, and centrifuge at 10 000×g for 30 minutes at 4 °C. Collect the supernatant as cytosol fraction. Resuspend the pellet in 0.1 mL mitochondrial extraction buffer mix containing DTT and protease inhibitors, vortex for 10 seconds and save as mitochondrial fraction. Both cytosolic fraction and mitochondrial fraction were stored at -80 °C until ready for Western blotting.

Preparation of proteins

Cells were seeded into flasks and grown to 50-60 % confluence, then seeded in serum-free medium for 24 hours. Cells were then placed in serum-free medium with or without 1:32 000 oil A for a period of 24 hours. In the end, proteins were extracted from attached and floating cells in lysis buffer [20 mM Tris-HCl (pH 7.4), 2 mM sodium vanadate, 1.0 mM sodium fluoride, 100 mM NaCl, 2.0 mM phosphate substrate, 1 % NP40, 0.5 % sodium deoxycholate, 20 mg/L each aprotinin and leupeptin, 25 mg/L pepstatin, and 2.0 mM each EDTA and EGTA] for further analysis. Protein concentrations were determined using the bicinchoninic acid assay with BSA as standard.

Western blotting

Western blotting was carried out using standard techniques. In brief, equal amounts of proteins in the cell lysates were separated on SDS-PAGE and the proteins then transferred onto nitrocellulose membranes. After blocking non-specific sites with fat free dried milk, membranes were incubated with the appropriate dilution of primary antibody. Then, membranes were incubated with a horseradish peroxidase conjugated secondary antibody. Proteins were detected using an enhanced chemiluminescence detection system, and light emission was captured on Kodak X-ray films.

RESULTS

Effect of oil A on activation of caspase 3 and cleavage of PARP, caspase 7 and caspase 9

The expression and activation of caspase 3 by cleavage as well as the specific cleavage of its downstream substrate, PARP during apoptosis were observed by Western blotting. The 32 kDa procaspase 3 was cleaved into products of lower molecular weight, including a band corresponding to the 17 kDa active form. The uncleaved 116 kDa pro-form of PARP was only seen in untreated controls while in oil A treatment resulted in

appearance of the active 85 kDa cleaved fragments. Caspase 7 and 9 degradation activation were also induced, and coincident with the induction of apoptosis (Figure 1).

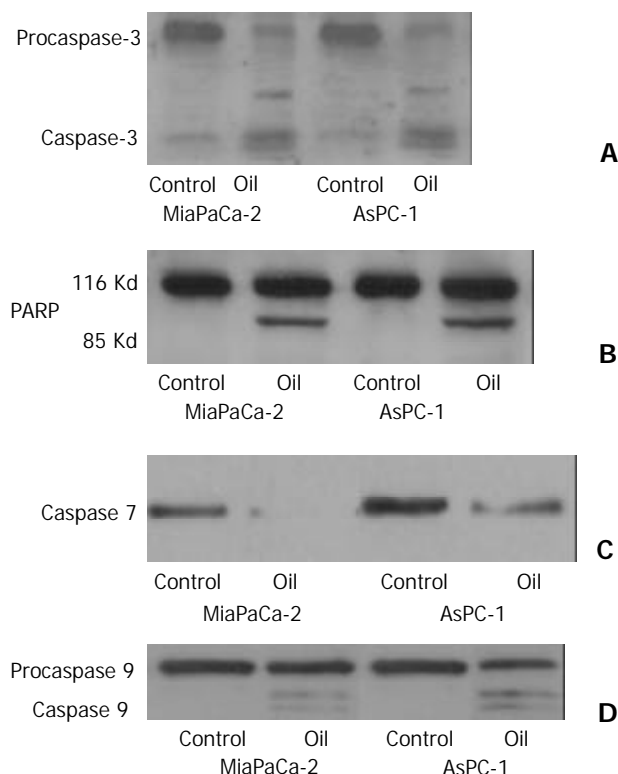


Figure 1 (A, B, C, D) Western blotting of the caspase-3, poly-ADP ribose polymerase (PARP), caspase 7 and caspase 9 in MiaPaCa-2 and AsPC-1 cells treated with 1:32 000 oil A for 24 hours. Proteins in whole cellular lysates were electrophoresed in SDS-PAGE gels and transferred to nitrocellulose membranes. Caspase-3, PARP, caspase 7 and caspase 9 were identified using specific antibodies.

Oil A induces cytochrome c release

Cytochrome c is a mitochondrial protein released from the mitochondria to cytosol during apoptosis when mitochondrial membrane permeability is disrupted. An increase in the amount of cytochrome c in the cytosolic fraction was seen in both cell lines after oil A treatment. Meanwhile, the amount of cytochrome c in the mitochondrial fraction was decreased also in both cell lines after oil A treatment (Figure 2).

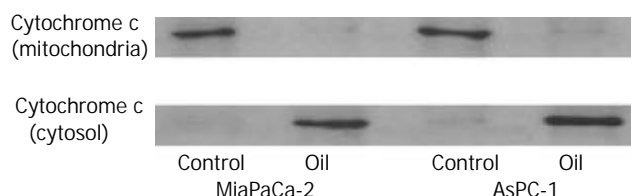


Figure 2 Western blotting of the cytochrome c protein in MiaPaCa-2 and AsPC-1 cells treated with 1:32 000 oil A for 24 hours. Proteins in cytosolic fraction and in mitochondria fraction were extracted. Proteins extracted from each sample were electrophoresed on an SDS-PAGE gel and transferred to nitrocellulose membrane. Cytochrome c was identified using a monoclonal cytochrome c antibody.

Effect of oil A on expression of Bax, Bcl-2, and Mcl-1 proteins

Expression of the anti-apoptosis proteins Bcl-2 and Mcl-1 was decreased and Bax increased following oil A treatment (Figure 3).

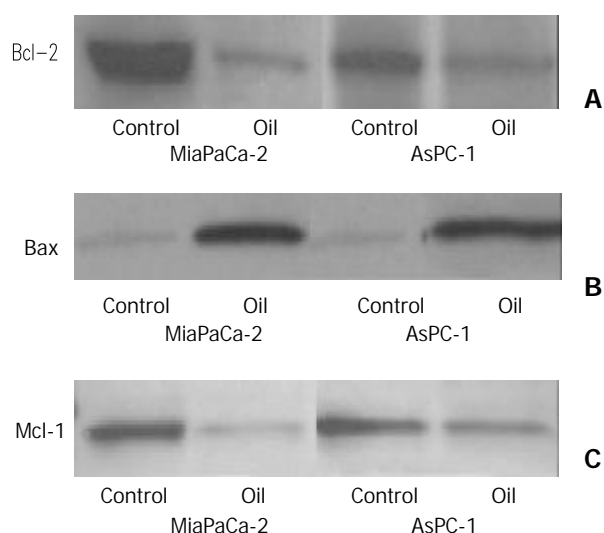


Figure 3 (A, B, C) Western blotting of the Bcl-2, Bax and Mcl-1 proteins in MiaPaCa-2 and AsPC-1 cells treated with 1:32 000 oil A for 24 hours. Whole cellular lysates were electrophoresed in SDS-PAGE gels and proteins were transferred to nitrocellulose membranes. Bcl-2, Bax and Mcl-1 were identified using specific antibodies.

Effect of oil A on cell cycle phase distribution

To understand the mechanism of induction of cell apoptosis, the redistribution of cell cycle phases were analyzed after the treatment with 1:32 000 oil A for 24 hours. The proportion of cells in the G₀/G₁ phase decreased in MiaPaCa-2 and AsPC-1 cell lines. Therefore, cells were significantly accumulated in the G₂/M-phase in these two cancer cell lines. The number of cells in S-phase was increased also in both cell lines when compared with control. The cells with a sub-G₀/G₁ DNA content, a hallmark of apoptosis, were seen following 24-hour exposure to oil A in both cell lines (Figure 4).

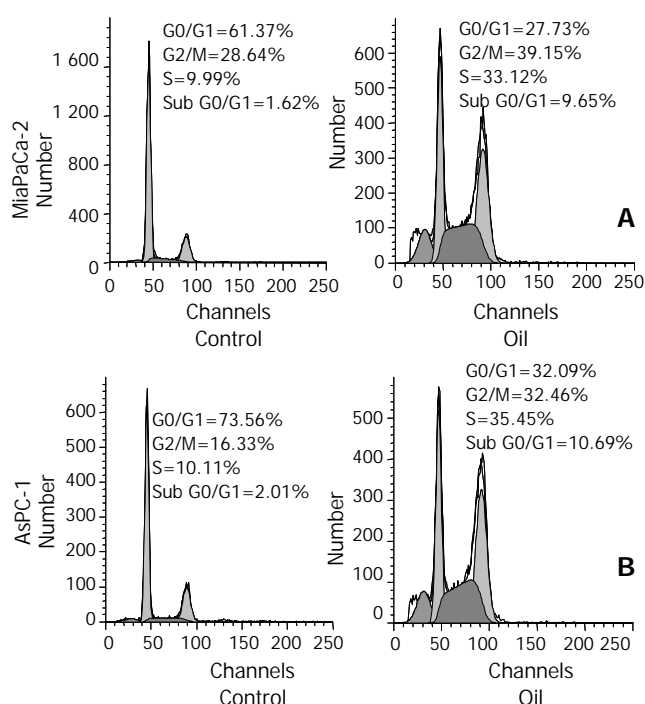


Figure 4 (A, B) Flow-cytometric analysis of cellular DNA content in control and oil A-treated MiaPaCa-2 and AsPC-1 cells, stained with propidium iodide. The cells were treated with 1:32 000 oil A in serum-free conditions for 24 hours. The distribution of cell cycle phases is expressed as % of total cells.

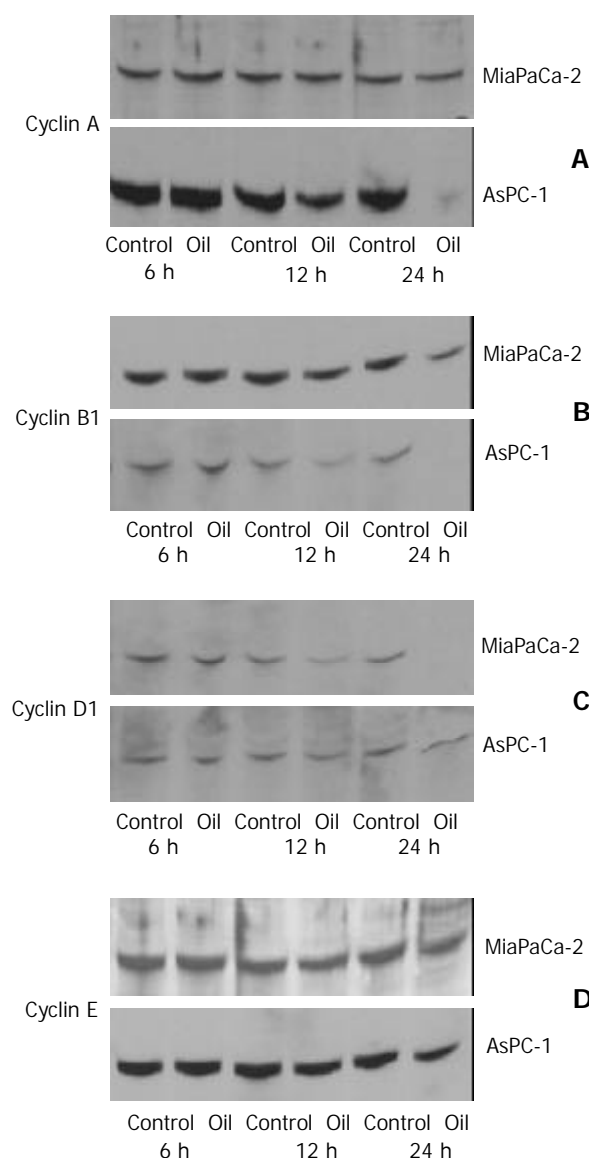


Figure 5 (A, B, C, D) Western blotting of the cyclin A, cyclin B1, cyclin D1 and cyclin E proteins in MiaPaCa-2 and AsPC-1 cells treated with 1:32 000 oil A for 24 hours. Whole cellular lysates were electrophoresed in SDS-PAGE gels and proteins were transferred to nitrocellulose membranes.

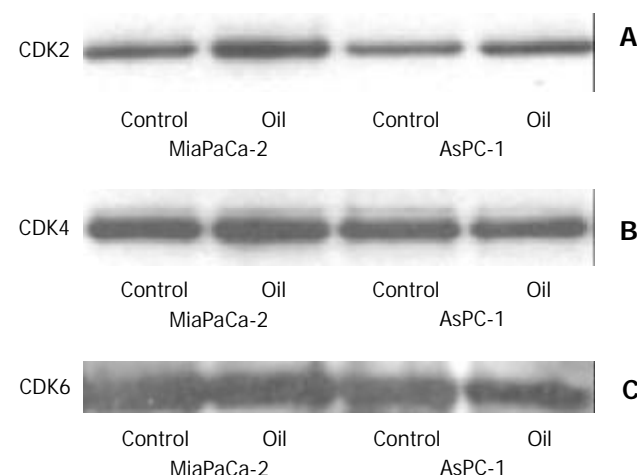


Figure 6 (A, B, C) Western blotting of the CDK2, CDK4 and CDK6 proteins in MiaPaCa-2 and AsPC-1 cells treated with 1:32 000 oil A for 24 hours. Whole cellular lysates were electrophoresed in SDS-PAGE gels and proteins were transferred to nitrocellulose membranes.

Effect of oil A on expression of cyclin proteins

The expression of cyclin A and cyclin B1 was slightly decreased and cyclin D1 levels were markedly decreased in MiaPaCa-2 cell line. The expression of cyclin A and cyclin B1 was markedly decreased and cyclin D1 levels were slightly decreased in AsPC-1 cell line, while cyclin E was unaffected and the levels of CDK2, CDK4, and CDK6 remained unchanged in MiaPaCa-2 and AsPC-1 cell lines (Figures 5 and 6).

Effect of oil A on expression of P21 and P27 proteins

In response to red oil A, P21 expression was increased, but P27 expression was not affected (Figure 7).

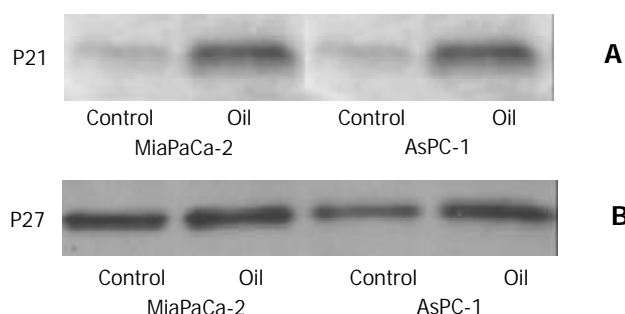


Figure 7 (A, B) Western blotting of the P21 and P27 proteins in MiaPaCa-2 and AsPC-1 cells treated with 1:32 000 oil A for 24 hours. Whole cellular lysates were electrophoresed in SDS-PAGE gels and proteins were transferred to nitrocellulose membranes. P21 and P27 were identified using specific antibodies.

Effect of oil A on expression of GADD

The expression of GADD 45 and GADD153 was enhanced in both pancreatic cancer cell lines following oil A treatment (Figure 8).

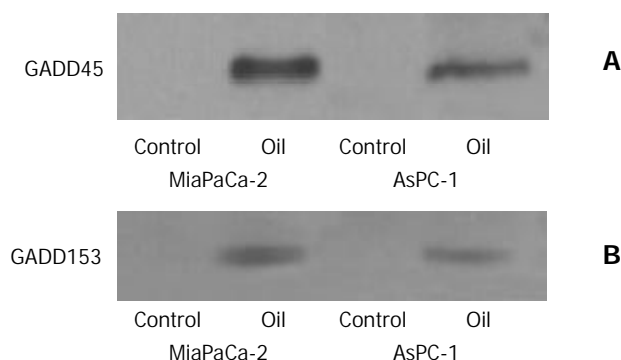


Figure 8 (A, B) Western blotting of GADD45 and GADD153 proteins in MiaPaCa-2 and AsPC-1 cells treated with 1:32 000 oil A for 24 hours. Whole cellular lysates were electrophoresed in SDS-PAGE gels and proteins were transferred to nitrocellulose membranes. GADD was identified using specific monoclonal antibodies.

DISCUSSION

Because of its significant medical properties, fish oil has been used for many years.

Recent studies indicate that diets containing a high proportion of long-chain n-3 polyunsaturated fatty acids were associated with inhibition of the growth and metastasis of human cancer including pancreatic cancer^[1-3]. Diets rich in linoleic acid (LA), an n-6 fatty acid, stimulate the progression of human cancer cell in athymic nude mice, whereas supplement of fish oil components, docosahexaenoic acid

(DHA) and eicosapentaenoic acid (EPA) exerts suppressive effects. Fish oil has been shown to reduce the induction of different cancer in animal models by a mechanism which may involve suppression of mitosis, increased apoptosis through long-chain n-3 polyunsaturated fatty acid EPA^[1,2,4-6]. In parallel, dietary supplementation with DHA is accompanied by reduced levels of 12- and 15-hydroxyeicosatetraenoic acids (12- and 15-HETE), suggesting that changes in eicosanoid biosynthesis may have been responsible for the observed decrease in tumor growth^[2,7-9]. Previous studies also have shown that the anticancer effect of fish oil is accompanied by a decreased production of cyclooxygenase and lipoxygenase metabolites^[10-13]. The efficacy of fish oil which we have found exhibits particularly potent anticancer effects that appear to be related to its content of lipoxygenase inhibitors rather than its EPA or DHA contents.

Oil A is lipid isolates from the epithelial layer of the echinoderm. Little attention of the mechanism of apoptosis induced by oil A has been paid to pancreatic cancer, which is a major cause of cancer death. The results from the present study indicate that oil A induces apoptosis on pancreatic cancer cells via caspase activities, release of cytochrome c from mitochondria, decreased expression of Bcl-2 and Mcl-1 proteins, increased expression of Bax, redistribution of cell cycle phases, increased expression of P21, GADD45 and GADD153, in association with different expression of cyclins^[14-21].

Caspases are cysteine proteases produced as inactive forms and activated during apoptosis. Caspase 3 is a major executioner protease, responsible for initiating in the apoptotic program^[22-24]. Caspase 3 plays an important role in the apoptotic program of cells^[22-28]. As a result, the caspase 3 and caspase 9 were activated, caspase 7 was decreased following oil A treatment. As a major executioner protease, the sequence alignment among caspase 3, 7 and 9 reveals the different structural basis of functions of caspase 3, 7 and 9. Caspase 3 and caspase 7 share the same sequence by 54 % and the backbone structures are nearly identical^[29]. The activation of an effector, caspase 3, is performed by an initiator, caspase 9 through proteolytic cleavage at specific internal asp residues and caspase 3 is responsible for initiating the apoptotic program^[22-24,30,31].

PARP cleavage could serve as a sensitive parameter for identification of early apoptosis^[32,33]. In parallel, PARP provided further evidence that this apoptotic pathway is activated.

Oil A induced cytochrome c release from the mitochondria to cytosol. Once cytochrome c is released from the mitochondria, it complexes with apoptotic protease-activating factor 1 to activate caspase 3^[34-37].

Also, the increase of Bax and the decrease of Bcl-2 and Mcl-1 indicate that Bcl proteins-mitochondria-caspase cascade play an important role in oil-induced apoptosis. To better understand the effect of oil A on apoptosis of pancreatic cancer cells, flow cytometric analysis of propidium iodide-stained cells was carried out. Cytometric analysis showed significant changes of cell cycle distribution in MiaPaCa-2 and AsPC-1 cells following oil treatment for 24 hours. At first (control), the proportion of cells was arrested in the G0/G1. The G2/M phase and S phase of cell cycle were accumulated after oil treatment. In the present study, we demonstrated that the distribution of cell cycle underwent changes from G0/G1 phase arrest to G2/M phase and S phase arrest following oil A treatment. The changes of cell cycle distribution suggest that apoptosis of pancreatic cancer cells may be related to some underlying mechanism, which may trigger an apoptosis signal. Thereafter, the cells with a sub-G0/G1 DNA content, a hallmark of apoptosis, were accumulated in both cell lines MiaPaCa-2 and AsPC-1 at 24 hours following exposure to oil A. The effects

of oil A persist throughout the course of cell growth, cells with DNA damage increase progressively and develop apoptosis successively. The typical peak of a sub-G0/G1 population of cells indicates oil-induced apoptosis of pancreatic cancer cells.

The cyclins and cyclin-dependent kinases (CDKs) are key components of the cell cycle machinery that is responsible for the progression through the G1/S and G2/M phases^[38]. In our experiments, the differential expression of cyclins and CDKs were observed in pancreatic cancer cells. During oil A treatment, no detectable changes of CDK2, 4, 6 were observed. When the cell cycle procession was arrested in G0/G1 phase at 24 hours of treatment, the expression of cyclins remained unchanged. Thereafter, when the cell cycle procession was arrested in G2/M phase at 24 hours of treatment, expression of cyclins was different between MiaPaCa-2 and AsPC-1 cells. Cyclin A and cyclin B1 levels were slightly decreased and cyclin D1 was markedly decreased in MiaPaCa-2 cells, whereas cyclin A and cyclin B1 levels were markedly decreased and cyclin D1 was slightly decreased in AsPC-1 cells. At the same time, expression of cyclin E was still constantly expressed. These changes of cyclins suggested underlying mechanism of cell cycle distribution in pancreatic cancer cells response to oil stress. How the cyclins are regulated remains unclear.

It has been reported that P21 mediated a significant response to DNA-damaging agents^[39,40]. The results show that oil induced an increased expression of P21, whereas the expression of P27 protein was not changed following oil treatment in the present work. These results suggested that P21 protein may play a key role in G0/G1 to G2/M phase arrest leading to apoptosis of pancreatic cancer cells.

The cell cycle is regulated by inhibitory proteins, such as GADDs, which are responsible for the maintenance of the cell cycle checkpoint that prevents inappropriate mitosis^[41-44]. GADDs expression played an important role in signal transduction pathway in response to DNA damage^[34,42-45]. Pancreatic cancer cells might respond to oil stress by activating signal transduction leading to cell cycle arrest. As an extracellular stress signal, oil A induced expression of GADDs in pancreatic cancer cells, which may be related to cell cycle arrest through G0/G1 to G2/M phases. The experimental findings suggest that GADD expression may modulate the sensitivity to oil-induced DNA damage leading to apoptosis. The GADD45 is considered to be functionally p53-dependent or p53-independent and GADD153 to be p53-independent. The increase in GADD45 and GADD153 along with a decrease in Bcl-2 and Mcl-1 were seen in pancreatic cancer cells that underwent growth arrest and apoptosis, which may provide clues concerning the mechanism of the effects of oil A. Although GADD expression with cell cycle redistributions are responsive to oil stress, the underlying mechanisms remain obscure. Further studies are required to elucidate how oil modulates the GADD proteins expression.

REFERENCES

- Fay MP**, Freedman LS, Clifford CK, Midthune DN. Effect of different types and amounts of fat on the development of mammary tumors in rodents: a review. *Cancer Res* 1997; **57**: 3979-3988
- Hawkins RA**, Sangster K, Arends MJ. Apoptotic death of pancreatic cancer cells induced by polyunsaturated fatty acids varies with double bond number and involves an oxidative mechanism. *J Pathol* 1998; **185**: 61-70
- Huang PL**, Zhu SN, Lu SL, Dai ZS, Jin YL. Inhibitor of fatty acid synthase induced apoptosis in human colonic cancer cells. *World J Gastroenterol* 2000; **6**: 295-297
- Calviello G**, Palozza P, Franceschelli P, Frattucci A, Piccioni E, Tessitore L, Bartoli GM. Eicosapentaenoic acid inhibits the growth of liver preneoplastic lesions and alters membrane phospholipid composition and peroxisomal beta-oxidation. *Nutr Cancer* 1999; **34**: 206-212
- Bartsch H**, Nair J, Owen RW. Dietary polyunsaturated fatty acids and cancers of the breast and colorectum: emerging evidence for their role as risk modifiers. *Carcinogenesis* 1999; **20**: 2209-2218
- Lai PB**, Ross JA, Fearon KC, Anderson JD, Carter DC. Cell cycle arrest and induction of apoptosis in pancreatic cancer cells exposed to eicosapentaenoic acid *in vitro*. *Br J Cancer* 1996; **74**: 1375-1383
- Falconer JS**, Ross JA, Fearon KC, Hawkins RA, O'Riordain MG, Carter DC. Effect of eicosapentaenoic acid and other fatty acids on the growth *in vitro* of human pancreatic cancer cell lines. *Br J Cancer* 1994; **69**: 826-832
- Karmali RA**, Donner A, Gobel S, Shimamura T. Effect of n-3 and n-6 fatty acids on 7, 12 dimethylbenz (a) anthracene-induced mammary tumorigenesis. *Anticancer Res* 1989; **9**: 1161-1167
- Rose DP**, Connolly JM. Antiangiogenicity of docosahexaenoic acid and its role in the suppression of breast cancer cell growth in nude mice. *Int J Oncol* 1999; **15**: 1011-1015
- Ding XZ**, Tong WG, Adrian TE. Cyclooxygenases and lipoxygenases as potential targets for treatment of pancreatic cancer. *Pancreatol* 2001; **1**: 291-299
- Larsen LN**, Hovik K, Bremer J, Holm KH, Myhren F, Borretzen B. Heneicosapentaenoate (21: 5n-3): its incorporation into lipids and its effects on arachidonic acid and eicosanoid synthesis. *Lipids* 1997; **32**: 707-714
- Noguchi M**, Earashi M, Minami M, Kinoshita K, Miyazaki I. Effects of eicosapentaenoic and docosahexaenoic acid on cell growth and prostaglandin E and Leukotriene B production by a human breast cancer cell line (MDA-MB-231). *Oncology* 1995; **52**: 458-464
- Eibl G**, Reber HA, Wente MN, Hines OJ. The selective cyclooxygenase-2 inhibitor nimesulide induces apoptosis in pancreatic cancer cells independent of COX-2. *Pancreas* 2003; **26**: 33-41
- Katz MH**, Spivack DE, Takimoto S, Fang B, Burton DW, Moossa AR, Hoffman RM, Bouvet M. Gene therapy of pancreatic cancer with green fluorescent protein and tumor necrosis factor-related apoptosis-inducing ligand fusion gene expression driven by a human telomerase reverse transcriptase promoter. *Ann Surg Oncol* 2003; **10**: 762-772
- Tassone P**, Tagliaferri P, Viscomi C, Palmieri C, Caraglia M, D'Alessandro A, Galea E, Goel A, Abbruzzese A, Boland CR, Venuta S. Zoledronic acid induces antiproliferative and apoptotic effects in human pancreatic cancer cells *in vitro*. *Br J Cancer* 2003; **88**: 1971-1978
- Buchler P**, Gukovskaya AS, Mouria M, Buchler MC, Buchler MW, Friess H, Pandolfi SJ, Reber HA, Hines OJ. Prevention of metastatic pancreatic cancer growth *in vivo* by induction of apoptosis with genistein, a naturally occurring isoflavonoid. *Pancreas* 2003; **26**: 264-273
- Saldeen J**, Tillmar L, Karlsson E, Welsh N. Nicotinamide- and caspase-mediated inhibition of poly(ADP-ribose) polymerase are associated with p53-independent cell cycle (G2) arrest and apoptosis. *Mol Cell Biochem* 2003; **243**: 113-122
- Shibayama-Imazu T**, Sakairi S, Watanabe A, Aiuchi T, Nakajo S, Nakaya K. Vitamin K(2) selectively induced apoptosis in ovarian TYK-nu and pancreatic MIA PaCa-2 cells out of eight solid tumor cell lines through a mechanism different from geranylgeraniol. *J Cancer Res Clin Oncol* 2003; **129**: 1-11
- Irawaty W**, Kay TW, Thomas HE. Transmembrane TNF and IFNgamma induce caspase-independent death of primary mouse pancreatic beta cells. *Autoimmunity* 2002; **35**: 369-375
- Marriott JB**, Clarke IA, Czajka A, Dredge K, Childs K, Man HW, Schafer P, Govinda S, Muller GW, Stirling DI, Dalglish AG. A novel subclass of thalidomide analogue with anti-solid tumor activity in which caspase-dependent apoptosis is associated with altered expression of bcl-2 family proteins. *Cancer Res* 2003; **63**: 593-599
- Thomas RP**, Farrow BJ, Kim S, May MJ, Hellmich MR, Evers BM. Selective targeting of the nuclear factor-kappaB pathway enhances tumor necrosis factor-related apoptosis-inducing ligand-mediated pancreatic cancer cell death. *Surgery* 2002; **132**: 127-134
- Thornberry NA**, Lazebnik Y. Caspase: enemies within. *Science* 1998; **281**: 1312-1316
- Mancini M**, Nicholson DW, Roy S, Thornberry NA, Peterson EP, Casciola-Rosen LA, Rosen A. The caspase-3 precursor has a cy-

- tosolic and mitochondrial distribution: implications for apoptotic signaling. *J Cell Biol* 1998; **140**: 1485-1495
- 24 **Kothakota S**, Azuma T, Reinhard C, Klippel A, Tang J, Chu K, McGarry TJ, Kirschner MW, Kohts K, Kwiatkowski DJ, Williams L. Caspase-3-generated fragment of gelsolin: effector of morphological change in apoptosis. *Science* 1997; **278**: 294-298
- 25 **Kobayashi D**, Sasaki M, Watanabe N. Caspase-3 activation downstream from reactive oxygen species in heat-induced apoptosis of pancreatic carcinoma cells carrying a mutant p53 gene. *Pancreas* 2001; **22**: 255-260
- 26 **Virkajarvi N**, Paakko P, Soini Y. Apoptotic index and apoptosis influencing proteins bcl-2, mcl-1, bax and caspases 3, 6 and 8 in pancreatic carcinoma. *Histopathology* 1998; **33**: 432-439
- 27 **Pirocanac EC**, Nassirpour R, Yang M, Wang J, Nardin SR, Gu J, Fang B, Moossa AR, Hoffman RM, Bouvet M. Bax-induction gene therapy of pancreatic cancer. *J Surg Res* 2002; **106**: 346-351
- 28 **Kirsch DG**, Doseff A, Chau BN, Lim DS, de Souza-Pinto NC, Hansford R, Kastan MB, Lazebnik YA, Hardwick JM. Caspase-3-dependent cleavage of Bcl-2 promotes release of cytochrome c. *J Biol Chem* 1999; **274**: 21155-21161
- 29 **Chai J**, Shiozaki E, Srinivasula SM, Wu Q, Datta P, Alnemri ES, Shi Y, Dataa P. Structure basis of caspase-7 inhibition by XIAP. *Cell* 2001; **104**: 769-780
- 30 **Akao Y**, Nakagawa Y, Akiyama K. Arsenic trioxide induces apoptosis in neuroblastoma cell lines through the activation of caspase-3 *in vitro*. *FEBS Lett* 1999; **455**: 59-62
- 31 **Jiang XH**, Wong BC, Yuen ST, Jiang SH, Cho CH, Lai KC, Lin MC, Kung HF, Lam SK, Chun YU, Wong B. Arsenic trioxide induces apoptosis in human gastric cancer cells through up-regulation of p53 and activation of caspase-3. *Int J Cancer* 2001; **91**: 173-179
- 32 **Decker P**, Isenberg D, Muller S. Inhibition of caspase-3-mediated poly (ADP-ribose) polymerase (PARP) apoptotic cleavage by human PARP autoantibodies and effect on cells undergoing apoptosis. *J Biol Chem* 2000; **275**: 9043-9046
- 33 **Sellers WR**, Fisher DE. Apoptosis and cancer drug targeting. *J Clin Invest* 1999; **104**: 1655-1661
- 34 **Tong WG**, Ding XZ, Witt RC, Adrian TE. Lipoxxygenase inhibitors attenuate growth of human pancreatic cancer xenografts and induce apoptosis through the mitochondrial pathway. *Mol Cancer Ther* 2002; **1**: 929-935
- 35 **Gerhard MC**, Schmid RM, Hacker G. Analysis of the cytochrome c-dependent apoptosis apparatus in cells from human pancreatic carcinoma. *Br J Cancer* 2002; **86**: 893-898
- 36 **Mouria M**, Gukovskaya AS, Jung Y, Buechler P, Hines OJ, Reber HA, Pandol SJ. Food-derived polyphenols inhibit pancreatic cancer growth through mitochondrial cytochrome C release and apoptosis. *Int J Cancer* 2002; **10**: 761-769
- 37 **Kluck RM**, Bossy-Wetzel E, Green DR, Newmeyer DD. The release of cytochrome c from mitochondria: a primary site for Bcl-2 regulation of apoptosis. *Science* 1997; **275**: 1132-1136
- 38 **Sherr CJ**. G1 phase progression: cycling on cue. *Cell* 1994; **79**: 551-555
- 39 **Waldman T**, Kinzler KW, Vogelstein B. p21 is necessary for the p53-mediated G1 arrest in human cancer cells. *Cancer Res* 1995; **55**: 5187-5190
- 40 **Waga S**, Hannon GJ, Beach D, Stillman B. The P21 inhibitor of cyclin-dependent kinases controls DNA replication by interaction with PCNA. *Nature* 1994; **369**: 574-578
- 41 **Takahashi S**, Saito S, Ohtani N, Sakai T. Involvement of the Oct-1 regulator element of the GADD45 promoter in the P53-independent response to ultraviolet irradiation. *Cancer Res* 2001; **61**: 1187-1195
- 42 **Patton GW**, Paciga JE, Shelley SA. NR8383 alveolar macrophage toxic growth arrest by hydrogen peroxide is associated with induction of growth-arrest and DNA damage-inducible genes GADD45 and GADD153. *Toxicol Appl Pharmacol* 1997; **147**: 126-134
- 43 **Ou YC**, Thompson SA, Kirchner SC, Kavanagh TJ, Faustman EM. Induction of growth arrest and DNA damage-inducible genes Gadd45 and Gadd153 in primary rodent embryonic cells following exposure to methylmercury. *Toxicol Appl Pharmacol* 1997; **147**: 31-38
- 44 **Carrier F**, Zhan Q, Alamo I, Hanaoka F, Fornace AJ Jr. Evidence for distinct kinase-mediated pathways in GADD gene responses. *Biochem Pharmacol* 1998; **55**: 853-861
- 45 **Zhan Q**, Fan S, Smith ML, Bae I, Yu K, Alamo I Jr, O' Connor PM, Fornace AJ Jr. Abrogation of p53 function affects Gadd gene responses to DNA base-damaging agents and starvation. *DNA Cell Biol* 1996; **15**: 805-815

Edited by Ma JY

Establishment and characterization of a rat pancreatic stellate cell line by spontaneous immortalization

Atsushi Masamune, Masahiro Satoh, Kazuhiro Kikuta, Noriaki Suzuki, Tooru Shimosegawa

Atsushi Masamune, Masahiro Satoh, Kazuhiro Kikuta, Noriaki Suzuki, Tooru Shimosegawa, Division of Gastroenterology, Tohoku University Graduate School of Medicine, Sendai, Japan
A.M. and M.S. equally contributed to this work

Supported by Grant-in-Aid for Encouragement of Young Scientists from Japan Society for the Promotion of Science (to A.M.), and Pancreas Research Foundation of Japan (to A.M.)

Correspondence to: Dr. Atsushi Masamune, Division of Gastroenterology, Tohoku University Graduate School of Medicine, 1-1 Seiryō-cho, Aoba-ku, Sendai 980-8574 Japan. amasamune@int3.med.tohoku.ac.jp

Telephone: +81-22-717-7171 **Fax:** +81-22-717-7177

Received: 2003-08-26 **Accepted:** 2003-09-15

Abstract

AIM: Activated pancreatic stellate cells (PSCs) have been implicated in the pathogenesis of pancreatic fibrosis and inflammation. Primary PSCs can be subcultured only several times because of their limited growth potential. A continuous cell line may therefore be valuable in studying molecular mechanisms of these pancreatic disorders. The aim of this study was to establish a cell line of rat PSCs by spontaneous immortalization.

METHODS: PSCs were isolated from the pancreas of male Wistar rats, and conventional subcultivation was performed repeatedly. Telomerase activity was measured using the telomere repeat amplification protocol. Activation of transcription factors was assessed by electrophoretic mobility shift assay. Activation of mitogen-activated protein (MAP) kinases was examined by Western blotting using anti-phosphospecific antibodies. Expression of cytokine-induced neutrophil chemoattractant-1 was determined by enzyme immunoassay.

RESULTS: Conventional subcultivation yielded actively growing cells. One clone was obtained after limiting dilution, and designated as SIPS. This cell line has been passaged repeatedly more than 2 years, and is thus likely immortalized. SIPS cells retained morphological characteristics of primary, culture-activated PSCs. SIPS expressed α -smooth muscle actin, glial acidic fibrillary protein, vimentin, desmin, type I collagen, fibronectin, and prolyl hydroxylases. Telomerase activity and p53 expression were negative. Proliferation of SIPS cells was serum-dependent, and stimulated with platelet-derived growth factor-BB through the activation of extracellular signal-regulated kinase. Interleukin-1 β activated nuclear factor- κ B, activator protein-1, and MAP kinases. Interleukin-1 β induced cytokine-induced neutrophil chemoattractant-1 expression through the activation of nuclear factor- κ B and MAP kinases.

CONCLUSION: SIPS cells can be useful for *in vitro* studies of cell biology and signal transduction of PSCs.

Masamune A, Satoh M, Kikuta K, Suzuki N, Shimosegawa T. Establishment and characterization of a rat pancreatic stellate cell line by spontaneous immortalization. *World J Gastroenterol* 2003; 9(12): 2751-2758

<http://www.wjgnet.com/1007-9327/9/2751.asp>

INTRODUCTION

Chronic pancreatitis as well as pancreatic cancer are accompanied by progressive fibrosis that is characterized by loss of functional tissue and its replacement by extracellular matrix rich connective tissues^[1,2]. In contrast to liver fibrosis, the molecular mechanisms of pancreatic fibrogenesis remain to be elucidated. In 1998, star-shaped cells in the pancreas, namely pancreatic stellate cells (PSCs), were identified and characterized^[3,4]. They are morphologically very similar to the hepatic stellate cells that play a central role in fibrosis of the liver^[5]. In normal pancreas, stellate cells are quiescent and can be identified by the presence of vitamin A-containing lipid droplets in the cytoplasm. In response to pancreatic injury or inflammation, they are transformed ("activated") from quiescent phenotype into highly proliferative myofibroblast-like cells which express the cytoskeletal protein α -smooth muscle actin (α -SMA), and produce type I collagen and other extracellular matrix components. Many of the morphological and metabolic changes associated with the activation of PSCs in animal models of fibrosis also occur when these cells are grown in culture on plastics in serum-containing medium. Therefore, culture of primary PSCs on plastics has been accepted as an established model that mimics the phenotypic changes that occur during the process of PSC activation following pancreatic injury. There is accumulating evidence that PSCs, like hepatic stellate cells, are responsible for the development of pancreatic fibrosis^[3,4,6]. Furthermore, PSCs might participate in the pathogenesis of acute pancreatitis through the expression of monocyte chemoattractant protein-1 and intercellular adhesion molecule-1^[7,8]. The activation of signaling pathways such as p38 mitogen-activated protein (MAP) kinase^[9] is likely to play a key role in PSC activation. However, the precise intracellular signaling pathways in PSCs are largely unknown.

Although primary stellate cell culture is a useful tool for studying molecular mechanisms of pancreatic fibrosis and inflammation *in vitro*, their isolation is time-consuming, yields are relatively low, and there is considerable heterogeneity between preparations. Several weeks in culture are required to obtain sufficient cells to perform experiments. In addition, primary cells can be subcultured only several times because of their limited life span *in vitro*. Because rat cells are known to be immortalized by spontaneous transformation, this study aimed to establish a rat PSC line by spontaneous immortalization.

MATERIALS AND METHODS

Materials

[γ -³²P]ATP was obtained from Amersham Biosciences UK, Ltd. (Buckinghamshire, England). Rat recombinant platelet-derived growth factor (PDGF)-BB was from R&D Systems (Minneapolis, MN). Recombinant human interleukin (IL)-1 β was from Roche Applied Science (Mannheim, Germany). Rabbit antibodies against phosphorylated MAP kinases, total MAP kinases, and inhibitor of nuclear factor κ B (NF- κ B)- α (I κ B- α) were purchased from Cell Technologies, Inc. (Beverly,

MA). Rabbit polyclonal antibody against p53 was from Santa Cruz Biotechnology (Santa Cruz, CA). Rabbit antibodies against rat type I collagen and prolyl hydroxylases (α , β) were from LSL Cosmo Bio (Tokyo, Japan). Rabbit anti-rat fibronectin antibody was from Chemicon International (Temecula, CA). Rabbit antibody against glyceraldehyde-3-phosphate dehydrogenase (G3PDH) was from Trevigen (Gaithersburg, MD). SP600125, U0126 and SB202190 were from Calbiochem (La Jolla, CA). All other reagents were products of Sigma-Aldrich (St. Louis, MO) unless specifically described.

Cell culture and immortalization

All animal procedures were performed in accordance with the National Institutes of Health Animal Care and Use Guidelines. Rat PSCs were prepared from the pancreas tissues of male Wistar rats (Japan SLC Inc., Hamamatsu, Japan) weighing 200-250 g as previously described^[3]. Isolated stellate cells were cultured in Ham's F-12 containing 10 % heat-inactivated fetal bovine serum (FBS; ICN Biomedicals, Aurora, OH), penicillin sodium, and streptomycin sulfate. When reaching confluent, the cells were trypsinized with 0.05 % trypsin/0.01 % EDTA. Initially, cells were passaged at a ratio of 1:3. After the 10th passage, cells were split at 1:5. A homogeneous population of cells, designated as SIPS, was cloned by limiting dilution, and expanded. SAM-K is another rat PSC line established by retrovirus-mediated introduction of simian virus 40 large T antigen^[10]. SAM-K cells and primary PSCs were maintained in Ham's F-12 containing 10 % FBS, penicillin sodium, and streptomycin sulfate.

Immunostaining

SIPS cells were grown directly on slides, serum-starved for 24 hours, and immunostaining for α -SMA was performed using a streptavidin-biotin-peroxidase complex detection kit (Histofine Kit; Nichirei, Tokyo, Japan) as previously described^[11]. Briefly, cells were fixed in 100 % methanol at -20 °C, and then endogenous peroxidase activity was blocked by incubation with hydrogen peroxide in methanol for 5 minutes. After immersion in normal rabbit serum, the slides were incubated with mouse anti- α -SMA antibody (at 1:200 dilution) at 4 °C overnight. The slides were incubated with biotinylated anti-mouse immunoglobulin antibody, and peroxidase-conjugated streptavidin. Finally, color was developed by incubating the slides with diaminobenzidine (Dojindo, Kumamoto, Japan). Expression of glial acidic fibrillary protein, vimentin, desmin, type I collagen, fibronectin, and prolyl hydroxylases (α , β) was examined in a similar manner.

Western blotting

The levels of activated, phosphorylated MAP kinases were determined by Western blotting as previously described^[12]. Briefly, cells were lysed in sodium dodecyl sulfate buffer (62.5 mM Tris-HCl at pH 6.8, 2 % sodium dodecyl sulfate, 10 % glycerol, 50 mM dithiothreitol, 0.1 % bromophenol blue) for 15 minutes on ice. The samples were then sonicated for 2 seconds, heated for 5 minutes, and centrifuged at 12 000×g for 5 minutes to remove insoluble cell debris. Cellular proteins (approximately 100 μ g) were fractionated on a 10 % sodium dodecyl sulfate-polyacrylamide gel. They were transferred to a nitrocellulose membrane (Bio-Rad, Hercules, CA), and the membrane was incubated overnight at 4 °C with rabbit anti-phosphospecific MAP kinase antibodies (at 1:1 000 dilution). After incubation with peroxidase-conjugated goat anti-rabbit secondary antibody for 1 hour, proteins were visualized using an ECL kit (Amersham Biosciences UK, Ltd.). Levels of total MAP kinases, p53, G3PDH, and I κ B- α were determined in a similar manner.

Telomerase activity

Telomerase activity was measured using the telomere repeat amplification protocol (TRAP) with the Telo TAGGG Telomerase PCR ELISAKit (Roche Applied Science). Briefly, SIPS, SAM-K, and primary PSCs (passage 3) were harvested separately, and the cell number was counted. The cell extracts were prepared from an equal number of cells, and used in telomerase-mediated elongation, adding the telomeric repeats to the 3' end of the biotin-labeled synthetic P1-TS-primer. These elongation products were amplified by PCR using the primers P1-TS and P2, generating PCR products with the telomerase-specific 6-nucleotide increments. An aliquot of the resulting PCR product was denatured, hybridized to a digoxigenin-labeled, telomeric repeat-specific detection probe, and immobilized to a streptavidin-coated microtiter plate. Then, peroxidase-conjugated anti-digoxigenin antibody was added to detect the immobilized PCR product, and the telomerase activity was determined, after the addition of 3,3', 5,5'-tetramethylbenzidine (substrate), as O.D.450-O.D.690. Ribonuclease A-treated cell extracts were used as negative controls. The mean of the absorbance readings of the negative control was subtracted from those of the samples, and the samples were regarded as telomerase positive if the O.D. difference was higher than 0.2.

Senescence-associated β -galactosidase (SA- β -Gal) staining

Senescence of SIPS, SAM-K, and primary PSCs (passage 20) was examined by SA- β -Gal staining^[13]. Cells were grown directly on slides, fixed, and stained with β -Gal staining solution (β -galactosidase staining kit; Mirus, Madison, WI), pH adjusted to 6.0, for 16 hours at 37 °C. After washed with phosphate-buffered saline, the slides were viewed under light microscope.

Cell proliferation assay

Serum-starved SIPS cells (approximately 80 % density) were treated with FBS at various concentrations or PDGF-BB (at 25 ng/ml). Cell proliferation was assessed using a commercial kit (Cell proliferation ELISA, BrdU; Roche Applied Science) according to the manufacturer's instructions. This is a colorimetric immunoassay based on the measurement of 5-bromo-2'-deoxyuridine (BrdU) incorporation during DNA synthesis^[14]. After 24-hour incubation with experimental reagents, cells were labeled with BrdU for 3 hours at 37 °C. Cells were then fixed, and incubated with peroxidase-conjugated anti-BrdU antibody. The peroxidase substrate 3,3', 5,5'-tetramethylbenzidine was added, and BrdU incorporation was quantitated by O.D.370-O.D.492.

Electrophoretic mobility shift assay

Following 1-hour-incubation, approximately 5×10^6 cells were harvested and nuclear extracts were prepared, and electrophoretic mobility shift assay was performed as previously described^[15]. Double-stranded oligonucleotide probes for NF- κ B (5' - AGTTGAGGGGACTTTCCAGGC-3'), and activator protein-1 (AP-1) (5' - CGCTTGATGAGTCAGCCGGAA-3') were end-labeled with [γ -³²P]ATP. Nuclear extracts (approximately 5 μ g) were incubated with the labeled oligonucleotide probe for 20 minutes at 22 °C, and electrophoresed through a 4 % polyacrylamide gel. Gels were dried and autoradiographed at -80 °C overnight. A 100-fold excess of unlabelled oligonucleotide was incubated with nuclear extracts for 10 minutes prior to the addition of the radiolabeled probe in the competition assays.

Enzyme immunoassay

After a 24 hour-incubation, cell culture supernatants were

harvested and stored at -80°C . CINC-1 levels in the culture supernatants were measured by enzyme immunoassay (Panapharm Laboratories, Udo, Japan) according to the manufacturer's instructions.

Statistical analysis

The results were expressed as mean \pm standard deviation (mean \pm SD). Luminograms and autoradiograms are representative of at least three experiments. Differences between experimental groups were evaluated by two-tailed unpaired Student's *t* test. A *P* value of less than 0.05 was considered statistically significant.

RESULTS

Establishment of an immortalized rat PSC line

PSCs were isolated from the pancreas of male Wistar rats, and conventional subcultivation was performed repeatedly. This procedure yielded actively growing cells. After limited dilution, one clone was obtained and designated as SIPS. SIPS cells were myofibroblast-like shaped, and morphologically very similar to primary, culture-activated PSCs. The characteristic fiber-like pattern of positive α -SMA staining was observed throughout the cytoplasm in SIPS cells (Figure 1A). In addition, SIPS cells showed positive staining for cytoskeletal proteins glial acidic fibrillary protein (Figure 1B), vimentin

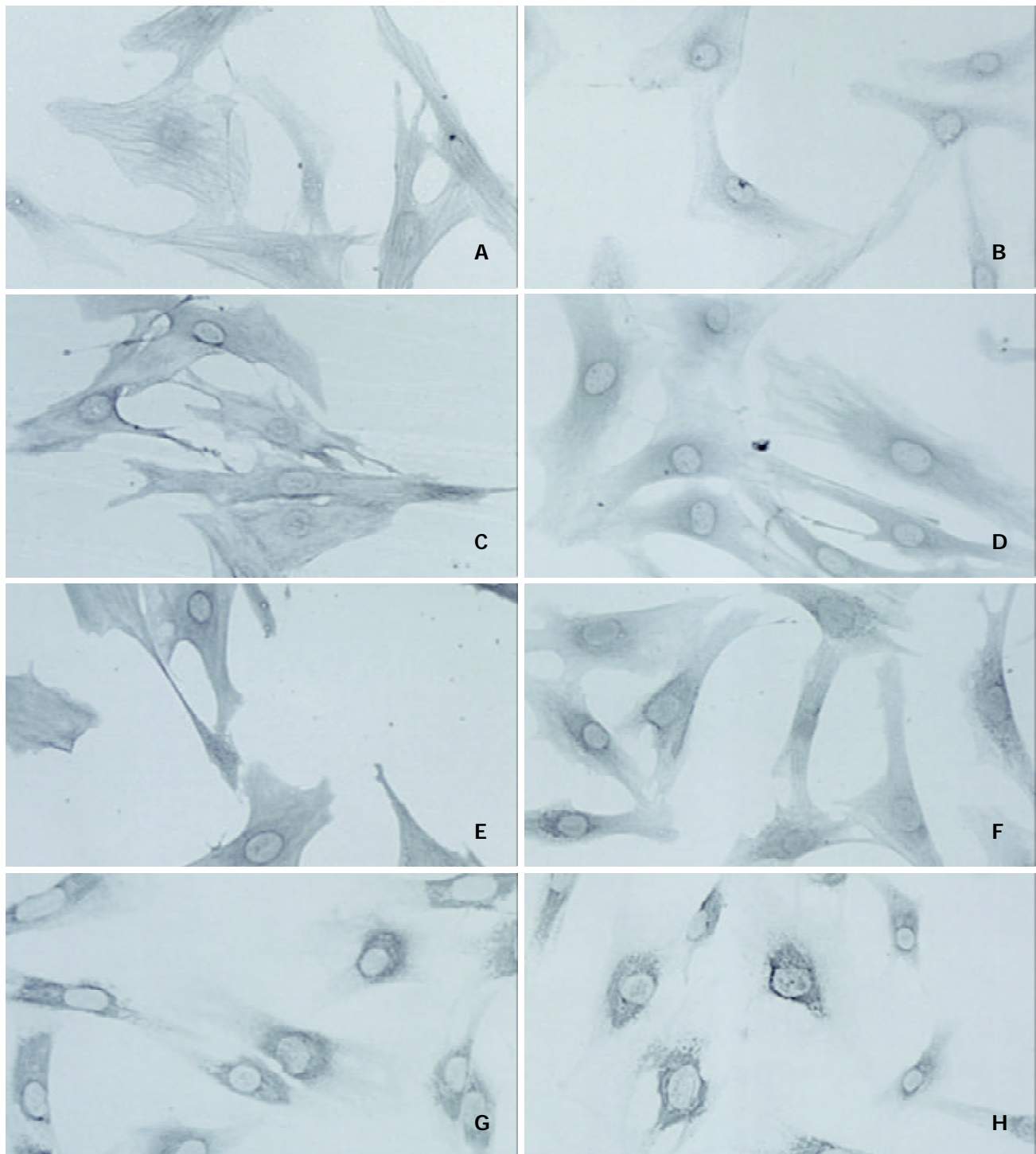


Figure 1 SIPS expressed cytoskeletal proteins and extracellular matrix proteins. Cells were grown directly on slides. Immunostaining for α -SMA (A), glial fibrillary acidic protein (B), vimentin (C), desmin (D), type I collagen (E), fibronectin (F), and prolyl hydroxylases (α) (G) and (β) (H) was performed using a streptavidin-biotin-peroxidase complex detection kit. Original magnification: $\times 20$ objective.

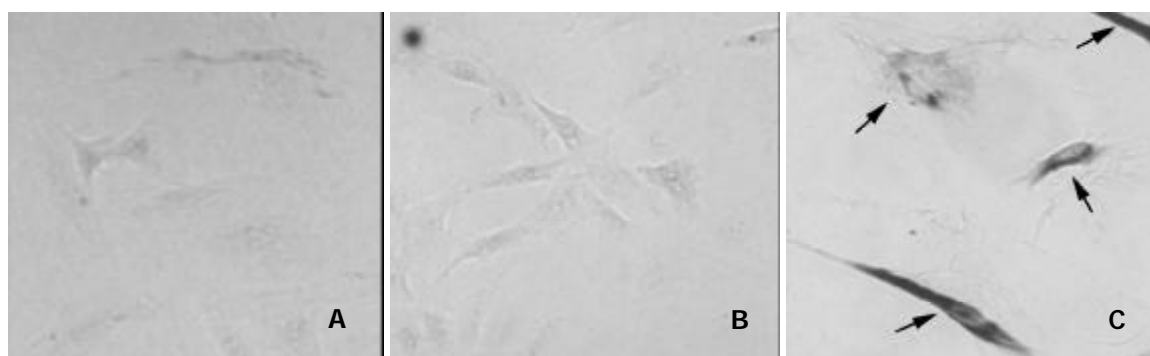


Figure 2 SIPS cells were negative for SA- β -Gal. SIPS cells (A), SAM-K cells (B), and late-passage (passage 20) PSCs (C) were grown directly on slides, fixed, and stained with β -Gal staining solution, adjusted to pH 6.0, for 16 hours at 37 °C. After washed, the slides were viewed under light microscope. SA- β -Gal was not detected in SIPS and in SAM-K cells, but was detected in late-passage PSCs (arrows). Original magnification: $\times 20$ objective.

(Figure 1C), and desmin (Figure 1D). SIPS cells also expressed extracellular matrix proteins type I collagen (Figure 1E) and fibronectin (Figure 1F). SIPS cells expressed prolyl hydroxylases (α , β) (Figure 1G, H), that are key enzymes in the hydroxylation of the proline residues in procollagen and are useful markers of collagen synthesis^[7]. These results suggest that SIPS cells shared many phenotypical and functional characteristics with primary, culture-activated PSCs. During the two years of culture, SIPS cells have been passaged repeatedly over 100 population doublings without showing any evidence of senescence. Indeed, SA- β -Gal, a biomarker of senescent cells^[13], was not detected in SIPS and in SAM-K cells (Figure 2A, B). In contrast, SA- β -Gal was detected in late-passage (passage 20) primary PSCs (Figure 2C). The phenotypic characteristics of SIPS remained unaltered, suggesting that they have acquired an immortalized phenotype. SIPS cells have conserved the characteristics of non-transformed cells since they did not form foci, and did not grow on soft agar (data not shown).

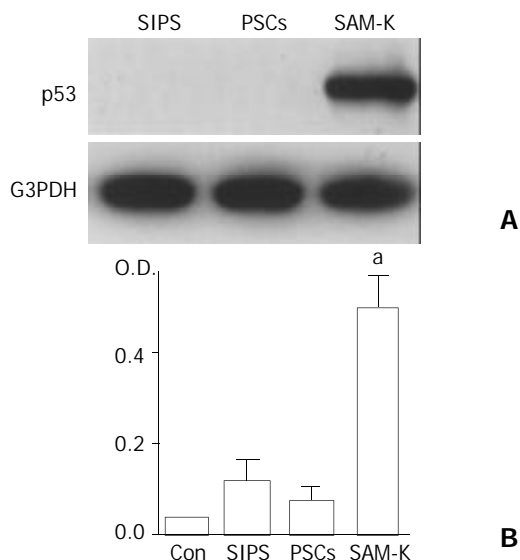


Figure 3 p53 expression and telomerase activity were negative in SIPS cells. (A) Total cell lysates (approximately 100 μ g) were prepared from SIPS, primary PSCs (passage 3), and SAM-K cells. The level of p53 was determined by Western blotting. The level of G3PDH was also determined as a loading control. (B) Telomerase activity was measured utilizing the TRAP by enzyme-linked immunosorbent assay. The telomerase activity was determined by differences in absorbance at O.D.450-O.D. 690. Negative control was prepared by incubating the total cell extracts with ribonuclease A. The mean of the absorbance in negative control was subtracted from those of the samples, and

the samples were regarded as telomerase positive ("a") if the difference in absorbance was higher than 0.2. Data are shown as mean \pm SD ($n=6$).

Negative p53 expression and telomerase activity in SIPS cells

We next examined telomerase activity and p53 expression, potentially important factors in cellular immortalization^[16,17]. p53 expression was not detected in SIPS cells and primary PSCs (passage 3), whereas the p53 level was very high in SAM-K cells (Figure 3A). As measured by the TRAP assay, SIPS cells and primary PSCs were negative for telomerase activity, whereas SAM-K cells were positive (Figure 3B).

Proliferation of SIPS stimulated by serum and PDGF

Previous studies have shown that proliferation of primary PSCs was stimulated by growth factors such as serum and PDGF-BB^[18-20]. Especially, PDGF-BB has been shown to be the most potent mitogen for PSCs, and is likely to be an important mediator of the increased proliferation of the cells both *in vivo* and *in vitro*^[18,19]. We examined whether proliferation of SIPS cells were also stimulated by serum and PDGF-BB. Treatment of the cells with FBS stimulated proliferation in a dose-dependent manner; serum-induced proliferation was significant at as low as 1 % ($P<0.05$) (Figure 4). In addition, PDGF-BB stimulated proliferation of SIPS cells; PDGF-BB (at 25 ng/ml) induced proliferation by approximately three fold in serum-free medium (Figure 4).

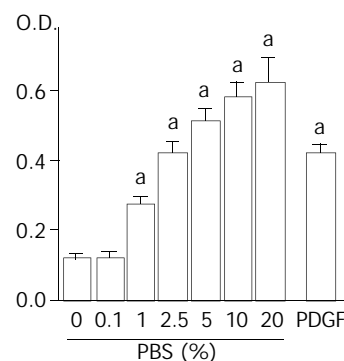


Figure 4 Proliferation of SIPS cells was serum-dependent and stimulated with PDGF-BB. SIPS cells were treated with FBS (at the indicated concentrations) or PDGF-BB (at 25 ng/ml). After 24-hour-incubation, cells were labeled with BrdU for 3 hours. Cells were then fixed, and incubated with peroxidase-conjugated anti-BrdU antibody. Then the peroxidase substrate 3,3', 5,5'-tetramethylbenzidine was added, and BrdU incorporation was quantitated by differences in absorbance at wavelength 370 minus 492 nm ("O.D."). Data are shown as mean \pm SD ($n=6$). ^a $P<0.01$ vs. serum-free medium only. O.D.: optical density.

IL-1 β activated NF- κ B and AP-1

We have previously shown that proinflammatory cytokines IL-1 β and tumor necrosis factor- α activated transcription factors NF- κ B and AP-1 in primary PSCs^[7,8]. We examined whether IL-1 β activated these transcription factors in SIPS cells. Nuclear extracts were prepared from SIPS cells treated with IL-1 β for 1 hour, and specific binding activities of NF- κ B and AP-1 were assessed by electrophoretic mobility shift assay. IL-1 β increased NF- κ B and AP-1 binding activities (Figure 5A, B). The specificity of these binding activities was confirmed by competition assays using 100-fold excess of unlabeled oligonucleotides (data not shown). Phosphorylation and degradation of I κ B- α is necessary for the activation of NF- κ B^[21]. We examined the effects of IL-1 β on the cellular I κ B- α levels by Western blotting. IL-1 β induced transient degradation of I κ B- α , further supporting that IL-1 β activated NF- κ B (Figure 5C).

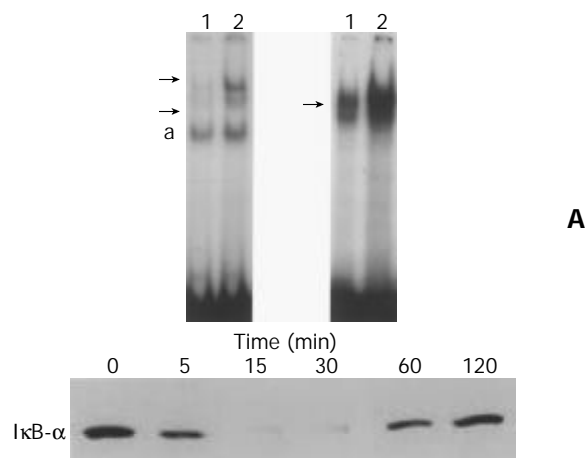


Figure 5 IL-1 β activated NF- κ B and AP-1 in SIPS cells. (A, B) SIPS cells were treated with IL-1 β (at 2 ng/ml, lane 2) for 1 hour. Nuclear extracts were prepared, and specific binding activities of NF- κ B (panel A) and AP-1 (panel B) were assessed by electrophoretic mobility shift assay. Arrows denote specific inducible complexes competitive with cold double-stranded oligonucleotide probes. Lane 1: control (medium only). a: non-specific band. (C) SIPS cells were treated with IL-1 β for indicated times. Total cell lysates (approximately 100 μ g) were prepared, and the level of I κ B- α was determined by Western blotting.

IL-1 β activated MAP kinases

Induction of the expression of AP-1 components c-Fos and c-Jun by a variety of stimuli such as growth factors and cytokines was mediated by the activation of three distinct MAP kinases: extracellular signal-regulated kinase (ERK) 1/2, c-Jun N-terminal kinase (JNK), p38 MAP kinase^[22]. Because the activation of these kinases occurred through phosphorylation, we examined whether IL-1 β activated these MAP kinases in SIPS cells by Western blotting using anti-phosphospecific MAP kinase antibodies. These antibodies recognized only phosphorylated form of MAP kinases, thus allowing the assessment of activation of these kinases. IL-1 β activated these three classes of MAP kinases in a time-dependent manner, peaking from 5 to 15 minutes (Figure 6). The levels of total MAP kinases were unaffected by the treatment, indicating that the lanes had been equally loaded.

PDGF-BB induced proliferation of SIPS cells through ERK pathway

We and others have shown that activation of ERK plays key roles in the PDGF-induced proliferation of PSCs^[20,23]. We examined whether PDGF-BB activated ERK in PSCs. PDGF-

BB activated ERK1/2 in a time-dependent manner (Figure 7A). U0126, a specific MAP kinase kinase inhibitor^[24], inhibited PDGF-induced proliferation in a dose-dependent manner (Figure 7B). Thus, activation of ERK plays a central role in the proliferation of SIPS, as is the case for primary PSCs.

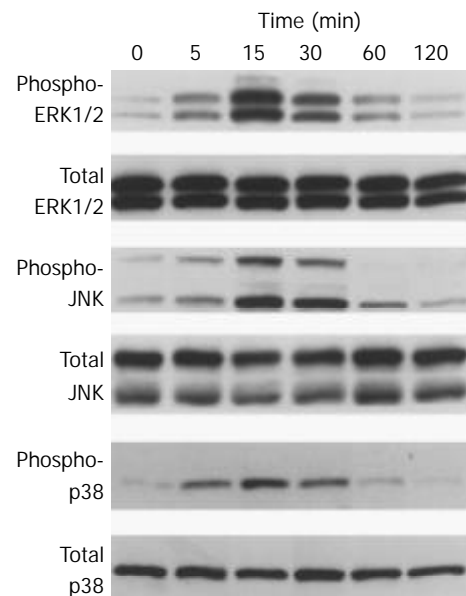


Figure 6 IL-1 β activated MAP kinases. SIPS cells were treated with IL-1 β (at 2 ng/ml) for the indicated time. Total cell lysates (approximately 100 μ g) were prepared, and the levels of activated, phosphorylated MAP kinases were determined by Western blotting. The levels of total MAP kinases were also determined.

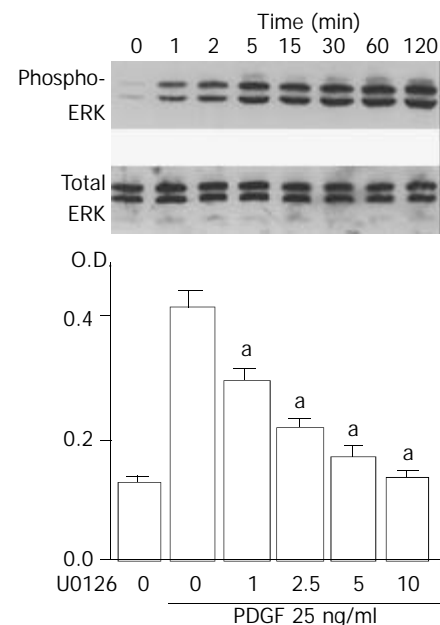


Figure 7 PDGF-BB induced proliferation of SIPS cells through ERK pathway. (A) SIPS cells were treated with PDGF-BB (at 25 ng/ml) for the indicated time. Total cell lysates (approximately 100 μ g) were prepared, and the level of activated, phosphorylated ERK was determined by Western blotting. The level of total ERK was also determined. (B) SIPS cells were treated with PDGF-BB (at 25 ng/ml) in the presence of U0126 at the indicated concentrations (at μ M). After 24-hour-incubation, cells were labeled with BrdU for 3 hours. Cells were fixed, and incubated with peroxidase-conjugated anti-BrdU antibody. Then the peroxidase substrate 3,3',5,5'-tetramethylbenzidine was added, and BrdU incorporation was

quantitated by differences in absorbance at O.D.370-O.D.492. Data are shown as mean \pm SD ($n=6$). $^aP<0.01$ versus PDGF only. O.D.: optical density.

IL-1 β induced CINC-1 expression

Activated PSCs acquire the proinflammatory phenotype; they may modulate the recruitment and activation of inflammatory cells through the expression of monocyte chemoattractant protein-1^[7] and intercellular adhesion molecule-1^[8]. Monocyte chemoattractant protein-1 is a C-C chemokine and potent mononuclear cell chemoattractant. CINC-1, a C-X-C chemokine, is a rat homologue of IL-8, and a potent neutrophil attractant^[25]. It remained unknown whether primary PSCs expressed CINC-1. We examined whether SIPS cells express CINC-1 in response to IL-1 β by enzyme immunoassay. SIPS cells constitutively produced CINC-1 at very low levels. IL-1 β significantly induced the production of CINC-1 (Figure 8). Ethanol and acetaldehyde at clinically relevant concentrations failed to induce CINC-1 production. To elucidate the roles of NF- κ B and MAP kinases for the expression of CINC-1 in SIPS cells, we used specific inhibitors to block these pathways. First, we treated SIPS cells with IL-1 β in the presence of pyrrolidine dithiocarbamate (PDTC), a specific inhibitor of NF- κ B activation^[26]. As shown in Figure 8, PDTC decreased the IL-1 β -induced CINC-1 production to near the basal levels. SP600125 is a reversible ATP-competitive inhibitor of JNK that inhibits c-jun phosphorylation and the expression of proinflammatory genes such as IL-2, and tumor necrosis factor- α ^[27]. SP600125 at 10 μ M decreased the IL-1 β -induced CINC-1 production approximately by 75 %. We next examined the effects of U0126^[24], a specific inhibitor of MAP kinase activation, which prevents the activation of ERK1/2. U0126 at 10 μ M partially inhibited inducible CINC-1 expression. A selective p38 MAP kinase inhibitor, SB202190^[28], at 25 μ M also partially inhibited inducible CINC-1 production. Similar results were obtained with tumor necrosis factor- α -induced CINC-1 expression (data not shown). In these experiments, the inhibitors at the indicated concentrations did not affect the cell viability during the incubation as assessed by trypan blue exclusion test (data not shown). However, at higher concentrations, some cytotoxic effects were observed during the incubation. These results suggested that activation of NF- κ B and JNK plays a key role in inducible CINC-1 expression in SIPS cells. Activation of ERK and p38 MAP kinase pathways is partially required for optimal CINC-1 expression.

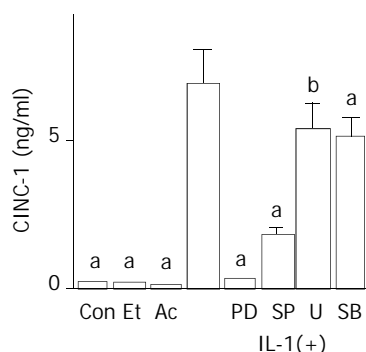


Figure 8 IL-1 β induced CINC-1 expression. SIPS cells were left untreated, or treated with IL-1 β (IL; at 2 ng/ml) in the absence or presence of PDTC ("PD" at 10 μ M), SP600125 ("SP" at 10 μ M), U0126 ("U" at 5 μ M), or SB202190 ("SB" at 25 μ M). After 24 hours, CINC-1 levels in the culture supernatant were determined by enzyme immunoassay. The effects of ethanol ("Et" at 50 mM) and acetaldehyde ("Ac" at 200 μ M) were also examined. Con: control (medium only). Data shown are expressed as means \pm SD ($n=6$). $^aP<0.01$, $^bP<0.05$ versus IL-1 β only.

DISCUSSION

In response to pancreatic injury or inflammation, PSCs undergo a transformation from quiescent cells to activated, proliferating myofibroblast-like cells, which produce cytokines and extracellular matrix proteins. It has been established that activated PSCs play an important role in the pathogenesis of pancreatic fibrosis and inflammation^[3,4,8]. Although primary stellate cell culture is a useful tool for studying molecular mechanisms of pancreatic fibrosis and inflammation *in vitro*, their isolation is time-consuming, yields are relatively low, and there is considerable heterogeneity between preparations. In addition, primary cells can be subcultured only several times because of their limited growth potential. To circumvent these problems, we have established and validated a new rat PSC line, named SIPS. This SIPS cell line has been developed through spontaneous immortalization, and can be passaged indefinitely compared with the limited number of passages for primary PSCs. SIPS cells have been passaged repeatedly without showing any evidence of senescence. Indeed, SA- β -Gal, a biomarker of senescent cells^[13], was not detected in SIPS cells. SIPS cells retained the morphologic characteristics of primary PSCs as well as the expression of the cytoskeletal proteins α -SMA and glial acidic fibrillary protein. SIPS cells maintained the functional characteristics of primary PSCs; SIPS cells showed positive staining for type I collagen, fibronectin, and prolyl hydroxylases. Proliferation of PSCs was stimulated by FBS and PDGF-BB. SIPS cells responded to IL-1 β , resulting in the activation of NF- κ B, AP-1, and MAP kinases. In addition, SIPS cells exhibited proinflammatory response; SIPS cells expressed CINC-1 in response to IL-1 β . Thus, SIPS cells retain several aspects of the primary and culture-activated PSCs.

We have previously established an immortalized cell line of rat PSCs, named SAM-K, by the introduction of the simian virus 40 T antigen^[10]. Although SAM-K cells were found to be useful for establishment of stable transfectants, it was also shown that large T antigen led to the alternation of genome such as p53 expression^[10]. The resulting genetic manipulations might limit the use of SAM-K cells for studies like defining genetic changes that occur during cell differentiation and transformation. In this study, we examined the expression of p53 and telomerase activity, both of which are shown to be associated with immortalization of mammalian cells^[16,17]. We found that p53 expression and telomerase activity was negative in SIPS cells as is the case for primary PSCs. This is in striking contrast to SAM-K cells, where p53 expression and telomerase activity were high. These results suggest that different mechanisms involved for immortalization of SIPS and SAM-K cells, and that SIPS cells have more similar phenotype to primary PSCs than SAM-K cells do. Obviously, further studies are necessary to clarify the molecular mechanisms responsible for immortalization of SIPS cells.

To our knowledge, this is the first report describing the establishment of stellate cell line of the pancreas by spontaneous immortalization. In culture, PSCs are morphologically very similar to the hepatic stellate cells. To date, several hepatic stellate cell lines have been established by spontaneous immortalization. Greenwel *et al*^[29] reported the characterization of two rat hepatic stellate cell lines, one from normal and the other from cirrhotic liver. Although both cell lines resembled primary cultures of hepatic stellate cells, significant differences in cell proliferation and IL-6 production between the two cell lines were found. Sauvant *et al*^[30] reported that immortalized rat hepatic stellate cells were able to convert retinol into retinoic acid. Rodent cells are known to undergo spontaneous immortalization with a frequency of 10^{-5} – 10^{-6} that makes isolation of immortal cell lines from rodent populations experimentally practical even without transfer of an oncogene, whereas the spontaneous immortalization of human cells is a

very rare event; the frequency is thought to be less than 10^{-12} ^[31]. Schnabl *et al.* reported immortal activated human hepatic stellate cells generated by ectopic telomerase expression^[32]. They showed that activated human hepatic stellate cells had little, if any, detectable telomerase activity. Telomerase-induced hepatic stellate cells did not undergo oncogenic transformation and showed morphologic characteristics of activated stellate cells. In addition, mRNA expression in telomerase-positive cells and -negative cells were very similar. It would be of particular interest to see if human PSC line could be established by the introduction of ectopic telomerase expression.

Proliferation of PSCs is a fundamental feature of pancreatic fibrosis. PDGF has been shown to be the most potent mitogen for PSCs *in vitro*^[18,19]. PDGF-BB stimulated proliferation of SIPS, and the stimulation was abolished in the presence of U126, a MAP kinase kinase inhibitor^[24]. This is in agreement with the previous studies showing that ERK is a key mediator of mitogenic signals in rat PSCs^[20,23].

Activated PSCs acquire the proinflammatory phenotype; they may modulate the recruitment and activation of inflammatory cells. We have shown that proinflammatory cytokines such as IL-1 β and tumor necrosis factor- α induced expression of monocyte chemoattractant protein-1 and intercellular adhesion molecule-1 in primary PSCs^[7,8]. In addition, we here showed for the first time that IL-1 β induced CINC-1 expression in SIPS cells. CINC-1 production in response to IL-1 β was also observed in primary PSCs (Satoh *et al.* manuscript in preparation). Although it has been shown that hepatic stellate cells express CINC-1 both *in vivo* and *in vitro*^[33], whether PSCs expressed CINC-1 and its regulatory mechanisms remained unknown. In this study, inducible CINC-1 production was abolished by PDTC, a specific inhibitor of NF- κ B activation, and strongly decreased by SP600125, an inhibitor of JNK. Inhibition of ERK pathway by U0126 and of p38 MAP kinase by SB202190 partially inhibited IL-1 β -induced CINC-1 production. Collectively, activation of NF- κ B and JNK plays a key role, and that of ERK and p38 MAP kinase plays a partial role for optimal CINC-1 expression in SIPS cells. This is in agreement with the regulatory mechanisms of IL-8, a human homologue of CINC-1^[34]. Maximal IL-8 amounts are generated by a combination of three different mechanisms: first, de-repression of the gene promoter; second, transcriptional activation of the gene by NF- κ B and JNK pathways; and third, stabilization of the mRNA by the p38 MAP kinase pathway. In addition, activation of ERK pathway contributes to IL-8 expression^[34]. Similar to PSCs^[35], ethanol and acetaldehyde at clinically relevant concentrations activated ERK, JNK and p38 MAP kinase (data not shown), but failed to induce CINC-1 expression in SIPS cells. Thus, activation of MAP kinases is required, but not sufficient for optimal CINC-1 expression in SIPS cells. We have previously shown that ethanol and acetaldehyde induced type I collagen gene expression through p38 MAP kinase in primary PSCs^[35]. Further studies are necessary to clarify whether ethanol and acetaldehyde induce the collagen gene expression in a similar manner.

In summary, SIPS cells are a newly established PSC line morphologically, phenotypically and functionally similar to primary, activated PSCs. Unlike SAM-K cells, immortalization was not associated with elevated p53 expression or telomerase activity. SIPS cells can be used for both transient and stable transfections (Masamune *et al.* unpublished observation), facilitating the overexpression of ectopic genes. Its phenotypic characteristics as well as its responsiveness to proinflammatory cytokines and growth factors make it a useful tool for investigation of the pathogenesis of pancreatic inflammation and fibrosis and thereby for future therapeutic development.

REFERENCES

- 1 **Etemad B**, Whitcomb DC. Chronic pancreatitis: diagnosis, classification, and new genetic developments. *Gastroenterology* 2001; **120**: 682-707
- 2 **Lankisch PG**. Natural course of chronic pancreatitis. *Pancreatol* 2001; **1**: 3-14
- 3 **Apte MV**, Haber PS, Applegate TL, Norton ID, McCaughan GW, Korsten MA, Pirola RC, Wilson JS. Periacinar stellate-shaped cells in rat pancreas: identification, isolation and culture. *Gut* 1998; **43**: 128-133
- 4 **Bachem MG**, Schneider E, Gross H, Weidenbach H, Schmid RM, Menke A, Siech M, Beger H, Grunert A, Adler G. Identification, culture, and characterization of pancreatic stellate cells in rats and humans. *Gastroenterology* 1998; **115**: 421-432
- 5 **Friedman SL**. Molecular regulation of hepatic fibrosis, an integrated cellular response to tissue injury. *J Biol Chem* 2000; **275**: 2247-2250
- 6 **Haber PS**, Keogh GW, Apte MV, Moran CS, Stewart NL, Crawford DH, Pirola RC, McCaughan GW, Ramm GA, Wilson JS. Activation of pancreatic stellate cells in human and experimental pancreatic fibrosis. *Am J Pathol* 1999; **155**: 1087-1095
- 7 **Masamune A**, Kikuta K, Satoh M, Sakai Y, Satoh A, Shimosegawa T. Ligands of peroxisome proliferator-activated receptor- γ block activation of pancreatic stellate cells. *J Biol Chem* 2002; **277**: 141-147
- 8 **Masamune A**, Sakai Y, Kikuta K, Satoh M, Satoh A, Shimosegawa T. Activated rat pancreatic stellate cells express intercellular adhesion molecule-1 (ICAM-1) *in vitro*. *Pancreas* 2002; **25**: 78-85
- 9 **Masamune A**, Satoh M, Kikuta K, Sakai Y, Satoh A, Shimosegawa T. Inhibition of p38 mitogen-activated protein kinase blocks activation of rat pancreatic stellate cells. *J Pharmacol Exp Ther* 2003; **304**: 8-14
- 10 **Satoh M**, Masamune A, Sakai Y, Kikuta K, Hamada H, Shimosegawa T. Establishment and characterization of a simian virus 40-immortalized rat pancreatic stellate cell line. *Tohoku J Exp Med* 2002; **198**: 55-69
- 11 **Masamune A**, Shimosegawa T, Kimura K, Fujita M, Sato A, Koizumi M, Toyota T. Specific induction of adhesion molecules in human vascular endothelial cells by rat experimental pancreatitis-associated ascitic fluids. *Pancreas* 1999; **18**: 141-150
- 12 **Masamune A**, Satoh K, Sakai Y, Yoshida M, Satoh A, Shimosegawa T. Ligands of peroxisome proliferator-activated receptor- γ induce apoptosis in AR42J cells. *Pancreas* 2002; **24**: 130-138
- 13 **Dimri GP**, Lee X, Basile G, Acosta M, Scott G, Roskelley C, Medrano EE, Linskens M, Rubelj I, Pereira-Smith O, Peacocke M, Campisi J. A biomarker that identifies senescent human cells in culture and in aging skin *in vivo*. *Proc Natl Acad Sci USA* 1995; **92**: 9363-9367
- 14 **Porstmann T**, Ternynck T, Avrameas S. Quantitation of 5-bromo-2-deoxyuridine incorporation into DNA: an enzyme immunoassay for the assessment of the lymphoid cell proliferative response. *J Immunol Methods* 1985; **82**: 169-179
- 15 **Masamune A**, Igarashi Y, Hakomori S. Regulatory role of ceramide in interleukin (IL)-1 β -induced E-selectin expression in human umbilical vein endothelial cells. Ceramide enhances IL-1 β action, but is not sufficient for E-selectin expression. *J Biol Chem* 1996; **271**: 9368-9375
- 16 **Banerjee A**, Srivatsan E, Hashimoto T, Takahashi R, Xu HJ, Hu SX, Benedict WF. Immortalization of fibroblasts from two patients with hereditary retinoblastoma. *Anticancer Res* 1992; **12**: 1347-1354
- 17 **Liu JP**. Studies of the molecular mechanisms in the regulation of telomerase activity. *FASEB J* 1999; **13**: 2091-2104
- 18 **Apte MV**, Haber PS, Darby SI, Rodgers SC, McCaughan GW, Korsten MA, Pirola RC, Wilson JS. Pancreatic stellate cells are activated by proinflammatory cytokines: implications for pancreatic fibrogenesis. *Gut* 1999; **44**: 534-541
- 19 **Luttenberger T**, Schmid-Kotsas A, Menke A, Siech M, Beger H, Adler G, Grunert A, Bachem MG. Platelet-derived growth factors stimulate proliferation and extracellular matrix synthesis of pancreatic stellate cells: implications in pathogenesis of pancreas fibrosis. *Lab Invest* 2000; **80**: 47-55
- 20 **Masamune A**, Kikuta K, Satoh M, Kume K, Shimosegawa T. Dif-

- ferential roles of signaling pathways for proliferation and migration of rat pancreatic stellate cells. *Tohoku J Exp Med* 2003; **199**: 69-84
- 21 **Grilli M**, Chiu JJ, Lenardo MJ. NF- κ B and Rel: participants in a multifactorial transcriptional regulatory system. *Int Rev Cytol* 1993; **143**: 1-62
- 22 **Karin M**, Liu Z, Zandi E. AP-1 function and regulation. *Curr Opin Cell Biol* 1997; **9**: 240-246
- 23 **Jaster R**, Sparmann G, Emmrich J, Liebe S. Extracellular signal regulated kinases are key mediators of mitogenic signals in rat pancreatic stellate cells. *Gut* 2002; **51**: 579-584
- 24 **Favata MF**, Horiuchi KY, Manos EJ, Daulerio AJ, Stradley DA, Feese WS, Van Dyk DE, Pitts WJ, Earl RA, Hobbs F, Copeland RA, Magolda RL, Scherle PA, Trzaskos JM. Identification of a novel inhibitor of mitogen-activated protein kinase. *J Biol Chem* 1998; **273**: 18623-18632
- 25 **Watanabe K**, Koizumi F, Kurashige Y, Tsurufuji S, Nakagawa H. Rat CINC, a member of the interleukin-8 family, is a neutrophil-specific chemoattractant *in vivo*. *Exp Mol Pathol* 1991; **55**: 30-37
- 26 **Schreck R**, Meier B, Mannel DN, Droge W, Baeuerle PA. Dithiocarbamates as potent inhibitors of nuclear factor kappa B activation in intact cells. *J Exp Med* 1992; **175**: 1181-1194
- 27 **Bennett BL**, Sasaki DT, Murray BW, O' Leary EC, Sakata ST, Xu W, Leisten JC, Motiwala A, Pierce S, Satoh Y, Bhagwat SS, Manning AM, Anderson DW. SP600125, an anthrapyrazolone inhibitor of Jun N-terminal kinase. *Proc Natl Acad Sci U S A* 2001; **98**: 13681-13686
- 28 **Lee JC**, Laydon JT, McDonnell PC, Gallagher TF, Kumar S, Green D, McNulty D, Blumenthal MJ, Heys JR, Landvatter SW, Strickler JE, McLaughlin MM, Siemens IR, Fisher SM, Livi GP, White JR, Adams JL, Young PR. A protein kinase involved in the regulation of inflammatory cytokine biosynthesis. *Nature* 1994; **372**: 739-746
- 29 **Greenwel P**, Schwartz M, Rosas M, Peyrol S, Grimaud JA, Rojkind M. Characterization of fat-storing cell lines derived from normal and CCl4-cirrhotic livers. Differences in the production of interleukin-6. *Lab Invest* 1991; **65**: 644-653
- 30 **Sauvant P**, Sapin V, Abergel A, Schmidt CK, Blanchon L, Alexandre-Gouabau MC, Rosenbaum J, Bommelaer G, Rock E, Dastugue B, Nau H, Azais-Braesco V. PAV-1, a new rat hepatic stellate cell line converts retinol into retinoic acid, a process altered by ethanol. *Int J Biochem Cell Biol* 2002; **34**: 1017-1029
- 31 **Hopfer U**, Jacobberger JW, Gruenert DC, Eckert RL, Jat PS, Whitsett JA. immortalization of epithelial cells. *Am J Physiol* 1996; **270**(1 Pt 1): C1-C11
- 32 **Schnabl B**, Choi YH, Olsen JC, Hagedorn CH, Brenner DA. Immortal activated human hepatic stellate cells generated by ectopic telomerase expression. *Lab Invest* 2002; **82**: 323-333
- 33 **Maher JJ**, Lozier JS, Scott MK. Rat hepatic stellate cells produce cytokine-induced neutrophil chemoattractant in culture and *in vivo*. *Am J Physiol* 1998; **275**(4 Pt 1): G847-G853
- 34 **Hoffmann E**, Dittrich-Breiholz O, Holtmann H, Kracht M. Multiple control of interleukin-8 gene expression. *J Leukoc Biol* 2002; **72**: 847-855
- 35 **Masamune A**, Kikuta K, Satoh M, Satoh A, Shimosegawa T. Alcohol activates activator protein-1 and mitogen-activated protein kinases in rat pancreatic stellate cells. *J Pharmacol Exp Ther* 2002; **302**: 36-42

Edited by Ma JY

Effects of bile acids on proliferation and ultrastructural alteration of pancreatic cancer cell lines

Zheng Wu, Yi Lü, Bo Wang, Chang Liu, Zuo-Ren Wang

Zheng Wu, Yi Lü, Bo Wang, Chang Liu, Zuo-Ren Wang,
Department of Hepatobiliary Surgery, The First Hospital of Xi'an Jiaotong University, Xi'an 710061, Shaanxi Province, China

Correspondence to: Yi Lü, Department of Hepatobiliary Surgery, The First Hospital of Xi'an Jiaotong University, 1 Jiankang Road, Xi'an 710061, Shaanxi Province, China. lvyi@newliver.net

Telephone: +86-29-5324009 **Fax:** +86-29-5323626

Received: 2003-03-02 **Accepted:** 2003-03-28

Abstract

AIM: Pancreatic cancer in the head is frequently accompanied by jaundice and high bile acid level in serum. This study focused on the direct effects of bile acids on proliferation and ultrastructural alteration of pancreatic cancer.

METHODS: Pancreatic cancer cell lines PANC-1, MIA PaCa-2 and PGHAM-1 were explored in this study. The cell lines were cultured in media supplemented with certain bile acids, CA, DCA, LCA, TCDC, TDCA and GCA. Their influence on cell growth was measured with MTT assay after 72 h of incubation. Cell cycles of PANC-1 cells in 40 μ M of bile acids media were analyzed by flow cytometry. Ultrastructural alteration of PANC-1 cells induced by DCA was observed using scanning and transmission electron microscope (SEM and TEM).

RESULTS: At various concentrations of bile acids and incubation time, no enhanced effects of bile acids on cell proliferation were observed. Significant inhibitory effects were obtained in almost all media with bile acids. DCA and CA increased the percentage of G₀+G₁ phase cells, while GCA and TDCA elevated the S phase cell number. After 48 h of incubation in DCA medium, PANC-1 cells showed some structural damages such as loss of their microvilli and vacuolization of organelles in cytoplasm.

CONCLUSION: Bile acids can reduce proliferation of pancreatic cancer cells due to their direct cytotoxicity. This result implies that elevation of bile acids in jaundiced serum may inhibit pancreatic cancer progression.

Wu Z, Lü Y, Wang B, Liu C, Wang ZR. Effects of bile acids on proliferation and ultrastructural alteration of pancreatic cancer cell lines. *World J Gastroenterol* 2003; 9(12): 2759-2763
<http://www.wjgnet.com/1007-9327/9/2759.asp>

INTRODUCTION

Pancreatic cancer is the fourth leading malignancy in terms of incidence in Western countries. Chemotherapy and radiotherapy could only produce minimal benefit. Extensive surgery is not boundless, either^[1]. Pancreatic cancer has been investigated in many institutes^[2-5], a great improvement of prognosis will only depend on clarifying molecular-biology of this grim tumor^[6]. Obstructive jaundice is the most common symptom of pancreatic cancer, especially in developing

countries and regions. Pancreatic cancer patients are always complicated with profound jaundice. About 70 % of pancreatic cancer patients already have obstructive jaundice at the time of diagnosis. Obstructive jaundice is a very life threatening pathophysiological disorder because elevation of bile acids in serum may attack many vital organs. Only two days after bile duct ligation, bile acids in serum have been reported to increase 30 fold compared to that of sham operated animals^[7]. Bile acids are amphiphilic compounds that behave as detergents in aqueous solution. The hydrophobicity-hydrophilicity determine the cytotoxicity of bile acids by destroying biomembrane specifically. No specific cytotoxicities of bile acids have been proved in hepatocytes, erythrocytes^[8] and intestinal mucous epithelium^[9] culture systems. However, proliferation of colonic epithelium stimulated by bile acids has been reported to occur with or without obvious cell surface damage^[10,11]. TUDC has been reported recently to enhance intrahepatic bile duct carcinogenesis in the hamster model. Although obstructive jaundice is very closely related to pancreatic cancer and both the pathophysiology of obstructive jaundice and biology of pancreatic cancer have already been investigated respectively, we know little of interaction between bile acids and biology of pancreatic cancer. In treatment of pancreatic cancer, the main purpose of surgery is to eliminate jaundice, and sometimes it is also a way to access extensive resection. If the biological effect of bile acids in serum on pancreatic cancer is clarified, it will be very helpful for treating pancreatic cancer with jaundice. In this study, three typical pancreatic cancer cell lines and six kinds of common bile acids were used to explore the direct effects of bile acids on proliferation and morphological changes of pancreatic cancer cells.

MATERIALS AND METHODS

Cell culture and treatment

Human pancreatic cancer cell lines PANC-1, MIA PaCa-2 (purchased from American Type Culture Collection) and hamster pancreatic cancer cell line PGHAM-1 (induced by BOP in the laboratory of First Department of Surgery, Nippon Medical School^[12]) were used in this study. PANC-1, MIA PaCa-2 were primarily cultured in a 75 cm² flask with the cell concentration of about 2.0×10^3 /ml in RPMI 1640 (GIBCO BRL, New York) medium. PGHAM-1 was incubated in Dulbecco's modified eagle medium (MEM: GIBCO BRL, New York) in the same way. Both media were supplemented with 10 % fetal bovine serum (FBS), 100 u/ml penicillin-streptomycin and 100 g/ml kanamycin and 100 g/ml amphotericin B (GIBCO, New York). Four days later, PANC-1, MIA PaCa-2 and PGHAM-1 cells were harvested and re-suspended in media supplemented with or without certain concentrations of bile acids including cholic acid (CA), deoxycholic acid (DCA), lithocholic acid (LCA), taurochenodeoxycholic acid (TCDC), taurodeoxycholic acid (TDCA) and glycocholic acid (GCA) (Sigma Chemical Co. USA). PANC-1, MIA PaCa-2 and PGHAM-1 cells in each group were treated and continuously cultured according to the protocols that the concentration of bile acid in each medium ranged from 10 μ mol/L to 60 μ mol/L. Cell density in the

suspension was adjusted to $6.0 \times 10^3/\text{ml}$. In the 96-well plates, 100 μl of cell suspension was added to each well, 6 wells for each group. The cells were incubated for 72 h and the viability of cells was measured by MTT assay. In another 96-well plate, PANC-1 cell suspension at very low concentration of bile acids (from 2 $\mu\text{mol/L}$ to 8 $\mu\text{mol/L}$) was incubated for 144 h and tested by MTT assay. The medium was changed every 2 days at the same concentration of bile acids. PANC-1 cell suspension was incubated in normal or 40 $\mu\text{mol/L}$ of bile acids (DCA, CA, GCA and TDCA) media in 25 cm^2 flasks for 72 h for cell cycle analysis. For scanning and transmission electron microscopic (SEM and TEM) investigations, 4 ml of PANC-1 cell suspension was incubated in normal or 20 $\mu\text{mol/L}$ or 40 $\mu\text{mol/L}$ DCA modified media in 25 cm^2 flasks for 48 h.

MTT assay

After 48 h or 96 h incubation, the viability of cells in each group was measured by 3-(4, 5-dimethylthiazol-2-yl)-2, 5-diphenyltetrazolium bromide (MTT) (Chemicon International Inc. Temecula, CA, USA) assay^[13]. Each group had six samples. With this method, 10 μl of (5 mg/ml) MTT was added to each cell suspension and the cells were incubated for 4 h. The purple formazan product formed by the action of mitochondrial enzymes in living cells was solubilized by the addition of acidic isopropanol. The absorbency of each cell suspension was measured using a microplate reader (Model 3550, Bio-Rad, CA, USA) at a test wavelength of 560 nm and a reference wavelength of 655 nm. The inhibitory rates were calculated according to the following formula: inhibitory rate = $(1 - \text{tested MTT viability} / \text{mean of control MTT viability}) \times 100\%$.

Flow cytometry

The cell cycles of PANC-1 cells incubated in 40 μM of bile acids added media for 24 h were measured by the following method. Cells were washed, permeabilised and exposed for 30 min at 4 $^{\circ}\text{C}$ to 800 μl of DNA-staining solution in 0.1 % Nonidet P-40 (Sigma-milan, Italy) and 25 $\mu\text{g/ml}$ propidium iodide (Sigma-Aldrich). The cellular DNA content was analysed by fluorescent activated cell sorter (FACS) can (Becton Dickinson Immunocytometry Systems, San Jose, CA, USA) using cell Quest software system for histograms of cell frequency *versus* propidium iodide fluorescence intensity.

SEM and TEM

PANC-1 cells in 25 cm^2 flasks were harvested by trypsinization after 24 h and 48 h of incubation. The cells were fixed with 2.5 % glutaraldehyde and 1 % osmium tetroxide (TAAB Laboratories Equipment Ltd. Berkshire, UK). The dehydration was carried out with an ethanol series. SEM specimens were dried using a critical point dryer (Hitachi Hcp-2), and the sputter was coated with Pt+Cd using an ion sputtering device (Hitachi Oie-102). The cell surface alteration was observed under a SEM device (Hitachi S-570). The dehydrated TEM samples were mixed with propylene oxide and Epok 812, which were embedded and prolymerilized. The semithin sections were stained with toluidine blue. Ultrathin sections were made using the ultra-microtome (Porter-Blum MTZ-B) and then were stained with uranyl acetate and lead citrate. The inner ultrastructure of the cells was investigated using the TEM Device (Hitachi H-500).

Statistical analyses

The digital data in this study were represented by $\bar{x} \pm s$ and assessed by the analysis of variance (ANOVA). Student's *t*-test (SPSS/PC7.5) was also used for cross comparison between different groups and different incubation times. Probabilities of less than 0.05 were considered as significant.

RESULTS

Inhibitory effects of bile acids on cultured pancreatic cancer cell lines

PANC-1 cell growth in 50 $\mu\text{mol/L}$ -1 000 $\mu\text{mol/L}$ of bile acids added RPMI-1640 medium was significantly inhibited in only 24 h compared with control (data not shown). When PANC-1 cells were cultured in 0.05 mmol/L to 1.0 mmol/L bile acid modified medium for 48 h, including unconjugated bile acids CA, DCA over the concentration of 0.5 mmol/L, LCA over 1.0 mmol/L and conjugated bile acids GCA over 1.0 mmol/L greater than 50 % growth inhibition was obtained (Figure 1). While PANC-1 treated with very low bile acid concentration of 2 $\mu\text{mol/L}$ to 8 $\mu\text{mol/L}$ for 96 h also produced certain inhibitory effect, but only exceeding 6 $\mu\text{mol/L}$ did DCA show significant effect (Figure 2). All of three cell lines: PANC-1, MIA PaCa-2 and PGHAM-1 were incubated in 10 $\mu\text{mol/L}$ -60 $\mu\text{mol/L}$ bile acid supplemented media for 72 h, cell proliferation was inhibited to a certain degree. But the unconjugated bile acids CA, DCA and LCA showed powerful inhibitive capacity (Figures 3, 4, 5).

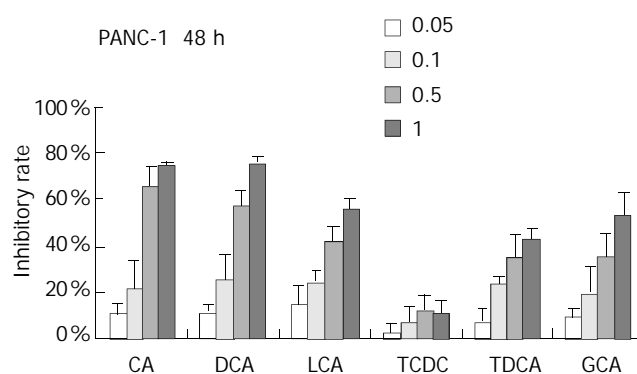


Figure 1 Bile acids (mmol/L) on PANC-1 for 48 h.

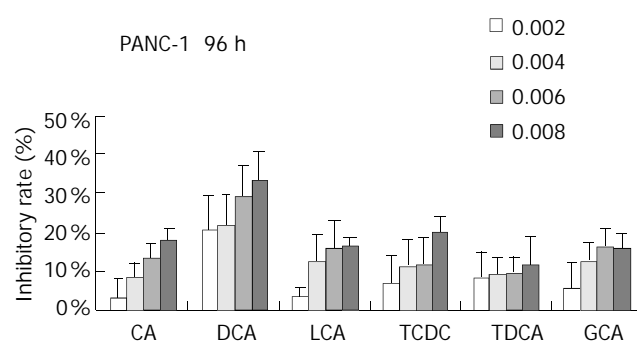


Figure 2 Bile acids (mmol/L) on PANC-1 for 96 h.

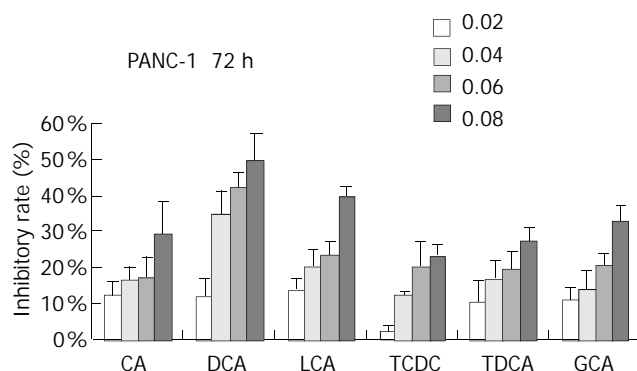


Figure 3 Bile acids (mmol/L) on PANC-1 for 72 h.

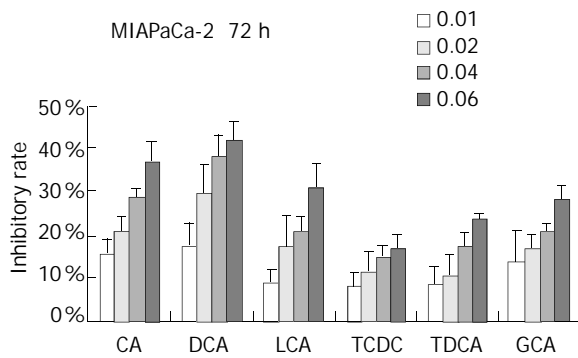


Figure 4 Bile acids (mmol/L) on MIA PaCa-2-1 for 72 h.

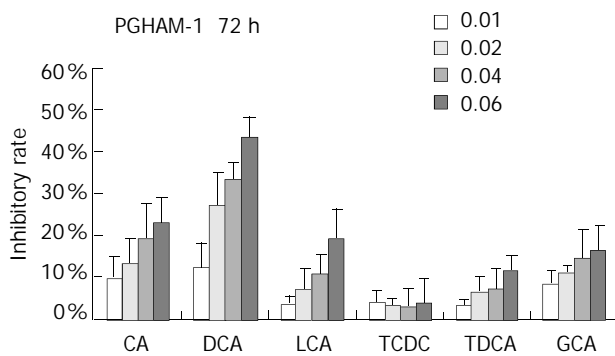


Figure 5 Bile acids (mmol/L) on PGHAM-1 for 72 h.

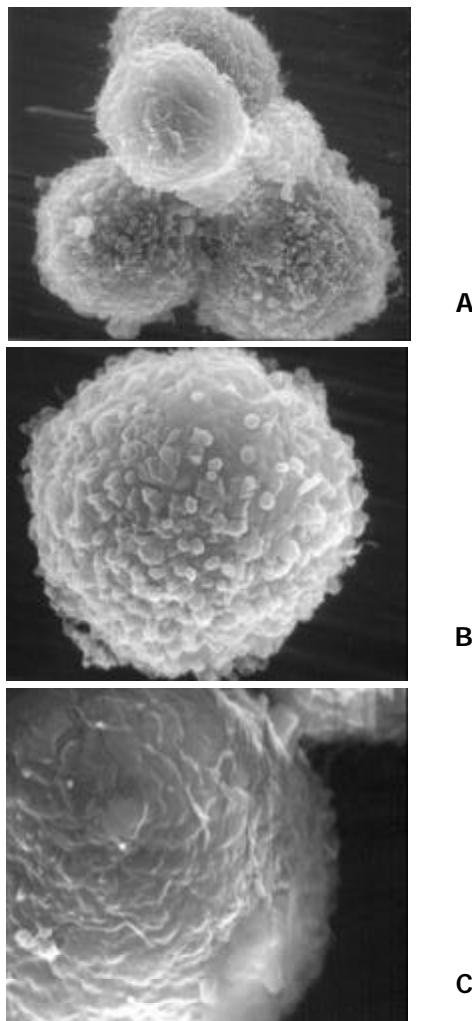


Figure 6 Ultrastructural alteration of PANC-1 viewed by SEM.

The inhibitive effects of all six bile acids were ranked in the following order: DCA>CA>LCA>GCA>TDCA>TCDC. Bile acid inhibition on the growth of three pancreatic cancer cells all showed a dosage dependent pattern. Among these bile acids, DCA produced the most powerful and obvious dosage-dependent inhibitory effect. Meanwhile PANC-1 cells were incubated in DCA (10-60 $\mu\text{mol/L}$) added medium supplemented with dexamethasone (50 μg per well), DCA's inhibitive effects could not be reversed by supplement of membrane stabilizer dexamethasone (data not shown).

Ultrastructural alteration of PANC-1 cells incubated in DCA added medium

The untreated PANC-1 cells, as viewed by SEM, were characteristic of spherical in shape with plentiful microvilli which could be described as floss, spherical and leaf like microvilli (Figure 6A \times 7 500). When PANC-1 cells were cultured in 20 $\mu\text{mol/L}$ DCA modified medium for 48 h, the majority of microvilli turned into spherical villi and the density of microvilli decreased obviously (Figure 6B \times 13 000). When PANC-1 cells were kept in 40 $\mu\text{mol/L}$ DCA treated medium for 48 h, some cell surfaces were dotted with huge leaf-like microvilli or big microhills. Most cells lost their microvilli, becoming a bear ball with only some microvilli remnants, micro-trench and prominences (Figure 6C \times 20 000).

Observation of intracellular ultrastructure with TEM showed the cells in control group had normal distribution of organelles, with the integrity of mitochondria and other organelles preserved. The nuclei were surrounded by double

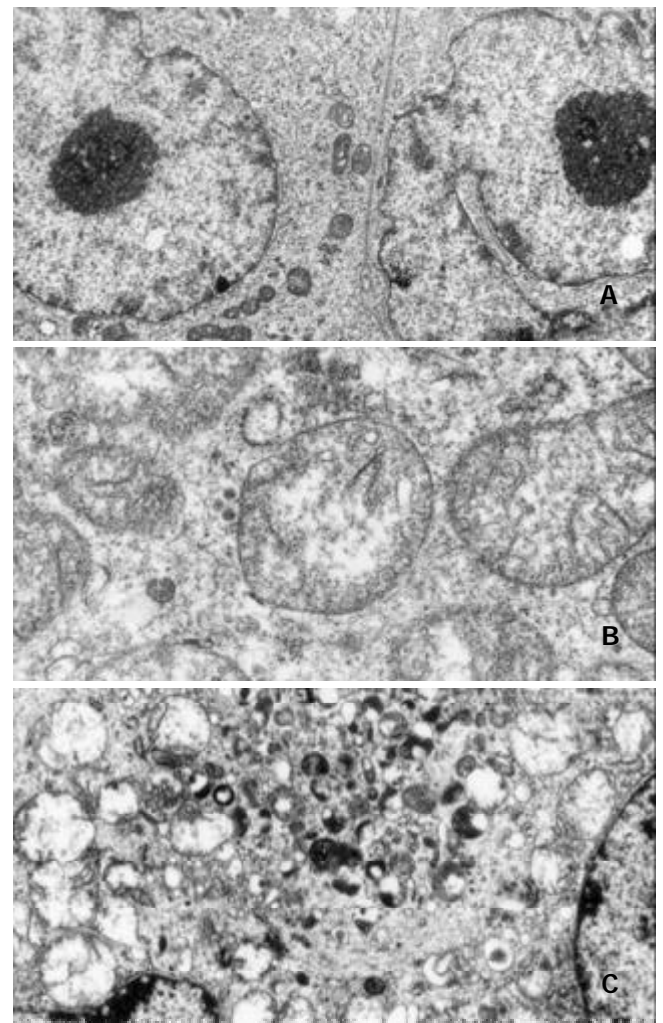


Figure 7 Ultrastructural alteration of PANC-1 viewed by TEM.

membrane envelope (Figure 7A×9 600). The cells growing in 20 $\mu\text{mol/L}$ DCA modified medium for 48 h exhibited greatly extended mitochondria and dilated rough endoplasmic reticulum. All the organelles located in cells disorderly and the obviously dilated mitochondria contained twisted and broken cristae. Injured organelles were frequently seen in plasm (Figure 7B×30 000). When DCA concentration was increased to 40 $\mu\text{mol/L}$ and incubated with cells for 48 h, exceedingly dilated mitochondria and vesicles formed by endoplasmic reticulum could be observed, some mitochondria lysed in cytoplasm were also seen. The lysosomes were also damaged and broken, which caused other surrounding organelles lysed in cytoplasm. The major portion of cytoplasm was occupied by vacuoles. The nuclear membrane double layer structure turned into indistinct and disconnected envelope. Rough granular masses against the inner surface of nuclear membrane could easily be observed (Figure 7C×12 000).

Cell cycles of PANC-1

The cell cycles of PANC-1 cells incubated in 40 μM of bile acids added media for 24 h were shown as follows. DCA and CA increased the percentage of G_0+G_1 phases cells, while GCA and TDCA elevated the S phase cell number compared with the control ($P<0.05$) (Figure 8).

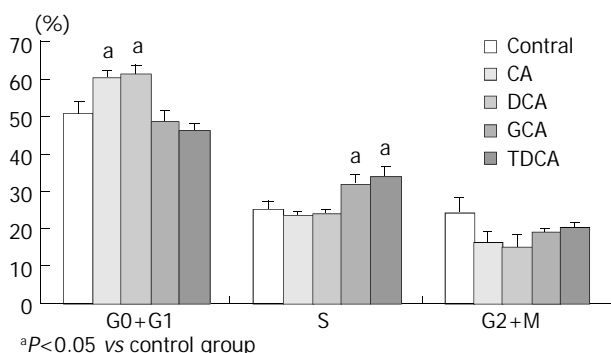


Figure 8 Cell cycles of PANC-1 cells incubated in 40 μM of bile acids added media for 24 h.

DISCUSSION

Pancreatic cancer frequently causes obstructive jaundice and elevates bile acid level in serum. For example, in non-pruritic jaundiced serum GCA concentration was 33.44 ± 16.90 $\mu\text{mol/L}$ [14]. Bile acids are steroid metabolites of cholesterol functioning as trophic factors for gut epithelium and as detergents for absorption of cholesterol and fat-soluble vitamins. The cytotoxicity of bile acids on various normal human cells [15,16] and a few malignant cells [17,18] has been demonstrated. It has been previously confirmed that bile acids could stimulate the growth of colonic epithelial cells but not that of colonic cancer cell lines [19]. While Debruyne *et al.* found recently that bile acids such as CA, chenodeoxycholic acid (CDCA), DCA, LCA could stimulate the invasion of HCT-8/E11 and PCmsrc human colorectal cancer cells into collagen type I gels [20]. Is there any interaction of elevated bile acids on human pancreatic cancer progression? However, how bile acids influence pancreatic cancer remains a subject of controversy. In order to investigate the direct effects of bile acids on pancreatic cancer, three typical pancreatic cancer cell lines (PANC-1, MIA PaCa-2 and PGHAM-1) and six common bile acids were selected and used in this study. Cultured pancreatic cancer cells have provided a model of pancreatic cancer free of other probable influencing factors such as immunoreaction and serum albumin in combination with bile acids in the body. MTT colorimetric assay is a very useful method for evaluating cell survival and

proliferation. The reliability and sensitivity of MTT assay have been demonstrated to be comparable to that of tritiated thymidine incorporation in cell proliferation and cytotoxicity assays [21]. To a certain extent, the results of MTT reflect the final effects of cell proliferation or cytotoxicity instead of only earlier events detected by tritiated thymidine incorporation.

In this study, PANC-1 cells were incubated in 50 $\mu\text{mol/L}$ to 1.0 mmol/L bile acid supplemented medium for 48 h, cell growth was inhibited to some extent at low concentration of bile acids and was also significantly inhibited by the higher concentration of bile acids. When bile acids concentration was reduced to only 2-8 $\mu\text{mol/L}$ and the incubation time was prolonged to 96 h, cell proliferation was also observed. In 6-8 $\mu\text{mol/L}$ of DCA supplemented medium significant inhibition could be obtained. Cell proliferation of PANC-1, MIA PaCa-2 and PGHAM-1 was significantly inhibited by bile acids supplemented media at certain concentrations for 72 h. The inhibitive effects of all six bile acids were ranked in the following order: DCA>CA>LCA>GCA>TDCA>TCDC. The inhibition exhibited a dosage-dependent manner, especially for DCA. Among these three cell lines, MIA PaCa-2 seemed to show the most sensitive response to all of the bile acids. The concentrations of bile acids resembled the elevation of some bile acids in jaundiced serum. Our investigation indicated that free bile acids in jaundiced serum might inhibit pancreatic cell growth and proliferation. Furthermore, we found that when PANC-1 cells were incubated in 40 μM of DCA or CA added media for 24 h, the percentage of G_0+G_1 phase cells was significantly increased compared with the control group ($P<0.05$). This implied that DCA and CA could induce cell cycle arrest, resulting in reduced proliferation and apoptosis of PANC-1 cells. Concerning its mechanism, Martinez *et al.* believed that cytotoxicity of DCA might be produced through induction of apoptosis via a protein kinase C-dependent signaling pathway [22].

According to our ultrastructural findings, the membrane and organelles were definitely damaged by supplement of bile acid DCA in medium, the inhibitory effects of bile acids on these pancreatic cancer cell lines might mainly depend on their cytotoxicity. Usually, cytotoxicity of bile acid is resulted from its hydrophobic features and hydrophobic-hydrophilic balance in serum. Lipophilic unconjugated bile acids have been shown to flip-flap rapidly across artificial lipid bilayers, so that unconjugated bile acids might enter the cytosol of every kind of cells even at a low concentration [23]. It has also been demonstrated that DCA or CDCA administration in rat colon could enhance cell membrane phospholipid turnover [24]. Hydrophobic bile acids, such as DCA, could damage cells by lysing membranes [25] and impairing mitochondrial function as well as increasing the generation of reactive oxygen radicals which can cause membrane lipid peroxidation and attack nucleic acids [26]. Velardi *et al.* have demonstrated that the cytotoxicity of bile acids is partially dependent on the cell membrane composition. Because cell membrane components such as glycolipids, receptors, and transport proteins vary in different cell lines depending on cell origin and differentiation, cell lines may also differ in regard to their response to bile acids. The over susceptibility of MIA PaCa-2 to bile acids might be due to their unique membrane lipid components. Under SEM, we also found that DCA could reduce microvilli density of PANC-1 cells. The microvilli on the surface of malignant cells could contribute to movement, attachment and invasion of malignant cells [27]. Reduction of microvilli might potentially inhibit PANC-1 cell invasion.

Biliary drainage has been shown to be an appropriate, definitive therapy for biliary obstruction due to unresectable pancreatic and peripancreatic malignancies. Some surgeons preferred to choose biliary drainage as a preoperative treatment

to reduce the level of jaundice. They expected patients to get a better operation tolerance before the radical cure. However, patients with jaundice had a higher risk of bleeding complications while those with preoperative biliary drainage (PBD) had more infective complications^[28]. Some researchers demonstrated that preoperative biliary drainage increased the risk of developing intraoperative infectious morbidity and postoperative infectious morbidity and mortality following pancreaticoduodenectomy. Preoperative biliary drainage should be avoided whenever possible in patients with potentially resectable lesions. Consequently, the effect of bile acids on pancreatic cancer should be evaluated. It is concluded that bile acids could inhibit proliferation of PANC-1, MIA PaCa-2 and PGHAM-1 cell lines *in vitro*^[29]. This may imply that bile acid can inhibit the growth of pancreatic cancer. Although the observation that bile acids inhibited proliferation of cultured cell lines could not completely reflect the complex pathophysiology of pancreatic cancer patients accompanied with obstructive jaundice, this study, at least, provides a clue that bile acids in jaundiced serum may have potentially inhibitory effects on pancreatic cancer progression. However, our investigation is an *in vitro* one, further studies are needed.

ACKNOWLEDGEMENT

We would like to express our thanks to Mr. Masahiko Onda and Mr. Eiji Uchida, from the First Department of Surgery, Nippon Medical School, Tokyo, Japan, for their valuable help in the work.

REFERENCES

- 1 **Yao GY**, Zhou JL, Lai MD, Chen XQ, Chen PH. Neuroendocrine markers in adenocarcinomas: an investigation of 356 cases. *World J Gastroenterol* 2003; **9**: 858-861
- 2 **Tan ZJ**, Hu XG, Cao GS, Tang Y. Analysis of gene expression profile of pancreatic carcinoma using cDNA microarray. *World J Gastroenterol* 2003; **9**: 818-823
- 3 **Rocha Lima CM**, Centeno B. Update on pancreatic cancer. *Curr Opin Oncol* 2002; **14**: 424-430
- 4 **Martignoni ME**, Wagner M, Krahenbuhl L, Redaelli CA, Friess H, Buchler MW. Effect of preoperative biliary drainage on surgical outcome after pancreatoduodenectomy. *Am J Surg* 2001; **181**: 52-59
- 5 **Sewnath ME**, Birjmohun RS, Rauws EA, Huibregtse K, Obertop H, Gouma DJ. The effect of preoperative biliary drainage on post-operative complications after pancreaticoduodenectomy. *J Am Coll Surg* 2001; **192**: 726-734
- 6 **McGrath PC**, Sloan DA, Kenady DE. Surgical management of pancreatic carcinoma. *Semin Oncol* 1996; **23**: 200-212
- 7 **Matsuzaki Y**, Bouscarel B, Le M, Ceryak S, Gettys TW, Shoda J, Fromm H. Effect of cholestasis on regulation of cAMP synthesis by glucagon and bile acids in isolated hepatocytes. *Am J Physiol* 1997; **273**(1 Pt 1): G164-G174
- 8 **Heuman DM**, Pandak WM, Hylemon PB, Vlahcevic ZR. Conjugates of ursodeoxycholate protect against cytotoxicity of more hydrophobic bile salts: *in vitro* studies in rat hepatocytes and human erythrocytes. *Hepatology* 1991; **14**: 920-926
- 9 **Velardi AL**, Groen AK, Elferink RP, Van Der Meer R, Palasciano G, Tytgat GN. Cell type-dependent effect of phospholipid and cholesterol on bile salt cytotoxicity. *Gastroenterology* 1991; **101**: 457-464
- 10 **Deschner E**, Cohen BI, Raicht RF. Acute and chronic effect of dietary cholic acid on colonic epithelial cell proliferation. *Digestion* 1981; **21**: 290-296
- 11 **Graven PA**, Pfanstiel J, Saito R, Derubertis FR. Relationship between loss of rat colonic surface epithelium induced by deoxycholate and initiation of the subsequent proliferative response. *Cancer Res* 1986; **46**: 5754-5759
- 12 **Yamamura S**, Onda M, Uchida E. Two types of peritoneal dissemination of pancreatic cancer cells in a hamster model. *Nippon Ika Daigaku Zasshi* 1999; **66**: 253-261
- 13 **Yoshida T**, Ohki S, Kanazawa M, Mizunuma H, Kikuchi Y, Satoh H, Andoh Y, Tsuchiya A, Abe R. Inhibitory effects of prostaglandin D2 against the proliferation of human colon cancer cell lines and hepatic metastasis from colorectal cancer. *Surg Today* 1998; **28**: 740-745
- 14 **Cabral DJ**, Small DM, Lilly HS, Hamilton JA. Transbilayer movement of bile acids in model membranes. *Biochemistry* 1987; **26**: 1801-1804
- 15 **Garner CM**, Mills CO, Elias E, Neuberger JM. The effect of bile salts on human vascular endothelial cells. *Biochim Biophys Acta* 1991; **1091**: 41-45
- 16 **Araki Y**, Fujiyama Y, Andoh A, Nakamura F, Shimada M, Takaya H, Bamba T. Hydrophilic and hydrophobic bile acids exhibit different cytotoxicities through cytolysis, interleukin-8 synthesis and apoptosis in the intestinal epithelial cell lines. IEC-6 and Caco-2 cells. *Scand J Gastroenterol* 2001; **36**: 533-539
- 17 **Lechner S**, Muller-Ladner U, Schlottmann K, Jung B, McClelland M, Ruschoff J, Welsh J, Scholmerich J, Kullmann F. Bile acids mimic oxidative stress induced upregulation of thioredoxin reductase in colon cancer cell lines. *Carcinogenesis* 2002; **23**: 1281-1288
- 18 **Shekels LL**, Lyftogt CT, Ho SB. Bile acid-induced alterations of mucin production in differentiated human colon cancer cell lines. *Int J Biochem Cell Biol* 1996; **28**: 193-201
- 19 **Shekels LL**, Beste JE, Ho SB. Tauroursodeoxycholic acid protects *in vitro* models of human colonic cancer cells from cytotoxic effects of hydrophobic bile acids. *J Lab Clin Med* 1996; **127**: 57-66
- 20 **Debruyne PR**, Bruyneel EA, Li X, Zimmer A, Gespach C, Mareel MM. The role of bile acids in carcinogenesis. *Mutat Res* 2001; **1**: 480-481: 359-369
- 21 **Denizot F**, Lang R. Rapid colorimetric assay for cell growth and survival: Modifications to the tetrazolium dye procedure giving improved sensitivity and reliability. *J Immunol Methods* 1986; **89**: 271-277
- 22 **Martinez JD**, Stratagoules ED, LaRue JM, Powell AA, Gause PR, Craven MT, Payne CM, Powell MB, Gerner EW, Earnest DL. Different bile acids exhibit distinct biological effects: the tumor promoter deoxycholic acid induces apoptosis and the chemopreventive agent ursodeoxycholic acid inhibits cell proliferation. *Nutr Cancer* 1998; **31**: 111-118
- 23 **Cabral DJ**, Small DM, Lilly HS, Hamilton JA. Transbilayer movement of bile acids in model membranes. *Biochemistry* 1987; **26**: 1801-1804
- 24 **Craven PA**, Pfanstiel J, DeRubertis FR. Role of activation of protein kinase C in the stimulation of colonic epithelial proliferation and reactive oxygen formation by bile acids. *J Clin Invest* 1987; **79**: 532-541
- 25 **Lichtenberg D**, Robson RJ, Dennis EA. Solubilization of phospholipids by detergents. Structural and kinetic aspects. *Biochim Biophys Acta* 1983; **737**: 285-304
- 26 **Ljubuncic P**, Fuhrman B, Oiknine J, Aviram M, Bomzon A. Effect of deoxycholic acid and ursodeoxycholic acid on lipid peroxidation in cultured macrophages. *Gut* 1996; **39**: 475-478
- 27 **Knyrim K**, Paweletz N. Cell interactions in a "bilayer" of tumor cells. A scanning electron microscope study. *Virchows Arch B Cell Pathol* 1977; **25**: 309-325
- 28 **Srivastava S**, Sikora SS, Kumar A, Saxena R, Kapoor VK. Outcome following pancreaticoduodenectomy in patients undergoing preoperative biliary drainage. *Dig Surg* 2001; **18**: 381-387
- 29 **Lu Y**, Onda M, Uchida E, Yamamura S, Yanagi K, Matsushita A, Kobayashi T, Fukuhara M, Aida K, Tajiri T. The cytotoxic effects of bile acids in crude bile on human pancreatic cancer cell lines. *Surg Today* 2000; **30**: 903-909

Loss of DPC4 expression and its correlation with clinicopathological parameters in pancreatic carcinoma

Zhan Hua, Yuan-Chun Zhang, Xiao-Ming Hu, Zhen-Geng Jia

Zhan Hua, Peking Union Medical College, China-Japan Friendship Institute of Clinical Medical Sciences, Beijing 100029, China

Yuan-Chun Zhang, Zhen-Geng Jia, Department of General Surgery, China-Japan Friendship Hospital, Beijing 100029, China

Xiao-Ming Hu, Department of Immunology, China-Japan Friendship Hospital, Beijing 100029, China

Correspondence to: Dr. Zhan Hua, Peking Union Medical College, China-Japan Friendship Institute of Clinical Medical Sciences, Beijing 100029, China. huazhan@hotmail.com

Telephone: +86-10-64221122-2353 **Fax:** +86-10-64278791

Received: 2003-05-10 **Accepted:** 2003-06-12

Abstract

AIM: DPC4 is a tumor suppressor gene on chromosome 18q21.1 that has high mutant frequencies in pancreatic carcinogenesis. The purpose of this study was to investigate the role of DPC4 alterations in tumorigenesis and progression of pancreatic carcinomas.

METHODS: We studied the immunohistochemical markers of DPC4 in 34 adenocarcinomas and 16 nonmalignant specimens from the pancreas. The 16 nonmalignant specimens from the pancreas included 8 non-neoplastic cysts and 8 normal pancreatic tissues. The relationship between DPC4 alterations and various clinicopathological parameters was evaluated by chi-square test or Fisher's exact test. Survivals were calculated using Kaplan-Meier method (by a log-rank test).

RESULTS: All the 16 nonmalignant cases of the pancreas showed expression of DPC4 gene. Loss of DPC4 expression was seen in 8 of 34 (23.5 %) pancreatic adenocarcinomas. The frequency of loss of DPC4 expression was higher in poorly differentiated adenocarcinoma (G3) than in well and moderately differentiated adenocarcinoma (G1 and G2) histologically ($P=0.037$). Loss of DPC4 expression of the patients at TNM stage IV was also higher than that of the patients at TNM stages I, II and III (60.0 % at stage IV, versus 14.3 % at stage I, 18.2 % at stage II, and 18.2 % at stage III) ($P=0.223$). The mean and median survival in patients with DPC4 expression was longer than those in patients with loss of DPC4 expression. Kaplan-Meier survival analysis demonstrated patients with DPC4 expression had a higher survival rate than patients with loss of DPC4 expression, but the difference did not reach statistical significance ($P=0.879$).

CONCLUSION: This study suggests that DPC4 is involved in the development of pancreatic carcinoma and is a late event in pancreatic carcinogenesis, DPC4 expression may be a molecular prognostic marker for pancreatic carcinoma.

Hua Z, Zhang YC, Hu XM, Jia ZG. Loss of DPC4 expression and its correlation with clinicopathological parameters in pancreatic carcinoma. *World J Gastroenterol* 2003; 9(12): 2764-2767
<http://www.wjgnet.com/1007-9327/9/2764.asp>

INTRODUCTION

The incidence of pancreatic carcinoma has increased in recent decades in the world, and this cancer has the lowest five-year survival rate among all cancers. The dismal survival of patients with pancreatic carcinomas is caused by the late diagnosis and low resection rates^[1,2]. However, understanding the molecular pathogenesis of pancreatic carcinomas may be the foundation upon which to develop novel strategies for identifying genetic markers useful for the early diagnosis and treatment. An association has been demonstrated between pancreatic carcinomas and various genetic alterations including genes K-ras^[3,4], Her-2/neu^[5], p16^[6], and p53^[7]. Recently, DPC4 (deleted in pancreatic carcinoma, locus 4; Smad4) located on chromosome 18q21.1, has received special attention as its alterations may play a role in activation of pancreatic carcinogenesis^[8].

DPC4 gene is a tumor suppressor gene, which has been shown to mediate the downstream effects of TGF- β superfamily signaling, resulting in growth inhibition^[9]. Inactivation of DPC4 tumor-suppressor gene is relatively specific for pancreatic carcinoma, although it has been shown to occur in a small percentage of primary carcinomas of the esophagus^[10,11], stomach^[11,12], head and neck^[13], breast, ovary^[14], colon^[15], and biliary tract^[16]. DPC4 can be inactivated by one of the two identified mechanisms: intragenic mutation of one allele coupled with loss of the other allele, or deletion of both alleles (homozygous deletions). Both mutations and homozygous deletions of DPC4 gene have been observed in a high proportion of pancreatic carcinomas^[8]. In contrast, the role of DPC4 in human pancreatic carcinoma remains less well defined. Recently, immunohistochemical labeling for the DPC4 gene product has become an extremely sensitive and specific marker for DPC4 gene alterations in pancreatic carcinomas, and has been shown to mirror the DPC4 genetic status of pancreatic carcinomas, because most mutations of DPC4 could result in a loss of the protein. Therefore, immunolabeling for DPC4 could provide a useful tool to examine genetic status in pancreatic adenocarcinomas^[17,18].

In the present study, we examined DPC4 expression in 34 adenocarcinomas and 16 nonmalignant specimens from the pancreas using a monoclonal antibody to human DPC4 protein by means of immunohistochemistry and studied the relation between expression of DPC4 and various clinicopathological parameters in order to elucidate whether altered DPC4 expression played a role in the tumorigenesis and progression of pancreatic carcinomas.

MATERIALS AND METHODS

Patients and samples

Thirty-four specimens of pancreatic adenocarcinomas were retrieved from the pathology archives of China-Japan Friendship Hospital between 1984 and 2000. There were 22 males and 12 females with pancreatic carcinomas, and the average age of the patients was 55.18 ± 1.29 years (mean \pm SD), with a range of 30-75 years. Twenty-eight patients were followed up until death or until the time of this study.

Histopathological grade and clinical staging were evaluated according to the criteria by Klöppel for pancreatic tumors^[19] and the International Union Against Cancer (UICC) TNM classification^[20]. Histopathologic examination revealed well differentiated adenocarcinoma in 10 patients, moderately differentiated adenocarcinoma in 15 patients, and poorly differentiated adenocarcinoma in 9 patients. Seven patients were at UICC stages I, 11 at stages II, 11 at stage III, and 5 at stage IV. In addition, 16 nonmalignant specimens from the pancreas including 8 non-neoplastic cysts and 8 normal pancreatic tissues were used as controls.

Immunohistochemistry

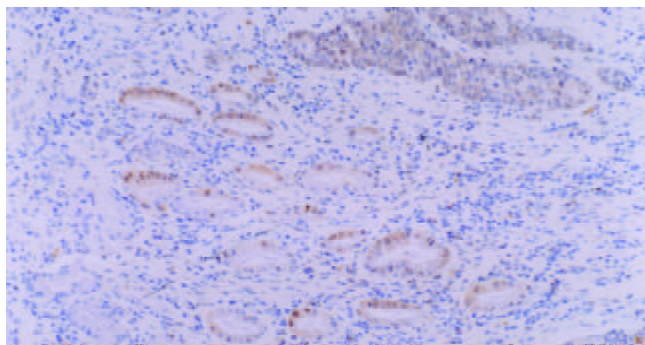
Tissues were routinely fixed in neutral formalin, embedded in paraffin, and 5 µm thick consecutive sections were cut. After deparaffinized, the slides were placed in a solution of 3 % hydrogen peroxide (1:1) for 10 minutes to block the activity of endogenous peroxidase, and then heated in a microwave for 5 minutes at 100 °C. After the slides were cooled for 30 minutes, nonspecific binding was blocked with a protein solution for 10 minutes, and then each slide was labeled with a 1:100 dilution of monoclonal antibody to DPC4 (clone B8, Santa Cruz, CA). Anti-DPC4 antibody was detected by adding biotinylated secondary antibodies, avidin-biotin complex, and 3,3'-diaminobenzidine. The sections were counterstained with hematoxylin. Positive cells were stained dark brown in the nuclei and/or cytoplasms, and the staining was graded into four categories: 0, no staining, 1+, weak staining, 2+, moderate staining, 3+, heavy staining. Positive staining was considered as expression of DPC4. Normal pancreatic ducts, islets of Langerhans, acini, lymphocytes, and stromal fibroblasts showing moderate to strong expression of DPC4 gene, served as positive internal controls for each section. For negative controls, the primary antibody was replaced with phosphate buffered solution (PBS).

Statistical analysis

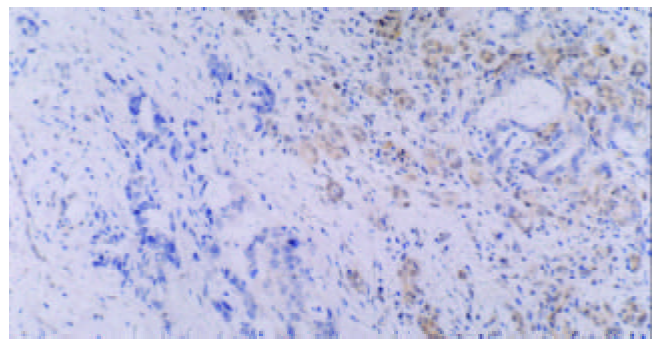
The data were analyzed with chi-square test or Fisher's exact test to compare the differences between the two subgroups of patients based on the results of DPC4 staining. All of the tests were two-tailed. Survivals were calculated using Kaplan-Meier method (by a log-rank test).

RESULTS

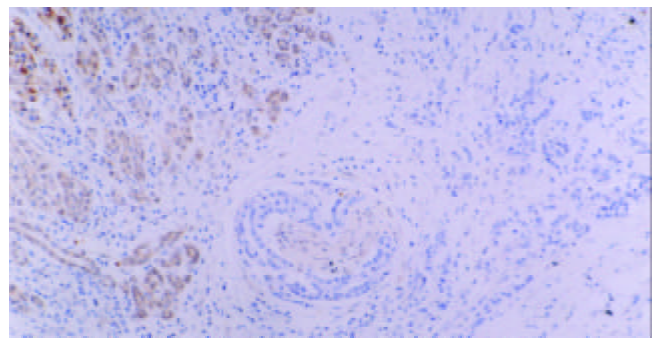
The results of DPC4 protein immunohistochemistry are summarized in Table 1, and typical examples of the positive and negative groups are shown in Figure 1 (A-E). It was observed that pancreatic carcinoma showed loss of DPC4 expression, whereas the adjacent normal pancreatic tissue had DPC4 expression (Figures 1B and C).



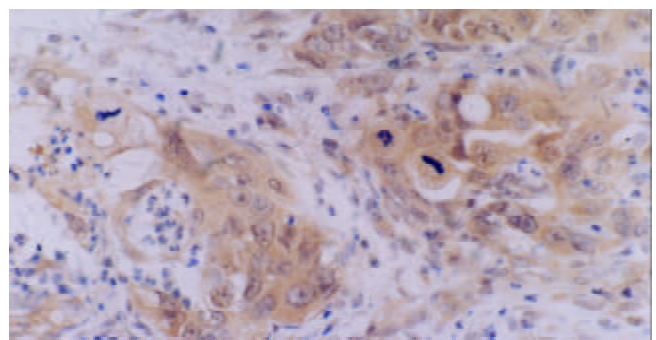
A: Well-differentiated pancreatic carcinoma showed DPC4 expression. hematoxylin counterstain. original magnification, ×100.



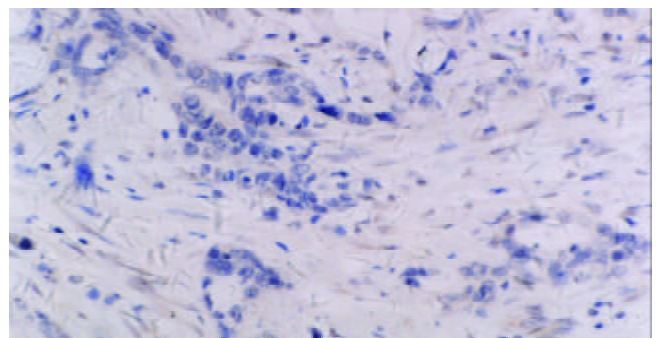
B: Well-differentiated pancreatic carcinoma showed loss of DPC4 expression (left), whereas the adjacent normal pancreatic tissue had DPC4 expression (right). hematoxylin counterstain. original magnification, ×200.



C: Moderately-differentiated pancreatic carcinoma showed loss of DPC4 expression (right), whereas the adjacent normal pancreatic tissue had DPC4 expression (left). Vortex in the middle shows invasion of pancreatic nerve. hematoxylin counterstain. original magnification, ×160.



D: Poorly-differentiated pancreatic carcinoma showed DPC4 expression. Hematoxylin counterstain. original magnification, ×400.



E: Poorly-differentiated pancreatic carcinoma showed loss of DPC4 expression. hematoxylin counterstain. original magnification, ×400.

Figure 1 Representative immunostaining results of DPC4 in pancreatic carcinoma (A-E). Positive cells were stained dark brown in the nuclei and/or cytoplasms (A-D).

All the 16 nonmalignant cases of the pancreas showed expression of DPC4 gene products. Loss of DPC4 expression was seen in 8 of 34 (23.5 %) pancreatic adenocarcinomas. The results of immunostaining of DPC4 expression in 34 pancreatic carcinomas and the correlation with various clinicopathological parameters are shown in Table 2. A significant difference was found in the frequency of loss of DPC4 expression between well and moderately differentiated adenocarcinomas (G1 and G2) and poorly differentiated adenocarcinoma (G3) histologically ($P=0.037$). Although loss of DPC4 expression in the patients at TNM staging IV was higher than that in those at stages I, II and III (60.0 % at stage IV, versus 14.3 % at stage I, 18.2 % at stage II, and 18.2 % at stage III), the difference did not reach any statistical significance ($P=0.223$). In addition, a higher frequency of loss of DPC4 expression in patients with lymph node-metastasis was also revealed, however the difference was not significant ($P=0.228$). The mean and median survival in patients with DPC4 expression was longer than that in patients with loss of DPC4 expression (Table 3). Kaplan-Meier survival analysis demonstrated patients with DPC4 expression had a higher survival rate than those with loss of DPC4 expression, but the difference did not reach any statistical significance ($P=0.879$) (Figure 2).

Table 1 Loss of DPC4 expression in pancreatic tissues (%)

Tissues	n	Loss expression of DPC4 (%)
Normal pancreas	8	0 (0)
Non-neoplastic cysts	8	0 (0)
Pancreatic carcinoma	34	8 (23.5)

Table 2 Correlations between loss expression of DPC4 and clinicopathological parameters in pancreatic carcinoma

Parameters	n	Loss expression of DPC4 (%)	P
Age (y)			
≥60	17	2 (11.8)	0.268
45≤x<60	11	4 (36.4)	
<45	6	2 (33.3)	
Sex			
Male	22	6 (27.3)	0.681
Female	12	2 (16.7)	
Pathological grade			
G1+G2	27	4 (14.8)	0.037
G3	7	4 (57.1)	
Tumor diameter			
≤4.5 cm	19	4 (21.2)	1.000
>4.5 cm	15	4 (26.7)	
Tumor location			
Head	24	6 (25.0)	0.842
Body and tail	10	2 (20.0)	
Lymph node			
Negative	20	3 (15.0)	0.228
Positive	14	5 (35.7)	
TNM staging			
I	7	1 (14.3)	0.223
II	11	2 (18.2)	
III	11	2 (18.2)	
IV	5	3 (60.00)	

G1, well differentiated; G2, moderately differentiated; G3, poorly differentiated.

Table 3 Mean and median survivals in pancreatic carcinomas

	Mean survival (days)	Median survival (days)
DPC4 expression	329.94±41.54	319.00±30.32
Loss of DPC4 expression	300.00±61.88	206.00±88.39

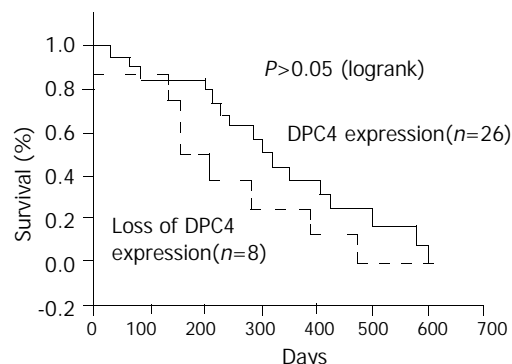


Figure 2 Kaplan-Meier survival curves comparing patients with DPC4 expression and patients with loss of DPC4 expression. Although patients with DPC4 expression had a higher survival rate than those with loss of DPC4 expression, the difference did not reach any statistical significance.

DISCUSSION

This study aimed to clarify the role of DPC4 in the development of pancreatic carcinoma. The product of DPC4 gene belongs to the evolutionally conserved family of Smad proteins which are linked to TGF- β superfamily of cytokines. Smad proteins are involved in the regulation of cell differentiation as well as the inhibition of cell proliferation, and their alterations could confer resistance to TGF- β and thereby contribute to tumorigenesis^[21,22]. DPC4 gene produces a 64-KD protein that influences gene transcription and growth arrest. In fact, DPC4 protein has three distinguishable domains, and mutations in each of these domains could lead to the loss of DPC4 function^[8,23,24].

There were different findings about the frequency of DPC4 alterations in pancreatic carcinomas in previous reports (9 %-55 %)^[8,25]. The discrepancies between studies might be due to differences in the study populations, techniques, or the statistical method. In our study, eight of the 34-pancreatic carcinoma specimens were immunohistochemically labeled for the loss of DPC4 protein (23.5 %). However, DPC4 immunohistochemical staining was found in all of the 16 nonmalignant specimens from the pancreas. This finding suggested that DPC4 might be involved in the tumorigenesis and development of pancreatic carcinoma.

Our study showed loss of DPC4 expression was correlated with the histological grade in patients with pancreatic carcinoma. Loss of DPC4 expression in those with poorly differentiated adenocarcinomas was significantly higher than that in those with well and moderately differentiated adenocarcinomas, which implied that DPC4 gene might preserve phenotypic characteristics under normal conditions and control the malignant progression of pancreatic carcinomas.

There was a trend toward a higher frequency of loss of DPC4 expression in patients at TNM staging IV in this study. When stratified by stage, the highest percentage of loss of DPC4 reactivity was found in carcinomas at stage IV (60.0 %), compared with 14.3 % at stage I, 18.2 % at stage II, and 18.2 % at stage III carcinomas. A higher frequency of loss of DPC4 expression in patients with lymph node-metastasis was also revealed. Survival analysis demonstrated patients with DPC4 expression had a higher survival rate than those with loss of DPC4 expression.

The data in our study were correlated fairly well with what has been reported. The results from Wilentz *et al* showed that DPC4 expression in duct lesions with a histologically low-grade (PanIN-1 and -2) was significantly higher than that in those with a histologically high-grade (PanIN-3)^[26]. Another study showed that DPC4 expression in PanIN could be

predictive of DPC4 expression in the subsequent invasive ductal adenocarcinoma. Additionally, DPC4 expression could be used to differentiate recurrent or persistent adenocarcinomas from a second primary adenocarcinoma. A recent study found that survival of patients whose tumors expressed DPC4 protein was significantly longer (19.2 months) as compared with 14.7 months of those without DPC4 protein expression, and DPC4 expression was correlated with a better prognosis of pancreatic carcinomas^[18]. Biankin *et al* also found DPC4/Smad4 expression had a potential as a prognostic indicator in patients with pancreatic carcinoma, and loss of DPC4 expression was associated with improved survival after resection, whereas resection did not improve the survival in patients whose tumor expressed DPC4.

These findings suggest that loss of DPC4 expression occurs biologically late in the neoplastic progression leading to the development of infiltrating pancreatic carcinoma, and indicates a poor prognosis for patients. It is reasonable to postulate that DPC4 plays a pivotal role in regulating all TGF- β superfamily signal pathways. Abrogation of DPC4 function might cause a breakdown in this signaling pathway and loss of transcription of genes critical to cell-cycle control. Cells might therefore become TGF- β resistant and escape from TGF- β -mediated growth control and apoptosis. Experimental evidences indicated that DPC4 could regulate an angiogenic switch by decreasing the expression of vascular endothelial growth factor (VEGF) and increasing the levels of angiogenesis inhibitor thrombospondin-1 (TSP-1).

In conclusion, our study shows that loss of DPC4 expression is involved in the carcinogenesis and development of pancreatic carcinoma and is a late event in pancreatic carcinogenesis. DPC4 expression may be a molecular prognostic marker for pancreatic carcinoma.

ACKNOWLEDGEMENTS

We thank Dr. Gonghua Zhao for her critical suggestions regarding this work and Mr. Jing Zhang for helping perform the immunohistochemical staining.

REFERENCES

- Bramhall SR**, Allum WH, Jones AG, Allwood A, Cummins C, Neoptolemos JP. Treatment and survival in 13,560 patients with pancreatic cancer, and incidence of the disease, in the West Midlands: an epidemiological study. *Br J Surg* 1995; **82**: 111-115
- Yeo CJ**, Cameron JL. Prognostic factors in ductal pancreatic cancer. *Langenbecks Arch Surg* 1998; **383**: 129-133
- Hruban RH**, van Mansfeld AD, Offerhaus GJ, van Weering DH, Allison DC, Goodman SN, Kensler TW, Bose KK, Cameron JL, Bos JL. K-ras oncogene activation in adenocarcinoma of the human pancreas. A study of 82 carcinomas using a combination of mutant-enriched polymerase chain reaction analysis and allele-specific oligonucleotide hybridization. *Am J Pathol* 1993; **143**: 545-554
- Robinson RA**. K-ras mutations and the diagnosis of pancreatic carcinoma. *Am J Clin Pathol* 1996; **105**: 257-259
- Safran H**, Steinhoff M, Mangray S, Rathore R, King TC, Chai L, Berzein K, Moore T, Iannitti D, Reiss P, Pasquariello T, Akerman P, Quirk D, Mass R, Goldstein L, Tantravahi U. Overexpression of the HER-2/neu oncogene in pancreatic adenocarcinoma. *Am J Clin Oncol* 2001; **24**: 496-499
- Hu YX**, Watanabe H, Ohtsubo K, Yamaguchi Y, Ha A, Okai T, Sawabu N. Frequent loss of p16 expression and its correlation with clinicopathological parameters in pancreatic carcinoma. *Clin Cancer Res* 1997; **3**: 1473-1477
- Li Y**, Bhuiyan M, Vaitkevicius VK, Sarkar FH. Molecular analysis of the p53 gene in pancreatic adenocarcinoma. *Diagn Mol Pathol* 1998; **7**: 4-9
- Hahn SA**, Schutte M, Hoque AT, Moskaluk CA, da Costa LT, Rozenblum E, Weinstein CL, Fischer A, Yeo CJ, Hruban RH, Kern SE. DPC4, a candidate tumor suppressor gene at human chromosome 18q21.1. *Science* 1996; **271**: 350-353
- Dai JL**, Turnacioglu KK, Schutte M, Sugar AY, Kern SE. Dpc4 transcriptional activation and dysfunction in cancer cells. *Cancer Res* 1998; **58**: 4592-4597
- Maesawa C**, Tamura G, Nishizuka S, Iwaya T, Ogasawara S, Ishida K, Sakata K, Sato N, Ikeda K, Kimura Y, Saito K, Satodate R. MAD-related genes on 18q21.1, Smad2 and Smad4, are altered infrequently in esophageal squamous cell carcinoma. *Jpn J Cancer Res* 1997; **88**: 340-343
- Lei J**, Zou TT, Shi YQ, Zhou X, Smolinski KN, Yin J, Souza RF, Appel R, Wang S, Cymes K, Chan O, Abraham JM, Harpaz N, Meltzer SJ. Infrequent DPC4 gene mutation in esophageal cancer, gastric cancer and ulcerative colitis-associated neoplasms. *Oncogene* 1996; **13**: 2459-2462
- Nishizuka S**, Tamura G, Maesawa C, Sakata K, Suzuki Y, Iwaya T, Terashima M, Saito K, Satodate R. Analysis of the DPC4 gene in gastric carcinoma. *Jpn J Cancer Res* 1997; **88**: 335-339
- Kim SK**, Fan Y, Papadimitrakopoulou V, Clayman G, Hittelman WN, Hong WK, Lotan R, Mao L. DPC4, a candidate tumor suppressor gene, is altered infrequently in head and neck squamous cell carcinoma. *Cancer Res* 1996; **56**: 2519-2521
- Schutte M**, Hruban RH, Hedrick L, Cho KR, Nadasdy GM, Weinstein CL, Bova GS, Isaacs WB, Cairns P, Nawroz H, Sidransky D, Casero RA Jr, Meltzer PS, Hahn SA, Kern SE. DPC4 gene in various tumor types. *Cancer Res* 1996; **56**: 2527-2530
- Takagi Y**, Kohmura H, Futamura M, Kida H, Tanemura H, Shimokawa K, Saji S. Somatic alterations of the DPC4 gene in human colorectal cancers *in vivo*. *Gastroenterology* 1996; **111**: 1369-1372
- Hahn SA**, Bartsch D, Schroers A, Galehdari H, Becker M, Ramaswamy A, Schwarte-Waldhoff I, Maschek H, Schmiegel W. Mutations of the DPC4/Smad4 gene in biliary tract carcinoma. *Cancer Res* 1998; **58**: 1124-1126
- Wilentz RE**, Su GH, Dai JL, Sparks AB, Argani P, Sohn TA, Yeo CJ, Kern SE, Hruban RH. Immunohistochemical labeling for dpc4 mirrors genetic status in pancreatic adenocarcinomas: a new marker of DPC4 inactivation. *Am J Pathol* 2000; **156**: 37-43
- Tascilar M**, Skinner HG, Rosty C, Sohn T, Wilentz RE, Offerhaus GJ, Adsay V, Abrams RA, Cameron JL, Kern SE, Yeo CJ, Hruban RH, Goggins M. The SMAD4 protein and prognosis of pancreatic ductal adenocarcinoma. *Clin Cancer Res* 2001; **7**: 4115-4121
- Klöppel G**. Pancreatic non-endocrine tumors. In: Klöppel G, Heitz PU ed. *Pancreatic pathology*. *Edinburg:Churchill Livingstone* 1984: 79-113
- Hermanek P**, Sobin LH. UICC TNM classification of malignant tumors. 4th ed. 2nd revision. *Berlin: Springer-Verlag* 1992: 71-73
- Zhang Y**, Feng X, We R, Derynck R. Receptor-associated Mad homologues synergize as effectors of the TGF- β response. *Nature* 1996; **383**: 168-172
- Chiao PJ**, Hunt KK, Grau AM, Abramian A, Fleming J, Zhang W, Breslin T, Abbruzzese JL, Evans DB. Tumor suppressor gene Smad4/DPC4, its downstream target genes, and regulation of cell cycle. *Ann N Y Acad Sci* 1999; **880**: 31-37
- Shi Y**, Hata A, Lo RS, Massague J, Pavletich NP. A structural basis for mutational inactivation of the tumour suppressor Smad4. *Nature* 1997; **388**: 87-93
- De Caestecker MP**, Hemmati P, Larisch-Bloch S, Ajmera R, Roberts AB, Lechleider RJ. Characterization of functional domains within Smad4/DPC4. *J Biol Chem* 1997; **272**: 13690-13696
- Moore PS**, Orlandini S, Zamboni G, Capelli P, Rigaud G, Falconi M, Bassi C, Lemoine NR, Scarpa A. Pancreatic tumours: molecular pathways implicated in ductal cancer are involved in ampullary but not in exocrine nonductal or endocrine tumorigenesis. *Br J Cancer* 2001; **84**: 253-262
- Wilentz RE**, Iacobuzio-Donahue CA, Argani P, McCarthy DM, Parsons JL, Yeo CJ, Kern SE, Hruban RH. Loss of expression of Dpc4 in pancreatic intraepithelial neoplasia: evidence that DPC4 inactivation occurs late in neoplastic progression. *Cancer Res* 2000; **60**: 2002-2006

G and D cells in rat antral mucosa: An immunoelectron microscopic study

Feng-Peng Sun, Yu-Gang Song

Feng-Peng Sun, Yu-Gang Song, Department of Gastroenterology, Nanfang Hospital, First Military Medical University, Guangzhou 510515, Guangdong Province, China

Supported by Natural Science Foundation of Guangdong Province, No. 010578; Technological and Social Development Project of Guangdong Province, No. 2002C31210; the Key Scientific Research Project of Guangzhou City, No. 2002Z3-E0131

Correspondence to: Feng-Peng Sun, Department of Gastroenterology, Nanfang Hospital, First Military Medical University, Guangzhou 510515, Guangdong Province, China. sci@china.com

Telephone: +86-20-85140114-87101

Received: 2002-10-08 **Accepted:** 2003-03-10

Abstract

AIM: To investigate the gastrin secreting cells (G cells) and the somatostatin secreting cells (D cells) of antral mucosa in rats at the ultrastructural level.

METHODS: Revised immunoelectron microscopic technique was used to detect the G cells and D cells in rat antral mucosa through gastrin and somatostatin antibodies labeled by colloidal gold. Also the relevant quantitative analysis regarding the granular number of colloidal gold in G cells and in D cells was conducted.

RESULTS: Immunological granules of colloidal gold were distributed in G cells and D cells. Gastrin labeled golden granules or somatostatin labeled ones presented mainly as lobation-like or island-like congeries. Most of the golden congeries were observed dissociated in cytoplasm of G cells or D cells, near the basement membrane. A few golden congeries were located in nuclei. The number of golden granules in one G cell was around 107.04 ± 19.68 and was 83.36 ± 17.58 in one D cell.

CONCLUSION: Gastrin secreting granules are located in cytoplasm and nuclei of G cells, and somatostatin secreting granules both in cytoplasm and in nuclei of D cells. The number of golden granules can be quantitatively analyzed to determine the relative amount of gastrin secreting granules or somatostatin secreting granules.

Sun FP, Song YG. G and D cells in rat antral mucosa: An immunoelectron microscopic study. *World J Gastroenterol* 2003; 9(12): 2768-2771

<http://www.wjgnet.com/1007-9327/9/2768.asp>

INTRODUCTION

Gastrointestinal hormones such as gastrin and somatostatin, regulate the secretion, motility, absorption, blood flow and cell nutrition of the digestive tract. Abnormality of their secretion often affects the normal functions of digestive tract, even cause clinical symptoms or syndromes. Pathological impairment of gastrointestinal tract could also result in changes of the level of gastrointestinal hormones. Gastrin is mainly secreted from

gastrin secreting cells (G cells) in antrum mucosa or upper small intestine. Medulla oblongata and dorsal nuclei of vagus nerve in central nervous system also have gastrin. Somatostatin is distributed in the body, hypothalamus and at other sites of the brain, peripheral nerve and gastrointestinal tract. In digestive system, for example, somatostatin is secreted from somatostatin secreting cells (D cells). D cells are distributed mainly in intestinal nerve plexus, stomach and pancreas^[1-4].

Although there are some methods to observe the shape of G cells and D cells, microscope or electron microscope could not decide G cells or D cells alone. Immunohistochemical method could not demonstrate G cells or D cells at ultrastructural levels. Thus investigations at the ultrastructural level by immunoelectron microscopy are effective^[5-8]. This study was to demonstrate G cells and D cells at the ultrastructural level by colloidal gold labeled immunoelectron microscopy technique.

MATERIALS AND METHODS

Guinea pigs and antral tissue processing

Seven healthy male Wistar rats weighing 230-250 g from the Center of Experimental Animals in Sun Yat-sen University of Medical Sciences (Guangzhou, China) were used. All rats received no special treatment before sacrificed. The rats were fasted overnight with free access to water. Four days later, the rat's abdomen, anesthetized with 3 % of sodium pentobarbital intraperitoneally at a dosage of 30 mg/kg, was cut open and its stomach was split from the greater curvature. The antral tissue of about 0.5 mm×0.5 mm was separated using ophthalmic scissors. Then the specimens were immersed into a mixture of 0.1 % glutaraldehyde and 3 % paraformaldehyde in 0.1M PBS, pH7.4, for 2 hr at room temperature for fixation.

Specimen preparation for immunoelectron microscopy

Two hours after fixation, the antral tissue specimens were washed four times for 15 min in 0.1M PBS, pH7.4, and then postfixed for 1 hr in solution of 1 % osmium tetroxide (1 % potassium dichromate, pH 7.2, 1 % osmium tetroxide, 0.85 % NaCl) at room temperature. The specimens were washed three times for 10 min in 0.1M PBS, pH7.4, and dehydrated at room temperature in 50 % acetone (15 min), 70 % acetone (15 min), 90 % acetone (15 min), and 100 % acetone (three times for 15 min each). The specimens were then infused in an open desiccator containing 50 % acetone: 50 % Spurr resin (1 hr), 33 % acetone: 67 % Spurr resin (2 hr), and 100 % Spurr resin overnight. When the resin was infused in the specimens, it was polymerized at 40 °C for 4 days. To orientate the samples, 1 μm thick sections were cut, put on an objective glass, and stained with 0.1 % toluidin blue. Appropriate regions were chosen, and the pyramids were further trimmed, cut on a Leica Reichert ultramicrotome into 60-80 nm ultrathin sections, put onto 300 nickel mesh grids. All ultrathin sections were divided into G cells group, D cells group, and control group.

Postembedded antibody incubation and immunoelectron microscopy

All the ultrathin sections were oxidized in H₂O₂ for 10 min,

washed three times for 5 min in water. Osmium tetroxide was removed in 1 % sodium periodate, washed three times for 5 min in 0.05 M TBS, pH7.4. The ultrathin sections were incubated for 30 min at room temperature in 1.5 % BSA (Sigma, USA) in PBS for blocking. The sections of G cells group were then incubated with rabbit anti-gastrin polyclonal antibody (Sigma, USA) at a concentration of 1:80 in PBS, the sections of D cells group were incubated with rabbit anti-somatostatin polyclonal antibody (ZYMED, USA) at a concentration of 1:80 in PBS, and the sections of control group were incubated with PBS only. All sections were incubated in a wet box at 4 °C overnight and then at 37 °C for 1 hr. The sections were washed three times for 10 min in 0.05M TBS, pH7.4, then one time for 10 min in 0.02 M TBS, pH7.4. The sections were again incubated for 30 min at room temperature in 1.5 % BSA in PBS for blocking and then incubated with a gold-conjugated secondary antibody, colloidal-gold/staphylococci-protein-A 1:80 (10 nm, Boster Biological Technology Co, Wuhan, China) in PBS, for 1 hr at 37 °C. The sections were washed three times for 5 min in water and stained with 5 % uranyl acetate (in water) at room temperature for 60 min, and with lead citrate for 60 min. At last the specimens were examined and photographed under an electron microscope (Philips CM10).

Image analysis of colloidal gold granules

A total of 50 cells in either G cells group or D cells group were randomly photographed from sections of their photos. They were input into the Quantimet-500 image analysis system (Leica Co. German) for calculation of the average number of colloidal gold granules. The data thus obtained were expressed in $\bar{x} \pm s$.

RESULTS

Immunoelectron microscopy of G cells

No immunological granules of colloidal gold in most antral mucosa cells were found, except those in G cells. Immunological granules of colloidal gold were well distributed in G cells, with the cells' ultrastructure clearly fixed. While the membrane of G cells was intact, rough endoplasmic reticles were increased, and mitochondria decreased. The nuclei of G cells were normal, and the chromatin was equally distributed. The gastrin labeled golden granules in G cells were clear, either round-shaped or oval-shaped, with a high electro-density. The granules presented mainly as lobation-like or island-like congeries, which were dispersed in cytoplasm of G cells, directing toward the basement membrane. A few golden congeries in the nuclei of G cells were mainly located in euchromatin area. No golden congeries were observed in heterochromatin area. There were immunological granules of colloidal gold in the nuclei of G cells as island-like congeries and penetrating nuclear pore in cytoplasm (Figure 1). The number of golden granules in a G cell was 107.04 ± 19.68 .

Immunoelectron microscopy of D cells

No immunological granules of colloidal gold were found in most antral mucosa cells, except those in D cells. Immunological granules of colloidal gold were found well distributed in D cells, with the ultrastructure clearly fixed. The membrane of D cells was intact, rough endoplasmic reticles were increased, and mitochondria decreased. The nuclei of D cells were normal, with their chromatin well distributed. The somatostatin labeled golden granules in D cells were clear, either round-shaped or olive-shaped, with a high electro-density. The granules presented mainly as lobation-like or island-like congeries, a few of them were dispersed in D cells while most of them were dissociated in cytoplasm of D cells, directing toward the basement membrane. Again, a few golden

congeries in the nuclei of D cells were mainly located in euchromatin area (Figure 2). No golden congeries were found in heterochromatin area. The number of golden granules in a D cell was 83.36 ± 17.58 . No colloidal gold-labeled cell was observed in control group.

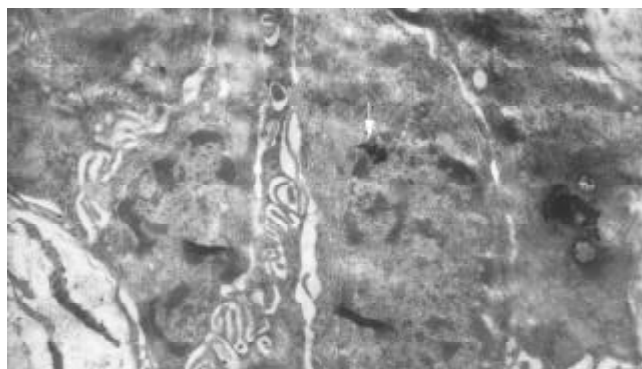


Figure 1 Immunological granules of colloidal gold located in nuclei of G cell as island-like congeries (↑), and penetrating nuclear pores into cytoplasm. $\times 21000$.

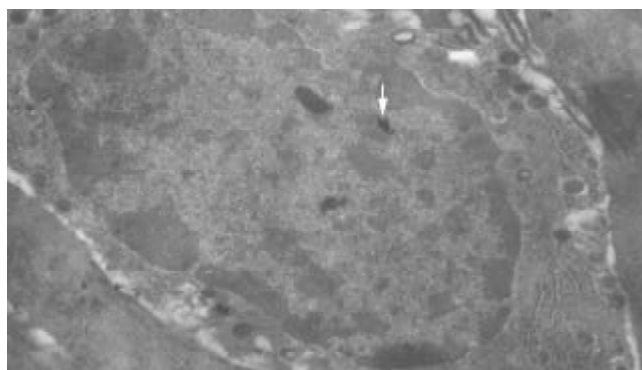


Figure 2 Immunological granules of colloidal gold locate in nuclei of D cell as island-like congeries (↑). $\times 8900$.

DISCUSSION

Gastric mucosa consists of highly organic multi-functional glands. In a single gastric gland there are at least five kinds of cells. They are the parietal cell, chief cell, endocrine cell, superficial epithelial cell and mucous cell. The stem cells of all these kinds of cells are in the neck area near the surface of the gland. When migrating upward to the surface of gland, they changed into the surface mucous cells. When migrating downward deeper into the gland, the proliferative stem cells changed into cells in forms of parietal cells, chief cells, and endocrine cells^[9-11].

The features of gastrin can be briefly summarized as follows. There are gastrin receptors both in parietal cells and in ECL cells. As the main regulating hormone of gastric acid secretion, gastrin stimulates parietal cells to secrete gastric acid directly via the gastrin receptors in parietal cells and also stimulates ECL cells to secrete histamine via the gastric receptors in the cells. Then histamine stimulates parietal cells to secrete gastric acid via H_2 receptors in parietal cells in a paracrine style. While accelerating the secretion of pepsin, secretin, pancreatic juice, and the secretion of water and salt in bile, gastrin also speeds up the releasing of insulin and calcitonin. It has both nutritional and accelerating effects on gastric mucosa. It also has a growth factor producing the similar effect. In the same way, the increase of gastrin would lead to the increasing number of both parietal cells and ECL cells.

Apart from all these, gastrin is also closely related with the occurrence of carcinoid tumor. Gastrin enhances the motion of gastrointestinal tract, thus increasing the contraction effect of the stomach, intestine and gall bladder. In addition, there are reports that G cells should be taken as the fourth histamine source in stomach besides chief cells, ECL cells, and intestinal nerve plexus. Increase of pH, intake of meal, increase of pressure in the stomach, and excitation introduced by vagus nerve or mucosa nerve plexus could make G cells secrete more gastrin. Decrease of pH stimulated by somatostatin or other gastrointestinal hormones, and excitation of sympathetic nerve could inhibit the secretion of gastrin^[12-17].

What characterizes somatostatin is presented as follows. The main physiological effect produced by somatostatin on digestive system is inhibition. Somatostatin could inhibit peristalsis of stomach, intestine, gall bladder and proliferation of mucosal cells, reduce blood flow of gastrointestinal tract and small intestine to absorb water, electrolyte, glucose, amino acid, and triglycerides, depress the secretion of gastric acid, pepsin, hepatic bile, small intestinal juice, and secretion of gastrin and other gastrointestinal hormones. Excitation of sympathetic nerve could inhibit D cells to secrete somatostatin, but that of vagus nerve could stimulate D cells to do so. Gastrin has a unique regional regulatory effect on secretion of somatostatin in stomach. Gastrin could directly stimulate D cells to secrete somatostatin. In some species, gastrin receptors have been detected in D cells of stomach. As shown in some investigations, endogenous histamine inhibited the secretion of somatostatin via paracrine effect on H₃ receptor. Others showed that endothelins inhibited the secretion of somatostatin via endothelin receptors^[18-23].

In histocyte, there are often different granules that are important symbols of classification. This includes neurosecretory granule of 80-600 nm with an electron-densed core, highly electron-densed zymogen granule of 1-2 μ m, large and light mucus granules and endocrine secretory granules. Although some endocrine secretory granules in endocrine cells had definite characteristics and are somewhat significant to evaluate the type of such endocrine cells, it was difficult to differentiate the features of endocrine simply according to endocrine cells and their secretory granules^[24-28].

Colloidal gold immunoelectron microscopic technique is the advanced method for microcosmic morphology. The colloidal gold probe is of high specification, high resolution, accurate localization and accurate quantity. The significance of colloidal gold immunoelectron microscopy is similar to common immunohistochemistry in testing specific antigens expressed in target cells. But it could not be more useful for immunoelectron microscopy to study the localization or the quantitative analysis of antigens at the ultrastructural level. There are many intervening factors in immunoelectron microscopy, the most important one is to protect the activity of antigen. In this aspect, improvement has been made in manipulating the integrating of samples, the fixative and embedding medium, the time of fixation, the temperature of aggregation, the purity and diluting ratio of antibody and colloidal gold, as well as the time of incubation^[29-32].

On the whole, the result was satisfactory. The ultrastructure of G cells and D cells was well protected. The ultrastructures of secretory granules of both gastrin and somatostatin were definitely localized. The secretory granules of gastrin in cytoplasm of G cells were also found in the nuclei of G cells. The secretory granules of somatostatin in cytoplasm of D cells were also found in the nuclei of D cells. Therefore, the conclusion is thus made that there are secretory granules of gastrin or somatostatin in nuclei of G cells or D cells. After they are gradually matured, the secretory granules penetrate the nuclear pores into cytoplasm. At last, gastrin or

somatostatin is secreted through the basement membrane into intercellular substances, playing their physiological roles. The lobe-like or island-like congeries of colloidal gold observed in G cells and D cells are in coincidence with the existing patterns of the secretory granules of gastrin or somatostatin. In our opinion, the size of secretory granules in congeries of colloidal gold could be subjected to quantitative analysis, though the quantitative scale of each piece of colloidal gold to bind gastrin or somatostatin has not been exactly decided. In this sense, the specific significance of colloidal gold number in congeries of G cells or D cells remains to be precisely interpreted.

REFERENCES

- 1 **Larsson LI**. Developmental biology of gastrin and somatostatin cells in the antropyloric mucosa of the stomach. *Microsc Res Tech* 2000; **48**: 272-281
- 2 **Portela-Gomes GM**, Albuquerque JP, Ferra MA. Serotonin and gastrin cells in rat gastrointestinal tract after thyroparathyroidectomy and induced hyperthyroidism. *Dig Dis Sci* 2000; **45**: 730-735
- 3 **Sun FP**, Song YG, Cheng W, Zhao T, Yao YL. Gastrin, somatostatin, G and D cells of gastric ulcer in rats. *World J Gastroenterol* 2002; **8**: 375-378
- 4 **Yao YL**, Xu B, Zhang WD, Song YG. Gastrin, somatostatin, and experimental disturbance of the gastrointestinal tract in rats. *World J Gastroenterol* 2001; **7**: 399-402
- 5 **Caplin ME**, Clarke P, Grimes S, Dhillon AP, Khan K, Savage K, Lewin J, Michaeli D, Pounder RE, Watson SA. Demonstration of new sites of expression of the CCK-B/gastrin receptor in pancreatic acinar AR42J cells using immunoelectron microscopy. *Regul Pept* 1999; **84**: 81-89
- 6 **Sereti E**, Gavril A, Agnantis N, Golematis VC, Voloudakis-Baltatzis IE. Immunoelectron study of somatostatin, gastrin and glucagon in human colorectal adenocarcinomas and liver metastases. *Anticancer Res* 2002; **22**: 2117-2123
- 7 **Takahashi M**, Hoshii Y, Kawano H, Setoguchi M, Gondo T, Yamashita Y, Nakayasu K, Kamei T, Ishihara T. Multihormone-producing islet cell tumor of the pancreas associated with somatostatin-immunoreactive amyloid: immunohistochemical and immunoelectron microscopic studies. *Am J Surg Pathol* 1998; **22**: 360-367
- 8 **Stahlman MT**, Gray ME. Immunogold EM localization of neurochemicals in human pulmonary neuroendocrine cells. *Microsc Res Tech* 1997; **37**: 77-91
- 9 **Bakke I**, Qvigstad G, Sandvik AK, Waldum HL. The CCK-2 receptor is located on the ECL cell, but not on the parietal cell. *Scand J Gastroenterol* 2001; **36**: 1128-1133
- 10 **Karam SM**, Alexander G. Blocking of histamine H2 receptors enhances parietal cell degeneration in the mouse stomach. *Histol Histopathol* 2001; **16**: 469-480
- 11 **Okamoto CT**, Forte JG. Vesicular trafficking machinery, the actin cytoskeleton, and H⁺-K⁺-ATPase recycling in the gastric parietal cell. *J Physiol* 2001; **532**(Pt 2): 287-296
- 12 **Buchan AM**, Squires PE, Ring M, Meloche RM. Mechanism of action of the calcium-sensing receptor in human antral gastrin cells. *Gastroenterology* 2001; **120**: 1128-1139
- 13 **Koh TJ**, Chen D. Gastrin as a growth factor in the gastrointestinal tract. *Regul Pept* 2000; **93**: 37-44
- 14 **Cui GL**, Sandvik AK, Munkvold B, Waldum HL. Effects of anaesthetic agents on gastrin-stimulated and histamine-stimulated gastric acid secretion in the totally isolated vascularly perfused rat stomach. *Scand J Gastroenterol* 2002; **37**: 750-753
- 15 **Kirton CM**, Wang T, Dockray GJ. Regulation of parietal cell migration by gastrin in the mouse. *Am J Physiol Gastrointest Liver Physiol* 2002; **283**: G787-793
- 16 **Cobb S**, Wood T, Tessarollo L, Velasco M, Given R, Varro A, Tarasova N, Singh P. Deletion of functional gastrin gene markedly increases colon carcinogenesis in response to azoxymethane in mice. *Gastroenterology* 2002; **123**: 516-530
- 17 **Pagliocca A**, Wroblewski LE, Ashcroft FJ, Noble PJ, Dockray GJ, Varro A. Stimulation of the gastrin-cholecystokinin(B) receptor promotes branching morphogenesis in gastric AGS cells. *Am J Physiol Gastrointest Liver Physiol* 2002; **283**: G292-299

- 18 **Zavros Y**, Paterson A, Lambert J, Shulkes A. Expression of progastrin-derived peptides and somatostatin in fundus and antrum of nonulcer dyspepsia subjects with and without *Helicobacter pylori* infection. *Dig Dis Sci* 2000; **45**: 2058-2064
- 19 **Iyo T**, Kaneko H, Konagaya T, Mori S, Kotera H, Uruma M, Rhue N, Shimizu T, Imada A, Kusugami K, Mitsuma T. Effect of intragastric ammonia on gastrin-, somatostatin- and somatostatin receptor subtype 2 positive-cells in rat antral mucosa. *Life Sci* 1999; **64**: 2497-2504
- 20 **Zhang QX**, Dou YL, Shi XY, Ding Y. Expression of somatostatin mRNA in various differentiated types of gastric carcinoma. *World J Gastroenterol* 1998; **4**: 48-51
- 21 **Arebi N**, Healey ZV, Bliss PW, Ghatei M, Van Noorden S, Playford RJ, Calam J. Nitric oxide regulates the release of somatostatin from cultured gastric rabbit primary D-cells. *Gastroenterology* 2002; **123**: 566-576
- 22 **Raderer M**, Traub T, Formanek M, Virgolini I, Osterreicher C, Fiebiger W, Penz M, Jager U, Pont J, Chott A, Kurtaran A. Somatostatin-receptor scintigraphy for staging and follow-up of patients with extraintestinal marginal zone B-cell lymphoma of the mucosa associated lymphoid tissue (MALT)-type. *Br J Cancer* 2001; **85**: 1462-1466
- 23 **Lippl F**, Schusdziarra V, Allescher HD. Effect of endomorphin on somatostatin secretion in the isolated perfused rat stomach. *Neuropeptides* 2001; **35**: 303-309
- 24 **Varro A**, Dockray GJ. Post-translational processing of progastrin: inhibition of cleavage, phosphorylation and sulphation by brefeldin A. *Biochem J* 1993; **295**(Pt 3): 813-819
- 25 **Gromada J**, Hoy M, Buschard K, Salehi A, Rorsman P. Somatostatin inhibits exocytosis in rat pancreatic alpha-cells by G(i2)-dependent activation of calcineurin and depriming of secretory granules. *J Physiol* 2001; **535**(Pt 2): 519-532
- 26 **Patel YC**, Galanopoulou AS, Rabbani SN, Liu JL, Ravazzola M, Amherdt M. Somatostatin-14, somatostatin-28, and prosomatostatin [1-10] are independently and efficiently processed from prosomatostatin in the constitutive secretory pathway in islet somatostatin tumor cells (1027B2). *Mol Cell Endocrinol* 1997; **131**: 183-194
- 27 **Konda Y**, Kamimura H, Yokota H, Hayashi N, Sugano K, Takeuchi T. Gastrin stimulates the growth of gastric pit with less-differentiated features. *Am J Physiol* 1999; **277**(4 Pt 1): G773-784
- 28 **Bakke I**, Qvigstad G, Brenna E, Sandvik AK, Waldum HL. Gastrin has a specific proliferative effect on the rat enterochromaffin-like cell, but not on the parietal cell: a study by elutriation centrifugation. *Acta Physiol Scand* 2000; **169**: 29-37
- 29 **Sierralta WD**. Immunoelectron microscopy in embryos. *Methods* 2001; **24**: 61-69
- 30 **Renno WM**. Post-embedding double-gold labeling immunoelectron microscopic co-localization of neurotransmitters in the rat brain. *Neurobiology* 2001; **9**: 91-106
- 31 **Dolapchieva S**, Eggers R, Kuhnel W. N- and R-cadherins expression in the rat sciatic nerve demonstrated by postembedding immunogold method on semi-thin sections. *Ann Anat* 2001; **183**: 405-411
- 32 **Ishida S**, Kaito M, Kohara M, Tsukiyama-Kohora K, Fujita N, Ikoma J, Adachi Y, Watanabe S. Hepatitis C virus core particle detected by immunoelectron microscopy and optical rotation technique. *Hepatol Res* 2001; **20**: 335-347

Edited by Wang XL

Effect of complex amino acid imbalance on growth of tumor in tumor-bearing rats

Yin-Cheng He, Yuan-Hong Wang, Jun Cao, Ji-Wei Chen, Ding-Yu Pan, Ya-Kui Zhou

Yin-Cheng He, Jun Cao, Ji-Wei Chen, Ding-Yu Pan, Ya-Kui Zhou, Department of General Surgery, Zhongnan Hospital, Wuhan University, Wuhan 430071, Hubei Province, China

Yuan-Hong Wang, Wuhan Centre for Disease Prevention and Control, Wuhan 430022, Hubei Province, China

Supported by grants from Hubei Provincial Health Bureau, No. W98016 and the Education Committee of Hubei Province, No. 2001A14005

Correspondence to: Dr. Yin-Cheng He, Department of General Surgery, Zhongnan Hospital, Wuhan University, Wuhan 430071, Hubei Province, China. w030508h@public.wh.hb.cn

Telephone: +86-27-67812963

Received: 2003-06-05 **Accepted:** 2003-08-16

Abstract

AIM: To investigate the effect of complex amino acid imbalance on the growth of tumor in tumor-bearing (TB) rats.

METHODS: Sprague-Dawley (SD) rats underwent jejunostomy for nutritional support. A suspension of Walker-256 carcinosarcoma cells was subcutaneously inoculated. TB rats were randomly divided into groups A, B, C and D according to the formula of amino acids in enteral nutritional solutions, respectively. TB rats received jejunal feedings supplemented with balanced amino acids (group A), methionine-depleted amino acids (group B), valine-depleted amino acids (group C) and methionine- and valine-depleted complex amino acid imbalance (group D) for 10 days. Tumor volume, inhibitory rates of tumor, cell cycle and life span of TB rats were investigated.

RESULTS: The G_0/G_1 ratio of tumor cells in group D (80.5 ± 9.0 %) was higher than that in groups A, B and C which was 67.0 ± 5.1 %, 78.9 ± 8.5 %, 69.2 ± 6.2 %, respectively ($P < 0.05$). The ratio of S/G_2M and PI in group D were lower than those in groups A, B and C. The inhibitory rate of tumor in groups B, C and D was 37.2 %, 33.3 % and 43.9 %, respectively ($P < 0.05$). The life span of TB rats in group D was significantly longer than that in groups B, C, and A.

CONCLUSION: Methionine/valine-depleted amino acid imbalance can inhibit tumor growth. Complex amino acids of methionine and valine depleted imbalance have stronger inhibitory effects on tumor growth.

He YC, Wang YH, Cao J, Chen JW, Pan DY, Zhou YK. Effect of complex amino acid imbalance on growth of tumor in tumor-bearing rats. *World J Gastroenterol* 2003; 9(12): 2772-2775 <http://www.wjgnet.com/1007-9327/9/2772.asp>

INTRODUCTION

Malnutrition is encountered everyday in cancer patients and is associated with severe protein-amino acid metabolic disorder, uncorrectable negative nitrogen balance and low immune function^[1-6]. Enteral nutrition (EN) and parenteral nutrition (PN)

are both safe and effective methods of administering nutrients in cancer patients^[7-9]. But PN with amino acid balanced solutions may prompt tumor growth^[10-12]. Based on Harper's concept of amino acid imbalance, EN/TPN preparations with depleted or enriched specific amino acids produce tumor growth inhibition^[13-18]. Previously, we found methionine/valine-depleted (0), low tyrosine (0.5 g/L) and arginine-enriched (6 g/L) complex amino acid imbalance solutions were the most rational formula in tumor-bearing (TB) rats^[19]. In this study, we aimed to investigate the effect of complex amino acid imbalance on the growth of tumor.

MATERIALS AND METHODS

Animals

SD rats weighing 170 ± 20 g were purchased from the Experimental Animal Center of Wuhan University (Wuhan, China) and fed with a stock rat diet *ad libitum*. The animals were maintained on a 12-hour light/12-hour dark cycle at ambient temperature of (23 ± 2) °C and housed for 7 days before the experiment.

Catheterization of jejunostomy

After fasted for 12 hours, the rats ($n=60$) were anesthetized by intraperitoneal administration of $40 \text{ mg} \cdot \text{kg}^{-1}$ pentobarbital. They were then undergone catheterization during jejunostomy (day 0). A silicone rubber catheter with an internal diameter of 2 mm and an external diameter of 3 mm was inserted into the proximal jejunum. The catheter passed through a subcutaneous tunnel and emerged between the scapulae. The catheter was then mounted on a harness, passed through a protective coil, and connected to a swivel so that the animals could move without any restrictions in individual metabolic cages. The cannulation system consisted of a microinfusion pump, a swivel, rat-harness and a silicone-tube-jejunostomy. The rats were fasted for 48 hours after operation but were provided with water *ad libitum*, and then given normal rat diet.

Preparation of TB rats

Walker-256 carcinosarcoma cells were purchased from Chinese Center of Culture Preservation. On day 0, the rats were subcutaneously inoculated in the right flank with 10^7 tumor cells of approximately 0.1 ml of cell suspension.

Tumor weights and inhibitory rates of tumor

Tumors were palpable 7 days after transplantation. Measurements were made at the tumor site. The lengths of the major, minor axes and depth were measured with calipers. Growth of the tumor was evaluated every 3 days. Tumor volumes during experiments were calculated according to the following equation: $V = LWDp/6$. Where V is the tumor volume (mm^3), L is the length, W is the width and D is the depth of a solid tumor (mm). Inhibitory rates of tumor = (tumor volume of control group - tumor volume of experimental group)/tumor volume of control group $\times 100$ %.

Experimental groups and jejunal feeding

On day 8, 48 TB rats were randomly divided into four groups

(12 rats per group) according to the solutions administered: an amino acid balance solution (group A), methionine-depleted amino acid solution (group B), valine-depleted amino acid solution (group C), and methionine and valine-depleted complex amino acid solution (group D). They were administered enteral nutritional solutions (jejunal feeding) for 10 days. During EN, the rats were individually housed in metabolic cages. The compositions of EN solution infused to each rat are summarized in Table 1.

Administration methods

TB rats received continuous jejunal tube infusion for nutritional support at a daily dose of 330 ml·kg⁻¹, by means of a microinfusion pump (Sino-Swed Pharmaceutical Corp. Ltd. China). Non-protein calorie per day was approximately 1 104 K J·kg⁻¹. TB rats were not fed during the entire infusion experiment, however, they had free access to water.

Compositions of amino acid solutions

Table 1 lists the components of amino acid solution in four groups.

Table 1 Compositions of amino acid solution (g·L⁻¹)

Amino acids	Group A	Group B	Group C	Group D
Isoleucine	5.5	5.5	5.5	5.5
Leucine	7.5	7.5	7.5	7.5
Lysine	7.0	7.0	7.0	7.0
Methionine	6.0	—	6.0	—
Phenylalanine	4.0	4.0	4.0	4.0
Threonine	5.0	5.0	5.0	5.0
Tryptophan	1.5	1.5	1.5	1.5
Valine	6.0	6.0	—	—
Arginine	6.0	6.0	6.0	6.0
Histidine	3.0	3.0	3.0	3.0
Proline	4.0	4.0	4.0	4.0
Tyrosine	1.0	1.0	1.0	1.0
Alanine	20.0	20.0	20.0	20.0
Glycine	7.5	7.5	7.5	7.5
Aspartic acid	4.0	4.0	4.0	4.0
Total amino acid	88.0	82.0	82.0	76.0
Total nitrogen	14.1	13.1	13.1	12.2

Compositions of EN solution

1 000 ml EN solution was composed of 350 ml of amino acid preparation (Table 1) supplemented with 300 ml of 50 % glucose, 100 ml of 20 % Intralipid (Sino-Swed Pharmaceutical Corp. Ltd. China), 20 ml of Soluvit, 20 ml of Vitalipid, 20 ml of Addamel and 190 ml of 0.9 % saline.

Specimen sampling

At the end of an administration period, 6 rats per group were respectively killed by cervical dislocation. The whole tumor was dissected and examined.

Cell cycle position measurement

Sections about 50 μm thick were cut from tumor tissues and washed 3 times in phosphate-buffered saline. Cell kinetics were measured by flow cytometry (FCM, PASIII, Partec Company, Germany).

Life span of TB rats

The remaining 6 rats per group were given solid food (Experimental Animal Center of Wuhan University, Wuhan,

China) and water *ad libitum* according to their body weight until they died of advanced cancer. The life span of each rat in terms of median survival time (MST) was observed.

Statistical analysis

All results were presented as mean ±SD. Comparisons of the four groups were made using Uni-variate ANOVA test. The difference was considered significant when *P* value was less than 0.05.

RESULTS

Animals

Two rats in groups A, C and two rats in group D died of intestinal fistula, diarrhea, infection of abdominal cavity during enteral nutrition, respectively.

Changes in tumor cell cycle

Tumor-selective cell cycle arrest occurred in the S-G₂ phase during methionine depleted enteral nutrition. The distribution of cancer cell cycle was not obviously affected during valine starvation. The percentages of tumor cells in G₀G₁ phase in groups B and D were significantly higher than that in group A while the percentages of S phase cells in groups B and D were obviously lower than that in group A (*P*<0.05). There was no statistical difference between the percentages of G₂M cells in groups B and D and that in group A (*P*>0.05, Table 2).

Table 2 Distribution of cancer cell cycle after EN treatment (%)

Phase	Group A	Group B	Group C	Group D
G ₀ G ₁	67.0±5.1	78.9±8.5 ^{ac}	69.2±6.2 ^b	80.5±9.0 ^{ac}
S	20.1±1.8	11.8±2.9 ^{ac}	19.9±3.0 ^b	10.2±2.1 ^{ac}
G ₂ +M	12.9±3.2	9.2±3.1	10.9±2.5	9.4±3.8
PI(S+G ₂ +M)	33.0±4.3	21.0±5.0 ^{ac}	30.8±5.6 ^b	20.5±2.8 ^{ac}

^a*P*<0.05, vs group A, ^b*P*<0.05, vs group B, ^c*P*<0.05, vs group C.

Tumor volumes and inhibitory rates of tumor

Tumor volume had no statistical difference among each group before treatment. On day 10 of enteral nutrition, tumor growth in amino acid imbalance groups (groups B, C and D) was significantly lower than that in control group. The most remarkable inhibitory effect on tumor growth was found in complex amino acid imbalance group (group D) (*P*<0.05). The inhibitory rate of tumor (IRT) in groups B, C and D was respectively 37.2 %, 33.3 % and 43.9 % (Table 3).

Table 3 Changes in tumor volumes, IRT and MST before and after treatment

Group	Tumor volumes		IRT(%)	MST(d)
	Before	After		
Group A	0.028±0.015	2.85±0.43	...	26.8±1.5
Group B	0.039±0.010	1.79±0.56 ^a	37.2	32.0±2.6 ^a
Group C	0.033±0.020	1.90±0.30 ^{ab}	33.3	35.6±3.2 ^a
Group D	0.031±0.011	1.60±0.40 ^{abc}	43.9	39.4±3.0 ^{abc}

^a*P*<0.05, vs group A, ^b*P*<0.05, vs group B, ^c*P*<0.05, vs group C.

Life span of TB rats

The median survival time (MST) in complex amino acid imbalance group was (39.4±3.0) days, as compared with (32.0±2.6) days in methionine-depleted group and (35.6±3.2) days in valine-depleted group (Table 3).

DISCUSSION

Influence of balanced amino acids on tumor growth

Compared with normal cells, the metabolism of tumor cells is significantly accelerated. *In vivo*, cancer cells have been known to have higher levels of protein synthesis, accompanied by a more active uptake of glucose and amino acids (nitrogen trap), and undergo more rapid differentiation and proliferation than healthy cells^[20]. Amino acids are important materials of protein synthesis. Supplement of balanced amino acids results in the greatest increase of tumor cell cycles, thus tumor tissues compete with host tissues for nitrogen substrates. Nucleic acid and protein synthesis are increased, and tumor growth is accelerated. Table 3 indicates the experimental results of the anticancer effects of various amino acid imbalance solutions. As clearly shown in this table, tumor volume was especially large, and the median survival time was short after TB rats were administrated with balanced amino acid solutions (group A).

Influence of methionine/valine-depleted amino acid imbalance on tumor growth

Methionine dependency of many malignant tumor cells has been demonstrated in previous studies. That is to say, these cells were arrested in late S/G₂ phase in methionine free cell culture media, and tumor cellular proliferation was inhibited, and normal cells were methionine independent after methionine was replaced by homocysteine^[21-26]. Methionine is the principal biological methyl donor via S-adenosyl-L-methionine (SAM). SAM can easily transfer its methyl group to a large variety of acceptor substrates including rRNA, tRNA, mRNA, DNA, proteins, phospholipids, biological amines, and a long list of small molecules. Methionine dependency might be due to overutilization of methionine for transmethylation reactions resulting in a low free methionine pool and a low S-adenosylmethionine/S-adenosylhomocysteine ratio^[27-31]. This directly inhibits the activity of transmethylation, thereby methionine depleted enteral nutrition can decrease methylation reaction of tumor tissues and lead to further reduction in nucleic acid synthesis and inhibition of cancer growth at molecular levels.

Our study demonstrated that tumor growth in group B was significantly slower than that in control group, the liver and peritoneum metastasis of cancer was much less in group B. It suggested that the invasive ability for metastasis be suppressed during methionine starvation. Breillout *et al* considered that methionine depletion disturbed the membrane lipids of tumor cells and inhibited their metastatic ability^[32].

It was also found that valine depleted imbalance solution (group C) had a great inhibitory effect on Walker-256 carcinosarcoma cells. One possible mechanism was the alterations of intracellular protein synthesis due to deprivation of essential amino acids (Valine)^[33-35]. Another possible mechanism seemed to be the inhibitory effect on the production of prolactin, which was likely to participate in tumor growth^[20].

Influence of complex amino acid imbalance on tumor growth

As shown in Table 3, the most remarkable inhibitory effect on cancer growth was seen in the methionine/valine depleted complex amino acid imbalance group, followed by the methionine depleted imbalance group and then the valine depleted group. It suggested that complex amino acid imbalance solutions had the most strong anticancer effects. However, are we able to prevent the development of side effects of complex imbalance due to starvation of essential amino acids? This still needs further studies.

REFERENCES

- 1 Nitenberg G, Raynard B. Nutritional support of the cancer patient: issues and dilemmas. *Crit Rev Oncol Hematol* 2000; **34**: 137-168
- 2 Xiao HB, Cao WX, Yin HR, Lin YZ, Ye SH. Influence of L-methionine-deprived total parenteral nutrition with 5-fluorouracil on gastric cancer and host metabolism. *World J Gastroenterol* 2001; **7**: 698-701
- 3 Karayiannakis AJ, Syrigos KN, Polychronidis A, Pitiakoudis M, Bounovas A, Simopoulos K. Serum levels of tumor necrosis factor-alpha and nutritional status in pancreatic cancer patients. *Anticancer Res* 2001; **21**: 1355-1358
- 4 Federico A, Iodice P, Federico P, Del Rio A, Mellone MC, Catalano G, Federico P. Effects of selenium and zinc supplementation on nutritional status in patients with cancer of digestive tract. *Eur J Clin Nutr* 2001; **55**: 293-297
- 5 Hatada T, Miki C. Nutritional status and postoperative cytokine response in colorectal cancer patients. *Cytokine* 2000; **12**: 1331-1336
- 6 Jagoe RT, Goodship TH, Gibson GJ. Nutritional status of patients undergoing lung cancer operations. *Ann Thorac Surg* 2001; **71**: 929-935
- 7 Buchman AL. Must every cancer patient die with a central venous catheter? *Clin Nutr* 2002; **21**: 269-271
- 8 Bozzetti F, Cozzaglio L, Biganzoli E, Chiavenna G, de Cicco M, Donati D, Gilli G, Percolla S, Pironi L. Quality of life and length of survival in advanced cancer patients on home parenteral nutrition. *Clin Nutr* 2002; **21**: 281-288
- 9 Buchman AL. Enteral versus parenteral nutrition following resection in malnourished patients with gastrointestinal cancer. *Curr Gastroenterol Rep* 2002; **4**: 322-323
- 10 Bozzetti F, Gavazzi C, Cozzaglio L, Costa A, Spinelli P, Viola G. Total parenteral nutrition and tumor growth in malnourished patients with gastric cancer. *Tumori* 1999; **85**: 163-166
- 11 Sasamura T, Matsuda A, Kokuba Y. Tumor growth inhibition and nutritional effect of d-amino acid solution in AH109A hepatoma-bearing rats. *J Nutr Sci Vitaminol* 1998; **44**: 79-87
- 12 Forchielli ML, Paolucci G, Lo CW. Total parenteral nutrition and home parenteral nutrition: an effective combination to sustain malnourished children with cancer. *Nutr Rev* 1999; **57**: 15-20
- 13 Komatsu H, Nishihira T, Chin M, Doi H, Shineha R, Mori S, Satomi S. Effect of valine depleted total parenteral nutrition on fatty liver development in tumor-bearing rats. *Nutrition* 1998; **14**: 276-281
- 14 Cao WX, Cheng QM, Fei XF, Li SF, Yin HR, Lin YZ. A study of preoperative methionine-depleting parenteral nutrition plus chemotherapy in gastric cancer patients. *World J Gastroenterol* 2000; **6**: 255-258
- 15 Nagahama T, Goseki N, Endo M. Doxorubicin and vincristine with methionine depletion contributed to survival in the Yoshida sarcoma bearing rats. *Anticancer Res* 1998; **18**: 25-31
- 16 Tang B, Li YN, Kruger WD. Defects in methylthioadenosine phosphorylase are associated with but not responsible for methionine-dependent tumor cell growth. *Cancer Res* 2000; **60**: 5543-5547
- 17 Komatsu H, Nishihira T, Chin M, Doi H, Shineha R, Mori S, Satomi S. Effects of caloric intake on anticancer therapy in rats with valine-depleted amino acid imbalance. *Nutr Cancer* 1997; **28**: 107-112
- 18 Yoshida S, Ohta J, Shirouzu Y, Ishibashi N, Harada Y, Yamana H, Shirouzu K. Effect of methionine-free total parenteral nutrition and insulin-like growth factor I on tumor growth in rats. *Am J Physiol* 1997; **273**(1 Pt 1): E10-16
- 19 Chen JW, He YC, Wang YH, Zhou YK, Liu QY, Shi HA. Rational formula of amino acids for nutritional supports in tumor-bearing rats. *Zhonghua Shiyan Waikexi* 2001; **18**: 378
- 20 Nishihira T, Takagi T, Kawarabayashi Y, Izumi U, Ohkuma S, Koike N, Toyoda T, Mori S. Anti-cancer therapy with valine-depleted amino acid imbalance solution. *Tohoku J Exp Med* 1988; **156**: 259-270
- 21 Sasamura T, Matsuda A, Kokuba Y. Nutritional effects of a D-methionine-containing solution on AH109A hepatoma-bearing rats. *Biosci Biotechnol Biochem* 1998; **62**: 2418-2420
- 22 Hoshiya Y, Kubota T, Inada T, Kitajima M, Hoffman RM. Methionine-depletion modulates the efficacy of 5-fluorouracil in human gastric cancer in nude mice. *Anticancer Res* 1997; **17**: 4371-4375

- 23 **Poirson-Bichat F**, Goncalves RA, Miccoli L, Dutrillaux B, Poupon MF. Methionine depletion enhances the antitumoral efficacy of cytotoxic agents in drug-resistant human tumor xenografts. *Clin Cancer Res* 2000; **6**: 643-653
- 24 **Poirson-Bichat F**, Lopez R, Bras Goncalves RA, Miccoli L, Bourgeois Y, Demerseman P, Poisson M, Dutrillaux B, Poupon MF. Methionine deprivation and methionine analogs inhibit cell proliferation and growth of human xenografted gliomas. *Life Sci* 1997; **60**: 919-931
- 25 **Sasamura T**, Matsuda A, Kokuba Y. Effects of D-methionine-containing solution on tumor cell growth *in vitro*. *Arzneimittel Forschung* 1999; **49**: 541-543
- 26 **Cao WX**, Ou JM, Fei XF, Zhu ZG, Yin HR, Yan M, Lin YZ. Methionine-dependence and combination chemotherapy on human gastric cancer cells *in vitro*. *World J Gastroenterol* 2002; **8**: 230-232
- 27 **Lu SC**. Methionine adenosyltransferase and liver disease: It's all about SMA. *Gastroenterology* 1998; **114**: 403-407
- 28 **Zhu SS**, Xiao SD, Chen ZP, Shi Y, Fang JY, Li RR, Mason JB. DNA methylation and folate metabolism in gastric cancer. *World J Gastroenterol* 2000; **6**(Suppl 3): 18
- 29 **Avila MA**, Carretero MV, Rodriguez EN, Mato JM. Regulation by hypoxia of methionine adenosyltransferase activity and gene expression in rat hepatocytes. *Gastroenterology* 1998; **114**: 364-371
- 30 **Wang XY**, Li N, Gu J, Li WQ, Li JS. The effects of the formula of amino acids enriched BCAA on nutritional support in traumatic patients. *World J Gastroenterol* 2003; **9**: 599-602
- 31 **Yoshioka T**, Wada T, Uchida N, Maki H, Yoshida H, Ide N, Kasai H, Hojo K, Shono K, Maekawa R, Yagi S, Hoffman RM, Sugita K. Anticancer efficacy *in vivo* and *in vitro*, synergy with 5-fluorouracil, and safety of recombinant methioninase. *Cancer Res* 1998; **58**: 2583-2587
- 32 **Breillout F**, Antoine E, Poupon MF. Methionine dependency of malignant tumors: a possible approach for therapy. *J Natl Cancer Inst* 1990; **82**: 1628-1632
- 33 **Samuels SE**, Knowles AL, Tilignac T, Debiton E, Madelmont JC, Attaix D. Protein metabolism in the small intestine during cancer cachexia and chemotherapy in mice. *Cancer Res* 2000; **60**: 4968-4974
- 34 **Poirson-Bichat F**, Gonfalone G, Bras-Goncalves RA, Dutrillaux B, Poupon MF. Growth of methionine-dependent human prostate cancer (PC-3) is inhibited by ethionine combined with methionine starvation. *Br J Cancer* 1997; **75**: 1605-1612
- 35 **He YC**, Cao J, Chen JW, Pan DY, Zhou YK. Influence of methionine/valine-depleted enteral nutrition on nucleic acid and protein metabolism in tumor-bearing rats. *World J Gastroenterol* 2003; **9**: 771-774

Edited by Zhu LH and Wang XL

Alterations of intestinal mucosa structure and barrier function following traumatic brain injury in rats

Chun-Hua Hang, Ji-Xin Shi, Jie-Shou Li, Wei Wu, Hong-Xia Yin

Chun-Hua Hang, Ji-Xin Shi, Wei Wu, Hong-Xia Yin, Medical College of Nanjing University; Department of Neurosurgery, Jinling Hospital, Nanjing 210002, Jiangsu Province, China

Jie-Shou Li, Research Institute of General Surgery, Jinling Hospital, Clinical School of Medicine, Nanjing University, Nanjing 210002, Jiangsu Province, China

Supported by the Scientific Research Foundation of the Chinese PLA Key Medical Programs during the 10th Five-Year Plan Period, No. 01Z011

Correspondence to: Chun-Hua Hang, Department of Neurosurgery, Jinling Hospital, 305 East Zhongshan Road, Nanjing 210002, Jiangsu Province, China. hang1965@public1.ptt.js.cn

Telephone: +86-25-4597342 **Fax:** +86-25-4810987

Received: 2003-07-12 **Accepted:** 2003-07-30

Abstract

AIM: Gastrointestinal dysfunction is a common complication in patients with traumatic brain injury (TBI). However, the effect of traumatic brain injury on intestinal mucosa has not been studied previously. The aim of the current study was to explore the alterations of intestinal mucosa morphology and barrier function, and to determine how rapidly the impairment of gut barrier function occurs and how long it persists following traumatic brain injury.

METHODS: Male Wistar rats were randomly divided into six groups (6 rats each group) including controls without brain injury and traumatic brain injury groups at hours 3, 12, 24, and 72, and on day 7. The intestinal mucosa structure was detected by histopathological examination and electron microscopy. Gut barrier dysfunction was evaluated by detecting serum endotoxin and intestinal permeability. The level of serum endotoxin and intestinal permeability was measured by using chromogenic limulus amoebocyte lysate and lactulose/mannitol (L/M) ratio, respectively.

RESULTS: After traumatic brain injury, the histopathological alterations of gut mucosa occurred rapidly as early as 3 hours and progressed to a serious state, including shedding of epithelial cells, fracture of villi, focal ulcer, fusion of adjacent villi, dilation of central chyle duct, mucosal atrophy, and vascular dilation, congestion and edema in the villous interstitium and lamina propria. Apoptosis of epithelial cells, fracture and sparseness of microvilli, loss of tight junction between enterocytes, damage of mitochondria and endoplasm, were found by electron microscopy. The villous height, crypt depth and surface area in jejunum decreased progressively with the time of brain injury. As compared with that of control group (183.7±41.8 EU/L), serum endotoxin level was significantly increased at 3, 12, and 24 hours following TBI (434.8±54.9 EU/L, 324.2±61.7 EU/L and 303.3±60.2 EU/L, respectively), and peaked at 72 hours (560.5±76.2 EU/L), then declined on day 7 (306.7±62.4 EU/L, $P<0.01$). Two peaks of serum endotoxin level were found at hours 3 and 72 following TBI. L/M ratio was also significantly higher in TBI groups than that in control group (control, 0.0172±0.0009; 12 h, 0.0303±0.0013; 24 h, 0.0354±0.0025;

72 h, 0.0736±0.0105; 7 d, 0.0588±0.0083; $P<0.01$).

CONCLUSION: Traumatic brain injury can induce significant damages of gut structure and impairment of barrier function which occur rapidly as early as 3 hours following brain injury and lasts for more than 7 days with marked mucosal atrophy.

Hang CH, Shi JX, Li JS, Wu W, Yin HX. Alterations of intestinal mucosa structure and barrier function following traumatic brain injury in rats. *World J Gastroenterol* 2003; 9(12): 2776-2781 <http://www.wjgnet.com/1007-9327/9/2776.asp>

INTRODUCTION

Gastrointestinal dysfunction occurs frequently in patients with traumatic brain injury (TBI)^[1]. Dysfunction of the different segments of gastrointestinal tract leads to corresponding symptoms such as gastrointestinal bleeding^[2-4], gastric reflux^[5,6] and decreased intestinal peristalsis^[7,8], mainly due to mucosal damage and alteration of gastrointestinal motility^[9]. Studies on gastrointestinal dysfunction associated with head injury in the literature concentrated on the gastric mucosa, gastric emptying and lower esophageal sphincter tone^[2-8]. However, the effect of TBI on intestinal mucosa has not been studied to date. Therefore, the alterations of intestinal mucosa morphology and barrier function following TBI remain unclear.

It is generally accepted that the intestine may serve as an important organ in the development of severe complications under critically ill conditions, including trauma, burns, shock, etc.^[10-12]. Major trauma and shock may initiate a cascade of intestinal events such as intestinal cytokine response^[13], increased intestinal permeability^[14,15], translocation of intestinal bacteria and endotoxin^[10,16], leading to systemic inflammatory response syndrome (SIRS) and sepsis with subsequent multiple organ failure^[12]. TBI is a severe pathological stress and critically ill condition usually complicated with gastric stress ulcer^[17]. Therefore, we hypothesized that TBI could also lead to significant gut structural alterations and barrier dysfunction as mentioned above in the same mechanism as trauma, hemorrhagic shock and burns. Additionally, brain-gut axis^[18,19] and hypothalamic-pituitary adrenal axis^[20] may also play a certain role in the development of gut dysfunction following TBI, but the potential mechanism underlying this action is not clear.

Studies have shown that cerebral inflammation following TBI occurs frequently and is associated with adverse outcomes^[21,22]. Bacterial endotoxin (lipopolysaccharide, LPS) may exacerbate the inflammatory response of injured brain, leading to invasion of granulocytes into the brain and breakdown of the blood-brain barrier^[23-26]. Severe extra-cerebral trauma can induce the expression of TNF- α mRNA in the brain of mice^[27]. Therefore, we suggest that intestinal cytokine, translocation of bacteria and endotoxin secondary to gut barrier dysfunction into the injured brain through blood circulation should activate the cerebral inflammatory response. Because enteral nutrition and enterogenous sepsis are two of the important factors affecting the outcomes of comatose patients with TBI, the maintenance of normal gut integrity is

believed to be beneficial in improving the outcomes of head-injured patients^[28,29].

Considering the important role of intestinal function in the rehabilitation of patients with TBI and no study reported previously on the intestinal aspects following TBI, additional studies need to be carried out to clarify the degree of mucosal damage and gut barrier dysfunction induced by TBI, and if possible, to explore the potential mechanisms that have not been interpreted yet. Therefore, we performed a series of studies on intestines of TBI rats. The purpose of this study was to explore the alterations of intestinal mucosa morphology and barrier function, and to determine how rapidly impairment of gut barrier function occurred and how long it persisted following TBI.

MATERIALS AND METHODS

Rat models of TBI

Male Wistar rats, weighing 220 g to 250 g, were purchased from Animal Center of Chinese Academy of Sciences, Shanghai, China. The rats were fed on rodent chow with free access to tap water and housed in temperature- and humidity-controlled animal quarters with a 12 hour light/dark cycle. All procedures were approved by the Institutional Animal Care Committee.

The rats were randomly divided into six groups (6 rats each group) including control group with right parietal bone window alone and no brain injury, and traumatic brain injury groups at hours 3, 12, 24, and 72, and on day 7, respectively. Following intraperitoneal anesthesia with urethane (1 000 mg.kg⁻¹), animal head was fixed in the stereotactic device. A right parietal bone window of 5 mm diameter was made under aseptic conditions with dental drill just behind the cranial coronal suture and beside midline. The dura was kept intact. Right parietal brain contusion was adopted using the impact method described by Feeney *et al.*^[30] and severe traumatic brain injury was made by dropping weight with a 4 mm impact diameter, a 5 mm depth and total impact energy of 1 000 g.cm. The control animals were killed for sample collection at 72 hours, and TBI group rats were decapitated at corresponding time points. Blood samples were obtained by right ventricle puncture and centrifuged with the plasma stored at -40 °C before the animals were sacrificed at each time point. A 3 cm segment of the jejunum 12 cm distal to Treitz ligament was taken for histopathological studies and 1 mm³ mucosa for ultrastructural observations.

Histopathological and ultrastructural examination

The 10 % buffered formalin-fixed jejunum was embedded in paraffin, sectioned at 4 µm thickness with a microtome and stained with hematoxylin and eosin. The sections were examined under light microscope. Villous height, diameter of middle villous segment and crypt depth in all tissues were

determined using the HPIAS-1000 colorful image analysis system (Champion Image Engineering Company, Wuhan, China). Villous surface area was calculated according to the following formula: surface area=πdh, (d: diameter, h: villous height). At least 10 well-oriented crypt-villous units per small intestinal sample were measured and averaged by a pathologist who was blind to animal groups.

Samples for electron microscopy were fixed in phosphate-buffered glutaraldehyde (2.5 %) and osmium tetroxide (1 %). Dehydration of the mucosa was accomplished in acetone solutions at increasing concentrations. The tissue was embedded in an epoxy resin. Semithin (1 µm) sections through the mucosa were then made and stained with toluidine blue. Then 600 angstrom-thin sections were made from a selected area of tissue defined by the semithin section, and these sections were stained with lead citrate and uranyl acetate. Ultrastructures of mucosa were observed under a transmission electron microscope (JEM-1200X).

Plasma endotoxin determination

The endotoxin content in plasma samples was assayed by the chromogenic limulus amebocyte lysate (LAL) test with a kinetic modification according to the test kit procedure.

Intestinal permeability

Intestinal permeability was quantified using the lactulose/mannitol (L/M) test as previously described^[19]. Six hours before the animals were sacrificed at each time point, the rats with their bladders emptied were given the test solution of 2.5 ml by gastric tube feeding, containing 60 mg lactulose and 30 mg mannitol. All urine was collected for 5 hours through the metabolic cage and stored at -40 °C for further analysis. Urinary lactulose and mannitol were measured using high-performance liquid chromatography (Waters Co., USA). Results were expressed as a ratio of percentage of the administered dose of the two molecules excreted.

Statistical analysis

Software SPSS 11.0 was used in the statistical analysis. Each parameter was expressed as mean ± SD, and compared using one-way ANOVA analysis of variance, followed by Tukey test. The level of significance was *P*<0.05.

RESULTS

Histopathology

Histopathological examination showed that the morphology of jejunal mucosa was approximately normal in control rats. After TBI, mucosal damage occurred as early as 3 hours and was maximal at 72 hours, then progressed to mucosal atrophy on day 7. The type of jejunal mucosa damages induced by TBI is shown in Table 1. Representative histopathologic sections of jejunal mucosa are shown in Figures 1-4.

Table 1 Main histopathological changes of jejunal mucosa after traumatic brain injury

Type of mucosal damages	Group of TBI
Shedding of epithelial cells from the top of villi	3 and 12 hours
Epithelial cell necrosis and disarrangement of villi	24 and 72 hours
Focal mucosa ulcer with exposure of submucosal interstitium	72 hours
Fusion of adjacent villi into piece	72 hours and 7 days
Dilation of central chyle duct	72 hours and 7 days
Inflammatory cell infiltration in intestinal wall	72 hours and 7 days
Mucosal atrophy	7 days
Vascular dilation, congestion and edema in villous interstitium and lamina propria	3 hours throughout 7 days

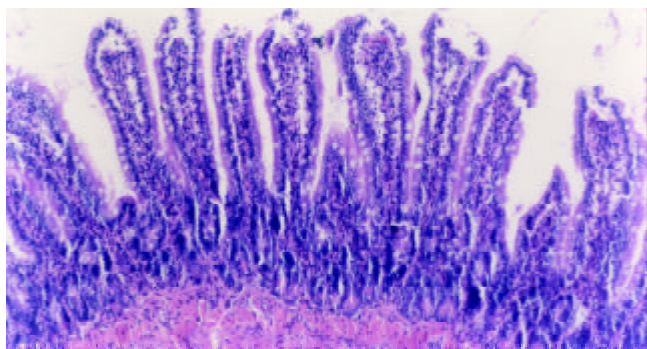


Figure 1 Epithelial cells shed from the top of villi with almost normal villous height and well defined arrangement of villi at 3 hours following TBI. H-E, magnification $\times 100$.

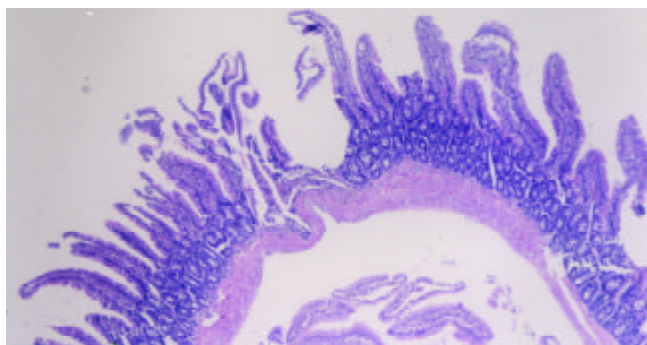


Figure 2 Markedly altered villous morphology and decreased height at 72 hours following TBI. Note the focal mucosa ulcer with exposure of submucosal interstitium and disarrangement of villi. H-E, magnification $\times 100$.

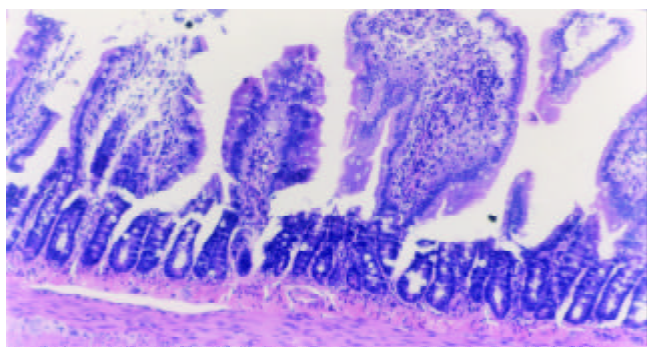


Figure 3 Marked alterations of villous morphology occurred 7 days following TBI, including mucosal atrophy, fusion of adjacent villi, inflammatory cell infiltration, and vascular dilation, congestion and edema in the villous interstitium and lamina propria. H-E, magnification $\times 100$.

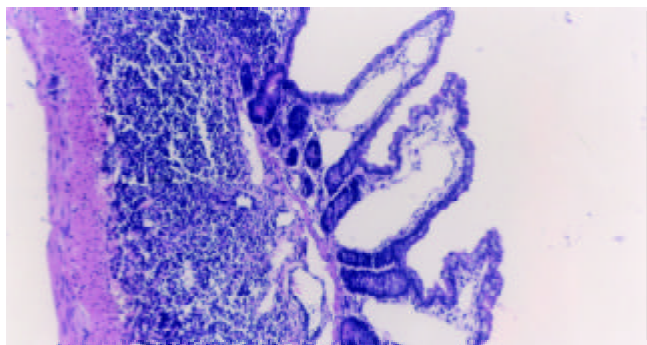


Figure 4 Dilation of central chyle duct of jejunal mucosa. H-E, magnification $\times 100$.

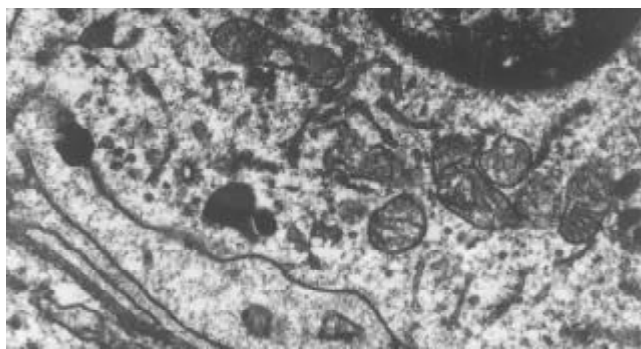


Figure 5 Reduction of mitochondrial matrix and disruption of its cristae at 72 hours following TBI. TEM, magnification $\times 15\text{ k}$.

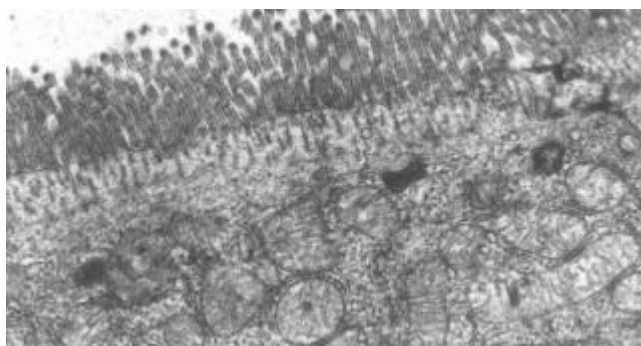


Figure 6 Ruptured, distorted and sparse microvilli at 24 hours following TBI. TEM, magnification $\times 10\text{ k}$.

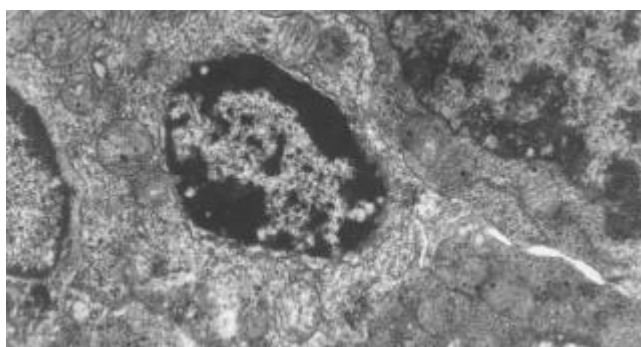


Figure 7 Apoptosis bodies in epithelial cytoplasm of jejunum following TBI. TEM, magnification $\times 8000$.

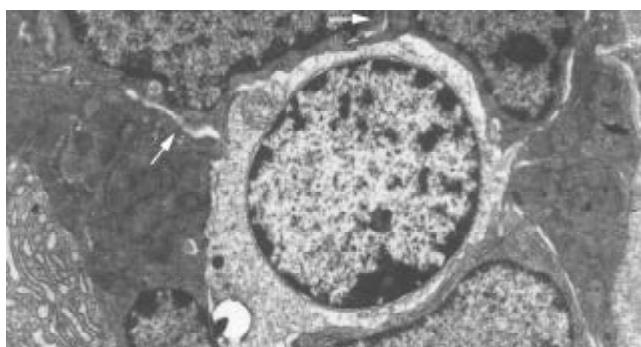


Figure 8 Disrupted and wider tight junction between epithelial cells at 72 hours and 7 days following TBI, shown as blank arrow. TEM, magnification $\times 5000$.

Histomorphometric studies

Villous height, crypt depth and villous surface area were determined as specific indices for the evaluation of mucosal

Table 2 Changes in villous height, diameter, crypt depth and surface area of mucosa

Groups	Villous height (μm)	Villous diameter (μm)	Crypt depth (μm)	Surface area (mm^2)
Control	229.2 \pm 18.1	37.4 \pm 5.5	79.3 \pm 9.6	0.0259 \pm 0.0048
TBI 3 hours	219.5 \pm 21.2	37.6 \pm 6.1	78.9 \pm 9.4	0.0258 \pm 0.0035
TBI 12 hours	214.5 \pm 22.5	35.6 \pm 3.1	74.0 \pm 6.9	0.0241 \pm 0.0037
TBI 24 hours	189.2 \pm 13.6 ^b	32.7 \pm 3.2	67.0 \pm 7.6 ^{bc}	0.0195 \pm 0.0012 ^{bc}
TBI 72 hours	150.8 \pm 10.4 ^{bc}	32.1 \pm 4.2	34.8 \pm 5.6 ^{bc}	0.0151 \pm 0.0010 ^{bc}
TBI 7 days	136.7 \pm 15.7 ^{bc}	30.8 \pm 5.8	38.3 \pm 6.1 ^{bc}	0.0130 \pm 0.0015 ^{bc}

Note: Values were expressed as mean \pm SD. ^b P <0.01 vs control, ^c P <0.01 vs group of 3 hour TBI.

damages. The alterations of these parameters following TBI are shown in Table 2. Qualitative analyses of the villi demonstrated that the villous height, crypt depth and surface area were significantly decreased at 24 hours after TBI as compared with control group and further declined to the degree of mucosal atrophy on day 7 following TBI.

Ultrastructural observations

Within 24 hours of TBI, the nuclei of epithelial cells appeared irregular, but their membranes were still intact. At 72 hours and on day 7 following TBI, obvious ultrastructural alterations were found, including reduction of matrix of mitochondria and disruption of their cristae (Figure 5), ruptured, distorted and sparse microvilli (Figure 6), apoptosis bodies in cytoplasm (Figure 7), disrupted and wider tight junction between epithelial cells (Figure 8), swollen and degenerated vascular endothelial cells.

Changes in plasma endotoxin concentration

As shown in Figure 9, plasma endotoxin was significantly increased at 3 hours following TBI, and peaked at 72 hours, then declined on day 7, but was still significantly higher than that of controls (P <0.01). A marked correlation was noted between the changes in plasma level of endotoxin and intestinal permeability throughout 12 hours and 7 days following TBI ($r=0.765$, P <0.01).

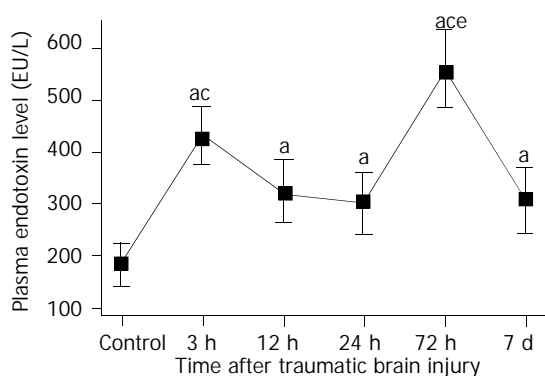


Figure 9 Significant increase of level of plasma endotoxin following TBI compared with control. Two peaks of plasma endotoxin existed at 3 h and 72 h postinjury, respectively. ^a P <0.05 vs control; ^c P <0.05 vs 12 h, 24 h and 72 h following TBI, ^e P <0.05 vs 3 h following TBI. Mean \pm SD of six animals, control: 183.7 \pm 41.8 EU/L, 3 h: 434.8 \pm 54.9 EU/L, 12 h: 324.2 \pm 61.7 EU/L, 24 h: 303.3 \pm 60.2 EU/L, 72 h: 560.5 \pm 76.2 EU/L, 7 d: 306.7 \pm 62.4 EU/L.

Intestinal permeability and L/M ratio

As shown in Figure 10, intestinal permeability was significantly increased at 12 hours after TBI, peaked at 72 hours, and declined gradually afterward, but was still higher on day 7 following TBI than that of control group.

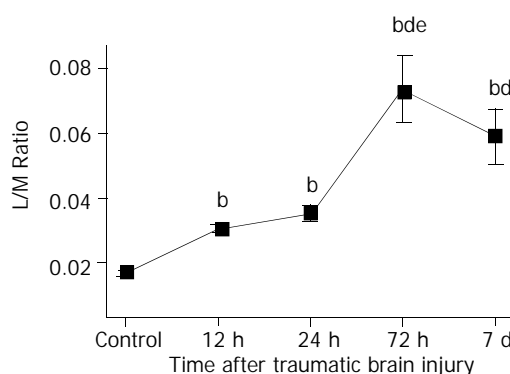


Figure 10 Significant increase of L/M ratio at 12 h, 24 h and 72 h following TBI compared with control and significant decline on day 7 compared with group at 72 h. The L/M ratio on day 7 was still significantly higher than that at 12 h and 24 h. ^b P <0.01 vs control, ^d P <0.01 vs 12 h and 24 h, ^e P <0.01 vs 7 d. Mean \pm SD of six animals, control: 0.0172 \pm 0.0009, 12 h: 0.0303 \pm 0.0013, 24 h: 0.0354 \pm 0.0025, 72 h: 0.0736 \pm 0.0105, 7 d: 0.0588 \pm 0.0083.

DISCUSSION

Major changes of gastrointestinal function following traumatic brain injury could be summarized in four aspects. The first was gastrointestinal mucosa ischemia, which usually resulted in stress ulcer and gastrointestinal bleeding^[3,4]. The second was motility dysfunction, which manifested as abdominal distention, diarrhea, gastric retention, and even toxic intestinal paralysis^[5-7,31]. The third was disruption of gut barrier, which led to bacterial and endotoxin translocation contributing to the development of SIRS and sepsis. The fourth was alteration of intestinal mucosal absorption of nutrients, which played an important role in malnutrition. Studies on stress ulcer and gastrointestinal bleeding after brain injury have been reported extensively^[2]. Stress ulcer was one of the most common gastrointestinal complications following head trauma with a reported incidence of 74-100 %^[3,4]. Endoscopic evidences of gastric mucosal lesions could appear within 24 hours, and 17 % of these erosions would progress to clinically significant gastrointestinal bleeding after severe brain injury.

Studies on intestinal mucosa structure and barrier function following TBI have not been found to date. In this study, we found that severe damage of intestinal mucosa occurred following TBI. The morphologic alterations of gut mucosa included shedding of epithelial cells, fracture of villi, focal ulcer, fusion of adjacent villi, dilation of central chyle duct, mucosal atrophy, and edema in the villous interstitium and lamina propria. Apoptosis of epithelial cells, fracture and sparseness of microvilli, disruption of tight junction between enterocytes, damage of mitochondria and endoplasm, were found by electron microscopy. These lesions occurred rapidly as early as 3 hours following TBI and lasted for more than 7 days. At the early stage (within 72 hours following TBI), it manifested as acute damages of intestinal epithelium, such as

epithelial necrosis and focal mucosa ulcer. On day 7 after TBI, the intestinal lesions were dominated by mucosal atrophy and edema of villous interstitium and lamina propria. Inflammatory cell infiltration in the small intestine was found 24 hours after TBI. Mucosal atrophy was considered to be associated with the necrosis and apoptosis of gut epithelium, which were induced by relative hypoperfusion (ischemia-reperfusion injury) and interaction of inflammatory mediators with their receptors located on the gut epithelial cells^[13].

Intestinal mucosal injury could also be assessed by measuring the permeability of mucosal barrier to small or large solutes. Lactulose and mannitol have previously been used to assess intestinal mucosal permeability in burn and critically ill patients^[12,14,15]. Mannitol, a smaller sugar, passes through aqueous pores in the cell membranes. Lactulose, a larger molecule, is absorbed paracellularly through tight junctions. Increased absorption of lactulose can reflect mucosal leakiness, and decreased absorption of mannitol can reflect decreased functional absorptive area. The current study demonstrated that the L/M ratio was significantly greater at 3 hours following TBI, and reached its peak at 72 hours, then declined on day 7 with the value still markedly higher than that of control group and 24 hour TBI group. Additionally, the results showed that increased intestinal permeability might persist for 7 days in rats with TBI, which conformed highly to the histopathological alterations, i.e. mucosal atrophy and disruption of tight junction between epithelial cells.

The level of plasma endotoxin was positively related to L/M ratio, and manifested as two peaks at 3 hours and 72 hours after TBI, respectively. The first peak might be the result of acute gut mucosal damage mainly induced by splanchnic ischemia due to the excited sympathetic nerve. With the resumption of liver anti-toxic function and the advent of specific antibodies to lipopolysaccharide, the plasma level of endotoxin was declined to some extent^[34]. The second peak of plasma endotoxin might be related to severe mucosal damages such as focal ulcer and epithelial necrosis which usually occurred at 72 hours following TBI. High L/M ratio and plasma level of endotoxin following TBI implied that the gut barrier function was disrupted.

The potential mechanism underlying the alterations of gut structure and impairment of barrier function following TBI might be related to several factors, including ischemia-reperfusion, intramucosal acidosis^[32], cytokines and inflammatory mediators^[13,33]. Splanchnic hypoperfusion is a common finding in trauma. In systemic pathological stresses such as TBI, an adaptive response mediated by neuro-endocrine exists, which leads to selective splanchnic vascular spasm in order to maintain the normal supply of vital organs such as the heart, lung and brain. The gut is highly susceptible to the consequent reduction in oxygenation, particularly mucosa of the stomach and intestine. This might induce increased gut permeability, alteration of enteral immune function, mucosal edema, epithelial necrosis and apoptosis, and even focal mucosa ulcer, which would contribute to bacterial and endotoxin translocation^[13,14,20]. Brain-gut axis and hypothalamus-pituitary-adrenal axis might play a potential role in gut mucosal damages^[18-20]. It may arise from the actions of parasympathetic centers of the hypothalamus with their connections to vagal nuclei in the medulla. Cytokines and inflammatory mediators such as TNF- α , IL-1, oxygen free radicals and nitric oxide could induce damages of microvilli, tight junction between enterocytes and paracellular junction, which would lead to increased intestinal permeability^[33].

Increased intestinal permeability has been implicated in the pathogenesis of both SIRS and progression to MODS^[10,11,14,15]. The gut origin hypothesis suggests that a failure of gut barrier function as a result of a major stress insult permits bacterial

and endotoxin translocation, which triggers systemic immunoinflammatory response to release cytokines and inflammatory mediators. These cytokines and mediators might exacerbate SIRS, sepsis and multiple organ failure^[10-13]. This concept was supported by the data from animal studies in experimental models, including surgical trauma^[14], malnutrition, jaundice, pancreatitis, hemorrhagic shock, and thermal injury^[28]. Results of the current study showed that gut barrier dysfunction occurred with high plasma level of endotoxin and increased intestinal permeability following TBI. Therefore, we suggest that SIRS and MODS secondary to traumatic brain injury be possibly related to the disruption of gut barrier. Otherwise, translocated endotoxin and gut-derived cytokines may enter the injured brain with circulating blood, which was assumed to activate or exacerbate the inflammation of brain, and cause "two-hit" insult^[22-26]. Circulating lipopolysaccharide and cytokines may stimulate the hypothalamic-pituitary-adrenal axis and sympathetic nervous system to affect the function of multiple organs. MODS is one of the common fatal complications following severe TBI.

ACKNOWLEDGEMENT

We would like to thank Dr. Genbao Feng, Fangnan Liu and Bo Wu for their technical assistance.

REFERENCES

- 1 **Pilitsis JG**, Rengachary SS. Complications of head injury. *Neurol Res* 2001; **23**: 227-236
- 2 **Lu WY**, Rhoney DH, Boling WB, Johnson JD, Smith TC. A review of stress ulcer prophylaxis in the neurosurgical intensive care unit. *Neurosurgery* 1997; **41**: 416-426
- 3 **Brown TH**, Davidson PF, Larson GM. Acute gastritis occurring within 24 hours of severe head injury. *Gastrointest Endosc* 1989; **35**: 37-40
- 4 **Kamada T**, Fusamoto H, Kawano S, Noguchi M, Hiramatsu K. Gastrointestinal bleeding following head injury: a clinical study of 433 cases. *J Trauma* 1977; **17**: 44-47
- 5 **Kao CH**, ChangLai SP, Chieng PU, Yen TC. Gastric emptying in head-injured patients. *Am J Gastroenterol* 1998; **93**: 1108-1112
- 6 **Saxe JM**, Ledgerwood AM, Lucas CE, Lucas WF. Lower esophageal sphincter dysfunction precludes safe gastric feeding after head injury. *J Trauma* 1994; **37**: 581-586
- 7 **Pedoto MJ**, O' Dell MW, Thrun M, Hollifield D. Superior mesenteric artery syndrome in traumatic brain injury: two cases. *Arch Phys Med Rehabil* 1995; **76**: 871-875
- 8 **Philip PA**. Superior mesenteric artery syndrome: an unusual cause of intestinal obstruction in brain-injured children. *Brain Inj* 1992; **6**: 351-358
- 9 **Jackson MD**, Davidoff G. Gastroparesis following traumatic brain injury and response to metoclopramide therapy. *Arch Phys Med Rehabil* 1989; **70**: 553-555
- 10 **Swank GM**, Deitch EA. Role of the gut in multiple organ failure: bacterial translocation and permeability changes. *World J Surg* 1996; **20**: 411-417
- 11 **Moore FA**. The role of the gastrointestinal tract in postinjury multiple organ failure. *Am J Surg* 1999; **178**: 449-453
- 12 **Doig CJ**, Sutherland LR, Sandham JD, Fick GH, Verhoef M, Meddings JB. Increased intestinal permeability is associated with the development of multiple organ dysfunction syndrome in critically ill ICU patients. *Am J Respir Crit Care Med* 1998; **158**: 444-451
- 13 **Grotz MR**, Deitch EA, Ding J, Xu D, Huang Q, Regel G. Intestinal cytokine response after gut ischemia: role of gut barrier failure. *Ann Surg* 1999; **229**: 478-486
- 14 **Langkamp-Henken B**, Donovan TB, Pate LM, Maull CD, Kudsk KA. Increased intestinal permeability following blunt and penetrating trauma. *Crit Care Med* 1995; **23**: 660-664
- 15 **Faries PL**, Simon RJ, Martella AT, Lee MJ, Machiedo GW. Intestinal permeability correlates with severity of injury in trauma patients. *J Trauma* 1998; **44**: 1031-1036

- 16 **Wang XD**, Soltesz V, Andersson R. Cisapride prevents enteric bacterial overgrowth and translocation by improvement of intestinal motility in rats with acute liver failure. *Eur Surg Res* 1996; **28**: 402-412
- 17 **Pepe JL**, Barba CA. The metabolic response to acute traumatic brain injury and implications for nutritional support. *J Head Trauma Rehabil* 1999; **14**: 462-474
- 18 **Glavin GB**, Hall AM. Brain-gut relationships: gastric mucosal defense is also important. *Acta Physiol Hung* 1992; **80**: 107-115
- 19 **Shanahan F**. Brain-gut axis and mucosal immunity: a perspective on mucosal psychoneuroimmunology. *Semin Gastrointest Dis* 1999; **10**: 8-13
- 20 **Grundy PL**, Harbuz MS, Jessop DS, Lightman SL, Sharples PM. The hypothalamo-pituitary-adrenal axis response to experimental traumatic brain injury. *J Neurotrauma* 2001; **18**: 1373-1381
- 21 **Morganti-Kossmann MC**, Rancan M, Otto VI, Stahel PF, Kossmann T. Role of cerebral inflammation after traumatic brain injury: a revisited concept. *Shock* 2001; **16**: 165-177
- 22 **Ghirnikar RS**, Lee YL, Eng LF. Inflammation in traumatic brain injury: role of cytokines and chemokines. *Neurochem Res* 1998; **23**: 329-340
- 23 **Bohatschek M**, Werner A, Raivich G. Systemic LPS injection leads to granulocyte influx into normal and injured brain: effects of ICAM-1 deficiency. *Exp Neurol* 2001; **172**: 137-152
- 24 **Ahmed SH**, He YY, Nassief A, Xu J, Xu XM, Hsu CY, Faraci FM. Effects of lipopolysaccharide priming on acute ischemic brain injury. *Stroke* 2000; **31**: 193-199
- 25 **Montero-Menei CN**, Sindji L, Garcion E, Mege M, Couez D, Gamelin E, Darcy F. Early events of the inflammatory reaction induced in rat brain by lipopolysaccharide intracerebral injection: relative contribution of peripheral monocytes and activated microglia. *Brain Res* 1996; **724**: 55-66
- 26 **Morganti-Kossmann MC**, Rancan M, Stahel PF, Kossmann T. Inflammatory response in acute traumatic brain injury: a double-edged sword. *Curr Opin Crit Care* 2002; **8**: 101-105
- 27 **Kamei H**, Yoshida S, Yamasaki K, Tajiri T, Ozaki K, Shirouzu K. Severity of trauma changes expression of TNF-alpha mRNA in the brain of mice. *J Surg Res* 2000; **89**: 20-25
- 28 **Zhu L**, Yang ZC, Li A, Cheng DC. Protective effect of early enteral feeding on postburn impairment of liver function and its mechanism in rats. *World J Gastroenterol* 2000; **6**: 79-83
- 29 **Suchner U**, Senftleben U, Eckart T, Scholz MR, Beck K, Murr R, Enzenbach R, Peter K. Enteral versus parenteral nutrition: effects on gastrointestinal function and metabolism. *Nutrition* 1996; **12**: 13-22
- 30 **Feeney DM**, Boyeson MG, Linn RT, Murray HM, Dail WG. Responses to cortical injury: I. Methodology and local effects of contusions in the rat. *Brain Res* 1981; **211**: 67-77
- 31 **Mackay LE**, Morgan AS, Bernstein BA. Factors affecting oral feeding with severe traumatic brain injury. *J Head Trauma Rehabil* 1999; **14**: 435-447
- 32 **Salzman AL**, Wang H, Wollert PS, Vandermeer TJ, Compton CC, Denenberg AG, Fink MP. Endotoxin-induced ileal mucosal hyperpermeability in pigs: role of tissue acidosis. *Am J Physiol* 1994; **266**(4 Pt 1): G633-646
- 33 **Gong JP**, Wu CX, Liu CA, Li SW, Shi YJ, Yang K, Li Y, Li XH. Intestinal damage mediated by Kupffer cells in rats with endotoxemia. *World J Gastroenterol* 2002; **8**: 923-927
- 34 **Buttenschoen K**, Berger D, Strecker W, Buttenschoen DC, Stenzel K, Pieper T, Beger HG. Association of endotoxemia and production of antibodies against endotoxins after multiple injuries. *J Trauma* 2000; **48**: 918-923

Edited by Zhang JZ and Wang XL

Changes of biological functions of dipeptide transporter (PepT1) and hormonal regulation in severe scald rats

Bing-Wei Sun, Xiao-Chen Zhao, Guang-Ji Wang, Ning Li, Jie-Shou Li

Bing-Wei Sun, Ning Li, Jie-Shou Li, Department of General Surgery, School of Medicine, Nanjing University, Nanjing 210093, Jiangsu Province, China

Bing-Wei Sun, Ning Li, Jie-Shou Li, Research Institute of General Hospital, Chinese PLA General Hospital of Nanjing Military Command, Nanjing 210002, Jiangsu Province, China

Xiao-Chen Zhao, Guang-Ji Wang, Center of Drug Metabolism and Pharmacokinetics, China Pharmaceutical University, Nanjing 210009, Jiangsu Province, China

Supported by National Natural Science Foundation of China, No. 39970862

Correspondence to: Bing-Wei Sun, Research Institute of General Hospital, Chinese PLA General Hospital of Nanjing Military Command, 305 East Zhongshan Road, Nanjing 210002, Jiangsu Province, China. sunbinwe@hotmail.com

Telephone: +86-25-3387871 Ext 58088 **Fax:** +86-25-4803956

Received: 2003-06-10 **Accepted:** 2003-08-16

Abstract

AIM: To determine the regulatory effects of recombinant human growth hormone (rhGH) on dipeptide transport (PepT1) in normal and severe scald rats.

METHODS: Male Sprague-Dawley rats with 30 % total body surface area (TBSA) III degree scald were employed as the model. In this study rhGH was used at the dose of 2 IU.kg⁻¹.d⁻¹. An everted sleeve of intestine 4 cm long obtained from mid-jejunum was securely incubated in Kreb's solution with radioactive dipeptide (³H-glycylsarcosine, ³H-Gly-Sar, 10 µCi/ml) at 37 °C for 15 min to measure the effects of uptake and transport of PepT1 of small intestinal epithelial cells in normal and severe scald rats.

RESULTS: Abundant blood supply to intestine and mesentery was observed in normal and scald rats administered rhGH, while less supply of blood to intestine and mesentery was observed in rats without rhGH. Compared with controls, the transport of dipeptide in normal rats with injection of rhGH was not significantly increased ($P=0.1926$), while the uptake was significantly increased ($P=0.0253$). The effects of transport and uptake of PepT1 in scald rats with injection of rhGH were significantly increased ($P=0.0082$, 0.0391).

CONCLUSION: Blood supply to intestine and mesentery of rats was increased following injection of rhGH. The effects of uptake and transport of dipeptide transporters in small intestinal epithelial cells of rats with severe scald were markedly up-regulated by rhGH.

Sun BW, Zhao XC, Wang GJ, Li N, Li JS. Changes of biological functions of dipeptide transporter (PepT1) and hormonal regulation in severe scald rats. *World J Gastroenterol* 2003; 9 (12): 2782-2785

<http://www.wjgnet.com/1007-9327/9/2782.asp>

INTRODUCTION

Small intestine is the major site of dietary protein absorption,

the main route of absorption protein is transport of protein in the form of small peptides (di/tripeptide) across the small intestinal wall. H⁺-coupled dipeptide transporter, PepT 1, is known to be located in the intestine and kidney, and plays an important role in the absorption of di/tripeptide. In addition, it mediates the intestinal absorption of β-lactam antibiotics, angiotension-converting enzyme inhibitors, and other peptide-like drugs^[1].

Knowledge about the regulation of PepT 1 activity is limited. A number of studies have shown that dietary protein load causes an increase in di/tripeptide transport in small intestine of rats and mice^[2,3]. Recent studies have shown that PepT1 in rat intestine is upregulated after a short period of fast via an increase in gene expression^[4-6]. Another interesting regulation of PepT 1 expression is that PepT1 in rat's small intestine is resistant to tissue damage induced by 5-fluorouracil, whereas other markers such as sucrase activity, D-glucose uptake are significantly decreased^[7]. This suggests that expression of PepT 1 is robust towards cellular damage.

Studies showed that some hormones metabolically regulated the expression of intestinal dipeptide transporter^[8,9]. For example, insulin could increase the membrane population of PepT 1 by increasing its translocation from a preformed cytoplasmic pool^[9]. Our previous study^[10] showed that rhGH markedly stimulated the uptake and transport of cephalixin in Caco-2 cells with normal or anoxia/reoxygenation management. These results indicate that rhGH greatly upregulates the physiological functions of dipeptide transporters (PepT1) of human cell line. Although rhGH has been shown to be a major regulator of peptide transport activity^[10], little is known about rhGH in regulation of peptide absorption *in vivo*, especially in rats with severe scald.

In this study, we determined whether rhGH could stimulate uptake and transport of small intestinal epithelial cells in normal or severe scald rats. We also investigated the *in vivo* application of 3H-glycylsarcosine (3H-Gly-Sar) as an ideal substrate for PepT1.

MATERIALS AND METHODS

Materials

[3H]-glycylsarcosine (special activity of 1Ci (37GBq)/mmol, radiochemical purity >=97 %, work concentration in this study: 10 µCi/ml) was purchased from Moravak Biochemicals, USA. Recombinant human growth hormone (rhGH, 2 IU.kg⁻¹.d⁻¹) was from Serono, Switzerland, Temperature-controlled surge culture device from Taicang Medical Instrument Co. Ltd, China. All other reagents were of analytical grade at least.

Animals

Adult male Sprague-Dawley (SD) rats (weighing 200±20 g) were housed in individual stainless steel cages in an air-conditioned room at 23±2 °C with a 12: 12-h light schedule and were fed normally. The weight of rats was measured daily during an experiment. The animals were treated in accordance with European Community Standards concerning the care and use of laboratory animals (INSERM and Ministère de l'Agriculture et de la Forêt, Paris, France).

Experimental groups

Rats were randomly divided into groups A, B, C and D. Group A (control group): normal feed rats, Group B: normal feed + injection of rhGH ($2 \text{ IU} \cdot \text{kg}^{-1} \cdot \text{d}^{-1}$) rats, Group C: scald rats and Group D: scald + injection of rhGH ($2 \text{ IU} \cdot \text{kg}^{-1} \cdot \text{d}^{-1}$) rats. The indices were observed on postburn days (PBDs) 0, 1, 3, 5 and 7 ($n=4$), respectively. Rats were killed by decapitation at every time point.

Scald injury models

Rats were anaesthetized with 2 % pentobarbital ($30 \text{ mg} \cdot \text{kg}^{-1}$ body weight) and scald on the back to 30 % total body surface area (TBSA) III degree, and 30 min later, they were resuscitated with Ringer's solution ($2 \text{ ml} \cdot \text{kg}^{-1}$ per 1 % body surface area).

Preparation of everted sleeve of rat small intestine

The rats were fasted overnight and water was available ad libitum throughout the study. The rat was killed by decapitation, a laparotomy was performed. We defined the region approximately 6 cm below the ligament of Treitz, then a 4-cm long segment of small intestine (mid-jejunum) was removed, ringed immediately with Kreb's buffer. One end of the intestinal fragment was ligated, an everted process was securely made by small tweezers, then an intact everted sleeve was formed after another terminal ligation. Each sleeve was weighed.

Uptake and transport measurement

We measured ^3H -Gly-Sar taken up into intestinal epithelial cells of the everted sleeve across the brush-border membrane. The everted sleeve was rinsed with Kreb's buffer, 0.2 ml Kreb's buffer was injected slowly into the lumen of the everted intestinal sleeve. The whole segment was then immersed into a 50 ml flask containing dipeptide (^3H -Gly-Sar) solution ($10 \mu\text{Ci}$) while 5 % CO_2 and 95 % O_2 were filled into the flask. The uptake and transport experiments were performed when the device was surged continually with a frequency of 100 r/min at 37°C for 15 min, then the everted sleeve was rinsed immediately with cold (4°C) Kreb's buffer to stop subsequent transport and uptake of PepT1 in epithelial cells. The transport sample was harvested from the lumen of the sleeve, a $0.5 \text{ cm} \times 0.5 \text{ cm}$ segment was removed from the middle of the sleeve, weighed and digested with HCl_4 to obtain the uptake sample. All samples were mixed with 10 ml of scintillation cocktail and the radioactivity was determined by liquid scintillation counter.

Statistical analysis

Data were expressed as mean \pm SD. Differences between groups were assessed by analysis of variance. Values less than 0.05 were considered statistically significant.

RESULTS

Blood Supply in bowel of rats

After killed by decapitation, a laparotomy was performed immediately at the different time point (0, 1, 3, 5 and 7 days) in rats (normal or scald) with or without injection of rhGH. Direct appearance of blood supply was observed in mesentery and the wall of intestine of rats. Abundant blood supply was shown in rats after injection of rhGH, while less blood supply was observed in rats without injection of rhGH (Figure 1, 2).

Uptake and transport in everted sleeve of normal rats after injection of rhGH

In comparison with the control, the transport of dipeptide (^3H -Gly-Sar) in normal rats after injection of rhGH was not

significantly increased ($P=0.1923$) while the uptake were markedly increased ($P=0.0253$) (Figure 3, 4).

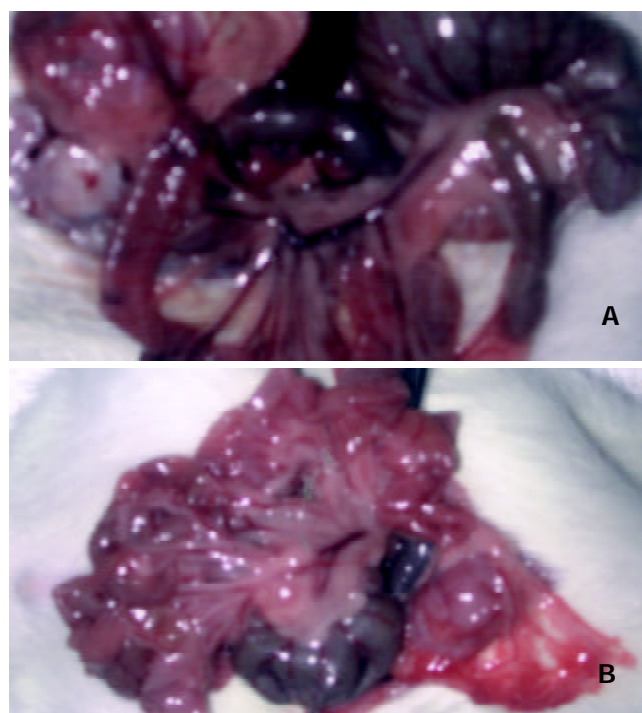


Figure 1 Blood supply to intestine and mesentery of rats 7 days after injection of rhGH was significantly abundant compared with controls. (A: rhGH group, B: control).

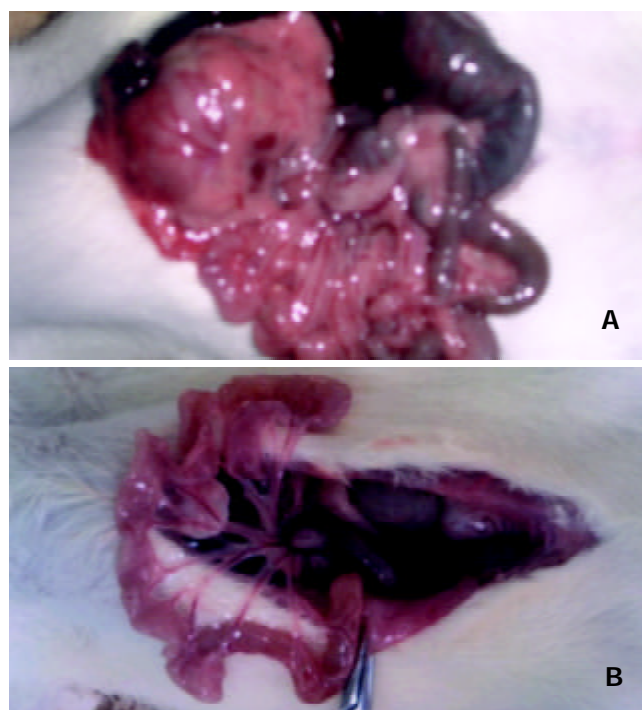


Figure 2 Blood supply to intestine and mesentery of rats with severe scald 7 days after injection of rhGH was significantly abundant compared with controls. (A: rhGH group, B: control).

Uptake and transport in everted sleeve of severe scald rats after injection of rhGH

The effects of transport and uptake of PepT1 in everted sleeve of severe scald rats after injection of rhGH were greatly increased compared with controls ($P=0.0082$, 0.0391) (Figure 5, 6).

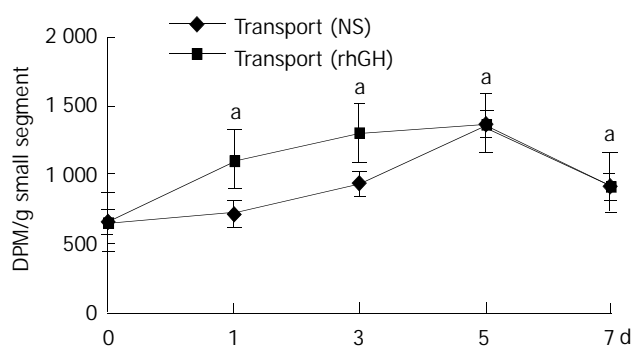


Figure 3 Transport of PepT1 in normal rats administered rhGH. Each point represents mean \pm s, $n=4$, ^a $P>0.05$ vs control.

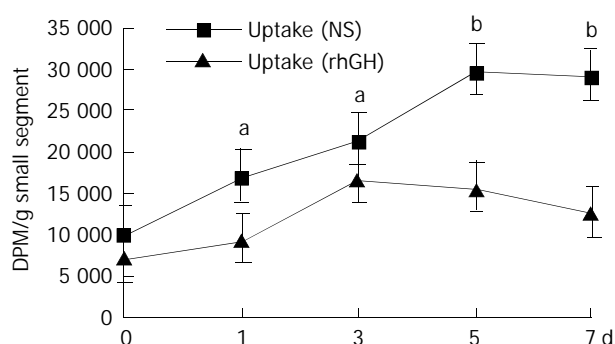


Figure 4 Uptake of PepT1 in normal rats administered rhGH. Each point represents mean \pm s, $n=4$, ^a $P<0.05$, ^b $P<0.01$ vs control.

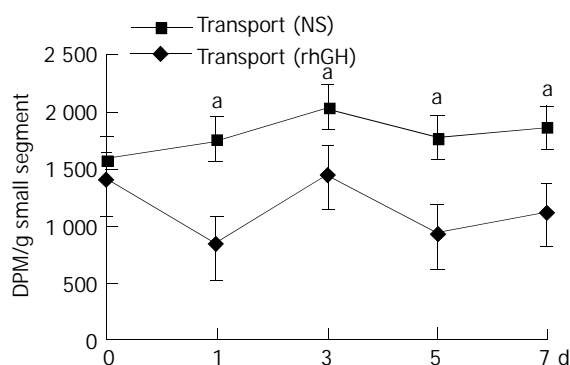


Figure 5 Transport of PepT1 in scald rats administered rhGH. Each point represents mean \pm s, $n=4$, ^a $P<0.05$ vs control.

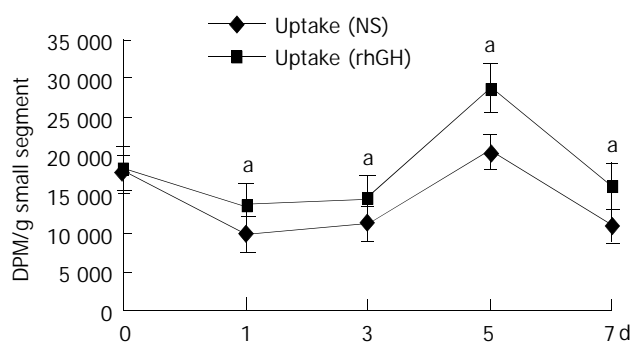


Figure 6 Uptake of PepT1 in scald rats administered rhGH. Each point represents mean \pm s, $n=4$, ^a $P<0.05$ vs control.

DISCUSSION

We found in this study that rhGH could significantly increase the transport and uptake of peptides across intestinal epithelial

barrier via proton-dependent transporter PepT1, suggesting that rhGH might be an important parameter in hormonal regulation of this transporter. It is well known that dietary proteins are absorbed as di- and tripeptides rather than free amino acids^[11-14]. This absorption process is carried out by intestinal brush board transporter PepT1, which transfers peptides from a region with low dipeptidase activity (intestinal lumen) to a region with high dipeptidase activity (enterocyte cytoplasm)^[15]. As a member of a family of transport proteins, PepT1 is located at the brush-border membranes of absorptive epithelial cells along the small intestine but absent in crypt and goblet cells^[16,17]. PepT1 allows the use of small peptides as a source of nitrogen for enteral feeding and the route for delivery of peptidomimetic drugs such as β -lactam antibiotics. Therefore, PepT1 appears to be essential for the efficient absorption of dietary proteins^[18]. Most studies on PepT1 have focused on its fundamental kinetic properties and its functional and structural characterization^[19-21].

Previous studies have shown that the functions of intestine (including PepT1) were changed under the influence of many factors^[22,23]. However, few reports have dealt with the hormonal regulation of PepT1. Insulin could stimulate dipeptide transport by increasing membrane insertion of PepT1 from a preformed cytoplasmic pool^[9], and cholera toxin could decrease dipeptide transport by inhibiting the activity of PepT1 through an increase in intracellular concentration of adenosine 3', 5'-cyclic monophosphate^[24]. Strong evidences have demonstrated that growth hormone (GH) was an important growth factor for intestine^[25]. Complete GH depletion due to hypophysectomy could cause pronounced hypoplasia of small intestinal mucosa with decreased villus height and reduced crypt cell proliferation^[26]. Simple replacement of GH could restore mucosal proliferative activity^[27], rhGH could promote normal growth and development in the body by changing chemical activity in cells. It activates protein production in muscle cells and release of energy from fats. rhGH could significantly improve anabolism in parenteral feeding^[28]. It has been typically used to stimulate growth of children with hormone deficiency, or to treat people with severe illness, burns or sepsis where destruction of human tissues and muscle occurs^[29-31]. It remains unclear, however, whether the key hormone, human growth hormone (hGH) also shows some significant importance in transport and uptake of PepT1. To examine the functional changes of PepT1, everted sleeves of small intestine were used as *in vivo* intestinal model, and severe scald (30 % TBSA III degree) rats with or without injection of rhGH were employed as animal model. The results in this study indicated that the blood supply in mesentery and the wall of rat's intestine (normal or severe scald) with injection of rhGH was abundant compared with the controls. It was suggested that rhGH could increase blood supply of animal bowel, therefore, upregulate directly the physiological functions of PepT1 of small intestine.

The data in this study confirmed that both transport and uptake of PepT1 in everted sleeves of severe scald rats administered rhGH were significantly increased compared with controls. It indicated that rhGH upregulated the biological functions of PepT1. This result was in accordance with our previous research^[10]. In our study, however, the transport of dipeptide in normal rats treated with rhGH was not markedly increased, while the uptake was greatly increased compared with controls. It might be due to the cytoplasmic level of dipeptidases, or a short period of experiment.

In conjunction with previous results^[10], the present study further testified the enhancement effect of peptide transport by rhGH. The biological mechanism might involve increased translocation of the cytoplasmic pool of PepT1 to the apical membrane, or increased level of PepT1 mRNA. Clearly,

further study on physiology and biology of PepT1 is required to clarify the mechanism of rhGH in upregulating the functions of PepT1.

REFERENCES

- Hsu CP**, Walter E, Merkle HP, Rothen-Rutishauser B, Wunderli-Allenspach H, Hilfinger JM, Amidon GL. Function and immunolocalization of overexpressed human intestinal H⁺/peptide cotransporter in adenovirus-transduced Caco-2 cells. *AAPS Pharm Sci* 1999; **1**: E12
- Erickson RH**, Gum JR Jr, Lindstrom MM, Mckean D, Kim YS. Regional expression and dietary regulation of rat small intestinal peptide and amino acid transporter mRNAs. *Biochem Biophys Res Commun* 1995; **216**: 249-257
- Ferraris RP**, Diamond J, Kwan WW. Dietary regulation of intestinal transport of the dipeptide carnosine. *Am J Physiol* 1998; **255** (2 Pt 1): G143-150
- Ihara T**, Tsuji Kawa T, Fujiyama Y, Bamba T. Regulation of PepT1 peptide transporter expression in the rat small intestine under malnourished conditions. *Digestion* 2000; **61**: 59-67
- Ogihara H**, Suzuki T, Nagamachi Y, Inui K, Takate K. Peptide transporter in the rat small intestine: ultrastructural localization and the effect of starvation and administration of amino acids. *Histochem J* 1999; **31**: 169-174
- Thamotharan M**, Bawani SZ, Zhou X, Adibi SA. Functional and molecular expression of intestinal oligopeptide transporter (PepT-1) after a brief fast. *Metabolism* 1999; **48**: 681-684
- Tanaka H**, Miyamoto KI, Morita K, Haga H, Segawa H, Shiraga T, Fujioka A, Kouda T, Taketani Y, Hisano S, Fukui Y, Kitagawa K, Takeda E. Regulation of the PepT1 peptide transporter in the rat small intestine in response to 5-fluorouracil-induced injury. *Gastroenterology* 1998; **114**: 714-723
- Thamotharan M**, Bawani SZ, Zhou X, Adibi SA. Hormonal regulation of oligopeptide transporter Pept-1 in a human intestinal cell line. *Am J Physiol* 1999; **276**(4 Pt 1): C821-826
- Nielsen CU**, Amstrup J, Steffansen B, Frøkjær S, Brodin B. Epidermal growth factor inhibits glycylsarcosine transport and hPepT1 expression in a human intestinal cell line. *Am J Physiol Gastrointest Liver Physiol* 2001; **281**: G191-199
- Sun BW**, Zhao XC, Wang GJ, Lin N, Li JS. Hormonal regulation of dipeptide transporter (PepT1) in Caco-2 cells with normal and anoxia/reoxygenation management. *World J Gastroenterol* 2003; **9**: 808-812
- Adibi SA**. The oligopeptide transporter Pept-1 in human intestine: biology and function. *Gastroenterology* 1997; **113**: 332-340
- Adibi SA**. Intestinal transport of dipeptides in man: relative importance of hydrolysis and intact absorption. *J Clin Invest* 1997; **50**: 2266-2275
- Hellier MD**, Holdsworth CD, McColl I, Perrett D. Dipeptide absorption in man. *Gut* 1972; **13**: 965-969
- Cook GC**. Comparison of intestinal absorption rates of glycine and glycylglycine in man and the effect of glucose in the perfusing fluid. *Clin Sci* 1972; **43**: 443-453
- Brodin B**, Nielsen CU, Steffansen B, Frøkjær S. Transport of peptidomimetic drugs by the intestinal Di/tri-peptide transporter, PepT₁. *Pharmacol Toxicol* 2002; **90**: 285-296
- Ogihara H**, Saito H, Shin BC, Terada T, Takenoshita S, Nagamachi Y, Inui K, Takata K. Immuno-localization of H⁺/peptide cotransporter in rat digestive tract. *Biochem Biophys Res Commun* 1996; **220**: 848-852
- Adibi SA**. The oligopeptide transporter (PepT1) in human intestine. *Biol Funct Gastroenterol* 1997; **113**: 332-340
- Buyse M**, Berlioz F, Guilmeaul S, Tsocas A, Voisin T, Peranzi G, Merlin D, Laburthe M, Lewin MJ, Roze C, Bado A. PepT₁-mediated epithelial transport of dipeptides and cephalixin is enhanced by luminal leptin in the small intestine. *J Clin Invest* 2001; **108**: 1483-1494
- Mackenzie B**, Fei YJ, Ganapathy V, Leibach FH. The human intestinal H⁺/oligopeptide cotransporter hPEPT1 transports differently-charged dipeptides with identical electrogenic properties. *Biochem Biophys Acta* 1996; **1284**: 125-128
- Chen XZ**, Steel A, Hediger MA. Functional roles of histidine and tyrosine residues in the H(+)-peptide transporter PepT₁. *Biochem Biophys Res Commun* 2000; **272**: 726-730
- Bolger MB**, Haworth IS, Yeung AK, Ann D, Von Grafenstein H, Hamm-Alvarez S, Okamoto CT, Kim KJ, Basu SK, Wu S, Lee VH. Structure, function, and molecular modeling approaches to the study of the intestinal dipeptide transporter PepT₁. *J Pharm Sci* 1998; **87**: 1286-1291
- Li YS**, Li JS, Li N, Jiang ZW, Zhao YZ, Li NY, Liu FN. Evaluation of various solutions for small bowel graft preservation. *World J Gastroenterol* 1998; **4**: 140-143
- Liang LJ**, Yin XY, Luo SM, Zheng JF, Lu MD, Huang JF. A study of the ameliorating effects of carnitine on hepatic steatosis induced by total parenteral nutrition in rats. *World J Gastroenterol* 1999; **5**: 312-315
- Ferraris RP**, Diamond J, Kwan WW. Dietary regulation of intestinal transport of the dipeptide carnosine. *Am J Physiol* 1988; **255**(2 Pt 1): G143-150
- Zhou X**, Li YX, Li N, Li JS. Effect of bowel rehabilitative therapy on structural adaptation of remnant small intestine: animal experiment. *World J Gastroenterol* 2001; **7**: 66-73
- Bastie MJ**, Balas D, Laval J, Senegas-Balas F, Bertrand C, Frexinos J, Ribet A. Histological variations of jejunal and ileal mucosa on days 8 and 15 after hypophysectomy in rat: morphometrical analysis on light and electron microscopy. *Acta Anat* 1982; **112**: 321-337
- Scow RO**, Hagan SN. Effect of testosterone Propionate and growth hormone on growth and chemical composition of muscle and other tissues in hypophysectomized male rats. *Endocrinology* 1965; **77**: 852-858
- Gu Y**, Wu ZH. The anabolic effects of recombinant human growth hormone and glutamine on parenterally fed, short bowel rats. *World J Gastroenterol* 2002; **8**: 752-757
- Jeschke MG**, Herndon DN, Wolf SE, Debroy MA, Rai J, Lichtenbelt BJ, Barrow RE. Recombinant human growth hormone alters acute phase reactant proteins, cytokine expression, and liver morphology in burned rats. *J Surg Res* 1999; **83**: 122-129
- Roth E**, Valentini L, Semsroth M, Holzenbei T, Winkler S, Blum WF, Ranke MB, Schemper M, Hammerle A, Karner J. Resistance of nitrogen metabolism to growth hormone treatment in the early phase after injury of patient with multiple injuries. *J Trauma* 1995; **38**: 136-141
- Postel-Vinay MC**, Finidori J, Sotiropoulos A, Dinerstein H, Martini JF, Kelly PA. Growth hormone receptor: structure and signal transduction. *Ann Endocrinol* 1995; **56**: 209-212

Edited by Ren SY and Wang XL

Protective effect of *angelica sinensis* polysaccharide on experimental immunological colon injury in rats

Shao-Ping Liu, Wei-Guo Dong, Dong-Fang Wu, He-Sheng Luo, Jie-Ping Yu

Shao-Ping Liu, Wei-Guo Dong, He-Sheng Luo, Jie-Ping Yu,
Department of Gastroenterology, Renmin Hospital of Wuhan University, 238 Jiefang Road, Wuhan 430060, Hubei Province, China
Dong-Fang Wu, Department of Pharmacy, Renmin Hospital of Wuhan University, 238 Jiefang Road, Wuhan 430060, Hubei Province, China

Supported by key Project in Scientific and Technological Researches of Hubei Province, No. 2001AA308B

Correspondence to: Professor Wei-Guo Dong, Renmin Hospital of Wuhan University, 238 Jiefang Road, Wuhan 430060, Hubei Province, China. dongwg@public.wh.hb.cn

Telephone: +86-27-88054511

Received: 2003-06-05 **Accepted:** 2003-09-18

Abstract

AIM: To study the effect of *angelica sinensis* polysaccharide (ASP) on immunological colon injury and its mechanisms in rats.

METHODS: Immunological colitis model of rats was induced by intracolonic enema with 2, 4, 6-trinitrobenzene sulfonic acid (TNBS) and ethanol. The experimental animals were randomly divided into normal control, model control, 5-aminosalicylic acid therapy groups and three doses of ASP therapy groups. The 6 groups were treated intracolonic with normal saline, normal saline, 5-aminosalicylic acid (100 mg·kg⁻¹), and ASP daily (8:00 am) at the doses of 200, 400 and 800 mg·kg⁻¹ respectively for 21 days 7 d following induction of colitis. The rat colon mucosa damage index (CMDI), the histopathological score (HS), the score of occult blood test (OBT), and the colonic MPO activity were evaluated. The levels of SOD, MDA, NO, TNF-α, IL-2 and IL-10 in colonic tissues were detected biochemically and immunoradiometrically. The expressions of TGF-β and EGF in colonic tissues were also determined immunochemically.

RESULTS: Enhanced colonic mucosal injury, inflammatory response and oxidative stress were observed in colitis rats, which manifested as significant increases of CMDI, HS, OBT, MPO activity, MDA and NO contents, as well as the levels of TNF-α and IL-2 in colonic tissues, although colonic TGF-β protein expression, SOD activity and IL-10 content were significantly decreased compared with the normal control ($P < 0.01$). However, these parameters were found to be significantly ameliorated in colitis rats treated intracolonic with ASP at the doses of 400 and 800 mg·kg⁻¹ ($P < 0.05-0.01$). Meantime, colonic EGF protein expression in colitis rats was remarkably up-regulated.

CONCLUSION: ASP has a protective effect on immunological colon injury induced by TNBS and ethanol enema in rats, which was probably due to the mechanism of antioxidation, immunomodulation and promotion of wound repair.

Liu SP, Dong WG, Wu DF, Luo HS, Yu JP. Protective effect of *angelica sinensis* polysaccharide on experimental immunological colon injury in rats. *World J Gastroenterol* 2003; 9(12): 2786-2790
<http://www.wjgnet.com/1007-9327/9/2786.asp>

INTRODUCTION

Angelica sinensis polysaccharide (ASP) possesses a variety of pharmacological effects including immunoregulation, anti-oxidation, anti-tumor, anti-irradiation injury, promotion of hematopoiesis^[1-6]. ASP not only has regulatory effects on cytokines, complements, immunocompetent cells such as lymphocyte, macrophage but also shows manifold immunoregulation according to different organism immunological status, drug dose and drug administration surroundings; In addition, ASP has been recently found to be effective in preventing gastrointestinal injury induced by a neutrophil-dependent lesion model in rats, to promote gastrointestinal wound healing in rats *in vitro* and *vivo*^[7-9].

Immunoregulation dysfunction plays a central role in the pathogenesis of inflammatory bowel disease (IBD) including Crohn's disease and ulcerative colitis, although their etiology and pathophysiology remain to be elucidated. Immunoregulation dysfunction is mainly manifested as increased pro-inflammatory cytokines and decreased anti-inflammatory cytokines, which introduce the generation of "inflammation cascade", result in overproduction of oxygen and nitrogen reactive species, thus leading to intestinal and/or colonic injury^[10-15]. Numerous studies have demonstrated that modulation of immunological disorders is an effective target for the treatment of IBD^[15-19].

Based on ASP's immunomodulatory feature with manifold efficacies, anti-oxidation property, promotion of gastrointestinal wound healing and safety in use, we therefore assumed that ASP might contribute to the treatment of IBD. To the best of our knowledge, there has been no report so far concerning the effect of ASP on IBD. The present study was to observe the effect of ASP on immunological colon injury in experimental colitis rats to test the hypothesis.

MATERIALS AND METHODS

Animals and reagents

Healthy Sprague-Dawley rats of both sexes, weighing 250±30 g, and C57BL/6J mice, weighing 20±2 g, supplied by the Animal Center of the Academy of Hubei Preventive Medical Sciences. The rats were allowed to take food and tap water *ad libitum*. ASP was isolated from *angelica sinensis* from Minxian County of China by water extraction and ethanol precipitation as described in the literature^[4,10] and dissolved in normal saline, sanitized by high pressure before use. TNBS (Lot. 51K5001), ConA, MTT were all purchased from Sigma Co (USA). 5-aminosalicylic acid (5-ASA) was provided by Guoyi Pharmaceutical Ltd (Lot. 20029477, China). Occult blood test paper was provided by Tonyar Biotech Co (USA). Bovine serum and RPMI-1640 medium were purchased from Gibco Co (USA). Recombinant human TNF-α was provided by BangDing Biotech Co (China). Actinomycin D was provided by HuaMei Biotech Co (China). L929 cells were provided by Biological Classic Culture Store Centre of Wuhan University in China. IL-10 radioimmunoassay kits were provided by Radio-immunity Institute of PLA General Hospital in Beijing. Polyclonal rabbit anti-rat-TGF-β and EGF were purchased

from Santa Cruz Co. and Zymed Co., respectively. S-P kits were supplied by Zhongshan Biological Technology CO. Ltd in Beijing. MPO, SOD, MDA, NO detection kits were purchased from Nanjing Jiancheng Bioengineering Institute. Other reagents used in the present study were all of analytical grade.

Experimental protocol

According to the references^[19,20], the rats were anesthetized with ether, then a flexible plastic rubber catheter with an outside diameter of 2 mm was inserted rectally into the colon, its tip was 8 cm proximal to the anus. TNBS (100 mg·kg⁻¹) dissolved in 50 % ethanol (v/v) was instilled into the colon lumen through the rubber catheter (the final volume was 0.25 mL), saline was instilled as control. The experimental animals were randomly divided into 6 groups: normal group, model group, 5-ASA therapy group and three doses of ASP therapy groups. The 6 groups were treated intracolically with normal saline, normal saline, 5-ASA (100 mg·kg⁻¹), and ASP daily (8:00 am) at the doses of 200, 400 and 800 mg·kg⁻¹ respectively for 21 days 7 d following induction of colitis in rats. Then the colon mucosa damage index (CMDI) and the histopathological score (HS) were evaluated and the colonic tissue was sampled for a variety of determinations after the animals were sacrificed by decapitation.

Assessment of CMDI, HS and OBT

The tissue of colon 10 cm proximal to anus of the sacrificed rats was excised, opened longitudinally, washed in saline buffer, and pinned out on a wax block. The colonic tissue samples for HS were prepared according to the reference^[19]. CMDI and HS in each colon were evaluated respectively by two independent observers. The assessment criteria of CMDI and HS were reported in previous literature^[19]. CMDI was as following: 0: normal mucosa, no damage on mucosal surface; 1: mild hyperemia and edema, no erosion or ulcer on mucosal surface; 2: moderate hyperemia and edema with erosion on mucosal surface; 3: severe hyperemia and edema with necrosis and ulcer on mucosal surface, the major ulcerative area extended less than 1 cm; 4: severe hyperemia and edema with necrosis and ulcer on mucosal surface, the major ulcerative area extended more than 1 cm. HS: (1) Infiltration of acute inflammatory cells: 0, without; 1, mild; 2, severe. (2) Infiltration of chronic inflammatory cells: 0, without; 1, mild; 2, severe. (3) Fibrin deposition: 0, negative; 1, positive. (4) Submucosal edema: 0, without; 1, focal; 2, diffuse. (5) Necrosis of epithelial cells: 0, without; 1, focal; 2, diffuse. (6) Mucosal ulcer: 0, negative; 1, positive. At the end of experiment, rat feces was collected for occult blood test (OBT) according to the instructions.

Determination of MPO, SOD activities and MDA and NO contents

The colon tissue samples taken for MPO detection were homogenized (50 g·L⁻¹) in ice-cold potassium phosphate buffer 50 mmol·L⁻¹ (pH 6.0) containing 0.5 % hexadecyltrimethylammonium bromide. The homogenates were frozen and thawed three times, then centrifuged at 4 000 rpm for 20 min at 4 °C. The level of MPO in supernatant was measured using a commercial kit according to its instructions. Other colon tissue samples were homogenized (50 g·L⁻¹) in ice-cold PBS (pH 7.4). The homogenates were centrifuged at 3 000 rpm for 10 min at 4 °C, and the supernatant was stored at -20 °C until determination for SOD, MDA and NO using corresponding commercial kits according to the instructions.

Measurement of TNF- α , IL-2, IL-10 levels

The colon tissue samples were homogenized (100 g·L⁻¹) in ice-cold phosphate buffer saline (pH 7.4) containing penicillin

100 u·ml⁻¹ and streptomycin 100 ug·ml⁻¹. The homogenates were centrifuged at 40 000 rpm for 10 min at 4 °C, and the supernatant was stored at -80 °C until determination for TNF- α , IL-2 and IL-10. The activity of TNF- α and IL-2 were measured by L929 cell cytotoxicity and C57BL/6J mice splenocytes using MTT colorimetry respectively as described in the literature^[19,21]. The content of IL-10 was detected by using a radioimmunoassay kit following the manufacturer's instructions.

Detection of colonic TGF- β and EGF expression

Immunohistochemical detection was performed using S-P technique. The experiment procedures were performed following the manufacturer's recommendations. Polyclonal rabbit anti-rat-TGF- β and EGF were diluted in PBS to 1:100, 1:150, and used as primary antibodies respectively. The dewaxed sections were incubated with polyclonal primary antibodies overnight at 4 °C after antigen repair. Biotinylated goat-anti-rabbit IgG was added as second antibody. Horseradish peroxidase labeled streptomycin-avidin complex was used to detect second antibody. Sections were stained with diaminobenzidine. Negative control sections were prepared by substituting primary antibodies with PBS. The blue stained nucleus was considered as negative while the brown or dark brown stained cytoplasm and/or cell membrane were considered as positive. Expressions of these target proteins were semiquantitated respectively with an automatic image analyzer (Nikon, Japan) and HPIAS-2000 image analyzing program, in which the average value of positive cell's absorbance (A) in ten randomly selected high power fields (400 \times) for each section was used to compare the target protein expression.

Statistical analysis

Experimental results were analyzed by ANOVA and *t*-test for multiple comparisons between the groups. Data were finally expressed as mean \pm SD. *P* value less than 0.05 was considered statistically significant.

RESULTS

Protective effect of ASP on colon injury

Results are shown in Table 1. CMDI, HS, OBT and MPO activity were regarded as main parameters that reflected the degree of colon injury and inflammation in inflammatory gut tissue. Compared with normal group, these parameters were significantly increased in model group (*P*<0.01). Both ASP (400, 800 mg·kg⁻¹) and 5-ASA (100 mg·kg⁻¹) could remarkably decrease these elevated parameters (*P*<0.05-0.01). Furthermore, the therapeutic effect of 800 mg·kg⁻¹ ASP was as effective as that of 5-ASA (100 mg·kg⁻¹).

Table 1 Effect of ASP on CMDI, HS, OBT and MPO activity in colonic tissue of colitis rats (*n*=8, $\bar{x}\pm s$)

Group	Dose (mg·kg ⁻¹)	CMDI	HS	OBT	MPO (U·g ⁻¹)
Control	-	0.0 \pm 0.0	0.7 \pm 1.1	0.0 \pm 0.0	29 \pm 18
Model	-	3.1 \pm 1.1 ^d	5.6 \pm 0.8 ^d	2.2 \pm 0.8 ^d	194 \pm 32 ^d
5-ASA	100	1.7 \pm 0.6 ^b	4.7 \pm 0.7 ^a	1.0 \pm 0.9 ^a	117 \pm 15 ^b
ASP	200	2.1 \pm 0.5 ^a	4.5 \pm 1.3	1.4 \pm 0.9	172 \pm 16
ASP	400	1.8 \pm 0.7 ^a	4.3 \pm 1.1 ^a	1.1 \pm 0.8 ^a	158 \pm 19 ^a
ASP	800	1.5 \pm 0.5 ^b	4.1 \pm 0.9 ^b	0.8 \pm 0.7 ^b	133 \pm 17 ^b

^a*P*<0.05, ^b*P*<0.01, vs model group; ^d*P*<0.01 vs normal group.

Effect of ASP on colonic oxidation of colitis rats

Compared with normal group, the contents of MDA and NO

were significantly elevated while SOD activity was significantly decreased in model group ($P<0.01$). ASP (400, 800 mg·kg⁻¹) not only obviously decreased MDA content but also evidently increased SOD activity ($P<0.05-0.01$). Furthermore, ASP (200, 400, 800 mg·kg⁻¹) remarkably reduced the elevated NO content in a dose-dependent manner ($P<0.05-0.01$) (Table 2).

Table 2 Effect of ASP on activity of SOD and contents of MDA and NO in colonic tissue of colitis rats ($n=8$, $\bar{x}\pm s$)

Group	Dose (mg·kg ⁻¹)	SOD (kU·g ⁻¹)	MDA (nmol·g ⁻¹)	NO (nmol·g ⁻¹)
Control	-	23.16±5.13	27.41±9.66	294±73
Model	-	8.41±3.17 ^d	83.47±22.53 ^d	568±65 ^d
5-ASA	100	15.26±2.14 ^b	55.32±8.61 ^b	367±26 ^b
ASP	200	11.95±3.22 ^a	67.31±13.84	496±52 ^a
ASP	400	14.84±2.45 ^b	58.52±14.36 ^a	445±47 ^b
ASP	800	16.27±1.96 ^b	49.14±10.73 ^b	381±34 ^b

^a $P<0.05$, ^b $P<0.01$, vs model group; ^d $P<0.01$ vs normal group.

Effect of ASP on colonic TNF- α , IL-2 and IL-10 levels

Compared with normal group, the levels of TNF- α , IL-2 were significantly increased while the content of IL-10 was obviously reduced in model group ($P<0.01$). ASP (400, 800 mg·kg⁻¹) not only obviously decreased the levels of TNF- α , IL-2 but also significantly increased the content of IL-10 in model group ($P<0.05-0.01$) (Table 3).

Table 3 Effect of ASP on levels of TNF- α , IL-2, IL-10 in colonic tissue of colitis rats ($n=8$, $\bar{x}\pm s$)

Group	Dose (mg·kg ⁻¹)	TNF- α (kU·g ⁻¹)	IL-2 (A)	IL-10 (ng·g ⁻¹)
Control	-	30.6±12.6	0.176±0.028	43±8
Model	-	82.8±18.6 ^d	0.381±0.069 ^d	15±5 ^d
5-ASA	100	45.3±21.9 ^b	0.264±0.042 ^b	22±10
ASP	200	61.9±25.6	0.318±0.032 ^a	23±11
ASP	400	57.4±20.8 ^a	0.303±0.036 ^a	23±8 ^a
ASP	800	51.7±21.5 ^b	0.285±0.031 ^b	26±10 ^a

^a $P<0.05$, ^b $P<0.01$, vs model group; ^d $P<0.01$ vs normal group.

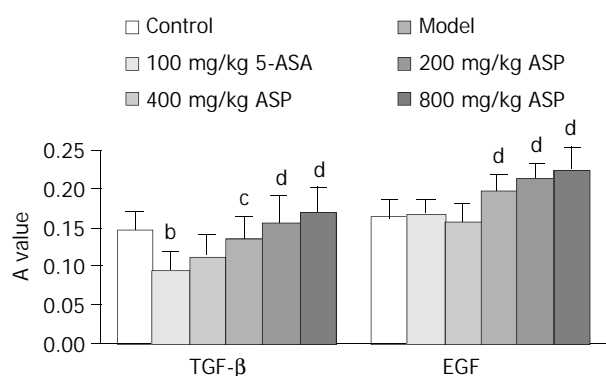


Figure 1 Effect of ASP on expressions of TGF- β and EGF in colonic tissue of colitis rats. $n=8$, $\bar{x}\pm s$, ^b $P<0.01$, vs normal control; ^c $P<0.05$, ^d $P<0.01$, vs model control.

Effect of ASP on colonic TGF- β and EGF expressions

As shown in Figures 1, 2 and 3, compared with normal group, TGF- β expression in model group was significantly decreased (0.096 ± 0.021 vs 0.145 ± 0.025 , $P<0.01$) and EGF expression was hardly changed. ASP (200, 400, 800 mg·kg⁻¹) remarkably up-regulated the expressions of TGF- β and EGF in a dose-dependent manner (TGF- β : 0.132 ± 0.031 , 0.154 ± 0.036 ,

0.169 ± 0.032 vs 0.096 ± 0.021 ; EGF: 0.197 ± 0.021 , 0.212 ± 0.023 , 0.225 ± 0.029 vs 0.166 ± 0.024 , $P<0.05-0.01$), whereas 5-ASA (100 mg·kg⁻¹) had no obvious effect on the expressions of TGF- β and EGF.

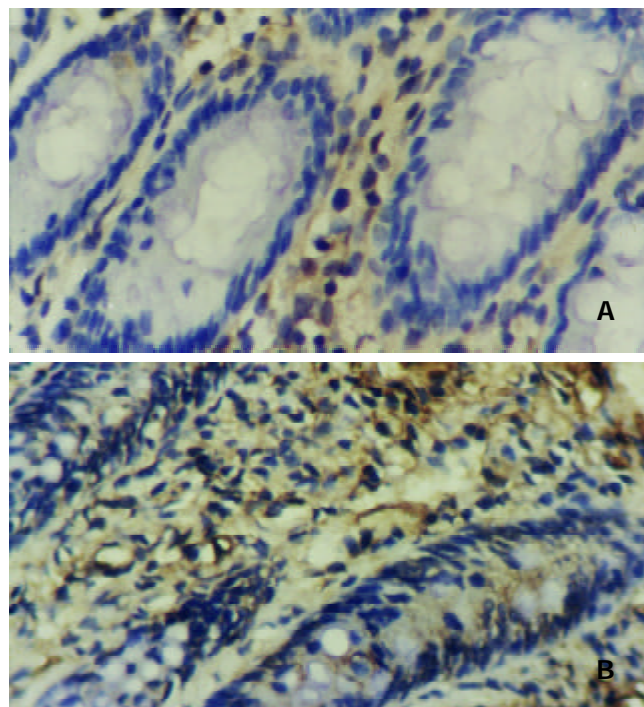


Figure 2 Expressions of TGF- β (A) and EGF (B) in inflammatory areas of colonic tissue from rats with colitis induced by TNBS and ethanol, respectively. Weakly positive signals were found. SP stain $\times 400$.

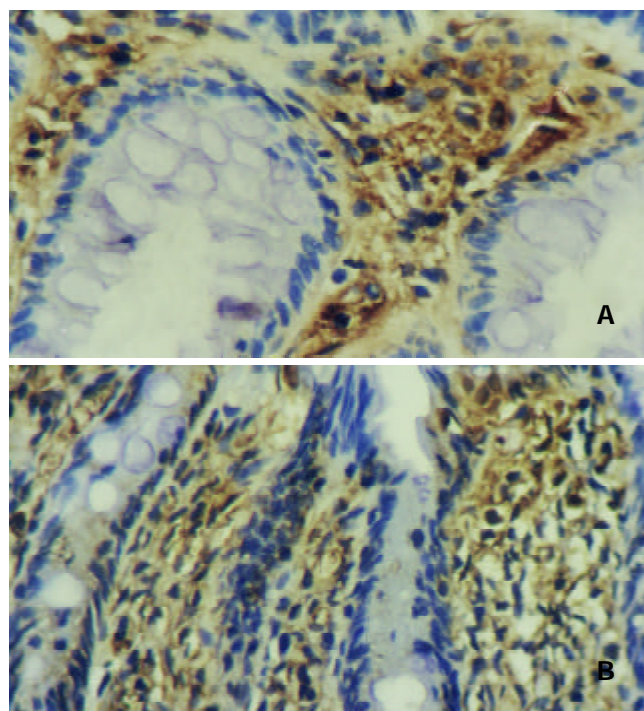


Figure 3 Significantly increased expressions of TGF- β (A) and EGF (B) were in colonic tissue from rats with colitis induced by TNBS and ethanol after treated with 800 mg·kg⁻¹ ASP. Strongly positive staining could be found. SP stain $\times 400$.

DISCUSSION

TNBS-induced rats colitis model established by Morris *et al*

was regarded as a classic model for immunological colon injury which shares many of the histopathological and clinical features and pathogenesis of human IBD. The whole process was summarized as following: after destruction of mucosa integrity by ethanol, hapten TNBS was bound to colon tissue proteins, and changed into a modified protein compound, which was recognized by macrophages as an abnormal antigen and presented quickly to the sensitized T lymphocytes. So a series of immunoresponsiveness and severe colon inflammation were initiated subsequently^[19,20]. In this study, an IBD model was successfully established, and intracolonic enema with ASP showed obviously protective effects on immunological colon injury, which might be related with ASP's antioxidation property and function of balancing cytokine generation and modulating immune.

Many studies have revealed that reactive metabolites of oxygen and nitrogen were a notable characteristic of IBD, which led to the pathological aggravation of a series of free radicals chain reactions and strongly attack DNA, proteins, enzymes, biological membranes as well as disruption of the integrity and function of intestinal mucosa barrier, activation of inflammatory mediators^[22-25]. Besides direct and severe impairment of the function of intestinal barrier, excessive NO participated in complicated web system between inflammatory cells and immunocytes in IBD^[12,15,22-25]. Our study showed that ASP, an anti-oxidant agent which can directly scavenge oxygen-derived free radicals, could not only remarkably decrease the elevated contents of MDA and NO, but also evidently increase the reduced SOD activity in colonic tissues of colitis rats. Reduction of NO by ASP might be related with its inhibition of nitric oxide synthase activity, which was proven by recent researches^[3,4].

As the most important cytokine in "inflammation cascade" of IBD, TNF- α could directly impair gut mucosa, promote production of inflammatory mediators and oxygen free radicals, up-regulate the expression of adhesive factors. Moreover, TNF- α is also a main activator for NF- κ B, a critical transcription factor, thus up-regulating many genes involved in proinflammatory and immune responses^[12,15,16,26]. In this article, ASP, an immunomodulatory reagent, obviously decreased the elevated colonic TNF- α level in colitis rats. As it is known, TNF- α and NO mainly came from activated macrophages in inflammatory gut^[12,19,26]. It deserves further investigation that whether inhibition of TNF- α and NO by ASP is related with its regulation of macrophage activation through the polysaccharide receptors on the surface of macrophages such as β -glucan receptor and mannose receptor^[27,28].

As it is known, imbalance of type 1 helper T lymphocyte (Th1) and Th2 in IBD could promote excretion of important pro-inflammatory cytokines including TNF- α , INF- γ , and activate macrophages, which mediate inflammatory and immunological injury. Moderate IL-2 level is important for keeping the dynamic balance of Th1 and Th2 in normal gut mucosa, whereas excessive IL-2 could up-regulate the activity of Th1^[29-31]. As a major anti-inflammatory cytokine mainly secreted by Th2, IL-10 could suppress inflammation by decreasing Th1 activation, reducing HLA class II expression, and diminishing production of pro-inflammatory cytokines from activated macrophages such as IL-1 α , IL-1 β , TNF- α and IL-8^[12,32-34]. Data obtained in this study indicated that ASP could not only significantly reduce the markedly elevated IL-2 level but also increase the reduced IL-10 level in colonic tissue of colitis rats, thus partly correcting the aberrant immunological status, which might be related with the marked induction of TGF- β by ASP. As a strong immunosuppressant and anti-inflammation cytokine mainly secreted by macrophages, TGF- β plays an important role in gut local immunity in IBD. TGF- β could not only suppress the immunoresponse of Th1

in intestine, depress the activity of activated macrophages but also induce production of IL-10^[12,18,34]. Investigations have demonstrated that deficiency of TGF- β in the intestine contributed to the development of IBD, whereas maintenance of TGF- β might be important in regulating immune homeostasis in the intestine^[18, 35].

Besides modulating immune response, TGF- β could control cell growth, differentiation and migration, stimulate synthesis of extracellular matrix proteins, and promote angiogenesis, thus promoting wound repair and tissue reconstruction. Its functions are similar to those of cytokine EGF^[36-41]. In addition, EGF could induce production of TGF- β and they showed cooperative effects^[40-42]. Researches have proven that TGF- β and EGF were crucial for maintaining the integrity and functions of intestine mucosa barrier, and could effectively prevent and ameliorate its injury and dysfunction induced by oxidants, thus contributing to the treatment of intestinal inflammation^[42-45]. Our study showed that ASP significantly increased the levels of EGF and markedly reduced TGF- β in colon tissue of colitis rats, thus accelerating repair of colon lesions, which agreed with investigations of Ye *et al.*^[18,9]. The underlying mechanism might be that ASP has pharmacological properties similar to heparin which can interact with a variety of proinflammatory chemokines and growth factors, thus promoting production of many growth factors^[7-9,42,47,48].

To sum up, the results of this study showed that intracolonic treatment with ASP at the doses of 400 mg·kg⁻¹ and 800 mg·kg⁻¹ could obviously attenuate experimental immunological colon injury in rats, suggesting that ASP in combination with well-established drugs, may contribute to the optimal therapy of IBD.

REFERENCES

- 1 **Xie L**, Yang LH, Li XH. Research on the pharmacologic effects of Angelica Sinensis. *Zhongyiyao Yanjiu* 2000; **16**: 56-58
- 2 **Ling XM**, Ding H, Luo SD, Zhang XJ, Zhang LH. Study on the pharmacological mechanism of angelica polysaccharide on the immunocompetence and the effects of its anti-oxidation. *Zhongguo Yiyuan Yaowu Zazhi* 2002; **22**: 584-586
- 3 **Ye YN**, Liu ES, Li Y, So HL, Cho CC, Sheng HP, Le SS, Cho CH. Protective effect of polysaccharides-enriched fraction from Angelica sinensis on hepatic injury. *Life Sci* 2001; **69**: 637-646
- 4 **Ding H**, Peng R, Yu J. Modulation of angelica sinensis polysaccharides on the expression of nitric oxide synthase and Bax, Bcl-2 in liver of immunological liver-injured mice. *Zhonghua Ganzhangbing Zazhi* 2001; **9**(Suppl): 50-52
- 5 **Yang TH**, Lu BH, Jia SM, Mei QB. Immunoregulation effect of Angelica polysaccharide isolated from Angelica sinensis on mice. *Zhongguo Yaolixue Tongbao* 2003; **19**: 448-451
- 6 **Xia XY**, Peng RX, Wang ZY. The effect of angelica sinensis polysaccharide and its ingredients on mice's immunocompetence. *Wuhan Daxue Xuebao(Medicine Edition)* 2001; **22**: 199-201
- 7 **Cho CH**, Mei QB, Shang P, Lee SS, So HL, Guo X, Li Y. Study of the gastrointestinal protective effects of polysaccharides from Angelica sinensis in rats. *Plant Med* 2000; **66**: 348-351
- 8 **Ye YN**, Koo MW, Li Y, Matsui H, Cho CH. Angelica sinensis modulates migration and proliferation of gastric epithelial cells. *Life Sci* 2001; **68**: 961-968
- 9 **Ye YN**, So HL, Liu ES, Shin VY, Cho CH. Effect of polysaccharides from Angelica sinensis on gastric ulcer healing. *Life Sci* 2003; **72**: 925-932
- 10 **Xia B**. Etiology and pathogenesis of inflammatory bowel disease. *Shijie Huaren Xiaohua Zazhi* 2001; **9**: 245-250
- 11 **Kirsner JB**. Historical origins of current IBD concepts. *World J Gastroenterol* 2001; **7**: 175-184
- 12 **Papadakis KA**, Targan SR. Role of cytokines in the pathogenesis of inflammatory bowel disease. *Annu Rev Med* 2000; **51**: 289-298
- 13 **Xia B**, Guo HJ, Crusius JBA, Deng CS, Meuwissen SGM, Pena A. *In vitro* production of TNF-alpha, IL-6 and sIL-2R in Chinese patients with ulcerative colitis. *World J Gastroenterol* 1998; **4**: 252-255

- 14 **Indaram AVK**, Nandi S, Weissman S, Lam S, Bailey B, Blumstein M, Greenberg R, Bank S. Elevated basal intestinal mucosal cytokine levels in asymptomatic first-degree relatives of patients with Crohn's disease. *World J Gastroenterol* 2000; **6**: 49-52
- 15 **Momeleone G**, Macdonald TT. Manipulation of cytokines in the management of patients with inflammatory bowel disease. *Ann Med* 2000; **32**: 552-560
- 16 **Blam ME**, Stein RB, Lichtenstein GR. Integrating anti-tumor necrosis factor therapy in inflammatory bowel disease: current and future perspectives. *Am J Gastroenterol* 2001; **96**: 1977-1997
- 17 **Das KM**, Farag SA. Current medical therapy of inflammatory bowel disease. *World J Gastroenterol* 2000; **6**: 483-489
- 18 **Fiocchi C**. TGF-beta/Smad signaling defects in inflammatory bowel disease: mechanisms and possible novel therapies for chronic inflammation. *J Clin Invest* 2001; **108**: 523-526
- 19 **Mei Q**, Yu JP, Xu JM, Wei W, Xiang L, Yue L. Melatonin reduces colon immunological injury in rats by regulating activity of macrophages. *Acta Pharmacol Sin* 2002; **23**: 882-886
- 20 **Morris GP**, Beck PL, Herridge MS, Depew WT, Szewczuk MR, Wallace JL. Hapten-induced model of chronic inflammation and ulceration in the rat colon. *Gastroenterology* 1989; **96**: 795-803
- 21 **Zhang JT**. Modern experimental methods in pharmacology. 1st ed. Beijing: Beijing Medical College Xiehe Medical College Pub 1997: 726-762
- 22 **Pavlick KP**, Laroux FS, Fuseler J, Wolf RE, Gray L, Hoffman J, Grisham MB. Role of reactive metabolites of oxygen and nitrogen in inflammatory bowel disease. *Free Radic Biol Med* 2002; **33**: 311-322
- 23 **Kriegelstein CF**, Cerwinka WH, Laroux FS, Salter JW, Russell JM, Schuermann G, Grisham MB, Ross CR, Granger DN. Regulation of murine intestinal inflammation by reactive metabolites of oxygen and nitrogen: divergent roles of superoxide and nitric oxide. *J Exp Med* 2001; **194**: 1207-1218
- 24 **Huang J**, Luo HS, Yang JX. Therapeutic effects of butyrate on nitric oxide abnormality in experimental ulcerative colitis in rats. *Shijie Huaren Xiaohua Zazhi* 2001; **9**: 967-969
- 25 **Bai AP**, Shen ZX, Yu JP, Yu BP, Luo Y. Nitric oxide and the acute injury in colitis model. *Shijie Huaren Xiaohua Zazhi* 1999; **7**: 900-901
- 26 **Li JH**, Yu JP, He XF, Xu XM. Expression of NF- κ B in rats with TNBS-induced ulcerative colitis. *Shijie Huaren Xiaohua Zazhi* 2003; **11**: 214-218
- 27 **Brown GD**, Taylor PR, Reid DM, Willment JA, Williams DL, Martinez-Pomares L, Wong SY, Gordon S. Dectin-1 is a major beta-glucan receptor on macrophages. *J Exp Med* 2002; **196**: 407-412
- 28 **Linehan SA**, Martinez-Pomares L, da Silva RP, Gordon S. Endogenous ligands of carbohydrate recognition domains of the mannose receptor in murine macrophages, endothelial cells and secretory cells; potential relevance to inflammation and immunity. *Eur J Immunol* 2001; **31**: 1857-1866
- 29 **Romagnani S**. Th1/Th2 cells. *Inflamm Bowel Dis* 1999; **5**: 285-294
- 30 **Van Damme N**, De Keyser F, Demetter P, Baeten D, Mielants H, Verbruggen G, Cuvelier C, Veys EM, De Vos M. The proportion of Th1 cells, which prevail in gut mucosa, is decreased in inflammatory bowel syndrome. *Clin Exp Immunol* 2001; **125**: 383-390
- 31 **Bemiss CJ**, Mahon BD, Henry A, Weaver V, Cantorna MT. Interleukin-2 is one of the targets of 1,25-dihydroxyvitamin D3 in the immune system. *Arch Biochem Biophys* 2002; **402**: 249-254
- 32 **Dejaco C**, Reinisch W, Lichtenberger C, Waldhoer T, Kuhn I, Tilg H, Gasche C. *In vivo* effects of recombinant human interleukin-10 on lymphocyte phenotypes and leukocyte activation markers in inflammatory bowel disease. *J Invest Med* 2000; **48**: 449-456
- 33 **Asseman C**, Mauze S, Leach MW, Coffman RL, Powrie F. An essential role for interleukin 10 in the function of regulatory T cells that inhibit intestinal inflammation. *J Exp Med* 1999; **190**: 995-1004
- 34 **Kitani A**, Fuss IJ, Nakamura K, Schwartz OM, Usui T, Strober W. Treatment of experimental (Trinitrobenzene sulfonic acid) colitis by intranasal administration of transforming growth factor (TGF)- β 1 plasmid: TGF- β 1-mediated suppression of T helper cell type 1 response occurs by interleukin (IL)-10 induction and IL-12 receptor beta2 chain downregulation. *J Exp Med* 2000; **192**: 41-52
- 35 **Hahn KB**, Im YH, Parks TW, Park SH, Markowitz S, Jung HY, Green J, Kim SJ. Loss of transforming growth factor beta signaling in the intestine contributes to tissue injury in inflammatory bowel disease. *Gut* 2001; **49**: 190-198
- 36 **Wiercinska-Drapalo A**, Flisiak R, Prokopowicz D. The role of transforming growth factors beta in pathogenesis of ulcerative colitis. *Pol Merkuriusz Lek* 2001; **10**: 177-179
- 37 **Fu XB**, Yang YH, Sun TZ, Gu XM, Jiang LX, Sun XQ, Sheng ZY. Effect of intestinal ischemia-reperfusion on expressions of endogenous basic fibroblast growth factor and transforming growth factor β in lung and its relation with lung repair. *World J Gastroenterol* 2000; **6**: 353-355
- 38 **Yuan YZ**, Lou KX, Gong ZH, Tu SP, Zhai ZK, Xu JY. Effects and mechanisms of emodin on pancreatic tissue EGF expression in acute pancreatitis in rats. *Shijie Huaren Xiaohua Zazhi* 2001; **9**: 128-130
- 39 **Xia L**, Yuan YZ, Xu CD, Zhang YP, Qiao MM, Xu JX. Effects of epidermal growth factor on the growth of human gastric cancer cell and the implanted tumor of nude mice. *World J Gastroenterol* 2002; **8**: 455-458
- 40 **Wu BW**, Wu Y, Wang JL, Lin JS, Yuan SY, Li A, Cui WR. Study on the mechanism of epidermal growth factor-induced proliferation of hepatoma cells. *World J Gastroenterol* 2003; **9**: 271-275
- 41 **Beck PL**, Podolsky DK. Growth factors in inflammatory bowel disease. *Inflamm Bowel Dis* 1999; **5**: 44-60
- 42 **Higashiyama S**, Abraham JA, Miller J, Fiddes JC, Klagsbrun M. A heparin-binding growth factor secreted by macrophage-like cells that is related to EGF. *Science* 1991; **251**: 936-939
- 43 **Chen DL**, Wang WZ, Wang JY. Epidermal growth factor prevents gut atrophy and maintains intestinal integrity in rats with acute pancreatitis. *World J Gastroenterol* 2000; **6**: 762-765
- 44 **Banan A**, Zhang Y, Losurdo J, Keshavarzian A. Carbonylation and disassembly of the F-actin cytoskeleton in oxidant induced barrier dysfunction and its prevention by epidermal growth factor and transforming growth factor alpha in a human colonic cell line. *Gut* 2000; **46**: 830-837
- 45 **Banan A**, Fields JZ, Talmage DA, Zhang L, Keshavarzian A. PKC-zeta is required in EGF protection of microtubules and intestinal barrier integrity against oxidant injury. *Am J Physiol Gastrointest Liver Physiol* 2002; **282**: G794-808
- 46 **Sandborn WJ**, Targan SR. Biologic therapy of inflammatory bowel disease. *Gastroenterology* 2002; **122**: 1592-1608
- 47 **Miller MD**, Krangel MS. Biology and biochemistry of the chemokines: a family of chemotactic and inflammatory cytokines. *Crit Rev Immunol* 1992; **12**: 7-46
- 48 **Li Y**, Wang HY, Cho CH. Association of heparin with basic fibroblast growth factor, epidermal growth factor, and constitutive nitric oxide synthase on healing of gastric ulcer in rats. *The J Pharmacol Exp Ther* 1999; **290**: 789-796

• BASIC RESEARCH •

Visceral hypersensitivity and altered colonic motility after subsidence of inflammation in a rat model of colitis

Jun-Ho La, Tae-Wan Kim, Tae-Sik Sung, Jeoung-Woo Kang, Hyun-Ju Kim, Il-Suk Yang

Jun-Ho La, Tae-Wan Kim, Tae-Sik Sung, Jeoung-Woo Kang, Hyun-Ju Kim, Il-Suk Yang, Department of Physiology, College of Veterinary Medicine, Seoul National University, Seoul, Republic of Korea

Correspondence to: Il-Suk Yang, Department of Physiology, College of Veterinary Medicine, Seoul National University, San 56-1 Sillim-Dong, Kwanak-Gu, Seoul, 151-742, Republic of Korea. isyang@snu.ac.kr

Telephone: +82-2-880-1261 **Fax:** +82-2-885-2732

Received: 2003-08-05 **Accepted:** 2003-09-17

Abstract

AIM: Irritable bowel syndrome (IBS) is a functional bowel disorder characterized by visceral hypersensitivity and altered bowel motility. There is increasing evidence suggesting the role of inflammation in the pathogenesis of IBS, which addresses the possibility that formerly established rat model of colitis could be used as an IBS model after the inflammation subsided.

METHODS: Colitis was induced by intracolonic instillation of 4 % acetic acid in male Sprague-Dawley rats. The extent of inflammation was assessed by histological examination and myeloperoxidase (MPO) activity assay. After subsidence of colitis, the rats were subjected to rectal distension and restraint stress, then the abdominal withdrawal reflex and the number of stress-induced fecal output were measured, respectively.

RESULTS: At 2 days post-induction of colitis, the colon showed characteristic inflammatory changes in histology and 8-fold increase in MPO activity. At 7 days post-induction of colitis, the histological features and MPO activity returned to normal. The rats at 7 days post-induction of colitis showed hypersensitive response to rectal distension without an accompanying change in rectal compliance, and defecated more stools than control animals when under stress.

CONCLUSION: These results concur largely with the characteristic features of IBS, visceral hypersensitivity and altered defecation pattern in the absence of detectable disease, suggesting that this animal model is a methodologically convenient and useful model for studying a subset of IBS.

La JH, Kim TW, Sung TS, Kang JW, Kim HJ, Yang IS. Visceral hypersensitivity and altered colonic motility after subsidence of inflammation in a rat model of colitis. *World J Gastroenterol* 2003; 9(12): 2791-2795

<http://www.wjgnet.com/1007-9327/9/2791.asp>

INTRODUCTION

Irritable bowel syndrome (IBS) is defined as a group of functional bowel disorders in which abdominal discomfort or pain is associated with defecation or a change in bowel habit

in the absence of an identifiable disease process^[1]. Clinical observations have revealed that patients with IBS show a disturbed colonic motor function and hypersensitivity to luminal distension, and these symptoms are generally accepted as cardinal features of IBS^[2].

Although IBS is known as one of the most common disorder encountered in clinical practice^[3], progress in the study of IBS in the basic scientific research fields has been hindered largely due to the lack of useful animal models that mimic the features of IBS^[4]. Since the pathophysiological processes involved in IBS are multifactorial, researchers have employed various kinds of symptom-generating stimulus to establish animal models of IBS. These include a stressful event in adult animals^[5], a chemical or mechanical irritation of colon in early life^[4], and neonatal maternal separation^[6].

Recently, attention has been directed to the role of inflammation in the pathogenesis of IBS^[3,7], and IBS after enteric infection, namely post-infectious IBS has begun to be studied using rodent models experimentally infected with *Nippostrongylus brasiliensis*^[8] or *Trichinella spiralis*^[9]. The infected animals underwent jejunitis and showed altered intestinal motor function or hypersensitivity to luminal distension even after the pathogens were eliminated. These inspiring reports addressed the possibility that the well-characterized rodent models of colitis could also exhibit some features of post-infectious IBS after resolution of colitis or, at least, in a certain period of time during the recovery course.

In the present study, we examined this possibility using one of the extensively studied rodent models of acute colitis, the rat model of acetic acid-induced colitis. Specifically, we aimed to find out whether the animal could show visceral hypersensitivity to rectal distension and altered defecation pattern under stress after the subsidence of colitis.

MATERIALS AND METHODS

Animals

Male Sprague-Dawley rats (270-310 g) were housed individually in an access-restricted room with controlled temperature (23 °C) and light-dark cycles (12:12 h). All the experimental protocols in this study were reviewed and approved by the Animal Care and Use Committee of Seoul National University.

Induction of colitis

After an overnight fast, the rats were lightly anesthetized with ether, and colitis was induced by intracolonic instillation of 1 ml 4 % acetic acid (Fluka, Buchs SG, Switzerland) at 8 cm proximal to the anus for 30 s. Then, 1 ml phosphate buffered saline was instilled to dilute the acetic acid and flush the colon. Control animals were handled identically except that 1 ml saline was instilled instead of 4 % acetic acid.

Myeloperoxidase (MPO) activity assay

MPO activity assay was performed to quantify the inflammation in distal colon according to the procedure described previously^[10]. Sixteen rats (4 animals at 2 and 7 days post-

enema in each group) were used for this study. These two time-points were selected according to previous reports^[10,11] to represent the overt inflammatory phase and the subsiding phase, respectively. Briefly, an 8 cm segment of distal colon was collected via laparotomy, minced in 1 ml of 50 mM potassium phosphate buffer (pH 6.0) containing 14 mM hexadecyltrimethylammonium bromide (Fluka), homogenized and sonicated. The lysates were frozen and thawed three-times, then centrifuged for 2 min in cold at 15 000 g. Aliquots of the supernatants were mixed with potassium phosphate buffer containing *o*-dianisidine-HCl (Sigma-Aldrich, St. Louis, MO, USA) and 0.0005 % H₂O₂. The change in absorbance at 460 nm was spectrophotometrically measured. MPO activity was expressed as units/g of wet tissue. The enzyme unit was defined as the conversion of 1 μ mol of H₂O₂ per min at 25 °C.

Histological examination of inflammation

To examine the extent of colonic inflammation, histological samples were collected at the selected time points. Sections with a thickness of 5 μ m were cut and processed for hematoxylin-eosin staining. The coded slides were analyzed by a pathologist blinded with regard to the treatment group and the time points.

Rectal distension procedure

At 7 days post-enema, eight rats from each group were used for studying visceral sensitivity to rectal distension. A disposable silicon balloon-urethral catheter for pediatric use (6 Fr, Sewoon Medical Co., Seoul, Korea) was used for this purpose. The maximal inflation volume for the balloon was 1.0 ml and the length of the maximally inflated balloon was 1.2 cm. After an overnight fast, the animals were lightly anesthetized with ether, and the balloon was carefully inserted into the rectum until the pre-marked line on the catheter (2 cm distal from the end of the balloon) was positioned to the anus, then the catheter was taped to the base of the tail to prevent displacement. After this procedure, the rats were placed in a transparent cubicle (20 cm \times 8 cm \times 8 cm) on a mirror-based elevated platform while still sedated, and were allowed to recover and acclimate for a minimum of 30 min before testing. The catheter was connected to a pressure transducer (RP-1500, Narco Bio-systems Inc., USA) via a 3-way connector, and a non-invasive pulse transducer (MLT125R, AD Instruments, Castle Hill, Australia) was attached so that the active site of the transducer was located on the ventral surface of the tail, directly below the caudal artery. The signals from both transducers were processed through PowerLab/400 (AD Instruments) and recorded on an IBM-compatible computer.

After the animals were fully awoken and acclimatized, ascending-limit phasic distension (0.1, 0.2, 0.3, 0.4, 0.6, 0.8 and 1 ml) was applied for 30 s every 4 min. The balloon was distended with pre-warmed (37 °C) water. We chose this protocol as hypersensitivity was reported to be best elicited by rapid phasic distension^[2]. In this experiment, the abdominal withdrawal reflex (AWR) was semiquantitatively scored as previously described^[4] and the concomitant change in arterial pulse rate was measured. The AWR score was assigned as follows: 0=no behavioral response to distension, 1=brief head movements followed by immobility, 2=contraction of abdominal muscle without lifting of abdomen, 3=lifting of abdomen, 4=body arching and lifting of pelvic structure.

After the experiments, the balloon was withdrawn and immersed in 37 °C tap water. Since the compliance of balloon was not infinite, we measured intraballoon pressure at each distension volume in 37 °C water, and digitally subtracted the value from that recorded during the rectal distension experiment to calculate the intrarectal pressure.

Restraint stress procedure

Fifteen animals of each group were used for this experiment. The rats were housed individually with no restrictions on food intake before testing. At 7 days post-enema, ten rats of each group were placed in restraint cages (5 cm \times 5 cm \times 20 cm) for 1 hr at room temperature. The feces excreted during restraint stress were divided into three types: hard pellet, soft pellet and formless stool, and counted separately. In another experiment, five rats of each group were left to be unrestrained for 1 hr and served as unstressed control. All the experiments were performed between 1 000 and 1 200 h.

Statistical analyses

Data were expressed as mean \pm SD. Significant difference between the two groups in MPO activity at the selected time-points and in the values (AWR score and the pulse rate change) at each distension volume was statistically analyzed using Mann-Whitney U-test with *P* value set at <0.05 significance level. The relationship between AWR score and the extent of pulse rate change was determined by linear regression analysis, and the estimated slope coefficients and intercepts were compared between groups using Student's *t*-test at 2N-4 (N=the number of data points) degrees of freedom (*d.f.*). The intraballoon volume-intrarectal pressure relationship of each group was also analyzed as above. The number of fecal output was compared using ANOVA and further analyzed using Newman-Keuls multiple comparison test, and considered significantly different from others when *P*<0.05.

RESULTS

Histological features and MPO activity

Figure 1 represents the histology of the distal colon in control (A), at 2 days (B) and at 7 days (C) post-induction of colitis (PIC). At 2 days PIC, mucosal hemorrhage with an inflammatory infiltrate in lamina propria and the edematous submucosa was observed. On the other hand, there was no remarkable inflammatory feature at 7 days PIC. Similar result was obtained from the MPO activity assay of colonic tissue. As shown in Figure 2, the enzyme activity was dramatically increased (8-fold) at 2 days PIC (*P*=0.0015, *n*=4), however it was not significantly different from the control value at 7 days PIC (*P*>0.5, *n*=4). These results indicated that at 7 days PIC, acute colonic inflammation was in subsiding phase.

Rectal distension-induced visceral nociception

Animals awoken in the cubicle showed regular arterial pulse after about 30 min acclimation. The pulse rate was 345.6 \pm 6.2 beat per minute (BPM) in control group (*n*=8) and 329.7 \pm 7.3 BPM in the 7 days PIC group (*n*=8), and the resting pulse rates of the two groups were not significantly different from each other. Pulse rate was instantly increased as the balloon inflated in the rectum and returned to nearly the resting level as it deflated. Animals at 7 days PIC showed hypersensitive response to the ascending-limit phasic rectal distension. The nociceptive threshold (distension volume that produced the AWR of score 2, i.e., abdominal contraction) was about 0.6 ml in the control group, and it was lowered to around 0.3 ml in the 7 days PIC group. The AWR score in rats at 7 days PIC was generally higher than that in control animals, which shifted the distension volume-response curve to left (Figure 3A). In addition, the extent of rectal distension-induced tachycardia was also significantly increased in the 7 days PIC group (Figure 3B).

We further analyzed these results by determining the relationship between the AWR score and the extent of pulse rate change (D pulse rate). The mean value with its standard error of D pulse rate at a given AWR score was plotted in

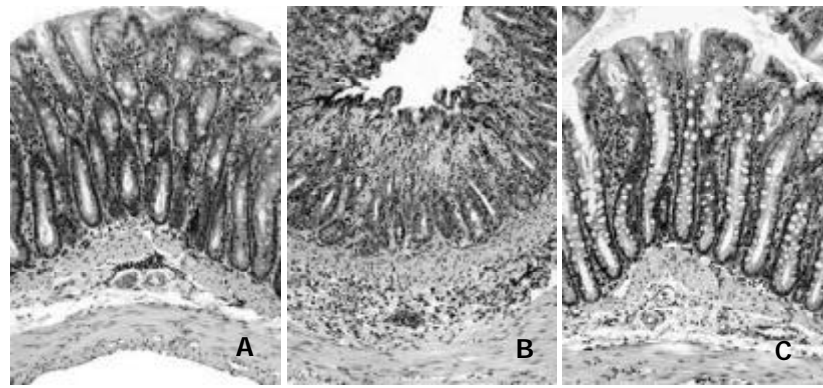


Figure 1 Photomicrographs of distal colons from control (A), at 2 days (B) and at 7 days (C) post-induction of colitis (PIC). At 2 days PIC, histological inflammatory features including mucosal hemorrhage, submucosal edema, and inflammatory infiltration in the lamina propria and the submucosa were observed. At 7 days PIC, there was no remarkable inflammatory feature compared with control.

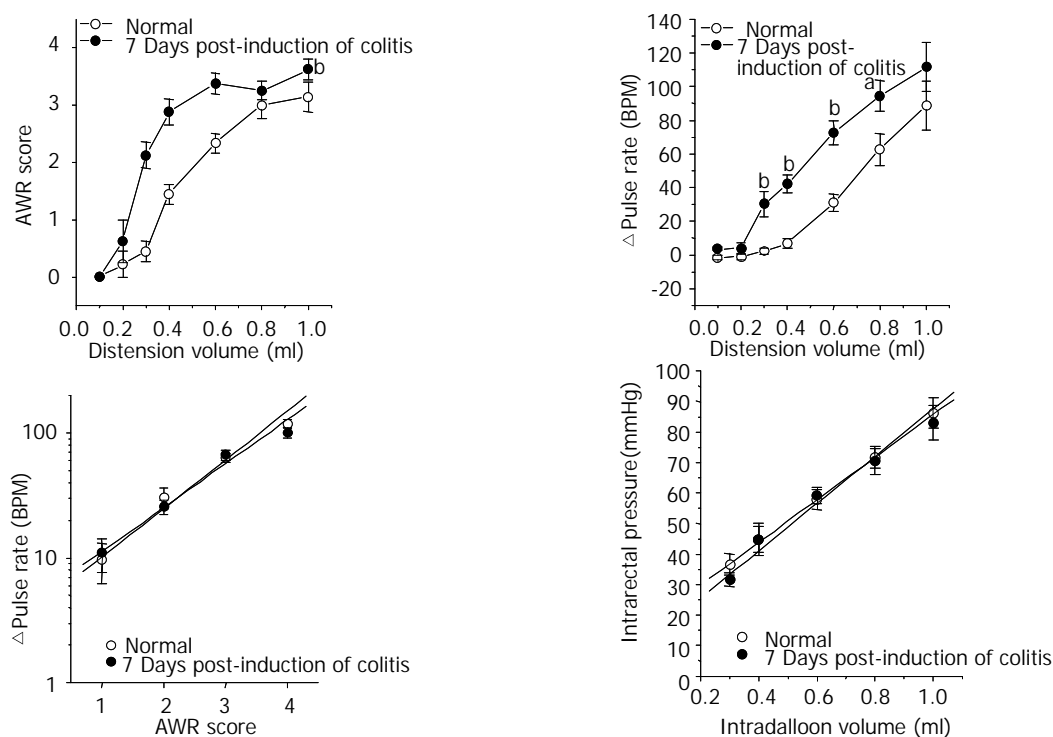


Figure 3 Summarized plots representing the rectal distension-induced AWR (A) and concomitant pulse rate change (B), the relationship between the AWR score and the extent of pulse rate change (C), and the relationship between intraballoon volume and intrarectal pressure (D) in each group. At 7 days PIC, AWR and tachycardia were exaggerated in response to rectal distension. Note the good linear correlation between the AWR score and the logarithmic D pulse rate, which was not significantly different between groups. Intrarectal pressure was linearly increased as the balloon inflated, and the fitted functions of two groups were not significantly different from each other. (^a $P < 0.05$, ^b $P < 0.01$).

logarithmic scale for a linear fit. As shown in Figure 3C, there was a good linear correlation between the AWR score and the logarithmic D pulse rate ($r = 0.99$, $P < 0.008$ in control; $r = 0.99$, $P < 0.007$ in the 7 days PIC group). The fitted functions of two groups were not significantly different from each other (slope coefficient: 0.39 ± 0.03 in control vs. 0.35 ± 0.01 in the 7 days PIC group ($P > 0.45$, $d.f. = 4$), intercept: 0.62 ± 0.07 in control vs. 0.69 ± 0.06 in the 7 days PIC group ($P > 0.43$, $d.f. = 4$)). This implied that scoring the AWR in the present study was a reliable method to quantify the animal's nociceptive response to rectal distension.

In order to examine whether the visceral hypersensitivity in rats at 7 days PIC was related to changes in rectal compliance, we compared the intraballoon volume-intrarectal pressure relationship of the two groups. The distension volume from 0.3 ml to 1.0 ml and the corresponding value of

calculated intrarectal pressure (refer MATERIALS AND METHODS) were plotted for regression analysis (Figure 3D). Intrarectal pressure was linearly increased as the balloon inflated ($r > 0.99$, $P < 0.0001$ in control; $r = 0.99$, $P = 0.0015$ in the 7 days PIC group). The fitted functions of the two groups were not significantly different from each other (slope coefficient: 69.83 ± 0.99 in control vs. 77.46 ± 6.81 in the 7 days PIC group ($P > 0.3$, $d.f. = 6$), intercept: 15.94 ± 0.64 in control vs. 10.15 ± 3.67 in the 7 days PIC group ($P > 0.17$, $d.f. = 6$)).

Restrain stress-induced defecation

As shown in Figure 4, the number of fecal pellet output for 1 hr was negligible in unrestrained animals regardless of the treatment. However, restraint stress significantly increased defecation. The restrained control rats defecated 2.1 ± 0.9 hard pellets, 1.9 ± 0.4 soft pellets, 1.2 ± 0.4 formless stool and a total

of 5.2 ± 0.5 feces in 1 hr ($n=10$). Comparatively, animals at 7 days PIC group defecated 4 ± 0.9 hard pellets, 3 ± 0.6 soft pellets, 2.7 ± 0.6 formless stool and 9.7 ± 0.8 feces in total during the 1 hr restraint stress ($n=10$). The number of formless stool and the total number of fecal output during 1 hr restraint stress in the 7 days PIC group were significantly larger than the corresponding values in control rats, which implied that the stress-induced increase in colonic motor function was enhanced in rats at 7 days PIC group.

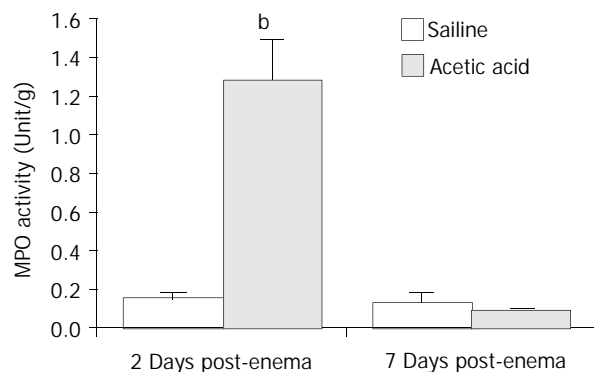


Figure 2 Tissue MPO activity at 2 and 7 days post-induction of colitis (PIC). MPO activity was increased about 8-fold at 2 days PIC. No statistically significant difference was detected between the saline-instilled and the acetic acid-instilled groups at day 7. (^b $P < 0.01$).

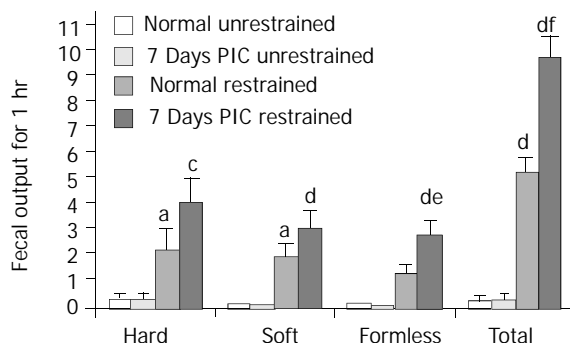


Figure 4 Restraint stress-induced defecation. The number of formless stool and the total number of defecation during 1 hr restraint stress in the 7 days PIC group were significantly larger than the corresponding values in control rats. (^a $P < 0.05$ restrained vs. unrestrained in control; ^b $P < 0.01$; ^c $P < 0.05$ restrained vs. unrestrained in 7 days PIC group; ^d $P < 0.01$; ^e $P < 0.05$ restrained 7 days PIC group vs. restrained control group; ^f $P < 0.01$).

DISCUSSION

In human study, patients with ulcerative colitis were reported to show visceral hypersensitivity even when their disease was in quiescent state^[12]. In the present study, we found that 7 days after the acetic acid-induced colitis subsided, the rats still showed visceral hypersensitivity, a generally accepted common feature of patients with IBS. Moreover, the rats at 7 days PIC defecated more stools in response to restraint stress than control animals, which was in good accordance with the clinical observations reporting the higher incidence of urgency to defecate and altered stool pattern under stress in IBS patients^[13]. These results suggested that along with the previously reported parasite-infected rat models, acetic acid-induced colitis model could be used for the study of a subset of IBS that developed from intestinal inflammation (post-inflammatory IBS).

Indeed, it was well documented that colitis caused motility alteration and visceral hypersensitivity in various models. For

instance, trinitrobenzene sulfonic acid (TNBS)/ethanol-induced colitis lowered the threshold for colorectal distension-induced visceromotor reflex at 3 days post-enema^[14], and progressively altered colonic muscle function^[15]. Similarly, acetic acid-induced colitis increased visceromotor response to colorectal distension at 6 and 24 h post-enema^[16], and decreased colonic circular muscle contractility^[17]. However, these studies mainly dealt with the alterations in acute or overt inflammatory phase, and few studies focused on the response of the animals with 'once' inflamed colon.

Advantages of our model as a post-inflammatory IBS model include not only a relatively short period required for the subsidence of inflammation but also an easy access to the affected sites, i.e., rectum and colon, which make it possible to measure behavioral and pseudoaffective responses in the awake animals. In the nematode-infected IBS models, the affected site is jejunum to which anesthesia and surgical procedures are required to access for experiments. Another potential advantage is a large body of literatures reporting the pathophysiological mechanisms of alterations occurred during active colitis. Scrutinizing those reports might help to find the pivotal inflammatory changes that induce the IBS symptoms.

The reasons for the exaggerated responses to rectal distension and restraint stress in our model have been unclear, but at least, it seemed not related to changes in rectal compliance since the intraballoon volume-intrarectal pressure relationship was not different between the groups. It was noteworthy that mast cells were found to be increased in a group of IBS patients^[3], and partially mediate functional disorder in the *N. brasiliensis*-infected rat model of post-infectious IBS^[8]. We are currently investigating whether mast cell also plays a role in the post-colitis IBS features in rat.

In summary, we found that the rat model of acetic acid-induced colitis showed major features of IBS after subsidence of the acute inflammation in colon. The results suggest that this model has several advantages as a useful model of post-inflammatory IBS.

ACKNOWLEDGEMENTS

This work was supported by the Research Institute of Veterinary Science, College of Veterinary Medicine, Seoul National University.

REFERENCES

- 1 Camilleri M, Heading RC, Thompson WG. Clinical perspectives, mechanisms, diagnosis and management of irritable bowel syndrome. *Aliment Pharmacol Ther* 2002; **16**: 1407-1430
- 2 Delvaux M. Role of visceral sensitivity in the pathophysiology of irritable bowel syndrome. *Gut* 2002; **51** (Suppl 1): i67-i71
- 3 Barbara G, De Giorgio R, Stanghellini V, Cremon C, Corinaldesi R. A role for inflammation in irritable bowel syndrome? *Gut* 2002; **51** (Suppl 1): i41-i44
- 4 Al-Chaer ED, Kawasaki M, Pasricha PJ. A new model of chronic visceral hypersensitivity in adult rats induced by colon irritation during postnatal development. *Gastroenterology* 2000; **119**: 1276-1285
- 5 Bradesi S, Eutamene H, Garcia-Villar R, Fioramonti J, Bueno L. Acute and chronic stress differently affect visceral sensitivity to rectal distension in female rats. *Neurogastroenterol Motil* 2002; **14**: 75-82
- 6 Coutinho SV, Plotsky PM, Sablad M, Miller JC, Zhou H, Bayati AI, McRoberts JA, Mayer EA. Neonatal maternal separation alters stress-induced responses to viscerosomatic nociceptive stimuli in rat. *Am J Physiol Gastrointest Liver Physiol* 2002; **282**: G307-G316
- 7 Tornblom H, Lindberg G, Nyberg B, Veress B. Full-thickness biopsy of the jejunum reveals inflammation and enteric neuropathy in irritable bowel syndrome. *Gastroenterology* 2002; **123**: 1972-1979

- 8 **Gay J**, Fioramonti J, Garcia-Villar R, Bueno L. Alterations of intestinal motor responses to various stimuli after *Nippostrongylus brasiliensis* infection in rats: role of mast cells. *Neurogastroenterol Motil* 2000; **12**: 207-214
- 9 **Barbara G**, Vallance BA, Collins SM. Persistent intestinal neuromuscular dysfunction after acute nematode infection in mice. *Gastroenterology* 1997; **113**: 1224-1232
- 10 **Al-Awadi FM**, Khan I. Studies on purine enzymes in experimental colitis. *Mol Cell Biochem* 1999; **194**: 17-22
- 11 **Conner EM**, Grisham MB. Animal models of colitis. In: Gaginella TS, eds. Experimental models of mucosal inflammation. New York: CRC press 1996: 97-109
- 12 **Rao SS**, Read NW, Davison PA, Bannister JJ, Holdsworth CD. Anorectal sensitivity and responses to rectal distention in patients with ulcerative colitis. *Gastroenterology* 1987; **93**: 1270-1275
- 13 **Drossman DA**, Sandler RS, McKee DC, Lovitz AJ. Bowel patterns among subjects not seeking health care. Use of a questionnaire to identify a population with bowel dysfunction. *Gastroenterology* 1982; **83**: 529-534
- 14 **Morteau O**, Hachet T, Caussette M, Bueno L. Experimental colitis alters visceromotor response to colorectal distension in awake rats. *Dig Dis Sci* 1994; **39**: 1239-1248
- 15 **Hosseini JM**, Goldhill JM, Bossone C, Pineiro-Carrero V, Shea-Donohue T. Progressive alterations in circular smooth muscle contractility in TNBS-induced colitis in rats. *Neurogastroenterol Motil* 1999; **11**: 347-356
- 16 **Burton MB**, Gebhart GF. Effects of intracolonic acetic acid on responses to colorectal distension in the rat. *Brain Res* 1995; **672**: 77-82
- 17 **Myers BS**, Martin JS, Dempsey DT, Parkman HP, Thomas RM, Ryan JP. Acute experimental colitis decreases colonic circular smooth muscle contractility in rats. *Am J Physiol* 1997; **273**: G928-G936

Edited by Zhu LH

• CLINICAL RESEARCH •

Relationship between clinical and pathologic findings in patients with chronic liver diseases

Lun-Gen Lu, Min-De Zeng, Yi-Min Mao, Ji-Qiang Li, De-Kai Qiu, Jing-Yuan Fang, Ai-Ping Cao, Mo-Bin Wan, Cheng-Zhong Li, Jun Ye, Xiong Cai, Cheng-Wei Chen, Ji-Yao Wang, Shan-Ming Wu, Jin-Shui Zhu, Xia-Qiu Zhou

Lun-Gen Lu, Min-De Zeng, Yi-Min Mao, Ji-Qiang Li, De-Kai Qiu, Jing-Yuan Fang, Ai-Ping Cao, Shanghai Institute of Digestive Disease, Renji Hospital, Shanghai Second Medical University, Shanghai 200001, China

Mo-Bin Wan, Cheng-Zhong Li, Department of Infectious Diseases, Changhai Hospital, Shanghai 200433, China

Jun Ye, Department of Infectious Diseases, Putuo District Central Hospital, Shanghai 200062, China

Xiong Cai, Department of Infectious Diseases, Changzheng Hospital, Shanghai 200003, China

Cheng-Wei Chen, Shanghai Liver Diseases Research Center of Nanjing Military Command, Shanghai 200233, China

Ji-Yao Wang, Department of Gastroenterology, Zhongshan Hospital, Shanghai 200032, China

Shan-Ming Wu, Shanghai Infectious Disease Hospital, Shanghai 200085, China

Jin-Shui Zhu, Department of Gastroenterology, Shanghai No.6 People's Hospital, Shanghai 200233, China

Xia-Qiu Zhou, Department of Infectious Diseases, Ruijin Hospital, Shanghai 200025, China

Supported by grants from the Key Project of Shanghai Medical Development Foundation, No.99ZDI001

Correspondence to: Dr. Lun-Gen Lu, MD, Shanghai Institute of Digestive Disease, Renji Hospital, Shanghai Second Medical University, Shanghai 200001, China. lulungen@online.sh.cn

Telephone: +86-21-33070824 **Fax:** +86-21-63364118

Received: 2003-03-28 **Accepted:** 2003-05-11

Abstract

AIM: To explore the relationship between clinical findings of patients with chronic liver diseases and the pathologic grading and staging of liver tissues.

METHODS: The inflammatory activity and fibrosis of consecutive liver biopsies from 200 patients were determined according to the diagnosis criteria of chronic hepatitis in China established in 1995. A comparative analysis was carried out for 200 patients with chronic liver diseases by comparing their clinical manifestations, serum biochemical markers with the grading and staging of liver tissues.

RESULTS: It was revealed that age, index of clinical symptoms and physical signs were obviously relevant to the pathologic grading and staging of liver tissues ($P < 0.05$). Blood platelet, red blood cells, aspartate aminotransferase (AST), N-terminal procollagen III (PIII NP) were apparently correlated with the degree of inflammation. PGA (prothrombin time, GGT, apoprotein A1) index, PGAA (PGA+ Δ 2-macroglobulin) index, albumin and albumin/globulin were relevant to both inflammation and fibrosis. Hyaluronic acid (HA) was an accurate variable for the severity of hepatic inflammation and fibrosis. The combination of serum markers for fibrosis could increase the diagnostic accuracy. It was notable that viral replication markers were not relevant to the degree of inflammation and fibrosis.

CONCLUSION: There is a good correlation between clinical

findings and the pathologic grading and staging of liver tissues, which may give aid to the noninvasive diagnosis of liver fibrosis.

Lu LG, Zeng MD, Mao YM, Li JQ, Qiu DK, Fang JY, Cao AP, Wan MB, Li CZ, Ye J, Cai X, Chen CW, Wang JY, Wu SM, Zhu JS, Zhou XQ. Relationship between clinical and pathologic findings in patients with chronic liver diseases. *World J Gastroenterol* 2003; 9(12): 2796-2800

<http://www.wjgnet.com/1007-9327/9/2796.asp>

INTRODUCTION

Liver fibrosis is a common sequel to diverse liver injuries. It is characterized by an accumulation of interstitial collagens and other matrix components^[1-4]. Chronic liver diseases usually develop into liver cirrhosis through the phase of liver fibrosis^[5-8]. In recent years, researchers have been making efforts to study the noninvasive diagnostic methods of liver fibrosis^[9-15]. Through a multi-center study, we carried out a comparative analysis of 200 patients with chronic liver diseases by comparing their clinical manifestations, serum biochemical markers with histopathological findings in liver biopsy, in order to appraise the relationship between clinical findings of patients with chronic liver diseases and the grading and staging of liver tissues, and to provide clues and basis for the noninvasive diagnosis of liver fibrosis.

MATERIALS AND METHODS

Patients recruitment

The study was organized and carried out by Shanghai Cooperative Group of Hepatic Fibrosis Project. The Cooperative Group was led by Renji Hospital and Changhai Hospital in Shanghai. Cases provided by the Cooperative Group were as follows: 37 from Changhai Hospital, 36 from Renji hospital, 30 from Putuo District Central Hospital, 22 from Shanghai Hepatic Disease Center of Nanjing Military Command, 20 from Changzheng Hospital, 14 from Zhongshan Hospital, 11 from Huashan Hospital, 9 from Shibe Hospital, 8 from Shanghai No. 6 People's Hospital, 6 from Shanghai Infectious Diseases Hospital, 3 from Ruijin Hospital, 3 from Shanghai No. 9 People's Hospital, 1 from Shanghai No. 1 People's Hospital. A total of 200 patients between July and October 1999 were recruited, including 156 male and 44 female patients. The average age of the patients was 34 years (range 15-60 years).

Histological examination

Within 1 week after admission, all the patients received liver puncture biopsy under the guidance of B ultrasound with the 14G quick-cut needle (8-light Company, Japan) or Menghini needle. The length of liver specimens was just 1 cm or longer. The samples were fixed with 10 % formaldehyde, embedded in paraffin and sliced, stained with hematoxylin-eosin, reticular fibers and collagenous fibers. According to the prevention and

treatment program for virus hepatitis set up in 1995^[16], all the patients were graded and staged for liver fibrosis and inflammatory activity. Three pathologists read the slides, respectively. The results were statistically analyzed with Kappa test. It was revealed that the consistency of the grading and staging by the pathologists was excellent. All the pathologic diagnoses of liver biopsy were performed by Department of Pathology, Medical College of Fudan University.

Clinical data

General data The general data included age (-25, 25-35, 35-), course of disease (from the time when hepatic symptoms or abnormal laboratory parameters appeared for the first time to the present study) and gender.

Degree of hepatitis The degree of hepatitis was clinically evaluated according to the criteria recommended at the meeting of prevention and treatment of viral hepatitis held in 1995.

Clinical symptoms According to the severity of clinical symptoms such as fatigue, inappetence, swelling, nausea, ache in hepatic region and gingival bleeding, it was scored as 0: no symptom, 1: with one kind of mild symptoms, 2: with one kind of symptoms between mild and severe, 3: with one kind of serious symptoms. It was further divided into 3 grades according to the totaled score: mild: 0-1, moderate: 2-3, severe: ≥ 4 .

Physical signs According to the degree of hepatomegaly and splenomegaly, it was scored as 0: no hyperplasia (maximal oblique diameter of the right liver <14 cm, thickness of the spleen <4.0 cm); 1: with hepatomegaly (maximal oblique diameter of the right liver >14 cm); 1.5: with mild splenomegaly (thickness of the spleen was between 4-6 cm); 3: with splenomegaly above moderate degree (thickness of the spleen ≥ 6.0 cm). It was further divided into 4 grades according to the totaled score: 0: no hyperplasia, 1: hepatomegaly, 1.5: mild splenomegaly, and ≥ 2.5 : splenomegaly above moderate degree or both splenomegaly and hepatomegaly.

Laboratory parameters

Routine blood test Red blood cells (RBC), white blood cells (WBC) and platelets (PLT) were counted.

Biochemical blood test Total serum bilirubin, AST, ALT, AST/ALT, GGT, albumin (A), albumin (A)/globulin (G), γ -globulin, prothrombin time (PT), apoprotein A1 (ApoA1), $\alpha 2$ -macroglobulin and α -fetoprotein (AFP) were detected. Among them, PT, GGT and Apo-A1 were integrated as PGA index. PGA and $\alpha 2$ -macroglobulin were integrated as PGAA index.

Serum viral markers HBsAg, HBeAg, anti-HBe, anti-HBc, HBV-DNA, anti-HCV and HCV-RNA were detected.

Serum fibrosis parameters Hyaluronic acid (HA), laminin (LN), N-terminal procollagen III (PIII NP), 7S collagen IV (7S-IV) were included.

Statistical analysis

Analysis of variance was carried out for all the data with SAS

software. $P < 0.05$ was considered statistically significant.

RESULTS

Relationship between general data and pathological grading and staging of liver tissues

It was revealed that there was a significant difference in inflammatory activity and fibrosis among different age groups (-25, 25-35, 35-) ($P < 0.05$). With the increase of age, the degree of fibrosis became more severe. However, there was no significant difference in inflammatory activity and fibrosis between different courses of disease (-1 year, 1-5 years, 5-years) and sexes ($P > 0.05$).

Relationship between clinical manifestations and pathological staging of liver fibrosis

The statistical results indicated that there was a significant difference between the severity of hepatitis and inflammatory grading, and fibrosis staging of liver tissues ($P < 0.01$) (Table 1).

The symptom accumulation score at different stages of liver fibrosis was significantly different ($P < 0.05$). With the increase of score, liver fibrosis tended to be more serious. However, there was no difference between symptom score and inflammatory grading. Statistical analysis of single symptom indicated that only nausea and gingival bleeding had a significant difference at different stages of liver fibrosis ($P < 0.05$ and $P < 0.01$, respectively).

Among different groups of inflammatory grading and fibrosis staging, the score of physical signs differed significantly ($P < 0.05$), with the increase of score, inflammatory and fibrosis became more serious.

When symptom score and physical signs were combined for a further analysis, all the subjects were divided into 6 groups (Table 1). There were correlations between the inflammatory activity and fibrosis staging, and the differences among different groups were significant ($P < 0.01$).

Relationship between biochemical parameters and inflammatory grading and fibrosis staging

The relationship between each single parameter and inflammatory grading and fibrosis staging is shown in Table 2.

From Table 2 we could find that the main biochemical parameters related only to inflammatory grading were RBC, PLT, AST, and PIIINP. With inflammation becoming serious, RBC and PLT tended to decrease, while the level of AST and PIIINP tended to increase. GGT, A, A/G, HA, 7S-IV and AFP were correlated with both inflammation grading and fibrosis staging, with the inflammation and fibrosis becoming more serious. A and A/G tended to decrease, while GGT and AFP tended to increase. There was no significant difference in PT at different stages and grades.

Table 1 Relationship between clinical manifestations and pathological grading and staging of liver tissues

Groups	Symptom score+physical signs	n	Inflammatory grading (G) (%)				Fibrosis staging (s) (%)				
			1	2	3	4	0	1	2	3	4
1	0~1+ no hepatomegaly and splenomegaly	15	46.7	40	13.3	0	33.3	26.7	40	0	0
2	0~1+ hepatomegaly and splenomegaly	14	28.6	28.6	28.6	14.3	7.1	35.7	28.6	14.3	14.3
3	~3+no hepatomegaly and splenomegaly	28	42.9	53.6	3.5	0	14.3	50	35.7	0	0
4	2~3 +hepatomegaly and splenomegaly	42	30.9	26.2	28.5	16.7	9.5	23.8	40.5	16.7	9.5
5	≥ 4 + no hepatomegaly and splenomegaly	32	43.7	25	15.6	15.6	12.5	34.3	25	15.6	12.5
6	≥ 4 + hepatomegaly and splenomegaly	69	23.3	21.7	34.8	15.9	2.9	29	29	15.9	23.2
			$P < 0.01$				$P < 0.01$				

Table 2 Relationship between biochemical parameters and inflammatory grading and fibrosis staging

Parameters	Inflammatory (G) (%)						Fibrosis staging (s) (%)									
	1~2	1~3	1~4	2~3	2~4	3~4	0~1	0~2	0~3	0~4	1~2	1~3	1~4	2~3	2~4	3~4
RBC			b		b	b				a			a		a	a
PLT			b		b	b										
AST		b	b	a	b											
ALT																
AST/ALT																
GGTa	a	b	b	b			b	b	b	b	b	b				
A				b		b				b			b		b	b
A/G				b		b				b			b		b	b
HA	b	b	b	b	b	b			b	b	b	b	b		b	b
LN																
7S-IV		a	b	a	b					a			a		a	
PIIINP			b		b											
AFP	b	b	b	b	b	b		b	b		b	b			b	
PT																

^a $P<0.05$, ^b $P<0.01$.

Table 3 Serologic parameters for diagnosing liver fibrosis and cirrhosis

Parameters	Fibrosis (S0/S1~4)			Cirrhosis (S1~3/S4)		
	Specificity(%)	Sensitivity(%)	Accuracy(%)	Specificity(%)	Sensitivity(%)	Accuracy(%)
HA	94.44	38.26	43.50	90.0	60.0	85.71
PIIINP	16.67	77.71	72.0	78.0	24.0	70.28
LN	55.26	50.29	50.10	54.0	52.0	53.71
7S-IV	50.22	24.67	51.0	93.29	24.0	89.08

Table 4 Serologic parameters for diagnosing liver fibrosis and cirrhosis

Parameters	Fibrosis (S0/S1~4)			Cirrhosis (S1~3/S4)		
	Specificity(%)	Sensitivity(%)	Accuracy(%)	Specificity(%)	Sensitivity(%)	Accuracy(%)
HA+7S-IV	88.89	37.93	42.50	89.93	60.0	85.63
HA+PIIINP	88.89	42.86	47.10	90.0	60.0	85.71
HA+7S-IV+PIIINP+LN	88.89	47.13	51.04	89.93	64.0	86.21
HA+TIMP	92.86	38.28	43.67	90.27	60.0	86.72
PGA+HA	60.0	60.44	60.40	89.41	66.67	87.91
PGAA+HA	70.0	62.64	63.67	89.41	66.67	87.91
PGA+7S-IV	61.12	50.22	50.31	90.59	33.33	86.80
PGAA+7S-IV	60.0	48.22	50.67	92.94	33.33	89.0

Relationship between PGA, PGAA index and pathological staging and grading

PGA score had a relationship with inflammation and fibrosis ($P<0.01$, $P<0.05$ respectively). Its sensitivity and accuracy for the diagnosis of liver fibrosis were 70.33 % and 67.33 %, respectively, both of which were higher than those for early liver cirrhosis (50.00 % and 57.14 %, respectively). PGAA also correlated with inflammation and fibrosis ($P<0.05$), the sensitivity and accuracy for the diagnosis of liver fibrosis were 63.74 % and 63.37 %, respectively, both of which were higher than those for early liver cirrhosis (33.33 % and 61.64 %, respectively).

Relationship between serum parameters of liver fibrosis and pathological grading and staging

With discriminatory analysis method, we evaluated the significance of assaying single or combined serum parameters of liver fibrosis, in the diagnosis of liver fibrosis and cirrhosis (Tables 3 and 4).

Relationship between viral markers and pathological staging and grading

The statistical results revealed that there was no relationship between viral replication parameters and degrees of inflammation and fibrosis.

DISCUSSION

This study suggested that age was correlated with inflammatory activity, but the course of disease did not. Maybe it is because most of the patients were unaware of the disease, but the course of disease was always calculated from the time when symptoms appeared or people saw a doctor. It could not reflect the course accurately. So it was difficult to discover the relationship between fibrosis severity and the course of the disease^[9,13,15].

With the integral method, we scored the severity of symptoms quantitatively, classified the total score, which could reflect the symptom severity comprehensively. The results indicated that there was no correlation between symptom score

and inflammatory activity ($P>0.05$), but the score correlated with fibrosis stage significantly ($P=0.0106$). With the symptoms becoming more prominent, fibrosis became more serious. At the same time, it was found that the score of physical signs had a strong relationship with inflammatory activity and fibrosis severity ($P<0.05$). The higher the physical sign score was, the more serious the inflammatory activity and fibrosis were. When the difference became more significant, the symptoms and signs were combined ($P<0.01$).

This study indicated that at different fibrosis stage and inflammatory grade of liver tissues, the serum level of HA differed remarkably ($P<0.01$), which could serve as a sensitive and accurate parameter to identify the severity of hepatic inflammation and fibrosis^[17-20]. In addition, HA was a specific and accurate parameter for the diagnosis of early liver cirrhosis, the specificity and accuracy were 90 % and 85 %, respectively. It was also found that PIIINP differed at the different inflammatory grades significantly ($P<0.01$), but not significantly at different fibrosis stages ($P<0.05$), indicating that its correlation with inflammatory severity was closer than that with fibrosis. Thus it might be of significance in determining the inflammatory severity.

One conclusion that differs from others is that this study did not agree with the significance of LN in the diagnosis of liver fibrosis. It has been claimed that the diagnostic efficiency would increase when HA was assayed in combination with other parameters, yet it needs to be proved^[21-28].

Based on the relationship between a single biochemical parameter and inflammation and fibrosis, we found that PLT, RBC and AST were important in identifying inflammatory severity rather than fibrosis. They differed significantly at grades 1, 2, 3 and 4, so they could help estimate the severity of inflammation. With the inflammation becoming serious, RBC and PLT tended to decrease. Both A and A/G ratio correlated with inflammation and fibrosis, and could be used to identify the severity. Additionally, our study proved that the level of AFP differed significantly at different inflammatory grades and fibrosis stages ($P<0.01$), indicating that it correlated with inflammation and fibrosis closely, and could be used as an adjuvant parameter^[29-32].

PGA (PT, GGT, and ApoA1) and PGAA (PGA+ α 2-macroglobulin) index were mainly used as liver function indicators put forward in the early 1990's by some experts to reflect the liver function of patients with alcoholic liver disease, and to screen or diagnose liver cirrhosis^[9,33-38].

In recent years, researchers in China have probed into applying PGA index or combining it with other serum parameters to the diagnosis of liver cirrhosis. To some extent, the results of our study are in accordance with the conclusion that both PGAA and PGA correlated with inflammation and fibrosis significantly. However, when the foreign criteria were used, the score of ApoA1 in most normal samples were 4, which were too high, resulting in the increase of total PGA and PGAA scores. Therefore, we considered it abnormal when PGA score was above 6. This difference might be due to the following reasons. First, there was an ethnic difference in the normal range of ApoA1, so it is necessary to set up PGA and PGAA criteria applicable in China. Second, the two parameters were mainly used in alcoholic liver diseases, but most of the patients in our study were viral hepatitis^[13-15,17,35,36,39,40].

Our study indicates that, viral replication parameters such as HBeAg and HBV DNA have no correlation with the severity of inflammation and fibrosis. We compared the inflammatory and fibrotic severity in patients with positive markers of hepatitis B only (141 cases) and in those with positive markers of both hepatitis B and C (10 cases), but no statistical difference was found between them. However, as the patients suffering from co-infection of hepatitis B and C were very few in the study, the conclusion needs to be verified by larger sample studies.

REFERENCES

- 1 **Albanis E**, Friedman SL. Hepatic fibrosis. Pathogenesis and principles of therapy. *Clin Liver Dis* 2001; **5**: 315-334
- 2 **Brenner DA**, Waterboer T, Choi SK, Lindquist JN, Stefanovic B, Burchardt E, Yamauchi M, Gillan A, Rippe RA. New aspects of hepatic fibrosis. *J Hepatol* 2000; **32**(1Suppl): 32-38
- 3 **Albanis E**, Safadi R, Friedman SL. Treatment of hepatic fibrosis: almost there. *Curr Gastroenterol Rep* 2003; **5**: 48-56
- 4 **Rockey DC**. The cell and molecular biology of hepatic fibrogenesis. Clinical and therapeutic implications. *Clin Liver Dis* 2000; **4**: 319-355
- 5 **Li D**, Friedman SL. Liver fibrogenesis and the role of hepatic stellate cells: new insights and prospects for therapy. *J Gastroenterol Hepatol* 1999; **14**: 618-633
- 6 **Friedman SL**. Molecular mechanisms of hepatic fibrosis and principles of therapy. *J Gastroenterol* 1997; **32**: 424-430
- 7 **Musca A**, Paoletti V, De Matteis A, Mammarella A, Labbadia G, Grassi M, Paradiso M. Liver fibrosis: what's the beginning of autonomic deficit? *Scand J Gastroenterol* 2002; **37**: 1235-1236
- 8 **Dai WJ**, Jiang HC. Advances in gene therapy of liver cirrhosis: a review. *World J Gastroenterol* 2001; **7**: 1-8
- 9 **Oberti F**, Valsesia E, Pilette C, Rousselet MC, Bedossa P, Aube C, Gallois Y, Rifflet H, Maiga MY, Penneau-Fontbonne D, Cales P. Noninvasive diagnosis of hepatic fibrosis or cirrhosis. *Gastroenterology* 1997; **113**: 1609-1616
- 10 **Tsutsumi M**, Takase S, Urashima S, Ueshima Y, Kawahara H, Takada A. Serum markers for hepatic fibrosis in alcoholic liver disease: which is the best marker, type III procollagen, type IV collagen, laminin, tissue inhibitor of metalloproteinase, or prolyl hydroxylase? *Alcohol Clin Exp Res* 1996; **20**: 1512-1517
- 11 **Aube C**, Oberti F, Korali N, Namour MA, Loisel D, Tanguy JY, Valsesia E, Pilette C, Rousselet MC, Bedossa P, Rifflet H, Maiga MY, Penneau-Fontbonne D, Caron C, Cales P. Ultrasonographic diagnosis of hepatic fibrosis or cirrhosis. *J Hepatol* 1999; **30**: 472-478
- 12 **Zaitoun AM**, Al Mardini H, Awad S, Ukabam S, Makadisi S, Record CO. Quantitative assessment of fibrosis and steatosis in liver biopsies from patients with chronic hepatitis C. *J Clin Pathol* 2001; **54**: 461-465
- 13 **Fontana RJ**, Lok AS. Noninvasive monitoring of patients with chronic hepatitis C. *Hepatology* 2002; **36**(5 Suppl 1): S57-S64
- 14 **Thabut D**, Simon M, Myers RP, Messous D, Thibault V, Imbert-Bismut F, Poynard T. Noninvasive prediction of fibrosis in patients with chronic hepatitis C. *Hepatology* 2003; **37**: 1220-1221
- 15 **Tran A**, Hastier P, Barjoan EM, Demuth N, Pradier C, Saint-Paul MC, Guzman-Granier E, Chevallier P, Tran C, Longo F, Schneider S, Piche T, Hebuterne X, Benzaken S, Rampal P. Non invasive prediction of severe fibrosis in patients with alcoholic liver disease. *Gastroenterol Clin Biol* 2000; **24**: 626-630
- 16 Prevention and treatment projects of virus hepatitis (tryout). *Zhonghua Neike Zazhi* 1995; **34**: 788-791
- 17 **Stickel F**, Urbaschek R, Schuppan D, Poeschl G, Oesterling C, Conradt C, McCuskey RS, Simanowski UA, Seitz HK. Serum collagen type VI and XIV and hyaluronic acid as early indicators for altered connective tissue turnover in alcoholic liver disease. *Dig Dis Sci* 2001; **46**: 2025-2032
- 18 **Guechot J**, Laudat A, Loria A, Serfaty L, Poupon R, Giboudeau J. Diagnostic accuracy of hyaluronan and type III procollagen amino-terminal peptide serum assays as markers of liver fibrosis in chronic viral hepatitis C evaluated by ROC curve analysis. *Clin Chem* 1996; **42**: 558-563
- 19 **Murawaki Y**, Ikuta Y, Okamoto K, Koda M, Kawasaki H. Diagnostic value of serum markers of connective tissue turnover for predicting histological staging and grading in patients with chronic hepatitis C. *J Gastroenterol* 2001; **36**: 399-406
- 20 **Pares A**, Deulofeu R, Gimenez A, Caballeria L, Bruguera M, Caballeria J, Ballesta AM, Rodes J. Serum hyaluronate reflects hepatic fibrogenesis in alcoholic liver disease and is useful as a marker of fibrosis. *Hepatology* 1996; **24**: 1399-1403
- 21 **Zheng M**, Cai WM, Weng HL, Liu RH. ROC curves in evaluation of serum fibrosis indices for hepatic fibrosis. *World J Gastroenterol* 2002; **8**: 1073-1076
- 22 **Zheng M**, Cai W, Weng H, Liu R. Determination of serum fibrosis indexes in patients with chronic hepatitis and its significance. *Chin Med J* 2003; **116**: 346-349

- 23 **Shahin M**, Schuppan D, Waldherr R, Risteli J, Risteli L, Savolainen ER, Oesterling C, Abdel Rahman HM, el Sahly AM, Abdel Razek SM. Serum procollagen peptides and collagen type VI for the assessment of activity and degree of hepatic fibrosis in schistosomiasis and alcoholic liver disease. *Hepatol* 1992; **15**: 637-644
- 24 **Ramadori G**, Zohrens G, Manns M, Rieder H, Dienes HP, Hess G, Meyer KH, Buschenfelde Z. Serum hyaluronate and type III procollagen aminoterminal propeptide concentration in chronic liver disease. Relationship to cirrhosis and disease activity. *Eur J Clin Invest* 1991; **21**: 323-330
- 25 **Hirayama C**, Suzuki H, Takada A, Fujisawa K, Tanikawa K, Igarashi S. Serum type IV collagen in various liver diseases in comparison with serum 7S collagen, laminin, and type III procollagen peptide. *J Gastroenterol* 1996; **31**: 242-248
- 26 **Fabris C**, Falleti E, Federico E, Toniutto P, Pirisi M. A comparison of four serum markers of fibrosis in the diagnosis of cirrhosis. *Ann Clin Biochem* 1997; **34**(Pt 2): 151-155
- 27 **Walsh KM**, Fletcher A, MacSween RN, Morris AJ. Comparison of assays for N-amino terminal propeptide of type III procollagen in chronic hepatitis C by using receiver operating characteristic analysis. *Eur J Gastroenterol Hepatol* 1999; **11**: 827-831
- 28 **Castera L**, Hartmann DJ, Chapel F, Guettier C, Mall F, Lons T, Richardet JP, Grimbet S, Morassi O, Beaugrand M, Trinchet JC. Serum laminin and type IV collagen are accurate markers of histologically severe alcoholic hepatitis in patients with cirrhosis. *J Hepatol* 2000; **32**: 412-418
- 29 **Lin DY**, Chu CM, Sheen IS, Liaw YF. Serum carboxy terminal propeptide of type I procollagen to amino terminal propeptide of type III procollagen ratio is a better indicator than each single propeptide and 7S domain type IV collagen for progressive fibrogenesis in chronic viral liver diseases. *Dig Dis Sci* 1995; **40**: 21-27
- 30 **Myers RP**, De Torres M, Imbert-Bismut F, Ratzu V, Charlotte F, Poynard T. Biochemical markers of fibrosis in patients with chronic hepatitis C: a comparison with prothrombin time, platelet count, and age-platelet index. *Dig Dis Sci* 2003; **48**: 146-153
- 31 **Imbert-Bismut F**, Ratzu V, Pieroni L, Charlotte F, Benhamou Y, Poynard T. Biochemical markers of liver fibrosis in patients with hepatitis C virus infection: a prospective study. *Lancet* 2001; **357**: 1069-1075
- 32 **Naveau S**, Montembault S, Balian A, Giraud V, Aubert A, Abella A, Capron F, Chaput JC. Biological diagnosis of the type of liver disease in alcoholic patients with abnormal liver function tests. *Gastroenterol Clin Biol* 1999; **23**: 1215-1224
- 33 **Myers RP**, Ratzu V, Imbert-Bismut F, Charlotte F, Poynard T. Biochemical markers of liver fibrosis: a comparison with historical features in patients with chronic hepatitis C. *Am J Gastroenterol* 2002; **97**: 2419-2425
- 34 **Pilette C**, Rousselet MC, Bedossa P, Chappard D, Oberti F, Rifflet H, Maiga MY, Gallois Y, Cales P. Histopathological evaluation of liver fibrosis: quantitative image analysis vs semi-quantitative scores. Comparison with serum markers. *J Hepatol* 1998; **28**: 439-446
- 35 **Naveau S**, Poynard T, Benattar C, Bedossa P, Chaput JC. Alpha-2-macroglobulin and hepatic fibrosis. Diagnostic interest. *Dig Dis Sci* 1994; **39**: 2426-2432
- 36 **Jiang JJ**, Salvucci M, Thepot V, Pol S, Ekindjian OG, Nalpas B. PGA score in diagnosis of alcoholic fibrosis. *Lancet* 1994; **343**: 803
- 37 **Teare JP**, Sherman D, Greenfield SM, Simpson J, Bray G, Catterall AP, Murray-Lyon IM, Peters TJ, Williams R, Thompson RP. Comparison of serum procollagen III peptide concentrations and PGA index for assessment of hepatic fibrosis. *Lancet* 1993; **342**: 895-898
- 38 **Croquet V**, Vuillemin E, Ternisien C, Pilette C, Oberti F, Gallois Y, Trossaert M, Rousselet MC, Chappard D, Cales P. Prothrombin index is an indirect marker of severe liver fibrosis. *Eur J Gastroenterol Hepatol* 2002; **14**: 1133-1141
- 39 **Cadranel JF**, Mathurin P. Prothrombin index decrease: a useful and reliable marker of extensive fibrosis? *Eur J Gastroenterol Hepatol* 2002; **14**: 1057-1059
- 40 **Lu LG**, Zeng MD, Wan MB, Li CZ, Mao YM, Li JQ, Qiu DK, Cao AP, Ye J, Cai X, Chen CW, Wang JY, Wu SM, Zhu JS, Zhou XQ. Grading and staging of hepatic fibrosis, and its relationship with noninvasive diagnostic parameters. *World J Gastroenterol* 2003; **9**: 2574-2578

Edited by Zhu LH and Wang XL

• CLINICAL RESEARCH •

Impact of endoscopically minimal involvement on IL-8 mRNA expression in esophageal mucosa of patients with non-erosive reflux disease

Yusei Kanazawa, Hajime Isomoto, Chun Yang Wen, Ai-Ping Wang, Vladimir A Saenko, Akira Ohtsuru, Fuminao Takeshima, Katsuhisa Omagari, Yohei Mizuta, Ikuo Murata, Shunichi Yamashita, Shigeru Kohno

Yusei Kanazawa, Hajime Isomoto, Ai-Ping Wang, Fuminao Takeshima, Katsuhisa Omagari, Yohei Mizuta, Shigeru Kohno, Second Department of Internal Medicine, Atomic Bomb Disease Institute, Nagasaki University School of Medicine, Nagasaki, Japan
Chun Yang Wen, Department of Molecular Pathology, Atomic Bomb Disease Institute, Nagasaki University School of Medicine, Nagasaki, Japan

Vladimir A Saenko, Akira Ohtsuru, Shunichi Yamashita, Department of Molecular Medicine, Atomic Bomb Disease Institute, Nagasaki University School of Medicine, Nagasaki, Japan

Ikuo Murata, Department of Pharmacotherapeutics, Nagasaki University Graduate School of Biomedical Sciences, Nagasaki, Japan

Correspondence to: Hajime Isomoto, M.D., Second Department of Internal Medicine, Nagasaki University School of Medicine, 1-7-1 Sakamoto, Nagasaki 852-8501, Japan. hajime2002@yahoo.co.jp
Telephone: +81-95-849-7567 **Fax:** +81-95-849-7568

Received: 2003-08-05 **Accepted:** 2003-10-12

Abstract

AIM: Little has been known about the pathogenesis of non-erosive reflux disease (NERD). Recent studies have implicated interleukin 8 (IL-8) in the development and progression of gastroesophageal reflux disease (GERD). The purpose of this study was to determine IL-8 RNA expression levels in NERD patients with or without subtle mucosal changes.

METHODS: We studied 26 patients with NERD and 13 asymptomatic controls. Biopsy sample was taken from the esophagus 3 cm above the gastroesophageal junction and snap frozen for measurement of IL-8 mRNA levels by real-time quantitative polymerase chain reaction (PCR). We also examined mRNA expression of IL-8 receptors, CXCR-1 and -2 by reverse transcriptase PCR. The patients were endoscopically classified into grade M (mucosal color changes without visible mucosal break) and N (neither minimal involvement nor mucosal break) of the modified Los Angeles classification.

RESULTS: The relative IL-8 mRNA expression levels were significantly higher in esophageal mucosa of NERD patients than those of the controls. There was a significant difference in IL-8 mRNA levels between grade M and N. The CXCR-1 and -2 mRNAs were constitutively expressed in esophageal mucosa.

CONCLUSION: Our results suggest that high IL-8 levels in esophageal mucosa may be involved in the pathogenesis of NERD through interaction with its receptors. NERD seems to be composed of a heterogeneous population in terms of not only endoscopically minimal involvement but also immune and inflammatory processes.

Kanazawa Y, Isomoto H, Wen CY, Wang AP, Saenko VA, Ohtsuru A, Takeshima F, Omagari K, Mizuta Y, Murata I, Yamashita S, Kohno S. Impact of endoscopically minimal

involvement on IL-8 mRNA expression in esophageal mucosa of patients with non-erosive reflux disease. *World J Gastroenterol* 2003; 9(12): 2801-2804

<http://www.wjgnet.com/1007-9327/9/2801.asp>

INTRODUCTION

Gastroesophageal reflux disease (GERD) is one of the most common chronic disorders in modern humans. In the United States, 44 % of the adult populations reported experiencing heartburn at least once a month, 14 % on a weekly basis, and 7 % daily^[1]. Esophageal erosions are the characteristic lesions of GERD seen on endoscopy^[2]. A small number of GERD patients develop stricture, Barrett's esophagus and adenocarcinoma of the esophagus. In fact, the majority of GERD patients have endoscopically normal-appearing esophageal mucosa; this group is termed non-erosive reflux disease (NERD) or endoscopy-negative reflux disease^[2,3].

The Los Angeles (LA) classification is widely used for endoscopic assessment of GERD^[4]. The slightest degree of esophagitis, i.e., grade A, is defined as one or more mucosal breaks confined to the mucosal folds, each no longer than 5 mm. Accordingly, this classification scheme ignores subtle mucosal damage in the absence of mucosal breaks. In this regard, Hoshihara *et al.*^[5,6] have proposed a modified LA system, in which grade O was subdivided into M and N, based on the concept of mucosal color changes. Thus, NERD patients can be classified into two subgroups (grade M and N) based on minimal esophageal involvement during endoscopy.

Recently, several studies have shown that mucosal immune and inflammatory responses, characterized by specific cytokine and chemokine profiles, may determine the diversity of esophageal phenotypes of GERD^[7-9]. Of note, Fitzgerald *et al.*^[7] reported significantly higher expression levels of interleukin 8 (IL-8) messenger ribonucleic acid (mRNA) in patients with reflux esophagitis (RE), assessed by competitive reverse transcriptase polymerase chain reaction (RT-PCR), compared with subjects with non-inflamed or Barrett's esophagus. Studies from our laboratories have also demonstrated high IL-8 protein levels in esophageal biopsy samples of patients with erosive esophagitis by enzyme linked immunosorbent assay (ELISA)^[8]. Furthermore, we also showed significantly high mucosal IL-8 production, which paralleled the endoscopic severity of RE^[8]. However, little has been known about the role of IL-8 in NERD.

The aim of the present study was to assess esophageal expression levels of IL-8 mRNA in NERD patients by quantitative real-time PCR procedure, with special reference to the difference between grade M and N subgroups of the modified LA scheme.

MATERIALS AND METHODS

Subjects and samples

We studied 26 patients with NERD and endoscopically confirmed normal-appearing esophageal mucosa who visited

the Outpatient Department between August 2002 and July 2003. They included 19 men and 7 women, aged between 28 and 80 years (mean, 62.0 years). The diagnosis of GERD was made with more than 6 points in the questionnaire for the diagnosis of reflux disease (QUEST) described by Carlsson *et al*^[10]. None of these patients had been treated with non-steroidal anti-inflammatory drugs, proton pump inhibitors, histamine H₂-receptor antagonists, anti-cholinergic agents or antibiotics within 4 weeks prior to the present study. Furthermore, patients with severe concomitant diseases, prior esophageal or gastric surgery, peptic ulcer diseases and comorbid conditions that might interfere with esophageal or gastric motility including diabetes mellitus, systemic sclerosis and neurological disorders were excluded. As a control group, we recruited 13 asymptomatic subjects with no hiatal hernia or any lesions in the esophagus, stomach and duodenum at endoscopy for a health check-up.

In each case, a biopsy specimen was obtained from the esophageal mucosa, 3 cm above the gastroesophageal junction^[8], snap-frozen in an ethanol-dry ice mixture for quantitative analysis of IL-8 mRNA expression and stored at -80 °C until use.

Endoscopic assessment of NERD

NERD was endoscopically classified into grade M and N in accordance with the modified Los Angeles (LA) classification system proposed by Hoshihara *et al*^[5,6]. The criteria were: grade M represents minimal changes (irregular redness or whiteness) without any mucosal breaks and grade N represents esophageal mucosa with neither the minimal changes nor mucosal injury. In addition, we also evaluated the presence of hiatal hernia by endoscopy^[11].

Real-time quantitative PCR

Total RNA from the biopsy samples was extracted using a commercial kit according to the instructions provided by the supplier (Isogen, Nippon Gene Co., Toyama, Japan). One µg of total RNA was reversely transcribed into complementary DNA (cDNA) in a volume of 25 µl with MuLV reverse transcriptase and random hexamers (both from PE Applied Biosystems, Warrington, UK).

Real-time PCR measurement of IL-8 cDNA was performed in the ABI PRISM 7700 sequence detector (PE Applied Biosystems) with TaqMan assay. The primers and probe sequences for IL-8 were synthesized (PE Applied Biosystems) as described previously^[12]: IL-8 forward primer, 5'-CTCTTGGCAGCCTTCCTGATT-3', reverse primer, 5'-TATGCACTGACATCTAAGTTCTTTAGCA-3' and probe, 5'-CTTGGCAAACCTGCACCTTCACACAGA-3', labeled with the reporter dye 6-carboxyfluorescein at the 5' end and quencher dye 6-carboxytetramethylrhodamine at the 3' end. PCR was performed in a total volume of 50 µl of each amplification mixture containing 1 µl of each RT product, 25 µl of 2×Universal Master Mix (PE Applied Biosystems), 200 nM IL-8 forward and reverse primers, 100 nM fluorogenic probe. Thermal cycling was initiated with at 50 °C for 2 min, followed by a first denaturation step at 95 °C for 10 min, and followed by 50 cycles of at 95 °C for 15 s and at 60 °C for 1 min.

The *tubulin alpha 3* gene cDNA (internal control) was quantified in the same machinery using SYBR Green PCR Core reagents kit (PE Applied Biosystems). The primers used were: forward, 5'-AGATCATTGACCTCGTGTGGA-3' and reverse, 5'-ACCAGTTCCCCACCAAAG-3', which correspond to nucleotides 437-458 and 537-519, respectively (*TUBA3*, GenBank accession number 17986282). PCR was performed in a total volume of 25 µl of each amplification mixture containing 1 µl of each RT product, 3 µl of 25 mM MgCl₂, 2.5 µl of 10×SYBR Green buffer, 2 µl of dNTP Mix (5 mM adenosine, deoxycytosine and deoxyguanosine

triphosphate and 2.5 mM deoxyuridine triphosphate), 0.625 U AmpliTaq Gold polymerase, 0.125 U AmpErase and 100 nM tubulin alpha 3 forward and reverse primers. Thermal cycling was initiated at 50 °C for 2 min, followed by a first denaturation step at 95 °C for 10 min, and continued with 40 cycles of at 95 °C for 15 s and at 59 °C for 1 min.

Each assay included a standard curve, a no-template control and cDNA samples in triplicate. The standard curve was generated by serial 5-fold dilutions of pooled cDNA obtained from gastric tissues that were found to contain high levels of mRNAs of both genes. Contents of the tubulin alpha 3 and IL-8 cDNAs were expressed in arbitrary units calculated according to the standard curve. The relative expression level of IL-8 was expressed as the ratio of IL-8/tubulin alpha 3 in arbitrary units^[13].

RT-PCR

Based on the technique described previously^[14] with slight modification, the target sequence of CXCR-1 mRNA was amplified through 35 cycles, each consisting of denaturation at 94 °C for 30 sec, annealing at 53 °C for 30 sec and extension at 72 °C for 30 min, followed by a final extension at 72 °C for 5 min with specific primers (forward, 5'-CAGATCCACAGATGTGGGAT-3' and reverse, 5'-TCCAGCCATTACCTTGAGAG-3') using an RT-PCR kit (Takara Shuzo Co., Otsu, Japan). Similarly, CXCR-2 mRNA expression was detected under the following conditions: amplification through 35 cycles, each consisting of denaturation at 94 °C for 30 sec, annealing at 60 °C for 30 sec and extension at 72 °C for 30 min, followed by a final extension at 72 °C for 5 min with specific primers (forward, 5'-AGCTGCTCTTCTGGAGGTGT-3' and reverse, 5'-TTAGAGAGTAGTGGGAAGTGTGC-3')^[14]. A 10-µl aliquot of each PCR product was analyzed by electrophoresis on 2 % agarose gel containing ethidium bromide, and the bands were examined under ultraviolet light for the presence of amplified DNA. Glyceraldehyde-3-phosphate dehydrogenase (G3PDH) gene transcript was also amplified as described previously^[15], and used as an internal control of the processed RNA for each preparation.

Detection of *Helicobacter pylori* infection

H. pylori status was assessed by serology (anti-*H. pylori* Immunoglobulin G antibody, HEL-p TEST, Amrad Co., Melbourne, Australia), rapid urease test (Helicocheck, Otsuka Pharmaceutical Co., Tokushima, Japan) and histopathology (hematoxylin-eosin and Giemsa staining) using additional biopsy specimens obtained during endoscopy from the antrum within 2 cm of the pyloric ring and the corpus along the greater curvature. Patients were considered positive for *H. pylori* infection when at least two of these examinations yielded positive results. On the other hand, patients were defined as *H. pylori*-negative if all the test results were negative^[16].

All the samples were obtained with written informed consent of the patients prior to their inclusion in this study, in accordance with the Helsinki Declaration.

Statistical analysis

Statistical analyses were performed using Fisher's exact, χ^2 , Student's *t*, Mann-Whitney U, and Kruskal-Wallis tests, whenever appropriate. A *P* value of less than 0.05 was accepted as statistically significant. Data are expressed as mean \pm standard deviation (SD).

RESULTS

Patient demographics

According to the modified LA system, 14 patients were classified as grade M and 12 as grade N. There were no

significant differences in age, gender, current tobacco use, alcohol intake, body mass index, the presence of hiatus hernia and *H pylori* status among the patients with grade M and N and the controls (Table 1). None had such complications as stricture, bleeding and columnar-lined esophagus. The overall incidence of *H pylori* infection in our series was 51.3 %.

Table 1 Baseline characteristics of the enrolled subjects

	Control group <i>n</i> =13	Nonerosive reflux disease group	
		Grade M ^a <i>n</i> =14	Grade N ^a <i>n</i> =12
Mean age, yr, (range)	61.6(39-80)	58.7(28-75)	62.5 (33-75)
Male/female	8/5	11/3	8/4
Smoker	53.8 %(7/13)	28.6 %(4/14)	33.3 %(4/12)
Alcohol drinker	46.2 %(6/13)	57.1 %(8/14)	33.3 %(4/12)
Hiatal hernia	0 %(0/13)	35.7 %(5/14)	50.0 %(6/12)
<i>H pylori</i> infection	53.8 %(7/13)	57.1 %(8/14)	41.7 %(5/12)

According to the modified Los Angeles system.

Relative expression levels of IL-8

We confirmed that both RT-PCR procedures for IL-8 and tubulin alpha 3 yielded 87- and 101-base pair (bp) specific bands, respectively (data not shown). As a whole, NERD patients had significantly higher expression levels of IL-8 than the controls (Figure 1, $P<0.05$). The expression levels of IL-8 in esophageal mucosa of grade M patients with NERD were significantly higher than those of grade N patients ($P<0.05$, Figure 2). In addition, the expression levels of IL-8 were higher in grade M than control group ($P<0.01$, Figure 2), but not significantly different between NERD-grade N and control group.

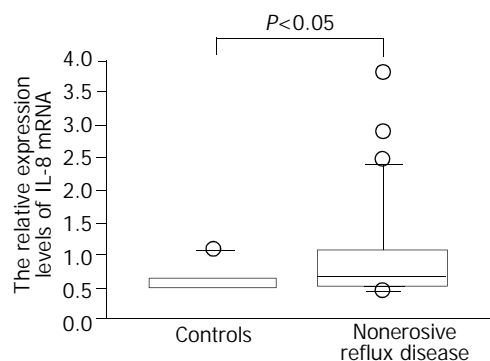


Figure 1 Relative interleukin 8 (IL-8) mRNA expression levels assessed by real-time quantitative polymerase chain reaction in patients with non-erosive reflux disease (NERD) and asymptomatic controls.

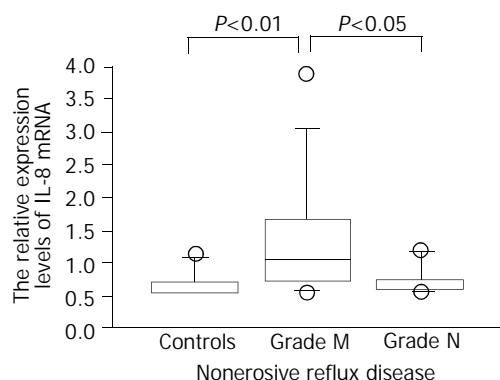


Figure 2 The expression levels of IL-8 assessed by real-time quantitative polymerase chain reaction in patients with non-erosive reflux disease (NERD) of grade M and N and asymptomatic controls.

Expression of CXCR-1 and CXCR-2 genes in esophageal mucosa

We identified the CXCR-1 and -2 gene-specific products as 257- and 1 154-bp bands, respectively, by RT-PCR (Figure 3). These mRNAs were constitutively expressed in each subject examined, irrespective of the presence of GERD-related symptoms or endoscopic grading. We confirmed that RT-PCR procedures for *G3PDH* housekeeping gene expression yielded 983 bp specific bands (data not shown).

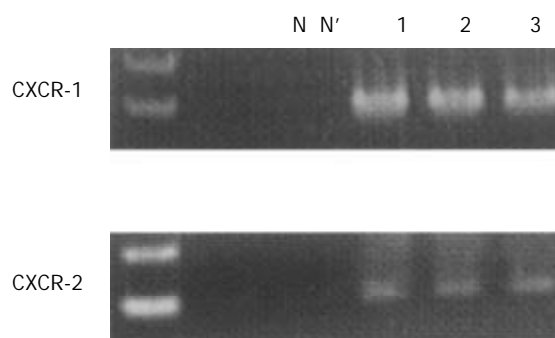


Figure 3 CXCR-1 and -2 mRNA transcripts were detected as 257 and 1 154 base pair (bp) bands with reverse transcription-polymerase chain reaction, respectively. Lane N; negative control, lane N'; RT (-) negative control, lane 1; asymptomatic normal control, lane 2; patient with NERD grade M, lane 3; patient with NERD grade N.

DISCUSSION

Several lines of evidence indicated that a prototype of CXC chemokine, IL-8, played a crucial role in the development and progression of erosive esophagitis^[7,8]. In the present study, we focused on the implication of this potent inflammatory mediator in NERD. We found significantly higher expression levels of IL-8 mRNA in esophageal mucosa of patients with NERD than those in asymptomatic controls, suggesting that IL-8 is implicated in the pathogenesis of this incipient form of GERD.

The striking finding of this study was that NERD patients classified as grade M subgroup based on the modified LA system had significantly higher expression levels of IL-8 mRNA compared to those of grade N. IL-8 mediated the recruitment of neutrophils into sites of inflammation^[17]. In addition, this potent chemoattractant acted on neutrophils to respiratory burst and release of a variety of reactive oxygen species (ROS), leading to tissue damage^[18]. In our previous work employing ELISA, we found a significant association between the presence of intraepithelial neutrophils and increased IL-8 levels in esophageal mucosa of patients with RE^[13]. Although we did not perform histopathological evaluation in the current study, elevated mucosal IL-8 expression may be involved even in such subtle mucosal changes as seen in the grade M subcategory, probably through its action on neutrophils, thus triggering chemotaxis and generating harmful ROS. This result also highlighted the possibility that NERD patients could encompass diverse subpopulations in terms of immune and inflammatory reactions. Further studies on the implication of other members of chemokines and proinflammatory cytokines can shed light on our understanding of the mechanisms underlying this poorly studied disorder.

In the present study, we demonstrated constitutive mRNA expression of CXCR-1 and -2 in esophageal biopsy samples by RT-PCR procedure. To date, CXCR-1 and -2 are two distinct receptors for IL-8^[19]. It is suggested that the increased IL-8 may facilitate trafficking of neutrophils into the mucosa

affected by GERD process through the interaction with these receptors. Again, recent data from our laboratories showed a significant correlation between IL-8 protein levels and basal layer hyperplasia as well as papillary elongation in patients with RE^[13]. IL-8 also exerted mitogenic actions directly or by binding to its receptors on epithelial cells^[20,21]. Taken together, it is possible that IL-8, together with other cytokines as well as growth factors^[14,22], could contribute to epithelial cell proliferation even in NERD, and could be eventually linked to carcinogenesis. Again, unlike CXCR-1, CXCR-2 is not specific for IL-8 and can bind to other chemokines such as growth related oncogene α , but it has 2- to 5-fold higher affinity for IL-8 than CXCR-1^[19]. Further studies on the distribution of diverse IL-8 receptors and the receptor-mediated signaling pathway may help to elucidate the pathogenesis of GERD via IL-8 action.

In conclusion, our study demonstrated significantly enhanced expression of IL-8 mRNA level in NERD by real-time PCR technology. The interaction of IL-8 with CXCR-1 and -2 is likely to be involved in the pathogenesis of NERD. We also showed a significant difference in IL-8 mRNA levels between grade M and N subgroups of the modified LA classification, indicating the heterogeneity of NERD patients both immunologically and endoscopically.

REFERENCES

- Fass R**, Ofman JJ. Gastroesophageal reflux disease-Should we adopt a new conceptual framework? *Am J Gastroenterol* 2002; **97**: 1901-1909
- Frierson HF Jr**. Histology in the diagnosis of reflux esophagitis. *Gastroenterol Clin N Am* 1990; **19**: 631-644
- Quigley EMM**. Factors that influence therapeutic outcomes in symptomatic gastroesophageal reflux disease. *Am J Gastroenterol* 2003; **98**(Suppl): S24-S30
- Armstrong D**, Bennett JR, Blum AL, Dent J, De Dombal FT, Galmiche JP, Lundell L, Margulies M, Richter JE, Spechler SJ, Tytgat GN, Wallin L. The endoscopic assessment of oesophagitis: a progress report on observer agreement. *Gastroenterology* 1996; **111**: 85-92
- Hoshihara Y**, Hashimoto M. Endoscopic classification of reflux esophagitis. *Nippon Rinsho* 2000; **58**: 1808-1812
- Nishiyama Y**, Koyama S, Andoh A, Moritani S, Kushima R, Fujiyama Y, Hattori T, Bamba T. Immunohistochemical analysis of cell cycle-regulating-protein (p21, p27, and Ki-67) expression in gastroesophageal reflux disease. *J Gastroenterol* 2002; **37**: 905-911
- Fitzgerald RC**, Onwuegbusi BA, Bajaj-Elliott M, Saeed IT, Burnham WR, Farthing MJ. Diversity in the oesophageal phenotypic response to gastro-oesophageal reflux: immunological determinants. *Gut* 2002; **50**: 451-459
- Isomoto H**, Wang A, Mizuta Y, Akazawa Y, Ohba K, Omagari K, Miyazaki M, Murase K, Hayashi T, Inoue K, Murata I, Kohno S. Elevated levels of chemokines in esophageal mucosa of patients with reflux esophagitis. *Am J Gastroenterol* 2003; **98**: 551-556
- Fitzgerald RC**, Abdalla S, Onwuegbusi BA, Sirieix P, Saeed IT, Burnham WR, Farthing MJ. Inflammatory gradient in Barrett's oesophagus: implications for disease complications. *Gut* 2002; **51**: 316-322
- Carlsson R**, Dent J, Bolling-Sternevald E, Johnsson F, Junghard O, Lauritsen K, Riley S, Lundell L. The usefulness of a structured questionnaire in the assessment of symptomatic gastroesophageal reflux disease. *Scand J Gastroenterol* 1998; **33**: 1023-1029
- Jones MP**, Sloan SS, Rabine JC, Ebert CC, Huang CF, Kahrilas PJ. Hiatal hernia size is the dominant determinant of esophagitis presence and severity in gastroesophageal reflux disease. *Am J Gastroenterol* 2001; **96**: 1711-1717
- Yuan A**, Yang PC, Yu CJ, Chen WJ, Lin FY, Kuo SH, Luh KT. Interleukin-8 messenger ribonucleic acid expression correlates with tumor progression, tumor angiogenesis, patient survival, and timing of relapse in non-small-cell lung cancer. *Am J Respir Crit Care Med* 2000; **162**: 1957-1963
- Rogounovitch TI**, Saenko VA, Shimizu-Yoshida Y, Abrosimov AY, Lushnikov EF, Roumiantsev PO, Ohtsuru A, Namba H, Tsyb AF, Yamashita S. Large deletions in mitochondrial DNA in radiation-associated human thyroid tumors. *Cancer Res* 2002; **62**: 7031-7041
- Kondo S**, Yoneta A, Yazawa H, Kamada A, Jimbow K. Downregulation of CXCR-2 but not CXCR-1 expression by human keratinocytes by UVB. *J Cell Physiol* 2000; **182**: 366-370
- Ohnita K**, Isomoto H, Mizuta Y, Maeda T, Haraguchi M, Miyazaki M, Murase K, Murata I, Tomonaga M, Kohno S. *Helicobacter pylori* infection in patients with gastric involvement by adult T-cell leukemia/lymphoma. *Cancer* 2002; **94**: 1507-1516
- Isomoto H**, Furusu H, Morikawa T, Mizuta Y, Nishiyama T, Omagari K, Murase K, Inoue K, Murata I, Kohno S. 5-day vs. 7-day triple therapy with rabeprazole, clarithromycin and amoxicillin for *Helicobacter pylori* eradication. *Aliment Pharmacol Ther* 2000; **14**: 1619-1623
- Mukaida N**. Interleukin-8: An expanding universe beyond neutrophil chemotaxis and activation. *Int J Hematol* 2000; **72**: 391-398
- Graca-Souza AV**, Arruda MA, de Freitas MS, Barja-Fidalgo C, Oliveira PL. Neutrophil activation by heme: implications for inflammatory processes. *Blood* 2002; **99**: 4160-4165
- Chuntharapai A**, Kim KJ. Regulation of the expression of IL-8 receptor A/B by IL-8: possible functions of each receptor. *J Immunol* 1995; **155**: 2587-2594
- Metzner B**, Hofmann C, Heinemann C, Zimpfer U, Schraufstatter I, Schopf E, Norgauer J. Overexpression of CXC-chemokines and CXC-chemokine receptor type 2 constitute an autocrine growth mechanism in the epidermoid carcinoma cells KB and A431. *Oncol Rep* 1999; **6**: 1405-1410
- Zachrisson K**, Neopikhanov V, Samali A, Uribe A. Interleukin-1, interleukin-8, tumour necrosis factor alpha and interferon gamma stimulate DNA synthesis but have no effect on apoptosis in small intestinal cell lines. *Eur J Gastroenterol Hepatol* 2001; **13**: 551-559
- Sfakianakis A**, Barr CE, Kreutzer DL. Localization of the chemokine interleukin-8 receptors in human gingival and cultured gingival keratinocytes. *J Periodont Res* 2002; **87**: 154-160

Edited by Zhu LH

• CLINICAL RESEARCH •

Endoscopic banding ligation can effectively resect hyperplastic polyps of the stomach

Ching-Chu Lo, Ping-I Hsu, Gin-Ho Lo, Hui-Hwa Tseng, Hui-Chun Chen, Ping-Ning Hsu, Chiun-Ku Lin, Hoi-Hung Chan, Wei-Lun Tsai, Wen-Chi Chen, E-Ming Wang, Kwok-Hung Lai

Ching-Chu Lo, Ping-I Hsu, Gin-Ho Lo, Hui-Hwa Tseng, Hui-Chun Chen, Ping-Ning Hsu, Chiun-Ku Lin, Hoi-Hung Chan, Wei-Lun Tsai, Wen-Chi Chen, E-Ming Wang, Kwok-Hung Lai, Division of Gastroenterology, Department of Internal Medicine, Pathology, Kaohsiung Veterans General Hospital and National Yang-Ming University, Taipei, Taiwan, China

Hui-Hwa Tseng, Division of Pathology, Kaohsiung Veterans General Hospital and National Yang-Ming University, Taipei, Taiwan, China
Hui-Chun Chen, Department of Radiation Oncology, Kaohsiung Chang-Gang Memorial Hospital, Chang-Gang University, Taoyuan, Taiwan, China

Ping-Ning Hsu, Graduate Institute of Immunology, National Taiwan University, Taipei, Taiwan, China

Supported by the research grant NSC-90-2314-B-075B-003 from the National Science Council and VGHKS-91-35 from Kaohsiung Veterans General Hospital, Taiwan

Correspondence to: Ping-I Hsu, MD. Division of Gastroenterology, Department of Internal Medicine, Kaohsiung Veterans General Hospital, 386, Ta-Chung 1st Road, Kaohsiung, Taiwan 813, China. williamhsup@yahoo.com.tw

Telephone: +86-7-3422121 Ext 2075 **Fax:** +86-7-3468237

Received: 2003-08-28 **Accepted:** 2003-10-12

Abstract

AIM: Bleeding and perforation are major and serious complications associated with endoscopic polypectomy. To develop a safe and effective method to resect hyperplastic polyps of the stomach, we employed rubber bands to strangulate hyperplastic polyps and to determine the possibility of inducing avascular necrosis in these lesions.

METHODS: Forty-seven patients with 72 hyperplastic polyps were treated with endoscopic banding ligation (EBL). At 14 days after endoscopic ligation, follow-up endoscopies were performed to assess the outcomes of the strangulated polyps.

RESULTS: After being strangulated by the rubber bands, all of the polyps immediately became congested (100 %), and then developed cyanotic changes (100 %) approximately 4 minutes later. On follow-up endoscopy 2 weeks later, all the polyps except one had dropped off. The only one residual polyp shrank with a rubber band in its base, and it also dropped off spontaneously during subsequent follow-up. No complications occurred during or following the ligation procedures.

CONCLUSION: Gastric polyps develop avascular necrosis following ligation by rubber bands. Employing suction equipment, EBL can easily capture sessile polyps. It is an easy, safe and effective method to eradicate hyperplastic polyps of the stomach.

Lo CC, Hsu PI, Lo GH, Tseng HH, Chen HC, Hsu PN, Lin CK, Chan HH, Tsai WL, Chen WC, Wang EM, Lai KH. Endoscopic banding ligation can effectively resect hyperplastic polyps of the stomach. *World J Gastroenterol* 2003; 9(12): 2805-2808
<http://www.wjgnet.com/1007-9327/9/2805.asp>

INTRODUCTION

Bleeding is the most common complication of electrocautery snare polypectomy for upper gastrointestinal polyps, with an incidence ranging from 6.0 to 7.2 % in prospective studies^[1-3]. To prevent polypectomy-elicited bleeding, epinephrine injection into the stalk^[2] or placement of a metallic clip^[4,5] before resection has been employed. Hachisu *et al.*^[6] also reported favorable results of preventive ligation during polypectomy with placement of detachable snares at the bases of polyps. However, it is difficult to place detachable snares on sessile polyps or on polyps situated in technically difficult areas.

Endoscopic ligation using suction equipment and rubber bands or detachable snare^[7-12] have been extensively applied in the management of bleeding esophageal and gastric varices. The varices are automatically eradicated through the use of ligation. In our pilot studies^[13,14], we used detachable snares to strangulate gastric polyps, and demonstrated that most gastric polyps (89 %) developed avascular necrosis following ligation. Those results implied that a strangulating technique alone can achieve the bloodless transection of gastrointestinal neoplasm. However, it is important to note that a significant portion of gastric polyps (11 %) remain alive following detachable snare ligation. The aim of this study was to assess the safety and efficacy of endoscopic banding ligation (EBL) for removal of hyperplastic polyps of the stomach.

MATERIALS AND METHODS

Patients

From June 2000 to October 2001, forty-five patients (30 men and 15 women) who had 70 hyperplastic polyps documented in previous endoscopic biopsies were electively treated with EBL. Another two male patients received emergent EBL to treat bleeding gastric polyps. The mean patient age was 59.9 years (range 14 to 75 years). Written informed consent was obtained from all the subjects. The characteristics of their polyps are analyzed and illustrated in Table 1. The mean diameter of the head of polyps was 9.3 mm (range 5 to 25 mm).

EBL procedure

EBL was carried out with a GIF XQ200 endoscope (Olympus Optical Co., Tokyo, Japan) and a 19 cm flexible overtube (Sumitomo Bakelite Co., Tokyo, Japan). We set a transparent hood at the end of a scope that was equipped with a pneumoactivated esophageal variceal ligation (EVL) device set (Sumitomo Bakelite Co., Tokyo, Japan). The EVL device set consisted of an air feeding tube, a sliding tube, an inner cylinder, and a rubber band (O-ring). Pumping through an air feeding tube made a sliding tube slide on an inner cylinder and, as a result, the rubber band slipped off, thus ligating a lesion aspirated into the hood.

As premedication, 20 mg of hyoscine-N-butylbromide was given intramuscularly 5 minutes before performing EBL. The endoscope with a flexible overtube attached to its base was inserted and the overtube was inserted gently over the

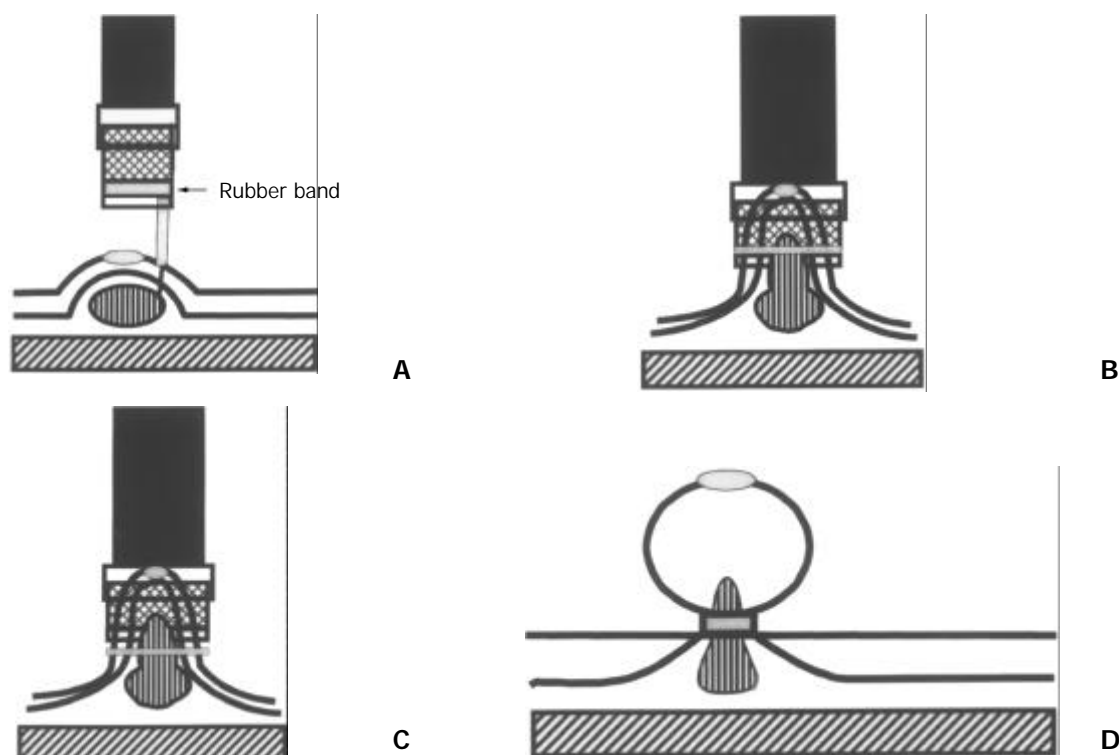


Figure 1 A: One to 4 ml of distilled water was injected locally into the submucosa adjacent to the polyp to lift the lesion from the muscle layer. B: The raised lesion was aspirated into the hood. C: The polyp was ligated by a rubber band after the air was pumped through the air feeding tube. D: The pneumoactivated EVL device set was removed.

endoscope to avoid mechanical injury to the thorax, larynx, and cervical esophagus. Before banding ligation, one to 4 ml of distilled water was injected into the submucosal layer near the lesion to tear and lift it off the muscle layer (Figure 1A). The endoscope was removed, and the pneumoactivated EVL device set was assembled on the instrument, which was then reinserted through the overtube. The raised lesion was aspirated into the hood (Figure 1B) and ligated with the rubber band after air was pumped through the air feeding tube (Figure 1C). Also, the polyp was observed for 5 minutes to investigate the sequential macroscopic changes of the strangulated lesion after EBL and biopsies were conducted later.

After the procedure, the patient was allowed to consume a liquid meal for a 24 hour period, and then issued a regular diet. An H₂-receptor antagonist was administered orally for 4 weeks. A follow-up endoscopy was performed 14 days after initial endoscopic ligation to assess the outcome of the strangulated polyp.

RESULTS

Table 1 summarizes the results of 47 patients treated with EBL. EBL was performed easily and safely in each case. Following strangulation with detachable snares, all of the polyps immediately became congested (100 %), and then developed cyanotic change (100 %) approximately 4 minutes later. Figure 2 displays the typical sequential changes of a strangulated polyp. Following ligation, biopsies were conducted, and almost no bleeding was induced by biopsy procedures from the strangulated polyps. Pathological examination revealed severe venous congestion in the lamina propria of the lesions (Figure 2F). In the case of the two patients with bleeding gastric polyps above the antrum, EBL achieved successful hemostasis. The biopsies of polyps following EBL disclosed that they were hyperplastic lesions.

The follow-up endoscopy 2 weeks later revealed that all the polyps except one had dropped off, and EBL-related ulcers

were found at the sites of the original lesions. The only one residual polyp shrank with a rubber band at its base. An additional follow-up endoscopy was performed for this lesion 1 month later, revealing that both the ligated polyp and rubber band had disappeared. No complications, such as bleeding or perforation, occurred during or after EBL and biopsies.

Table 1 Clinical characteristics and treatment results of endoscopic banding ligation in patients with hyperplastic gastric polyps

Variables	Number
Number of cases (M/F)	47 (32/15)
Age (years±SD)	59.9±15.1
Number of polyps	72
Mean size of polyps	9.3 mm (5-25 mm)
Morphology of polyps	
Sessile	70 (97.2 %)
Pedunculated	2 (2.8 %)
Location of polyps	
Cardia (superior, inferior, anterior, posterior)	(0, 1, 0, 2)
Fundus (superior, inferior, anterior, posterior)	(1, 4, 4, 1)
Antrum (superior, inferior, anterior, posterior)	(4, 5, 9, 7)
Body (superior, inferior, anterior, posterior)	(5, 10, 4, 15)
Initial endoscopic findings after ligation	
Congestion	72 (100 %)
Cyanosis	72 (100 %)
Endoscopic findings at second look	
Shrunk polyps	1 (1.4 %) ^a
Ligation-related ulcer	71 (98.6 %)

^aThe polyp dropped off spontaneously in subsequent follow-up.

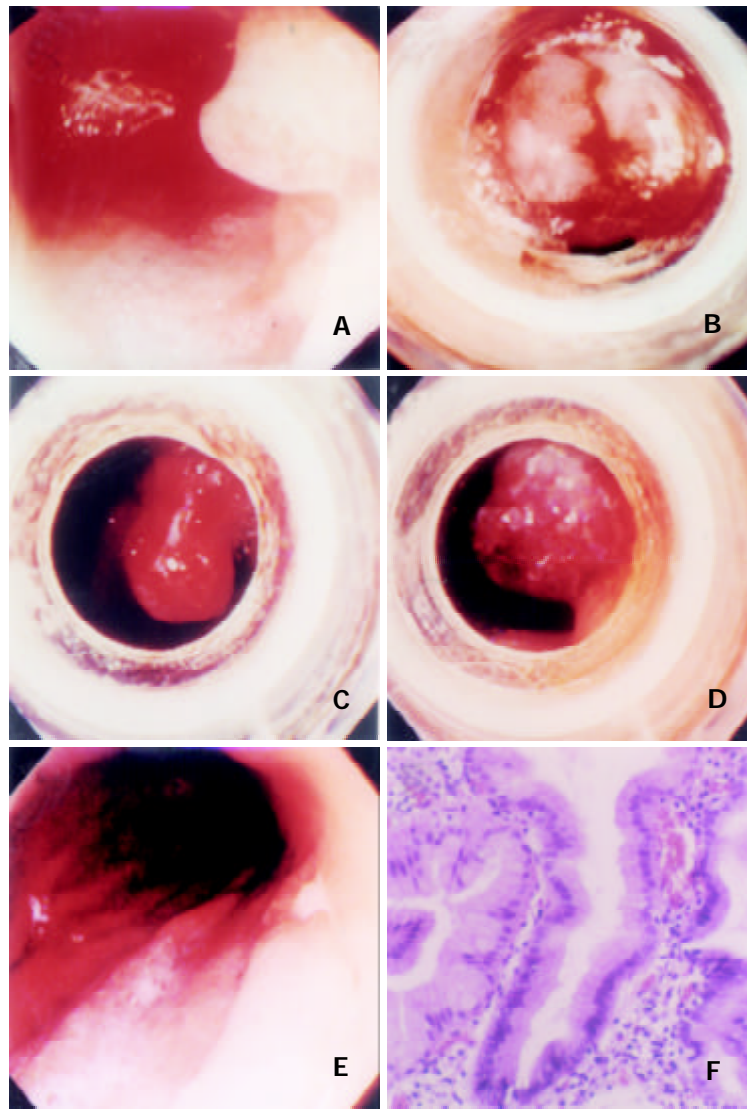


Figure 2 EBL for a hyperplastic polyp. A: A polyp over the posterior wall of corpus. B: The polyp was aspirated into the hood and ligated with a rubber band after local injection of distilled water into the submucosa. C: The polyp congested immediately after ligation. D: The polyp developed cyanotic change about 4 minutes later. E: An artificial ulcer presented at the previous ligation site. F: Pathological examination of the strangulated polyp revealed both foveolar hyperplasia of the gastric mucosa and severe venous congestion in the lamina propria.

DISCUSSION

The current study has confirmed that gastric hyperplastic polyps develop ED avascular necrosis following EBL. A strangulated polyp became congested immediately after ligation, and developed cyanotic changes within a few minutes. These important findings herein have not been documented before. Our study also reveals that EBL can be applied not only in the elective treatment of asymptomatic hyperplastic polyps, but also in the management of bleeding lesions. A strangulated polyp was bloodlessly transected without complications following the banding ligation.

Hyperplastic polyp is the most common polyp in the stomach, comprising 75 to 90 % of gastric polyps^[15-17]. Most of the hyperplastic gastric polyps are asymptomatic. However, malignant transformation of hyperplastic polyps has been reported in several long-term follow-up studies^[18,19]. They therefore should be resected when incidentally detected. Bleeding is a common complication of electrocautery snare polypectomy for gastric polyps. In a well-conducted prospective study^[2], bleeding was observed in 16 of 222 snare polypectomies (7.2 %). Recently, various endoscopic mucosal resection (EMR) techniques have been developed. They included strip biopsy^[20], double snare polypectomy^[21] and cap-

fitted panendoscopy^[22]. However, complications (bleeding and perforation) of these new techniques were also high with an incidence ranging from 2.7 % to 23.9 %^[23-25]. These studies underscored the importance of proficiency in endoscopic hemostatic techniques by the endoscopic team as a prerequisite for performing polypectomy in the stomach.

To prevent hemorrhage following polypectomy, preventive ligation could be conducted before the procedure^[6]. However, bleeding can be encountered if a polyp is resected by electrocautery in cases where the distance above the detachable snare or rubber band is inadequate. According to our results, single ligation could effectively remove all the gastric polyps without requiring further electrocautery. No complications occurred during or after ligation. The low bleeding rate associated with EBL seemed to be attributed mainly to both a ligation of the vessels at the polyp bases and the avoidance of resecting polyps with a high-frequency electrocautery. Additionally, perforation was prevented by lifting the lesion from the muscle layer.

Our results further demonstrated that the ligating method could be employed to treat actively bleeding polyps. In the two patients with bleeding gastric polyps, EBL successfully achieved hemostasis for their bleeding polyps. Furthermore,

the strangulated polyps were bloodlessly transected without complications following the banding.

Conventional snare polypectomy or EMR methods encounter difficulties in effectively managing lesions located in the lesser curvature side, posterior wall and cardia of the stomach. Employing the EBL method allowed a lesion to be easily captured into the transparent hood, even in cases where it was situated tangentially.

Sessile polyps pose another dilemma for traditional electrocautery polypectomy, and it is difficult for snare to capture these polyps. EMR with cap-fitted panendoscopy^[22] may solve this problem, but bleeding and perforation remain very problematic. Employing the proposed EBL procedure allowed these polyps to be easily captured after submucosal injection with distilled water followed by suction. However, our EBL technique is not suitable for treating gastric adenoma, which has a high risk of carcinomatous conversion^[16,17]. In managing such lesions, additional electrocautery is still required to assess the possibility of malignant transformation of polyps.

Previously, we also employed the endoscopic detachable snare ligation method to treat hyperplastic gastric polyps^[13], and found that cyanotic change was an important predictor of the outcome of strangulated polyps. All the polyps with cyanotic changes developed avascular necrosis, but those without cyanotic changes remained alive following ligation by detachable snares. This study demonstrated that all the polyps became cyanotic following ligation by rubber bands, and that all the cyanotic polyps then developed avascular necrosis.

In conclusion, gastric polyps congest immediately following strangulation by rubber bands, and then develop cyanotic change within a few minutes. Avascular necrosis occurs in all the gastric polyps following banding ligation. Employing suction equipment, EBL can easily capture sessile polyps. It is an easy, safe and effective method to eradicate gastric hyperplastic polyps. Additionally, the new technique may be the choice of therapy for bleeding gastrointestinal polyps.

ACKNOWLEDGEMENTS

The authors would like to express their deep appreciation to Dr. Chang-Bih Shie, Jeng-Jie Pzeng, Miss Yu-San Chen, and Hsuan-Chun Huang for their invaluable support to this study.

REFERENCES

- 1 **Lanza FL**, Graham DY, Nelson RS, Godines R, Mckechnie JC. Endoscopic upper gastrointestinal polypectomy. Report of 73 polypectomies in 63 patients. *Am J Gastroenterol* 1981; **75**: 345-348
- 2 **Muehldorfer SM**, Stole M, Hahn EG, Ell C. Diagnostic accuracy of forceps biopsy versus polypectomy for gastric polyps: a prospective multicentre study. *Gut* 2002; **50**: 465-470
- 3 **Hsieh YH**, Lin HJ, Tseng GY, Perng CL, Li AF, Chang FY, Lee SD. Is submucosal epinephrine injection necessary before polypectomy? A prospective comparative study. *Hepatogastroenterology* 2001; **48**: 1379-1382
- 4 **Chang FY**. Endoscopic ligation for removal of stomach hyperplastic polyp: less risk or saving money? *Chin Med J* 2001; **64**: 615-616
- 5 **Sobrino-Faya M**, Martinez S, Gomez Balado M, Lorenzo A, Iglesias-Garcia J, Iglesias-Canle J, Dominquez Munoz JE. Clip for the prevention and treatment of polypectomy bleeding. *Res Esp Enferm Dig* 2002; **94**: 457-462
- 6 **Hachisu T**. A new detachable snare for hemostasis in the removal of large polyps or other elevated lesions. *Surg Endosc* 1991; **5**: 70-74
- 7 **Cipolletta L**, Bianco MA, Rotondano G, Piscopo R, Prisco A, Garofano ML. Emergency endoscopic ligation of actively bleeding gastric varices with a detachable snare. *Gastrointest Endosc* 1998; **47**: 400-403
- 8 **Lo GH**, Lai KH, Cheng JS, Chen MH, Huang HC, Hsu PI. Endoscopic variceal ligation plus nadolol and sucralfate compared with ligation alone for the prevention of variceal rebleeding: a prospective, randomized trial. *Hepatology* 2000; **32**: 461-465
- 9 **Lo GH**, Lai KH, Cheng JS, Lin CK, Hsu PI, Chiang HT. Prophylactic banding ligation of high-risk esophageal varices in patients with cirrhosis: a prospective randomized trial. *J Hepatol* 1999; **31**: 451-456
- 10 **Lo GH**, Chen WC, Chen MH, Hsu PI, Lin CK, Tai WL, Lai KH. Banding ligation versus nadolol and isosorbide mononitrate for the prevention of esophageal variceal rebleeding. *Gastroenterology* 2002; **123**: 728-734
- 11 **Hou MC**, Chen WC, Lin HC, Lee FY, Chang FY, Lee SD. A new "sandwich" method of combined endoscopic variceal ligation and sclerotherapy versus ligation alone in the treatment of esophageal variceal bleeding: a randomized trial. *Gastrointest Endosc* 2001; **53**: 572-578
- 12 **Deschenes M**, Barkun AN. Comparison of endoscopic ligation and propranolol for the primary prevention of variceal bleeding. *Gastrointest Endosc* 2000; **51**: 630-633
- 13 **Hsu PI**, Lai KH, Lo GH, Lin CK, Lo CC, Wang EM, Wang YY, Tsai WL, Lin CP, Tseng HH, Chen HC, Chen JL. Sequential changes of gastric hyperplastic polyps following endoscopic ligation. *Chin Med J* 2001; **64**: 609-614
- 14 **Hsu PI**, Lai KH, Lo GH, Lin CK, Lo CC, Wang EM, Wang YY, Tsai WL, Lin CP, Tseng HH, Chen HC, Chen JL. Sequential changes of gastric polyps following endoscopic ligation. *Gastrointest Endosc* 2001; **53**(Suppl): AB218
- 15 **Koch HK**, Lesch R, Cremer M, Oehlert W. Polyp and polypoid foveolar hyperplasia in gastric biopsy specimens and the pre-cancerous prevalence. *Front Gastrointest Res* 1979; **4**: 183-191
- 16 **Laxen F**, Sipponen P, Ihamaiki T, Hakkiuoto A, Dortscheva Z. Gastric polyps; their morphological and endoscopic characteristics and relation to gastric carcinoma. *Acta Pathol Microbiol Scand* 1982; **90**: 221-228
- 17 **Rosch W**. Epidemiology, pathogenesis, diagnosis, treatment of benign gastric tumors. *Front Gastrointest Res* 1980; **6**: 167-184
- 18 **Daibo M**, Itabashi M, Hirota T. Malignant transformation of gastric hyperplastic polyps. *Am J Gastroenterol* 1987; **82**: 1016-1025
- 19 **Kamiya T**, Morishita T, Asakura H. Histoclinical long-standing follow-up study of hyperplastic polyps of the stomach. *Am J Gastroenterol* 1981; **75**: 275-281
- 20 **Karta M**, Tada M, Okita K. The successive strip biopsy partial resection technique for large early gastric and colon cancers. *Gastrointest Endosc* 1992; **38**: 174-178
- 21 **Takekoshi T**, Takagi K, Kato Y. Radical endoscopic treatment of early gastric cancer. *Gann Monogr Cancer Res* 1990; **37**: 111-126
- 22 **Inoue H**, Takeshita K, Hori H, Muraoka Y, Yoneshima H, Endo M. Endoscopic mucosal resection with a cap-fitted panendoscopy for esophagus, stomach and colon mucosal lesions. *Gastrointest Endosc* 1993; **39**: 58-62
- 23 **Hirao M**, Asanuma T, Masuda K. Endoscopic resection of early gastric cancer following locally injecting hypertonic saline-epinephrine. *Stomach Intest* 1988; **23**: 399-409
- 24 **Yokota K**, Tanabe Y, Komatsu H. Safety and risk in the endoscopic mucosal resection of gastric disease: the strip biopsy method. *Endoscopia Digestiva* 1996; **8**: 465-471
- 25 **Ahmad NA**, Kochman ML, Long WB, Furth EE, Ginsberg GG. Efficacy, safety, and clinical outcomes of endoscopic mucosal resection: a study of 101 cases. *Gastrointest Endosc* 2002; **55**: 390-396

Edited by Zhu LH

• CLINICAL RESEARCH •

Clinical manifestations and prognostic factors in patients with gastrointestinal stromal tumors

Shee-Chan Lin, Ming-Jer Huang, Chen-Yuan Zeng, Tzang-In Wang, Zen-Liang Liu, Ray-Kuan Shiay

Shee-Chan Lin, Tzang-In Wang, Division of Gastroenterology, Department of Internal Medicine, Mackay Memorial Hospital, Taipei, Taiwan and Mackay Junior College of Nursing, Taipei, Taiwan, China
Ming-Jer Huang, Ray-Kuan Shiay, Division of Hematology-Oncology, Department of Internal Medicine, Mackay Memorial Hospital, Taipei, Taiwan, China

Chen-Yuan Zeng, Department of Pathology, Mackay Memorial Hospital, Taipei, Taiwan, China

Zen-Liang Liu, Department of Surgery, Mackay Memorial Hospital, Taipei, Taiwan and Mackay Junior College of Nursing, Taipei, Taiwan, China

Correspondence to: Dr. Shee-Chan Lin, Chief of Division of Gastroenterology, Department of Internal Medicine, Mackay Memorial Hospital, 92, Sec. 2, Chung San North Road, Taipei, Taiwan, China. sheechan@ms2.mmh.org.tw

Telephone: +86-2-25433535 **Fax:** +86-2-25433642

Received: 2003-08-11 **Accepted:** 2003-10-12

Abstract

AIM: To investigate the incidence of CD117-positive immunohistochemical staining in previously diagnosed GI tract stromal tumors (GIST) and to analyze the tumors' clinical manifestations and prognostic factors.

METHODS: We retrospectively reviewed 91 cases with a previous diagnosis of GI stromal tumor, leiomyoma, or leiomyosarcoma. Tissue samples were assessed with CD117, CD34, SMA and S100 immunohistochemical staining. Clinical and pathological characteristics were analyzed for prognostic factors.

RESULTS: CD117 was positive in 81 (89 %) of 91 tissue samples. There were 59 cases (72.8 %) positive for CD34, 13 (16 %) positive for SMA, and 12 (14.8 %) positive for S100. There was no gender difference in patients with CD117-positive GIST. Their mean age was 65 years. There were 44 (54 %) tumors located in the stomach and 29 (36 %) in the small intestine. The most frequent presenting symptoms were abdominal pain and GI bleeding. The mean tumor size was 7.5±5.7 cm. There were 35 cases (43.2 %) with tumors >5 cm. The tumor size correlated significantly with tumor mitotic count and resectability. Tumor size, mitotic count, and resectability correlated significantly with tumor recurrence and survival. There was recurrent disease in 39 % of our patients, and their mean survival after recurrence was 16.6 months. Most recurrences were at the primary site or metastatic to the liver. Twenty-six percent of our patients died of their disease.

CONCLUSION: Traditional histologic criteria are not specific enough to diagnose GIST. This diagnosis must be confirmed with CD117 immunohistochemical staining. Prognosis is dependent on tumor size, mitotic count, and resectability.

Lin SC, Huang MJ, Zeng CY, Wang TI, Liu ZL, Shiay RK. Clinical manifestations and prognostic factors in patients with gastrointestinal stromal tumors. *World J Gastroenterol* 2003; 9 (12): 2809-2812

<http://www.wjgnet.com/1007-9327/9/2809.asp>

INTRODUCTION

Leiomyoma of the gastrointestinal (GI) tract has a typical pathologic picture with parallel spindle cells arranged in a fascicular pattern^[1,2]. However, a number of tumors have atypical findings, with epithelioid cells or pleomorphic cells instead of spindle cells or even characteristics of neurons that stain for neuron-specific enolase. Therefore, pathologists used the umbrella term "stromal tumor" to refer to such atypical mesenchymal tumors. It has been thought that these tumors might originate from mesenchymal or stromal cells within the muscle layer of the GI tract^[3-5]. Molecular biochemical studies have revealed expression of kit protein (CD117) in the primitive mesenchymal cells. CD117 can be demonstrated by immunohistochemical staining using anti-kit antibodies^[6]. It has been found that most mesenchymal or stromal cell tumors of the GI tract are positive for CD117^[7]. Leiomyoma or leiomyosarcoma of the GI tract with typical pathologic features also stain positive for CD117. There is therefore now a consensus that these tumors originate from a common cell and that the term gastrointestinal stromal tumors (GIST) be reserved for CD117-positive neoplasms^[8].

These tumors arise from primitive cells with dual characteristics of muscle and neural cells, similar to interstitial cell of Cajal^[9]. Cytogenetic analysis shows that most of these tumors have a mutation of the c-kit gene. Oncogenic mutations enable the kit protein, a transmembrane tyrosine kinase receptor, to phosphorylate various substrate proteins, leading to activation of signal transduction cascades which regulate cell proliferation, apoptosis, chemotaxis, and adhesion^[9]. Additional chromosomal derangements in 22q or 24q may promote GIST development^[10,11]. C-kit gene mutation and kit protein over-expression appear to be essential for the pathogenesis of GIST. Imatinib is a tyrosine kinase inhibitor that has resulted in remarkable myxoid degeneration and fibrosis of GIST in clinical trials^[12]. Since specifically targeted therapy is thus becoming available, it is important to know if tumors with histology consistent with GIST in fact express the kit protein^[13]. We retrospectively reviewed cases in our hospital in the past 13 years with a tissue diagnosis of leiomyoma, leiomyosarcoma, or GIST to assess their immunohistochemical staining patterns, clinical manifestations, and prognostic factors.

MATERIALS AND METHODS

Patients

Using our hospital database, we collected records with a pathologic diagnosis of leiomyoma or leiomyosarcoma or stromal cell tumor of the GI tract from 1988 until 2001. There were 91 such cases. All the patients had undergone surgical resection of their tumor. We recorded the patients' age, gender, clinical manifestations, tumor site, maximal tumor diameter, duration of surgery, resectability of the tumor, the presence and date of local recurrence or distance metastasis, and the outcome, including date of death. The data of patients who were still alive in January 2002 were censored.

Immunohistochemistry

The tumor samples from all the 91 cases were examined for

various markers by using immunohistochemistry with commercially available antibodies against CD117 (1:50 dilution), S-100 protein (1:1 500), desmin (1:50), and SMA (1:100) (Dako, Carpinteria, CA). Immunoreaction was detected according to the manufacturer's instructions (Ventana Medical Systems, Tucson, AZ). The risk of aggressive behavior of the tumors was calculated according to the NIH consensus statement of 2001^[13]. Briefly, a tumor size <2 cm and mitotic count <5/50 high power fields (HPF) was graded as very low risk, a tumor between 2 and 5 cm and a mitotic count <5/50 HPF as low risk, a tumor <5 cm and mitotic count between 5/50 HPF and 10/50 HPF or a tumor between 5 and 10 cm and a mitotic count less than 5/50 HPF as intermediate risk, and a tumor >10 cm or mitotic count >10/50 HPF or a tumor >5 cm and mitotic count >5/50 HPF as high risk.

Statistic analysis

Statistic analysis was performed with SPSS software (SPSS for Window 9.0). Student's *t* test was used to compare continuous variables. And a χ^2 test was used for dichotomous variables. Survival was calculated from the day of diagnosis until death or the last day of a patient's visit to the outpatient clinic. The disease-free survival was calculated from the first diagnosis until tumor recurrence or distant metastases were found. Kaplan Meier analysis with a log rank test was used to compare survival and disease-free survival. The Cox proportional hazard method was used to evaluate prognostic factors.

RESULTS

Of the 91 tissue samples tested, 81 (89 %) were positive for CD117 staining. There were no significant differences in the distribution of previous pathologic diagnoses between CD117-positive and -negative samples. The highest incidence of CD117 positivity was in samples previously diagnosed as malignant GIST (Table 1). Of the 10 cases negative for CD117, 6 tumors were located in the stomach, 2 in the small bowel, and 1 each in the colon and retroperitoneum. Three of these tumors were positive for CD34, 3 for SMA, and 3 S100 (Table 2). These 10 cases were excluded from further analysis.

Table 1 Immunohistochemical staining for CD117 in tumors with a previous pathologic diagnosis of leiomyoma, leiomyosarcoma or GIST

Previous pathologic diagnosis	CD117-positive (n)	CD117-negative (n)
Leiomyoma	6 (86 %)	1 (14 %)
Leiomyosarcoma	14 (78 %)	4 (22 %)
Benign GIST	10 (77 %)	3 (23 %)
Malignant GIST	51 (96 %)	2 (4 %)
Total	81 (89 %)	10 (11 %)

Table 2 Previous pathologic diagnoses, tumor site, and other immunohistochemical markers in CD117-negative patients

Previous pathologic diagnosis	n	Site	CD34	SMA	S100
Leiomyoma	1	Stomach	+	-	-
Leiomyosarcoma	1	Stomach	-	-	-
	1	Small bowel	-	-	+
	1	Colon	-	-	-
	1	Other	-	+	-
Benign GIST	2	Stomach	-	-	+
	1	Stomach	+	+	+
Malignant GIST	1	Stomach	+	-	-
	1	Small bowel	-	+	-

Of the 81 patients with CD117-positive tumors, there were 42 males and 39 females. Their ages ranged from 21 to 91 years (mean 65.2±13.6 years), with over half (44/81, 54 %) between 60 and 79 years of age (Table 3). Additional immunohistochemical staining showed that the tissue samples were positive for CD34 in 59 cases (73 %), for SMA in 13 (16 %), and for S100 in 12 cases (15 %).

Table 3 Age distribution of patients with CD117-positive GIST

Age range	No. of cases (n)	Percentage (%)
<30	1	1
30-39	2	3
40-49	7	9
50-59	15	19
60-69	19	24
70-79	26	32
80-89	10	12
>90	1	1
Total	81	100

The tumors were located in the stomach in 44 cases (54 %), the small intestine in 29 (36 %), the colon in 5 (6 %), and the retroperitoneum or mesentery in 3 (4 %). The most frequent presenting symptoms were GI tract bleeding and abdominal pain in 27 cases (33 %) each, abdominal fullness and discomfort in 14 (17 %). Four patients had anemia on presentation, 7 had a palpable abdominal mass, and 1 presented with vaginal bleeding due to a rectal GIST involving the uterus. One patient was asymptomatic and was incidentally found to have a 3.5 cm GIST in her stomach on routine physical examination.

On pathology of the resected tumors, the mean size was 7.5±5.7 cm, 10 (12 %) were <2 cm, 25 (31 %) between 2 and 5 cm, 27 (33 %) between 5 and 10 cm, and 19 (24 %) >10 cm. Mitotic counts were <5/50 HPF in 38 cases (47 %), between 5 and 10/50 HPF in 21 (26 %), and >10/50 HPF in 22 (27 %). There was a significant correlation between tumor size and mitotic count (Pearson correlation coefficient = 0.541, *P*<0.001, Table 4). There was ulceration of the tumor in 47 % (38/81), hemorrhage in 53 % (43), tumor necrosis in 54 % (44), and tumor perforation in 25 % (20). Sixty-two (77 %) of the tumors were completely resected. There was a significant correlation between tumor size and resectability (Pearson correlation coefficient = 0.505, *P*<0.001, Table 5).

Table 4 Correlation between tumor size and mitotic count in CD117-positive GIST

Tumor size	Mitotic counts/50 HPF ^a		
	<5	5-10	>10
≤2 cm	10 (100 %)	0	0
2 to 5 cm	14 (56 %)	8 (32 %)	3 (12 %)
5 to 10 cm	12 (44 %)	8 (30 %)	7 (26 %)
>10 cm	2 (11 %)	5 (26 %)	12 (63 %)

Pearson correlation = 0.541, *P*<0.001, ^aHPF=High power fields.

Table 5 Correlation between tumor size and resectability in CD117-positive GIST

Tumor sizes	Complete resection	Incomplete resection
≤2 cm	10 (100 %)	0
2 to 5 cm	25 (100 %)	0
5 to 10 cm	18 (69 %)	8 (30.8 %)
>10 cm	9 (47 %)	10 (52.6 %)

Pearson correlation = 0.505, *P*<0.001.

There were 31 patients (39 %) with local recurrence or distant metastasis, which was statistically associated with tumor size ($P<0.001$, Figure 1). The 31 included 3 of 25 (12 %) whose primary tumor had been between 2 and 5 cm, 13 of 27 (48 %) whose tumor had been between 5 and 10 cm, and 15 of 19 (79 %) whose tumor had been greater than 10 cm. Recurrence was also significantly associated with mitotic count, occurring in 5 of 38 (13 %) with counts $<5/50\text{HPF}$, 10 of 21 (48 %) with counts between 5 and 10/50HPF, 16 of 22 (73 %) with counts $>10/50\text{HPF}$ ($P<0.001$, Figure 2).

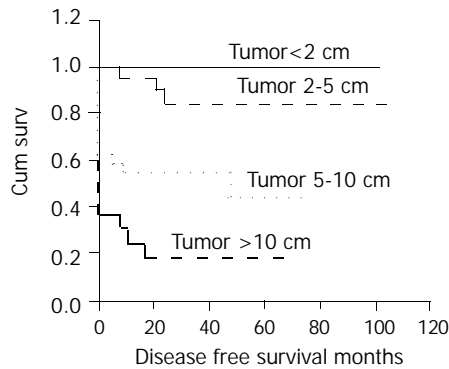


Figure 1 Cumulative disease-free survival for patients with CD117-positive GIST based on tumor size.

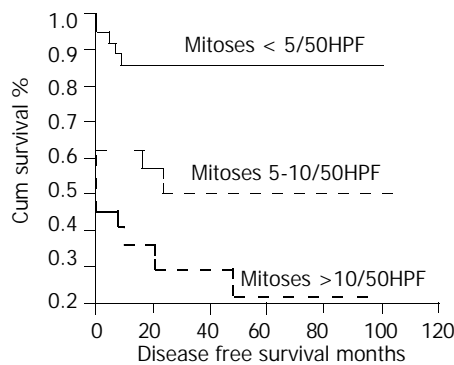


Figure 2 Cumulative disease-free survival for patients with CD117-positive GIST based on mitotic count.

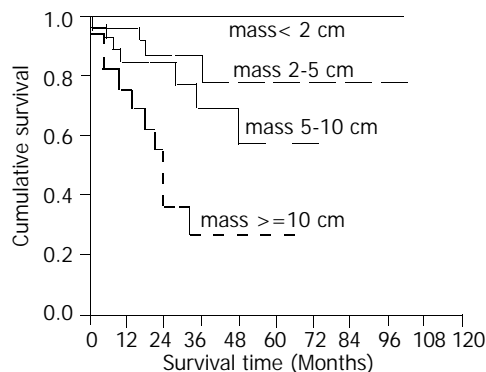


Figure 3 Cumulative survival for patients with CD117-positive GIST based on tumor size.

Twenty-one patients (26 %) died during follow up. The mean survival time after recurrence was 16.6 ± 14.5 months. Tumor size, mitotic count, and resectability were significantly associated with survival (Figures 3,4,5). The 5-year survival was 78 % (mean survival 85.5 ± 8.13 months) for patients with tumors between 2 and 5 cm, 57 % (mean survival 53.8 ± 6.09 months) for those with tumors between 5 and 10 cm, and 27 % (mean survival 30.0 ± 6.41 months) for those with tumors larger

than 10 cm (Figure 3, log rank test, $P<0.001$). The 5-year survival was 76 % (mean survival 80.7 ± 6.77 months) for patients with mitotic counts $<5/50\text{HPF}$, 73 % (mean survival 80.9 ± 10.5 months) for those with counts between 5 and 10/50HPF, and 31 % (mean survival time 44.2 ± 9.53 months) for those with counts $>10/50\text{HPF}$ (Figure 4, $P<0.02$). Patients whose tumors were completely resected had a 5-year survival of 73 % (mean survival 82.0 ± 5.78 months) while those without complete resection had a 5-year survival of 26 % (mean survival 27.0 ± 5.23 months) (Figure 5, $P<0.05$).

The survival was also significantly correlated with the score for risk of aggressive behaviors (Figure 6, $P<0.0001$).

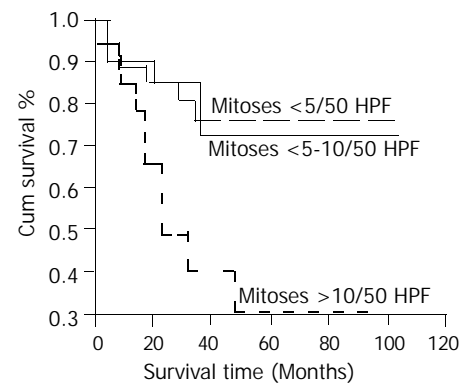


Figure 4 Cumulative survival for patients with CD117-positive GIST based on mitotic count.

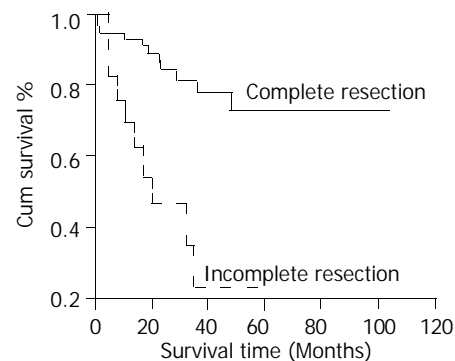


Figure 5 Cumulative survival for patients with CD117-positive GIST based on resectability.

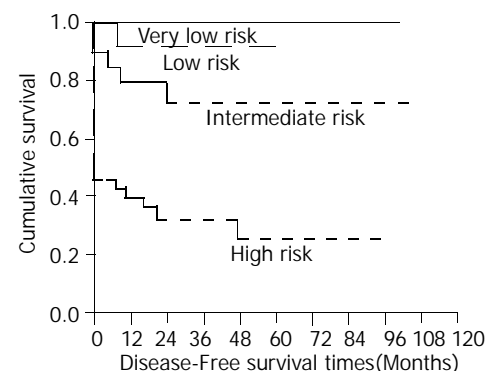


Figure 6 Cumulative disease-free survival for patients with CD117-positive GIST based on risk of aggressive behaviors.

DISCUSSION

Before the development of imatinib, surgical resection was the only treatment for tumors classified pathologically as GIST^[14,15]. Tumor size was an independent prognostic factor, with tumors >10 cm having a disease-specific 5-year survival

of only 20 % after resection^[16]. The tumors are often soft and fragile and prone to rupture or intraperitoneal dissemination during resection. The primary goal of surgery is complete resection of the disease, because rupture at surgery is another poor prognostic factor^[17]. A number of other pathologic features have also been correlated with survival, including mitotic index, aneuploidy, cellular morphometry, proliferative index, and percent S-phase fraction^[18]. Most patients with malignant stromal tumor or leiomyosarcoma have had either local recurrence or metastasis to the liver^[14]. Locally recurrent tumors were usually not amenable to complete resection because of peritoneal implantation^[19], nor has chemotherapy been very effective^[20]. Solitary liver metastasis could be surgically resected^[21], but multiple liver metastases are difficult to manage. Transcatheter arterial embolization has been used, but the partial response rate was low.

Our study confirms the contention that pathology alone is inadequate to confirm GIST by the current diagnostic criterion of CD117 immunohistochemical staining. Of the 91 tissue samples in our series, only 81 (89 %) were CD117-positive. Of the 10 negative samples, 2 were positive for SMA but negative for CD34 and S100 and therefore may be leiomyosarcomas. Another 3 were positive for S100 but negative for CD34 and SMA and therefore may be schwannomas. One case was positive and 2 were negative for all the 3 markers (that is, CD34, SMA and S100). The diagnosis in these cases is still unclear. A search for a gene mutation other than in the C-kit gene, for example PDGFR, might be helpful to clarify the diagnosis.

Among the 81 cases positive for CD117, 73 % were also positive for CD34, 16 % for SMA, and 15 % for S100. These data are similar to that of previous reports.

Esophagogastroduodenoscopy is usually performed in Taiwan for any patient complaining of abdominal discomfort. As a result, we can, on occasion, find small submucosal tumors in the stomach. Most of our cases with a tumor less than 5 cm were located in the stomach. This accounted for 43 % of our patients with tumors less than 5 cm in size, all of whom had completely resectable lesions. None of our patients with tumors less than 4 cm in size died (data not shown). Our findings confirmed that complete resection of the tumor is one of the most important factors related to survival^[16]. In our analysis, tumor size was significantly correlated with mitotic count and resectability, with larger tumors usually having higher mitotic counts and being more likely to be unresectable. Most of our patients with small intestinal GIST had lesions larger than 5 cm and a poorer outcome than those with gastric tumors. At the present time it is probably unwise to characterize any GIST as benign^[13]. This diagnosis mandates treatment.

Tumor grade was correlated, as expected, with mortality. No patients with very low grade tumors died, but the mortality increased as tumor grade increased, 14 % for low grade tumor, 30 % for moderate grade, and 35 % for high grade. Thirty-nine percent of our patients had recurrence, with a mean survival of 16.6 months after recurrence. Twenty-six percent of our patients died of their diseases.

We have done a clinical trial using imatinib 800 mg daily for 3 months in 11 patients with recurrent GIST. There was partial response in 3 cases and stable disease in 6 cases (unpublished data).

In conclusion, two recent developments are important with regard to GIST. The first is the ability to diagnose the tumor based on immunohistochemical staining. Our study confirms that traditional histologic criteria alone are not specific enough. The second is the development of imatinib, which specifically targets CD117, providing us a new tool to combat

GIST. Early diagnosis and complete resection remain the ideal, as surgical removal provides the best prognosis. However, specific molecular diagnosis and treatment are expanding our ability to manage this disease.

REFERENCES

- 1 **Ranchod M**, Kempson RL. Smooth muscle tumors of the gastrointestinal tract and retroperitoneum. *Cancer* 1977; **39**: 255-262
- 2 **Akwari OE**, Dozois RR, Weiland LH, Beahrs OH. Leiomyosarcoma of the small and large bowel. *Cancer* 1978; **42**: 1375-1384
- 3 **Casper ES**. Gastrointestinal stromal tumors. *Curr Treat Options Oncol* 2000; **1**: 267-273
- 4 **Schalldenbrand JD**, Appelman HD. Solitary solid stromal gastrointestinal tumors in von Recklinghausen's disease with minimal smooth muscle differentiation. *Hum Pathol* 1984; **15**: 229-232
- 5 **Mazur MT**, Clark HB. Gastric stromal tumors: Reappraisal of histogenesis. *Am J Surg Pathol* 1983; **7**: 507-519
- 6 **Huizinga JD**, Thunberg L, Kluppel M, Malysz J, Mikkelsen HB, Bernstein A. W/klt gene required for interstitial cells of Cajal and for intestinal pacemaker activity. *Nature* 1995; **373**: 347-349
- 7 **Corless CL**, McGreevey L, Haley A, Town A, Heinrich MC. KIT mutations are common in incidental gastrointestinal stromal tumors one centimeter or less in size. *Am J Pathol* 2002; **160**: 1567-1572
- 8 **Miettinen M**, Majidi M, Lasota J. Pathology and diagnostic criteria of gastrointestinal stromal tumors (GISTs): a review. *Eur J Cancer* 2002; **38**(Suppl 5): S39-51
- 9 **Heinrich MC**, Rubin BP, Longley BJ, Fletcher JA. Biology and genetic aspects of gastrointestinal stromal tumors: KIT activation and cytogenetic alterations. *Hum Pathol* 2002; **33**: 484-495
- 10 **Andersson J**, Sjogren H, Meis-Kindblom JM, Stenman G, Aman P, Kindblom LG. The complexity of KIT gene mutations and chromosome rearrangements and their clinical correlation in gastrointestinal stromal (pacemaker cell) tumors. *Am J Pathol* 2002; **160**: 15-22
- 11 **Gunawan B**, Bergmann F, Hoer J, Langer C, Schumpelick V, Becker H, Fuzesi L. Biological and clinical significance of cytogenetic abnormalities in low-risk and high-risk gastrointestinal stromal tumors. *Hum Pathol* 2002; **33**: 316-321
- 12 **Croom KF**, Perry CM. Imatinib mesylate: in the treatment of gastrointestinal stromal tumours. *Drugs* 2003; **63**: 513-522
- 13 **Fletcher CD**, Berman JJ, Corless C, Gorstein F, Lasota J, Longley BJ, Miettinen M, O'Leary TJ, Remotti H, Rubin BP, Shmookler B, Sobin LH, Weiss SW. Diagnosis of gastrointestinal stromal tumors: a consensus approach. *Int J Surg Pathol* 2002; **10**: 81-89
- 14 **Blanke CD**, Eisenberg BL, Heinrich MC. Gastrointestinal stromal tumors. *Curr Treat Options Oncol* 2001; **2**: 485-491
- 15 **Shiu MH**, Farr GH, Papachristou DN, Hajdu SI. Myosarcomas of the stomach: natural history, prognostic factors and management. *Cancer* 1982; **49**: 177-187
- 16 **DeMatteo RP**, Lewis JJ, Leung D, Mudan SS, Woodruff JM, Brennan MF. Two hundred gastrointestinal stromal tumors: Recurrence patterns and prognostic factors for survival. *Ann Surg* 2000; **231**: 51-57
- 17 **Ng EH**, Pollock RE, Munsell MF, Atkinson EN, Romsdahl MM. Prognostic factors influencing survival in gastrointestinal leiomyosarcomas. Implications for surgical management and staging. *Ann Surg* 1992; **215**: 68-77
- 18 **Miettinen M**, Sarlomo-Rikala M, Lasota J. Gastrointestinal stromal tumors: recent advances in understanding of their biology. *Hum Pathol* 1999; **30**: 1213-1220
- 19 **DeMatteo RP**, Heinrich MC, El-Rifai WM, Demetri G. Clinical management of gastrointestinal stromal tumors: before and after STI-571. *Hum Pathol* 2002; **33**: 466-477
- 20 **Plaa BE**, Hollema H, Molenaar WM, Torn Broers GH, Pijpe J, Mastik MF, Hoekstra HJ, van den Berg E, Scheper RJ, van der Graaf WT. Soft tissue leiomyosarcomas and malignant gastrointestinal stromal tumors: Differences in clinical outcome and expression of multidrug resistance proteins. *J Clin Oncol* 2000; **18**: 3211-3220
- 21 **DeMatteo RP**, Shah A, Fong Y, Jarnagin WR, Blumgart LH, Brennan MF. Results of hepatic resection for sarcoma metastatic to liver. *Ann Surg* 2001; **234**: 540-548

• CLINICAL RESEARCH •

Eosinophilic gastroenteritis: Clinical experience with 15 patients

Ming-Jen Chen, Cheng-Hsin Chu, Shee-Chan Lin, Shou-Chuan Shih, Tsang-En Wang

Ming-Jen Chen, Cheng-Hsin Chu, Shee-Chan Lin, Shou-Chuan Shih, Tsang-En Wang, Division of Gastroenterology, Department of Internal Medicine, Mackay Memorial Hospital, Taipei, Taiwan, China
Correspondence to: Dr. Cheng-Hsin Chu, Division of Gastroenterology, Department of Internal Medicine, Mackay Memorial Hospital, 92, Section 2, Chungshan North Road, Taipei, Taiwan, China. jessierc@ms28.hinet.net

Telephone: +86-225433535 Ext 2260

Received: 2003-08-05 **Accepted:** 2003-10-12

Abstract

AIM: To evaluate the clinic features of eosinophilic gastroenteritis and examine the diagnosis, treatment, long-term outcome of this disease.

METHODS: Charts with a diagnosis of eosinophilic gastroenteritis from 1984 to 2002 at Mackay Memorial Hospital were reviewed retrospectively. There were 15 patients diagnosed with eosinophilic gastroenteritis. The diagnosis was established in 13 by histologic evaluation of endoscopic biopsy or operative specimen and in 2 by radiologic imaging and the presence of eosinophilic ascites.

RESULTS: All the patients had gastrointestinal symptoms and 12 (80 %) had hypereosinophilia (absolute eosinophil count 1 008 to 31 360/cm³). The most common symptoms were abdominal pain and diarrhea. Five of the 15 patients had a history of allergy. Seven patients had involvement of the mucosa, 2 of muscularis, and 6 of subserosa. One with a history of seafood allergy was successfully treated with an elimination diet. Another patient improved spontaneously after fasting for several days. The remaining 13 patients were treated with oral prednisolone, 10 to 40 mg/day initially, which was then tapered. The symptoms in all the patients subsided within two weeks. Eleven of the 15 patients were followed up for more than 12 months (12 to 104 months, mean 48.7), of whom 5 had relapses after discontinuing steroids (13 episodes). Two of these patients required long-term maintenance oral prednisolone (5 to 10 mg/day).

CONCLUSION: Eosinophilic gastroenteritis is a rare condition of unclear etiology characterized by relapses and remissions. Short courses of corticosteroids are the mainstay of treatment, although some patients with relapsing disease require long-term low-dose steroids.

Chen MJ, Chu CH, Lin SC, Shih SC, Wang TE. Eosinophilic gastroenteritis: Clinical experience with 15 patients. *World J Gastroenterol* 2003; 9(12): 2813-2816
<http://www.wjgnet.com/1007-9327/9/2813.asp>

INTRODUCTION

Eosinophilic gastroenteritis is a rare disease characterized by eosinophilic infiltration into one or more layers of the gastrointestinal (GI) tract. It affects adults as well as children. The pathogenesis is poorly understood. Up to 40 % of cases were reported to have an underlying allergic basis^[1]. It might

involve any area of the gastrointestinal tract from the esophagus to the rectum^[2,3], although the stomach and proximal small bowel were most commonly affected. Klein *et al.*^[4] suggested a classification, based on the histology of the lesion: mucosal, muscularis, and subserosal disease. Clinical features depend on which layer and site are involved. Mucosal involvement leads to protein-losing enteropathy, fecal blood loss, and malabsorption, muscularis disease often causes gastric outlet or small bowel obstruction, and subserosal involvement manifests as eosinophilic ascites. The disease often waxes and wanes in severity. Only a few studies have described the long-term outcome^[5] and none have evaluated risk factors for relapse. In this study, we described the clinical manifestations of 15 patients with eosinophilic gastroenteritis.

MATERIALS AND METHODS

Charts with a diagnosis of eosinophilic gastroenteritis from 1984 to 2002 at Mackay Memorial Hospital were reviewed retrospectively. The diagnostic criteria included 1) the presence of gastrointestinal symptoms, 2) an eosinophilic infiltrate on a biopsy or operative specimen from the GI tract or else a high eosinophil count in ascitic fluid, 3) absence of parasite infestation, 4) no eosinophilic disease outside the GI tract, and 5) exclusion of intestinal lymphoma, Crohn's disease or other tumors. As peripheral blood hypereosinophilia was not a universal finding in eosinophilic gastroenteritis, hypereosinophilia was not required for the diagnosis. Data collected from the charts included age, sex, presenting symptoms, allergy history (drug or food allergy, atopy, asthma, hay fever, etc), absolute eosinophil count, endoscopic, sonographic and radiological findings, operative records, histology of biopsies or operative specimens, response to medication, length of follow-up, and number of relapses.

An eosinophilic infiltrate was defined as at least 20 eosinophils per high power field. Klein's criteria were followed: 1) mucosal disease was defined as infiltration of the mucosa without involvement of the muscularis or serosa, 2) muscular disease was defined as complete or incomplete intestinal obstruction and eosinophilic infiltration of the muscularis without eosinophilic ascites, and 3) subserosal disease was defined as eosinophilic infiltration of the GI tract with eosinophilic ascites.

RESULTS

Fifteen patients (6 men, 9 women), with a mean age of 38.4±14.2 (3 to 58) years, were diagnosed as eosinophilic gastroenteritis according to the above criteria. The patients are listed in Table 1 according to Klein's classification. Hypereosinophilia (1 008 to 31 360/cm³) in peripheral blood was noted in 12 (80 %) cases. The most common symptoms and signs in our series are shown in Table 2.

Endoscopic biopsies were performed in 12 patients from 30 different sites in the gastric antrum, duodenum, and colon. Sixteen specimens were positive, yielding the diagnosis in 12. Another 20-year-old female underwent endoscopic laparotomy for refractory ascites and was diagnosed as subserosal eosinophilic gastroenteritis based on a biopsy. The other two patients had general bowel wall thickening on CT scan and

eosinophils in their ascitic fluid. Although eosinophilic ascites might also be seen in parasitic disease and abdominal lymphoma, these entities were excluded by the clinical findings and response to treatment.

Table 1 General characteristics of patients with eosinophilic gastroenteritis according to histologic classification

Group/Patient	Sex	Age	WBC/cm ³	Eos count	% of Eos
I 1	M	43	13 800	1 380	13
2	F	65	12 720	2 540	18
3	F	38	11 220	4 704	41
4	F	57	33 010	19 475	59
5	F	34	7 900	2 291	27
6	M	45	10 400	3 340	34
7	F	64	13 700	3 973	29
II 8	M	31	14 500	6 960	43
9	F	58	9 900	396	5
III 10	M	17	24 800	11 016	42
11	F	38	13 400	1 008	12
12	F	20	11 720	3 984	36
13	M	35	5 650	621	10
14	M	53	31 360	14 500	68
15	F	3	8 800	264	3

Group I: mucosal, group II: muscular and group III: subserosal disease. Eos=eosinophil.

Table 2 Presenting symptoms and signs of the 15 patients

Symptoms and signs	n=15
Abdominal pain	12
Diarrhea	11
Bloating /fullness	10
Nausea/vomiting	9
Hypoalbuminemia (<3.5 g/dL)	11
Fecal blood loss	6

Table 3 Characteristics of patients with and without relapse

No.	Sex	Age	Klein classification Relapsing (number of episodes)	Followed up >12 m	Allergy
4	F	57	Mucosal (3)	+	+
9	F	58	Muscular (4)	+	+
10	M	17	Subserosal (1)		+
12	F	20	Subserosal (3)		+
15	F	3	Subserosal (4)		+
			Non-relapsing		
1	M	43	Mucosal	+	
2	F	65	Mucosal	+	
3	F	38	Mucosal	+	+
5	F	34	Mucosal		
6	M	45	Muscular	+	
7	F	64	Muscular		
8	M	31	Muscular		+
11	F	38	Subserosal	+	+
13	M	35	Subserosal		
14	M	53	Subserosal	+	

The endoscopic findings were nonspecific, with most patients having only hyperemic mucosa, although 2 patients had ulcers in the antrum and duodenum. A barium study of the small intestine showed thickening of the duodenal wall in 1 patient with subserosal disease and ischemic changes in the proximal ileum in 1 patient with muscular disease. CT scan or sonography were performed on all the patients with muscular and subserosal diseases (Figures 1 and 2). Intestinal wall

thickening was noted in the 2 with muscular disease and in 3 of 6 with subserosal disease. Ascites was present in all the 6 who had subserosal disease.



Figure 1 Abdominal computed tomography with intravenous contrast medium showing general thickening in the small bowel wall (white arrows), characteristic of the distribution of eosinophilic gastroenteritis.

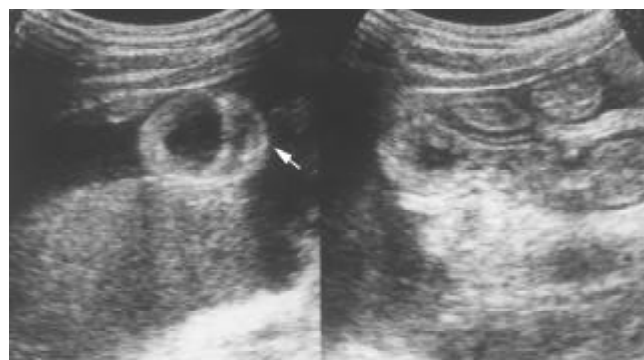


Figure 2 Transverse sonography of the proximal small bowel in the right subcostal area showing general thickening of the wall (white arrow) and ascites.

A history of allergy was noted in 5 of the 15 (34 %) patients (1 mucosal, 1 muscular, and 3 subserosal). One patient with mild mucosal disease and allergy to shellfish was successfully treated with an elimination diet. The mucosal disease in another patient (who had no history of allergy) remitted spontaneously after a fast of several days. Symptoms in both of these patients resolved within one week, and neither patient had a relapse over more than three years of follow up. Thirteen patients were treated with prednisolone, 10 to 40 mg/day initially, which was then gradually tapered over 4 to 6 weeks. Of these 13, 11 had relief of symptoms within one week, while 2 patients with subserosal disease improved within two weeks. The average hospital stay was 14.8 days (5 to 27 days).

Eleven of our patients have been followed up for more than one year (12 to 102 months). Of them, 5 (1 with mucosal, 1 with muscular and 3 with subserosal disease) had a total of 13 relapses after discontinuing steroids. A 58-year-old female with muscular disease had a relapse after discontinuing steroids and had an ileal perforation associated with ischemia. She underwent ileal resection. In general, an additional short course of steroids resulted in resolution, although 2 patients maintained on low-dose prednisolone (5 to 10 mg/day) to prevent relapses. Patients with and without relapse are compared in Table 3.

DISCUSSION

The pathogenesis of eosinophilic gastroenteritis is still unknown, but speculation has focused on the selective release

of eosinophil major proteins leading to intestinal epithelial damage. Keshavarzian *et al* demonstrated that the number of activated degranulated eosinophils in the mucosa correlated with the severity of eosinophilic gastroenteritis^[6]. The disease was reportedly more prevalent in patients with seasonal allergies, food sensitivities^[7], eczema, allergic rhinitis, and asthma^[8]. There have been a few cases related to exposure to medications^[9,10]. The evidence of elevations in IgE suggested that atopy might be involved in the pathogenesis of the disease^[11,12], however a history of allergy may be of little help in establishing the diagnosis. In our study 34 % of patients had a history of allergy, a proportion similar to that of other studies^[1], but there was no correlation between an allergy history and the histologic type of disease.

Hypereosinophilia in the peripheral blood was absent in at least 20 % of the cases^[1]. In our series, the results were similar. Therefore, the absence of hypereosinophilia should not exclude consideration of the diagnosis of eosinophilic gastroenteritis in patients with unexplained GI symptoms. Eleven of our patients had hypoalbuminemia (serum albumin <3.5 g/dl). Such a finding in patients with vague symptoms may be a hint to this disease, a chronic, organic rather than a transient, functional character.

Radiologically, the hallmark of eosinophilic gastroenteritis on CT is nodular and irregular thickening of the folds in the distal stomach and proximal small bowel^[13,14]. However, similar thickening may also be seen in Menetrier's disease, lymphoma, *scirrhous* carcinoma, Crohn's disease, and granulomatous disease. It is thus not a specific sign of eosinophil gastroenteritis. Mesenteric inflammation as well as ascites are not uncommon but are still nonspecific. Sonography is a useful tool for detecting non-mucosal eosinophilic gastroenteritis in patients without peripheral hypereosinophilia. It may reveal generalized thickening of the intestinal wall as well as ascites, which prompted us to do cytological examination of ascitic fluid or endoscopic biopsy. Based on these sonographic abnormalities, we were able to diagnose eosinophilic gastroenteritis in 3 patients who had a normal serum eosinophil count (396 to 621/cm³). In our series, all the 6 patients with subserosal disease had ascites on sonography, and 5 patients (3 with subserosal and 2 with muscular disease) had a thickened wall. Sonography could also evaluate the response to treatment by measuring the thickness of the affected layer^[15].

The endoscopic appearance in eosinophilic gastroenteritis is nonspecific, including erythematous, friable, nodular, and occasional ulcerative changes. In our study, 10 patients had only nonspecific gastritis or colitis, while 2 had shallow gastric or duodenal ulcers. These were most likely peptic ulcers, because no eosinophilic infiltrate was found on biopsy.

Definitive diagnosis requires histological evidence of eosinophilic infiltration. Eosinophilic infiltrates are usually patchy in distribution and may be present in otherwise normal, non-inflamed bowel wall. Therefore, multiple biopsies may be required to avoid missing the diagnosis. In our study, the definitive diagnosis was established by endoscopic biopsy in 12 patients. Several different examinations, such as gastroduodenoscopy and colonoscopy, and multiple deep biopsies may be necessary to establish the diagnosis. Even then it may be difficult to evaluate accurately the degree and extent of disease in most patients, given the patchy distribution of the infiltrates. A new technique using Tc-99m HMPAO-labeled WBC SPECT may be useful in assessing the extent of disease and response to treatment. Lee *et al*, have proposed a grading system using this technology^[16].

Eosinophilic gastroenteritis may present with symptoms suggesting an acute abdomen. There have been reports of the disease mimicking acute appendicitis, an obstructing cecal

mass, pancreatitis, giant refractory duodenal ulcer, and intussusception^[17-25]. If such patients have peripheral hypereosinophilia, the correct diagnosis of eosinophilic gastroenteritis might be suspected, avoiding an unnecessary operation. Surgery in eosinophilic gastroenteritis should be reserved for obstruction or perforation. One 53-year-old male with subserosal disease in our series underwent surgery twice, once for a refractory ulcer that had perforated, and again for an acute abdomen without definitive etiology, before the diagnosis of eosinophilic gastroenteritis. It is possible that the acute symptoms at the second time were a manifestation of eosinophilic gastroenteritis.

Once the diagnosis has been made, it is useful to look for specific food allergies, as an elimination diet may be successful if a limited number of food allergies are identified. One of our patients with mucosal disease had improvement after elimination of seafood. Katz *et al* reported that an elimination diet might fail to prevent recurrence^[26], but our patient has remained well for more than 3 years. In general, patients responded quickly and well to steroids^[27,28], as was true in our series. The appropriate duration of steroid treatment has been unknown, but short courses followed by a repeat course for a relapse have been described^[29]. Patients with refractory relapsing disease are usually placed on long-term low-dose steroids or immunosuppressive therapy. Some authors have described the use of sodium cromoglycate (a stabilizer of mast cell membranes)^[30] or montelukast (a selective, competitive leukotriene receptor antagonist)^[31] as steroid-sparing agents.

We were able to follow 11 of our patients for more than one year and found that 5 of them had relapses. Three of the 5 relapse patients were all younger than 20 years old in our series. Our numbers are too small to draw firm conclusions, but this observation does raise the possibility that young age may be a risk factor for relapse. Larger series or a meta-analysis would be needed to investigate this possibility.

We found the incidence of subserosal disease (6/15=40 %) to be higher than in other studies, for example, 4.5 % to 9 % in Japan and 13 % in the USA^[32,1]. Ascites as a manifestation of subserosal disease may be a more worrisome symptom, leading to a more aggressive approach to diagnosis. This in itself would not explain regional differences, but it might be that we under-diagnosed cases of mucosal and muscular disease, attributing vague symptoms to functional GI disease.

The diagnosis of eosinophilic gastroenteritis is problematic because the final diagnosis requires histological confirmation. However, this entity should be considered in the patient with unexplained chronic and relapsing gastrointestinal symptoms.

REFERENCES

- 1 **Talley NJ**, Shorter RG, Phillips SF, Zinsmeister AR. Eosinophilic gastroenteritis: a clinicopathological study of patients with disease of the mucosa, muscle layer, and subserosal tissues. *Gut* 1990; **31**: 54-58
- 2 **Matsushita M**, Hagiuro K, Morita Y, Takakuwa H, Suzuki T. Eosinophilic gastroenteritis involving the entire digestive tract. *Am J Gastroenterol* 1995; **90**: 1868-1870
- 3 **Liawouras CA**, Markowitz JE. Eosinophilic esophagitis: A subset of eosinophilic gastroenteritis. *Curr Gastroenterol Rep* 1999; **1**: 253-258
- 4 **Klein NC**, Hargrove RL, Sleisenger MH, Jeffries GH. Eosinophilic gastroenteritis. *Medicine* 1970; **49**: 299-319
- 5 **Lee CM**, Changchien CS, Chen PC, Lin DY, Sheen IS, Wang CS, Tai DI, Sheen-Chen SM, Chen WJ, Wu CS. Eosinophilic gastroenteritis: 10 years experience. *Am J Gastroenterol* 1993; **88**: 70-74
- 6 **Keshavarzian A**, Savarymattu S, Tai PC, Thompson M, Barter S, Spry C. Activated eosinophils in familial eosinophilic gastroenteritis. *Gastroenterology* 1985; **88**: 1041-1049
- 7 **Kelly KJ**. Eosinophilic gastroenteritis. *J Pediatr Gastroenterol Nutr*

- 2000; **30**: S28-35
- 8 **Von Wattenwyl F**, Zimmermann A, Netzer P. Synchronous first manifestation of an idiopathic eosinophilic gastroenteritis and bronchial asthma. *Eur J Gastroenterol Hepatol* 2001; **13**: 721-725
- 9 **Lee JY**, Medellin MV, Tumpkin C. Allergic reaction to gemfibrozil manifesting as eosinophilic gastroenteritis. *South Med J* 2000; **93**: 807-808
- 10 **Barak N**, Hart J, Sitrin MD. Enalapril-induced eosinophilic gastroenteritis. *J Clin Gastroenterol* 2001; **3**: 157-158
- 11 **Cello JP**. Eosinophilic gastroenteritis—a complex disease entity. *Am J Med* 1979; **67**: 1097-1104
- 12 **Von Wattenwyl F**, Zimmermann A, Netzer P. Synchronous first manifestation of an idiopathic eosinophilic gastroenteritis and bronchial asthma. *Eur J Gastroenterol Hepatol* 2001; **13**: 721-725
- 13 **Marco-Domenech SF**, Gil-Sanchez S, Jornet-Fayos J, Ambit-Capdevila S, Gonzalez-Anon M. Eosinophilic gastroenteritis: percutaneous biopsy under ultrasound guidance. *Abdom Imaging* 1998; **23**: 286-288
- 14 **Horton KM**, Corl FM, Fishman EK. CT of nonneoplastic diseases of the small bowel: spectrum of disease. *J Comput Assist Tomogr* 1999; **23**: 417-428
- 15 **Maroy B**. Nonmucosal eosinophilic gastroenteritis: sonographic appearance at presentation and during follow-up of response to prednisone therapy. *J Clin Ultrasound* 1998; **26**: 483-486
- 16 **Lee KJ**, Hahm KB, Kim YS, Kim JH, Cho SW, Jie H, Park CH, Yim H. The usefulness of Tc-99m HMPAO labeled WBC SPECT in eosinophilic gastroenteritis. *Clin Nucl Med* 1997; **22**: 536-541
- 17 **Box JC**, Tucker J, Watne AL, Lucas G. Eosinophilic colitis presenting as a left-sided colocolonic intussusception with secondary large bowel obstruction: an uncommon entity with a rare presentation. *Am Surg* 1997; **63**: 741-743
- 18 **Tran D**, Salloum L, Tshibaka C, Moser R. Eosinophilic gastroenteritis mimicking acute appendicitis. *Am Surg* 2000; **66**: 990-992
- 19 **Redondo Cerezo E**, Moreno Platero JJ, Garcia Dominguez E, Gonzalez Aranda Y, Cabello Tapia MJ, Martinez Tirado P, Lopez de Hierro Ruiz M, Gomez Garcia M. Comments to a report: eosinophilic gastroenteritis presenting as an obstructing cecal mass: review literature and our own experience. *Am J Gastroenterol* 2000; **95**: 3655-3657
- 20 **Tsai MJ**, Lai NS, Huang YF, Huang YH, Tseng HH. Allergic eosinophilic gastroenteritis in a boy with congenital duodenal obstruction. *J Microbiol Immunol Infect* 2000; **33**: 197-201
- 21 **Markowitz JE**, Russo P, Liacouras CA. Solitary duodenal ulcer: a new presentation of eosinophilic gastroenteritis. *Gastrointest Endosc* 2000; **52**: 673-676
- 22 **Shweiki E**, West JC, Klena JW, Kelley SE, Colley AT, Bross RJ, Tyler WB. Eosinophilic gastroenteritis presenting as an obstructing cecal mass—a case report and review of the literature. *Am J Gastroenterol* 1999; **94**: 3644-3645
- 23 **Kristopaitis T**, Neghme C, Yong SL, Chejfec G, Aranha G, Keshavarzian A. Giant antral ulcer: a rare presentation of eosinophilic gastroenteritis—case report and review of the literature. *Am J Gastroenterol* 1997; **92**: 1205-1208
- 24 **Scolapio JS**, DeVault K, Wolfe JT. Eosinophilic gastroenteritis presenting as a giant gastric ulcer. *Am J Gastroenterol* 1996; **91**: 804-805
- 25 **Siahanidou T**, Mandyla H, Dimitriadis D, Van-Vliet C, Anagnostakis D. Eosinophilic gastroenteritis complicated with perforation and intussusception in a neonate. *J Pediatr Gastroenterol Nutr* 2001; **32**: 335-337
- 26 **Katz AJ**, Twarog FJ, Zeiger RS, Fslshck ZM. Milk-sensitive and eosinophilic gastroenteropathy: similar clinical features with contrasting mechanisms and clinical course. *J Allergy Clin Immunol* 1984; **74**: 72-78
- 27 **Malaguarnera M**, Restuccia N, Pistone G, Panebianco MP, Giugno I, Grasso G, Seminara G. Eosinophilic gastroenteritis. *Eur J Gastroenterol Hepatol* 1997; **9**: 533-537
- 28 **Liacouras CA**, Wenner WJ, Brown K, Ruchelli E. Primary eosinophilic esophagitis in children: successful treatment with oral corticosteroids. *J Pediatr Gastroenterol Nutr* 1998; **26**: 380-385
- 29 **Naylor AR**. Eosinophilic gastroenteritis. *Scott Med J* 1990; **35**: 163-165
- 30 **Perez-Millan A**, Martin-Lorente JL, Lopez-Morante A, Yuguero L, Saez-Royuela F. Subserosal eosinophilic gastroenteritis treated efficaciously with sodium cromoglycate. *Dig Dis Sci* 1997; **42**: 342-344
- 31 **Schwartz DA**, Pardi DS, Murray JA. Use of montelukast as steroid-sparing agent for recurrent eosinophilic gastroenteritis. *Dig Dis Sci* 2001; **46**: 1787-1790
- 32 **Miyamoto T**, Shibata T, Matsuura S, Kagesawa M, Ishizawa Y, Tamiya K. Eosinophilic gastroenteritis with ileus and ascites. *Intern Med* 1996; **35**: 779-782

Edited by Zhu LH

• CLINICAL RESEARCH •

Correlation of P-glycoprotein expression with poor vascularization in human gallbladder carcinomas

Yu Tian, Li-Li Zhu, Ren-Xuan Guo, Chui-Feng Fan

Yu Tian, Ren-Xuan Guo, Department of General Surgery, First Affiliated Hospital, China Medical University, Shenyang 110001, Liaoning Province, China

Li-Li Zhu, Department of General Surgery, Second Affiliated Hospital, China Medical University, Shenyang 110004, Liaoning Province, China

Chui-Feng Fan, Department of Pathology, China Medical University, Shenyang 110001, Liaoning Province, China

Correspondence to: Dr. Yu Tian, Department of General Surgery, First Affiliated Hospital, China Medical University, Shenyang 110001, Liaoning Province, China. tianyu5460@21cn.com

Telephone: +86-24-23256666-6237 **Fax:** +86-24-23896804

Received: 2003-06-05 **Accepted:** 2003-07-24

Abstract

AIM: To investigate the relationship between the expression of P-glycoprotein (P-gp) and the degree of vascularization in gallbladder carcinomas.

METHODS: P-gp was stained with streptavidin-peroxidase complex immunohistochemical method in routine paraffin-embedded sections of gallbladder carcinomas. Microvessel counts (MVC) were determined using factor-VIII-related antigens.

RESULTS: The average MVC in 32 cases of gallbladder carcinomas was (34 ± 10) /HP. The value of MVC was closely correlated with Nevin staging and tumor differentiation ($P < 0.01$ and $P < 0.05$). The total expression rate of P-gp was 62.5 %. The P-gp expression rate in cases of Nevin staging S1-S3 (78.6 %) was higher than that of S4-S5 (50.0 %) with no statistical significance. The P-gp expression rate was not correlated with tumor differentiation or pathologic types. The value of MVC in P-gp (+) cases was markedly lower than that in P-gp (-) cases ($P < 0.01$). The positive rate of P-gp was significantly higher in cases of smaller MVC than those of bigger MVC ($P < 0.05$).

CONCLUSION: MVC may be used as one of the important parameters to reflect the biological behaviors of gallbladder carcinomas. As a major cause of drug resistance, the overexpression of P-gp is closely correlated with the poor vascularization in gallbladder carcinomas.

Tian Y, Zhu LL, Guo RX, Fan CF. Correlation of P-glycoprotein expression with poor vascularization in human gallbladder carcinomas. *World J Gastroenterol* 2003; 9(12): 2817-2820
<http://www.wjgnet.com/1007-9327/9/2817.asp>

INTRODUCTION

Because the rate of neovascularization (angiogenesis) frequently fails to keep pace with tumor growth, tumor vasculature is often insufficient in supplying the tumor mass, therefore many solid tumors contain subpopulation of hypoxic cells. Some researches showed that the drug resistance was

partially due to the poor tumor vascularization in reducing the influx of cytotoxic agents. Additionally, the hypoxic environment due to poor vascularization could also inhibit tumor cell proliferation, yet noncycling cells would be expected to be less sensitive to many agents. In recent years, some biochemical mechanisms of drug resistance have been identified; one of them is the overexpression of transmembrane transport protein and P-glycoprotein. We therefore linked angiogenesis assessed by microvessel counts with the expression of P-gp in human gallbladder carcinomas. The aim of the present study was to investigate whether MVC could be used as an important parameter to reflect the biological behaviors of gallbladder carcinomas and to illustrate the relationship between P-gp expression and vascularization.

MATERIALS AND METHODS

Clinical materials

Thirty-two cases of gallbladder carcinomas were randomly selected and diagnosed histologically. All the patients were treated surgically in our hospital. No chemotherapy or anti-angiogenesis therapy was used prior to surgery. There were 17 males and 15 females with an average age of 56 years. Histological types included 4 cases of papillary adenocarcinoma (12.5 %), 25 cases of tubal adenocarcinoma (78.1 %) and 3 cases of mucous adenocarcinoma (9.4 %). Twelve cases had well-differentiated gallbladder carcinomas (37.5 %), 9 cases moderate-differentiated gallbladder carcinomas (28.1 %) and 11 cases poor-differentiated gallbladder carcinomas (34.4 %). The Nevin staging (Table 1) was determined based on clinical features: 14 cases at stages S1, S2 and S3, and 18 cases at stages S4 and S5. All available hematoxylin and eosin-stained sections in each case were reviewed.

Table 1 Nevin staging system for gallbladder cancer^[1]

Stage	Definition
1	Tumor invades mucosa only
2	Tumor invades muscularis and mucosa
3	Tumor invades subserosa, muscularis and mucosa
4	Tumor invades all layers of gallbladder wall plus cystic lymph node
5	Tumor extends into liver bed or distant spread

Immunohistochemical stains

Four micrometer-thick sections from formalin-fixed and paraffin-embedded tissues were placed on poly-L-lysine-coated slides for immunohistochemistry study. The expression of P-gp was assessed by SP immunohistochemical method using a mouse-anti-human P-gp monoclonal antibody (JSB1) and a UltraSensitive™ S-P kit (kit 9710). Blood vessels were highlighted by staining endothelial cells for factor VIII-related antigens. The deparaffinized sections were boiled in citrate buffer at high temperature and high pressure for antigen retrieval for staining of P-gp, pepsin digestion for factor VIII-related antigen staining, and then incubated with each antibody

at 4 °C overnight. Immunohistochemical staining was then performed according to the UltraSensitive™ S-P kit manual. All reagents were supplied by Maixin-Bio Co, Fuzhou, China. The cells with brown-yellow granules in cytoplasm or on cytomembranes were considered as positive for P-gp expression.

Immunostaining

P-gp Stained slide was examined by two independent observers and scored semi-quantitatively. Staining intensity was assessed in comparison with positive slide of colon cancer, supplied by Maixin-Bio Co, Fuzhou, China. The staining intensity was scored as none (0), weak (1), moderate (2) and strong (3). The slides were classified as negative (0), positive (1), strong positive (2) and strongest positive (3) with corresponding rates of positive cells at <10 %, 10-20 %, 20-40 %, and >40 %, respectively. When the mean score in each group was 3 or more, the slide was considered as positive. Negative controls were stained without primary antibody.

Microvessel counts

MVCs were assessed according to Weidner *et al*^[2]. The hot spots were selected under a microscope (40x), then individual counts were made under 200x field (Olympus BH-2 microscope, 0.74 mm² per field). The average counts in 5 fields were recorded. Any single highlighted endothelial cell or endothelial cell cluster clearly separated from adjacent microvessel, and distinct clusters of brown-staining endothelial cells were counted as separate microvessels. Vessel lumens were not the sole criteria in identifying a microvessel.

Statistical analysis

Statistical analysis was performed using the Chi-square test and *t* test with SPSS software (Ver.10.0). *P*<0.01 or *P*<0.05 was considered as significant.

RESULTS

Expression of P-gp and MVC

The microvessels in malignant tissues were heterogeneously distributed. These highly neovascularized areas distributed within the tumor and dominated around the tumor margins (Figure 1). The P-gp was stained in cytoplasm and on the cytomembranes of gallbladder carcinoma cells (Figure 2).

Clinicopathologic characteristics of MVC and P-gp expressions

The average MVC in 32 cases of gallbladder carcinoma was (34±10)/HP. The number of MVC was markedly higher in cases of Nevin stages S4-S5 than in those of Nevin stages S1-S3 (*t*=2.833, *P*=0.008). MVC in moderately or poorly differentiated group was higher than that in well-differentiated group (*t*=2.581, *P*=0.015). The differences of MVC among the different pathologic types were not statistically significant (*P*=0.313, 0.822, 0.168) (Table 2).

The P-gp expression rate was 62.5 % in these 32 cases. The positive rate of P-gp was higher in cases of Nevin stages S1-S3 (78.6 %) than in those of Nevin stages S4-S5 (50.0 %) with no statistical significance ($\chi^2=2.743$, *P*>0.05). The expression rate of P-gp was not correlated with tumor differentiation or pathologic types (*P*>0.05) (Table 3).

Relationship between expression of P-gp and MVC

The value of MVC in P-gp (+) cases was 30±9/HP which was significantly lower than that in P-gp (-) cases (40±8/HP) (*t*=2.987, *P*=0.006). The P-gp expression rate was significantly higher in cases with less median MVC (33.6/HP) than in those with MVC over median MVC (81.3 % vs 43.8 %, $\chi^2=4.800$, *P*<0.05).

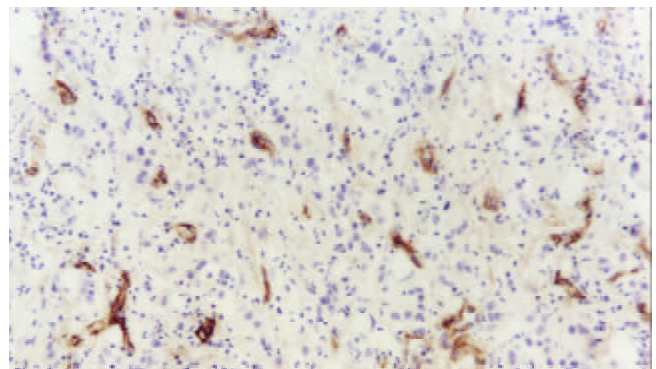


Figure 1 Distribution of microvessels in section of gallbladder carcinoma (S-P ×200).

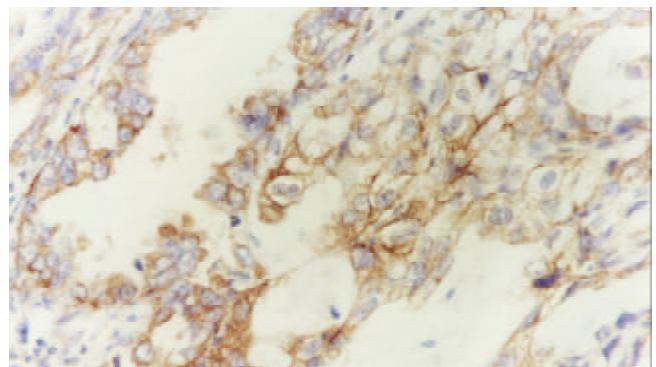


Figure 2 Expressed P-gp in gallbladder carcinoma (S-P ×400).

Table 2 Characteristics of MVC in gallbladder carcinoma

Characteristics	<i>n</i>	MVC
Pathologic types		
Papillary adenocarcinoma	4	27±8 ^a
Tubal adenocarcinoma	25	35±10 ^a
Mucous adenocarcinoma	3	32±10 ^a
Tumor differentiation		
Well	12	28±9 ^b
Moderate-poor	20	37±9 ^b
Nevin staging		
S1, S2, S3	14	28±10 ^c
S4, S5	18	38±8 ^c

^a*P*>0.05, ^b*P*<0.05, ^c*P*<0.01.

Table 3 Characteristics of P-gp expression in gallbladder carcinoma

Characteristics	<i>n</i>	+	%
Pathologic types			
Papillary adenocarcinoma	4	3	75.0 ^a
Tubal adenocarcinoma	25	15	60.0 ^a
Mucous adenocarcinoma	3	2	66.7 ^a
Tumor differentiation			
Well	12	9	75.0 ^b
Moderate-poor	20	11	55.0 ^b
Nevin staging			
S1, S2, S3	14	11	78.6 ^c
S4, S5	18	9	50.0 ^c

^a*P*>0.05, ^b*P*>0.05, ^c*P*>0.05.

DISCUSSION

In 1971, Folkman proposed that tumor growth be dependent on angiogenesis, and then considerable evidences showed that tumor growth was angiogenesis dependent, and the neovascularization was closely associated with the growth, invasion, metastasis, staging and prognosis of tumors^[2-15]. Our study indicated that MVC was correlated to Nevin staging and tumor differentiation. The case at later stage and with poorer differentiation had higher level of MVC in gallbladder carcinomas. MVC might be one of the most important parameters in reflecting the biologic behaviors of gallbladder carcinomas.

Though tumor growth depends on the angiogenesis, its rate often fails to keep pace with tumor growth, as tumor vasculature is inadequate for the tumor mass. Therefore, many solid tumors have subpopulations of hypoxic cells. Studies showed that the hypoxic tumor cells were relatively resistant to certain cytotoxic drugs^[16]. In the past, authors proposed that drug resistance be partly caused by poor tumor vascularization in reducing the influx of cytotoxic agents. Additionally, the hypoxic environment due to poor vascularization inhibited proliferation of tumor cells, yet noncycling cells would be expected to be less sensitive to many agents. In recent years, the identified biochemical mechanism of drug resistance was the overexpression of the transmembrane transport protein, P-glycoprotein (P-gp). P-gp is an ATP-binding-cassette transporter that is ubiquitously expressed, and often has high concentrations on plasma membrane of cancer cells, where it causes multidrug resistance by pumping lipophilic drugs out of the cell. The expression of P-gp influenced the efficacy of postoperative chemotherapy^[17-24]. In our study, P-gp expression rate was 62.5 % which was similar to the result of another report on hepatocellular carcinoma^[25]. Our result showed that overexpression of P-gp in gallbladder carcinoma tissue might be an important cause of drug resistance.

Recent studies showed that hypoxia-induced resistance to doxorubicin and methotrexate was attributed to an amplification of the P-gp gene and the dihydrofolate reductase gene^[26-29]. Recently, it has also been shown that poor vascularization in lung carcinomas correlated with an up-regulation of drug-resistance enzymes, such as glutathione S-transferase- \bar{I} , metallothionein and thymidylate synthase^[30]. In another study on rectal cancer, poor angiogenesis was also linked to an expression of glutathione S-transferase and metallothionein^[31]. Moreover, lung tumors with low vessel density and low VEGF expression have been found to be more frequently resistant to doxorubicin *in vitro* than tumors with high vessel counts and high expression of VEGF^[32]. In our study, the value of MVC was markedly lower in P-gp (+) cases than in P-gp (-) cases. The positive rate of P-gp was significantly higher in cases with small MVC than in cases with big MVC.

In conclusion, the finding that poor vascularization links to overexpression of the most important multidrug resistance enzyme—P-gp provides us an additional insight into drug resistance in gallbladder carcinomas.

REFERENCES

- 1 **Nevin JE**, Moran TJ, Kay S, King R. Carcinoma of the gallbladder: staging, treatment and prognosis. *Cancer* 1976; **37**: 141-148
- 2 **Weidner N**, Semple JP, Welch WR, Folkman J. Tumor angiogenesis and metastasis—correlation in invasive breast carcinoma. *N Engl J Med* 1991; **324**: 1-8
- 3 **Macchiarini P**, Fontanini O, Hardin MJ, Squartini F, Angeletti CA. Relation of neovascularization to metastasis of non-small-cell lung cancer. *Lancet* 1992; **340**: 145-146
- 4 **Song ZJ**, Gong P, Wu YE. Relationship between the expression of iNOS, VEGF, tumor angiogenesis and gastric cancer. *World J Gastroenterol* 2002; **8**: 591-595
- 5 **Liu XP**, Song SB, Li G, Wang DJ, Zhao HL, Wei LX. Correlations of microvessel quantitation in colorectal tumors and clinicopathology. *Shijie Huaren Xiaohua Zazhi* 1999; **7**: 37-39
- 6 **Gao GL**, Yang Y, Yang SF, Ren CW. Relationship between proliferation of vascular endothelial cells and gastric cancer. *Shijie Huaren Xiaohua Zazhi* 2000; **8**: 282-284
- 7 **Jia L**, Chen TX, Sun JW, Na ZM, Zhang HH. Relationship between microvessel density and proliferating cell nuclear antigen and prognosis in colorectal cancer. *Shijie Huaren Xiaohua Zazhi* 2000; **8**: 74-76
- 8 **Liu H**, Wu JS, Li LH, Yao X. The expression of platelet-derived growth factor and angiogenesis in human colorectal carcinoma. *Shijie Huaren Xiaohua Zazhi* 2000; **8**: 661-664
- 9 **Giatromanolaki A**, Sivridis E, Koukourakis MI, Polychronidis A, Simopoulos C. Prognostic role of angiogenesis in operable carcinoma of the gallbladder. *Am J Clin Oncol* 2002; **25**: 38-41
- 10 **Niedergethmann M**, Hildenbrand R, Wostbrock B, Hartel M, Sturm JW, Richter A, Post S. High expression of vascular endothelial growth factor predicts early recurrence and poor prognosis after curative resection for ductal adenocarcinoma of the pancreas. *Pancreas* 2002; **25**: 122-129
- 11 **Ng IO**, Poon RT, Lee JM, Fan ST, Ng M, Tso WK. Microvessel density, vascular endothelial growth factor and its receptors Flt-1 and Flk-1/KDR in hepatocellular carcinoma. *Am J Clin Pathol* 2001; **116**: 838-845
- 12 **Niemoller K**, Jakob C, Heider U, Zavrski I, Eucker J, Kaufmann O, Possinger K, Sezer O. Bone marrow angiogenesis and its correlation with other disease characteristics in multiple myeloma in stage I versus stage II-III. *J Cancer Res Clin Oncol* 2003; **129**: 234-238
- 13 **Takahashi R**, Tanaka S, Kitadai Y, Sumii M, Yoshihara M, Haruma K, Chayama K. Expression of vascular endothelial growth factor and angiogenesis in gastrointestinal stromal tumor of the stomach. *Oncology* 2003; **64**: 266-274
- 14 **Onogawa S**, Tanaka S, Oka S, Morihara M, Kitadai Y, Sumii M, Yoshihara M, Shimamoto F, Haruma K, Chayama K. Clinical significance of angiogenesis in rectal carcinoid tumors. *Oncol Rep* 2002; **9**: 489-494
- 15 **Joo YE**, Sohn YH, Joo SY, Lee WS, Min SW, Park CH, Rew JS, Choi SK, Park CS, Kim YJ, Kim SJ. The role of vascular endothelial growth factor (VEGF) and p53 status for angiogenesis in gastric cancer. *Korean J Intern Med* 2002; **17**: 211-219
- 16 **Teicher BA**. Hypoxia and drug resistance. *Cancer Metastasis Rev* 1994; **13**: 139-168
- 17 **Chung HC**, Rha SY, Kim JH, Roh JK, Min JS, Lee KS, Kim BS, Lee KB. P-glycoprotein: the intermediate end point of drug response to induction chemotherapy in locally advanced breast cancer. *Breast Cancer Res Treat* 1997; **42**: 65-72
- 18 **Chen CY**, Zhu ZH. Relationship between expression of P-glycoprotein and efficacy of chemotherapy in gastric cancer. *Shijie Huaren Xiaohua Zazhi* 2003; **11**: 36-38
- 19 **Cao L**, Peng S, Duchrow M. Expression of P-glycoprotein in benign and malignant gallbladder neoplasms. *Zhonghua Zhongliu Zazhi* 1999; **21**: 119-121
- 20 **Cao L**, Duchrow M, Windhovel U, Kujath P, Bruch HP, Broll R. Expression of MDR1 mRNA and encoding P-glycoprotein in archival formalin-fixed paraffin-embedded gall bladder cancer tissues. *Eur J Cancer* 1998; **34**: 1612-1617
- 21 **Monden N**, Abe S, Hishikawa Y, Yoshimura H, Kinugasa S, Dhar DK, Tachibana M, Nagasue N. The role of P-glycoprotein in human gastric cancer xenografts in response to chemotherapy. *Int J Surg Invest* 1999; **1**: 3-10
- 22 **Yokoyama Y**, Sato S, Fukushi Y, Sakamoto T, Futagami M, Saito Y. Significance of multi-drug-resistant proteins in predicting chemotherapy response and prognosis in epithelial ovarian cancer. *J Obstet Gynaecol Res* 1999; **25**: 387-394
- 23 **Baekelandt MM**, Holm R, Nesland JM, Trope CG, Kristensen GB. P-glycoprotein expression is a marker for chemotherapy resistance and prognosis in advanced ovarian cancer. *Anticancer Res* 2000; **20**: 1061-1067
- 24 **Warnakulasuriya S**, Jia C, Johnson N, Houghton J. p53 and P-

- glycoprotein expression are significant prognostic markers in advanced head and neck cancer treated with chemo/radiotherapy. *J Pathol* 2000; **191**: 33-38
- 25 **Kong XB**, Yang ZK, Liang LJ, Huang JF, Lin HL. Overexpression of P-glycoprotein in hepatocellular carcinoma and its clinical implication. *World J Gastroenterol* 2000; **6**: 134-135
- 26 **Rice GC**, Hoy C, Schimke RT. Transient hypoxia enhances the frequency of dihydrofolate reductase gene amplification in Chinese hamster ovary cells. *Proc Natl Acad Sci U S A* 1986; **83**: 5978-5982
- 27 **Rice GC**, Ling V, Schimke RT. Frequencies of independent and simultaneous selection of Chinese hamster cells for methotrexate and doxorubicin (adriamycin) resistance. *Proc Natl Acad Sci U S A* 1987; **84**: 9261-9264
- 28 **Kalra R**, Jones AM, Kirk J, Adams GE, Stratford IJ. The effect of hypoxia on acquired drug resistance and response to epidermal growth factor in Chinese hamster lung fibroblasts and human breast-cancer cells *in vitro*. *Int J Cancer* 1993; **54**: 650-655
- 29 **Luk CK**, Veinot-Drebot L, Tjan E, Tannock IF. Effect of transient hypoxia on sensitivity to doxorubicin in human and murine cell lines. *J Natl Cancer Inst* 1990; **82**: 684-692
- 30 **Koomagi R**, Mattern J, Volm M. Up-regulation of resistance-related proteins in human lung tumors with poor vascularization. *Carcinogenesis* 1995; **16**: 2129-2133
- 31 **Mattern J**, Kallinowski F, Herfarth C, Volm M. Association of resistance-related protein expression with poor vascularization and low levels of oxygen in human rectal cancer. *Int J Cancer* 1996; **67**: 20-23
- 32 **Volm M**, Koomagi R, Mattern J. Interrelationships between microvessel density, expression of VEGF and resistance to doxorubicin of non-small lung cell carcinoma. *Anticancer Res* 1996; **16**: 213-217

Edited by Ren SY and Wang XL

• CLINICAL RESEARCH •

Clinical predictors of severe gallbladder complications in acute acalculous cholecystitis

Ay-Jiun Wang, Tsang-En Wang, Ching-Chung Lin, Shee-Chan Lin, Shou-Chuan Shih

Ay-Jiun Wang, Tsang-En Wang, Ching-Chung Lin, Shee-Chan Lin, Shou-Chuan Shih, Division of Gastroenterology, Department of Internal Medicine, Mackay Memorial Hospital, Taipei, Taiwan, China
Correspondence to: Dr. Ay-Jiun Wang, Division of Gastroenterology, Department of Internal Medicine, Mackay Memorial Hospital, 92, Sec. 2, Chung San North Road, Taipei, Taiwan, China. ajw@ms2.mmh.org.tw
Telephone: +86-2-25433535 **Fax:** +86-2-25574800

Received: 2003-08-26 **Accepted:** 2003-10-12

Abstract

AIM: To evaluate the relationship between clinical information (including age, laboratory data, and sonographic findings) and severe complications, such as gangrene, perforation, or abscess, in patients with acute acalculous cholecystitis (AAC).

METHODS: The medical records of patients hospitalized from January 1997 to December 2002 with a diagnosis of acute cholecystitis were retrospectively reviewed to find those with AAC, confirmed at operation or by histologic examination. Data collected included age, sex, white blood cell count, AST, total bilirubin, alkaline phosphatase, bacteriology, mortality, and sonographic findings. The sonographic findings were recorded on a 3-point scale with 1 point each for gallbladder distention, gallbladder wall thickness >3.5 mm, and sludge. The patients were divided into 2 groups based on the presence (group A) or absence (group B) of severe gallbladder complications, defined as perforation, gangrene, or abscess.

RESULTS: There were 52 cases of AAC, accounting for 3.7 % of all cases of acute cholecystitis. Males predominated. Most patients were diagnosed by ultrasonography (48 of 52) or computed tomography (17 of 52). Severe gallbladder complications were present in 27 patients (52 %, group A) and absent in 25 (group B). Six patients died with a mortality of 12 %. Four of the 6 who died were in group A. Patients in group A were significantly older than those in group B (mean 60.88 y vs. 54.12 y, $P=0.04$) and had a significantly higher white blood cell count (mean 15 885.19 vs. 9 948.40, $P=0.0005$). All the 6 patients who died had normal white blood cell counts with an elevated percentage of band forms. The most commonly cultured bacteria in both blood and bile were *E. coli* and *Klebsiella pneumoniae*. The cumulative sonographic points did not reliably distinguish between groups A and B, even though group A tended to have more points.

CONCLUSION: Older patients with a high white cell count are more likely to have severe gallbladder complications. In these patients, earlier surgical intervention should be considered if the sonographic findings support the diagnosis of AAC.

Wang AJ, Wang TE, Lin CC, Lin SC, Shih SC. Clinical predictors of severe gallbladder complications in acute acalculous cholecystitis. *World J Gastroenterol* 2003; 9(12): 2821-2823
<http://www.wjgnet.com/1007-9327/9/2821.asp>

INTRODUCTION

Acute acalculous cholecystitis (AAC) is rare, occurring in only 5 % to 10 % of patients with acute cholecystitis^[1]. It is more likely to be found in patients with recent severe trauma, critical illness, cardiovascular surgery^[2,3] or severe burns. AAC has also been found in association with total parenteral nutrition^[4], mechanical ventilation, and the use of narcotic analgesics. Major cardiovascular disorders, complicated diabetes mellitus, autoimmune disease^[5-8], and AIDS^[9] have all been recognized as possible inciting factors for AAC.

AAC is a surgical emergency. Without immediate treatment, there may be rapid progression to perforation or gangrenous cholecystitis, with a mortality as high as 65 %^[10]. With early diagnosis and intervention, the mortality drops to 7 %^[11]. Therefore, it is important to understand the clinical variables that may assist in making an early diagnosis of this condition. The aim of the present retrospective study was to assess what clinical information might accurately predict AAC.

MATERIALS AND METHODS

We retrospectively reviewed the charts of patients in a medical center from January 1997 to December 2002 and found 1395 cases of acute cholecystitis. Gallstones were present in 1234 cases. We excluded patients with carcinoma of the gallbladder, pancreas, or biliary tract, common bile duct stones, intrahepatic stones, and patients who recovered without surgery, leaving 52 cases of AAC confirmed surgically or histologically. We divided the patients into two groups based on the presence (group A) or absence (group B) of severe complications involving the gallbladder, defined as perforation, gangrene, or abscess. We recorded the following data: age, sex, white blood cell count, AST, total bilirubin, alkaline phosphatase, sonographic findings, bacteriology, and mortality. The sonographic findings were scored, with 1 point each given for gallbladder distention, wall thickness greater than 3.5 mm, and sludge.

Student's *t*-test was used to analyze differences in means between the two groups. Sonographic scores for the severity of gallbladder condition were analyzed using the χ^2 test. A *P* value <0.05 was considered significant.

RESULTS

The 52 cases of AAC in our study accounted for 3.7 % of the totally 1 359 cases of acute cholecystitis seen during the study period. Males predominated, with 37 cases. The mean age of males was 56.5 years and of females, 60.5 years (Table 2). Most of our cases were diagnosed by ultrasonography (48 of 52) or computed tomography (17 of 52), with 13 patients having both examinations. Severe complications of the gallbladder were encountered in 27 (52 %) patients (group A). Six patients (12 %), all men, died, of whom 4 were in group A. The underlying conditions in these 4 patients were major surgery in 2, sepsis in 1, and bacteremia caused by *Salmonella* gr. D in 1. Of the 2 patients in group B who died, 1 had severe burns and 1 had *Aeromonas* bacteremia. The predisposing conditions for all

the patients are shown in Table 1.

There were no significant differences between the two groups in terms of liver biochemistry, length of hospital stay, or thickness of the gallbladder wall. The white blood cell count and age were significantly higher in group A ($P < 0.05$, Table 2). In 10 patients in both groups, the percentage of band forms was over 10 %, including the 6 patients who died. Blood cultures were positive in 24 % and bile cultures in 66 % (Table 3). *E. coli* and *Klebsiella pneumoniae* were the most frequently cultivated organisms in both blood and bile (Tables 4 and 5).

Most patients had a score of at least 2 points for sonographic findings. There was a tendency for group A to have higher scores, but the difference was not statistically significant (Table 6).

Table 1 Predisposing factors in patients with acute acalculous cholecystitis

Predisposing factor	Total (n)
Shock	7
Trauma	2
Burn	1
Major surgery	2
Bacteremia	11
DM	8
HTN	13
Heart disease ^a	14
CVA	3
TPN	1
Hyperlipidemia	5

a: Heart disease includes atrial fibrillation, congestive heart failure, hypertensive cardiovascular disease, hypertrophic cardiomyopathy and dilated cardiomyopathy.

Table 2 Demographic and clinical data in patients with acute acalculous cholecystitis with and without severe complications

	Group A n=27	Group B n=25	P
Gender			
Female	8	7	0.28
Male	19	18	0.71
Age (years)	60.88	54.12	0.04
Hospital stay (days)	19.74	18.84	0.42
WBC/mm ³	15 885.19	9 948.40	0.0005
AST (u/l)	138.04	141.87	0.48
Bilirubin (mg/dl)	2.46	2.37	0.46
Alkaline phosphatase (u/l)	106.19	130.59	0.07
Gallbladder wall (mm)	8.8	8.55	0.38

Table 3 Results of blood and bile culture for bacteria in patients with acute acalculous cholecystitis

Culture	Blood (n)	Bile (n)
No growth	34 (76%)	14 (34%)
Bacteria(+)	11 (24%)	27 (66%)

Table 4 Bacteria cultured from blood in patients with acute acalculous cholecystitis

	Group A (n)	Group B (n)	Total (n)
<i>E. coli</i>	3	3	6
<i>Klebsiella pneumoniae</i>	1	2	3
<i>Aeromonas sp</i>	0	1	1
<i>Salmonella gr.D</i>	1	0	1
<i>G(+)</i> Bacilli	1	0	1

Table 5 Bacteria cultured from bile in patients with acute acalculous cholecystitis

	Group A (n)	Group B (n)	Total (n)
<i>E. coli</i>	12	1	13
<i>Klebsiella pneumoniae</i>	6	1	7
<i>Aeromonas</i>	0	1	1
<i>Salmonella gr.D</i>	1	1	2
<i>Enterobacter sp.</i>	2	0	2
<i>Pseudomonas sp.</i>	1	1	2
<i>Burkholderia cepacia</i>	1	0	1
<i>Candida albican</i>	0	1	1
<i>Citro. Freundii</i>	1	0	1
<i>Enterococcus</i>	1	0	1
<i>Providencia</i>	0	1	1
<i>Staphy. Coagulase (-)</i>	1	0	1

Table 6 Sonographic findings recorded including gallbladder thickening, distention, and sludge

Sonographic finding	1 point	2 points	3 points	Total
Group A	4	11	9	24
Group B	9	11	4	24
Subtotal	13	22	13	48
$\chi^2=3.85$	$P>0.05$			

DISCUSSION

Most of our patients had multiple conditions that probably predisposed them to AAC (Table 1). Bile stasis, gallbladder ischemia, cystic duct obstruction, and systemic infection have been considered to be the most important factors in the pathogenesis of AAC^[12].

The bacteria we cultured from blood and bile were similar to those reported by others. Gastrointestinal flora such as *E. coli* and *Klebsiella pneumoniae* were most commonly cultured, as was true in our series. However, uncommon microorganisms have also been isolated from the bile, including *Leptospira spp*^[13,14], *Salmonella spp*^[15], *Vibrio cholerae*^[16], or *Listeria monocytogenes*. We had two patients with *Salmonella group D* infection, one of whom died of gangrene of the gallbladder with sepsis.

Rapid and accurate diagnosis is essential because ischemia may progress rapidly to gangrene and perforation. If an operation was performed within 48 hours from the onset of symptoms, severe complications would be reduced^[17]. AAC should be considered in every patient who is critically ill or injured and who has clinical findings of sepsis with no obvious source. Fever, right upper quadrant pain, and leukocytosis are common manifestations but are very nonspecific. However, our study revealed that a high white blood cell count and older age were associated with a higher incidence of gallbladder gangrene and perforation. More aggressive management should be considered in these patients. Patients with greater than 10 % band neutrophils might have an especially poor outcome.

Abdominal ultrasonography is the primary diagnostic modality for AAC. The most significant ultrasonographic findings are thickening of the gallbladder wall of more than 3.5 mm, gallbladder distention, a positive sonographic Murphy's sign, pericholecystic fluid, and a sonolucent intraluminal layer^[18,19]. We did not find the 3 sonographic findings we used were adequate to predict those patients likely to have severe gallbladder complications, although there was a trend toward higher scores in the group with complications. It may be that a study with a larger sample might find this to be a useful criterion.

In a discussion of diagnostic strategies for AAC, Kalliafas *et al* reported that morphine cholescintigraphy had the highest sensitivity (9 of 10, 90 %), followed by computed tomography (8 of 12, 67 %) and ultrasonography (2 of 7, 29 %). They reported a mortality of 41 % and a morbidity (that is, gangrene, perforation, or abscess) of 82 %^[20]. However, in our series, the mortality was only 11.5 % and morbidity 52 %. Why are the results so different? We diagnosed most of our cases by ultrasonography (48 of 52) or computed tomography (17 of 52), only two patients had cholescintigraphy. Further studies are needed to elucidate the relationship between the diagnostic modality and prediction of the morbidity and mortality of AAC.

The mainstay of therapy for AAC is cholecystectomy, which was traditionally performed by open laparotomy^[21]. Recently, laparoscopic cholecystectomy was performed in a small study with no complications from the procedure^[22]. Cholecystostomy has become a potentially lifesaving alternative in patients too weak to undergo general anesthesia^[23]. Percutaneous cholecystostomy by computed tomography or echo guidance is gaining acceptance as an alternative to an open procedure^[24]. In the future, laparoscopy for early diagnosis and treatment may be further developed as a useful method to decrease the mortality of AAC.

Finally, early diagnosis and early operation are the key to managing acute acalculous cholecystitis. Older patients with a high white cell count are more likely to have severe gallbladder complications. In these patients, earlier surgical intervention should be considered if the sonographic findings support the diagnosis of AAC.

REFERENCES

- 1 **Howard R.** Acute acalculous cholecystitis. *Am J Surg* 1981; **141**: 194-198
- 2 **Saito A,** Shirai Y, Ohzeki H, Hoyashi J, Eguchi S. Acute acalculous cholecystitis after cardiovascular surgery. *Surg Today* 1997; **27**: 907-909
- 3 **Hagino RT,** Valentine RJ, Claggett GP. Acalculous cholecystitis after aortic reconstruction. *J Am Coll Surg* 1997; **184**: 245-248
- 4 **Hatada T,** Kobayashi H, Tanigawa A, Fujiwara Y, Hanada Y, Yamamura T. Acute acalculous cholecystitis in a patient on total parenteral nutrition: case report and review of the Japanese literature. *Hepato-Gastroenterology* 1999; **46**: 2208-2211
- 5 **Kamimura T,** Mimori A, Takeda A, Masuyama J, Yoshio T, Okazaki H, Kano S, Minota S. Acute acalculous cholecystitis in systemic lupus erythematosus: a case report and review of the literature. *Lupus* 1998; **7**: 361-363
- 6 **Date K,** Shirai Y, Hatakeyama K. Antiphospholipid antibody syndrome presenting as acute acalculous cholecystitis. *Am J Gastroenterol* 1997; **92**: 2127-2128
- 7 **Parangi S,** Oz MC, Blume RS, Bixon R, Laffey KJ, Perzin KH, Buda JA, Markowitz AM, Nowygrod R. Hepatobiliary complications of polyarteritis nodosa. *Arch Surg* 1991; **126**: 909-912
- 8 **Imai H,** Nakamoto Y, Nakajima Y, Miura AB. Allergic granulomatosis and angiitis (Churg-Strauss syndrome) presenting as acalculous cholecystitis. *J Rheumatol* 1990; **17**: 247-249
- 9 **Jannuzzi C,** Belghiti J, Erlinger S, Menu Y, Fekete F. Cholangitis associated with cholecystitis in patients with acquired immunodeficiency syndrome. *Arch Surg* 1990; **125**: 1211-1213
- 10 **Flancbaum L,** Choban PS. Use of morphine cholescintigraphy in the diagnosis of acute cholecystitis in critically ill patients. *Intensive Care Med* 1995; **21**: 120-124
- 11 **Adam A,** Roddie ME. Acute cholecystitis: radiological management. *Baillieres Clin Gastroenterol* 1991; **5**: 787-816
- 12 **Barie PS,** Fischer E. Acute acalculous cholecystitis. *J Am Coll Surg* 1995; **180**: 232-244
- 13 **Vilaichone RK,** Mahachai V, Wilde H. Acute acalculous cholecystitis in leptospirosis. *J Clin Gastroenterol* 1999; **29**: 282-283
- 14 **Baelen E,** Roustan J. Leptospirosis associated with acute acalculous cholecystitis, Surgical or medical treatment. *J Clin Gastroenterol* 1997; **25**: 704-706
- 15 **McCarron B,** Love WC. Acalculous nontyphoidal salmonella cholecystitis requiring surgical intervention despite ciprofloxacin therapy: report of three cases. *Clin Infect Dis* 1997; **24**: 707-709
- 16 **West BC,** Silberman R, Otterson WN. Acalculous cholecystitis and septicemia caused by non-O1 *Vibrio cholerae*: first reported case and review of biliary infections with *Vibrio cholerae*. *Diagn Microbial Infect Dis* 1998; **30**: 187-191
- 17 **Hsu JC,** Yang TL, Wang TC. Acute acalculous cholecystitis. *Chin Med J* 1993; **51**: 266-2704
- 18 **Deitch EA,** Engel JM. Acute acalculous cholecystitis: ultrasonic diagnosis. *Am J Surg* 1981; **142**: 290-292
- 19 **Becker CD,** Burckhardt B, Terrier F. Ultrasound in postoperative acalculous cholecystitis. *Gastrointest Radiol* 1986; **11**: 47-50
- 20 **Kalliafas S,** Ziegler DW, Flancbaum L, Choban PS. Acute acalculous cholecystitis: incidence, risk factors, diagnosis, and outcome. *Am Surg* 1998; **64**: 471-475
- 21 **Glenn F,** Becker CG. Acute acalculous cholecystitis: an increasing entity. *Ann Surg* 1982; **195**: 131-136
- 22 **McClain T,** Gilmore BT, Peetz M. Laparoscopic cholecystectomy in the treatment of acalculous cholecystitis in patients after thermal injury. *J Burn Care Rehabil* 1997; **18**: 141-146
- 23 **Glenn F.** Cholecystostomy in the high-risk patient with biliary tract disease. *Ann Surg* 1977; **185**: 185-191
- 24 **Vauthey JN,** Lerut J, Martini M, Becker C, Gertsch P, Blumgart LH. Indications and limitations of percutaneous cholecystostomy for acute cholecystitis. *Surg Gynecol Obstet* 1993; **176**: 49-54

Edited by Zhu LH

• CLINICAL RESEARCH •

Imaging diagnosis of pancreato-biliary diseases: A control study

Liang Zhong, Qiu-Ying Yao, Lei Li, Jian-Rong Xu

Liang Zhong, Qiu-Ying Yao, Lei Li, Jian-Rong Xu, Department of Radiology, Renji Hospital, Shanghai Second Medical University, Shanghai 200001, China

Correspondence to: Dr. Liang Zhong, Department of Radiology, Renji Hospital, 145 Shandong Zhonglu, Shanghai 200001, China. zhong-liang@online.sh.cn

Telephone: +86-21-63260930 **Fax:** +86-21-63730455

Received: 2003-05-13 **Accepted:** 2003-06-04

Abstract

AIM: To evaluate the clinical value of various imageological methods in diagnosing the pancreato-biliary diseases and to seek the optimal procedure.

METHODS: Eighty-two cases of pancreato-biliary diseases confirmed by surgery and pathology were analyzed. There were 38 cases of cholelithiasis, 34 cases of pancreato-biliary tumors and 10 other cases. The imageological methods included B-US, CT, ERCP, PTC, cross-sectional MRI and MR cholangiopancreatography (MRCP).

RESULTS: The accuracy rate of MRCP in detecting the location of pancreato-biliary obstruction was 100 %. In differentiating malignant from benign obstruction, the sensitivity of the combination of MRCP and cross-sectional MRI was 82.3 %, the specificity was 93.8 %, and the accuracy rate was 89.0 %. The accuracy rate for determining the nature of obstruction was 87.8 %, which was superior to that of B-US ($P=0.0000$) and CT ($P=0.0330$), but there was no significant difference between direct cholangiopancreatography and the combination of MRCP and conventional MRI ($P=0.6666$).

CONCLUSION: In most cases, MRCP can substitute direct cholangiopancreatography for diagnosis. The combination of MRCP and cross-sectional MRI should be considered as an important means in diagnosing the pancreato-biliary diseases, pre-operative assessment and post-operative follow-ups.

Zhong L, Yao QY, Li L, Xu JR. Imaging diagnosis of pancreato-biliary diseases: A control study. *World J Gastroenterol* 2003; 9(12): 2824-2827

<http://www.wjgnet.com/1007-9327/9/2824.asp>

INTRODUCTION

Pancreato-biliary disorders are common diseases that often involve the biliary system to produce the symptom of obstructive jaundice. It is the precondition to investigate the obstructive location and causes of pancreato-biliary diseases. In this study, 82 cases of pancreato-biliary diseases confirmed by surgery and pathology were analyzed. The aims of the prospective study were to evaluate the clinical value of various imageological methods in diagnosing the pancreato-biliary diseases and to seek the optimal examination procedure.

MATERIALS AND METHODS

Patients

The study subjects included 82 patients (54 men and 28 women, mean age 60.0 years, range 11-82 years), 67 (81.7 %) cases had the symptom of obstructive jaundice. All patients underwent B-US, MR cholangiopancreatography (MRCP) and cross-sectional MRI examination. Fifty-seven patients underwent enhanced or un-enhanced CT scan. In addition, 48 patients had undergone direct cholangiopancreatography (41 ERCP and 7 PTC). However, direct cholangiopancreatography was unsuccessful in 4 cases due to difficult cannulation (2 ERCP), post-gastroenterostomy (1 ERCP) and sick patient (1 PTC). ERCP was incomplete in another 4 cases because only the pancreatic duct could be demonstrated and the biliary tree was not opacified. Therefore, 40 direct cholangiopancreatographies (34 ERCP and 6 PTC) were performed in all 82 cases, 1 patient had complication of acute pancreatitis after ERCP. All patients with pancreato-biliary diseases were confirmed by surgical findings and pathology, including 12 by laparoscopic cholecystectomy (LC), 6 by endoscopic sphincter tenotomy (EST) and 1 by PTC drainage (PTCD). Among the 82 cases, 38 were diagnosed as cholelithiasis, 34 as pancreato-biliary tumors and 10 as other diseases (Table 1).

Table 1 Pancreato-biliary diseases (n=82)

Pancreato-biliary diseases	No. of cases
Cholelithiasis ^a	38
Gallbladder stone	14
Intrahepatic bile duct stone	7
Choledocholithiasis	17
Pancreato-biliary tumor ^b	34
Gallbladder carcinoma	6
Cholangiocarcinoma	9
Ampullary carcinoma	3
Pancreatic head carcinoma	11
Bile papilla carcinoma	5
Other diseases	10
Bile duct injury	2
Choledochal cyst	2
Sclerosing cholangitis	2
Chronic pancreatitis	4

^aGallbladder stone mixed with intra- or extra-hepatic stone 15, Mirizzi syndrome 2; ^bHepatic invasion or metastasis 5, lymphadenectasis 3.

Techniques

MR imaging was performed with a 1.0T superconductive unit (Philips Gyroscan T10-NT, software version 4.6.2) containing a body coil. The patients were examined in the supine position, quiet breathing and abdominal band compression. The routine upper abdominal axial T1WI, T2WI and coronal T2WI MR examinations with Turbo Spin-Echo (TSE) sequence were performed first, and followed by the additional axial T2WI and/or T1WI fat-suppressed sequence (spectral saturation

inversion recovery, SPIR). The routine axial images served as guides to locate the MR cholangiopancreatography (MRCP). MRCP was performed with coronal, multislices, heavily T2-weighted TSE sequence (TR=2 000 ms, TE=700 ms). A non-breath-hold, respiratory-triggering technique was used to decrease the respiratory motion artifact. The MRCP source images were three-dimensionally (3D) reconstructed using a maximum-intensity-projection (MIP) algorithm. The total imaging time was approximately 30 min.

Computed tomography (CT) used a whole body CT scan unit (Picker PQ-2000). All CT examinations were performed after the patients had fasted for 4-8 hours and took 5 00-1 000 ml oral contrast (0.5-1 % Meglumine Diatrizoate) before CT scanning. Enhanced CT examination used 80-100 ml non-ion intravenous contrast agents injected through antecubital vein in a bolus at the rate of 2-3 ml/s.

Direct cholangiopancreatography (ERCP and PTC) was performed with a digital imaging unit (Philips Diagnost 93).

Imaging analysis

All image data of 82 cases were carefully reviewed to observe the enlargement or stricture of pancreato-biliary tract. The study protocol included detecting the obstructive locations, distinguishing the malignant from benign causes and evaluating the clinical value of various imaging methods (including B-US, CT, MRCP, ERCP/PTC) in diagnosing the pancreato-biliary diseases. SAS software was used for all statistical analyses.

The diagnostic principles and evaluating criteria for direct cholangiopancreatography and MRCP were identical, but in MRCP it was more important to carefully review both the source images and the MIP reconstructed images. According to the findings of the dilatation or stricture of pancreato-biliary tree and gallbladder, the obstructive locations of pancreato-biliary duct were divided into three parts: intra-hepatic or extra-hepatic bile duct and main pancreatic duct. Normal gallbladder was 7-10 cm in length and 3-4 cm in width. Dilatation of the common bile duct was defined as larger than 8 mm in maximal diameter in patients without histories of cholecystectomy and 10 mm in patients with prior cholecystectomy. Dilatation of the intra-hepatic bile duct and main pancreatic duct was defined as larger than 3 mm in maximal diameter^[1-4].

The cause of pancreato-biliary abnormality was evaluated using a five-point scale to assign a confidence level: 1. definitely benign, 2. probably benign, 3. indeterminate, 4. probably malignant, and 5. definitely malignant^[5]. If the cause of pancreato-biliary abnormality was assumed to be malignant, the reasons were chosen from the following findings: visualization of tumor, double duct sign, abrupt obstruction of bile duct, irregularity of obstructed margin, or asymmetric obstruction of the distal margin of the dilated bile duct. Receiver operating characteristic (ROC) curve analysis was performed to compare the results of readings of MRCP images versus the results of readings of the combination of MRCP images and routine MR images and versus the results of readings of ERCP images. Binormal ROC curves were fitted using *ROCKIT 0.9B* software. The diagnostic capability was determined by calculating the area under the ROC curve (Az). Ratings of 1 or 2 indicated a reading of a benign lesion, ratings of 4 or 5 indicated a rating of a malignant lesion. Ratings of 3 were considered to indicate an indeterminate diagnosis. Sensitivity, specificity and accuracy of ERCP, MRCP and the combination of MRCP and routine MR imaging in differentiating malignant from benign causes of pancreato-biliary tract obstruction were calculated.

RESULTS

MRCP image quality

MR cholangiopancreatography was successfully performed in

all 82 patients and the images of MRCP were similar to those of direct cholangiopancreatography. MRCP studies of diagnostic quality were obtained in 79 (96.3 %) subjects with fine contrast between the pancreato-biliary structure and the surrounding background. In the remaining 3 patients with pancreato-biliary tumor, the presence of ascitic fluid in the upper abdomen and the fluid-containing organs due to gastrointestinal obstruction obscured visualization of the pancreato-biliary tree and degraded the quality of the MRCP image. In 8 (16.7 %) patients in whom direct cholangiopancreatography was unsuccessful or incomplete, MRCP examinations all succeeded and the MRCP images were satisfactory.

Diagnosis of obstructive location

Among the 82 patients with pancreato-biliary diseases, 8, 60 and 21 cases had pancreato-biliary obstructive locations in intra-hepatic, extra-hepatic bile duct and main pancreatic duct, respectively (totally 89 locations). MRCP could clearly visualize the dilatation of pancreato-biliary ducts above the obstructive level in their native state, thus being more suitable for demonstrating the extra-hepatic bile duct obstruction. The total accuracy of MRCP in detecting the location of pancreato-biliary obstruction was 100 %, which was superior to that of B-US ($P=0.0002$) and CT ($P=0.0422$), but there was no significant difference between MRCP and direct cholangiopancreatography ($P=0.1487$) (Table 2).

Table 2 Accuracy of pancreato-biliary obstruction level (%) by different imageological methods

Level	Intra-hepatic	Extra-hepatic	Main pancreatic	Total
B-US	100.0 (8/8)	81.7 (49/60)	90.5 (19/21)	85.4 (76/89)
CT	100.0 (4/4)	93.0 (40/43)	100.0 (19/19)	95.5 (63/66)
ERCP/PTC	100.0 (5/5)	96.7 (29/30)	100.0 (8/8)	97.7 (42/43)
MRCP	100.0 (8/8)	100.0 (60/60)	100.0 (21/21)	100.0 (89/89)

Differentiation of malignant from benign obstruction

The sensitivity, specificity and accuracy of MRCP in distinguishing malignant from benign causes of pancreato-biliary obstruction were 64.7 %, 81.2 % and 74.4 %, respectively, while those of ERCP/PTC were 77.8 %, 86.4 % and 82.5 %, respectively. The difference was not significant between MRCP and ERCP/PTC in Az area under the ROC curve ($P=0.4590$). The combination of MRCP and routine MR imaging could obviously improve the diagnostic capability of differentiating the causes of pancreato-biliary obstruction with a sensitivity of 82.3 %, a specificity of 93.8 % and an accuracy of 89.0 %. The difference was significant between MRCP and the combination of MRCP and routine MR imaging ($P=0.0489$) (Table 3 and Figure 1).

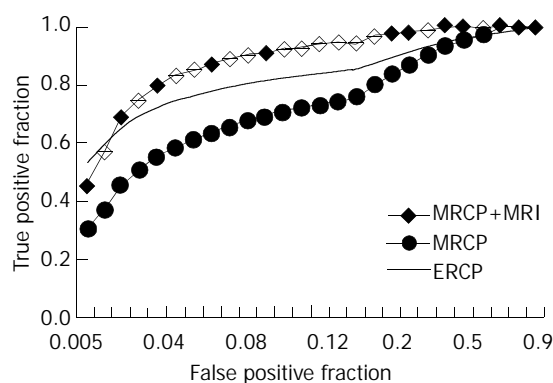


Figure 1 ROC curve analysis of differentiation between malignant and benign causes of pancreato-biliary obstruction.

Table 3 ROC analysis of pancreato-biliary obstruction

	ERCP/PTC (n=40)	MRCP (n=82)	MRCP+MRI (n=82)
True-positive	14	22	28
True-negative	19	39	45
False-positive	3	9	3
False-negative	4	12	6
Sensitivity (%)	77.8	64.7	82.3
Specificity (%)	86.4	81.2	93.8
Accuracy (%)	82.5	74.4	89.0
Az Values±SD	0.9281±0.0455	0.8833±0.0400	0.9687±0.0168

Diagnosis of obstructive causes

The total accuracy of MRCP in diagnosing the causes of pancreato-biliary obstruction was 75.6 %, which was similar to that of direct cholangiopancreatography (ERCP/PTC) ($P=0.2345$) and CT ($P=0.7970$), but superior to that of B-US ($P=0.0131$). The combination of MRCP and routine MR imaging significantly improved the clinical diagnostic ability with an accuracy of 87.8 %, which was superior to that of CT ($P=0.0330$) and US ($P=0.0000$).

The diagnostic rate by the combination of MRCP and routine MR imaging was 92.1 % and 94.1 %, for cholelithiasis and choledocholithiasis respectively, which was superior to that of CT ($P=0.0428$) and US ($P=0.0049$). But the difference between ERCP/PTC and the combined MRCP and routine MR imaging was not significant ($P=0.6445$). The accuracy of CT, ERCP/PTC, MRCP and the combined MRCP and routine MR imaging in distinguishing the various pancreato-biliary tumors was significantly higher than that of US ($P=0.0002$) (Table 4).

Table 4 Accuracy of diagnosis of obstructive causes (%)

	B-US	CT	ERCP /PTC	MRCP	MRCP +MRI
Cholelithiasis					
Gallbladder stone	71.4	75.0	80.0	78.5	92.9
Intrahepatic bile duct stone	85.7	100.0	100.0	71.4	85.7
Choledocholithiasis	52.9	63.6	87.5	88.2	94.1
Pancreato-biliary tumor					
Gallbladder carcinoma	50.0	75.0	60.0	50.0	66.7
Cholangiocarcinoma	33.3	75.0	83.3	77.8	88.9
Ampullary carcinoma	33.3	50.0	100.0	66.7	66.7
Pancreatic head carcinoma	63.6	81.8	100.0	90.9	100.0
Bile papilla carcinoma	40.0	66.7	100.0	60.0	80.0
Other diseases					
Bile duct injury	50.0		100.0	100.0	100.0
Choledochal cyst	100.0	100.0	100.0	100.0	100.0
Sclerosing cholangitis	0	50.0	0	0	50.0
Chronic pancreatitis	75.0	75.0	100.0	50.0	75.0
Total	57.3	73.7	85.0	75.6	87.8

DISCUSSION

US or CT examination (including endoscopic US and spiral CT) has been the first choice in diagnosing the pancreato-biliary diseases^[6-9]. Direct cholangiopancreatography obtained through ERCP or PTC has served as “golden standard” in pancreato-biliary imageology.

Magnetic resonance cholangiopancreatography (MRCP), advocated by German researcher Wallner BK and his group in 1991^[10], has offered a new imaging modality for diagnosing pancreato-biliary system disorders^[10-15]. In the present study, MRCP was successfully performed in all 82 patients and the images of MRCP were similar to those of direct

cholangiopancreatography. MRCP studies of diagnostic quality were obtained in 79 cases (96.3 %), including 8 (16.7 %) in which direct cholangiopancreatography were unsuccessful or incomplete. Therefore, MRCP might provide an efficient alternative to direct cholangiopancreatography when diagnostic ERCP and PTC were unsuccessful or inadequate^[11,16].

In our study, the accuracy of MRCP in detecting the location of pancreato-biliary obstruction was 100 %, which was superior to that of B-US and CT, but was not significantly different between MRCP and direct cholangiopancreatography. Compared with ERCP/PTC examination, the noninvasive MRCP could exhibit the whole pancreato-biliary duct system and demonstrate the level, degree and range of obstruction as well as morphological characteristics. In addition, MRCP could provide a plenty of valuable imageological information and help determine the best approach for palliative drainage and other interventional treatment for the patients with unresectable tumors^[17,18].

In pancreato-biliary system imageology, it is very important in diagnosing and differentiating malignant from benign causes of pancreato-biliary obstruction. The combined MRCP and routine MR imaging could significantly improve the clinical diagnostic capability by exhibiting the pathological changes of the surrounding structures^[19-22]. For pancreato-biliary tumors, MRCP could define the location and morphological characteristics of pancreato-biliary obstruction, and evaluate the range of tumors involvement and the surgical resectability. Furthermore, with the advantages of both CT and direct cholangiopancreatography examination, the combined routine MR imaging and MRCP might exhibit the pertinent surrounding structures and raise the clinical diagnostic accuracy^[17,23,24].

US and CT techniques are most frequently used in the initial evaluation of patients with cholelithiasis and both have a high accuracy in diagnosing gallbladder and intrahepatic duct stones. The sensitivity of MRCP in diagnosing gallbladder and intrahepatic duct stones varied with the size, number and location of the stones and MRCP being more suitable for the diagnosis of choledocholithiasis. In summary, the MRCP could mainly detect the stones in common bile duct and exclude other pancreato-biliary obstructive diseases^[25-27].

With the development of laparoscopic technique, laparoscopic cholecystectomy (LC) and endoscopic sphincter tenotomy (EST) have been widely used in the biliary surgery^[28]. MRCP can depict the whole anatomic structure of biliary tree and help guarantee the success of laparoscopic cholecystectomy. Before surgical dissection, to identify the anatomic variants of the biliary tree with MRCP could result in a decreased risk of bile duct injury during laparoscopic cholecystectomy^[29]. Now, ERCP is no longer the routine examination in patients with choledocholithiasis, and endoscopic sphincter tenotomy is chiefly used instead to remove stones in common bile duct.

As to the benign strictures, due to cholangitis, surgical injury or chronic pancreatitis, MRCP may have some difficulties in showing the mini-changes of pancreato-biliary duct. But the use of dynamic MRCP with secretin stimulation might be useful for diagnosing pancreatic papillary stenosis or dysfunction and for detecting reduced pancreatic exocrine reserve^[30-32]. In addition, the literature indicates that MRCP could be used initially in evaluating choledochal cyst^[33].

In conclusion, in recent optimal imageological procedures of diagnosing the pancreato-biliary diseases, B-US is still the first choice for evaluation. The combination of MRCP and routine MR imaging provides an efficient method to diagnose various pancreato-biliary obstructions, differentiate malignant from benign causes and carry out post-operative follow-ups. Cross-sectional MR imaging and CT are complementary modalities for pre-operative diagnosis and

assessment of pancreato-biliary tumors. Direct diagnostic cholangiopancreatography (ERCP/PTC) is chiefly used for difficult cases and combined with other interventional treatment, including EST or PTCD (Figure 2).

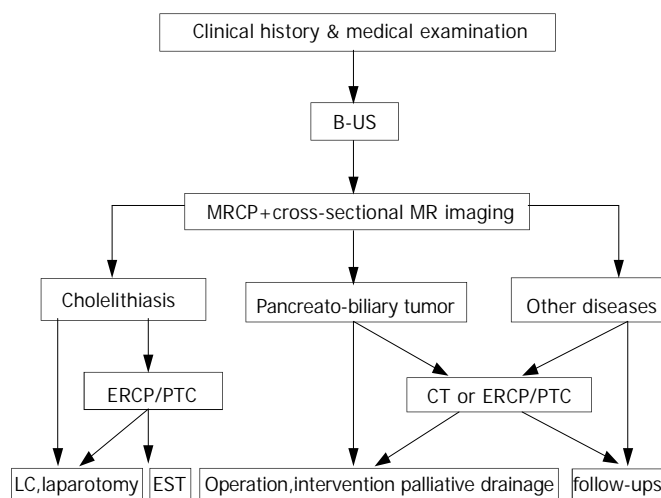


Figure 2 Optimal imageological examination procedure of pancreato-biliary diseases.

REFERENCES

- Soto JA, Yucel EK, Barish MA, Chuttani R, Ferrucci JT. MR cholangiopancreatography after unsuccessful or incomplete ERCP. *Radiology* 1996; **199**: 91-98
- Guibaud L, Bret PM, Reinhold C, Atri M, Barkun AN. Bile duct obstruction and choledocholithiasis: diagnosis with MR cholangiography. *Radiology* 1995; **197**: 109-115
- Reinhold C, Bret PM. Current status of MR cholangiopancreatography. *AJR* 1996; **166**: 1285-1295
- Barish MA, Soto JA. MR cholangiopancreatography: techniques and clinical applications. *AJR* 1997; **169**: 1295-1303
- Irie H, Honda H, Tajima T, Kuroiwa T, Yoshimitsu K, Masuda K. Optimal MR cholangiopancreatographic sequence and its clinical application. *Radiology* 1998; **206**: 379-387
- Kanemaki N, Nakazawa S, Inui K, Yoshino J, Yamao J, Okushima K. Three-dimensional intraductal ultrasonography: preliminary results of a new technique for the diagnosis of disease of the pancreatobiliary system. *Endoscopy* 1997; **29**: 726-731
- de Ledinghen V, Lecesne R, Raymond JM, Gense V, Amouretti M, Drouillard J, Couzigou P, Silvain C. Diagnosis of choledocholithiasis: EUS or magnetic resonance cholangiography? A prospective controlled study. *Gastrointest Endosc* 1999; **49**: 26-31
- Zeman RK, Fox SH, Silverman PM, Davros WJ, Carter LM, Griego D, Weltman DI, Ascher SM, Cooper CJ. Helical (spiral) CT of the abdomen. *AJR* 1993; **160**: 719-725
- Stockberger SM, Sherman S, Kopecky KK. Helical CT cholangiography. *Abdom Imaging* 1996; **21**: 98-104
- Wallner BK, Schumacher KA, Weidenmaier W, Friedrich JM. Dilated biliary tract: evaluation with MR cholangiography with a T₂-weighted contrast-enhanced fast sequence. *Radiology* 1991; **181**: 805-808
- Takehara Y. Fast MR imaging for evaluating the pancreaticobiliary system. *Eur J Radiol* 1999; **29**: 211-232
- Jara H, Barish MA, Yucel EK, Melhem ER, Hussain S, Ferrucci JT. MR hydrography: theory and practice of static fluid imaging. *AJR* 1998; **170**: 873-882
- Hirohashi S, Hirohashi R, Uchida H, Kitano S, Ono W, Ohishi H, Mikanishi S. MR cholangiopancreatography and MR urography: improved enhancement with a negative oral contrast agent. *Radiology* 1997; **203**: 281-285
- Papanikolaou N, Karantanas A, Maris T, Gourtsoyiannis N. MR cholangiopancreatography before and after oral blueberry juice administration. *J Comput Assist Tomogr* 2000; **24**: 229-234
- Fulcher AS, Turner MA. MR cholangiopancreatography. *Radiol Clin North Am* 2002; **40**: 1363-1376
- Owens GR, Shutz SM. Value of magnetic resonance cholangiopancreatography (MRCP) after unsuccessful endoscopic retrograde cholangiopancreatography (ERCP). *Gastrointest Endosc* 1999; **49**: 265-266
- Bret PM, Reinhold C. Magnetic resonance cholangiopancreatography. *Endoscopy* 1997; **29**: 472-486
- Macaulay SE, Schulte SJ, Sekijima JH, Obregon RG, Simon HE, Rohrmann CA Jr, Freeny PC, Schmiedl UP. Evaluation of a non-breath-hold MR cholangiography technique. *Radiology* 1995; **196**: 227-232
- Boraschi P, Braccini G, Gigoni R, Geloni M, Perri G. MR cholangiopancreatography: value of axial and coronal fast Spin-Echo fat-suppressed T₂-weighted sequences. *Eur J Radiol* 1999; **32**: 171-181
- Lee MG, Lee HJ, Kim MH, Kang EM, Kim YH, Lee SG, Kim PN, Ha HK, Auh YH. Extrahepatic biliary diseases: 3D MR cholangiopancreatography compared with endoscopic retrograde cholangiopancreatography. *Radiology* 1997; **202**: 663-669
- Kim MJ, Mitchell DG, Ito K, Outwater EK. Biliary dilatation: differentiation of benign from malignant causes—value of adding conventional MR imaging to MR cholangiopancreatography. *Radiology* 2000; **214**: 173-181
- Qin LX, Tang ZY. Hepatocellular carcinoma with obstructive jaundice: diagnosis, treatment and prognosis. *World J Gastroenterol* 2003; **9**: 385-391
- Pavone P, Laghi A, Catalano C, Panebianco V, Fabiano S, Passariello R. MRI of the biliary and pancreatic ducts. *Eur Radiol* 1999; **9**: 1513-1522
- Pavone P, Laghi A, Passariello R. MR cholangiopancreatography in malignant biliary obstruction. *Semin Ultrasound CT MR* 1999; **20**: 317-323
- Varghese JC, Liddell RP, Farrell MA, Murray FE, Osborne DH, Lee MJ. Diagnostic accuracy of magnetic resonance cholangiopancreatography and ultrasound compared with direct cholangiography in the detection of choledocholithiasis. *Clin Radiol* 2000; **55**: 25-35
- Boraschi P, Neri E, Braccini G, Gigoni R, Caramella D, Perri G, Bartolozzi C. Choledocholithiasis: diagnostic accuracy of MR cholangiopancreatography. Three-year experience. *Magn Reson Imaging* 1999; **17**: 1245-1253
- Chan YL, Chan AC, Lam WW, Lee DW, Chung SS, Sung JJ, Cheung HS, Li AK, Metrewell C. Choledocholithiasis: comparison of MR cholangiography and endoscopic retrograde cholangiography. *Radiology* 1996; **200**: 85-89
- Fulcher AS, Turner MA, Capps GW, Zfass AM, Baker KM. Half-Fourier RARE MR cholangiopancreatography: experience in 300 subjects. *Radiology* 1998; **207**: 21-32
- Yeh TS, Jan YY, Tseng JH, Hwang TL, Jeng LB, Chen MP. Value of magnetic resonance cholangiopancreatography in demonstrating major bile duct injuries following laparoscopic cholecystectomy. *Br J Surg* 1999; **86**: 181-184
- Matos C, Metens T, Deviere J, Nicaise N, Braude P, Van Yperen G, Cremer M, Struyven J. Pancreatic duct: morphologic and functional evaluation with dynamic MR pancreatography after secretin stimulation. *Radiology* 1997; **203**: 435-441
- Takehara Y. MR pancreatography. *Semin Ultrasound CT MR* 1999; **20**: 324-339
- Manfredi R, Costamagna G, Brizi MG, Maresca G, Vecchioli A, Colagrande C, Marano P. Severe chronic pancreatitis versus suspected pancreatic disease: dynamic MR cholangiopancreatography after secretin stimulation. *Radiology* 2000; **214**: 849-855
- Irie H, Honda H, Jimi M, Yokohata K, Chijiwa K, Kuroiwa T, Hanada K, Yoshimitsu K, Tajima T, Matsuo S, Suita S, Masuda K. Value of MR cholangiopancreatography in evaluating choledochal cysts. *AJR* 1998; **171**: 1381-1385

Overexpression of Caspase-1 in adenocarcinoma of pancreas and chronic pancreatitis

Yin-Mo Yang, Marco Ramadani, Yan-Ting Huang

Yin-Mo Yang, Yan-Ting Huang, Department of Surgery, The First Teaching Hospital, Health Science Center, Beijing University, Beijing 100034, China

Marco Ramadani, Department of General Surgery, University of Ulm, 89075 Ulm, Germany

Correspondence to: Professor Yin-Mo Yang, Department of Surgery, The First Teaching Hospital, Health Science Center, Beijing University, Beijing 100034, China. yangyinmo@263.net

Telephone: +86-10-66171122

Received: 2003-05-12 **Accepted:** 2003-06-12

Abstract

AIM: To identify the expression of Caspase-1(interleukin-1 β converting enzyme) and its role in adenoma of the pancreas and chronic pancreatitis.

METHODS: The expression of Caspase-1 was assessed in 42 pancreatic cancer tissue samples, 38 chronic pancreatitis specimens, and 9 normal pancreatic tissues by immunohistochemistry and Western blot analysis.

RESULTS: Overexpression of Caspase-1 was observed in both disorders, but there were differences in the expression patterns in distinct morphologic compartments. Pancreatic cancer tissues showed a clear cytoplasmatic overexpression of Caspase-1 in tumor cells of 71 % of the tumors, whereas normal pancreatic tissues showed only occasional immunoreactivity. In chronic pancreatitis, overexpression of Caspase-1 was found in atrophic acinar cells (89 %), hyperplastic ducts (87 %), and dedifferentiating acinar cells (84 %). Although in atrophic cells a clear nuclear expression was found, hyperplastic ducts and dedifferentiating acinar cells showed clear cytoplasmic expression. Western blot analysis revealed a marked expression of the 45 kDa precursor of Caspase-1 in pancreatic cancer and chronic pancreatitis (80 % and 86 %, respectively). Clear bands at 30 kDa, which suggested the p10-p20 heterodimer of active Caspase-1, were found in 60 % of the cancer tissue and 14 % of the pancreatitis tissue specimens, but not in normal pancreatic tissues.

CONCLUSION: Overexpression of Caspase-1 is a frequent event in pancreatic disorders and its differential expression patterns may reflect two functions of the protease. One is its participation in the apoptotic pathway in atrophic acinar cells and tumor-surrounding pancreatitis tissue, the other is its possible role in proliferative processes in pancreatic cancer cells and hyperplastic duct cells and dedifferentiating acinar cells in chronic pancreatitis.

Yang YM, Ramadani M, Huang YT. Overexpression of Caspase-1 in adenocarcinoma of pancreas and chronic pancreatitis. *World J Gastroenterol* 2003; 9(12): 2828-2831

<http://www.wjgnet.com/1007-9327/9/2828.asp>

INTRODUCTION

Caspase-1 was the first described member of a group of cysteine

proteases called Caspases. It was formerly designated as interleukin-1 β converting enzyme, and was originally characterized by its ability to cleave the inactive precursor of interleukin-1 β to generate the active 17.5 kDa proinflammatory cytokine IL-1 β ^[1]. It has been found to express in many tissues as an inactive 45 kDa precursor protein (p45) from which the active enzyme is generated by an autocatalytic cleavage process^[2]. Caspase-1 was first isolated from human monocytic cell line THP 1. Because of its similarity in sequence to the death gene product CED-3 of nematode *Caenorhabditis elegans*, it has been regarded as a key enzyme of the apoptotic pathway^[3]. Today, more than 10 Caspases have been identified and their roles in apoptosis are well known^[4-6].

Several new members of the group of Caspases have been identified and described. Similar to Caspase-1, overexpression of any of these enzymes would lead to apoptosis in a variety of cell types^[7-9]. We investigated the expression of apoptosis-related enzyme Caspase-1 in pancreatic cancer and chronic pancreatitis. Interestingly, we found a clear overexpression of Caspase-1 in pancreatic cancer tissue as well as in chronic pancreatitis specimens.

MATERIALS AND METHODS

Tissue samples

Pancreatic tissue samples were obtained from 42 patients with pancreatic cancer and 38 patients with chronic pancreatitis who underwent surgery at the Department of General Surgery, University of Ulm. The median age of the patients with pancreatic cancer (20 women and 22 men) was 61.8 years (range 38 to 78 years). The group of patients with chronic pancreatitis was composed of 13 women and 25 men. The median age of this group was 52.2 years (range 22 to 73 years). The main indication for pancreatic head resection was long-lasting pain (36 of 38 patients) and obstruction of the common bile duct (19 of 38 patients). In all patients, duodenum-preserving pancreatic head resection was performed.

Tissues were collected after surgical removal, immediately snap-frozen in liquid nitrogen, and stored at -80 °C, or fixed in 4 % formalin for 24 hours at room temperature, processed, and embedded in paraffin. All 42 pancreatic cancer tissue and 38 chronic pancreatitis tissue samples were used for immunohistochemical analysis. Five normal pancreatic tissue samples from organ donors and four normal pancreatic tissue samples from patients undergoing surgery for pancreatic cancer served as control specimens. Twenty pancreatic cancer tissues, 14 chronic pancreatitis tissues, and seven normal pancreatic tissues underwent Western blot analysis.

Immunohistochemistry

Paraffin-embedded tissues were cut into 5 μ m-thick sections and adhered to silanized slides, deparaffinized, and hydrated. Endogenous peroxidase activity was blocked with 3 % hydrogen peroxide in methanol. The tissue sections were covered with 5 % normal goat serum (DAKO, Glostrup, Denmark) in Tris-buffered saline for 60 minutes and incubated overnight with polyclonal rabbit antihuman caspase-1 antibody (Upstate Biotechnology, Lake Placid, NY, USA.) in a dilution

of 1:100. For each case, a corresponding section was incubated in Tris-buffered saline without the primary antibody as a control for nonspecific staining. Further negative controls consisted of normal rabbit serum instead of specific antiserum. Biotinylated pig anti-rabbit secondary antibody was added for 45 minutes, followed by avidin-biotinylated peroxidase complex for an additional 45 minutes. Staining was achieved using 3,3'-diaminobenzidine. The sections were then counterstained with Mayer's hemalum and mounted.

Grading of immunohistochemical findings

Immunohistochemical findings were scored depending on the extent and intensity of staining. Both intensity and extent were assessed in regions with hyperplastic ducts and atrophic acinar cells. All sections were graded by two experienced investigators who had no knowledge of the clinical data. At least 10 randomly selected high-power fields were scored. The intensity of staining was graded on a four points scale of 0=no staining, 1=weak, 2=moderate, and 3=strong. The extent of positive immunoreactivity was graded by the percentage of stained cells in the region of interest: 0 point=0 %, 1 point \leq 20 %, 2 points=20-50 %, and 3 points \geq 50 %. An overall score was obtained by the product of intensity and extent of positive staining. Cases with 0 points were considered to be negative, cases with a final score of 1-3 were considered to be weakly positive, cases with a score of 4-7 were considered to be moderately positive, and cases with a final score greater than 7 were considered to be strongly positive.

Western blot analysis

Frozen pancreatic samples were finely diced with a surgical blade and washed twice with ice-cold phosphate-buffered saline. After swelling on ice for 60 minutes, the samples were dissociated by sonication. The lysates were centrifuged and the protein fraction was aliquoted and stored at -80 °C until further analysis. For immunoblotting, the lysates were boiled in sodium dodecyl sulfate-gel sample buffer for 5 minutes. Thirty micrograms of protein were electrophoretically resolved on denaturing 15 % polyacrylamide gels with a 3 % stacking gel. Proteins were transferred to nitrocellulose membranes using a transblot apparatus (Phase, Lubeck, Germany). Nonspecific interactions were blocked by preincubation of the membranes with a milk powder suspension overnight at 4 °C. After incubation of the membranes with monoclonal antibodies, the binding of antibodies was detected using the ECL-system (Amersham Pharmacia Biotech, Piscataway, NJ, USA). The autocleavage experiments of the monocytic cell line THP1 were performed as previously described^[10].

RESULTS

Immunohistochemical findings

Staining of pancreatic tissue specimens with a polyclonal rabbit antiserum recognizing Caspase-1 revealed a marked overexpression of Caspase-1 in pancreatic cancer and chronic pancreatitis. Although normal pancreatic tissue showed only occasional slight staining (Figure 1A), we found predominantly cytoplasmic immunoreactivity of cancer cells in 71 % of the pancreatic tumors (Figure 1B). In primary chronic pancreatitis tissue samples, Caspase-1 overexpression was found in atrophic acinar cells, hyperplastic ducts, and acinar cells that appeared to dedifferentiate to form tubular structures. Hyperplastic ducts showed clear cytoplasmic staining in 87 % (Figure 1C). Atrophic acinar cells with pyknotic nuclei were stained positive in 89 % of the pancreatitis tissues, but the immunoreactivity was predominantly nuclear (Figure 1D). Dedifferentiating acinar cells showed positive cytoplasmic immunostaining with Caspase-1 antiserum in 84 %. In chronic pancreatitis tissues,

which often surrounded pancreatic carcinoma because of tumor obstruction, we also found strong Caspase-1 expression, but immunoreactivity differed from that of chronic pancreatitis tissue specimens from patients without malignancy. The staining in tumor-surrounding pancreatitis tissues was generally stronger than that in non-tumor-related pancreatitis tissues, and the distinct distribution pattern found in primary chronic pancreatitis could not be observed. In addition to this tissue-specific staining, a positive immunoreactivity of tissue-infiltrating lymphocytes was found in 73 % of the tissues.

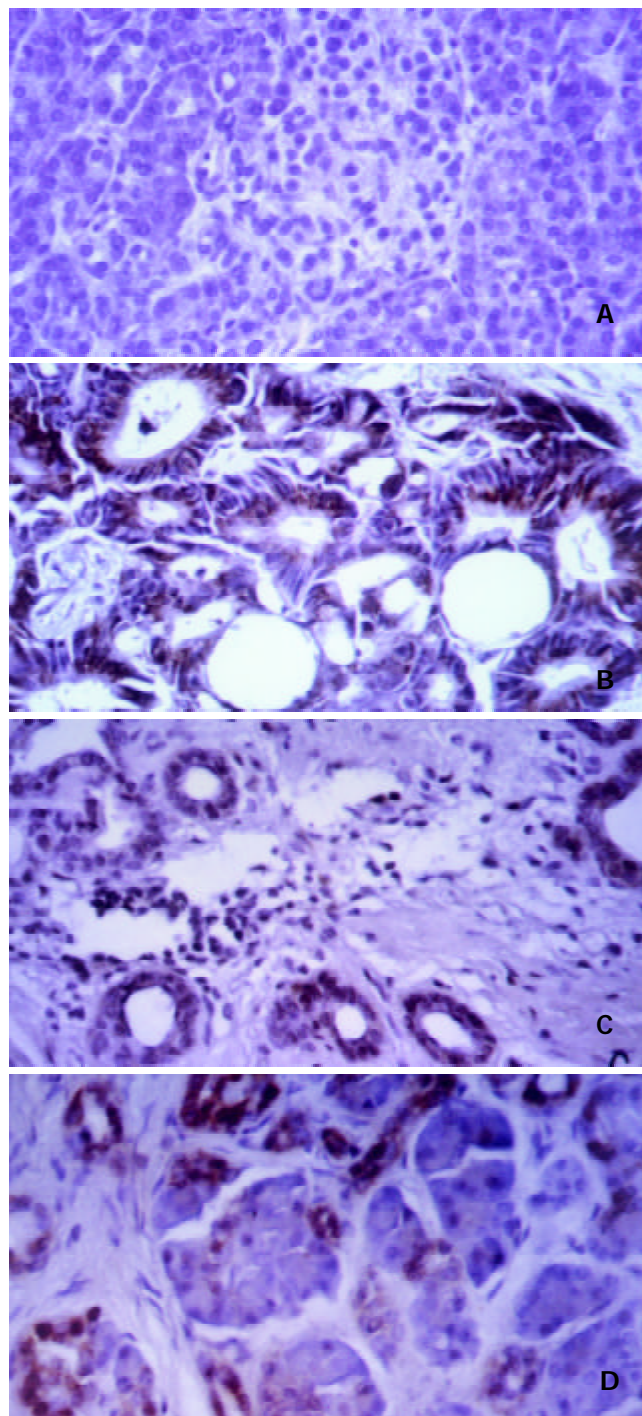


Figure 1 Immunohistochemical staining of pancreatic tissues using antiserum against human Caspase-1. A: Normal pancreas showed only occasional slight staining. B: Pancreatic cancer cells showed a clear cytoplasmic immunoreactivity in 71 %. C: Hyperplastic ducts in chronic pancreatitis tissues also showed cytoplasmic staining in 87 % of the tissues, whereas in atrophic acinar cells (D) a predominantly nuclear staining could be observed in 89 %.

Western blot analysis

To confirm the overexpression of Caspase-1 seen in immunohistochemical staining, Western blot analysis was performed with monoclonal antibody CAL against human Caspase-1. This antibody was developed to detect the 20 kDa subunit of active Caspase-1^[11], but also detect the p45 precursor. Pancreatic cancer tissue as well as chronic pancreatitis tissue specimens showed specific bands migrating at 45 kDa (Figure 2) which suggested the p45 precursor protein of Caspase-1. This band was found in 80 % of cancer tissues and 86 % of chronic pancreatitis tissues.

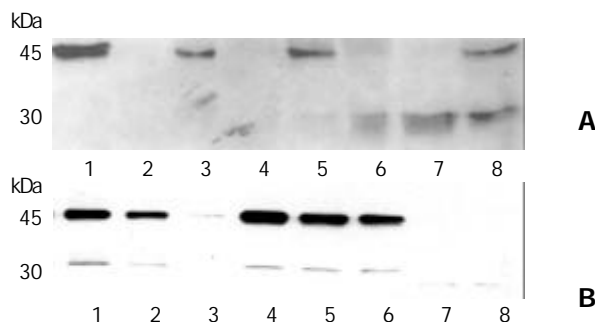


Figure 2 Western blot analysis of pancreatic tissues with anti-Caspase-1 antibody. The 45 kDa precursor of Caspase-1 was found in 86 % of chronic pancreatitis samples (A, Lanes 3-8) and 80 % of pancreatic cancer samples (B, Lanes 1-8). In 60 % of cancer specimens and 14 % of chronic pancreatitis tissue samples, the active 30 kDa p10-p20 heterodimer was found. In normal pancreatic tissues (A, lane 2), neither p45 precursor nor active Caspase-1 could be detected. Lane 1 (A) shows the positive control of THP 1 cells.

Lysates from THP-1 cells served as control specimens for active Caspase-1. In monocytic THP1 cells, p45 Caspase-1 precursor has been known to be cleaved by an autocatalytic process to the active Caspase-1 enzyme when kept at room temperature for 24 hours^[11]. In 60 % of the cancer probes and 14 % of the pancreatitis lysates, and in lysates from the autocleavage experiments of THP1 cells, a further band at 30 kDa was detectable, which was suggested the active p10-p20 heterodimer of active Caspase-1. In pancreatic tissue of healthy organ donors, no signal was obtained using monoclonal antibody against human Caspase-1, suggesting an overexpression of Caspase-1 protein in pancreatic cancer and chronic pancreatitis. Since lysates from pancreatic cancer tissue and chronic pancreatitis specimens also showed the 30 kDa band, it was plausible that Caspase-1 was at least partly activated in these disorders.

Correlation with clinicopathological features

To assess the clinical importance of Caspase-1 overexpression in pancreatic cancer, we correlated the immunohistochemical findings with age, sex, tumor extent, lymph node metastasis, and grading. As a result, no correlation was found between Caspase-1 expression and any of these clinicopathologic features. In addition, no statistical difference was found with regard to postoperative survival. In patients with chronic pancreatitis, we correlated the expression of Caspase-1 with age, sex, onset of disease, need for analgesic drugs, and endocrine and exocrine pancreatic function. As in patients with pancreatic cancer, no correlation with any of the tested features could be found.

DISCUSSION

Caspases play an important role in the apoptotic pathway in a variety of cell types. However, little is known about the

physiologic roles of different homologues during apoptosis. We assessed the expression of Caspase-1 in pancreatic cancer and chronic pancreatitis. Interestingly, immunohistochemical analysis revealed a clear overexpression of this enzyme in both disorders, but also differences in the expression patterns in distinct morphologic compartments. Furthermore, Western blot analysis of pancreatic cancer tissues and chronic pancreatitis tissues showed that Caspase-1 was at least partially activated in these diseases.

Caspase-1 is described as a cytosolic protein. However, in our experiments we found a clear nuclear staining with the antibody against human Caspase-1 in atrophic acinar cells in chronic pancreatitis specimens. Interestingly, most of the known substrates for Caspases in apoptosis were structural or catalytic nuclear proteins, the cleavage fragments of which were found in apoptotic bodies^[12]. The nuclear immunoreactivity of atrophic acinar cells in chronic pancreatitis may, therefore, be an indication of ongoing apoptotic processes. In contrast, the marked cytoplasmatic overexpression of Caspase-1 in tumor cells could hardly be explained by apoptosis, since some tumors showed Caspase-1 overexpression in nearly all cancer cells. Furthermore, we found a clear correlation between Caspase-1 overexpression in pancreatic carcinoma and cyclin D1, which has been known to be involved in cellular proliferation and to contribute to an aggressive behavior in many tumors^[13-16]. EGF and EGF-R have been shown to play a crucial role in autocrine stimulation of human pancreatic carcinoma^[17]. In the pancreatic cancer tissues we investigated, the cytoplasmatic expression of Caspase-1 in pancreatic cancer cells also correlated significantly with the expression of EGF and EGF-R. Interestingly, it has recently been shown that EGF was also able to inhibit cell growth and induce apoptosis via Caspase-1 induction^[18]. However, with regard to the fact that cyclin D1, EGF, and EGF-R overexpression was associated with poor prognosis in human pancreatic cancer^[13,19], it is hard to believe that these factors could be an indication for the apoptotic state of these tumors.

Chronic pancreatitis is histologically characterized by the destruction of the pancreatic parenchyma, irregular sclerosis, and focal duct cell proliferation. Besides the predominantly nuclear staining with the antibody against Caspase-1 in atrophic acinar cells, we found a clear cytoplasmatic overexpression in two other distinct morphologic compartments in chronic pancreatitis—in hyperplastic ducts and in areas with tubularly dedifferentiating acinar cells. Cyclin D1, EGF, and EGF-R were also altered in chronic pancreatitis^[20,21], which lend support to the hypothesis that chronic pancreatitis is a progressive process. Furthermore, we have recently found that positive nuclear MIB-1 (Ki67) expression in pancreatitis tissues might be an indication for proliferative processes^[22,23]. Tumor surrounding pancreatitis tissues from patients with pancreatic cancer showed a strong positive immunoreactivity with antiserum against Caspase-1, but the differential expression pattern seen in primary chronic pancreatitis could not be observed. Nuclear and cytoplasmatic expression of Caspase-1 was found in atrophic acinar cells and in duct cells as well. One explanation for this overexpression might be the dramatic course of pancreatitis due to tumor obstruction. Another explanation might be that Caspase-1 was upregulated through paracrine stimulation with tumor-derived EGF in these cells. Nevertheless, destruction of pancreatic parenchyma due to tumor growth and invasion was likely to be associated with apoptosis of normal pancreatic cells.

In summary, Caspase-1 is overexpressed in atrophic acinar cells of chronic pancreatitis and tumor-surrounding pancreatitis tissues and is markedly expressed in cytoplasm of pancreatic cancer cells and hyperplastic duct cells and dedifferentiating acinar cells in chronic pancreatitis.

REFERENCES

- 1 **Kostura MJ**, Tocci MJ, Limjuco G, Chin J, Cameron P, Hillman AG, Chartrain NA, Schmidt JA. Identification of a monocyte specific pre-interleukin 1 beta convertase activity. *Proc Natl Acad Sci U S A* 1989; **86**: 5227-5231
- 2 **Thornberry NA**, Bull HG, Calaycay JR, Chapman KT, Howard AD, Kostura MJ, Miller DK, Molineaux SM, Weidner JR, Aunins J. A novel heterodimeric cysteine protease is required for interleukin-1 beta processing in monocytes. *Nature* 1992; **356**: 768-774
- 3 **Yuan J**, Shaham S, Ledoux S, Ellis HM, Horvitz HR. The *C. elegans* cell death gene *ced-3* encodes a protein similar to mammalian interleukin-1 beta-converting enzyme. *Cell* 1993; **75**: 641-652
- 4 **Enari M**, Hug H, Nagata S. Involvement of an ICE-like protease in Fas-mediated apoptosis. *Nature* 1995; **375**: 78-81
- 5 **Zhu H**, Fearnhead HO, Cohen GM. An ICE-like protease is a common mediator of apoptosis induced by diverse stimuli in human monocytic THP. 1 cells. *FEBS Lett* 1995; **374**: 303-308
- 6 **Jacobsen MD**, Weil M, Raff MC. Role of Ced-3/ICE-family proteases in staurosporine-induced programmed cell death. *J Cell Biol* 1996; **133**: 1041-1051
- 7 **Duan H**, Chinnaiyan AM, Hudson PL, Wing JP, He WW, Dixit VM. ICE-LAP3, a novel mammalian homologue of the *Caenorhabditis elegans* cell death protein Ced-3 is activated during Fas- and tumor necrosis factor-induced apoptosis. *J Biol Chem* 1996; **271**: 1621-1625
- 8 **Faucheu C**, Diu A, Chan AW, Blanchet AM, Miossec C, Herve F, Collard Dutilleul V, Gu Y, Aldape RA, Lippke JA. A novel human protease similar to the interleukin-1 beta converting enzyme induces apoptosis in transfected cells. *Embo J* 1995; **14**: 1914-1922
- 9 **Kumar S**, Kinoshita M, Noda M, Copeland NG, Jenkins NA. Induction of apoptosis by the mouse *Nedd2* gene, which encodes a protein similar to the product of the *Caenorhabditis elegans* cell death gene *ced-3* and the mammalian IL-1 beta-converting enzyme. *Genes Dev* 1994; **8**: 1613-1626
- 10 **Miossec C**, Decoen MC, Durand L, Fassy F, Diu-Hercend A. Use of monoclonal antibodies to study interleukin-1 beta-converting enzyme expression: only precursor forms are detected in interleukin-1 beta-secreting cells. *Eur J Immunol* 1996; **26**: 1032-1042
- 11 **Gu Y**, Wu J, Faucheu C, Lalanne JL, Diu A, Livingston DJ, Su MS. Interleukin-1 beta converting enzyme requires oligomerization for activity of processed forms in vivo. *Embo J* 1995; **14**: 1923-1931
- 12 **Casciola Rosen LA**, Anhalt GJ, Rosen A. DNA-dependent protein kinase is one of a subset of autoantigens appecifically cleaved early during apoptosis. *J Exp Med* 1995; **182**: 1625-1634
- 13 **Gansauge S**, Gansauge F, Ramadani M, Stobbe H, Rau B, Harada N, Beger HG. Overexpression of cyclin D1 in human pancreatic carcinoma is associated with poor prognosis. *Cancer Res* 1997; **57**: 1634-1637
- 14 **Toyoda H**, Nakamura T, Shinoda M, Suzuki T, Hatooka S, Kobayashi S, Ohashi K, Seto M, Shiku H, Nakamura S. Cyclin D1 expression is useful as a prognostic indicator for advanced esophageal carcinomas, but not for superficial tumors. *Dig Dis Sci* 2000; **45**: 864-869
- 15 **Sallinen SL**, Sallinen PK, Kononen JT, Syrjakoski KM, Nupponen NN, Rantala IS, Helen PT, Helin HJ, Haapasalo HK. Cyclin D1 expression in astrocytomas is associated with cell proliferation activity and patient prognosis. *J Pathol* 1999; **188**: 289-293
- 16 **Keum JS**, Kong G, Yang SC, Shin DH, Park SS, Lee JH, Lee JD. Cylin D1 overexpression ia an indicator of poor prognosis in resectable non-small cell lung cancer. *Br J cancer* 1999; **81**: 127-132
- 17 **Korc M**, Chandrasekar B, Shah GN. Differential binding and biological activities of epidermal growth factor and transforming growth factor alpha in a human pancreatic cancer cell line. *Cancer Res* 1991; **51**(23 Pt 1): 6243-6249
- 18 **Chin YE**, Kitagawa M, Kuida K, Flavell RA, Fu XY. Activation of the STAT signaling pathway can cause expression of caspase1 and apoptosis. *Mol Cell Biol* 1997; **17**: 5328-5337
- 19 **Yamanaka Y**, Friess H, Kobrin MS, Buchler M, Beger HG, Korc M. Coexpression of epidermal growth factor receptor and ligands in human pancreatic cancer is associated with enhanced tumor aggressiveness. *Anticancer Res* 1993; **13**: 565-569
- 20 **Korrmann M**, Ishiwata T, Arber N, Beger HG, Korc M. Increased cyclin D1 expression in chronic pancreatitis. *Pancreas* 1998; **17**: 158-162
- 21 **Korc M**, Friess H, Yamanaka Y, Kobrin MS, Buchler M, Beger HG. Chronic pancreatitis is associated with increased concentrations of epidermal growth factor receptor, transforming growth factors alpha, and phospholipase C gamma. *Gut* 1994; **35**: 1468-1473
- 22 **Gansauge S**, Gansauge F, Yang Y, Muller J, Seufferlein T, Ramadani M, Beger HG. Interleukin 1 beta-converting enzyme (caspase-1) is overexpressed in adenocarcinoma of the pancreas. *Cancer Res* 1998; **58**: 2703-2706
- 23 **Ramadani M**, Yang Y, Gansauge F, Gansauge S, Beger HG. Overexpression of caspase-1 (interleukin-1 β converting enzyme) in chronic pancreatitis and its participation in apoptosis and proliferation. *Pancreas* 2001; **22**: 383-387

Edited by Ma JY

• CLINICAL RESEARCH •

Spider angiomas in patients with liver cirrhosis: Role of vascular endothelial growth factor and basic fibroblast growth factor

Chung-Pin Li, Fa-Yauh Lee, Shinn-Jang Hwang, Rei-Hwa Lu, Wei-Ping Lee, Yee Chao, Sung-Sang Wang, Full-Young Chang, Jacqueline Whang-Peng, Shou-Dong Lee

Chung-Pin Li, Fa-Yauh Lee, Shinn-Jang Hwang, Rei-Hwa Lu, Wei-Ping Lee, Sung-Sang Wang, Full-Young Chang, Shou-Dong Lee, Division of Gastroenterology, Department of Medicine, Taipei Veterans General Hospital and Institute of Clinical Medicine, National Yang-Ming University School of Medicine, Taipei, Taiwan, China
Yee Chao, Cancer Center, Taipei Veterans General Hospital and National Yang-Ming University School of Medicine, Taipei, Taiwan, China
Jacqueline Whang-Peng, Cancer Research Division, National Health Research Institutes and Institute of Clinical Medicine, National Yang-Ming University School of Medicine, Taipei, Taiwan, China
Correspondence to: Chung-Pin Li, Division of Gastroenterology, Department of Medicine, Taipei Veterans General Hospital, No. 201, Sec. 2, Shih-Pai Road, Taipei, 11217, Taiwan. cpli@vghtpe.gov.tw
Telephone: +886-2-28757308 **Fax:** +886-2-28739318
Received: 2003-08-23 **Accepted:** 2003-10-12

Abstract

AIM: To investigate whether vascular endothelial growth factor (VEGF) and basic fibroblastic growth factor (bFGF) are associated with spider angiomas in patients with liver cirrhosis.

METHODS: Eighty-six patients with liver cirrhosis were enrolled and the number and size of the spider angiomas were recorded. Fifty-three healthy subjects were selected as controls. Plasma levels of VEGF and bFGF were measured in both the cirrhotics and the controls.

RESULTS: Plasma VEGF and bFGF were increased in cirrhotics compared with controls (122 ± 13 vs. 71 ± 11 pg/mL, $P=0.003$ for VEGF; 5.1 ± 0.5 vs. 3.4 ± 0.5 pg/mL, $P=0.022$ for bFGF). In cirrhotics, plasma VEGF and bFGF were also higher in patients with spider angiomas compared with patients without spider angiomas (185 ± 28 vs. 90 ± 10 pg/mL, $P=0.003$ for VEGF; 6.8 ± 1.0 vs. 4.1 ± 0.5 pg/mL, $P=0.017$ for bFGF). Multivariate logistic regression showed that young age and increased plasma levels of VEGF and bFGF were the most significant predictors for the presence of spider angiomas in cirrhotic patients (odds ratio [OR]=6.64, 95 % confidence interval [CI]=2.02-21.79, $P=0.002$; OR=4.35, 95 % CI=1.35-14.01, $P=0.014$; OR=5.66, 95 % CI=1.72-18.63, $P=0.004$, respectively).

CONCLUSION: Plasma VEGF and bFGF are elevated in patients with liver cirrhosis. Age as well as plasma levels of VEGF and bFGF are significant predictors for spider angiomas in cirrhotic patients.

Li CP, Lee FY, Hwang SJ, Lu RH, Lee WP, Chao Y, Wang SS, Chang FY, Peng JW, Lee SD. Spider angiomas in patients with liver cirrhosis: Role of vascular endothelial growth factor and basic fibroblast growth factor. *World J Gastroenterol* 2003; 9 (12): 2832-2835

<http://www.wjgnet.com/1007-9327/9/2832.asp>

INTRODUCTION

Liver cirrhosis is a major disease in Asian countries and causes

marked morbidity and mortality. Spider angioma is a common presentation of liver cirrhosis^[1,2]. It appears frequently in alcoholic cirrhotics or when liver function deteriorates^[2-4] and may be associated with esophageal variceal bleeding^[5]. However, the exact pathogenesis has been unclear.

Angiogenesis is a possible mechanism in the pathogenesis of spider angiomas and has not been well investigated. Serum vascular growth factors, such as vascular endothelial growth factor (VEGF) and basic fibroblast growth factor (bFGF), have been found to be elevated in cirrhotic patients^[6-9]. These vascular growth factors may play a role in the neovascularization and formation of spider angiomas in patients with liver cirrhosis.

The aim of this study was to evaluate the predictive value of plasma VEGF and bFGF for the presence of spider angiomas in patients with liver cirrhosis.

MATERIALS AND METHODS

Study patients

Eighty-six consecutive liver cirrhotic patients from Taipei Veterans General Hospital were enrolled into this study. Fifty-three age- and sex-matched subjects from apparently healthy adults who were admitted to our hospital for routine physical checkups were randomly selected as healthy controls. The etiologies of liver cirrhosis included hepatitis B in 37 patients (43 %), hepatitis C in 18 patients (21 %), alcoholism in 12 patients (14 %), primary biliary cirrhosis in 2 patients (2 %), hepatitis B and alcoholism in 7 patients (8 %), hepatitis C and alcoholism in 6 patients (7 %), and being cryptogenic in 4 patients (5 %). The diagnosis of cirrhosis was confirmed by liver biopsy or peritoneoscopy in 8 patients, and based on typical clinical findings (splenomegaly, ascites, and/or esophageal varices), imaging studies (abdominal sonography^[10], computerized tomography, and/or angiography), and characteristic laboratory findings in the remaining 78 patients. The severity of cirrhosis was categorized according to the Child-Pugh classification^[11]. Patients with hypertension, diabetes mellitus, atherosclerosis, uremia, and peripheral vascular occlusive diseases were excluded. None of these patients had received antibiotics or vasoactive drugs in the previous week before blood sampling. All the subjects gave informed consent to participate in this study, which was approved by the Hospital Ethics Committee. This study also conformed to the provisions of the World Medical Association Declarations of Helsinki.

All the patients received a complete physical examination to reveal the number and size of the spider angiomas. Serum albumin (reference range 3.7-5.3 g/dL), bilirubin (0.2-1.6 mg/dL), aspartate transaminase (AST, 5-45 U/L), alanine transaminase (ALT, 0-40 U/L), creatinine (0.7-1.5 mg/dL), and blood urea nitrogen (7-20 mg/dL) concentrations were measured in each patient using standard laboratory methods (Hitachi Model 736 automatic analyzer, Tokyo, Japan) on the same day the blood was sampled for assays of plasma vascular growth factors. Each cirrhotic patient underwent an upper GI endoscopy (Olympus GIF-XQ240; Olympus Corp., Taipei, Taiwan) to

document the presence of esophageal varices. The severity of varices was graded F1: small straight varices, F2: enlarged tortuous varices, and F3: largest-sized coil-shaped varices, as suggested by Beppu *et al*^[12].

Determination of plasma levels of VEGF and bFGF

All the plasma samples were centrifuged at 3 000 rpm for 10 minutes at 4 °C and stored at -80 °C until tested. Samples from all the patients and controls were coded so that the technicians running the assays were blind to the sources of the samples. Plasma levels of VEGF and bFGF were measured by using commercially available enzyme-linked immunoabsorbent assay kits (R&D Systems Inc., Minneapolis, MN) according to the manufacturer's instructions. Standard curves were constructed using serial dilutions of recombinant VEGF and bFGF. Optical densities were determined using a micro-titer plate reader (Bio-Kinetics Reader, Bio-Tek Instruments, VT). Tests were performed in duplicate. The intra- and inter-assay variations of these assays were less than 10 %.

Statistical analysis

Results were expressed as mean \pm SD. Unpaired Student *t*-test was used to analyze continuous variables between groups. Chi-square test or Fisher's exact test was used for comparison of categorical variables. Pearson correlation coefficient was used to determine the relationship between numerical variables, such as plasma levels of VEGF and the size of spider angiomas. Cut-off values were determined for each serum angiogenic factor according to the best discrimination between patients with or without spider angiomas regarding optimal values of sensitivity and specificity using the receiver operating characteristics (ROC) curve analysis. Logistic regression was used to assess the relationship of independent variables with the presence of spider angiomas in cirrhotic patients. Statistical analyses were performed using the SPSS software (SPSS 10.0, SPSS Inc., Chicago, IL, USA). Results were considered statistically significant at $P < 0.05$.

RESULTS

Plasma angiogenic factors in patients with liver cirrhosis

Plasma VEGF and bFGF levels in patients with liver cirrhosis are listed in Table 1. Plasma levels of VEGF and bFGF were increased in patients with liver cirrhosis compared with healthy controls ($P < 0.05$). There was no difference in age, sex, and serum levels of creatinine between the two groups (data not shown).

Table 1 Plasma levels of VEGF and bFGF

Parameters	Healthy controls (<i>n</i> =53)	Cirrhotics (<i>n</i> =86)	<i>P</i> Value
VEGF (pg/mL)	71 \pm 11	122 \pm 13	0.003
bFGF (pg/mL)	3.4 \pm 0.5	5.1 \pm 0.5	0.022

VEGF=vascular endothelial growth factor, bFGF=basic fibroblast growth factor.

Patient characteristics

Characteristics of the 86 patients with liver cirrhosis are listed in Table 2. Plasma VEGF and bFGF were increased in the 31 cirrhotic patients with spider angiomas compared with the 55 patients without spider angiomas (185 \pm 28 pg/mL *vs.* 90 \pm 10 pg/mL, $P=0.003$ for VEGF; 6.8 \pm 1.0 pg/mL *vs.* 4.1 \pm 0.5 pg/mL, $P=0.017$ for bFGF). Plasma VEGF was also higher in the 26 patients with alcohol-related liver cirrhosis compared with the 60 patients with non-alcoholic liver cirrhosis (167 \pm 29 pg/mL *vs.* 103 \pm 13 pg/mL, $P=0.04$).

Table 2 Characteristics of patients'

	No. of patients	VEGF (pg/mL)	bFGF (pg/mL)
Sex			
Male	67	121 \pm 14	4.8 \pm 0.5
Female	19	123 \pm 27	6.1 \pm 1.5
Age			
≤ 60 years	36	149 \pm 24	5.2 \pm 0.8
> 60 years	50	103 \pm 13	5.1 \pm 0.6
Etiology			
Alcohol-related	26	167 \pm 29*	4.6 \pm 0.7
Non-alcoholic	60	103 \pm 13	5.4 \pm 0.6
Albumin (g/dL)			
≤ 3.6	48	132 \pm 15	5.1 \pm 0.7
> 3.6	38	109 \pm 21	5.2 \pm 0.7
Creatinine (mg/dL)			
≤ 1.5	83	122 \pm 13	5.2 \pm 0.5
> 1.5	3	125 \pm 73	4.5 \pm 2.6
ALT (U/L)			
≤ 40	37	136 \pm 22	4.1 \pm 0.6
> 40	49	111 \pm 15	5.9 \pm 0.7
Total bilirubin (mg/dL)			
≤ 1.6	54	115 \pm 16	5.2 \pm 0.6
> 1.6	32	133 \pm 20	5.0 \pm 0.9
Child-Pugh score			
A	47	98 \pm 19	5.5 \pm 0.7
B, C	39	141 \pm 16	4.8 \pm 0.7
Prothrombin time prolongation > 4 s			
Yes	27	145 \pm 23	5.0 \pm 1.0
No	59	112 \pm 15	5.3 \pm 0.6
Platelet count (/ μ L)			
$\leq 150\ 000$	71	109 \pm 12 [†]	6.8 \pm 1.5
$> 150\ 000$	15	204 \pm 41	4.7 \pm 0.5
Esophageal varices			
Yes	59	122 \pm 14	5.0 \pm 0.6
No	27	119 \pm 28	5.8 \pm 1.0
Spider angioma			
Yes	31	185 \pm 28 ^b	6.8 \pm 1.0 ^a
No	55	90 \pm 10	4.1 \pm 0.5

Data were presented as mean \pm SD. ^a $P < 0.05$, ^b $P < 0.005$. VEGF=vascular endothelial growth factor, bFGF=basic fibroblast growth factor.

Plasma angiogenic factors and clinical features

Table 3 summarizes the clinical features of cirrhotic patients with spider angiomas and those without. Cirrhotic patients with spider angiomas were younger (54 \pm 2 years *vs.* 66 \pm 1 years, $P < 0.001$) and had higher serum bilirubin (3.1 \pm 0.5 mg/dL *vs.* 1.7 \pm 0.2 mg/dL, $P=0.03$), longer prothrombin time (16.6 \pm 0.7 sec *vs.* 14.8 \pm 0.4 sec, $P=0.015$), and higher proportion of alcoholism (45 % *vs.* 20 %, $P=0.014$) than those without. Sex, serum albumin, creatinine, AST, ALT, platelet count, size of esophageal varices, and Child-Pugh score did not differ between the two groups.

In the cirrhotics, plasma VEGF was significantly correlated with the size of spider angiomas ($r=0.38$, $P < 0.001$). Plasma VEGF level also showed correlation with serum bilirubin level ($r=0.3$, $P=0.006$) and platelet count ($r=0.5$, $P < 0.001$).

Univariate analysis of predictive factors for spider angiomas

Univariate analysis of factors predicting the presence of spider angiomas in patients with liver cirrhosis by using logistic regression is shown in Table 4. The cut-off values of 134 pg/mL

for VEGF and 4.8 pg/mL for bFGF obtained by the ROC analysis were used in the univariate analysis. Young age, elevated serum AST and bilirubin, prolonged prothrombin time, elevated plasma VEGF and bFGF, and alcoholism were associated with the presence of spider angiomas in cirrhotic patients.

Table 3 Clinical features of cirrhotic patients with and without spider angiomas

Parameters	Spider (+) (n=31)	Spider (-) (n=55)	P Value
Age (years)	54±2	66±1	<0.001
Sex (male/female)	27/4	41/14	0.17
Albumin (g/dL)	3.4±0.1	3.5±0.1	0.69
Creatinine (mg/dL)	1.0±0.1	1.1±0.1	0.24
AST (U/L)	91±9	89±13	0.93
ALT (U/L)	59±9	72±11	0.36
Platelet count (/uL)	108 097±12 379	94 762±7 541	0.33
Esophageal varices (nil/F1/F2/F3)	7/6/12/6	18/12/14/11	0.88
Child-Pugh score	8.2±0.5	7.3±0.3	0.99
Bilirubin (mg/dL)	3.1±0.5	1.7±0.2	0.03
Prothrombin time (s)	16.6±0.7	14.8±0.4	0.015
Alcoholism	14 (45 %)	11 (20 %)	0.014

AST=aspartate transaminase, ALT=alanine transaminase.

Table 4 Univariate analysis of predictive factors for spider angiomas

Parameters	Odds ratio	95 % Confidence interval	P Value
Age (≤60 years)	5.12	1.97-13.28	0.001
Albumin (≥3.7 g/dL)	0.66	0.27-1.64	0.369
Creatinine (>1.5 mg/dL)	0.58	0.06-5.81	0.642
AST (>45 U/L)	5.76	1.56-21.3	0.009
ALT (>40 U/L)	1.24	0.51-3.02	0.634
Bilirubin (>1.6 mg/dL)	2.71	1.09-6.74	0.031
Platelet count (>150 000/uL)	1.41	0.44-4.52	0.563
Prothrombin time prolongation (>4 s)	2.96	1.15-7.58	0.024
Child-Pugh score C	1.64	0.59-4.53	0.344
VEGF (≥134 pg/mL)	5.33	1.93-14.74	0.001
bFGF (≥4.8 pg/mL)	4.38	1.67-11.5	0.003
Alcoholism	3.29	1.25-8.67	0.016

AST=aspartate transaminase, ALT=alanine transaminase, VEGF=vascular endothelial growth factor, bFGF=basic fibroblast growth factor.

Table 5 Multivariate analysis of predictive values of VEGF, bFGF, and age for spider angiomas

Parameters	Odds ratio	95% confidence interval	P Value
Age (≤60 years)	6.64	2.02-21.79	0.002
VEGF (≥134 pg/mL)	4.35	1.35-14.01	0.014
bFGF (≥4.8 pg/mL)	5.66	1.72-18.63	0.004

VEGF=vascular endothelial growth factor, bFGF=basic fibroblast growth factor.

Multivariate analysis of plasma VEGF and bFGF, age and their predictive values for spider angiomas

Multivariate analysis with logistic regression showed that young age and elevated plasma levels of VEGF and bFGF were the most independent predictive factors for spider

angiomas in cirrhotic patients, as shown in Table 5. The predictive values of plasma VEGF for spider angiomas were the following: sensitivity, 53 %; specificity, 82 %; positive predictive value, 64 %; and negative predictive value, 75 %. The predictive values of plasma bFGF for spider angiomas were: sensitivity, 60 %; specificity, 75 %; positive predictive value, 58 %; and negative predictive value, 76 %.

DISCUSSION

Spider angioma has been commonly seen in patients with liver cirrhosis^[1,2]. The pathogenesis is still unknown. Neovascularization is a likely mechanism, but has not been proved. In the current study, we found significantly elevated plasma levels of VEGF and bFGF in cirrhotic patients compared with healthy controls. Elevated plasma VEGF was correlated with the size of spider angiomas. To our knowledge, this is the first study to demonstrate that age and plasma VEGF and bFGF are the most significant independent predictors of spider angiomas in cirrhotic patients.

VEGF has been found to be a glycoprotein that selectively induces endothelial proliferation, angiogenesis, and capillary hyperpermeability^[13-15]. VEGF gene was expressed in a wide variety of normal human tissues, including the liver^[16,17]. Blood levels of VEGF in patients with cirrhosis remain controversial^[6,18]. Our results showed that plasma VEGF was elevated in patients with liver cirrhosis. In addition, plasma VEGF levels were negatively correlated with liver function reserve in patients with liver cirrhosis. The elevated VEGF might be due to ischemic or damaged liver cells, which released cellular VEGF to facilitate damage repair by stimulating angiogenesis^[19]. Increased production of VEGF by the cirrhotic liver has also been reported^[20], and may subsequently lead to the formation of spider angiomas.

bFGF has also been found to be a potent stimulator of endothelial cell proliferation, migration, and angiogenesis^[21]. Our results showed that plasma bFGF was elevated in patients with liver cirrhosis which was consistent with previous reports^[7-9]. The elevated bFGF might be due to a release from damaged liver cells^[22] or increased production by the cirrhotic liver^[9]. bFGF could also stimulate the production of VEGF and enhance angiogenesis^[23].

The presence of spider angiomas has been reported to be associated with esophageal variceal bleeding^[5]. The pathophysiological mechanism has been unclarified. Spider angiomas originate from arterioles, while esophageal varices are one kind of veins. They are different in nature. In this study, there was no relationship between the presence of spider angiomas and the degree of esophageal varices. In addition, there was no association between esophageal varices and these angiogenic factors.

A positive correlation was also found between serum VEGF level and the platelet count. This result was in accordance with the findings reported by others^[24]. Platelets release a variety of vasoactive substances, including VEGF, and promote angiogenesis, endothelial permeability, and endothelial growth^[25]. Although there was a positive correlation between the serum VEGF level and platelet count, there was no significant association between platelet count and spider angioma in the present study. Serum VEGF level was an independent predictor of spider angioma.

Plasma VEGF was increased in alcoholic cirrhotics compared with non-alcoholic cirrhotics in our study. Ethanol could induce expression of vascular endothelial growth factor and stimulate angiogenesis^[26]. This may lead to the high prevalence of spider angiomas in alcoholic cirrhotic patients.

Young age was a significant predictor for the presence of spider angiomas in cirrhotics in our study. This was in

conformity with previous reports^[1]. The underlying mechanism is unknown. A decline in angiogenic capacity in the aged^[27,28] may cause impaired neovascularization and formation of spider angiomas in cirrhotic patients.

In summary, plasma VEGF and bFGF are elevated in patients with liver cirrhosis, especially in those with spider angiomas. Age-related angiogenic capacity as well as VEGF and bFGF may play important roles in the formation of spider angiomas in cirrhotic patients.

ACKNOWLEDGMENT

This work was supported by grant NSC 89-2315-B-075-004 from the National Science Council, and grant VGH 90-070 from Taipei Veterans General Hospital, Taiwan.

REFERENCES

- 1 **Bean WB**. The cutaneous arterial spider: a survey. *Medicine* 1945; **24**: 243-331
- 2 **Sherlock S**, Dooley J. Hepato-cellular failure In: Sherlock S, Dooley J, eds. *Diseases of the Liver and Biliary System*. 11th ed. Oxford: Blackwell Science 2002: 81-92
- 3 **Schenker S**, Balint J, Schiff L. Differential diagnosis of jaundice: report of a prospective study of 61 proved cases. *Am J Dig Dis* 1962; **7**: 449-463
- 4 **Li CP**, Lee FY, Hwang SJ, Chang FY, Lin HC, Lu RH, Hou MC, Chu CJ, Chan CC, Luo JC, Lee SD. Spider angiomas in patients with liver cirrhosis: role of alcoholism and impaired liver function. *Scand J Gastroenterol* 1999; **34**: 520-523
- 5 **Foutch PG**, Sullivan JA, Gaines JA, Sanowski RA. Cutaneous vascular spiders in cirrhotic patients: correlation with hemorrhage from esophageal varices. *Am J Gastroenterol* 1988; **83**: 723-726
- 6 **Rosmorduc O**, Wendum D, Corpechot C, Galy B, Sebbagh N, Raleigh J, Housset C, Poupon R. Hepatocellular hypoxia-induced vascular endothelial growth factor expression and angiogenesis in experimental biliary cirrhosis. *Am J Pathol* 1999; **155**: 1065-1073
- 7 **Hsu PI**, Chow NH, Lai KH, Yang HB, Chan SH, Lin XZ, Cheng JS, Huang JS, Ger LP, Huang SM, Yen MY, Yang YF. Implications of serum basic fibroblast growth factor levels in chronic liver diseases and hepatocellular carcinoma. *Anticancer Res* 1997; **17**: 2803-2809
- 8 **Jin-no K**, Tanimizu M, Hyodo I, Kurimoto F, Yamashita T. Plasma level of basic fibroblast growth factor increases with progression of chronic liver disease. *J Gastroenterol* 1997; **32**: 119-121
- 9 **Napoli J**, Prentice D, Niinami C, Bishop GA, Desmond P, McCaughan GW. Sequential increases in the intrahepatic expression of epidermal growth factor, basic fibroblast growth factor, and transforming growth factor beta in a bile duct ligated rat model of cirrhosis. *Hepatology* 1997; **26**: 624-633
- 10 **Di Lelio A**, Cestari C, Lomazzi A, Beretta L. Cirrhosis: diagnosis with sonographic study of the liver surface. *Radiology* 1989; **172**: 389-392
- 11 **Pugh RN**, Murray-Lyon IM, Dawson JL, Pietroni MC, Williams R. Transection of the oesophagus for bleeding oesophageal varices. *Br J Surg* 1973; **60**: 646-649
- 12 **Beppu K**, Inokuchi K, Koyanagi N, Nakayama S, Sakata H, Kitano S, Kobayashi M. Prediction of variceal hemorrhage by esophageal endoscopy. *Gastrointest Endosc* 1981; **27**: 213-218
- 13 **Shweiki D**, Itin A, Soffer D, Keshet E. Vascular endothelial growth factor induced by hypoxia may mediate hypoxia-initiated angiogenesis. *Nature* 1992; **359**: 843-845
- 14 **Plate KH**, Breier G, Weich HA, Risau W. Vascular endothelial growth factor is a potential tumour angiogenesis factor in human gliomas *in vivo*. *Nature* 1992; **359**: 845-848
- 15 **Shi BM**, Wang XY, Mu QL, Wu TH, Liu HJ, Yang Z. Angiogenesis effect on rat liver after administration of expression vector encoding vascular endothelial growth factor D. *World J Gastroenterol* 2003; **9**: 312-315
- 16 **Berse B**, Brown LF, Van de Water L, Dvorak HF, Senger DR. Vascular permeability factor (vascular endothelial growth factor) gene is expressed differentially in normal tissues, macrophages, and tumors. *Mol Biol Cell* 1992; **3**: 211-220
- 17 **Warren RS**, Yuan H, Matli MR, Gillett NA, Ferrara N. Regulation by vascular endothelial growth factor of human colon cancer tumorigenesis in a mouse model of experimental liver metastasis. *J Clin Invest* 1995; **95**: 1789-1797
- 18 **Akiyoshi F**, Sata M, Suzuki H, Uchimura Y, Mitsuyama K, Matsuo K, Tanikawa K. Serum vascular endothelial growth factor levels in various liver diseases. *Dig Dis Sci* 1998; **43**: 41-45
- 19 **Klagsbrun M**, Dmora PA. Regulation of angiogenesis. *Annu Rev Physiol* 1991; **53**: 217-239
- 20 **El-Assal ON**, Yamanoi A, Soda Y, Yamaguchi M, Igarashi M, Yamamoto A, Nabika T, Nagasue N. Clinical significance of microvessel density and vascular endothelial growth factor expression in hepatocellular carcinoma and surrounding liver: possible involvement of vascular endothelial growth factor in the pathogenesis of cirrhotic liver. *Hepatology* 1998; **27**: 1554-1562
- 21 **Duthu GS**, Smith JR. *In vitro* proliferation and lifespan of bovine aorta endothelial cells: effect of culture conditions and fibroblast growth factor. *J Cell Physiol* 1980; **103**: 285-392
- 22 **Dmora PA**. Modes of FGF release *in vivo* and *in vitro*. *Cancer Metastasis Rev* 1991; **9**: 227-238
- 23 **Seghezzi G**, Patel S, Ren CJ, Gualandris A, Pintucci G, Robbins ES, Shapiro RL, Galloway AC, Rifkin DB, Mignatti P. Fibroblast growth factor-2 (FGF-2) induces vascular endothelial growth factor (VEGF) expression in the endothelial cells of forming capillaries: an autocrine mechanism contributing to angiogenesis. *J Cell Biol* 1998; **141**: 1659-1673
- 24 **Salgado R**, Vermeulen PB, Benoy I, Weytjens R, Huget P, Van Marck E, Dirix LY. Platelet number and interleukin-6 correlate with VEGF but not with bFGF serum levels of advanced cancer patients. *Br J Cancer* 1999; **80**: 892-897
- 25 **Maloney JP**, Silliman CC, Ambruso DR, Wang J, Tudor RM, Voelkel NF. *In vitro* release of vascular endothelial growth factor during platelet aggregation. *Am J Physiol* 1998; **275**: H1054-1061
- 26 **Gu JW**, Elam J, Sartin A, Li W, Roach R, Adair TH. Moderate levels of ethanol induce expression of vascular endothelial growth factor and stimulate angiogenesis. *Am J Physiol Regul Integr Comp Physiol* 2001; **281**: R365-372
- 27 **Rivard A**, Fabre JE, Silver M, Chen D, Murohara T, Kearney M, Magner M, Asahara T, Isner JM. Age-dependent impairment of angiogenesis. *Circulation* 1999; **99**: 111-120
- 28 **Reed MJ**, Corsa AC, Kudravy SA, McCormick RS, Arthur WT. A deficit in collagenase activity contributes to impaired migration of aged microvascular endothelial cells. *J Cell Biochem* 2000; **77**: 116-126

Edited by Zhu LH

• CLINICAL RESEARCH •

Copper metabolism after living related liver transplantation for Wilson's disease

Xue-Hao Wang, Feng Cheng, Feng Zhang, Xiang-Cheng Li, Jian-Ming Qian, Lian-Bao Kong, Hao Zhang, Guo-Qiang Li

Xue-Hao Wang, Feng Cheng, Feng Zhang, Xiang-Cheng Li, Jian-Ming Qian, Lian-Bao Kong, Hao Zhang, Guo-Qiang Li, Liver Transplantation Center, First Affiliated Hospital of Nanjing Medical University, Nanjing 210029, Jiangsu Province, China

Supported by the Basic Research Program Foundation of Jiangsu Province, No.BJ98025

Correspondence to: Feng Cheng, Liver Transplantation Center, First Affiliated Hospital of Nanjing Medical University, Nanjing 210029, Jiangsu Province, China. docchengfeng@sohu.com

Telephone: +86-25-3718836-6476

Received: 2003-06-28 **Accepted:** 2003-08-16

Abstract

AIM: Liver transplantation is indicated for Wilson's disease (WD) patients with the fulminant form and end-stage liver failure. The aim of this study was to review our experience with living-related liver transplantation (LRLT) for WD.

METHODS: A retrospective review was made for WD undergoing LRLT at our hospital from January 2001 to February 2003.

RESULTS: LRLT was carried out in 15 patients with WD, one of them had fulminant hepatic failure and the others had end-stage hepatic insufficiency. The mean age of the patients was 14.5 ± 2.5 years (range 6 to 20 years). All the recipients had low serum ceruloplasmin levels with a mean value of 126.8 ± 34.8 mg/L before transplantation. The serum ceruloplasmin levels increased to an average of 238.6 ± 34.4 mg/L after LRLT at the latest evaluation, between 2 and 27 months after transplantation. A marked reduction in urinary copper excretion was observed in all the recipients after transplantation. Among the eight recipients with preoperative Kayser-Fleischer (K-F) rings, this abnormality resolved completely after LRLT in five patients and partially in three. All the recipients are alive and remain well, and none has developed signs of recurrent WD after a mean follow-up period of 15.4 ± 9.3 months (range 2-27 months) except one who died of severe rejection. The donors were 14 mothers and 1 father. The serum ceruloplasmin levels were within normal limits in all the donors (mean: 220 ± 22.4 mg/L). The mean donor age was 35.0 ± 4.0 years (range, 30 to 45 years). Two donors had biliary leakage and required reoperation. Grafts were harvested as follows: four right lobe grafts without hepatic middle vein and eleven left lobe grafts with hepatic middle vein. The grafts were blood group-compatible in all recipients. Two patients had hepatic artery thrombosis and underwent retransplantation.

CONCLUSION: LRLT is a curative procedure in Wilson's disease manifested as fulminant hepatic failure and/or end-stage hepatic insufficiency. After liver transplantation, the serum ceruoplasmin level can increase to its normal range while urinary copper excretion decreases. Grafts chosen from heterozygote carriers do not appear to confer any risk of recurrence in recipients.

Wang XH, Cheng F, Zhang F, Li XC, Qian JM, Kong LB, Zhang H, Li GQ. Copper metabolism after living related liver transplantation for Wilson's disease. *World J Gastroenterol* 2003; 9(12): 2836-2838

<http://www.wjgnet.com/1007-9327/9/2836.asp>

INTRODUCTION

Wilson's disease (WD) is an autosomal recessive disease. Its clinical and pathological manifestations are the consequence of an excessive accumulation of copper in tissues, particularly in the liver, brain, cornea, and kidneys. Liver transplantation is indicated for fulminant form and end-stage liver disease of WD^[1,2]. Cadaveric liver transplantation has been reported to normalize copper metabolism in recipients^[3,4]. Recently, LRLT has also been used for WD^[5-14]. Asonuma *et al*^[8] reported that LRLT from heterozygous carriers of the WD gene could also resolve clinical signs and symptoms of WD and correct the parameters of copper metabolism. In this study, we reported our experience with LRLT for hepatic complications of WD from January 2001 to February 2003.

MATERIALS AND METHODS

Clinical and laboratory data were obtained from a review of the files of patients from 2001 to 2003 at Liver Transplantation Center of Jiangsu Province. All treatments had an informed consent of the children's parents and the approval of the Ethics Committee of Nanjing Medical University. Donors were selected based on blood type, liver function, negative serological test results (hepatitis B virus, hepatitis C, HIV), physical examination, psychosocial evaluation including alcohol abuse and liver volumes assessed by Doppler ultrasound equipment and computed tomography. The donors were 14 mothers and 1 father. The serum ceruloplasmin levels were within the normal limits in all donors (mean: 220 ± 22.4 mg/L). The mean donor age was 35.0 ± 4.0 years (range, 30 to 45 years). Serum ceruloplasmin and copper level were also normal in all donors who gave an informed consent.

The diagnosis of WD was made on the basis of a combination of the findings, including hepatic and/or neurological clinical abnormalities, the presence of Kayser-Fleischer rings (KFR), elevated 24-hr urine copper (>100 μ g/24 hr), low ceruloplasmin level (reference range 200-500 mg/L). The above mentioned routine laboratory data were obtained by using standard methods. No patient received any chelating agent and presented clinical signs of WD after LRLT.

Among the 15 patients with WD, one had fulminant hepatic failure and the others had end-stage hepatic insufficiency. Their mean age was 14.5 ± 2.5 years (range 6 to 20 years). Before transplantation, all recipients had a low serum ceruloplasmin level with a mean value of 126.8 ± 34.8 mg/L and a high urinary copper excretion with a mean value of 1825.6 ± 187.4 μ g/24 h. Eight recipients had preoperative Kayser-Fleischer (K-F) rings. Grafts were harvested as follows: four right lobe grafts without hepatic middle vein and eleven left lobe grafts with hepatic middle vein. The grafts were blood group-compatible in all recipients.

RESULTS

Donors

All the donors were discharged from the hospital after a mean hospital stay of 9-14 days, and then resumed their normal life without any significant adverse sequelae. Two complications of bile leaks occurred, and required reoperation.

Recipients

Two patients had hepatic artery thrombosis and underwent retransplantation. All the recipients enjoyed normal health with a good quality of life, and none had signs of recurrent WD after a mean follow-up period of 15.4 ± 9.3 months (range 2-27 months). One patient died of severe rejection. Copper metabolism of the WD recipients and the presence of K-F rings were compared before and after transplantation. After LRLT, all the recipients had normal serum ceruloplasmin concentrations in the first month. Marked reduction of urinary copper excretion occurred in the first three months, which became normal 6-9 months after operation. Kayser-Fleischer (K-F) rings were resolved completely after LRLT in five patients and partially in three.

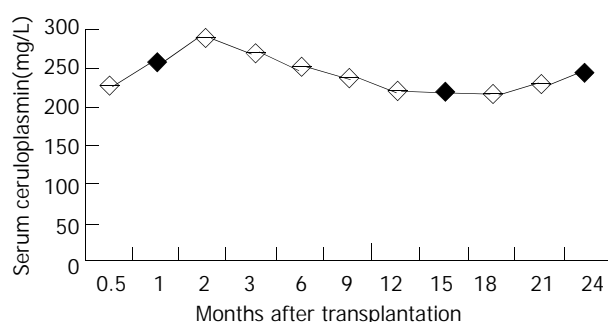


Figure 1 Changes in serum ceruloplasmin of postoperative recipients (Normal: 200-500 mg/L).

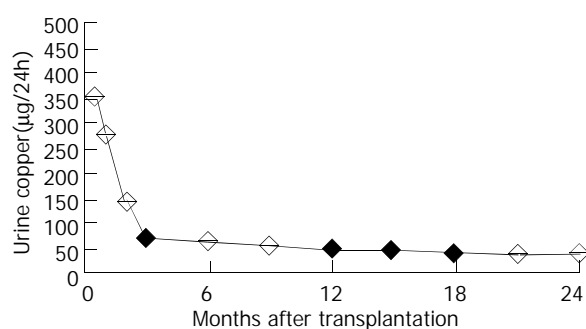


Figure 2 Changes in urine copper of postoperative recipients (Normal: <50 μg/24 h).

DISCUSSION

Wilson's disease, first described by Kinneir Wilson in 1912, is an autosomal recessive condition with a prevalence in one of 30 000^[15]. Its clinical and pathological manifestations are the consequence of an excessive accumulation of copper in tissues, particularly in the liver, brain, cornea, and kidneys. The WD gene is localized on the long arm of chromosome 13 and was recently cloned by several different research groups^[16-19]. The gene product ATP7B is a copper transporting type ATPase. Establishing the diagnosis of Wilson's disease is usually straightforward if the major clinical and laboratory features are manifested as: typical hepatic and/or neurological symptoms and signs, Kayser-Fleischer rings, low serum caeruloplasmin concentrations, and increased urinary copper excretion.

It has been reported that the prognosis of fulminant WD is extremely poor and liver transplantation is currently the only available form of curative therapy when penicillamine therapy has failed or is no longer appropriate^[20-22]. Cadaveric liver transplantation has been reported to normalize copper metabolism in recipients^[3,4]. As scarcity of cadaveric donors is a serious problem in many countries, LRLT represents a critical form of rescue therapy in endstage liver disease. Recently, because of the shortage of donors for cadaveric liver transplantation, LRLT has also been indicated for WD^[5-14]. Asonuma *et al*^[8] reported that LRLT from heterozygous carriers of the WD gene could also resolve clinical signs and symptoms of WD and correct the parameters of copper metabolism.

The advantage of LRLT is that the donor liver can be obtained in an urgent situation when conservative therapy has failed. A successful transplantation of a liver from a living donor was performed in Australia in 1989 by Strong and colleagues^[23], and the technique had been practised worldwide now, particularly in countries where cadaveric organs are not available. In general, the most important ethical dilemma with LRLT is that the process subjects a healthy person to a major operation. More than 1500 such surgeries in children have been performed throughout the world. Only two donors died. One died from pulmonary embolism, and the other died from an anesthetic accident. The patient with pulmonary embolisms was probably a poor surgical candidate. In neither case were there any technical complications related to the procedure. Both cases showed the importance of donor evaluation and selection in preventing living donor mortalities. In this study, 15 donors were discharged from the hospital and all resumed their normal life style without any significant adverse sequelae after a mean hospital stay of 15 days after the operation. Two complications of bile leakage occurred, and required a relaparotomy. The results, along with those from other centers, confirmed the general safety of the donor operation^[24,25]. Hepatic arterial reconstruction is one of the most difficult procedures in living-donor liver transplantation (LDLT) because the artery used is generally small in diameter and has a short stalk. If hepatic artery thrombosis (HAT) occurred, the recipient clinical course would be unstable^[26-30]. The introduction of microvascular hepatic arterial reconstruction has significantly decreased the incidence of HAT. In our group, HATs were recognized in 2 cases (13 %), retransplantations saved the patients. So surgeons who perform hepatic arterial reconstruction in LDLT should be well trained in microvascular techniques to decrease the incidence of HAT.

In this study, Copper metabolism in the WD recipients and the presence of K-F rings were compared before and after transplantation. After LRLT, all the recipients had a normal serum ceruloplasmin concentration and marked reduction in urinary copper excretion. All the donor ceruloplasmin levels were within the normal range, as were the post-transplant levels in the recipients. In addition to normal laboratory profiles of copper abnormalities, five out of eight patients with Kayser-Fleischer rings had a complete resolution and the remaining three showed improvement following transplantation. Despite these results, it is important to remember that about 10 % of WD heterozygotes would have low ceruloplasmin levels, so that they might be unsuitable as donors^[31]. Based on the findings of this study, living related liver transplantation can be used safely in WD when appropriate cadaveric organs are unavailable. Despite the excellent results of the reported cases, there are some questions to be studied, such as screening of potential WD heterozygote donors for uncommon abnormalities of copper metabolism, *etc.*

Furthermore, it is still unclear whether de-coppering after LRLT from heterozygote donors is slower than de-coppering after cadaveric transplantation from non-related donors. We

are reassured, however, by the fact that none of our transplanted recipients had persistent neurological abnormalities after LRLT, and K-F rings disappeared in most of the recipients, indicating that LRLT was indeed an effective and safe modality of therapy for patients with Wilsonian fulminant hepatic failure and end-stage hepatic insufficiency. After liver transplantation, serum ceruoplasmin level increased to normal range and urinary copper excretion decreased. Grafts chosen from heterozygote carriers did not appear to confer any risk of recurrence in the recipients, at least in the short term. Long-term follow-up should be continued to evaluate this specific therapy.

REFERENCES

- Bellary S**, Hassanein T, Van Thiel DH. Liver transplantation for Wilson's disease. *J Hepatol* 1995; **23**: 373-381
- Sternlieb I**. Wilson's disease: indications for liver transplants. *Hepatology* 1984; **4**(Suppl): 15s-17s
- Emre S**, Atillasoy EO, Ozdemir S, Schilsky M, Rathna Varma CV, Thung SN, Sternlieb I, Guy SR, Sheiner PA, Schwartz ME, Miller CM. Orthotopic liver transplantation for Wilson's disease: a single-center experience. *Transplantation* 2001; **72**: 1232-1236
- Burdelski M**, Rogiers X. Liver transplantation in metabolic disorders. *Acta Gastroenterol Belg* 1999; **62**: 300-305
- Komatsu H**, Fujisawa T, Inui A, Sogo T, Sekine I, Kodama H, Uemoto S, Tanaka K. Hepatic copper concentration in children undergoing living related liver transplantation due to Wilsonian fulminant hepatic failure. *Clin Transplant* 2002; **16**: 227-232
- Tanaka K**, Uemoto S, Inomata Y, Tokunaga Y, Ueda M, Tokka A, Sato B, Yamaoka Y. Living-related liver transplantation for fulminant hepatic failure in children. *Transpl Int* 1994; **7**(Suppl 1): S108-110
- Tanaka K**, Uemoto S, Tokunaga Y, Fujita S, Sano K, Yamamoto E, Sugano M, Awane M, Yamaoka Y, Kumada K. Living related liver transplantation in children. *Am J Surg* 1994; **168**: 41-48
- Asonuma K**, Inomata Y, Kasahara M, Uemoto S, Egawa H, Fujita S, Kiuchi T, Hayashi M, Tanaka K. Living related liver transplantation from heterozygote genetic carriers to children with Wilson's disease. *Pediatr Transplant* 1999; **3**: 201-205
- Terajima H**, Tanaka K, Okajima K, Inomata Y, Yamaoka Y. Timing of transplantation and donor selection in living related liver transplantation for fulminant Wilson's disease. *Transplant Proc* 1995; **27**: 1177-1178
- Wang X**, Zhang F, Li X, Qian J, Kong L, Huang J, Huang Z, Zhang H, Li G, Cheng F, Wang K, Lu S. A clinical report of 12 cases-times of living related liver transplantation. *Zhonghua Yixue Zazhi* 2002; **82**: 435-439
- Hattori H**, Higuchi Y, Tsuji M, Inomata Y, Uemoto S, Asonuma K, Egawa H, Kiuchi T, Furusho K, Yamaoka Y, Tanaka K. Living-related liver transplantation and neurological outcome in children with fulminant hepatic failure. *Transplantation* 1998; **65**: 686-692
- Wang X**, Li G, Li X, Zhang F, Qian J, Kong L, Zhang H, Sun B. Multimodal approach to clinical liver transplantation. *Zhonghua Waike Zazhi* 2002; **40**: 758-761
- Kobayashi S**, Ochiai T, Hori S, Suzuki T, Shimizu T, Gunji Y, Shimada H, Yamamoto S, Ogawa A, Kohno Y, Sunaga M, Shimazu M, Tanaka K. Copper metabolism after living donor liver transplantation for hepatic failure of Wilson's disease from a gene mutated donor. *Hepatogastroenterology* 2001; **48**: 1259-1261
- Sakoguchi T**, Nishizaki T, Suehiro T, Nomoto K, Hashimoto K, Ohta R, Minagawa R, Hiroshige S, Terashi T, Ninomiya M, Nagata S, Shiotani S, Shimada M, Sugimachi K. Living donor liver transplantation in Kyushu University. *Fukuoka Igaku Zasshi* 2000; **91**: 198-202
- Schilsky ML**. Wilson's disease: genetic basis of copper toxicity and natural history. *Semin Liver Dis* 1996; **16**: 83-95
- Steindl P**, Ferenci P, Dienes HP, Grimm G, Pabinger I, Madl C, Maier-Dobersberger T, Herneth A, Dragosics B, Meryn S, Knoflach P, Granditsch G, Gangl A. Wilson's disease: in patients presenting with liver disease: a diagnostic challenge. *Gastroenterology* 1997; **113**: 212-218
- Tanzi RE**, Petrukhin K, Chernov I, Pellequer JL, Wasco W, Ross B, Romano DM, Parano E, Pavone L, Brzustowicz LM. The Wilson disease gene is a copper transporting ATPase with homology to the Menkes disease gene. *Nat Genet* 1993; **5**: 344-350
- Petrukhin K**, Fischer SG, Pirastu M, Tanzi RE, Chernov I, Devoto M, Brzustowicz LM, Cayanis E, Vitale E, Russo JJ. Mapping cloning and genetic characterization of the region containing the Wilson disease gene. *Nat Genet* 1993; **5**: 338-343
- Yamaguchi Y**, Heiny ME, Gitlin JD. Isolation and characterization of a human liver cDNA as a candidate gene for Wilson disease. *Biochem Biophys Res Commun* 1993; **197**: 271-277
- Nazer H**, Ede RJ, Mowat AP, Williams R. Wilson's disease: clinical presentation and use of prognostic index. *Gut* 1986; **27**: 1377-1381
- Rakela J**, Kurtz SB, McCarthy JT, Ludwig J, Ascher NL, Bloomer JR, Claus PL. Fulminant Wilson's disease treated with postdilution hemofiltration and orthotopic liver transplantation. *Gastroenterology* 1986; **90**: 2004-2007
- Stampfl DA**, Munoz SJ, Moritz MJ, Rubin R, Armenti VT, Jarrell BE, Maddrey WC. Heterotopic liver transplantation for fulminant Wilson's disease. *Gastroenterology* 1990; **99**: 1834-1836
- Strong RW**, Lynch SV, Ong TH, Matsunami H, Koido Y, Balderson GA. Successful liver transplantation from a living donor to her son. *N Engl J Med* 1990; **322**: 1505-1507
- Sugawara Y**, Makuuchi M, Takayama T, Imamura H, Kaneko J, Ohkubo T. Safe donor hepatectomy for living related liver transplantation. *Liver Transpl* 2002; **8**: 58-62
- Miller CM**, Gondolesi GE, Florman S, Matsumoto C, Munoz L, Yoshizumi T, Artis T, Fishbein TM, Sheiner PA, Kim-Schluger L, Schiano T, Shneider BL, Emre S, Schwartz ME. One hundred nine living donor liver transplants in adults and children: a single-center experience. *Ann Surg* 2001; **234**: 301-311
- Dalgic A**, Dalgic B, Demirogullari B, Ozbay F, Latifoglu O, Ersoy E, Mahli A, Ilgit E, Ozdemir H, Arac M, Akyol G, Tatlicioglu E. Clinical approach to graft hepatic artery thrombosis following living related liver transplantation. *Pediatr Transplant* 2003; **7**: 149-152
- Goldstein MJ**, Salame E, Kapur S, Kinkhabwala M, LaPointe-Rudow D, Harren NPP, Lobritto SJ, Russo M, Brown RS Jr, Cataldegirmen G, Weinberg A, Renz JF, Emond JC. Analysis of failure in living donor liver transplantation: differential outcomes in children and adults. *World J Surg* 2003; **27**: 356-364
- Uchiyama H**, Hashimoto K, Hiroshige S, Harada N, Soejima Y, Nishizaki T, Shimada M, Suehiro T. Hepatic artery reconstruction in living-donor liver transplantation: a review of its techniques and complications. *Surgery* 2002; **131**(1 Supp 1): S200-S204
- Suehiro T**, Ninomiya M, Shiotani S, Hiroshige S, Harada N, Ryosuke M, Soejima Y, Shimada M, Sugimachi K. Hepatic artery reconstruction and biliary stricture formation after living donor adult liver transplantation using the left lobe. *Liver Transpl* 2002; **8**: 495-499
- Hatano E**, Terajima H, Yabe S, Asonuma K, Egawa H, Kiuchi T, Uemoto S, Inomata Y, Tanaka K, Yamaoka Y. Hepatic artery thrombosis in living related liver transplantation. *Transplantation* 1997; **64**: 1443-1446
- Gollan JL**, Gollan TJ. Wilson disease in 1998: genetic, diagnostic and therapeutic aspects. *J Hepatol* 1998; **28**(Suppl): 28-36

Edited by Xu JY and Wang XL

• CLINICAL RESEARCH •

Clinical relationship between EDN-3 gene, EDNRB gene and Hirschsprung's disease

Xiang-Long Duan, Xian-Sheng Zhang, Guo-Wei Li

Xiang-Long Duan, Guo-Wei Li, Department of General Surgery, Second Hospital of Xi'an Jiaotong University, Xi'an 710004, Shaanxi Province, China

Xian-Sheng Zhang, Department of Pediatric Surgery, Second Hospital of Xi'an Jiaotong University, Xi'an 710004, Shaanxi Province, China

Supported by the Natural Science Foundation of Shaanxi Province, No. 2000SM58

Correspondence to: Dr. Duan-Xiang Long, Department of General Surgery, Second Hospital of Xi'an Jiaotong University, Xi'an 710004, Shaanxi Province, China. duanxl@21cn.com

Telephone: +86-29-8402350 **Fax:** +86-29-5535250

Received: 2003-05-11 **Accepted:** 2003-06-02

Abstract

AIM: To investigate the mutation of EDNRB gene and EDN-3 gene in sporadic Hirschsprung's disease (HD) in Chinese population.

METHODS: Genomic DNA was extracted from bowel tissues of 34 unrelated HD patients which were removed by surgery. Exon 3, 4, 6 of EDNRB gene and Exon 1, 2 of EDN-3 gene were amplified by polymerase chain reaction (PCR) and analyzed by single strand conformation polymorphism (SSCP).

RESULTS: EDNRB mutations were detected in 2 of the 13 short-segment HD. One mutant was in the exon 3, the other was in the exon 6. EDN-3 mutation was detected in one of the 13 short-segment HD and in the exon 2. Both EDNRB and EDN-3 mutations were detected in one short-segment HD. No mutations were detected in the ordinary or long-segment HD.

CONCLUSION: The mutations of EDNRB gene and EDN-3 gene are found in the short-segment HD of sporadic Hirschsprung's disease in Chinese population, which suggests that the EDNRB gene and EDN-3 gene play important roles in the pathogenesis of HD.

Duan XL, Zhang XS, Li GW. Clinical relationship between EDN-3 gene, EDNRB gene and Hirschsprung's disease. *World J Gastroenterol* 2003; 9(12): 2839-2842

<http://www.wjgnet.com/1007-9327/9/2839.asp>

INTRODUCTION

Hirschsprung's disease (HD) is a congenital malformation with an incidence of one in 5 000 live newborns. The absence of intramural intestinal ganglia of Meissner and Auerbach results in poor coordination of propulsive movement, and hence functional intestinal obstruction. Patients were treated surgically with removal of the affected intestine^[1-4]. In 1994, two major genes associated with HD were recognized. First, in the RET (receptor tyrosin kinase) gene, there are inactivating mutations in isolated HD. RET accounts for up to 20 % of sporadic and 50 % of familial cases^[5-11]. The second major

gene is the EDNRB (endothelin receptor B) gene. EDNRB accounts for 5-10 % of all HD cases. Heterozygous mutations in the EDNRB gene were reported in nonsyndromic HD^[12-16]. The preferred ligand for the G-protein coupled transmembranous receptor EDNRB was EDN-3 (endothelin-3). The interaction between EDN-3 and EDNRB was reported to be essential for normal development of enteric ganglia. The importance of the EDN-3-EDNRB interaction in promoting the normal development of neural crest cells has been clearly demonstrated. Human mutations in the EDN-3 gene have been reported recently: heterozygous missense mutations in two cases of sporadic HD^[17-19]. However, there are fewer reports about mutations of EDNRB gene and EDN-3 gene in HD in Chinese population. In order to further investigate the pathogenic mechanism of HD, we examined mutations on exon 3, 4, 6 of EDNRB gene and exon 1, 2 of EDN-3 gene in 34 sporadic HD cases with the single strand conformation polymorphism analysis of polymerase chain reaction products (PCR-SSCP).

MATERIALS AND METHODS

Tissue preparation and extraction of DNA

Thirty-four specimens of sporadic HD cases were collected after operation in the Second Hospital of Xi'an Jiaotong University between 1999 and 2001, and the pathological statement was approved pathologically. There are four cases of long-segment HD, seventeen cases of common HD, and thirteen cases of short-segment HD based on Romen's division. At the same time, normal recta and sigmoid flexure tissues were collected, serving as a control group. All specimens were put into liquid nitrogen to freeze quickly after cut off in 15 minutes, and stored at a temperature of -80 °C. DNA was extracted according to the standard protocols.

PCR amplification

The designed primers were synthesized by Bioasia Company. The specific primer sequences of exon 3, 4, 6 of EDNRB gene and exon 1, 2 of EDN-3 gene are summarized in Table 1. The PCR mixture (total volume: 30 µL) contained 2 µL of template-DNA, 3 µL of 10×PCR buffer, 3 µL of 2.5 mmol/L MgCl₂, 3 µL of 2.5 mmol/L dNTPs, 1 µL each of two fragment-specific primers, 17 µL of triplex distilled water, and 1 unit of Taq DNA polymerase. Thirty-five PCR amplification cycles were performed with the following condition of temperature: 94 °C for 35 seconds, 55 °C for 50 seconds and 72 °C for 1 minute. Amplifications were performed with a final extension for 10 minutes at 72 °C. The amplified fragments were run in 15 g/L agarose gel, and were confirmed to be in existence.

SSCP analysis

A conventional electrophoresis apparatus (PC-3000 Mini Electrophoresis Unit; Bio-Red Company, USA) was used with a constant temperature of 10 °C for SSCP. For SSCP, the PCR products were heated for 10 min at 94 °C, transferred into an ice-cold water bath for 3 min, and then run on 60 g/L polyacrylamide gel for 3 hours. The gel was stained by ethidium bromide for 10 - 20 min to visualize DNA band patterns.

Table 1 EDNRB and EDN-3 primer sequences

Gene	Exon		Primer	bp
EDNRB	3	Forward	ATCTTCAGATATCGAGCTGTT	223 bp
		Reverse	TGAAATTTACCTGCATGAAAG	
	4	Forward	ATCCCTATAGTTTACAAGACAGC	170 bp
		Reverse	ATTTTCTTACCTGCTTTAGGTG	
	6	Forward	ACAGAAGCTACAATGACTAC	240 bp
		Reverse	GAAAGGCTTATATTGAGCC	
EDN-3	1	Forward	CAAGCGGCCGTCCTCCTGGTCCGGT	180 bp
		Reverse	CTTCTCCGCGCCTCGGTCC	
	2A	Forward	CCCTCCTCAGGTGTTTGGG	239 bp
		Reverse	TCGGCCGCTGCTCCTGC	
	2B	Forward	TGGCGAGGAGACTGTGGCT	218 bp
		Reverse	TGGCGAGGAGACTGTGGCT	

RESULTS

Analysis of PCR products

EDNRB gene PCR products The increment of all DNA samples from HD patients was a single strand with a length of 223 bp, 170 bp and 240 bp and so was the normal control, which indicated that a large fragment insertion and deletion did not exist in the region of EDNRB gene exon 3, 4 and 6 among 34 HD patients.

EDN-3 gene PCR products The increment of all DNA samples from HD patients was a single strand with a length of 180 bp, 239 bp and 219 bp and so was the normal control, which indicated that a large fragment insertion and deletion did not exist in the region of EDN-3 gene exon 1, 2A and 2B among 34 HD patients.

were found in 2 unrelated HD. EDNRB mutations were detected in 2 of the 17 short-segment HD. One mutant was in the exon 3 (Figure 1), the other was in the exon 6 (Figure 2). EDN-3 mutation was detected in 1 of the 17 short-segment HD and in the exon 2 (Figure 3). Both EDNRB mutation and EDN-3 mutation were detected in one short-segment HD (Figure 4). The mutation was absent in the ordinary, long-segment HD and normal control group samples.

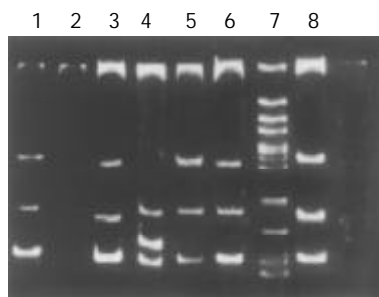


Figure 1 The abnormal shifted SSCP band in exon 3 of EDNRB. 1, 3, 5, 6: Normal shifted SSCP bands; 7: PGEM-3zf/*Hae* III marker; 8: Positive control; 2: Negative control; 4: Abnormal shifted SSCP band.

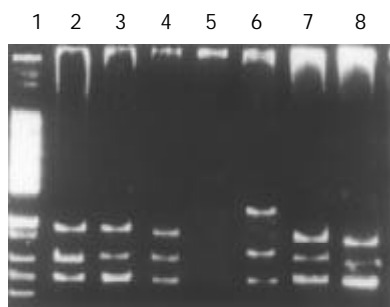


Figure 2 The abnormal shifted SSCP band in exon 6 of EDNRB. 1: PGEM-3zf/*Hae* III marker; 2: Positive control; 5: Negative control; 6: Abnormal shifted SSCP band. 3, 4, 7, 8: Normal shifted SSCP bands.

Results of SSCP

Among the 34 HD patients, abnormal SSCP migration patterns

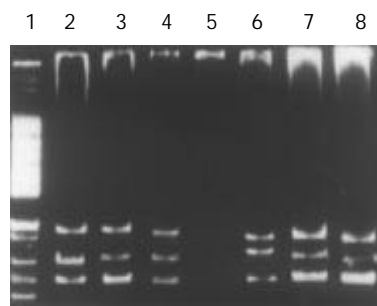


Figure 3 The abnormal shifted SSCP band in exon 2A of EDN-3. 1: PGEM-3zf/*Hae* III marker; 2: Positive control; 5: Negative control; 6: Abnormal shifted SSCP band. 3, 4, 7, 8: Normal shifted SSCP bands.

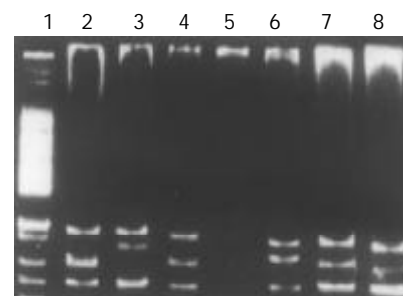


Figure 4 The abnormal shifted SSCP band in exon 2A of EDN-3 and exon 6 of EDNRB. 1: PGEM-3zf/*Hae* III marker; 2: Normal shifted SSCP band; 3: Abnormal shifted SSCP band; 4: Normal control; 5: Negative control; 6: Abnormal shifted SSCP band; 7: positive control; Lane 8: normal shifted SSCP band.

DISCUSSION

The endothelin peptide family of secreted peptides comprises four members to date: EDN-1, EDN-2, EDN-3, and VIP (vasoactive intestinal polypeptide)^[20,21]. A diverse set of pharmacologic activities with different potencies are exerted by endothelin family peptides, suggesting the existence of

endothelin receptor subtypes.

The EDNRB gene encodes a heptahelical receptor that is involved in the G-protein-mediated intracellular signaling pathway. The human EDNRB gene lies on chromosome band 13q22 and comprises 7 exons, with a length of about 24 kb^[22-27]. The predicted protein had 442 amino acids with a transmembrane topology similar to that of other G protein-coupled receptors which, when activated by a ligand, induce a calcium flux into the cells. Activation of EDNRB may result in upregulation of secretion of the endothelins, thereby amplifying their effects.

The EDN-3 gene encodes a large inactive preproendothelin-3 precursor which yields a biologically active 21 amino acid peptide containing four cysteines involved in two disulphide bonds. The human EDN-3 gene lies on chromosome band 20q13.3 and comprises 5 exons^[28-30]. The EDN-3 is produced by a two-step proteolytic cleavage of a larger precursor molecule, preproendothelin. This molecule is enzymatically processed to an inactive progenitor (big endothelin) which is subsequently converted to the active peptide by a specific endothelin-converting enzyme 1. The mature peptide mediates its effect through two receptors, one of which is the EDNRB.

We have examined mutations on exon 3, 4, 6 of EDNRB gene and exon 1, 2 of EDN-3 gene in 34 sporadic Chinese HD patients with PCR-SSCP. The PCR result revealed that the increment of all DNA samples from HD patients was a single strand with a length of 223 bp, 170 bp and 240 bp and so was that from normal control, which indicated that a large fragment insertion and deletion did not exist in the region of EDNRB gene exon 3, 4 and 6 among 34 HD patients. And the increment of all DNA samples from HD patients was a single strand with a length of 180 bp, 239 bp and 219 bp and so was that from normal control, which indicated that a large fragment insertion and deletion did not exist in the region of EDN-3 gene exon 1, 2A and 2B among 34 HD patients. Among the 34 HD patients, we found abnormal SSCP migration patterns in 2 unrelated HD. EDNRB mutations were detected in 2 of the 17 short-segment HDs. One mutant was in the exon 3, the other in the exon 6. EDN-3 mutation was detected in 1 of the 17 short-segment HD and in the exon 2. Both EDNRB and EDN-3 mutations were detected in one short-segment HD. The mutation is absent in the ordinary, long-segment HD and normal control group samples. Due to the mutation of EDNRB, there would be no upregulation of secretion of the endothelins and amplification of endothelin effect, and the total amount of endothelin produced would be too small to initiate migration. Alteration of the structure of the preproendothelin by the mutation may conceivably result in a less efficient cleavage, or even a complete failure of cleavage of the preproendothelin, resulting in EDN-3 deficiency during development. This might lead to an incomplete colonization of the bowel by ganglion cells. We should bear in mind that EDNRB is the receptor for EDN-3, so it is reasonable to assume that the mutations of EDNRB and EDN-3 caused the maldevelopment of the enteric nervous system.

Similar to the receptor-ligand relationship between RET and GDNF observed in the etiology of some HD patients, in human fetuses, both EDNRB and EDN-3 have been demonstrated on enteric neurons and gut mesenchyme cells^[31], suggesting that EDN-3 and EDNRB may regulate interactions between neural crest and gut mesenchyme cells, necessary for normal migration. There are reports on HSCR patients with GDNF-RET or NTN-RET gene mutation combinations, as well as a case with mutations in both RET and EDNRB^[32-39]. So far, there has been no report on an EDN-3 mutation in combination with a mutation in other HSCR genes. In the present study, we found an EDN-3 mutation in combination with an EDNRB mutation in one short-segment HD patient.

To date, at least 16 different mutations or alterations of the EDNRB gene and 4 different mutations or alterations of the EDN-3 gene have been identified in HD patients. A variety of frameshift, nonsense, or missense mutations scattered along EDNRB gene and EDN-3 gene has been identified in HD patients^[40, 41]. The combined results of our study for mutations in EDN3 and EDNRB may indicate the contributions of these genes to the HD phenotype. EDNRB and EDN3 mutations seem to account for a minority of cases. The majority of HSCR cases cannot be explained by mutations in any of the genes analysed so far, suggesting that other genes or additional factors may contribute to the occurrence of HD phenotype and that HD is a multifactorial disease.

REFERENCES

- 1 **Bates MD.** Development of the enteric nervous system. *Clin Perinatol* 2002; **29**: 97-114
- 2 **Amiel J, Lyonnet S.** Hirschsprung disease, associated syndromes, and genetics: a review. *J Med Genet* 2001; **38**: 729-739
- 3 **Meier-Ruge WA, Brunner LA.** Morphometric assessment of Hirschsprung's disease: associated hypoganglionosis of the colonic myenteric plexus. *Pediatr Dev Pathol* 2001; **4**: 53-61
- 4 **Li JC, Mi KH, Zhou JL, Busch L, Kuhnel W.** The development of colon innervation in trisomy 16 mice and Hirschsprung's disease. *World J Gastroenterol* 2001; **7**: 16-21
- 5 **Borrego S, Wright FA, Fernandez RM, Williams N, Lopez-Alonso M, Davuluri R, Antinolo G, Eng C.** A founding locus within the RET proto-oncogene may account for a large proportion of apparently sporadic Hirschsprung disease and a subset of cases of sporadic medullary thyroid carcinoma. *Am J Hum Genet* 2003; **72**: 88-100
- 6 **Griseri P, Pesce B, Patrone G, Osinga J, Puppo F, Sancandi M, Hofstra R, Romeo G, Ravazzolo R, Devoto M, Ceccherini I.** A rare haplotype of the RET proto-oncogene is a risk-modifying allele in hirschsprung disease. *Am J Hum Genet* 2002; **71**: 969-974
- 7 **Sancandi M, Ceccherini I, Costa M, Fava M, Chen B, Wu Y, Hofstra R, Laurie T, Griffiths M, Burge D, Tam PK.** Incidence of RET mutations in patients with Hirschsprung's disease. *J Pediatr Surg* 2000; **35**: 139-143
- 8 **Fitze G, Cramer J, Ziegler A, Schierz M, Schreiber M, Kuhlisch E, Roesner D, Schackert HK.** Association between c135G/A genotype and RET proto-oncogene germline mutations and phenotype of Hirschsprung's disease. *Lancet* 2002; **359**: 1200-1205
- 9 **Pasini B, Rossi R, Ambrosio MR, Zatelli MC, Gullo M, Gobbo M, Collini P, Aiello A, Pansini G, Trasforini G, degli Uberti EC.** RET mutation profile and variable clinical manifestations in a family with multiple endocrine neoplasia type 2A and Hirschsprung's disease. *Surgery* 2002; **131**: 373-381
- 10 **Julies MG, Moore SW, Kotze MJ, du Plessis L.** Novel RET mutations in Hirschsprung's disease patients from the diverse South African population. *Eur J Hum Genet* 2001; **9**: 419-423
- 11 **Shimotake T, Go S, Inoue K, Tomiyama H, Iwai N.** A homozygous missense mutation in the tyrosine kinase domain of the RET proto-oncogene in an infant with total intestinal aganglionosis. *Am J Gastroenterol* 2001; **96**: 1286-1291
- 12 **Newby DE, Strachan FE, Webb DJ.** Abnormal endothelin B receptor vasomotor responses in patients with Hirschsprung's disease. *Q J Med* 2002; **95**: 159-163
- 13 **Von Boyen GB, Krammer HJ, Suss A, Dembowski C, Ehrenreich H, Wedel T.** Abnormalities of the enteric nervous system in heterozygous endothelin B receptor deficient (spotting lethal) rats resembling intestinal neuronal dysplasia. *Gut* 2002; **51**: 414-419
- 14 **Zaahl MG, du Plessis L, Warnich L, Kotze MJ, Moore SW.** Significance of novel endothelin-B receptor gene polymorphisms in Hirschsprung's disease: predominance of a novel variant (561C/T) in patients with co-existing Down's syndrome. *Mol Cell Probes* 2003; **17**: 49-54
- 15 **Fuchs S, Amiel J, Claudel S, Lyonnet S, Corvol P, Pinet F.** Functional characterization of three mutations of the endothelin B receptor gene in patients with Hirschsprung's disease: evidence for selective loss of Gi coupling. *Mol Med* 2001; **7**: 115-124
- 16 **Matsushima Y, Shinkai Y, Kobayashi Y, Sakamoto M, Kunieda**

- T, Tachibana M. A mouse model of Waardenburg syndrome type 4 with a new spontaneous mutation of the endothelin-B receptor gene. *Mamm Genome* 2002; **13**: 30-35
- 17 **Bidaud C**, Salomon R, Van Camp G, Pelet A, Attie T, Eng C, Bonduelle M, Amiel J, Nihoul-Fekete C, Willems PJ, Munnich A, Lyonnet S. Endothelin-3 gene mutations in isolated and syndromic Hirschsprung disease. *Eur J Hum Genet* 1997; **5**: 247-251
- 18 **Pingault V**, Bondurand N, Lemort N, Sancandi M, Ceccherini I, Hugot JP, Jouk PS, Goossens M. A heterozygous endothelin 3 mutation in Waardenburg-Hirschsprung disease: is there a dosage effect of EDN3/EDNRB gene mutations on neurocristopathy phenotypes? *J Med Genet* 2001; **38**: 205-209
- 19 **Svensson PJ**, Von Tell D, Molander ML, Anvret M, Nordenskjold A. A heterozygous frameshift mutation in the endothelin-3 (EDN-3) gene in isolated Hirschsprung's disease. *Pediatr Res* 1999; **45**(5 Pt 1):714-717
- 20 **Goraca A**. New views on the role of endothelin (minireview). *Endocr Regul* 2002; **36**: 161-167
- 21 **Milla PJ**. Endothelins, pseudo-obstruction and Hirschsprung's disease. *Gut* 1999; **44**: 148-149
- 22 **Gariépy CE**, Williams SC, Richardson JA, Hammer RE, Yanagisawa M. Transgenic expression of the endothelin-B receptor prevents congenital intestinal aganglionosis in a rat model of Hirschsprung disease. *J Clin Invest* 1998; **102**: 1092-1101
- 23 **Shanske A**, Ferreira JC, Leonard JC, Fuller P, Marion RW. Hirschsprung disease in an infant with a contiguous gene syndrome of chromosome 13. *Am J Med Genet* 2001; **102**: 231-236
- 24 **Shin MK**, Levorse JM, Ingram RS, Tilghman SM. The temporal requirement for endothelin receptor-B signalling during neural crest development. *Nature* 1999; **402**: 496-501
- 25 **Tanoue A**, Koshimizu TA, Tsuchiya M, Ishii K, Osawa M, Saeki M, Tsujimoto G. Two novel transcripts for human endothelin B receptor produced by RNA editing/alternative splicing from a single gene. *J Biol Chem* 2002; **277**: 33205-33212
- 26 **Syrris P**, Carter ND, Patton MA. Novel nonsense mutation of the endothelin-B receptor gene in a family with Waardenburg-Hirschsprung disease. *Am J Med Genet* 1999; **87**: 69-71
- 27 **Tanaka H**, Moroi K, Iwai J, Takahashi H, Ohnuma N, Hori S, Takimoto M, Nishiyama M, Masaki T, Yanagisawa M, Sekiya S, Kimura S. Novel mutations of the endothelin B receptor gene in patients with Hirschsprung's disease and their characterization. *J Biol Chem* 1998; **273**: 11378-11383
- 28 **Dupin E**, Glavieux C, Vaigot P, Le Douarin NM. Endothelin 3 induces the reversion of melanocytes to glia through a neural crest-derived glial-melanocytic progenitor. *Proc Natl Acad Sci U S A* 2000; **97**: 7882-7887
- 29 **Kenny SE**, Hofstra RM, Buys CH, Vaillant CR, Lloyd DA, Edgar DH. Reduced endothelin-3 expression in sporadic Hirschsprung disease. *Br J Surg* 2000; **87**: 580-585
- 30 **Woodward MN**, Kenny SE, Vaillant C, Lloyd DA, Edger DH. Time-dependent effects of endothelin-3 on enteric nervous system development in an organ culture model of Hirschsprung's disease. *J Pediatr Surg* 2000; **35**: 25-29
- 31 **McCallion AS**, Chakravarti A. EDNRB/EDN3 and Hirschsprung disease type II. *Pigment Cell Res* 2001; **14**: 161-169
- 32 **Angrist M**, Bolk S, Halushka M, Lapchak PA, Chakravarti A. Germline mutations in glial cell line-derived neurotrophic factor (GDNF) and RET in a Hirschsprung disease patient. *Nat Genet* 1996; **14**: 341-344
- 33 **Carrasquillo MM**, McCallion AS, Puffenberger EG, Kashuk CS, Nouri N, Chakravarti A. Genome-wide association study and mouse model identify interaction between RET and EDNRB pathways in Hirschsprung disease. *Nat Genet* 2002; **32**: 237-244
- 34 **Auricchio A**, Griseri P, Carpentieri ML, Betsos N, Staiano A, Tozzi A, Priolo M, Thompson H, Bocciardi R, Romeo G, Ballabio A, Ceccherini I. Double heterozygosity for a RET substitution interfering with splicing and an EDNRB missense mutation in Hirschsprung disease. *Am J Hum Genet* 1999; **64**: 1216-1221
- 35 **Tomiyama H**, Shimotake T, Ono S, Kimura O, Tokiwa K, Iwai N. Relationship between the type of RET/GDNF/NTN or SOX10 gene mutations and long-term results after surgery for total colonic aganglionosis with small bowel involvement. *J Pediatr Surg* 2001; **36**: 1685-1688
- 36 **Svensson PJ**, Anvret M, Molander ML, Nordenskjold A. Phenotypic variation in a family with mutations in two Hirschsprung-related genes (RET and endothelin receptor B). *Hum Genet* 1998; **103**: 145-148
- 37 **Inoue K**, Shimotake T, Tomiyama H, Iwai N. Mutational analysis of the RET and GDNF gene in children with hypoganglionosis. *Eur J Pediatr Surg* 2001; **11**: 120-123
- 38 **Ivanchuk SM**, Myers SM, Eng C, Mulligan LM. De novo mutation of GDNF, ligand for the RET/GDNFR-alpha receptor complex in Hirschsprung disease. *Hum Mol Genet* 1996; **5**: 2023-2026
- 39 **McCallion AS**, Stames E, Conlon RA, Chakravarti A. Phenotype variation in two-locus mouse models of Hirschsprung disease: tissue-specific interaction between Ret and Ednrb. *Proc Natl Acad Sci U S A* 2003; **100**: 1826-1831
- 40 **Parisi MA**, Kapur RP. Genetics of Hirschsprung disease. *Curr Opin Pediatr* 2000; **12**: 610-617
- 41 **Gath R**, Goessling A, Keller KM, Koletzko S, Coerdet W, Muntefering H, Wirth S, Hofstra RM, Mulligan L, Eng C, Von Deimling A. Analysis of the RET, GDNF, EDN3, and EDNRB genes in patients with intestinal neuronal dysplasia and Hirschsprung disease. *Gut* 2001; **48**: 671-675

Edited by Ma JY

• CLINICAL RESEARCH •

Plasma matrix metalloproteinase-1 and tissue inhibitor of metalloproteinases-1 as biomarkers of ulcerative colitis activity

Alicja Wiercinska-Drapalo, Jerzy Jaroszewicz, Robert Flisiak, Danuta Prokopowicz

Alicja Wiercinska-Drapalo, Jerzy Jaroszewicz, Robert Flisiak, Danuta Prokopowicz, Department of Infectious Diseases, Intestinal Diseases Unit, Medical University of Bialystok, Poland

Correspondence to: Alicja Wiercinska-Drapalo MD., Department of Infectious Diseases, Medical University of Bialystok, 15-540 Bialystok, Zurawia str., 14, Poland. alicja@priv.onet.pl
Telephone: +48-85-7416921

Received: 2003-08-05 **Accepted:** 2003-10-12

Abstract

AIM: Overexpression of mucosal metalloproteinases (MMP) have been demonstrated recently in inflammatory bowel disease. Their activity can be counterbalanced by the tissue inhibitor of metalloproteinases (TIMP). The aim of this study was to evaluate the effect of ulcerative colitis (UC) on MMP-1 and TIMP-1 plasma concentrations, as two possible biomarkers of the disease activity.

METHODS: MMP-1 and TIMP-1 plasma concentrations were measured with an enzyme immunoassay in 16 patients with endoscopically confirmed active UC.

RESULTS: Plasma concentrations of both MMP-1 (13.7 ± 0.2 ng/ml) and TIMP-1 (799 ± 140 ng/ml) were significantly elevated in UC patients in comparison to healthy controls (11.9 ± 0.9 ng/ml and 220 ± 7 ng/ml respectively). There was no correlation between TIMP-1 and MMP-1 concentrations ($r = -0.02$). TIMP-1 levels revealed significant positive correlations with scored endoscopic degree of mucosal injury, disease activity index and clinical activity index values as well as C-reactive protein concentration. There was no correlation between MMP-1 and laboratory, clinical or endoscopic indices of the disease activity.

CONCLUSION: These results confirm the role of both MMP-1 and TIMP-1 in the pathogenesis of ulcerative colitis. However only TIMP-1 can be useful as a biomarker of the disease activity, demonstrating association with clinical and endoscopic pictures.

Wiercinska-Drapalo A, Jaroszewicz J, Flisiak R, Prokopowicz D. Plasma matrix metalloproteinase-1 and tissue inhibitor of metalloproteinases-1 as biomarkers of ulcerative colitis activity. *World J Gastroenterol* 2003; 9(12): 2843-2845
<http://www.wjgnet.com/1007-9327/9/2843.asp>

INTRODUCTION

Pathogenesis of ulcerative colitis (UC) is focused on abnormal immune response and diminished ability of mucosal protection and regeneration. These processes are controlled by signaling between epithelial cells involving complex network of cytokines, growth factors and other bioactive substances, responsible for cell proliferation and differentiation, as well as regulation of immune response^[1-3]. Alterations in synthesis and breakdown of extracellular matrix components are known

to play a crucial role in tissue remodeling during inflammation and wound healing. Inflammatory bowel disease (IBD) is sometimes complicated by stricture formation and muscle hypertrophy resulting from extracellular matrix (ECM) changes related to matrix metalloproteinases (MMPs) activity^[4]. Overexpression of mucosal MMPs have been demonstrated recently in inflammatory bowel disease^[5-7]. Effects of MMPs activity can be counterbalanced by the tissue inhibitor of metalloproteinases-1 (TIMP-1)^[8]. The MMP/TIMP ratio imbalance plays an important role in many diseases including not only inflammatory bowel disease but also chronic liver injury^[8] and carcinogenesis^[9]. As we demonstrated recently, elevated plasma concentration of TGF- β_1 , known as TIMP-1 stimulator, was related to inflammation activity and should be considered as a possible biomarker in UC patients^[11,12]. According to Sch ppan and Hahn^[10] blockade of certain MMPs could be a novel therapeutic approach, and therefore some novel mucosa derived parameters, such as MMP-1 and TIMP-1, may prove useful to assess prognosis, disease activity, and treatment response in inflammatory bowel disease.

The aim of this study was to evaluate effect of ulcerative colitis on MMP-1 and TIMP-1 plasma concentrations, as two possible biomarkers of the disease activity.

MATERIALS AND METHODS

Patients

MMP-1 and TIMP-1 concentrations were measured in the plasma of 16 patients (6 females and 10 males) with active ulcerative colitis (UC), and age ranging from 25 to 68 years (mean: 42.5 ± 3.8). All the patients had a history of diagnosed ulcerative colitis that required typical clinical and endoscopic signs of distal part of bowel involvement. MMP-1 and TIMP-1 plasma concentrations were compared with endoscopic picture scored according to Meyers *et al.*^[13], the disease activity index (DAI) according to Schroeder *et al.*^[14], clinical activity index (CAI) as previously described^[11] and laboratory indices of UC activity such as C-reactive protein (CRP), sedimentation rate (SR), white blood count (WBC) and hemoglobin concentration. Plasma MMP-1 and TIMP-1 concentrations were also compared with those of 12 healthy controls (mean age: 40.8 ± 2.7 years). The study was approved by the Bioethical Committee of the Medical University in Bialystok. Informed consent was obtained from each patient.

MMP-1 and TIMP-1 measurement

Venous blood was collected on ice using vacutainer tubes with EDTA as an anticoagulant and centrifuged at $1\,000 \times g$ within 30 minutes of collection. Obtained plasma was additionally centrifuged at $10\,000 \times g$ for 10 minutes at $-2-8^\circ\text{C}$ for complete platelet removal and stored at -20°C . The samples were diluted 1:40 with 0.1M phosphate buffer before assay and then incubated in duplicate in microtitre wells precoated with anti-TIMP-1 or anti-MMP-1 antibodies (Amersham Pharmacia Biotech, Little Chalfont, Buckinghamshire, England). Any TIMP-1 or MMP-1 remained in the microtitre wells after four cycles of washing and aspiration were detected by peroxidase

labelled specific antibodies. The amount of peroxidase bound to each well was determined by the addition of tetramethylbenzidine substrate. The reaction was stopped by acidification and optical density was read with a microtitre plate photometer Stat Fax® 2100 (Alab/Poland) at 450 nm. The concentration of MMP-1 or TIMP-1 in the sample was determined by interpolation from a standard curve prepared with standard samples supplied by the manufacturer.

Statistical methods

Values were expressed by their mean and standard error of the mean (\pm SEM). The significance of the difference was calculated by two-tailed Student's *t* test. Correlation analysis was calculated by the non-parametric Spearman rank order correlation test. Values of $P < 0.05$ were considered to be significant.

RESULTS

Plasma mean concentration of MMP-1 measured in patients with active UC was significantly elevated (13.7 ± 0.2 ng/ml) in comparison to that of healthy controls (11.9 ± 0.9 ng/ml) (Figure 1). Mean TIMP-1 plasma concentration in UC patients (799 ± 140 ng/ml) also exceeded normal values significantly (220 ± 7 ng/ml), and the difference was much more apparent (Figure 2). Even the lowest TIMP-1 value (456 ng/ml) doubled the mean concentration from the controls. As demonstrated in Table 1, the majority of patients had CRP and SR values exceeding the upper limit of normal range. Moreover evaluation of the disease activity through CAI, DAI and endoscopic score demonstrated severe course of the present relapse (Table 1). There was no correlation between TIMP-1 and MMP-1 plasma concentrations ($r = -0.02$, $P = 0.95$). As shown in Table 2 plasma TIMP-1 levels analyzed in UC patients revealed significant positive correlations with scored endoscopic degree of mucosal injury, DAI and CAI values as well as CRP concentration. There was no correlation between MMP-1 and laboratory, clinical or endoscopic indices of the disease activity (Table 2).

Table 1 Laboratory and clinical indices of ulcerative colitis activity in the patients

	Normal range	Mean	\pm SEM	Minimum	Maximum	Median
CRP (mg/dl)	0-5	17.7	4.6	6	62	6
SR (mm/h)	0-12	22.7	4.7	2	68	17
WBC ($\times 10^3/\mu$ l)	4-10	6.8	0.5	3.5	11.5	6.2
HGB (mg/dl)	12-16	13.3	0.3	10.5	14.9	13.4
CAI	0	10.6	0.75	7	15	9
DAI	0	6.4	0.7	3	10	5
Endoscopic score	0	11.6	0.8	8	16	10

CAI: clinical activity index, DAI: disease activity index.

Table 2 Correlation between plasma TIMP-1 or MMP-1 concentrations and values of selected laboratory indices, demonstrated through "r" values. Statistically significant correlation: ^a $P < 0.05$; ^b $P < 0.01$

	TIMP-1 (r)	MMP-1 (r)
CRP (mg/dl)	0.60 ^a	0.05
SR (mm/h)	0.17	-0.07
WBC ($\times 10^3/\mu$ l)	0.24	-0.10
HGB (mg/dl)	-0.19	-0.10
CAI (clinical activity index)	0.55 ^a	-0.18
DAI (disease activity index)	0.66 ^b	-0.27
Score	0.66 ^b	-0.11

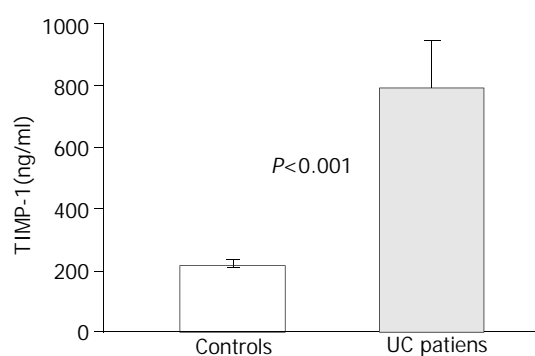


Figure 1 Comparison of mean (\pm SEM) TIMP-1 plasma concentrations in group of patients with ulcerative colitis and controls.

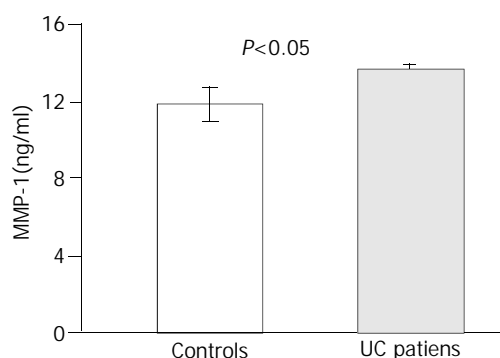


Figure 2 Comparison of mean (\pm SEM) MMP-1 plasma concentrations in group of patients with ulcerative colitis and controls.

DISCUSSION

Matrix metalloproteinases are involved in mucosal degradation causing tissue remodelling and ulcerations related to inflammatory bowel diseases. Enhanced expression of MMP-1, MMP-2 and MMP-3 has been demonstrated recently in inflamed mucosa from patients with UC and Crohn disease^[5,6]. According to Arihiro *et al.*^[15] in both UC and CD, MMP-1, MMP-9 and TIMP-1 were expressed by inflammatory cells, fibroblastic cells as well as by vascular smooth muscle cells most prominently in actively inflamed areas in ulcer bases. Stimulation of T lymphocytes in inflammatory lesions seemed to be responsible for activation of several MMPs^[7,16,17]. TNF- α released by T lymphocytes was a powerful inducer of fibroblasts that were the prime source of MMPs^[19,20]. This created link between mucosal inflammation and destruction of the subepithelial matrix, and MMP-1 expression in the mucosa might be related to the initial step of ulceration in UC^[14]. According to Baugh *et al.*^[20] the expression of matrix metalloproteinases 1, 2, 3 and 9 was significantly higher in inflamed areas of UC patients mucosa compared with noninvolved regions. In the study carried out by von Lampe *et al.*^[5] MMP-1 and -3 correlated well with the histological degree of acute inflammation resulting in more than 15-fold increased levels in inflamed versus normal colon samples from patients with UC. In another study MMP-1 and -2 concentrations measured (using sandwich ELISA) in samples from pouchitis and active UC doubled the values obtained in samples of uninflamed mucosa. Mesenchymal cells were identified as major producers of MMP-1 and -2^[6]. MMPs were implicated in the tissue destruction associated with inflammatory diseases and the role of MMPs in the pathogenesis of inflammatory bowel disease was also confirmed through improvement of experimentally induced colitis after treatment with a matrix metalloproteinase inhibitor^[21].

Apart from protease-inhibitory action TIMP-1 serves

additional functions. Several investigators have demonstrated its growth-promoting properties and stimulation of tumor growth by inhibiting apoptosis indicating the role of TIMP-1 in cancer progression^[22,23]. According to Holten-Andersen *et al.*^[24] plasma TIMP-1 levels could be used to identify patients with colorectal cancer with a sensitivity of 63 % and a specificity of 98 %, so it was suggested as a marker for early identification of this cancer.

According to Heuschkel *et al.*^[25] TIMP-1 measured in biopsies from patients with active IBD remained unchanged. In the study of Louis *et al.*^[26] the production of TIMP-1 was undetectable in the majority of uninflamed biopsy samples from controls, UC and CD patients. However in inflamed mucosa, the production of TIMP-1 was increased significantly in both UC and CD. Its elevated plasma concentration, demonstrated in our study, can reflect situation in bowel mucosa. Enhanced expression of TIMP-1 can be a result of the stimulatory effect of transforming growth factor TGF- β_1 . As we demonstrated recently, enhanced production of TGF- β_1 could be related to inflammation activity in UC patients^[11]. This profibrogenic cytokine accelerated healing but during chronic inflammation might lead to excessive collagen deposition and eventually fibrosis^[4]. In our recent study successful treatment of the disease resulted in decrease of its levels both in plasma and rectal mucosa, but better response has been achieved in patients with higher baseline TGF- β_1 concentrations^[12].

MMP-1 is the main enzyme responsible for degradation of fibrillar collagen and therefore we decided to use it as a possible biomarker in our study^[6]. We demonstrated a significant increase of both MMP-1 and TIMP-1 plasma concentrations in UC patients, which could reflect their over-expression in the bowel mucosa. However significant correlation with clinical and endoscopical signs of UC activity was proved only for TIMP-1. Moreover the only laboratory parameter that showed any association with TIMP-1 was C-reactive protein.

In conclusion, our data confirm the role of both MMP-1 and TIMP-1 in the pathogenesis of ulcerative colitis. However only TIMP-1 may be useful as a biomarker of the disease activity, demonstrating association with clinical and endoscopic pictures.

REFERENCES

- 1 **Beck PL**, Podolsky DK. Growth factors in inflammatory bowel disease. *Inflamm Bowel Dis* 1999; **5**: 44-60
- 2 **Fiocchi C**. IBD: Etiology and Pathogenesis. *Gastroenterology* 1998; **115**: 182-205
- 3 **Zimmerman CM**, Padgett RW. Transforming growth factor b signaling mediators and modulators. *Gene* 2000; **249**: 17-30
- 4 **Mourelle M**, Salas A, Guarner F, Crespo E, Garcia-Lafuente A, Malagelada JR. Stimulation of transforming growth factor beta-1 by enteric bacteria in the pathogenesis of rat intestinal fibrosis. *Gastroenterology* 1998; **114**: 519-526
- 5 **von Lampe B**, Barthel B, Coupland SE, Riecken EO, Rosewicz S. Differential expression of matrix metalloproteinases and their tissue inhibitors in colon mucosa of patients with inflammatory bowel disease. *Gut* 2000; **47**: 63-73
- 6 **Stallmach A**, Chan CC, Ecker KW, Feifel G, Herbst H, Schuppan D, Zeitz M. Comparable expression of matrix metalloproteinases 1 and 2 in pouchitis and ulcerative colitis. *Gut* 2000; **47**: 415-422
- 7 **Salmela MT**, MacDonald TT, Black D, Irvine B, Zhuma T, Saarialho-Kere U, Pender SL. Upregulation of matrix metalloproteinases in a model of T cell mediated tissue injury in the gut: analysis by gene array and in situ hybridisation. *Gut* 2002; **51**: 540-547
- 8 **Nie QH**, Cheng YQ, Xie YM, Zhou YX, Bai XG, Cao YZ. Methodologic research on TIMP-1, TIMP-2 detection as a new diagnostic index for hepatic fibrosis and its significance. *World J Gastroenterol* 2002; **8**: 282-287
- 9 **Fan YZ**, Zhang JT, Yang HC, Yang YQ. Expression of MMP-2, TIMP-2 protein and the ratio of MMP-2/TIMP-2 in gallbladder carcinoma and their significance. *World J Gastroenterol* 2002; **8**: 1138-1143
- 10 **Schuppan D**, Hahn EG. MMPs in the gut: inflammation hits the matrix. *Gut* 2000; **47**: 12-14
- 11 **Wiercinska-Drapalo A**, Flisiak R, Prokopowicz D. Effect of ulcerative colitis activity on plasma concentration of transforming growth factor β_1 . *Cytokine* 2001; **14**: 343-346
- 12 **Wiercinska-Drapalo A**, Flisiak R, Prokopowicz D. Effect of ulcerative colitis treatment on transforming growth factor β_1 in plasma and rectal mucosa. *Regul Pept* 2003; **113**: 57-61
- 13 **Meyers S**, Sachar DB, Present DH, Janowitz HD. Olsalazine in the treatment of ulcerative colitis among patients intolerant of sulphasalazine: a prospective, randomized, placebo controlled double blind, dose-ranging clinical trial. *Scand J Gastroenterol* 1988; **23** (Suppl 148): 29-35
- 14 **Schroeder KW**, Tremaine WJ, Ilstrup DM. Coated oral 5-aminosalicylic acid therapy for mildly to moderately active ulcerative colitis. *N Engl J Med* 1987; **317**: 1625-1629
- 15 **Arihiro S**, Ohtani H, Hiwatashi N, Torii A, Sorsa T, Nagura H. Vascular smooth muscle cells and pericytes express MMP-1, MMP-9, TIMP-1 and type 1 procollagen in inflammatory bowel disease. *Histopathology* 2001; **39**: 50-59
- 16 **MacDonald TT**, Bajaj-Elliott M, Pender SL. T cells orchestrate intestinal mucosal shape and integrity. *Immunology Today* 1999; **20**: 505-510
- 17 **Pender SL**, Tickle SP, Docherty AJ, Howie D, Wathen NC, MacDonald TT. A major role of matrix metalloproteinases in T cell injury in the gut. *J Immunol* 1997; **158**: 1582-1590
- 18 **Pender SL**, Breese EJ, Gunther U, Howie D, Wathen NC, Schuppan D, MacDonald TT. Suppression of T cell mediated injury in human gut by interleukin-10: role of matrix metalloproteinases. *Gastroenterology* 1998; **115**: 573-583
- 19 **Daum S**, Bauer U, Foss HD, Schuppan D, Stein H, Riecken EO, Ullrich R. Increased expression of mRNA for matrix metalloproteinase -1 and -3 and tissue inhibitor of metalloproteinases-1 in intestinal biopsy specimens from patients with coeliac disease. *Gut* 1999; **44**: 17-25
- 20 **Baugh MD**, Perry MJ, Hollander AP, Davies DR, Cross SS, Lobo AJ, Taylor CJ, Evans GS. Matrix metalloproteinase levels are elevated in inflammatory bowel disease. *Gastroenterology* 1999; **117**: 814-822
- 21 **Sykes AP**, Bhogal R, Brampton C, Chander C, Whelan C, Parsons ME, Bird J. The effect of an inhibitor of matrix metalloproteinases on colonic inflammation in a trinitrobenzenesulphonic acid rat model of inflammatory bowel disease. *Aliment Pharmacol Ther* 1999; **13**: 1535-1542
- 22 **Li G**, Fridman R, Kim HR. Tissue inhibitor of metalloproteinase-1 inhibits apoptosis of human breast epithelial cells. *Cancer Res* 1999; **59**: 6267-6275
- 23 **Pellegrini P**, Contasta I, Berghella AM, Gargano E, Mammarella C, Adorno D. Simultaneous measurement of soluble carcinoembryogenic antigen and the tissue inhibitor of metalloproteinase TIMP-1 serum levels for use as markers of pre-invasive to invasive colorectal cancer. *Cancer Immunol Immunother* 2000; **49**: 388-394
- 24 **Holten-Andersen MN**, Christensen IJ, Nielsen HJ, Stephens RW, Jensen V, Nielsen OH, Sorensen S, Overgaard J, Lilja H, Harris A, Murphy G, Brunner N. Total levels of tissue inhibitor of metalloproteinases 1 in plasma yield high diagnostic sensitivity and specificity in patients with colon cancer. *Clin Cancer Res* 2002; **8**: 156-164
- 25 **Heuschkel RB**, MacDonald TT, Monteleone G, Bajaj-Elliott M, Smith JA, Pender SL. Imbalance of stromelysin-1 and TIMP-1 in the mucosal lesions in children with inflammatory bowel disease. *Gut* 2000; **47**: 57-62
- 26 **Louis E**, Ribbens C, Godon A, Franchimont D, De Groote D, Hardy N, Boniver J, Belaiche J, Malaise M. Increased production of matrix metalloproteinase-3 and tissue inhibitor of metalloproteinase-1 by inflamed mucosa in inflammatory bowel disease. *Clin Exp Immunol* 2000; **120**: 241-246

Gastric pseudolipomatosis, usual or unusual? Re-evaluation of 909 endoscopic gastric biopsies

Murat Alper, Yusuf Akcan, Olcay K Belenli, Selma Çukur, Kamuran A Aksoy, Mazlume Suna

Murat Alper, Olcay K Belenli, Selma Çukur, Kamuran A Aksoy, Mazlume Suna, Department of Pathology, Medical School of Düzce, Abant İzzet Baysal University, Turkey

Yusuf Akcan, Department of Gastroenterology, Medical School of Düzce, Abant İzzet Baysal University, Turkey

Correspondence to: Assistant Professor. Dr. Murat Alper, Düzce Tıp Fakültesi Patoloji ABD, Konuralp/Düzce 81650, Turkey. muratalper@tusdata.com

Fax: +90-212-5311616

Received: 2003-08-02 **Accepted:** 2003-10-22

Abstract

Microvesicular pneumatosis intestinalis, also called "pseudolipomatosis" for resembling fatty infiltration, is characterized by the presence of small gas voids in the gastrointestinal wall, especially in mucosa. These voids are not lined with epithelia. There are few reported cases about colon, duodenum and skin. Because there is only one case report about pseudolipomatosis in the stomach, we re-evaluated 909 endoscopic biopsies taken from gastric corpus to check the presence of pseudolipomatosis. We determined pseudolipomatosis foci in 3 percent ($n=27$) of biopsies. In two cases there were pseudolipomatosis foci in endoscopic biopsies having otherwise normal histologic findings, while there were pseudolipomatosis foci in endoscopic biopsies of 25 patients with gastritis. *Helicobacter pylori* was found in 85 % of biopsies having pseudolipomatosis foci. In this study, we presented some histopathologic characteristics of pseudolipomatosis seen in gastric mucosa.

Alper M, Akcan Y, Belenli OK, Çukur S, Aksoy KA, Suna M. Gastric pseudolipomatosis, usual or unusual? Re-evaluation of 909 endoscopic gastric biopsies. *World J Gastroenterol* 2003; 9(12): 2846-2848

<http://www.wjgnet.com/1007-9327/9/2846.asp>

INTRODUCTION

Microvesicular pneumatosis intestinalis which is also called "pseudolipomatosis" for resembling fatty infiltration, is characterized by the presence of small gas voids in the gastrointestinal wall, especially in mucosa^[1]. These gas voids are not lined with epithelial cells. Since we came across only one letter about gastric mucosa while searching literature for our previous case report, in which we presented a case of pseudolipomatosis in the stomach, duodenum and colon, although recently in gastrointestinal system pseudolipomatosis was defined particularly in the colon, duodenum and skin, we investigated endoscopic biopsies with regard to pseudolipomatosis^[1-8].

MATERIALS AND METHODS

In this study, 909 endoscopic gastric biopsies were investigated at the Department of Pathology of Düzce Medical Faculty

Abant İzzet Baysal University, between December 1998 and June 2003. Biopsies taken from the corpus for various reasons other than cancer were included in this study. Biopsies were fixed in 10 % formaldehyde and subjected to automatic tissue follow-up procedures. We re-examined the 4-5 micron thick samples stained with hematoxyline eosin and modified Giemsa by a light microscope. When pseudolipomatosis was found, the presence and grade of inflammation, the presence of intestinal metaplasia, and the presence and concentration of *Helicobacter pylori* were determined. The absence of inflammation was designated as (0), and the presence of inflammation was classified as mild (1), moderate (2) and severe (3). The absence of *Helicobacter pylori* was designated as (0), and the presence was classified as scarce (1), moderate (2) and diffuse (3). Intestinal metaplasia was evaluated as present or absent, and atrophy as present or absent, if present as mild, moderate or severe. Three hundred and sixty-four (40 %) subjects were female and 545 (60 %) were male. The ages of patients ranged between 19 and 78 years with a mean of 46 years.

RESULTS

Pseudolipomatosis was found in 27 of 909 re-evaluated cases. Of these 27 patients, 15 were male and 12 were female. Male patients were between 28 and 56 years old, with a mean of 39 years, female patients were aged between 22 and 65 years, with a mean of 41 years. Mucosal vacuolation was characterized by empty spaces, 30-250 micron in diameter, associated with neither fibrosis/sclerosis nor a lymphocytic infiltrate. There was no evidence of true adipocyte differentiation, vascular markers, e.g. S-100 protein, F-VIII and F-XIII were negative. Vacuoles were found in different parts of the mucosa, although they could be seen beneath epithelia, in a few cases they were detected within muscularis mucosa as well (Figures 1-2). Twenty five of the patients with pseudolipomatosis had gastritis. Of these patients 23 were *Helicobacter pylori* positive. Among the *Helicobacter pylori* positive patients, five had scarce, ten had moderate, and eight had diffuse bacteria. Among the 25 patients with gastritis, 5 had mild, 13 had moderate, and 7 had severe chronic inflammation. In 8 cases with gastritis, intestinal metaplasia was encountered. In all the cases with metaplasia goblet cells and in 4 cases Paneth cells were noticed. Two cases of gastritis had severe atrophy, and one case had mild atrophy. Four patients with gastritis had prior endoscopy for gastric complaints. The previous biopsy results were *Helicobacter pylori* gastritis with severe inflammatory activity in three cases, and *Helicobacter pylori* gastritis with moderate inflammatory activity in one case. Pseudolipomatosis was not found in previous endoscopic gastric biopsies of these four patients. However, in one of these patients, pseudolipomatosis was detected in duodenal and colonic biopsies^[8]. Two other patients had undergone colonoscopy while being searched for malignancy. In samples taken from the colon pseudolipomatosis was not detected.

The patients who were *Helicobacter pylori* positive were given a course of treatment for *Helicobacter pylori* eradication composed of lansoprazol 30 mg daily for 15 days, clarithromycin

bid 500 mg and amoxicillin bid 1 000 mg for 10 days. One month later control biopsies were performed for 5 patients whose complaints were not fully resolved. We found that in two of them pseudolipomatosis continued while in the other three biopsies pseudolipomatosis was not found. In those cases in which pseudolipomatosis continued, we noticed that although *Helicobacter pylori* was decreased, it was not completely eradicated, and in the other three patients we saw that *Helicobacter pylori* was eradicated and the gastritis continued though decreased. Control biopsies were not performed for the remaining patients. In two patients with pseudolipomatosis, a 45-year-old female and a 39-year-old man, biopsies taken for non-specific abdominal pain showed no *Helicobacter pylori*, inflammation or metaplasia. In these patients no pathologic finding except mild edema could be demonstrated. These patients had no previous endoscopies. Vacuoles were seen in small foci in lamina propria, and were considered as pseudolipomatosis.

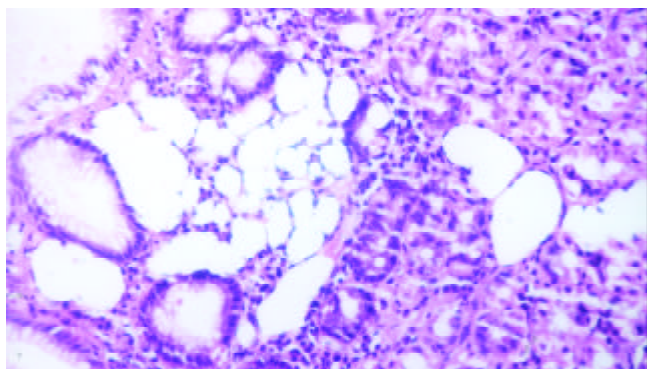


Figure 1 Presence of many vacuoles beneath epithelium in gastric mucosa (H & E ×200).

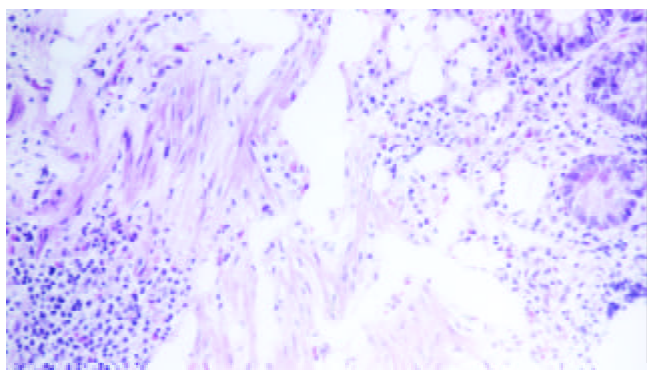


Figure 2 Presence of many vacuoles in muscularis mucosa and lamina propria as well (H & E ×200).

DISCUSSION

Mucosal pseudolipomatosis is a recently described endoscopic finding, most likely caused by intramucosal air. Because of their gross and microscopical similarity to fat, however, the term “pseudolipomatosis” is proposed. Although the etiopathogenesis of pseudolipomatosis is not so clear yet, some probable causes of it in the colon, duodenum and skin have been mentioned^[1-8]. We could find only one case-report about gastric pseudolipomatosis except our one^[6]. For this reason we searched how often pseudolipomatosis, yet its rate in colon increased continuously, was found in gastric mucosa.

Pneumatosis coli is a rare condition characterized by multiple gas-filled cysts within the bowel wall. Mechanical, bacterial and biochemical theories have been available to

explain the pathogenesis of pneumatosis in the colon^[5]. Pneumatosis cystoides intestinalis has been reported to be present together with other conditions such as pseudomembranous enterocolitis, necrotizing enterocolitis, bowel infarction, chronic obstructive pulmonary disease, intestinal obstruction, collagen vascular diseases (scleroderma, dermatomyositis, mixed connective tissue disease), systemic amyloidosis and iatrogenic conditions (after surgery or endoscopy), late-stage AIDS with cryptosporidial diarrhea, and Crohn’s disease^[5]. Gagliardi *et al.* detected mucosal pseudolipomatosis foci in colon of 5 cases among 25 pneumatosis coli patients in their study^[5]. Micropneumatosis was reported to be caused by disinfectant hydrogen peroxide solution^[3]. It might also be a result of colonoscopy application and usually disappeared three weeks after the procedure^[4]. Commercially available endoscope disinfecting hydrogen peroxide solution could cause the unique form of colitis referred as pseudolipomatosis^[3]. It was also reported in asymptomatic patients as an air pressure-related colonoscopy complication^[4]. Mucosal pseudolipomatosis of the colon is an infrequent condition that occurs mainly in elderly males, usually involves the left colon, and is manifested clinically by passage of blood per rectum. Colonoscopy showed solitary or multiple whitish-yellowish plaques, which were localized or involved several segments^[1]. Superficial dermal vacuoles resembling fatty infiltration of the skin have also been reported as pseudolipomatosis cutis^[2]. Dermal vacuoles likely represent an artifact of tissue fixation or processing and are unrelated to the underlying pathologic process. Trotter *et al.* suggested the name pseudolipomatosis cutis, analogous to insufflation-induced colonic vacuolation, to distinguish this phenomenon from true dermal fatty infiltration and to emphasize its incidental, likely artifactual nature^[2]. As in colon and duodenum, histologic studies in the stomach demonstrated microscopic cavities in mucosa, measuring 20 to 300 micron in diameter. Histochemical stains showed that these cavities contained no lipids, suggesting that they were filled with gas. In the study of Gagliardi *et al.*, 14 patients were treated with antidiarrhoeals and anti-inflammatory drugs, improvement was detected in 9 cases. There was a high recurrence rate, but with further courses of continued therapy remission was achieved in five patients. According to Gagliardi *et al.*, the associations of pneumatosis coli with psychiatric disorders and mucosal pseudolipomatosis were new and of possible pathogenetic^[5].

In our study, 23 out of 27 patients had *Helicobacter pylori*. In our previous case report, one patient was diagnosed as micropneumatosis on the first and second colonoscopy specimens at a four week interval^[8]. After another four weeks during the first half of *Helicobacter pylori* gastritis treatment of the patient, colonoscopy was repeated for the third time, and micropneumatosis foci were not observed on pathological sections. In the present study, when control biopsy was performed one month later for 5 patients whose complaints were not resolved it was noticed that pseudolipomatosis continued in two of them while pseudolipomatosis was not seen in the other three in control biopsies. In those cases with persistent pseudolipomatosis, it was noticed that although *Helicobacter pylori* was decreased, it was not completely eradicated, and in the other three patients it was seen that *Helicobacter pylori* was eradicated and the gastritis findings were decreased. It is also possible that the control endoscopic biopsies may be taken from sites that are free of pseudolipomatosis. Since the conditions of some patients improved after the eradication therapy for *Helicobacter pylori*, this finding implicates that *Helicobacter pylori* may be one of the causative factors for micropneumatosis and pneumatosis cystoides intestinalis. It can also be speculated that micropneumatosis grows with time and may lead to pneumatosis

cyctoides intestinalis. The fact that micropneumatosis foci are also reported in most pneumatosis cyctoides intestinalis cases is supportive for this suggestion. The pseudolipomatosis type changes seen in mucosal biopsies should not be ignored by just considering them as artifacts. We think that, in order to determine the etiopathogenesis and significance of gastric mucosal pseudolipomatosis, more case reports are required.

REFERENCES

- 1 **Ben Rejeb A**, Khedhiri F. Mucosal pseudo-lipomatosis of the colon. Apropos of a case with a review of the literature. *Arch Anat Cytol Pathol* 1989; **37**: 254-257
- 2 **Trotter MJ**, Crawford RI. Pseudolipomatosis cutis: superficial dermal vacuoles resembling fatty infiltration of the skin. *Am J Dermatopathol* 1998; **20**: 443-447
- 3 **Ryan CK**, Potter GD. Disinfectant colitis. Rinse as well as you wash. *J Clin Gastroenterol* 1995; **21**: 6-9
- 4 **Waring JP**, Manne RK, Wadas DD. Mucosal pseudolipomatosis: an air pressure-related colonoscopy complication. *Gastrointest Endosc* 1989; **35**: 93-94
- 5 **Gagliardi G**, Thompson IW, Hershman MJ. Pneumatosis coli: a proposed pathogenesis based on study of 25 cases and review of the literature. *Int J Colorectal Dis* 1996; **11**: 111-118
- 6 **Stebbing J**, Wyatt JL. Gastric 'pseudolipomatosis'. *Histopathology* 1998; **32**: 283-284
- 7 **Cook DS**, Williams GT. Duodenal 'pseudolipomatosis'. *Histopathology* 1998; **33**: 394-395
- 8 **Belenli OK**, Akcan Y, Alper M. Micropneumatosis (pseudolipomatosis) coexistent with *Helicobacter pylori* and its improvement. *Indian J Gastroenterol* 2003 (in press)

Edited by Wang XL

Oddi sphincter function after canine auto-pancreas transplantation with bladder drainage

Gui-Chen Li, Chun-Hui Yuan, Ying Cheng, Yong-Feng Liu

Gui-Chen Li, Chun-Hui Yuan, Ying Cheng, Yong-Feng Liu,
Department of Surgery and Organ Transplant Unit, the First Affiliated Hospital, China Medical University, Shenyang 110001, Liaoning Province, China

Supported by programs foundation of Ministry of Education of Liaoning Province, No.202013146

Correspondence to: Dr. Gui-Chen Li, Department of Surgery and Organ Transplant Unit, the First Affiliated Hospital, China Medical University, Shenyang 110001, Liaoning Province, China. lgc763@sohu.com

Telephone: +86-24-23265284

Received: 2003-05-12 **Accepted:** 2003-06-02

Abstract

AIM: Several neural and hormonal factors are known to affect motility of sphincter of Oddi (SO). The major roles of SO are to regulate the flow of bile and pancreatic juice into the duodenum and to prevent the reflux of duodenal contents into the biliary and pancreatic duct. After pancreas transplantation, graft SO was denervated and graft pancreatitis might have relations to SO motility. The motility of SO after canine pancreas transplantation with bladder drainage was investigated.

METHODS: Normal canine SO manometry and pancreas graft SO manometry after pancreas transplantation with bladder drainage were performed in seven dogs respectively before and after cholecystokinin (CCK) administration. Data of SO basal pressure, contraction frequency, amplitude and motility index after transplantation and CCK administration were compared with that in controls and before CCK administration.

RESULTS: SO showed regular contractions with a certain basal pressure in control dogs. After transplantation, the graft SO basal pressure and contraction frequency were higher than that in controls, but the amplitude decreased ($P < 0.01$). There was no great difference in SO motility index. CCK administration could relax normal SO but stimulate graft SO after pancreas transplantation with bladder drainage. After CCK administration, SO basal pressure, frequency and motility index were increased significantly ($P < 0.05$), in comparison with that before administration. The amplitude remained unchanged ($P > 0.05$), in comparison with that before CCK administration.

CONCLUSION: After auto-pancreas transplantation with bladder drainage, canine SO motility was inhibited. Basal pressure and frequency increased but amplitude decreased. CCK administration after transplantation had an inhibitory effect on canine SO instead of a relaxation effect observed in normal canine SO. This will increase the resistance of SO to the pancreatic juice flow and induce pancreatic juice stagnation and can not prevent reflux of urine and duodenal contents when the bladder pressure is increased to a certain extent, which may cause graft pancreatitis.

Li GC, Yuan CH, Cheng Y, Liu YF. Oddi sphincter function after canine auto-pancreas transplantation with bladder drainage. *World J Gastroenterol* 2003; 9(12): 2849-2852

<http://www.wjgnet.com/1007-9327/9/2849.asp>

INTRODUCTION

The major roles of the sphincter of Oddi (SO) are to regulate the flow of bile and pancreatic juice into the duodenum and to prevent the reflux of duodenal contents into the biliary and pancreatic duct. SO motility is composed of tonic contraction and phasic contraction. Neural factors, hormones and some drugs play important roles in the control of SO motility. SO motility is related to migrating motor complex (MMC) of the duodenum. Graft pancreatitis is one of the factors for graft dysfunction with bladder drainage. Reflux of urine and pancreatic juice can cause graft pancreatitis. After transplantation, the graft was denervated and graft duodenum lost its MMC. Little is known about the function of SO and its effect on the graft function after pancreas transplantation with bladder drainage. The aim of this paper was to study canine SO function after pancreas transplantation with bladder drainage and its effect on the graft.

MATERIALS AND METHODS

Preparation of animal

Fourteen healthy adult mongrel dogs, weighing 13-18 kg were anesthetized with 35 mg/kg intravenous pentobarbital sodium, and maintained under adequate anesthesia with 15 mg/kg intravenous pentobarbital sodium as required. System blood pressure was monitored through a catheter placed into the femoral artery. The femoral vein was cannulated and used for systemic administration of solutions and drugs.

Normal canine SO manometry

After an upper medium laparotomy using aseptic technique, the biliary tree was identified. A small longitudinal incision was made in the common bile duct. A triple lumen catheter was cannulated and tied in the bile duct to avoid any leakage and occlusion of the orifice of the catheters. The triple lumen catheter, measuring 1.7 mm of outer diameter and 0.5 mm of inner diameter, with three holes at 2-mm intervals, was perfused with sterile water at a rate of 0.25 ml/min per channel by means of a low-compliance pneumohydraulic pump, and connected via transducers to a computerized recording system. The catheter was sent into the duodenum. Intraduodenal pressure was taken as zero reference. By 1-mm station pull through technique, the catheter was placed just at the site of SO. After a stable basal recording for at least 2 min was obtained at the level of SO high pressure zone, 20 mg/kg cholecystokinin (CCK) diluted in 5 ml saline was injected intravenously and registration continued for a few more minutes until 2 min of stable recording was obtained during drug infusion. SO basal pressure above duodenal zero, amplitude above basal pressure, and frequency of phasic contractions before and after CCK

injection were calculated as well as the motility (amplitude per frequency).

Pancreas graft SO manometry

The dogs were fasted and anesthetized the same as the control group. After a midline celiotomy with aseptic techniques, the tail of the pancreas was mobilized by division of the veins which drain the distal pancreas into the spleen vein. The head of the pancreas was then mobilized without cutting the pancreaticoduodenal vessels. After the common bile duct at its entry into the duodenum was ligated and divided, the lesser omentum was opened. At least 1 cm of gastroduodenal artery and vein were dissected from the bifurcation. The proximal duodenum was cut 1 cm distal to pylorus and closed. After inferior pancreaticoduodenal vessels were cut out, the distal duodenum was divided at the end of the second part of duodenum. Thus the donor was skeletonized with intact vascular connections. Finally, the gastroduodenal artery was ligated and divided as far as possible from the bifurcation of proper hepatic arteries, and the gastroduodenal vein was removed with a cuff of portal venous wall. The graft was immediately immersed in and flushed with cold ringer solution while the portal vein wall was repaired. Reconstruction of vascular connections to the autograft was accomplished by an end-to-side anastomosis of the gastroduodenal vein to the right common iliac artery and end-to-end anastomosis of the accompanying artery to the internal iliac artery. After reperfusion, the distal pancreas was resected. Gastrointestinal continuity was restored by the Roux-en-Y technique with cholecystojejunum, gastrojejunum and graft-duodenal-host bladder anastomosis. Average graft ischemia time was 30-40 min. The bile duct residual of graft was placed under the skin. Fluid and antibiotics were given for 5 days. Oral alimentation was started on the second postoperative day. Serum and urinary amylase, free blood sugar and insulin were determined on days 1, 3, 5 postoperatively. Five days after operation, the same manometry procedure from the residual bile duct before and after CCK injection was performed as for the control dogs.

Statistical analysis

All values were expressed as mean \pm SD. Comparison of values between the two groups was made with analysis of variance and paired *t* tests. Differences were regarded as significant when *P* value was less than 0.5.

RESULTS

1.Changes of SO activity before and after transplantation are shown in Table 1.

Table 1 SO activity in control and transplanted dogs

	Basal pressure (mmHg)	Amplitude (mmHg)	Frequency (min ⁻¹)	Motility index
Control	18.5 \pm 2.8	47.1 \pm 5.5	9.7 \pm 1.5	235.6 \pm 56.1
Transplant	27.8 \pm 2.8	7.2 \pm 1.4	13.1 \pm 1.9	211.3 \pm 33.2

SO showed regular contractions with a certain basal pressure in control dogs.

After transplantation, the graft SO basal pressure and contraction frequency increased as compared with that in controls, but the amplitude decreased (*P*<0.01). There was no great difference in SO motility index.

2.Changes of SO activity before and after administration of CCK in normal dogs are shown in Table 2.

Table 2 SO activity before and after CCK administration in normal dogs

	Basal pressure (mmHg)	Amplitude (mmHg)	Frequency (min ⁻¹)	Motility index
Before CCK	18.5 \pm 2.8	47.1 \pm 5.5	9.7 \pm 1.5	235.6 \pm 56.1
After CCK	10.2 \pm 2.2	18.7 \pm 5.3	5.0 \pm 1.2	49.6 \pm 16.9

CCK administration could relax SO motility. SO basal pressure, contraction frequency and amplitude decreased significantly after CCK administration in comparison with controls (*P*<0.01).

3.SO activity of grafts before and after CCK administration is shown in Table 3.

Table 3 SO activity of grafts before and after CCK administration

	Basal pressure (mmHg)	Amplitude (mmHg)	Frequency (min ⁻¹)	Motility index
Before CCK	27.8 \pm 2.8	7.2 \pm 1.4	13.1 \pm 1.9	211.3 \pm 33.2
After CCK	35.5 \pm 5.1	9.7 \pm 2.1	18.9 \pm 1.9	515.4 \pm 42.3

CCK administration stimulated graft SO motility. After CCK administration, SO basal pressure, frequency and motility index increased significantly in comparison with those before administration (*P*<0.05), while the amplitude remained unchanged (*P*>0.05).

4.After transplantation, there was no great difference in serum amylase, blood sugar and blood insulin as compared with those on day 0 (*P*<0.05). Urine amylase that reflects graft function increased significantly. These data showed a good pancreas graft function (Table 4).

Table 4 Pancreas graft function after transplantation

	Day 0	Day 1	Day 3	Day 5
Serum amylase (IU/L)	22 \pm 5	30 \pm 11	26 \pm 7	24 \pm 4
Urine amylase (IU/L)	80 \pm 38	25 400 \pm 12 100	45 100 \pm 1 780	14 900 \pm 2 100
Blood sugar (mmol/L)	4.5 \pm 1.2	5.1 \pm 0.7	3.8 \pm 1.3	3.6 \pm 0.4
Blood insulin (IU/L)	8.5 \pm 2.2	7.3 \pm 3.2	7.0 \pm 2.4	5.5 \pm 1.0

DISCUSSION

Canine segmental pancreas auto-transplantation and pancreaticoduodenal allotransplantation were often carried out in other studies. In order to investigate the SO motility after pancreas transplantation, we excluded the effect of rejection on the graft and also the graft must have intact SO. So, we established a canine auto-pancreaticoduodenal transplantation model. The results of serum and urine amylase, free blood sugar and insulin level after transplantation showed that the endocrine and exocrine functions of the pancreas graft were both good enough for SO manometry. The transplantation model was stable and suitable for SO manometry.

Canine SO plays an important role in controlling the flow of bile and pancreatic juice into the duodenum and acts as a variable resistor to prevent the reflux of duodenal contents^[1-4]. SO is a complex neuromuscular structure located at the choledochopancreaticoduodenal junction. Canine SO exhibits regular phasic contractions superimposed on a low basal pressure under neurohormonal control. After pancreas transplantation with bladder drainage, the graft was denervated. Little was known about the SO motility after pancreas

transplantation. Several reports suggested that SO dysfunction played an important role in acute recurrent pancreatitis^[5-7]. Graft pancreatitis was a serious complication after pancreas transplantation with bladder drainage. The late graft pancreatitis might be related to SO dysfunction caused by graft SO denervation. Our present study on canine SO motility after auto-pancreas transplantation with bladder drainage showed: (1) Canine SO exhibited regular contractions with a certain basal pressure. After transplantation, graft SO basal pressure and contraction frequency increased and amplitude decreased significantly. But there was no great difference in SO motility index. (2) CCK administration could relax normal canine SO, but stimulate graft SO after canine pancreas transplantation with bladder drainage. The denervated graft duodenum lost its normal migrating motor complex (MMC). These data suggested that the tonic contraction of SO remained and created a higher basal pressure than that before transplantation, and phasic contraction decreased significantly. This resulted in the obstruction of pancreatic juice flowing into the graft duodenum. Furthermore, when bladder pressure increased to a certain extent because of urine stasis, the urine would reflux into pancreatic duct and induce acute pancreatitis.

The role of extrinsic nerves in the control of SO motility has not been fully investigated. The SO was richly innervated by cholinergic, adrenergic and peptidergic neurons^[8]. Direct neural pathways couple the duodenum with the gallbladder and SO, and the SO with the gallbladder. Several surgical procedures, such as gastrectomy^[9], vagotomy^[10] and cholecystectomy^[11,12] have been known to alter SO motility by disrupting certain aspects of the innervations. Numerous reports described SO motility after transection or electrical stimulation of extrinsic nerves, such as the vagal and splanchnic nerves^[13-16]. Different effects of innervation on SO motility reflect the difference both in species and in experimental designs. Complete denervation using tetrodotoxin increased tonic pressure and amplitude of SO phasic contraction in the cats^[10]. Ohtsuke reported increased biliary sphincter basal pressure and amplitude after neural isolation of the pancreatoduodenal region by surgical procedure in conscious dogs^[17]. The present study showed that extrinsic innervation to the pancreatoduodenal region had an inhibitory effect on SO motility. The main role of extrinsic nerves was to regulate phasic contraction and relax SO. Under normal condition, the relaxing effect of extrinsic nerve on canine SO motility was better than the stimulation effect. But the amplitude decreased significantly after transplantation instead of increasing observed in Ohtsuke's study. This is probably because the motility of graft SO was not affected by duodenum MMC. Furthermore, the effect of gastrointestinal hormone on SO motility may be different from that in normal canines because of its anastomosis to system vessels. Further investigations are needed to identify this guess.

CCK is the major physiological hormone regulating tone and motility of biliary system. It normally inhibited biliary sphincter motor activity in human and dogs but stimulated SO under various circumstances, which is known as a paradoxical response^[18,19]. It is believed that these SO relaxant responses to CCK were induced via nonadrenergic, noncholinergic inhibitory neurons since cholinergic and adrenergic antagonists could not inhibit these relaxant responses^[20]. Our present study showed that CCK could relax canine SO and lower SO basal pressure. But denervated SO after transplantation apparently produced paradoxical response of SO to CCK, which was likely caused by the direct effect of CCK on the smooth muscle of SO. Based on these data, we could consume that the paradoxical response of SO to CCK in SO dysfunctional patients might also be caused by the direct stimulation of CCK to SO smooth muscle because of injury of inhibitory nerves of SO.

Gancio reported that reflux pancreatitis was chemically induced by reflux of urine through SO into pancreatic duct during the voiding phase with high detrusor pressure (over 70 cmH₂O)^[21]. Others hypothesized that this could be caused by an incompetent SO or by either pressure exerted on the pancreatic duct due to a large volume bladder or micturition narrowing the duodenocystostomy and obstructing it^[22,23]. The current study showed that canine SO lost its normal contraction rhythm, increased basal pressure causing an obstruction of pancreatic juice into graft duodenum. When bladder pressure overrode the basal pressure, SO probably could not prevent the reflux of urine and duodenal contents into pancreatic duct. All these would contribute to graft pancreatitis.

In conclusion, after auto-pancreas transplantation with bladder drainage, canine SO motility was inhibited. Basal pressure and frequency increased but amplitude decreased. CCK administration after transplantation showed an inhibitory effect on canine SO instead of a relaxation effect to normal canine SO. This will increase the resistance of SO to the pancreatic juice flow and induce pancreatic juice stagnation and can not prevent reflux of urine and duodenal contents when the bladder pressure is increased to a certain extent, which may cause graft pancreatitis.

REFERENCES

- 1 **Torsoli A**, Corazziari E, Habib FI, De Masi E, Biliotti D, Mazzarella R, Giubilei D, Fegiz G. Frequencies and cyclical pattern of the human sphincter of Oddi phasic activity. *Gut* 1986; **27**: 363-369
- 2 **Liu YF**, Saccone GT, Thune A, Baker RA, Harvey JR, Tooouli J. Sphincter of Oddi regulates flow by acting as a variable resistor to flow. *Am J Physiol* 1992; **263**(5 Pt 1): G683-689
- 3 **Yokohata K**, Kimura H, Ogawa Y, Naritomi G, Tanaka M. Biliary motility. Changes in detailed characteristics correlated to duodenal migrating motor complex and effects of morphine and motilin in dogs. *Dig Dis Sci* 1994; **39**: 1294-1301
- 4 **Tanaka M**. Advances in research and clinical practice in motor disorders of the sphincter of Oddi. *J Hepatobiliary Pancreat Surg* 2002; **9**: 564-568
- 5 **Sakorafas GH**, Tsiotou AG. Etiology and pathogenesis of acute pancreatitis: current concepts. *J Clin Gastroenterol* 2000; **30**: 343-356
- 6 **Frulloni L**, Cavallini G. Acute recurrent pancreatitis and dysfunction of the sphincter of Oddi: Comparison between invasive and non-invasive techniques. *JOP* 2001; **2**: 406-413
- 7 **Lai KH**. Sphincter of Oddi and acute pancreatitis: A new treatment option. *JOP* 2002; **3**: 83-85
- 8 **Tooouli J**, Baker RA. Innervation of the sphincter of Oddi: physiology and considerations of pharmacological intervention in biliary dyskinesia. *Pharmacol Ther* 1991; **49**: 268-281
- 9 **Odani K**, Nimura Y, Yasui A, Akita Y, Shionoya S. Paradoxical response to cerulein on sphincter of Oddi in the patients with gastrectomy. *Dig Dis Sci* 1992; **37**: 904-911
- 10 **Behar J**, Biancani P. Neural control of the sphincter of Oddi. Physiologic role of enkephalins on the regulation of basal sphincter of Oddi motor activity in the cat. *Gastroenterology* 1984; **86**: 134-141
- 11 **Grace PA**, Pitt HA. Cholecystectomy alters the hormonal response of the sphincter of Oddi. *Surgery* 1987; **102**: 186-194
- 12 **Wei JG**, Wang YC, Liang GM, Wang W, Chen BY, Xu JK, Song LJ. The study between the dynamics and the X-ray anatomy and regularizing effect of gallbladder on bile duct sphincter of the dog. *World J Gastroenterol* 2003; **9**: 1014-1019
- 13 **Shafik A**. Cholecysto-sphincter inhibitory reflex: identification of a reflex and its role in bile flow in a canine model. *J Invest Surg* 1998; **11**: 199-205
- 14 **Nabae T**, Yokohata K, Otsuka T, Inoue K, Yamaguchi K, Chijiwa K, Tanaka M. Effect of truncal vagotomy on sphincter of Oddi cyclic motility in conscious dogs. *Ann Surg* 2002; **236**: 98-104
- 15 **Takahashi I**, Dodds WJ, Hogan WJ, Itoh Z, Baker K. Effect of vagotomy on biliary-tract motor activity in the opossum. *Dig*

- Dis Sci* 1988; **33**: 481-489
- 16 **Tansy MF**, Mackowiak RC, Chaffee RB. A vagosympathetic pathway capable of influencing common bile duct motility in the dog. *Surg Gynecol Obstet* 1971; **133**: 225-236
- 17 **Ohtsuka T**, Yokohata K, Inoue K, Nabae T, Takahata S, Tanabe Y, Sugitani A, Tanaka M. Biliary sphincter motility after neural isolation of the pancreatoduodenal region in conscious dogs. *Surgery* 2002; **131**: 139-148
- 18 **Toouli J**, Hogan WJ, Geenen JE, Dodds WJ, Arndorfer RC. Action of cholecystokinin-octapeptide on sphincter of Oddi basal pressure and phasic wave activity in humans. *Surgery* 1982; **92**: 497-503
- 19 **Toouli J**, Roberts-Thomson IC, Dent J, Lee J. Manometric disorders in patients with suspected sphincter of Oddi dysfunction. *Gastroenterology* 1985; **88**(5 Pt 1): 1243-1250
- 20 **Behar J**, Biancani P. Pharmacologic characterization of excitatory and inhibitory cholecystokinin receptors of the cat gallbladder and sphincter of Oddi. *Gastroenterology* 1987; **92**: 764-770
- 21 **Ciancio G**, Burke GW, Roth D, Luque CD, Coker D, Miller J. Reflux pancreatitis after simultaneous pancreas-kidney transplantation treated by α 1-blocker. *Transplantation* 1995; **60**: 760-761
- 22 **Stephanian E**, Gruessner RW, Brayman KL, Gores P, Dunn DL, Najarian JS, Sutherland DE. Conversion of exocrine secretions from bladder to enteric drainage in recipients of whole pancreaticoduodenal transplants. *Ann Surg* 1992; **216**: 663-672
- 23 **Boudreaux JP**, Nealon WH, Carson RC, Fish JC. Pancreatitis necessitating urinary diversion in a bladder-drained pancreas transplant. *Transplant Proc* 1990; **22**: 641-642

Edited by Ma JY and Wang XL

Incidence and treatment of hepatic artery complications after orthotopic liver transplantation

Ji-Chun Zhao, Shi-Chun Lu, Lu-Nan Yan, Bo Li, Tian-Fu Wen, Yong Zeng, Nan-Sheng Cheng, Jing Wang, Yan Luo, Yu-Lan Pen

Ji-Chun Zhao, Shi-Chun Lu, Lu-Nan Yan, Bo Li, Tian-Fu Wen, Yong Zeng, Nan-Sheng Cheng, Jing Wang, Department of General Surgery, West China Hospital, Sichuan University, Chengdu 610041, Sichuan Province, China

Yan Luo, Yu-Lan Pen, Department of Ultrasound Diagnosis, West China Hospital, Sichuan University, Chengdu 610041, Sichuan Province, China

Correspondence to: Dr. Ji-Chun Zhao, Department of General Surgery, West China Hospital, Sichuan University, Chengdu 610041, Sichuan Province, China. jichunzhao@hotmail.com

Telephone: +86-28-85422474

Received: 2003-03-19 **Accepted:** 2003-04-24

Abstract

AIM: To investigate the incidence and treatment of hepatic artery complications after orthotopic liver transplantation.

METHODS: From February 1999 to May 2002, orthotopic liver transplantations (OLT) were performed in 72 patients with end-stage liver diseases with an average age of 40.2 ± 13.6 years (ranged from 11 to 68 years), 56 were males and 16 females. The preoperative evaluation for the 72 patients was performed using duplexsonography, abdominal CT scan, and angiography of the hepatic artery. All donor grafts were perfused and preserved in University of Wisconsin solution at 4 °C. OLT was performed with standard techniques with or without a veno-venous bypass. Reconstructions of hepatic artery were performed between the branch patches of gastroduodenal/hepatic or splenic/common hepatic artery confluence of the donors and recipients, and an end-to-end anastomosis between other arterial vessels of the donors and recipients was done. Arterial anastomosis was performed with interrupted 7-0/8-0 monofilament polypropylene suture under 3.5 x loupe magnification. Diagnosis of the complications of hepatic artery after OLT was based on the clinical presentations, ultrasound findings and arterial angiography. All patients were followed up regularly for duplex ultrasound scan after discharge.

RESULTS: The overall incidence of arterial complications in 72 patients after OLTs was 1.4 % (1/72). One 3 cm pseudoaneurysm at the side of anastomotic site of hepatic artery was found by urgent arteriogram due to hemoperitoneum secondary to bile leakage after OLT. Subsequently the pseudoaneurysm was successfully embolized and the blood flow toward the donor liver in hepatic artery remained. The overall postoperative 30-day mortality rate was 8.33 %. The one-year survival rate was 83.72 % in 50 patients with benign diseases and was 71.43 % in 22 patients with malignant diseases following OLT. No death associated with complications of hepatic artery occurred.

CONCLUSION: Careful preoperative evaluations and intraoperative microsurgical technique for hepatic artery reconstructions are the keys in prevention of hepatic artery complications after OLT.

Zhao JC, Lu SC, Yan LN, Li B, Wen TF, Zeng Y, Cheng NS, Wang J, Luo Y, Pen YL. Incidence and treatment of hepatic artery complications after orthotopic liver transplantation. *World J Gastroenterol* 2003; 9(12): 2853-2855

<http://www.wjgnet.com/1007-9327/9/2853.asp>

INTRODUCTION

Vascular complications after orthotopic liver transplantation (OLT) ranges from 2 % to 25 % in most publications^[1,2]. The most frequent complications involve the hepatic artery (2 % to 12 % in adults)^[3-5], in which the hepatic artery thrombosis (HAT) is most common^[6,7]. The complications of hepatic artery are usually associated with technical, hemodynamic, immunological and infectious factors^[2,8,9], which may result in biliary tract complications or sepsis^[10,11], and even a retransplantation may be required^[12,13]. In the present study, we report the incidence and treatment of hepatic artery complications in 72 patients with end-stage liver diseases after OLT from February 1999 to May 2002.

MATERIALS AND METHODS

Patients

From February 1999 to May 2002, OLTs were performed in 72 patients with an average age of 40.2 ± 13.6 years (range 11 to 68 years, and 56 males, 16 females). Indications for OLT included post-inflammatory liver cirrhosis complicated with hepatitis B and liver function failure (34 cases), primary hepatocellular carcinoma (19 cases), end-stage liver hydatid cyst disease complicated with liver function failure (4 cases), Caroli's disease (3 cases), cholestatic liver cirrhosis complicated with hepatolithiasis (2 cases), polycystic liver disease complicated with liver function failure (2 cases), primary sclerosing cholangitis (2 cases), Budd-Chiari syndrome complicated with liver function failure (2 cases), cholangiocarcinoma (2 cases), alcoholic cirrhosis (one case) and secondary hepatic malignancy (gallbladder cancer) (one case).

Methods

The preoperative evaluation for the 72 patients was performed using duplexsonography, abdominal CT scan, and angiography of the hepatic artery. All donor grafts were perfused and preserved in University of Wisconsin solution at 4 °C. OLT was performed with standard techniques and a veno-venous bypass was used in 61 patients, and no veno-venous bypass was used in 5 patients. Retro-hepatic vena cava was resected in 66 patients, and an end-end interposition of donor vena cava together with donor liver was performed. Hepatectomy was performed according to the classical technique with preservation of retrohepatic vena cava (piggy back) in the remaining 6 patients. Reconstruction of the portal vein was performed by an end-to-end veno-venous anastomosis. The reconstruction of hepatic artery was variable and dependent on hepatic artery anatomy of the donors and recipients. Arterial anastomosis was performed between the branch patches of gastroduodenal/hepatic or splenic/common hepatic artery

confluence of the donors and recipients in 22 out of the 72 cases. End-to-end anastomosis was done between the proper hepatic artery of the donors and recipients in 18 out of the 72 cases, and the remaining anastomosis was performed between the proper hepatic artery of the donors and the right hepatic artery or the common hepatic artery of the recipients respectively in 6 and 5 out of the 72 cases. Anastomoses were performed between the proper hepatic artery of the donors and the splenic artery, between the left gastric artery and the left hepatic artery of the recipients in one case each, and between the splenic artery of the donors and the proper hepatic artery, the common hepatic artery or the left hepatic artery of the recipients in 6, 4 and one case respectively, between the common hepatic artery of the donors and the proper hepatic artery or the left hepatic artery of the recipients in 3 and one case respectively, and between the coeliac trunk of the donors and the common hepatic artery of the recipients in 3 cases. Arterial reconstruction was performed by microsurgical techniques with interrupted 7-0/8-0 monofilament polypropylene suture under 3.5 x loupe magnification, interposition grafting with same donor's part of common hepatic conduit was used selectively in one case with end-to-end anastomosis between the proper hepatic arteries of the donors and recipients when anastomotic thrombosis was suspected before closure of the abdominal incision^[14,15]. Diagnosis of complications of hepatic artery after OLTs was based on the clinical presentations, ultrasound findings and arteriography of hepatic artery. The hepatic artery was detected with routine duplex sonography intraoperatively after completion of hepatic artery reconstruction and daily in the first week after OLTs^[16,17]. When the patients had elevated hepatic enzymes, cholestasis, bile leakage and high fever in the absence of acute rejection and drug toxicity, spiral CT scan or angiography of hepatic artery should be considered. No anticoagulable pharmacotherapy to maintain arterial patency was used intraoperatively and postoperatively in this group, but laboratory examination of coagulation state should be done regularly. All the patients received immunosuppressive therapy including cyclosporine or FK506 regimens and were followed up from 3 to 34 months. Hepatic artery of liver transplant patients was detected regularly by duplex ultrasound scan three or six months after discharge.

Statistical methods

The Kaplan-Meier method was used to calculate survival rate, and statistical calculations for mean values and standard deviations were performed using the SPSS software package.

RESULTS

The overall incidence of arterial complications in the 72 patients after OLTs was 1.4 % (1/72) and no HAT and hepatic artery stenosis were found after OLTs. A 3 cm anastomotic pseudoaneurysm of hepatic artery was found in 1 case by urgent arteriogram due to hemoperitoneum secondary to bile leakage about one month after OLT. The pseudoaneurysm at the side of anastomotic site of hepatic artery was successfully embolized, and blood flow toward the donor liver in hepatic artery remained. This patient was fully recovered and discharged one month later when bile leakage was stopped. The patient was doing well 1 year after OLT. The overall postoperative 30-day mortality rate was 8.33 % (6 deaths in 72 patients). The one-year survival rate was 83.72 % in 50 patients with benign diseases and was 71.43 % in 22 patients with malignant diseases after OLTs. No death occurred due to complications of hepatic artery.

DISCUSSION

Vascular reconstructions are critical to a successful outcome

in orthotopic liver transplantation (OLT), complications associated with hepatic artery reconstructions are one of the major causes of graft loss and mortality after OLT. Hepatic artery complications after OLT include HAT, hepatic artery stenosis, hepatic artery pseudoaneurysm (HAP) and hepatic artery fistula. The early complications of hepatic artery were usually caused by technical problems^[11-13]. The late complications of hepatic artery were usually associated with hypercoagulable state, over transfusion of platelets and fresh-frozen plasma during the surgery, severe rejection and bile leakage^[11,18,19]. The hepatic artery is relatively small (3 to 6 mm in diameter in adults) during the vascular reconstructions of OLT with a very fragile intima that requires highly careful atraumatic manipulating technique during the reconstruction of hepatic artery. The anatomical variations^[20-22], diameter and length of hepatic artery, and injury to vessels including prolonged clamping of hepatic artery, kinking of a long artery, and hematoma of artery wall from improper flushing after clamping during operation, and the quality of recipient vessels and mismatch between donor and recipient arterial vessels should be carefully considered and managed preoperatively and intraoperatively^[2,15]. The incidence of arterial complications after OLTs varied between 2 % and 25 % among the liver transplant patients^[2], HAT was most common^[6,7], and caused irreversible graft damage and often required immediate revascularization of hepatic artery, even retransplantation of the liver^[12,13]. HAP occurred in less than 1 % patients after OLT^[23,24]. The incidence of hepatic artery complications was low in this group. The technique of microsurgical hepatic artery reconstruction contributed greatly to the reduction of incidence of HAT and hepatic stenosis^[6,15,25]. Current HAT rate reported after hepatic arterial reconstruction was 1.44 % via the branch patch technique using the hepatic-gastroduodenal bifurcation and interrupted suture of 7/0 monofilament polypropylene suture^[6,20]. We found a single case of hepatic artery pseudoaneurysm whose opening was at the side of anastomotic site of hepatic artery as the complication following OLT and the pseudoaneurysm was embolized successfully. The reported incidence of pseudoaneurysm of hepatic artery was low, but this complication could be devastating with a high mortality rate due to massive bleeding that often required immediate revascularization^[26,27], and even retransplantation^[12,13]. Extrahepatic pseudoaneurysms of hepatic artery were associated with local infection, bile leakage while intrahepatic pseudoaneurysms were caused by liver punctures^[2,5]. The most frequent presentations of hepatic artery pseudoaneurysm were hemorrhages including gastrointestinal hemorrhage, hemoperitoneum and hemobilia^[5,19], which often occurred within the first two months after liver transplantation, and might lead to death due to massive bleeding or loss of the donor graft^[5,28,29]. Although ultrasound and CT scanning were useful in the diagnosis of hepatic artery pseudoaneurysms^[30-32], arteriography was more accurate^[10,33], and might demonstrate clearly an anastomotic pseudoaneurysm of the hepatic artery with bleeding into peritoneum cavity or bile tract^[23,29,33]. The treatment for hepatic artery pseudoaneurysm remains a challenging problem. The current treatment options include ligation or embolization, excision and immediate revascularization of hepatic arterial pseudoaneurysm with or without a donor iliac artery or autogenous saphenous vein, and retransplantation. However, ligation resulted in an extremely high morbidity and mortality^[12,26,34,35], especially at the early stage after liver transplantation. The excision and immediate revascularization of hepatic arterial pseudoaneurysm appeared to be the best choice^[26,27]. At the time of revascularization, bile leakage should be also repaired^[26], and the donor iliac artery or autogenous saphenous vein was often used for arterial revascularization^[34,35]. If an adequate donor

iliac artery or autogenous saphenous vein was not available, an autogenous radial artery could be used^[36]. Embolization therapy of hepatic artery pseudoaneurysm after OLT was seldom reported. In our study, pseudoaneurysm at the side of the anastomotic site of hepatic artery was embolized successfully and the patency of the hepatic artery toward the donor liver remained, which salvaged the donor liver as well as the recipient by the mini-invasive percutaneous endovascular techniques. This case provides a good example of safe and effective approach in the management of pseudoaneurysm of hepatic artery, but more experience is expected.

REFERENCES

- Turroni VS**, Alvira LG, Jimenez M, Lucena JL, Ardaiz J. Incidence and results of arterial complications in liver transplantation: experience in a series of 400 transplants. *Transplant Proc* 2002; **34**: 292-293
- Settmacher U**, Stange B, Haase R, Heise M, Steinmuller T, Bechstein WO, Neuhaus P. Arterial complications after liver transplantation. *Transpl Int* 2000; **13**: 372-378
- Sanchez-Bueno F**, Robles R, Acosta F, Ramirez P, Lujan J, Munitiz V, Rios A, Parrilla P. Hepatic artery complications in a series of 300 orthotopic liver transplants. *Transplant Proc* 2000; **32**: 2669-2670
- Stange B**, Settmacher U, Glanemann M, Nussler NC, Bechstein WO, Neuhaus P. Hepatic artery thrombosis after orthotopic liver transplantation. *Transplant Proc* 2001; **33**: 1408-1409
- Almogy G**, Bloom A, Verstandig A, Eid A. Hepatic artery pseudoaneurysm after liver transplantation. A result of transhepatic biliary drainage for primary sclerosing cholangitis. *Transpl Int* 2002; **15**: 53-55
- Proposito D**, Loinaz Seguro C, Garcia Garcia I, Jimenez C, Gonzalez Pinto I, Gomez Sanz R, De La Cruz J, Moreno Gonzalez E. Assessment of risk factors in the incidence of hepatic artery thrombosis in a consecutive series of 687 liver transplantations. *Ann Ital Chir* 2001; **72**: 187-205
- Abou Ella KA**, Al Sebayel MI, Ramirez CB, Rabea HM. Hepatic artery thrombosis after orthotopic liver transplantation. *Saudi Med J* 2001; **22**: 211-214
- Abou El-Ella K**, Al Sebayel M, Ramirez C, Hussien R. Outcome and risk factors of hepatic artery thrombosis after orthotopic liver transplantation in adults. *Transplant Proc* 2001; **33**: 2712-2713
- Pastacaldi S**, Teixeira R, Montalto P, Rolles K, Burroughs AK. Hepatic artery thrombosis after orthotopic liver transplantation: a review of nonsurgical causes. *Liver Transpl* 2001; **7**: 75-81
- Cavallari A**, Nardo B, Catena F, Montalti R, Cavallari G, Bellusci R, Golfieri R, Rossi C. Mini-invasive treatment of arterial and biliary complications after orthotopic liver transplantation. *Transplant Proc* 2001; **33**: 2001
- Leonardi LS**, Boin IF, Neto FC, de Oliveira GR, Leonardi MI. Biliary reconstructions in 150 orthotopic liver transplantations: an experience with three techniques. *Transplant Proc* 2002; **34**: 1211-1215
- Dudek K**, Nyckowski P, Zieniewicz K, Michalowicz B, Pawlak J, Malkowski P, Krawczyk M. Liver retransplantation: indications and results. *Transplant Proc* 2002; **34**: 638-639
- Bramhall SR**, Minford E, Gunson B, Buckels JA. Liver transplantation in the UK. *World J Gastroenterol* 2001; **7**: 602-611
- Zhao JC**, Lu SC, Huang FG, Yan LN, Li B, Jin LR, Wen TF, Wang J, Luo Y, Peng YL, Yuan ZX. Reconstruction of hepatic artery in orthotopic liver transplantation. *Zhongguo Xiandai Shoushuxue Zazhi* 2001; **5**: 24-26
- Zhao JC**, Huang FG, Lu SC, Yan LN, Li B, Jin LR, Wen TF, Wang J, Luo Y, Peng YL. Reconstructions of hepatic artery in orthotopic liver transplantation. *Zhonghua Qiguan Yizhi Zazhi* 2002; **23**: 37-39
- Lin M**, Crawford M, Fisher J, Hitos K, Verran D. Hepatic artery thrombosis and intraoperative hepatic artery flow rates in adult orthotopic liver transplantation. *ANZ J Surg* 2002; **72**: 798-800
- De Candia A**, Como G, Tedeschi L, Zanardi R, Vergendo M, Rositani P, Bazzocchi M. Color doppler sonography of hepatic artery reconstruction in liver transplantation. *J Clin Ultrasound* 2002; **30**: 12-17
- Bhattacharjya S**, Gunson BK, Mirza DF, Mayer DA, Buckels JA, McMaster P, Neuberger JM. Delayed hepatic artery thrombosis in adult orthotopic liver transplantation—a 12-year experience. *Transplantation* 2001; **71**: 1592-1596
- Hidalgo E**, Cantarell C, Charco R, Murio E, Lazaro JL, Bilbao I, Margarit C. Risk factors for late hepatic artery thrombosis in adult liver transplantation. *Transplant Proc* 1999; **31**: 2416-2417
- Proposito D**, Loinaz Seguro C, Garcia Garcia I, Jimenez C, Gonzales Pinto I, Gomez Sanz R, Moreno Gonzalez E. Role of anatomic variations and methods of hepatic artery reconstruction in the incidence of thrombosis following liver transplantation. *Ann Ital Chir* 2001; **72**: 303-314
- Gruttadauria S**, Foglieni CS, Doria C, Luca A, Lauro A, Marino IR. The hepatic artery in liver transplantation and surgery: vascular anomalies in 701 cases. *Clin Transplant* 2001; **15**: 359-363
- Jones RM, Hardy KJ**. The hepatic artery: a reminder of surgical anatomy. *J R Coll Surg Edinb* 2001; **46**: 168-170
- Marshall MM**, Mulesan P, Srinivasan P, Kane PA, Rela M, Heaton ND, Karani JB, Sidhu PS. Hepatic artery pseudoaneurysms following liver transplantation: incidence, presenting features and management. *Clin Radiol* 2001; **56**: 579-587
- Stange B**, Settmacher U, Glanemann M, Nuessler NC, Bechstein WO, Neuhaus P. Aneurysms of the hepatic artery after liver transplantation. *Transplant Proc* 2000; **32**: 533-534
- Egawa H**, Asonuma K, Sakamoto Y, Iwasaki M, Kim I, Tanaka K. Surgical techniques for vascular reconstruction of the portal vein and hepatic artery in living-donor liver transplantation. *Nippon Geka Gakkai Zasshi* 2001; **102**: 798-804
- Bonham CA**, Kapur S, Geller D, Fung JJ, Pinna A. Excision and immediate revascularization for hepatic artery pseudoaneurysm following liver transplantation. *Transplant Proc* 1999; **31**: 443
- Sellers MT**, Haustein SV, McGuire BM, Jones C, Bynon JS, Diethelm AG, Eckhoff DE. Use of preserved vascular homografts in liver transplantation: hepatic artery aneurysms and other complications. *Am J Transplant* 2002; **2**: 471-475
- Busenius-Kammerer M**, Ott R, Wutke R, Grunewald M, Hohenberger W, Reck T. Pseudoaneurysm of the hepatic artery—a rare complication after orthotopic liver transplantation. *Chirurg* 2001; **72**: 78-81
- Glehen O**, Feugier P, Ducerf C, Chevalier JM, Baulieux J. Hepatic artery aneurysms. *Ann Chir* 2001; **126**: 26-33
- Garcia-Criado A**, Gilabert R, Nicolau C, Real I, Arguis P, Bianchi L, Vilana R, Salmeron JM, Garcia-Valdecasas JC, Bru C. Early detection of hepatic artery thrombosis after liver transplantation by Doppler ultrasonography: prognostic implications. *J Ultrasound Med* 2001; **20**: 51-58
- Quiroga S**, Sebastia MC, Margarit C, Castells L, Boye R, Alvarez-Castells A. Complications of orthotopic liver transplantation: spectrum of findings with helical CT. *Radiographics* 2001; **21**: 1085-1102
- Katyal S**, Oliver JH 3rd, Buck DG, Federle MP. Detection of vascular complications after liver transplantation: early experience in multislice CT angiography with volume rendering. *Am J Roentgenol* 2000; **175**: 1735-1739
- Cavallari A**, Vivarelli M, Bellusci R, Jovine E, Mazziotti A, Rossi C. Treatment of vascular complications following liver transplantation: multidisciplinary approach. *Hepatogastroenterology* 2001; **48**: 179-183
- Zamboni F**, Franchello A, Ricchiuti A, Fop F, Rizzetto M, Salizzoni M. Use of arterial conduit as an alternative technique in arterial revascularization during orthotopic liver transplantation. *Dig Liver Dis* 2002; **34**: 122-126
- Meyer C**, Riehm S, Perrot F, Cag M, Nizand G, Audet M, Veillon F, Jaeck D, Wolf P. Donor iliac artery used for arterial reconstruction in liver transplantation. *Transplant Proc* 2000; **32**: 2791
- Rogers J**, Chavin KD, Kratz JM, Mohamed HK, Lin A, Baillie GM, Shafizadeh SF, Baliga PK. Use of autologous radial artery for revascularization of hepatic artery thrombosis after orthotopic liver transplantation: case report and review of indications and options for urgent hepatic artery reconstruction. *Liver Transpl* 2001; **7**: 913-917

Management of choledocholithiasis: Comparison between laparoscopic common bile duct exploration and intraoperative endoscopic sphincterotomy

Qi Wei, Jian-Guo Wang, Li-Bo Li, Jun-Da Li

Qi Wei, Li-Bo Li, Jun-Da Li, Department of General Surgery, Sir Run Run Shaw Hospital, Zhejiang University, Hangzhou 310016, Zhejiang Province, China

Jian-Guo Wang, Department of Gastroenterology, Sir Run Run Shaw Hospital, Zhejiang University, Hangzhou 310016, Zhejiang Province, China

Correspondence to: Qi Wei, Department of General Surgery, Sir Run Run Shaw Hospital, Zhejiang University, Hangzhou 310016, Zhejiang Province, China. weiqi@hzcn.com

Telephone: +86-571-86437761

Received: 2003-06-21 **Accepted:** 2003-07-24

Abstract

AIM: Choledocholithiasis is present in 5 to 10 percent of patients who have cholelithiasis. In the area of laparoscopic cholecystectomy (LC), laparoscopic common bile duct exploration (LCBDE) and intraoperative endoscopic sphincterotomy (IOES) have been used to treat choledocholithiasis. The purpose of this study was to compare the clinical outcomes and hospital costs of LCBDE with IOES.

METHODS: Between November 1999 and October 2002, patients with choledocholithiasis undergoing LC plus LCBDE (Group A, $n=45$) were retrospectively compared to those undergoing LC plus IOES (Group B, $n=57$) at a single institution.

RESULTS: Ductal stone clearance rates were equivalent for the two groups (88 % versus 89 %, $P=0.436$). The conversion rate was higher for Group B (8.8 % versus 4.4 %, $P=0.381$), as was the morbidity (12.3 % versus 6.7 %, $P=0.336$). There were no other significant differences between the two groups. The complications were mainly related to endoscopic sphincterotomy (ES), and the hospital costs were significantly increased in this subset of Group B (median, 23 910 versus 14 955 RMB yuan, $P=0.03$). Although hospital stay was longer in Group A (median, 7 versus 6 days, $P=0.041$), the patients in Group A had a significantly decreased cost of hospitalization compared with those in Group B (median, 11 362 versus 15 466 RMB yuan, $P=0.000$).

CONCLUSION: The results demonstrate equivalent ductal stone clearance rates for the two groups. LCBDE management appears safer, and is associated with a significantly decreased hospital cost. The findings suggest LCBDE for choledocholithiasis is a better option.

Wei Q, Wang JG, Li LB, Li JD. Management of choledocholithiasis: Comparison between laparoscopic common bile duct exploration and intraoperative endoscopic sphincterotomy. *World J Gastroenterol* 2003; 9(12): 2856-2858

<http://www.wjgnet.com/1007-9327/9/2856.asp>

INTRODUCTION

Laparoscopic cholecystectomy (LC) has become the standard

method for cholecystectomy, but the same cannot be said of the management of choledocholithiasis. There is still no standard algorithm. Laparoscopic common bile duct exploration (LCBDE) and intraoperative endoscopic sphincterotomy (IOES) have been used to treat choledocholithiasis for many years in clinical practice^[1-6]. The purpose of this study was to determine the most cost-effective approach for patients with choledocholithiasis.

MATERIALS AND METHODS

Between November 1999 and October 2002, patients with choledocholithiasis undergoing LC plus LCBDE (Group A, $n=45$) were retrospectively compared to those undergoing LC plus IOES (Group B, $n=57$) at a single institution.

The clinical demographic details and the pretreatment biochemical findings are shown in Table 1. There were no significant differences between the groups. Preoperative investigations included liver function tests and external ultrasound examination of the gallbladder and bile duct. Four patients in Group A underwent preoperative ERCP. Endoscopic sphincterotomy (ES) was unsuccessful in three patients, and another ERCP was performed but no stones were found. Five patients in Group B underwent preoperative ERCP. ES was not performed in two patients. The three other patients underwent ERCP but no stones were found.

Table 1 Clinical and demographic details in patients of groups A and B

	Group A	Group B
Total no.	45	57
Age range (yr)	29-79	18-75
Male patients	17	20
Female patients	28	37
Abnormal LFTa	40	38
Jaundice	18	19
Acute cholecystitis	19	12
Pancreatitis	11	6
Preoperative ERCP	4	5

a: Liver function test.

Laparoscopic ductal stone clearance was performed either by the transcystic duct route ($n=10$) or by direct CBDE with placement of T-tube ($n=35$). Intraoperative cholangiography (IOC) was done in all patients. Complete clearance of the ductal stones was determined by the end of IOC. The necessity to convert to a different technique or the presence of an unexpected retained stone was considered as a failure. LCBDE was performed at the same institution by experienced surgeons. Two experienced gastroenterologists performed IOES^[5,6]. The exact technique was left up to the individual physician.

All hospital cost data were obtained from the hospital admission department. The cost of complications the patients

incurred was included in the cost data. If LCBDE or IOES failed and the patient required postoperative ES or chledochoscopy through the sinus tract, the cost of that intervention was included. The cost of additional anesthesia or IOC was also included.

Data and statistical analysis

Statistical analysis was performed using chi square test with a likelihood ratio and Mann-Whitney test for nonparametric data. Significance was set at the 5 % level.

RESULTS

Outcome of Group A (LCBDE)

Ductal stone clearance was successful in 40 out of 45 patients (88 %). There were two cases of conversions to open surgery (4.4 %)(Table 2). One patient had large impact stones, the other had multiple stones. Two patients (4.4 %) had unexpected retained stones, one requiring ES at readmission, the other choledochoscopy through the sinus tract.

Postoperative complications occurred in 3 patients (6.7 %) (Table 3). Two patients had infection around the T-tube, and the other had bile leak after the T-tube was removed.

The cost ranged from 6 979 to 23 813 RMB yuan with a median 11 362 RMB yuan (Table 2). Of the 42 patients having uncomplicated hospital stays, the median cost was 11210 RMB yuan compared with a cost of 15121 RMB yuan for the three patients with complications (Table 4). The hospital stay ranged from four to eighteen days with a median stay of seven days. The median postoperative stay was four days (range, 2-14) (Table 2).

Outcome of Group B (IOES)

Ductal stone clearance was successful in 51 out of 57 patients (89 %). There were five cases of conversions to open surgery (8.8 %) (Table 2). One had a microperforation of the duodenum, one had bleeding at the sphincterotomy, and the other three patients had unsuccessful ES. One patient (1.8 %) had an unrecognized retained stone and required ES at a second admission.

Seven cases had complications (12.3 %)(Table 3). Three patients developed pancreatitis, two of them had severe pancreatitis, and the other required open surgery for an abdominal abscess that resulted in a 51-day hospital stay

with a cost of 133 239 RMB yuan. Two patients developed postoperative pneumonia.

The cost ranged from 8 823 to 133 239 RMB yuan with a median of 15 466 RMB yuan (Table 2). Of the 50 patients having uncomplicated hospital stays, the median cost was 14 955 RMB yuan compared with a cost of 23910 RMB yuan for the seven patients with complications (Table 4). The hospital stay ranged from 2 to 51 days with a median stay of six days. The median postoperative stay was three days (range, 1-51)(Table 2).

Table 3 Morbidity of two groups

	Group B	Group A
Patient no(%)	7 (12.3)	3 (6.7)
Bleeding	1	
Microperforation	1	
Pancreatitis	3	
Pneumonia	2	
Infection with t-tube		2
Bile leak		1

Comparison of clinical outcome and hospital costs of two groups

Statistical analysis and comparison between Groups A (LCBDE) and B (IOES) are presented in Table 2.

The ductal stone clearance rates were equivalent in the two groups (88 % versus 89 %, $P=0.436$). The conversion rate was higher in Group B (8.8 % versus 4.4 %, $P=0.381$), as was the morbidity (12.3 % versus 6.7 %, $P=0.336$). The operating time was shorter in Group B (median, 155 min versus 180 min, $P=0.661$). But there were no significant differences between the two groups. Although the hospital stay was longer in Group A (median, 7 versus 6 days, $P=0.041$), the patients in Group A had a significantly decreased cost of hospitalization compared with those in Group B (median, 11 362 versus 15 466 RMB yuan, $P=0.000$), and the hospital costs significantly increased in complicated Group B (Table 4).

DISCUSSION

The presence of common bile duct stones (CBDS) significantly increases the morbidity, mortality, and cost of patients with gallstones. The potential complications of choledocholithiasis,

Table 2 Comparison of clinical outcome and cost between groups A and B

	Group A	Group B	$\chi^2(Z)$	P value
Ductal stone clearance (%)	88	89	0.607	0.436 ^b
Conversion to open surgery (%)	4.4	8.8	0.767	0.381 ^b
Morbidity (%)	6.7	12.3	0.927	0.336 ^b
Operative time(min)	180,130-220 ^a	155,130-210 ^a	(-0.439)	0.661 ^c
Hospital stay(days)	7,6-9 ^a	6,4.5-8 ^a	(-2.046)	0.041 ^c
Postoperative stay(days)	4,3-6 ^a	3,2-5 ^a	(-2.259)	0.024 ^c
Cost (RMB)	11362,10196-14822 ^a	15466,13555-17689 ^a	(-4.822)	0.000 ^c

a: Median, 25-75 % quartile range; b: Chi square test with a likelihood ratio; c: Mann-Whitney test.

Table 4 Comparison of cost with or without complication between two groups

	Without complication cost (RMB)	n	With complication cost (RMB)	n	P value
Group A	11210,10119-14380 ^a	42	15121,11706-19895 ^a	3	0.08 ^b
Group B	14955,12650-16793 ^a	50	23910,20746-111289 ^a	7	0.03 ^b
P value		0.000 ^b		0.000 ^b	

a: Median, 25-75 % quartile range; b: Mann-Whitney test.

cholangitis, and pancreatitis could be life-threatening^[7,8]. The safest and most cost-effective approach for patients with CBDS could decrease suffering and disability and save millions of health care us dollars each year^[9,10].

ES was first described in 1974. Today, ES for choledocholithiasis remains the most difficult and dangerous procedure routinely performed by endoscopists. The application of ES to CBDS was advocated for patients with cholangitis, acute biliary pancreatitis, and for elderly high-risk patients^[11]. Gong *et al* from China reported a ductal stone clearance rate of 91.7 % and a complication rate of 8.8 %^[12]. In our experience, the ductal stone clearance rate was 89 %, the morbidity was 12.3 %. Although IOES was performed by experienced gastroenterologists, it still resulted in procedure-related complications that could be life-threatening^[13-16]. The cost was significantly increased in complicated Group B (IOES) (median, 23 910 versus 14 955 RMB yuan, $P=0.03$)(Table 4), and the hospital stay was much longer.

Successful LCBDE has been reported in several large series in 57 to 98 percent of cases^[17]. Our experience compared favorably with these results. LCBDE was used in our recent management of choledocholithiasis for the vast majority of patients, whereas early IOES was more commonly performed in the past two years. The clearance rate in Group A (LCBDE) was 88 %, and the complication rate was 6.7 %. With the experience and new instrumentation, the limiting factor in successful LCBDE was not the CBD access but the CBD pathologic alterations such as large impact stones or multiple stones^[17].

On the other hand, Group A was associated with a significantly decreased cost of hospitalization compared with Group B (median, 11 362 versus 15 466 RMB yuan, $P=0.000$)(Table 2). The total hospital cost of Group B included two parts, and was higher even for uncomplicated patients (median, 14 955 versus 11 210 RMB yuan, $P=0.000$). The cost of complicated patients was significantly increased (Table 4). Therefore, a thorough evaluation and consideration of management options would reduce the risk of complications and the cost of CBDS management.

Although the hospital stay was longer in Group A (LCBDE), it was mainly related to postoperative stay (median, 4 versus 3 days, $P=0.024$) with placement of T-tube. Therefore, primary closure of CBD without T-tube would be more cost-effective.

The operation time was shorter in Group B (IOES) (median, 155 min versus 180 min, $P=0.661$). In most situations, we had to wait for gastroenterologists, and the waiting time was not included in the operation time. The actual procedure time was delayed, which partially contributed to an increased hospital cost^[18].

The results demonstrate that the ductal stone clearance rate was equivalent in the two groups. The conversion rate and morbidity were higher in Group B (IOES), and mainly related to ES. The hospital cost was significantly increased in complicated Group B patients. LCBDE management appears safer, and has no life-threatening complications, and can significantly decrease the hospital cost. The findings suggest LCBDE for CBDS is a better option.

ACKNOWLEDGMENTS

We thank Dr. C. Welch for editorial assistance and helpful suggestions.

REFERENCES

- 1 **Paganini AM**, Feliciotti F, Guerrieri M, Tamburini A, De Sanctis A, Campagnacci R, Lezoche E. Laparoscopic common bile duct exploration. *J Laparoendosc Adv Surg Tech A* 2001; **11**: 391-400
- 2 **Lilly MC**, Arregui ME. A balanced approach to choledocholithiasis. *Surg Endosc* 2001; **15**: 467-472
- 3 **Moroni J**, Haurie JP, Juddhak I, Fuster S. Single-stage laparoscopic and endoscopic treatment for choledocholithiasis: A novel approach. *J Laparoendosc Adv Surg Tech A* 1999; **9**: 69-74
- 4 **Sgourakis G**, Karaliotas K. Laparoscopic common bile duct exploration and cholecystectomy versus endoscopic stone extraction and laparoscopic cholecystectomy for choledocholithiasis. A prospective randomized study. *Minerva Chir* 2002; **57**: 467-474
- 5 **Wang YD**, Gao M, Zhang QY, Wang JG, yuan XM, Cai XJ, Wang XF. Single-stage laparoscopic cholecystectomy and endoscopic sphincterotomy for management of patients with cholecystocholedocholithiasis. *Zhonghua Putong Waikē Zazhi* 2000; **15**: 108-109
- 6 **Hong DF**, Gao M, Bryner U, Cai XJ, Mou YP. Intraoperative endoscopic sphincterotomy for common bile duct stones during laparoscopic cholecystectomy. *World J Gastroenterol* 2000; **6**: 448-450
- 7 **Zhang WZ**, Chen YS, Wang JW, Chen XR. Early diagnosis and treatment of severe acute cholangitis. *World J Gastroenterol* 2002; **8**: 150-152
- 8 **Kohut M**, Nowak A, Nowakowska-Duiawa E, Marek T. Presence and density of common bile duct microlithiasis in acute biliary pancreatitis. *World J Gastroenterol* 2002; **8**: 558-561
- 9 **Liberman MA**, Phillips EH, Carroll BJ, Fallas MJ, Rosenthal R, Hiatt J. Cost-effective management of complicated choledocholithiasis: laparoscopic transcystic duct exploration or endoscopic sphincterotomy. *J Am Coll Surg* 1996; **182**: 488-494
- 10 **Urbach DR**, Khajanchee YS, Jobe BA, Standage BA, Hansen PD, Swanstrom LL. Cost-effective management of common bile duct stones: a decision analysis of the use of endoscopic retrograde cholangiopancreatography (ERCP), intraoperative cholangiography, and laparoscopic bile duct exploration. *Surg Endosc* 2001; **15**: 4-13
- 11 **Cuschieri A**, Lezoche E, Morino M, Croce E, Lacy A, Tooouli J, Faggioni A, Ribeiro VM, Jakimowicz J, Visa J, Hanna GB. E.A.E. S. multicenter prospective randomized trial comparing two-stage vs single-stage management of patients with gallstone disease and ductal calculi. *Surg Endosc* 1999; **13**: 952-957
- 12 **Gong JP**, Zhou YB, Han BL, Li ZH. Endoscopic sphincterotomy in treatment of secondary common bile duct stones. *Shijie Huaren Xiaohua Zazhi* 1999; **7**: 320-322
- 13 **He GH**, Cai Y, Qian XY, Feng GH, Ying RC, Xu Q, Jia PH. Surgical management of the complications after endoscopic sphincterotomy. *Zhonghua Putong Waikē Zazhi* 2002; **17**: 469-470
- 14 **Freeman ML**, DiSario JA, Nelson DB, Fennerty MB, Lee JG, Bjorkman DJ, Overby CS, Aas J, Ryan ME, Bochna GS, Shaw MJ, Snady HW, Erickson RV, Moore JP, Roel JP. Risk factors for post-ERCP pancreatitis: a prospective, multicenter study. *Gastrointest Endosc* 2001; **54**: 425-434
- 15 **Vandervoort J**, Soetikno RM, Tham TC, Wong RC, Ferrari AP Jr, Montes H, Roston AD, Slivka A, Lichtenstein DR, Ruymann FW, Van Dam J, Hughes M, Carr-Locke DL. Risk factors for complications after performance of ERCP. *Gastrointest Endosc* 2002; **56**: 652-656
- 16 **Masci E**, Toti G, Mariani A, Curioni S, Lomazzi A, Dinelli M, Minoli G, Crosta C, Comin U, Fertitta A, Prada A, Passoni GR, Testoni PA. Complications of diagnostic and therapeutic ERCP: a prospective multicenter study. *Am J Gastroenterol* 2001; **96**: 417-423
- 17 **Heili MJ**, Wintz NK, Fowler DL. Choledocholithiasis: endoscopic versus laparoscopic management. *Am Surg* 1999; **65**: 135-138
- 18 **Wright BE**, Freeman ML, Cumming JK, Quickel RR, Mandal AK. Current management of common bile duct stones: is there a role for laparoscopic cholecystectomy and intraoperative endoscopic retrograde cholangiopancreatography as a single-stage procedure? *Surgery* 2002; **132**: 729-735

Edited by Zhang JZ and Wang XL

Influence of liver nonparenchymal cell infusion combined with cyclosporin A on rejection of rat small bowel transplantation

Yan-Ling Yang, Ji-Peng Li, Ke-Feng Dou, Kai-Zong Li

Yan-Ling Yang, Ji-Peng Li, Ke-Feng Dou, Kai-Zong Li,
Department of Hepatobiliary Surgery, Xijing Hospital, Fourth Military Medical University, Xi'an 710032, Shaanxi Province, China
Supported by the National Natural Science Foundation of China, No. 30070741

Correspondence to: Kai-Zong Li, Department of Hepatobiliary Surgery, Xijing Hospital, Fourth Military Medical University, Xi'an 710032, Shaanxi Province, China. gdwk@fmmu.edu.cn
Telephone: +86-29-3375259 **Fax:** +86-29-3375561
Received: 2003-06-06 **Accepted:** 2003-07-24

Abstract

AIM: To investigate the effect of liver nonparenchymal cell infusion combined with cyclosporin A (CsA) on rejection of heterostrain rat small bowel transplantation.

METHODS: The liver nonparenchymal cell suspension was prepared by density gradient centrifugation method with Percoll centrifugal solution. Heterotopic small bowel transplantation was performed. Then the rats were divided into four groups. Group one: homogenic transplantation (F344/N→F344/N), group two: allotransplantation (F344/N→Wistar), group three: allotransplantation (F344/N→Wistar) + CsA, with CsA 10 mg·kg⁻¹·d⁻¹ after transplantation, group four: allotransplantation + CsA (F344/N→Wistar) + liver nonparenchymal cell infusion + CsA (F344/N→Wistar), in which recipient Wistar rats had been injected with 2×10⁸ F344/N liver nonparenchymal cells 20 days before transplantation, and treated with CsA after transplantation. Finally, the survival time after small bowel transplantation, gross and histopathological examination, and IL-2 levels in serum were observed.

RESULTS: The survival time after small bowel transplantation was 7.14±0.33 d, 16.32±0.41 d and 31.41±0.74 d in group 2, 3, and 4, respectively. The survival time was significant longer (*P*<0.01) in group 4. The gross and histopathological examination showed that the rejection degree in group 4 was lower than those in groups 2 and 3. Serum IL-2 level in group 4 was also lower than those in groups 2 and 3 (*P*<0.01).

CONCLUSION: Liver nonparenchymal cell infusion combined with CsA can prolong the survival time of rat small bowel transplantation, and the anti-rejection effect is good.

Yang YL, Li JP, Dou KF, Li KZ. Influence of liver nonparenchymal cell infusion combined with cyclosporin A on rejection of rat small bowel transplantation. *World J Gastroenterol* 2003; 9 (12): 2859-2862

<http://www.wjgnet.com/1007-9327/9/2859.asp>

INTRODUCTION

In clinical practice, rejection responses induced by organ transplants necessitate the use of potent immunosuppressive drugs. It should be noted, however, that excessive dosage of

immunosuppressive agents may result in severe side effects such as hypertension and hepatic and/or renal toxicity. Moreover, prolonged usage of immunosuppressants often leads to severe infection and increased susceptibility to malignant tumors, thus critically affecting the health of recipients^[1-5]. It is therefore imperative to assess, as an alternative to immunosuppressants, the protective effect of induced immune tolerance on organ transplantation. The ideal strategy is to induce a immune tolerance state or a low reactive state toward donors' grafts in the recipients, while preserving normal immunological functions for the recognition of tumor antigens and prevention of infection. Thus immunosuppressive agents can be avoided or used at a dramatically reduced dosage. The key steps toward a successful transplantation therefore include either attenuated immune reactions or induced immune tolerance to grafts^[6-10].

Small bowel transplantation is an ideal method to treat short bowel syndrome and other end stage small bowel dysfunctions, and thus can free the patients from total parenteral nutrition, returning to normal life pattern^[11,12]. But because of the rich lymphatic tissue in small bowel and its mesentery, the mesenteric lymph nodes and lymphatic plexus are transplanted along with small bowel transplantation. So small bowel transplantation has more severe immune rejection compared with other organ transplantation, which is the main cause leading to failure of small bowel transplantation^[13-16]. The liver is an immunologically privileged organ, and after liver transplantation, the incidence rate and degree of rejection are much lower than other solid organ transplantations. Liver transplantation can also induce tolerance in recipients to organs, such as the heart, kidneys, skin, etc, which are susceptible to be rejected^[17-19]. Both in experimental study and in clinical practice of recent years, liver nonparenchymal cells (including lymphocytes, dendritic cells, Kupffer cells, etc) play an important role in immune tolerance induction^[20-22]. In the present study, we took the advantage of liver nonparenchymal cell infusion combined with cyclosporin A (CsA) on rat small bowel transplantation. Some parameters were tested in order to confirm the anti-rejection effect of liver nonparenchymal cell infusion combined with CsA.

MATERIALS AND METHODS

Animals

Male FK344/N rats weighing 230-260 g as donors and male Wistar rats weighing 200-240 g as recipients were obtained from the Laboratory Animal Center of Beijing Medical University, and fed with standard rat chow.

Preparation of rat liver nonparenchymal cells from donor liver

Rats were anaesthetized with intraperitoneal pentobarbital and the abdomens were shaved and cleansed with betadine solution. The peritoneal cavity was widely exposed, with the inferior vena cava cannulated, the portal vein divided, and the suprahepatic vena cava ligated. The liver was perfused at a rate of 3-4 ml/min at 37 °C *in situ* with a Hank's calcium-free solution for 5 min followed by perfusion with a 0.05 % collagenase (Sigma, type V) solution for 15 min. Hepatic

attachments were divided and the liver was transferred to a Petri dish, where the liver substance was gently minced and filtered (100 μ m) to remove large aggregates, followed by incubation for 45 min in 50 ml of Hank's containing 0.05 % collagenase at 37 °C with continuous stirring. 0.5 mg DNAase in 1.0 ml of PBS was added 20 and 40 min after this incubation period. The cell suspension was filtered (40 μ m) and nonparenchymal cells were separated by discontinuous density gradients of Percoll (Pharmacia Biotech) at 1.044 g/ml and 1.07 g/ml. The final cell suspension was prepared in PBS/15 % FCS at a concentration of 5×10^8 /ml. Cell viability counting (usually greater than 95 %) was done using trypan blue exclusion test, the cell suspension was used for infusion within 4 hours of preparation^[23,24].

Rat small bowel transplantation

Donor rats were fasted for 24 hours. All procedures were performed under inhalation anesthesia with ether. The entire small bowel from the ligament of Treitz to the ileocecal valve was isolated with the superior mesenteric artery on a segment of aorta and portal vein. After donor systemic heparinization (300 U), the graft was perfused with 20 ml of cold lactated Ringer's solution via the aorta. The lumen was also washed in 20 ml of the same solution. In the recipient, end-to-side vascular anastomoses were performed between the graft aorta and recipient infrarenal aorta and between the graft portal vein and recipient inferior vena cava with 10-0 sutures using the standard microsurgical technique. Superior extremity of transplanted small bowel was ligated and distal small bowel stoma was performed on left abdominal wall. Animals that died within 3 days were considered as technical failures and excluded from data collection^[25-28].

Experimental groups and postoperative care

The rats were divided into the following four groups. Group 1: homogenic transplantation group (F344/N→F344/N), Group 2: allotransplantation group (F344/N→Wistar), Group 3: allotransplantation group +CsA group (F344/N→Wistar), in which recipient rats received CsA 10 mg·kg⁻¹·d⁻¹ after transplantation, Group 4: allotransplantation +CsA+nonparenchymal cells infusion group (F344/N→Wistar), in which nonparenchymal cell infusion was performed 20 days prior to transplantation, and CsA applied after transplantation. Animals were fasted with access to water on the day of surgery, fed with only sugar water (7 g/day) on day 1, and rat chow and water on day 2 and thereafter. The rats' psyche status, appetite and ejection liquid of small bowel stoma were observed.

Graft histology

Rats' small bowel allografts were excised from stoma or by laparotomy and fixed in 10 % formalin. The fixed tissue was paraffin embedded, and tissue sections were stained with hematoxylin and eosin (H-E). Rejection was evaluated according to the following scoring system: grade 0, intact mucosa with complete villi; grade 1, mucosa with shortened villi and initial cellular infiltration; grade 2, mucosa with incomplete and damaged villi or complete loss of villi, usually with cryptitis and lymphocyte infiltration; grade 3, no mucosa with extensive necrosis and fibrosis^[29-31].

Detection of interleukin-2 (IL-2)

The serum samples were collected on days 3, 5, and 7 after transplantation. Serum concentration of IL-2 was measured with ELISA kits (Beijing East Asia Immunological Technique Institute).

Graft survival

All recipients were followed by visual inspection, and

submitted to autopsy as soon as they died. Graft survival time was defined as death of recipient due to acute rejection.

Statistics

All the data were analyzed by Student's *t* test and expressed as mean \pm SD. The statistical difference $P < 0.05$ was considered significant and $P < 0.01$ as very significant.

RESULTS

Gross observation

The rats awaked soon after operation, then reactivated. In homogenic transplantation group (group 1), the psyche of rats was good with normal diet and activity. Mucosa of abdominal wall stoma was ruddy, and secretion was mucous. Exploratory laparotomy showed that intestinal graft was rubicund, mesentery blood vessel pulsated obviously, and the intestinal adhesion was seldom. In allotransplantation group (Group 2), the rats presented various degrees of lethargy, anorexia hair disorder, unresponsive to outside stimulation and body weight loss, until died. Exploratory laparotomy showed that intestinal graft was hoar, intestinal luminal amplified with massive adhesion and gradually aggravated, accompanying mass purulent discharge, intestinal perforation occurred in some severe cases. In allotransplantation +CsA group (Group 3), the rats were vigorous, sensitive to outside stimulation, and low-grade adhesion occurred 7 days after transplantation. In allotransplantation +CsA+ nonparenchymal cell infusion group (Group 4), the manifestations were similar to those in Group 1.

Histopathologic examination

In group 1, the rats represented rejection of grade 0, with no rejection pathological finding but a few of lymphocytic infiltration in stroma. In group 2, rejection of grade 1 was found 3 days after transplantation, rejection of grade 2 was found 5 days after transplantation, and rejection of grade 3 was found 7 days after transplantation. In group 3, rejection of grade 1 was found 5 or 7 days after transplantation. In group 4, histopathologic examination showed similar results as in group 1.

Detection of IL-2

Expression level of IL-2 was low in group 1, and increased in group 2 on days 5 and 7 after transplantation. IL-2 level in group 3 was mildly increased, but was lower than that in group 2 on days 3, 5 and 7 after transplantation. IL-2 level in group 4 was significantly lower than those in group 2 and group 3 ($P < 0.01$), and was slightly increased on days 5 and 7 after transplantation.

Table 1 IL-2 level after small bowel transplantation in rats ($\bar{x} \pm s$, ng/ml)

Group	IL-2 level		
	3 d	5 d	7 d
Group 1	1.46 \pm 0.02	1.73 \pm 0.01	1.61 \pm 0.05
Group 2	2.44 \pm 0.07	5.15 \pm 0.31	5.83 \pm 0.52
Group 3	1.72 \pm 0.11	2.17 \pm 0.09	2.43 \pm 0.06
Group 4 ^b	1.62 \pm 0.08	1.81 \pm 0.05	2.06 \pm 0.13

^b $P < 0.01$ vs group 2 and group 3

Survival time after transplantation

The survival time after small bowel transplantation was 7.14 \pm 0.33 d in group 2, 16.32 \pm 0.41 d in group 3, 31.41 \pm 0.74 d in group 4 which was significantly longer than that in other groups ($P < 0.01$).

DISCUSSION

Small bowel transplantation is the ultimate therapy for patients with short-bowel syndrome or end stage intestinal function failure. But the small bowel is the maximal immunological organ in human body, the mesenteric lymph nodes and lymphatic plexus are transplanted along with the small bowel transplantation, thus the rejection of small bowel transplantation is much more fiercer than that of other organ transplantations. The failure of small bowel transplantation was more often due to severe rejection^[32-34]. So rejection induced by small bowel transplantation necessitates the use of large potent immunosuppressive drugs. It should be noted, however, that excess dosage of immunosuppressive agents may result in severe side effects such as hypertension and hepatic and/or renal toxicity. Moreover, prolonged usage of immunosuppressants often leads to severe infection and increased susceptibility to malignancy, thus critically affecting the health of recipients. The ideal strategy is to induce a low responsiveness or irresponsiveness in recipients toward grafts from donors, while preserving normal immunological functions for the recognition of tumor antigens and prevention of infection. Thus immunosuppressive agents can be avoided or used at a dramatically reduced dosage. The key steps toward successful transplantation therefore should include either attenuated immune reactions or induced immune tolerance to grafts^[35-38].

The liver is an immunologically privileged organ, the rejection incidence rate and degree of liver transplantation are much lower than other solid organs. Liver transplantation can also induce tolerance of other organ transplantations, such as the heart, kidneys, skin, *etc.* Experimental and clinical researches also showed that liver combined with small bowel transplantation could alleviate the rejection of small bowel transplantation. Investigations in recent years showed that liver nonparenchymal cells (including lymphocytes, dendritic cells, Kupffer cells, *etc.*) played an important role in inducing tolerance. Donor rat's intrahepatic leucocytes were eliminated by rays before transplantation, acute rejection would happen after liver transplantation, and the recipients' survival time was shortened. Yet after intrahepatic leucocyte infusion to recipients with rays treated donor liver, the recipients' survival time was obviously prolonged^[39-41]. So in our experiment, liver nonparenchymal cell transfusion combined with ciclosporin A was used to suppress the rejection of rat small bowel transplantation. It was observed that the rejection was effectively suppressed, indicating the feasibility of tolerance induction by this method. Compared with small bowel associated with liver transplantation, the method of donor liver nonparenchymal cell transfusion has the advantage of less demanding on manipulation and technique requirements. Its postoperative complications are relative less, yet the suppressive effect on rejection of small bowel transplantation is good. So the donor liver nonparenchymal cell transfusion is a simple and practical method, which has the prospect of becoming a new way to suppress rejection of small bowel transplantation in clinical practice. Further work is needed to reveal if chimerism is induced by liver nonparenchymal cells transfusion, and its possible influence on the immune system of graft recipients such as graft versus host reaction.

REFERENCES

- 1 **Yoo SJ**, Kahan BD. Combination treatment with sirolimus and ciclosporin in clinical renal transplantation: A comprehensive review. *Drugs Today* 2001; **37**: 385-400
- 2 **Qian YB**, Cheng GH, Huang JF. Multivariate regression analysis on early mortality after orthotopic liver transplantation. *World J Gastroenterol* 2002; **8**: 128-130
- 3 **Bramhall SR**, Minford E, Gunson B, Buckels JA. Liver transplantation in the UK. *World J Gastroenterol* 2001; **7**: 602-611
- 4 **Szabo A**, Muller V. Causes of late renal transplant dysfunction. *Orv Hetil* 2002; **143**: 2811-2819
- 5 **Becker BN**, Hullett DA, O' Herrin JK, Malin G, Sollinger HW, DeLuca H. Vitamin D as immunomodulatory therapy for kidney transplantation. *Transplantation* 2002; **74**: 1204-1206
- 6 **Yang YL**, Dou KF, Li KZ. Influence of intrauterine injection of rat fetal hepatocytes on rejection of rat liver transplantation. *World J Gastroenterol* 2003; **9**: 137-140
- 7 **Guo R**, Zou P, Fan HH, Gao F, Shang QX, Cao YL, Lu HZ. Repression of allo-cell transplant rejection through CIITA ribonuclease P(+) hepatocyte. *World J Gastroenterol* 2003; **9**: 1077-1081
- 8 **Zhang AB**, Zheng SS, Jia CK, Wang Y. Effect of 1,25-dihydroxyvitamin D3 on preventing allograft from acute rejection following rat orthotopic liver transplantation. *World J Gastroenterol* 2003; **9**: 1067-1071
- 9 **Jia CK**, Zheng SS, Li QY, Zhang AB. Immunotolerance of liver allotransplantation induced by intrathymic inoculation of donor soluble liver specific antigen. *World J Gastroenterol* 2003; **9**: 759-764
- 10 **Ding J**, Guo CC, Li CN, Sun AH, Guo XG, Miao JY, Pan BR. Post-operative endoscopic surveillance of human living-donor small bowel transplantations. *World J Gastroenterol* 2003; **9**: 595-598
- 11 **Platell CF**, Coster J, McCauley RD, Hall JC. The management of patients with the short bowel syndrome. *World J Gastroenterol* 2002; **8**: 13-20
- 12 **Westergaard H**. Short bowel syndrome. *Semin Gastrointest Dis* 2002; **13**: 210-220
- 13 **Nishida S**, Levi D, Kato T, Nery JR, Mittal N, Hadjis N, Madariaga J, Tzakis AG. Ninety-five cases of intestinal transplantation at the University of Miami. *J Gastrointest Surg* 2002; **6**: 233-239
- 14 **Kato T**, Ruiz P, Thompson JF, Eskind LB, Weppeler D, Khan FA, Pinna AD, Nery JR, Tzakis AG. Intestinal and multivisceral transplantation. *World J Surg* 2002; **26**: 226-237
- 15 **Cicalese L**, Rastellini C, Sileri P, Abcarian H, Benedetti E. Segmental living related small bowel transplantation in adults. *J Gastrointest Surg* 2001; **5**: 168-172
- 16 **Reyes J**. Intestinal transplantation for children with short bowel syndrome. *Semin Pediatr Surg* 2001; **10**: 99-104
- 17 **Dresske B**, Lin X, Huang DS, Zhou X, Fandrich F. Spontaneous tolerance: experience with the rat liver transplant model. *Hum Immunol* 2002; **63**: 853-861
- 18 **Knolle PA**, Gerken G. Local control of the immune response in the liver. *Immunol Rev* 2000; **174**: 21-34
- 19 **Bishop GA**, Wang C, Sharland AF, McCaughan G. Spontaneous acceptance of liver transplants in rodents: evidence that liver leucocytes induce recipient T-cell death by neglect. *Immunol Cell Biol* 2002; **80**: 93-100
- 20 **Kreisel D**, Petrowsky H, Krasinskas AM, Krupnick AS, Szeto WY, McLean AD, Popma SH, Gelman AE, Traum MK, Furth EE, Moore JS, Rosengard BR. The role of passenger leukocyte genotype in rejection and acceptance of rat liver allografts. *Transplantation* 2002; **73**: 1501-1507
- 21 **Morelli AE**, O'Connell PJ, Khanna A, Logar AJ, Lu L, Thomson AW. Preferential induction of Th1 responses by functionally mature hepatic (CD8alpha- and CD8alpha+) dendritic cells: association with conversion from liver transplant tolerance to acute rejection. *Transplantation* 2000; **69**: 2647-2657
- 22 **Meyer D**, Loffeler S, Otto C, Czub S, Gassel HJ, Timmermann W, Thiede A, Ulrichs K. Donor-derived alloantigen-presenting cells persist in the liver allograft during tolerance induction. *Transpl Int* 2000; **13**: 12-20
- 23 **Vrochides D**, Papanikolaou V, Pertoft H, Antoniadis AA, Heldin P. Biosynthesis and degradation of hyaluronan by nonparenchymal liver cells during liver regeneration. *Hepatology* 1996; **23**: 1650-1655
- 24 **Fiegel HC**, Park JJ, Lioznov MV, Martin A, Jaeschke-Melli S, Kaufmann PM, Fehse B, Zander AR, Kluth D. Characterization of cell types during rat liver development. *Hepatology* 2003; **37**: 148-154
- 25 **Nakao A**, Tahara K, Inoue S, Tanaka N, Kobayashi E. Experimental models of small intestinal transplantation in rats: orthotopic versus heterotopic model. *Acta Med Okayama* 2002; **56**: 69-74
- 26 **Motohashi H**, Masuda S, Katsura T, Saito H, Sakamoto S, Uemoto S, Tanaka K, Inui KI. Expression of peptide transporter following intestinal transplantation in the rat. *J Surg Res* 2001; **99**: 294-300

- 27 **Wu XT**, Li JS, Zhao XF, Zhuang W, Feng XL. Modified techniques of heterotopic total small intestinal transplantation in rats. *World J Gastroenterol* 2002; **8**: 758-762
- 28 **Nakao A**, Kobayashi E, Shen SD, Yoshino T, Tanaka N. Impact of tacrolimus and bone marrow augmentation on intestinal allograft survival and intra-graft cytokine expression in rats. *J Med* 2001; **32**: 207-230
- 29 **Timmermann W**, Hoppe H, Otto C, Gasser M, Vowinkel T, Gassel AM, Meyer D, Gassel HJ, Ulrichs K, Thiede A. Videomicroscopic imaging of graft mucosa for monitoring immunosuppressive therapy after small intestinal transplantation in rats. *Transplantation* 1999; **67**: 1555-1561
- 30 **Hoppe H**, Gasser M, Gassel AM, Vowinkel T, Timmermann W, Otto C, Tykal K, Thiede A. Noninvasive videomicroscopic monitoring of rat small-bowel rejection. *Microsurgery* 1999; **19**: 89-94
- 31 **Furukawa T**, Kimura O, Go S, Iwai N. Small bowel allografts maintained by administration of Bombesin while under immunosuppression. *J Pediatr Surg* 2003; **38**: 83-87
- 32 **Veenendaal RA**, Ringers J, Baranski A, van Hoek B, Lamers CB. Clinical aspects of small-bowel transplantation. *Scand J Gastroenterol Suppl* 2000; **232**: 65-68
- 33 **Gilroy R**, Sudan D. Liver and small bowel transplantation: therapeutic alternatives for the treatment of liver disease and intestinal failure. *Semin Liver Dis* 2000; **20**: 437-450
- 34 **Goulet O**, Lacaille F, Jan D, Ricour C. Intestinal transplantation: indications, results and strategy. *Curr Opin Clin Nutr Metab Care* 2000; **3**: 329-338
- 35 **Xu MQ**, Yao ZX. Functional changes of dendritic cells derived from allogeneic partial liver graft undergoing acute rejection in rats. *World J Gastroenterol* 2003; **9**: 141-147
- 36 **Bagley J**, Iacomini J. Gene Therapy Progress and Prospects: Gene therapy in organ transplantation. *Gene Ther* 2003; **10**: 605-611
- 37 **Ohdan H**, Sykes M. B cell tolerance to xenoantigens. *Xenotransplantation* 2003; **10**: 98-106
- 38 **Diao TJ**, Yuan TY, Li YL. Immunologic role of nitric oxide in acute rejection of golden hamster to rat liver xenotransplantation. *World J Gastroenterol* 2002; **8**: 746-751
- 39 **Meyer D**, Otto C, Rummel C, Gassel HJ, Timmermann W, Ulrichs K, Thiede A. "Tolerogenic effect" of the liver for a small bowel allograft. *Transpl Int* 2000; **13**(Suppl): S123-126
- 40 **Meyer D**, Thorwarth WM, Otto C, Gassel HJ, Timmermann W, Ulrichs K, Thiede A. Orthotopic liver/small bowel transplantation in rats: a microsurgical model inducing tolerance. *Microsurgery* 2001; **21**: 156-162
- 41 **Otto C**, Kauczok J, Martens N, Steger U, Moller I, Meyer D, Timmermann W, Ulrichs K, Gassel HJ. Mechanisms of tolerance induction after rat liver transplantation: intrahepatic CD4(+) T cells produce different cytokines. *J Gastrointest Surg* 2002; **6**: 455-463

Edited by Zhang JZ and Wang XL

Expression of PCNA and CD44mRNA in colorectal cancer with venous invasion and its relationship to liver metastasis

Shu-Qiang Yue, Yan-Ling Yang, Ke-Feng Dou, Kai-Zong Li

Shu-Qiang Yue, Yan-Ling Yang, Ke-Feng Dou, Kai-Zong Li,
Department of Hepatobiliary Surgery, Xijing Hospital, Fourth Military Medical University, Xi'an 710032, Shaanxi Province, China
Correspondence to: Kai-Zong Li, Department of Hepatobiliary Surgery, Xijing Hospital, Fourth Military Medical University, 710032 Xi'an, Shaanxi Province, China. gdwk@fmmu.edu.cn
Telephone: +86-29-3375259 **Fax:** +86-29-3375561
Received: 2003-05-13 **Accepted:** 2003-06-02

Abstract

AIM: To investigate the expression of proliferating cell nuclear antigen (PCNA) and CD44mRNA in colorectal cancer with venous invasion and its relationship with liver metastasis.

METHODS: Reverse transcriptase-polymerase chain reaction (RT-PCR) was used to detect the expression of PCNA and CD44mRNA in 31 cases of colorectal cancer with venous invasion.

RESULTS: Positive expression rates of PCNA and CD44mRNA in colorectal cancer were higher than those without liver metastasis ($P < 0.05$ and $P < 0.01$). In case of colorectal cancer with liver metastasis, strongly positive rates of PCNA and CD44mRNA were 94.1 % and 70.6 %, respectively, significantly higher than those without liver metastasis. There was a positive relationship between the expressions of PCNA and CD44mRNA ($r = 0.67$, $P < 0.05$).

CONCLUSION: Detection of PCNA and CD44mRNA expression in colorectal cancer may be useful for evaluating liver metastasis of cancer cells.

Yue SQ, Yang YL, Dou KF, Li KZ. Expression of PCNA and CD44mRNA in colorectal cancer with venous invasion and its relationship to liver metastasis. *World J Gastroenterol* 2003; 9 (12): 2863-2865

<http://www.wjgnet.com/1007-9327/9/2863.asp>

INTRODUCTION

Many mechanisms are involved in liver metastasis of colorectal cancer, of which venous invasion is considered to be the chief process^[1-6]. Previous studies showed that the degree of venous invasion was positively related to the rate of liver metastasis. But it is unknown which factors participate in liver metastasis of colorectal cancer. PCNA is a chief marker reflecting the activity of cell proliferation, which is closely related to invasion and metastasis of malignant neoplasms and their prognosis^[7-10]. Cell adhesion molecules (CAMs) correlate to the invasion and metastasis of tumor cells, and play an important role in occurrence, development and metastasis of neoplasms^[11,12]. The goal of this study was to test the expression of PCNA and adhesion molecule CD44mRNA in colorectal cancer with venous invasion by RT-PCR and its relationships with liver metastasis.

MATERIALS AND METHODS

Materials

According to the pathological diagnosis standards, the severity of venous invasion was classified as V0- V3^[13]. Thirty-one patients with severe venous invasion of colorectal cancer in V3 stage were chosen as study subjects (male 20, female 11), aged 44-82 years (average 66 years), of them 17 cases had liver metastasis. After operations, neoplasm samples were kept in liquid nitrogen. RNA extract reagent was purchased from Gibco Co., Taq enzyme from Takara Co., PCNA, CD44mRNA and β -actin primer were synthesized by BoYa Shanghai Co.. PCNA's sequence of up-stream primer was 5' -GCCGAGATC-TCAGCCATATT-3', that of down-stream primer was 5' -ATGTACTTAGAGGTACAAAT-3'. CD44's sequence of up-stream primer was 5' -CTTCATCCCAGTGACC-3', that of down-stream primer was 5' -TGCCACTGTTGATCAC-3'. β -actin's sequence of up-stream primer was 5' -CACCATGTACCCTGGCATTG-3', that of down-stream primer was 5' -TAACGCAACTAAGTCATAGT-3'. The size of anticipatively amplified products was 452 bp, 446 bp and 243 bp, respectively.

Methods

Using TRIzol reagent kit, total RNA was extracted according to the method previously described^[14-20]. The purity and content of RNA were measured by a spectrophotometer, and kept at -80 °C. Total RNA 5 μ g, 5 \times reaction buffer 10 μ l, 10 mmol \cdot L⁻¹ dNTPs 5 μ l, RNasin 20 U, oligo(dT)₁₂₋₁₈ 0.25 μ g, reverse transcriptase (M-MLV, Gibco) 200 U and 0.1 mol \cdot L⁻¹ DTT 0.5 μ l were added to reaction volume of 50 μ l, incubated at 37 °C for 1 h, then heated at 65 °C for 5 min to stop reaction. cDNA 0.1 μ g, 10 \times PCR buffer 2.5 μ l, 2 mmol \cdot L⁻¹ dNTPs 2.5 μ l, 25 mmol \cdot L⁻¹ MgCl₂ 2.5 μ l, PCR primer 20 pmol and Taq DNA polymerase (Takara) 5 U were added to reaction volume of 25 μ l. Using PTC-100 equipment (MJ Research), PCR conditions were as follows: pre-denaturing at 93 °C for 1 min, then 35 cycles at 93 °C for 30 s, at 52 °C for 30 s and 72 °C for 1 min, followed by extension at 72 °C for 8 min. Each amplified product of 10 μ l was detected via 3 g \cdot L⁻¹ sepharose electrophoresis, bromide staining, and analyzed by using a UVP gel imaging system and Labworks software. The ratio of density of positive PCNA and CD44 to that of β -actin was considered to be PCNA and CD44 relative expression quantity^[21-28]. Expression intensity was classified into 3 grades: +: 1-30 % β -actin density, ++: 31-65 %, +++: 66-100 %.

Statistics

All the data were analyzed by χ^2 -test, and a value of $P < 0.05$ was considered significant and $P < 0.01$ very significant.

RESULTS

Expression of PCNA and CD44mRNA in colorectal cancer tissue

PCNA, CD44 and β -actin gene expressions were detected in colorectal cancer tissues by RT-PCR, the size of amplified fragment was coincident with that of anticipation (Figure 1). All cases had expression of PCNA, the positive rate was 100 %,

but the expression levels were different among different cases (Figure 1A). Twenty cases had positive expression of CD44 mRNA, the positive rate was 64.5 %. The expression levels were different among different cases. As an inter-control, the expression level of β -actin was basically coincident among different cases (Figure 1C).

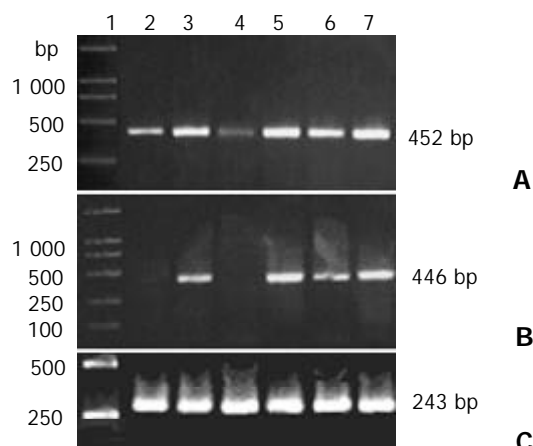


Figure 1 Expression of PCNA (A), CD44 (B) and β -actin (C) in colorectal cancer by PCR amplification. 1: DL2000 DNA marker (Takara), 2-7: Colorectal cancer tissues at various venous invasion stages.

Relationship between expression of PCNA and CD44mRNA and liver metastasis

In 17 cases of liver metastasis, 16 cases had strongly positive expression of PCNA mRNA (++, +++) (94.1 %), significantly higher than those without liver metastasis (28.6 %, $P < 0.01$). There was a positive relationship between the expression of PCNA and colorectal cancer with liver metastasis ($r = 0.82$, $P < 0.01$). In 17 cases of liver metastasis, 12 cases had strongly positive expression of CD44mRNA (70.6 %), significantly higher than those without liver metastasis (21.4 %, $P < 0.01$). There was a positive relationship between the expression of CD44mRNA and colorectal cancer with liver metastasis ($r = 0.82$, $P < 0.01$).

Relationship between expressions of PCNA and CD44mRNA in colorectal cancer

Of the 16 cases with strongly positive expression of CD44mRNA, 12 cases had strongly positive expression of PCNA (75.0 %). Of the 15 cases with weak or negative expression of CD44mRNA, 7 cases had strongly positive expression of PCNA (46.7 %), and there was a significant difference ($P < 0.05$). There was a positive relationship between the expressions of PCNA and CD44mRNA ($r = 0.67$, $P < 0.05$).

DISCUSSION

Venous invasion of cancer cells was the first step of neoplasm's liver metastasis^[29]. However, in clinical cases, venous invasion by histological detection was not definitely related to liver metastasis. It implies that, besides venous invasion, other factors might also participate in the process of liver metastasis^[30-32].

PCNA is a kind of non-histone nuclear polypeptide with 36 000 molecular weight, as an assistant protein to DNA polymerase, its content could reflect the degree of cell proliferation^[33-37]. Previous studies showed that there was a significant relationship between PCNA labelling and degree of malignancy, vessel invasion, distant metastasis and prognosis^[38-42]. In this study, we found that under the condition of venous invasion, the strong expression rate of PCNA mRNA

in venous invasion of colorectal cancer with liver metastasis, was significantly higher than that without liver metastasis. This showed that there was a positive relationship between the strong expression of PCNA and colorectal cancer with liver metastasis. All these indicate that colorectal cancer cells with higher proliferating activity are much more easier to proceed liver metastasis.

CD44 is a kind of cell adhesion molecules. Under normal conditions, CD44 acts as the receptor of hyaluronic acid, and chiefly participates in intra-cells and cell-stroma specific adhesion^[43-46]. Recent studies showed that CD44 could be expressed in different neoplasm tissues. Bhatavdekar *et al* found that over-expression of CD44 was associated with clinical staging of colorectal cancer. Furthermore, positive expression of CD44 is an important prognostic factor associated with colorectal cancer patients' relapse and total survival time. Further studies found that CD44 could make cancer cells be able to metastasize, adhere to vessel endothelium, accelerate cancer metastasis. We found that the strong expression rate of CD44 mRNA in colorectal cancer with liver metastasis was significantly higher than that without liver metastasis, further suggesting that CD44 might play an important role in colorectal cancer with liver metastasis. But it is still in argument whether CD44 can be taken as an independent marker for progress and metastasis of colorectal cancer.

We also found that under the condition of venous invasion in colorectal cancer patients with liver metastasis, the expression of PCNA and CD44mRNA was strong at the same time. All these indicate that there is a positive relationship between colorectal cancer with liver metastasis and expression of PCNA and CD44mRNA ($r = 0.82$, $P < 0.01$). Moreover, in colorectal cancer tissue with strong expression of CD44mRNA, PCNA mRNA was significantly higher than that with weak or negative expression, showing that there was a positive relationship between the expressions of CD44 and PCNA ($r = 0.67$, $P < 0.05$). Taken together, we conclude that detection of PCNA and CD44 expression in colorectal cancer may be useful for evaluating liver metastasis of cancer cells.

REFERENCES

- 1 Gu J, Ma ZL, Li Y, Li M, Xu GW. Angiography for diagnosis and treatment of colorectal cancer. *World J Gastroenterol* 2003; **9**: 288-290
- 2 Liu LX, Zhang WH, Jiang HC. Current treatment for liver metastases from colorectal cancer. *World J Gastroenterol* 2003; **9**: 193-200
- 3 Cui JH, Krueger U, Henne-Bruns D, Kremer B, Kalthoff H. Orthotopic transplantation model of human gastrointestinal cancer and detection of micrometastases. *World J Gastroenterol* 2001; **7**: 381-386
- 4 Minagawa N, Nakayama Y, Hirata K, Onitsuka K, Inoue Y, Nagata N, Itoh, H. Correlation of plasma level and immuno-histochemical expression of vascular endothelial growth factor in patients with advanced colorectal cancer. *Anticancer Res* 2002; **22**: 2957-2963
- 5 Berglund A, Edler D, Molin D, Nordlinder H, Graf W, Glimelius B. Thymidylate synthase and p53 expression in primary tumor do not predict chemotherapy outcome in metastatic colorectal carcinoma. *Anticancer Res* 2002; **22**: 3653-3659
- 6 Takashima T, Onoda N, Ishikawa T, Ogawa Y, Kato Y, Fujimoto Y, Sowa M, Hirakawa Y, Chung K. Proliferating cell nuclear antigen labeling index and p53 expression predict outcome for breast cancer patients with four or more lymph node metastases. *Int J Mol Med* 2001; **8**: 159-163
- 7 Shen LJ, Zhang HX, Zhang ZJ, Li JY, Chen MQ, Yang WB, Huang R. Detection of HBV, PCNA and GST-pi in hepatocellular carcinoma and chronic liver diseases. *World J Gastroenterol* 2003; **9**: 459-462
- 8 Terada R, Yasutake T, Nakamura S, Hisamatsu T, Nakagoe T, Ayabe H, Tagawa Y. Evaluation of metastatic potential of gastric tumors by staining for proliferating cell nuclear antigen and chromosome 17 numerical aberrations. *Ann Surg Oncol* 2001; **8**: 525-532

- 9 **Huang ZH**, Fan YF, Xia H, Feng HM, Tang FX. Effects of TNP-470 on proliferation and apoptosis in human colon cancer xenografts in nude mice. *World J Gastroenterol* 2003; **9**: 281-283
- 10 **Chen H**, Wang LD, Guo M, Gao SG, Guo HQ, Fan ZM, Li JL. Alterations of p53 and PCNA in cancer and adjacent tissues from concurrent carcinomas of the esophagus and gastric cardia in the same patient in Linzhou, a high incidence area for esophageal cancer in northern China. *World J Gastroenterol* 2003; **9**: 16-21
- 11 **Satyamoorthy K**, Herlyn M. Cellular and molecular biology of human melanoma. *Cancer Biol Ther* 2002; **1**: 14-17
- 12 **Gdor Y**, Timme TL, Miles BJ, Kadmon D, Thompson TC. Gene therapy for prostate cancer. *Expert Rev Anticancer Ther* 2002; **2**: 309-321
- 13 **Shirouzu K**, Isomoto H, Kakegawa T, Morimatsu M. A prospective clinicopathologic study of venous invasion in colorectal cancer. *Am J Surg* 1991; **162**: 216-222
- 14 **Zhang DL**, Li JS, Jiang ZW, Yu BJ, Tang XM, Zheng HM. Association of two polymorphisms of tumor necrosis factor gene with acute biliary pancreatitis. *World J Gastroenterol* 2003; **9**: 824-828
- 15 **Yang XL**, Zhang YL, Lai ZS, Xing FY, Liu YH. Pleckstrin homology domain of G protein-coupled receptor kinase-2 binds to PKC and affects the activity of PKC kinase. *World J Gastroenterol* 2003; **9**: 800-803
- 16 **Wen CY**, Ito M, Wang H, Chen LD, Xu ZM, Matsuu M, Shichijo K, Nakayama T, Nakashima M, Sekine I. IL-11 up-regulates Tie-2 expression during the healing of gastric ulcers in rats. *World J Gastroenterol* 2003; **9**: 788-790
- 17 **Wang HT**, Chen S, Wang J, Ou QJ, Liu C, Zheng SS, Deng MH, Liu XP. Expression of growth hormone receptor and its mRNA in hepatic cirrhosis. *World J Gastroenterol* 2003; **9**: 765-770
- 18 **Jeon MJ**, Shin JH, Suh SP, Lim YC, Ryang DW. TT virus and hepatitis G virus infections in Korean blood donors and patients with chronic liver disease. *World J Gastroenterol* 2003; **9**: 741-744
- 19 **Baptista M**, Kramvis A, Jammeh S, Naicker J, Galpin JS, Kew MC. Follow up of infection of chacma baboons with inoculum containing a and non-a genotypes of hepatitis B virus. *World J Gastroenterol* 2003; **9**: 731-735
- 20 **Fang J**, Jin HB, Song JD. Construction, expression and tumor targeting of a single-chain Fv against human colorectal carcinoma. *World J Gastroenterol* 2003; **9**: 726-730
- 21 **Hu HY**, Liu XX, Jiang CY, Zhang Y, Bian JF, Lu Y, Geng Z, Liu SL, Liu CH, Wang XM, Wang W. Cloning and expression of ornithine decarboxylase gene from human colorectal carcinoma. *World J Gastroenterol* 2003; **9**: 714-716
- 22 **Huang XH**, Sun LH, Lu DD, Sun Y, Ma LJ, Zhang XR, Huang J, Yu L. Codon 249 mutation in exon 7 of p53 gene in plasma DNA: maybe a new early diagnostic marker of hepatocellular carcinoma in Qidong risk area, China. *World J Gastroenterol* 2003; **9**: 692-695
- 23 **Ikeda O**, Egami H, Ishiko T, Ishikawa S, Kamohara H, Hidaka H, Mita S, Ogawa M. Expression of proteinase-activated receptor-2 in human pancreatic cancer: A possible relation to cancer invasion and induction of fibrosis. *Int J Oncol* 2003; **22**: 295-300
- 24 **Zhan J**, Tang XD. Expression of cyclooxygenase-2 in human transitional cell bladder carcinomas. *Ai Zheng* 2002; **21**: 1212-1216
- 25 **Tan Z**, Hu X, Ying K, Li Y, Tang R, Cao G, Tang Y, Jin G. cDNA microarray in the gene expression pattern in lymphatic metastasis of pancreatic carcinoma. *Zhonghua Zhongliu Zazhi* 2002; **24**: 243-246
- 26 **Diamond MP**, El-Hammady E, Wang R, Saed G. Metabolic regulation of collagen I in fibroblasts isolated from normal peritoneum and adhesions by dichloroacetic acid. *Am J Obstet Gynecol* 2002; **187**: 1456-1460
- 27 **Murphy N**, Ring M, Killalea AG, Uhlmann V, O'Donovan M, Mulcahy F, Turner M, McGuinness E, Griffin M, Martin C, Sheils O, O'Leary JJ. p16INK4A as a marker for cervical dyskaryosis: CIN and cGIN in cervical biopsies and ThinPrep smears. *J Clin Pathol* 2003; **56**: 56-63
- 28 **Schneider T**, Osl F, Friess T, Stockinger H, Scheuer WV. Quantification of human Alu sequences by real-time PCR—an improved method to measure therapeutic efficacy of anti-metastatic drugs in human xenotransplants. *Clin Exp Metastasis* 2002; **19**: 571-582
- 29 **Hanke B**, Wein A, Martus P, Riedel C, Voelker M, Hahn EG, Schuppan D. Serum markers of matrix turnover as predictors for the evolution of colorectal cancer metastasis under chemotherapy. *Br J Cancer* 2003; **88**: 1248-1250
- 30 **Yamauchi T**, Watanabe M, Hasegawa H, Nishibori H, Ishii Y, Tatematsu H, Yamamoto K, Kubota T, Kitajima M. The potential for a selective cyclooxygenase-2 inhibitor in the prevention of liver metastasis in human colorectal cancer. *Anticancer Res* 2003; **23**: 245-249
- 31 **Brenner AS**, Thebo JS, Senagore AJ, Duepree HJ, Gramlich T, Ormsby A, Lavery IC, Fazio VW. Analysis of both NM23-h1 and NM23-H2 expression identifies "at-risk" patients with colorectal cancer. *Am Surg* 2003; **69**: 203-208
- 32 **Kuwai T**, Kitadai Y, Tanaka S, Onogawa S, Matsutani N, Kaio E, Ito M, Chayama K. Expression of hypoxia-inducible factor-1 α is associated with tumor vascularization in human colorectal carcinoma. *Int J Cancer* 2003; **105**: 176-181
- 33 **Sano B**, Sugiyama Y, Kunieda K, Sano J, Saji S. Antitumor effects induced by the combination of TNP-470 as an angiogenesis inhibitor and lentinan as a biological response modifier in a rabbit spontaneous liver metastasis model. *Surg Today* 2002; **32**: 503-509
- 34 **Farre L**, Casanova I, Guerrero S, Trias M, Capella G, Manguers R. Heterotopic implantation alters the regulation of apoptosis and the cell cycle and generates a new metastatic site in a human pancreatic tumor xenograft model. *FASEB J* 2002; **16**: 975-982
- 35 **Martins AC**, Faria SM, Cologna AJ, Suaid HJ, Tucci S Jr. Immunoeexpression of p53 protein and proliferating cell nuclear antigen in penile carcinoma. *J Urol* 2002; **167**: 89-92
- 36 **Kawasaki G**, Kato Y, Mizuno A. Cathepsin expression in oral squamous cell carcinoma: relationship with clinicopathologic factors. *Oral Surg Oral Med Oral Pathol Oral Radiol Endod* 2002; **93**: 446-454
- 37 **Dong Y**, Sui L, Watanabe Y, Sugimoto K, Tokuda M. Aberrant expression of cyclin A in laryngeal squamous cell carcinoma. *Anticancer Res* 2002; **22**: 83-89
- 38 **Kouvaraki M**, Gorgoulis VG, Rassidakis GZ, Liodis P, Markopoulos C, Gogas J, Kittas C. High expression levels of p27 correlate with lymph node status in a subset of advanced invasive breast carcinomas: relation to E-cadherin alterations, proliferative activity, and ploidy of the tumors. *Cancer* 2002; **94**: 2454-2465
- 39 **Van Poznak C**, Tan L, Panageas KS, Arroyo CD, Hudis C, Norton L, Seidman AD. Assessment of molecular markers of clinical sensitivity to single-agent taxane therapy for metastatic breast cancer. *J Clin Oncol* 2002; **20**: 2319-2326
- 40 **Yue H**, Na YL, Feng XL, Ma SR, Song FL, Yang B. Expression of p57(kip2), Rb protein and PCNA and their relationships with clinicopathology in human pancreatic cancer. *World J Gastroenterol* 2003; **9**: 377-380
- 41 **Jiang YA**, Zhang YY, Luo HS, Xing SF. Mast cell density and the context of clinicopathological parameters and expression of p185, estrogen receptor, and proliferating cell nuclear antigen in gastric carcinoma. *World J Gastroenterol* 2002; **8**: 1005-1008
- 42 **Takahima T**, Onoda N, Ishikawa T, Ogawa Y, Kato Y, Fujimoto Y, Sowa M, Hirakawa K. Prognostic value of combined analysis of estrogen receptor status and cellular proliferative activity in breast cancer patients with extensive lymph node metastases. *Oncol Rep* 2002; **9**: 589-594
- 43 **Qin LX**, Tang ZY. The prognostic molecular markers in hepatocellular carcinoma. *World J Gastroenterol* 2002; **8**: 385-392
- 44 **Xin Y**, Li XL, Wang YP, Zhang SM, Zheng HC, Wu DY, Zhang YC. Relationship between phenotypes of cell-function differentiation and pathobiological behavior of gastric carcinomas. *World J Gastroenterol* 2001; **7**: 53-59
- 45 **Neumayer R**, Rosen HR, Reiner A, Sebesta C, Schmid A, Tuchler H, Schiessel R. CD44 expression in benign and malignant colorectal polyps. *Dis Colon Rectum* 1999; **42**: 50-55
- 46 **Nanashima A**, Yamaguchi H, Sawai T, Yasutake T, Tsuji T, Jibiki M, Yamaguchi E, Nakagoe T, Ayabe H. Expression of adhesion molecules in hepatic metastases of colorectal carcinoma: relationship to primary tumours and prognosis after hepatic resection. *J Gastroenterol Hepatol* 1999; **14**: 1004-1009

Relationship between expression of CD105 and growth factors in malignant tumors of gastrointestinal tract and its significance

Jian-Xian Yu, Xiao-Tun Zhang, Yong-Qiang Liao, Qi-Yi Zhang, Hua Chen, Mei Lin, Shant Kumar

Jian-Xian Yu, Xiao-Tun Zhang, Hua Chen, Department of Pathology, Qingdao Municipal Hospital, Qingdao 266011, Shandong Province, China

Qi-Yi Zhang, Department of Internal Medicine, Qingdao Municipal Hospital, Qingdao 266011, Shandong Province, China

Mei Lin, Shant Kumar, Department of Pathology, Manchester University, Manchester, United Kingdom

Yong-Qiang Liao, Department of Pathology, Xiamen People's Hospital, Xiamen, Fujian Province, China

Correspondence to: Dr. Jian-Xian Yu, Department of Pathology, Qingdao Municipal Hospital, No.1 Jiaozhou Lu, Qingdao 266011, Shandong Province China. yujianxian@hotmail.com

Telephone: +86-532-2827971-4345 **Fax:** +86-532-2827971-4345

Received: 2003-04-04 **Accepted:** 2003-05-21

Abstract

AIM: Angiogenesis is an important step in the growth of solid malignant tumors. A number of angiogenic factors have been found such as transforming growth factor β 1 (TGF- β 1) and vascular endothelial growth factor (VEGF). However, the roles of TGF β 1 and VEGF in gastrointestinal carcinogenesis are still unclear. This study was to investigate the expressions of TGF- β 1 and VEGF in gastrointestinal tract malignant tumors, as well as their association with microvessel density (MVD). At the same time, we also observed the localization of TGF- β 1 and its receptor CD105 in gastric malignant tumors.

METHODS: The expressions of TGF- β 1 and CD105 were detected in 55 fresh specimens of gastric carcinoma and VEGF and CD105 in 44 fresh specimens of colorectal carcinoma by immunohistochemical staining (S-ABC). TGF- β 1 and CD105 in 55 gastric carcinoma tissues on the same slide were detected by using double-stain Immunohistochemistry (DS-ABC).

RESULTS: Among the 55 cases of gastric carcinoma tissues, 30 were positive for TGF- β 1 (54.55 %). The MVD of TGF- β 1 strong positive group ($++\sim+++$ 23.22 \pm 5.8) was significantly higher than that of weak positive group ($+17.56\pm7.2$) and negative group (-17.46 ± 3.9) ($q=4.5$, $q=5.3207$, respectively, $P<0.01$). In the areas of high expression of TGF- β 1, MVD and the expression of CD105 were also high. Among the 44 cases of colonic carcinoma tissues, 26 were positive for VEGF (59.1 %). The expressions of both VEGF and CD105 (MVD) were related with the depth of invasion ($F=5.438$, $P<0.05$; $F=4.168$, $P=0.05$), lymph node metastasis ($F=10.311$, $P<0.01$; $F=20.282$, $P<0.01$) and Dukes stage ($F=6.196$, $P<0.01$; $F=10.274$, $P<0.01$), but not with histological grade ($F=0.487$, $P>0.05$). There was a significant correlation between the expression of VEGF and CD105 (MVD) ($r=0.720$, $P<0.01$).

CONCLUSION: Over-expression of TGF- β 1 and VEGF acts as stimulating factors of angiogenesis in gastrointestinal tumors. CD105, as a receptor of TGF- β 1, can regulate the biological effect of TGF- β 1 in tumor angiogenesis. MVD marked by CD105 is more suitable for detecting newborn blood vessels.

Yu JX, Zhang XT, Liao YQ, Zhang QY, Chen H, Lin M, Kumar S. Relationship between expression of CD105 and growth factors in malignant tumors of gastrointestinal tract and its significance. *World J Gastroenterol* 2003; 9(12): 2866-2869

<http://www.wjgnet.com/1007-9327/9/2866.asp>

INTRODUCTION

Angiogenesis occurs in diverse physiological and pathological situations and particularly in tumour growth. The development of a new blood vessel is a complex phenomenon and the result of a sequence of events, among which the release of growth factors of interstitial cells is the most important step. At present, many growth factors have been identified including transforming growth factor (TGF)- β 1 and endothelial cell growth factor (VEGF). TGF- β 1 is a potent inhibitor of endothelial cells (EC) proliferation and migration *in vitro* and an angiogenesis promoter *in vivo*. It has aroused much interests in study of the relationship between TGF- β 1 and angiogenesis. In this research, we used CD105, a new EC marker, to count the intratumor microvessel density (MVD), and to detect the expression of TGF- β 1 in 55 gastric carcinoma tissues. Because CD105 is one of the receptors of TGF- β 1, we hoped to find out the biological effect of TGF- β 1 by studying the relationship between the ligand and the receptor. We also detected the expression of VEGF and CD105 (MVD) in 44 colorectal carcinoma tissues and analyzed the effect of VEGF in angiogenesis of colorectal carcinoma tissues. Furthermore we demonstrated the confidence level and superiority of CD105 in studying tumor angiogenesis.

MATERIALS AND METHODS

Patients

Two groups of patients were chosen and examined. Group A: Fifty-five specimens of freshly resected malignant gastric tissues were collected from 55 patients with gastric carcinoma (median age 57.65 \pm 5.3 years, range 29-77 years) who were operated in Qingdao Municipal Hospital and the Affiliated Hospital of Medical College, Qingdao University (Shandong, China) from October 2000 to April 2001. Four cases were well-differentiated adenocarcinoma, nine moderately-differentiated adenocarcinoma and forty-two poorly-differentiated adenocarcinoma. Among the 55 cases, 36 cases had lymph node metastasis and five cases had distant metastasis. Normal tissue samples located at least 8 cm away from the margins of cancers, and 51 normal gastric tissue samples were frozen in liquid nitrogen. Group B: Forty-four freshly resected malignant intestinal tissue samples were collected from 44 patients with intestinal carcinoma (median age 62.5 \pm 6.2 years, range 31-79 years) who were operated in Qingdao Municipal Hospital and the Affiliated Hospital of Medical College, Qingdao University from July 2001 to March 2002. The group included one case of well-differentiated adenocarcinoma, thirty-eight cases of moderately-differentiated adenocarcinoma and five cases of poorly-differentiated adenocarcinoma. Among the 44 tumor patients, 20 cases had lymph node metastasis. 20 normal

intestinal tissue samples taken at least 8 cm away from the margins of cancers were frozen in liquid nitrogen.

None of the patients in groups A and B received any chemotherapy or radiation therapy prior to surgery. Fresh tissue samples were collected within 4 hours after resection. The pathological diagnosis was made on the basis of the size, infiltrating depth, histological grade, lymph node and distant metastasis. The grading standard was in accordance with "Practical and surgical pathology" (Chen-Zhong Nian, published by ShangHai Medical University, first edition). Written informed consent was obtained from each patient.

Methods

Immunohistochemistry Biopsy specimens were snap frozen in liquid nitrogen and serial cryostat sections were cut into 7 μm thick. Paraffin-embedded sections were cut into 4 μm thick. Immunohistochemical staining (S-ABC) and immunohistochemical double staining (DS-ABC) were performed in accordance with the introduction of the kit. PBS was used as the negative controls instead of Mab.

Identification of immunohistochemical staining results TGF- β 1/VEGF staining was classified into four grades. +++, most carcinoma cells were stained with a very strong intensity, and distributed in clusters. ++, a large number of carcinoma cells were stained with a moderate intensity, and distributed in clusters occasionally. +, a few carcinoma cells were stained with a slight intensity. -, no staining of carcinoma cells.

Counting of MVD in carcinoma tissues was in accordance with Weidner's standards with a minor modification. The slide was searched for the hot spots rich in vessels, which were located in or near the area of tumor tissues under a low power microscope (100 \times). MVD was counted under a high power (400 \times) or low power (100 \times) microscope according to the standards that any stained endothelial cell or cells were identified as an independent vessel. These vessels must be clearly separated from each other. However, apparent vasa or vasa with red blood cells could be regarded as vessels. Five different HP vision fields were chosen on each of the slides, and the stained vessels were counted simultaneously by two doctors under a multi-ocular len microscope. The results were averaged, which was the relative value of the amount of vessels per unit area.

Statistic analysis

The relation between MVD and expression of TGF- β 1 was studied with analysis of variance and Q-test. The analysis of variance and χ^2 -test were used for statistical analysis of the relation between MVD and expression of VEGF.

RESULTS

Results of TGF- β 1 staining in gastric carcinoma tissues

Among the 55 specimens in group A, 30 were positively stained and 25 negatively stained, with a positive rate of 54.55 %. TGF- β 1 was mainly existed in cytoplasm of carcinoma cells. In the 51 specimens of normal gastric tissues, TGF- β 1 was mainly expressed in gastric mucosa epithelial cells.

Results of VEGF staining in colorectal carcinoma tissues

Among the 44 cases in group B, 26 were positively stained and 18 negatively stained, with a positive rate of 59.1 %. VEGF was mainly existed in cytoplasm of colorectal carcinoma cells.

Expression of CD105 and counting of MVD in carcinoma tissues

In both group A and group B CD105 was mainly expressed in cytoplasm and plasmalemma of newborn endothelial cells in cryostat section. CD105 was weakly expressed or absent in native blood vessels with thick walls and large lumina. MVD of gastric carcinoma tissues is listed in Figure 1.

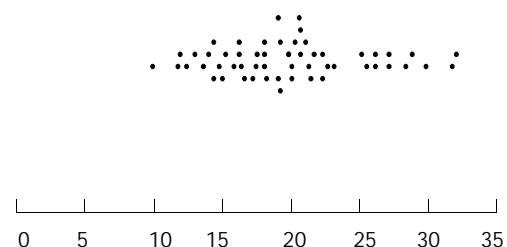


Figure 1 MVD marked by CD105 in 55 cases of gastric carcinoma tissues.

Table 1 Relations between MVD and TGF- β 1 (under 400 \times)

Grade of TGF- β 1 staining	n	%	MVD	P value
+++~++	21	38.18	23.22 \pm 5.8	<0.01 ^a
+	9	16.36	17.56 \pm 7.2	>0.05 ^b
-	25	45.46	17.46 \pm 3.9	<0.01 ^c
Total	55	100		

^a P <0.01, TGF- β 1 +++ group vs. + group, ^b P >0.05, TGF- β 1 + group vs. - group, ^c P <0.01, TGF- β 1, group vs. +++ group.

Relation between TGF- β 1 and MVD in gastric carcinoma tissues

When the gastric carcinoma tissues were double stained for CD105 and TGF- β 1 in one cryostat section, TGF- β 1 was highly

Table 2 Relations between VEGF/MVD and clinical pathological parameters in colorectal carcinoma (under 100 \times)

Clinical pathological parameters	Cases (n)	VEGF	P_x value	MVD (CD105)	P value
Histological grade					
Well differentiation	1	18.50		143.1	
Moderate differentiation	38	22.28 \pm 14.49	>0.05	144.8 \pm 31.9	>0.05
Poor differentiation	5	21.89 \pm 14.44		146.4 \pm 47.4	
Infiltrating depth					
Serous membrane (-)	5	9.37 \pm 4.79	<0.05	119.0 \pm 17.2	=0.05
Serous membrane (+)	39	22.55 \pm 12.32		150.0 \pm 32.7	
Lymph node metastasis					
(-)	24	14.76 \pm 9.62	<0.01	126.3 \pm 20.8	<0.01
(+)	20	27.31 \pm 12.17		167.7 \pm 30.3	
Dukes stage					
A	3	9.37 \pm 4.79	<0.01	119.0 \pm 17.2	<0.01
B	16	17.00 \pm 10.37		129.3 \pm 22.1	
C and D	25	27.31 \pm 12.16		167.7 \pm 30.3	

expressed and so was CD105 in the same area. It was also found that newborn vessels were present around carcinoma nests whereas TGF- β 1 was observed mainly in cytoplasm of carcinoma cells. The relation between MVD and TGF- β 1 is shown in Table 1. Analysis of variance and Q -test were used to analyze the difference of MVD counting among the three different TGF- β 1 staining groups. It showed that MVD of TGF- β 1 strong positive group was significantly higher than weak positive group and negative group, and the MVD between the two groups of TGF- β 1 staining weak positive “+” and negative “-” had no significant difference.

Relation between VEGF/MVD and clinical pathological parameters in colorectal carcinoma

Analysis of variance showed the expression of VEGF was correlated with infiltrating depth ($F=5.438$, $P<0.05$), lymph node metastasis ($F=10.311$, $P<0.01$) and Duke's staging ($F=6.196$, $P<0.01$), but had no relation with histological stage ($F=0.487$, $P>0.05$). MVD was correlated with infiltrating depth ($F=4.168$, $P=0.05$), lymph nodes metastasis ($F=20.282$, $P<0.01$) and Duke's staging ($F=10.274$, $P<0.01$), but had no relation with histological stage ($F=0.006$, $P>0.05$), (Table 2).

DISCUSSION

Angiogenesis refers to the formation of new blood vessels from native blood vessels, which is essential for the unrestricted growth and metastasis of solid tumors^[1]. Thus, highly hyperplastic microvessels are usually recognized as a marker of malignant tumor development. At present, many growth factors have been identified including TGF- β 1 and VEGF. These factors could be paracrine by tumor cells^[2]. However, the potential roles of these factors, especially TGF- β 1, are not clearly known.

Human TGF- β is a large family consisting of 3 isomers: TGF- β 1, TGF- β 2 and TGF- β 3. TGF- β 1, the most widely studied protein of the three TGF- β isomers, derived from a 390-amino acid precursor cleaved to produce a 112-amino acid carboxy-terminal peptide, is the predominant form in humans. TGF- β 1 influences the proliferation rate of many cell types, acting as a growth inhibitor in most but not all cases. In addition, TGF- β 1 controls the processes of epithelial cell differentiation. In normal cells, TGF- β 1 generally enhances adhesion through increased matrix production and decreased proteolysis. Resistance to the negative growth regulating properties of TGF- β 1 has been observed in epithelial and mesenchymal tumors. In addition to a stimulator of angiogenesis, TGF- β 1 also influences the growth of tumor cells directly or indirectly. Tumor cells can escape the inhibiting effect of TGF- β 1 on normal cells at post-transcription level, receptor level or post-receptor level. When tumor cells are insensitive, TGF- β 1 also can promote tumor metastasis through enhancing angiogenesis, adjusting the character of matrix, or adjusting the body's immune response to tumor growth. TGF- β 1 seems to affect tumor angiogenesis and play an important role in tumor progression in non-small cell lung carcinoma and lung adenocarcinoma. A significant correlation between TGF- β 1 protein level and prognosis was detected by multivariate analysis^[3]. Maehara^[4] found that TGF- β 1 was closely related to the invasion and metastasis of gastric cancer, and production of TGF- β 1 in the tumor did not contribute to the total amount of TGF- β 1 in the blood circulation. TGF- β 1 might be associated with tumor progression by modulating angiogenesis in colorectal cancer and it could be used as a possible biomarker^[5].

In the present study, 55 cases of gastric carcinoma tissues were stained for TGF- β 1. 54.55 % of these tissues were positively stained including 21 strong positive cases “+++~++”, 9 positive cases “+”, 25 negative cases “-”. MVD between the two groups of “+” and “-” staining had no significant difference

($P>0.05$), but MVD of the group of “+++~++” was significantly higher than the groups of “+” and “-” ($P<0.01$). Therefore, we propose that overexpression of TGF- β 1 be positively correlated with MVD in tumors and one of the bio-effects of TGF- β 1 act as a stimulating factor of angiogenesis *in vivo*. In our other studies, TGF- β 1 was highly expressed in gastric carcinoma tissues with lymph node metastasis and distant metastasis.

TGF- β 1 exerts its functions through binding its receptors. Receptors for TGF- β family include type I, type II, type III and CD105. CD105 could act as an auxiliary protein in the ligand-receptor compound and regulate the function of TGF- β 1^[6]. It has been found to mainly localize in vascular endothelial cells in normal or tumor tissues. Calabro^[7] detected soluble TGF- β 1 and CD105 (sCD105) in hematopoietic malignancies, and showed that high levels of sCD105 were present in myeloid malignancies characterized by a high cellular proliferation rate, and suggested that an altered balance between sCD105 and sTGF- β 1 might favor disease progression and clinical complications.

In this study we used double staining to detect the expression of CD105 and TGF- β 1 in one gastric carcinoma section, and found that CD105 was highly expressed around these cancer cells with more TGF- β 1.

VEGF, also named vascular permeability factor, can specifically direct to endothelial cells and is one of the most important factors to induce, up-regulate and migrate angiogenesis. VEGF is a kind of dimer glycoproteins, with a molecular weight of 34-50 kD. VEGF specifically promotes the mitosis and proliferation of endothelial cells by paracrine. Furthermore, VEGF can induce angiogenesis, increase the permeability of vessels and stimulate endothelial cells to produce protease and other low molecule proteins. In addition, VEGF can significantly prolong the life span of endothelial cells, increasing the mitosis to 15-20 fold. Further studies showed VEGF could improve the function of vesicles in endothelial cells, thus increasing the permeability of vessels, which facilitates tumor cells to invade the vessels and distant migration. Therefore, VEGF can effectively promote angiogenesis and maintain its existence.

Kaio^[8] found that lymph node metastasis and VEGF expression were significant risk factors in advanced colorectal carcinoma patients. Song^[9] noticed VEGF was closely related to gastric carcinoma angiogenesis, and involved in tumor progression and lymph node metastasis. Some other studies showed that high VEGF expression or high MVD would indicate a poor prognosis in breast carcinoma patients^[10] or high VEGF could be a marker of metastasis and invasion in squamous cell carcinomas^[11]. In our study, VEGF and MVD marked by CD105 were highly expressed in colorectal carcinoma tissues. The expression of VEGF and MVD in colorectal carcinoma tissues was closely related to infiltrating depth, lymph node metastasis and Duke's staging but not related to histological staging. These observations suggested that the expression of VEGF and MVD in colorectal carcinoma tissues was important in monitoring tumor invasion, lymph node metastasis and Duke's staging.

Our previous correlation analysis showed that the expression of VEGF was positively related to MVD, further proving the causality of VEGF and MVD, i.e., VEGF could stimulate angiogenesis through paracrine in colorectal carcinoma tissues and thus promoting the growth, infiltration and metastasis of tumors.

Newborn blood vessels have their own construction features. For example, the new vessels in tumor tissues do not further differentiate or rebuild corresponding arteries and veins, which means that newborn vessels have no smooth muscle and cannot contract. Newborn vessels in tumors are highly winded, sinusoid and slender. Functionally, blood stream in new vessels is irregular, tending to result in thrombosis or

hemorrhage spontaneously. In this case, tumor cells invade into new vessels and are carried to other organs, continuing to grow and become a metastasis. The more the newborn blood vessels are, the greater the possibilities of metastasis are. Because of the important effects of newborn vessels, great attention has been paid to the studies of angiogenesis.

While counting newborn blood vessels, most researchers selected several normal endothelial cell markers, such as CD31, CD34 and von Willerbrand (vWF). VWF, a factor VIII related antigen (VIII-RA), is a kind of EC marker that exists on EC of normal tissues. Many experiments showed that VIII-RA mainly existed in completely mature vessels, and the chapter restricts its utilization in angiogenesis of tumor tissues. CD31, a member of cell adhesion molecules, often participates in the adhesiveness of platelets in inflammation and wound. Parums pointed out that anti-CD31 monoclonal antibody could also bind normal blood vessels. CD34 is a transmembrane glycoprotein with a MW of 110 kD, and can express on endothelial cells. Ewoto^[12] found that it was difficult to identify native or newborn vessels by using CD34. For this reason, CD34 is not an ideal marker of endothelial cells in the research of newborn vessels. Because of the heterogeneity of endothelial cells, the markers of normal endothelial cells are apparently unfit for the studies of angiogenesis in tumor tissues.

CD105, also called endoglin, is a new kind of cell adhesion molecules, first found by Quackenbush in pre-B cell line HOON^[13]. CD105 mainly locates in EC and has become a new marker of EC^[14]. CD105 is an endothelial homodimeric membrane antigen with 633 amino acid residues and its molecular mass is 180 kD. The gene of CD105 is located on 9q34, which is the target gene of HHT-I. Therefore, the expression of CD105 in EC showed it was highly related to the structure and function of EC^[15]. Although CD105 can express in normal vessels, many studies showed CD105 could be detected more easily and reacted more strongly in tissues with angiogenesis.

Mab E9, a new murine anti-human monoclonal antibody, was produced by the Experimental Pathology Institute, Manchester University in early 1990's. It belongs to immunoglobulin G (IgG). Mab E9 does not react with large vessels but with microvessels in tumor tissues strongly. The series of responses of Mab E9 showed its uniqueness from other antibodies. Wang stained the vessels in breast carcinoma tissues with antibody Mab5.6E (anti-CD31) and Mab E9 (anti-CD105), and found blood vessels in or around tumor tissues stained intensely for Mab E9, whereas the same blood vessels were either weakly positive or did not stain at all for CD31. Furthermore, in most cases, unlike Mab 5.6E, Mab E9 failed to stain (a) some apparently normal blood vessels in tumor tissues and (b) a few apparently normal blood vessels in normal tissues were entrapped within a tumor mass. In several normal breast tissues, Mab E9 alone stained only a proportion of blood vessels (~20 %) that were positive for Mab 5.6E. Kumar stained CD34 and CD105 in series cryostat sections with Mab QBEND-10 and Mab E9, and found there was no relation between the two groups of MVD. The group of MVD marked with CD34 was only related to the size of tumors, while the group marked with CD105 could be the independent prognostic marker for patients with breast cancer. Further observation showed, in the same sites the native vessels were CD34 stained, and the newborn vessels were CD105 stained^[16].

Because of the heterogeneity of endothelial cells, the markers of normal endothelial cells are apparently unfit for the studies of angiogenesis in tumor tissues. The growth of tumors includes not only the increase of blood vessels in number but also the change of protein molecules in structure of ECs. An ideal EC marker for angiogenesis should detect

the newborn vessel quality as well as its quantity. Only in this way can we improve the sensitivity and credibility in detecting angiogenesis. From the above, it is reasonably believed that CD105 is a better marker of angiogenesis compared with CD34, CD31 and VIII-RA. Mab E9 increases the credibility in detecting angiogenesis. In our study, we used Mab E9 to stain MVD in malignant tumors of the gastrointestinal tract, so the credibility was high. We were able to prevent the possibility of mistaking native vessels for newborn vessels.

REFERENCES

- 1 **Griffioen AW**, Molema G. Angiogenesis: potentials for pharmacologic intervention in the treatment of cancer, cardiovascular diseases, and chronic inflammation. *Pharmacol Rev* 2000; **52**: 237-268
- 2 **De Jong JS**, van Diest PJ, van der Valk P, Baak JP. Expression of growth factors, growth-inhibiting factors, and their receptors in invasive breast cancer. II: Correlations with proliferation and angiogenesis. *J Pathol* 1998; **184**: 53-57
- 3 **Hasegawa Y**, Takanashi S, Kanehira Y, Tsushima T, Imai T, Okumura K. Transforming growth factor-beta1 level correlates with angiogenesis, tumor progression, and prognosis in patients with nonsmall cell lung carcinoma. *Cancer* 2001; **91**: 964-971
- 4 **Maehara Y**, Kakeji Y, Kabashima A, Emi Y, Watanabe A, Akazawa K, Baba H, Kohnoe S, Sugimachi K. Role of transforming growth factor-beta 1 in invasion and metastasis in gastric carcinoma. *J Clin Oncol* 1999; **17**: 607-614
- 5 **Xiong B**, Gong LL, Zhang F, Hu MB, Yuan HY. TGF beta1 expression and angiogenesis in colorectal cancer tissue. *World J Gastroenterol* 2002; **8**: 496-498
- 6 **Li C**, Hampson IN, Hampson L, Kumar P, Bernabeu C, Kumar S. CD105 antagonizes the inhibitory signaling of transforming growth factor beta1 on human vascular endothelial cells. *FASEB J* 2000; **14**: 55-64
- 7 **Calabro L**, Fonsatti E, Bellomo G, Alonci A, Colizzi F, Sigalotti L, Altomonte M, Musolino C, Maio M. Differential levels of soluble endoglin (CD105) in myeloid malignancies. *J Cell Physiol* 2003; **194**: 171-175
- 8 **Kaio E**, Tanaka S, Kitadai Y, Sumii M, Yoshihara M, Haruma K, Chayama K. Clinical significance of angiogenic factor expression at the deepest invasive site of advanced colorectal carcinoma. *Oncology* 2003; **64**: 61-73
- 9 **Song ZJ**, Gong P, Wu YE. Relationship between the expression of iNOS, VEGF, tumor angiogenesis and gastric cancer. *World J Gastroenterol* 2002; **8**: 591-595
- 10 **Li HJ**, Jing J, Zhao YB, Zhu JQ, Zhang SY, Shi ZD. Tumor angiogenesis in node-negative breast carcinoma. *Ai Zheng* 2002; **21**: 75-78
- 11 **Sauter ER**, Nesbit M, Watson JC, Klein-Szanto A, Litwin S, Herlyn M. Vascular endothelial growth factor is a marker of tumor invasion and metastasis in squamous cell carcinomas of the head and neck. *Clin Cancer Res* 1999; **5**: 775-782
- 12 **Emoto M**, Iwasaki H, Mimura K, Kawarabayashi T, Kikuchi M. Difference in the angiogenesis of benign and malignant ovarian tumors, demonstrated by analyses of color Doppler ultrasound, immunohistochemistry, and microvessel density. *Cancer* 1997; **80**: 899-907
- 13 **Fonsatti E**, Del Vecchio L, Altomonte M, Sigalotti L, Nicotra MR, Coral S, Natali PG, Maio M. Endoglin: An accessory component of the TGF-beta-binding receptor-complex with diagnostic, prognostic, and bioimmunotherapeutic potential in human malignancies. *J Cell Physiol* 2001; **188**: 1-7
- 14 **Miller DW**, Graulich W, Karges B, Stahl S, Ernst M, Ramaswamy A, Sedlacek HH, Muller R, Adamkiewicz J. Elevated expression of endoglin, a component of the TGF-beta-receptor complex, correlates with proliferation of tumor endothelial cells. *Int J Cancer* 1999; **81**: 568-572
- 15 **Bodey B**, Bodey B Jr, Siegel SE, Kaiser HE. Over-expression of endoglin (CD105): a marker of breast carcinoma-induced neovascularization. *Anticancer Res* 1998; **18**: 3621-3628
- 16 **Kumar S**, Ghellal A, Li C, Byrne G, Haboubi N, Wang JM, Bundred N. Breast carcinoma: vascular density determined using CD105 antibody correlates with tumor prognosis. *Cancer Res* 1999; **59**: 856-861

A case of pedunculated rectal carcinoid removed by endoscopic mucosal resection

Hisayuki Hamada, Saburo Shikuwa, Chun-Yang Wen, Hajime Isomoto, Kazuhiko Nakao, Kosei Miyashita, Manabu Daikoku, Koji Yano, Masahiro Ito, Yohei Mizuta, Long-Dian Chen, Zhao-Min Xu, Ikuo Murata, Shigeru Kohno

Hisayuki Hamada, Saburo Shikuwa, Kosei Miyashita, Manabu Daikoku, Koji Yano, Masahiro Ito, Institute for Clinical Research Center, WHO Collaborating Center for Reference and Research on Viral Hepatitis, National Nagasaki Medical Center, Nagasaki, Japan, Kubara 2-1001-1, Omura 852-8562, Nagasaki, Japan

Chun-Yang Wen, Department of Molecular Pathology, Atomic Bomb Disease Institute, Nagasaki University Graduate School of Biomedical Science, 1-12-4 Sakamoto, Nagasaki 852-8523, Japan

Chun-Yang Wen, Long-Dian Chen, Zhao-Min Xu, Department of Digestive Disease, Nanjing Drum Tower Hospital, Medical School of Nanjing University, Nanjing 210008, Jiangsu Province, China

Hajime Isomoto, Kazuhiko Nakao, Yohei Mizuta, Shigeru Kohno, Second Department of Internal Medicine, School of Medicine, Nagasaki University, 1-7-1 Sakamoto, Nagasaki, 852-8523 Japan

Ikuo Murata, Department of Pharmacotherapeutics, Nagasaki University, Graduate School of Biomedical Sciences, 1-14 Bunkyo-machi, Nagasaki 852-8521, Japan

Correspondence to: Chun-Yang Wen M.D Ph.D, Department of Molecular Pathology, Atomic Bomb Disease Institute, Nagasaki University Graduate School of Biomedical Science, 1-12-4 Sakamoto, Nagasaki 852-8523, Japan. cywen518@net.nagasaki-u.ac.jp
Telephone: +81-95-849-7107 **Fax:** +81-95-849-7108

Received: 2003-08-06 **Accepted:** 2003-10-23

Abstract

Carcinoid tumors generally appear as yellow/gray or tan submucosal nodules. We experienced a case of pedunculated rectal carcinoid showing a mushroom-like appearance. The case was a forty years old woman who was admitted to our hospital due to rectal bleeding. Colonoscopy revealed a pedunculated polyp presenting a mushroom-shaped appearance measuring 13 mm in diameter in the rectum. The histological diagnosis of specimens obtained by biopsy was adenocarcinoma and transanal ultrasonography revealed the tumor localization within the submucosal layer in the rectum. Endoscopic mucosal resection (EMR) was performed. Histopathological examination established the diagnosis of carcinoid tumor in the rectum. Frequencies of the pedunculated type in rectal carcinoids were reported to be 2.4 % to 7.1 % in the literature. Because of its rarity, pedunculated configuration may confuse the endoscopic diagnosis of carcinoids. Treatment for carcinoids of 1 to 1.5 cm in size remains controversial. Although such tumors are technically respectable by EMR, careful attention must be paid in dealing with these tumors because there may be unexpected behaviors of the tumors.

Hamada H, Shikuwa S, Wen CY, Isomoto H, Nakao K, Miyashita K, Daikoku M, Yano K, Ito M, Mizuta Y, Chen LD, Xu ZM, Murata I, Kohno S. A case of pedunculated rectal carcinoid removed by endoscopic mucosal resection. *World J Gastroenterol* 2003; 9 (12): 2870-2872

<http://www.wjgnet.com/1007-9327/9/2870.asp>

INTRODUCTION

Carcinoid tumors characteristically appear as yellow/gray or

tan submucosal nodules, but they are occasionally polypoid or sessile. However, there have been few reports describing a pedunculated type of carcinoid. We presented here an extremely rare case with a pedunculated rectal carcinoid showing a mushroom-like appearance, and referred to the diagnosis and treatment of this rare tumor.

CASE REPORT

A 40 years old woman was admitted to our hospital due to rectal bleeding. Physical examination and laboratory data including serum tumor markers and hormones such as urinary 5-hydroxyindoleacetic acid (5-HIAA) were normal. Barium enema contrast examination showed a fungiform polyp in the rectum. Colonoscopy revealed a pedunculated polyp presenting a mushroom-shaped appearance in the rectum (Figures 1A, B). There was a hemispherical protrusion with a shallow central erosion in the top, surrounded by a marked mucosal bulge of the edge. Magnifying endoscopy (OLYMPUS CF-type XQ240ZI, Olympus, Tokyo, Japan) revealed no absence of the pit pattern in the center and enlarged pits at the edge, corresponding to the non-structure type of the pit pattern classification proposed by Kudo *et al*^[1] (Figure 1C). Endoscopic ultrasonography (EUS), using a miniature probe (12-20 Hz) with a water-filling method, demonstrated a homogeneous hypoechoic mass, but the structure deeper than the third layer of the rectal wall was unclear (Figure 2). Therefore, we employed a soft-balloon technique using an ultrasonic probe with a balloon filled with deaerated water, which provided a clear ultrasonographic picture of the deeper part of the rectum. Judging from findings on EUS, abdominal computed tomography and chest roentgenography, there were no signs of metastasis in the regional lymph nodes or distant organs. Histology of the biopsy specimens suggested an adenocarcinoma, yielding a diagnosis of polypoid type of early rectal cancer. The depth of mural invasion was estimated to be limited to the submucosa by magnifying endoscopy and EUS. After an injection of saline in the submucosa, the lesion was excised by EMR. Macroscopically, the lesion was located in the submucosal layer. The mass was white-yellowish and solid, measuring 13 mm in diameter (Figure 3). Microscopically, the tumor was composed of small uniform cells, arranged in small nests and cords and with an anastomosing ribbon-like pattern in the submucosal layer (Figure 4). There were no atypical histopathologic features such as mitosis or nuclear atypism. Histochemically, the tumor cells possessed an argyrophil but not an argentaffin nature. Immunohistologically, the tumor cells were positive for neuron specific enolase (NSE) and chromogranin A, but were negative for p53 and Ki67. These findings established the diagnosis of carcinoid tumor in the rectum.

DISCUSSION

Carcinoid tumors are enigmatic slow growing malignancies

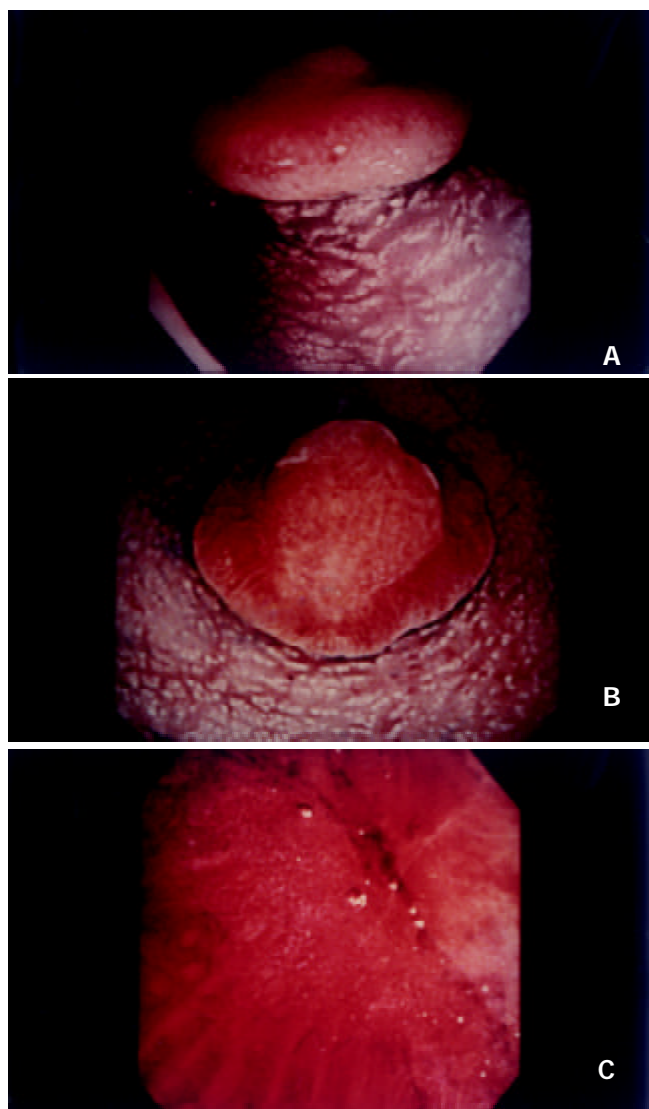


Figure 1 A: Pedunculated polypoid lesion presenting a mushroom appearance in the rectum; B: A round and shallow erosion in the center and a marked mucosal bulge at the edge of polyp; C: A non-structural pit pattern in the center with elongated pits at the edge revealed in magnifying endoscopy.

and controversy remains as to their origin^[2]. Gastrointestinal carcinoid is regarded as a tumor arising from subepithelial neuroendocrine cells or the totipotential crypt cells in the deep mucosa, usually presenting as a submucosal tumor. Therefore, endoscopic diagnosis is difficult unless biopsy provides a correct histological diagnosis. Macroscopically, a gastrointestinal carcinoid tumor appears as a yellow-gray tan nodule beneath the mucosa and develops a round or oval, sessile polyp as it grows^[3]. A pedunculated polyp of carcinoid tumor is extremely rare in the rectum. To our knowledge, only nine cases of rectal carcinoid, including the present case, have been reported^[4-9]. Frequencies of the pedunculated type in rectal carcinoids were reported to be 2.4 % to 7.1 % in the literature^[5,6]. Because of its rarity, pedunculated configuration may confuse the endoscopic diagnosis of carcinoids.

Recently, Kudo *et al.* reported the usefulness of the pit pattern observation using magnifying endoscopy and stereomicroscopy in the diagnosis of epithelial neoplasms of the large intestine^[1]. They classified the pit patterns into five types based on fine morphology of the surface, histology and size. Type V pit pattern showed an irregular or nonstructural surface, which was frequently seen in carcinomas^[1]. In this case, we misdiagnosed this tumor as carcinoma because it



Figure 2 An endoscopic ultrasonography demonstrated homogeneous hypoechoic mass.

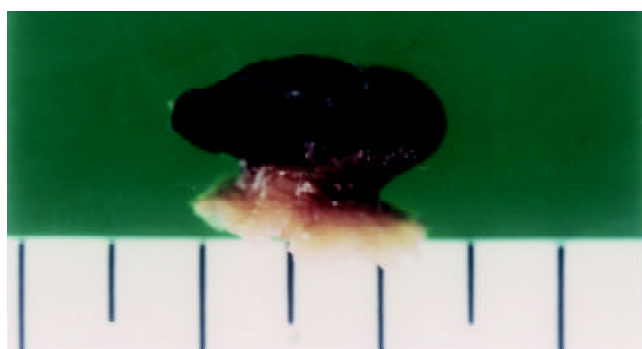


Figure 3 Gross appearance of excised polyp showing a white-yellowish and solid tumor, measuring 13×10 mm with a pedicle.

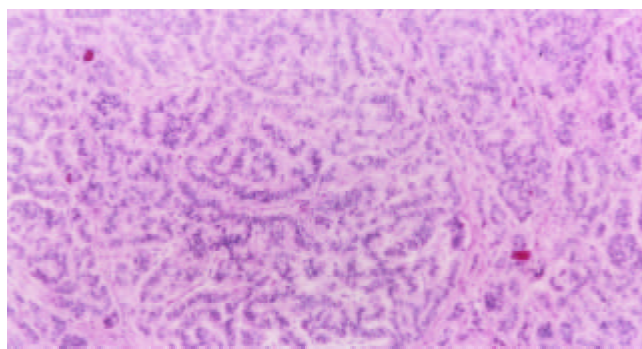


Figure 4 Histology of tumor showing small uniform cells arranged in small nests and cords with an anastomosing ribbon-like pattern in the submucosal layer.

showed the V pit pattern and pathological diagnosis of biopsy specimens was not correct. It was suggested that the carcinoid in the present case showed non-structural pit patterns because overlying mucosa of the tumor disappeared. It appears inappropriate, therefore, to use pit pattern analysis for evaluation of nature of the tumor in this case.

The size of carcinoid has been accepted as an important factor predicting its prognosis. Several surgical studies have shown that tumors less than 1 cm seldom metastasize, whereas tumors greater than 2 cm have a high incidence of metastasis^[2,3,10]. As for the risk of metastasis from rectal carcinoid, Bates *et al.* reported an incidence of 1.7 % for tumors less than 9 mm in size, 10 % for tumor of 10 to 19 mm and 82 % for tumors larger than 20 mm^[11]. It is uncertain whether gross appearance of the carcinoids is a predicting factor, although Haraguchi *et al.*^[12] reported that no metastasis was observed in pedunculated carcinoid in a review of 496 cases of rectal carcinoid.

These reports indicated that the most effective therapy for

rectal carcinoid was a complete surgical excision, particularly in tumors greater than 2 cm^[3,13]. Recently, endoscopic treatment has been applied for gastrointestinal tumors including carcinoids. Ishikawa *et al.* suggested the following indications of conventional endoscopic polypectomy for rectal carcinoid tumors. They were tumors less than 15 mm in diameter, flat tumors with normal or yellow color, tumors consisting of nodular nests or trabecular or ribbon-like structures in histology^[14]. This guideline of endoscopic treatment for rectal carcinoid may remain controversial. We do not recommend a conventional endoscopic polypectomy for common rectal carcinoid because there was a high incidence of tumor residue after treatment^[15]. Recently, endoscopic mucosal resection (EMR) has been generally accepted as a choice of treatment for rectal carcinoid tumors less than 1 cm^[9,14,16,17]. Treatment for carcinoids of 1 to 1.5 cm in size remains controversial. Although such tumors have been technically respectable by endoscopic aspiration mucosectomy using the hood technique or a ligating device^[18], careful attention must be paid to these tumors because there may be unexpected behaviors of the tumors.

The carcinoid in the present case was negative for p53 and Ki-67. Hasegawa *et al.* reported that carcinoid tumors expressing p53 and Ki-67 had a high malignant potential and metastatic activity^[4]. In future, the induction of molecular biology may be helpful in predicting the prognosis of carcinoid tumors^[19,20].

REFERENCES

- 1 **Kudo S**, Rubio CA, Teixeira CR, Kushida H, Kogure E. Pit pattern in colorectal neoplasia: endoscopic magnifying view. *Endoscopy* 2001; **33**: 367-373
- 2 **Koura AK**, Giacco GG, Curley SA, Skibber JM, Feig BW, Ellis LM. Carcinoid tumor of the rectum. *Cancer* 1997; **79**: 1294-1298
- 3 **Lauffer IM**, Zhang T, Modlin IM. Current status of gastrointestinal carcinoid. *Aliment Pharmacol Ther* 1999; **13**: 271-287
- 4 **Hasegawa O**, Iwashita A, Futami T, Kitamura K, Arima S. Pathological study of rectal carcinoid. *J the Japan society of colon Proctology* 1997; **50**: 163-176
- 5 **Ponka JL**, Walke L. Carcinoid tumor of rectum. *Dis Col Rect* 1971; **14**: 46-56
- 6 **Quan SHQ**, Bader G, Berg JW. Carcinoid of rectum. *Dis Col Rect* 1964; **7**: 197-206
- 7 **Masumori S**, Nogaki M, Ozeki T, Ktsuragi T, Koshimura Y, Higaki A, Hosoda S. The rectal carcinoid-clinicopathologic Study of five cases. *Jap J Cancer Clin* 1975; **21**: 1181-1188
- 8 **Kira J**, Fuchigami T, Murakami M, Koga A, Iwashita A. A case report of rectal carcinoid and an analysis of rectal carcinoids reported in Japan. *I to Cho(Stomach and Intestine)* 1980; **15**: 1105-1110
- 9 **Kobayashi K**, Katsumata T, Otani Y, Naka H. Diagnosis and treatment of rectal carcinoid. *Nippon Rinsho* 1991; **12**: 233-237
- 10 **Soga J**. Carcinoids of the rectum: An evaluation of 1271 reported cases. *Jpn J Surg* 1997; **27**: 112-119
- 11 **Bates HR Jr**. Carcinoid tumors of the rectum. A statistical review. *Dis. Colon Rectum* 1966; **9**: 90
- 12 **Haraguchi M**, Makiyama K, Yamakawa M, Yamasaki K, Iwanaga S, Mizuta Y, Ide T, Komori M, Tanaka T, Osabe M, Murata I, Imanishi T, Hara K. Six cases of rectal carcinoid treated by endoscopic polypectomy. *Gastroenterol Endosc* 1998; **30**: 2612-2620
- 13 **Kulke MH**, Mayer RJ. Carcinoid tumors. *N Engl J Med* 1999; **18**: 358-368
- 14 **Ishikawa H**, Imanishi K, Otani T, Okuda S, Tatsuta M, Ishiguro S. Effectiveness of endoscopic treatment of carcinoid tumors of the rectum. *Endoscopy* 1998; **21**: 133-135
- 15 **Okamoto T**, Higaki K, Kawabata K. Autopsy case of malignant carcinoid tumor of the ascending colon. *Gan No Rinsho* 1983; **29**: 1361-1365
- 16 **Fujimura Y**, Mizuno M, Takeda M, Sato I, Hoshika K, Uchida J, Kihara T, Mure T, Sano K, Moriya T. A carcinoid tumor of the rectum removed by strip biopsy. *Endoscopy* 1993; **25**: 428-430
- 17 **Higaki S**, Nishiaki M, Mitani N, Yanai H, Tada M, Okita K. Effectiveness of local endoscopic resection of rectal carcinoid tumors. *Endoscopy* 1997; **29**: 171-175
- 18 **Shikuwa S**, Matsunaga K, Osabe M, Ofukuji M, Omagari K, Mizuta Y, Takeshima F, Murase K, Otani H, Ito M, Shimokawa I, Fujii M, Kohno S. Esophageal granular cell tumor treated by endoscopic mucosal resection using a ligating device. *Gastrointest Endosc* 1998; **47**: 529-532
- 19 **Lundqvist M**, Wilander E. Subepithelial neuroendocrine cells and carcinoid tumours of the human small intestine and appendix. A comparative immunohistochemical study with regard to serotonin, neuron-specific enolase and S-100 protein reactivity. *J Pathol* 1986; **148**: 141-147
- 20 **Moyana TN**, Satkunam N. Crypt cell proliferative micronests in rectal carcinoids. An immunohistochemical study. *Am J Surg Pathol* 1993; **17**: 350-356

Edited by Wang XL

Bouveret's syndrome complicated by a distal gallstone Ileus

Rasim Gencosmanoglu, Resit Inceoglu, Caglar Baysal, Sertac Akansel, Nurdan Tozun

Rasim Gencosmanoglu, Unit of Surgery, Marmara University Institute of Gastroenterology, Istanbul, Turkey

Resit Inceoglu, Department of General Surgery, Marmara University School of Medicine, Istanbul, Turkey

Resit Inceoglu, Unit of General Surgery, Acibadem Hospital, Istanbul, Turkey

Caglar Baysal, Nurdan Tozun, Unit of Gastroenterology, Acibadem Hospital, Istanbul, Turkey

Sertac Akansel, Unit of Radiology, Acibadem Hospital, Istanbul, Turkey

Nurdan Tozun, Sub-department of Gastroenterology, Marmara University School of Medicine, Istanbul, Turkey

Correspondence to: Rasim Gencosmanoglu, M.D., Unit of Surgery, Marmara University Institute of Gastroenterology, Basibuyuk, Maltepe, PK: 53, TR-81532, Istanbul, Turkey. rgencosmanoglu@marmara.edu.tr

Telephone: +90-216-383-3057 **Fax:** +90-216-399-9912

Received: 2003-08-11 **Accepted:** 2003-10-12

Abstract

AIM: Gastric outlet obstruction caused by duodenal impaction of a large gallstone migrated through a cholecystoduodenal fistula has been referred as Bouveret's syndrome. Endoscopic lithotomy is the first-step treatment. However, surgery is indicated in case of failure or complication during this procedure.

METHODS: We report herein an 84-year-old woman presenting with features of gastric outlet obstruction due to impacted gallstone. She underwent an attempt of endoscopic retrieval which was unsuccessful and was further complicated by distal gallstone ileus. Physical examination was irrelevant.

RESULTS: Endoscopy revealed multiple erosions around the cardia, a large stone in the second part of the duodenum causing complete obstruction, and wide ulceration in the duodenal wall where the stone was impacted. Several attempts of endoscopic extraction by using foreign body forceps failed and surgical intervention was mandatory. Preoperative ultrasound evidenced pneumobilia whilst computerized tomography showed a large stone, 5×4×3 cm, logging at the proximal jejunum and another one, 2.5×2×2 cm, in the duodenal bulb causing closed-loop syndrome. She underwent laparotomy and the jejunal stone was removed by enterotomy. Another stone reported as located in the duodenum preoperatively was found to be present in the gallbladder by intraoperative ultrasound. Therefore, cholecystoduodenal fistula was broken down, the stone was retrieved and cholecystectomy with duodenal repair was carried out. She was discharged after an uneventful postoperative course.

CONCLUSION: As the simplest and the least morbid procedure, endoscopic stone retrieval should be attempted in the treatment of patients with Bouveret's syndrome. When it fails, surgical lithotomy consisting of simple enterotomy may solve the problem. Although cholecystectomy and cholecystoduodenal fistula breakdown is unnecessary

in every case, conditions may urge the surgeon to perform such operations even though they carry high morbidity and mortality.

Gencosmanoglu R, Inceoglu R, Baysal C, Akansel S, Tozun N. Bouveret's syndrome complicated by a distal gallstone Ileus. *World J Gastroenterol* 2003; 9(12): 2873-2875

<http://www.wjgnet.com/1007-9327/9/2873.asp>

INTRODUCTION

Gallstones are completely asymptomatic in the majority of patients (60 %-80 %)^[1]. When they become symptomatic, biliary colic is the most frequently encountered manifestation. Patients with mild symptoms have a higher risk of developing gallstone-related complications such as acute cholecystitis, choledocholithiasis with or without cholangitis, gallstone pancreatitis or gallstone ileus^[2]. Biliary fistula occurs in 3 % to 5 % of the cases^[3]. Gallstones can migrate into the terminal ileum through a cholecystoduodenal fistula and cause an intestinal obstruction at this level but they may also anchor at the duodenum and produce the symptoms of gastric outlet obstruction in rare cases as first described by Bouveret in 1893^[4]. Since this syndrome is usually observed in older patients with poor medical status, a non-surgical approach such as endoscopic stone removal has been used as the first-line treatment. This may be performed by simple endoscopic lithotomy with snare or specific stone baskets designed for endoscopic retrograde cholangio-pancreatography. When feasible, stones are attempted to fragment into small pieces followed by endoscopic removal. Laser lithotripsy either with percutaneous or transendoscopic routes and extracorporeal shock-wave lithotripsy (ESWL) are the alternative treatment modalities^[5-7]. In the case of unsuccessful stone removal or its distal migration resulting in mechanical intestinal obstruction, particularly with larger stones, these techniques may be ineffective and surgery may be needed. The main purpose of surgical intervention should be to remove the obstructing stone by enterotomy without cholecystectomy and cholecystoduodenal fistula breakdown to minimize the risks of surgery. However, when it is necessary as the case presented hereby, gallbladder excision can be performed successfully.

CASE REPORT

An 84-year-old woman presenting with 5 days of nausea and vomiting, hematemesis, loss of appetite, and a severe upper abdominal pain located to the periumbilical region was admitted to the emergency unit of the Marmara University Institute of Gastroenterology and referred to Acibadem Hospital according to her will. The physical examination did not show remarkable abdominal distention or any changes in bowel sounds. Abdominal ultrasound evidenced pneumobilia but the gallbladder was not visualized due to excess gas related to gastric and duodenal dilatation. Upper gastrointestinal endoscopy revealed multiple erosions around the cardia, ascribed to Mallory-Weiss syndrome, a large stone in the second part of the duodenum causing complete obstruction, and wide ulceration in the duodenal wall where the stone was

impacted (Figure 1). Although, no clear cholecystoduodenal fistula was demonstrated endoscopically, the typical appearance of the stone indicated its gallbladder origin. Attempts for mechanical fragmentation and retrieval of the stone at the same endoscopic session were unsuccessful. Computerized tomography of the abdomen showed pneumobilia, remarkable distention of stomach, and a 5 cm mass with a calcified rim in the jejunum (Figure 2A). Another mass of 2.5 cm in diameter, sharing similar radiologic features at the right upper abdominal quadrant (Figure 2B) was reported by radiologists as a second gallstone obstructing the duodenal lumen and resulting in a closed-loop syndrome.

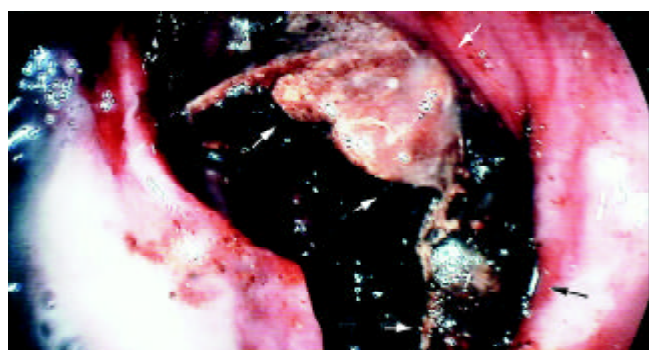


Figure 1 Endoscopic appearance of a large duodenal stone (black arrows) causing complete obstruction. Note the irregular edges of the stone (white arrows), which indicate its fragmentation.

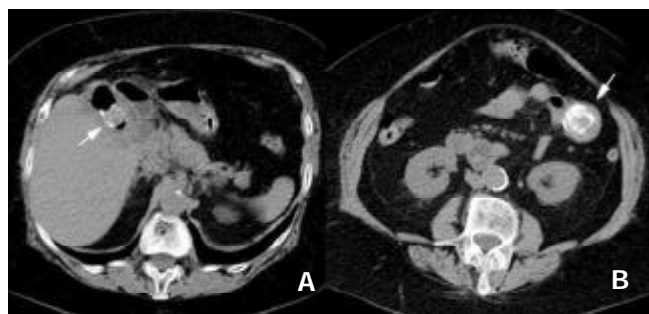


Figure 2 CT shows: A: A large, 5×3 cm, intraluminal stone (arrow) in the proximal jejunum, B: Another stone in the duodenal bulb (arrow).



Figure 4 After the adhesions between the gallbladder (arrow) and the adjacent organs were dissected, cholecystoduodenal fistula (arrow head) was broken down and then the retained stone was removed.

The features of the stone, the failure of endoscopic retrieval and the general status of the patient urged to undertake a surgical lithotripsy by laparotomy and enterotomy. At

laparotomy, the stone was palpated in the jejunum about 15 cm distal to the ligament of Treitz with a complete mechanical obstruction which was easily diagnosed with the presence of remarkable dilation of the proximal jejunal segment (Figure 3A). There were dense adhesions between the gallbladder and the duodenum, greater omentum, and right part of the transverse colon. The jejunum was opened and the large stone was removed (Figure 3B). Two small pieces of the stone were also removed from the proximal lumen (Figure 3C).

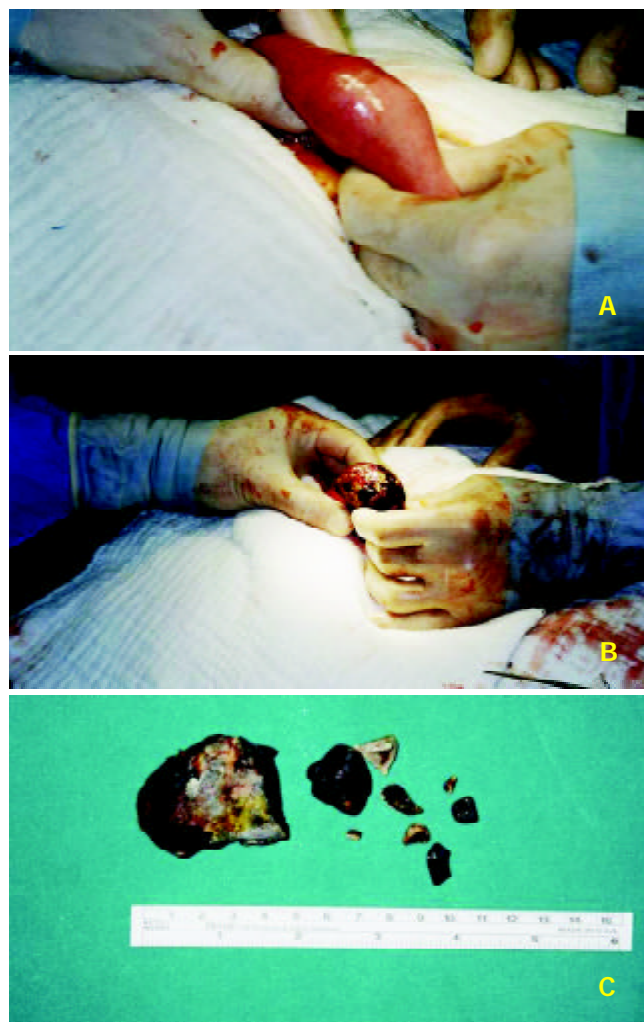


Figure 3 Intraoperative views: A: The obstructed proximal jejunal segment, note a large intraluminal stone causing complete intestinal obstruction at this level, B: Removal of the stone with enterotomy, C: Macroscopic view of the fragmented gallstone which had a very hard outer shell with a soft core.

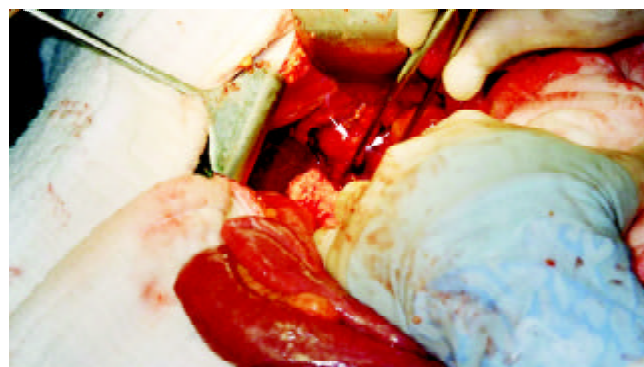


Figure 5 Intraoperative ultrasound revealed that the suspicious stone was in the gallbladder instead of the duodenal lumen.

Then the jejunum was primarily closed with double-layer running stitches of an absorbable material. Since the location of the other stone could not be detected by palpation and the subsequent operative strategy was dependent on its site, an intra-operative ultrasound was performed (Figure 4). Once the other stone was shown to be located in the gallbladder lumen, a cholecystectomy and a duodenal repair was undertaken to avoid further migration of the retained large fragment of the stone which would result in intestinal obstruction. Hence the gallbladder was opened, cholecystoduodenal fistula was broken down, and the stone was retrieved from the lumen followed by antegrade cholecystectomy (Figure 5). Duodenal lumen was also cleared from small stone fragments (Figure 3C) then the duodenal opening was closed by a transverse single-layer running stitch of an absorbable material. The post-operative period was uneventful and the patient was discharged on the eighth postoperative day. She has been symptom-free in the 3-month period of follow-up.

DISCUSSION

Bouveret's syndrome as described by gastric outlet obstruction caused by a large gallstone passing into the duodenal bulb through a biliogastric or bilioduodenal fistula usually develops in older patients with poor medical conditions and surgical treatment consisting of cholecystectomy and duodenal repair following extraction of the stone through the broken-down cholecystoduodenal fistula or a separate duodenotomy results in considerable morbidity and mortality^[8]. Developments in surgical techniques have reduced the reported mortality rate of 30 % before 1968 to 12 % in recent years. Accordingly, surgical aim has gradually shifted from a radical procedure in which the gallbladder is removed and the cholecystoduodenal fistula is repaired to a simple approach consisting of enterotomy and stone extraction. Alternatives to surgical lithotomy such as simple endoscopic lithotomy and laser or ESWL have been reported with successful outcomes in some cases^[5].

Bouveret's syndrome was reported to occur more frequently in females (65 %) with a median age of 69 years. Diagnosis is made usually during the upper GI endoscopy further supported by abdominal ultrasound findings. Computerized tomography is helpful in demonstrating the exact level of obstruction, the biliary site of duodenal fistula, and the status of gallbladder especially in cases of gallbladder rupture. Endoscopic lithotomy is the first line approach to treatment; however, it may be unsuccessful in some cases particularly with impacted large stones. Stones, usually larger than 2.5 cm in diameter, have been reported in cases with Bouveret's syndrome^[3]. Smaller stones generally pass through the duodenum and do not cause gastric outlet obstruction. Endoscopic extraction of stones up to 3 cm in size has been reported^[3]. However, larger stones usually get impacted in the duodenum and cause an ischemic ulceration on its wall. On the other hand, large gallstones of mixed type tend to have a very hard outer shell, even though their core may be softer^[5]. This feature may hamper their mechanical fragmentation with endoscopic forceps. Although these large stones can be broken down by ESWL, the irregular shape and the relatively large sizes of the fragments may hinder their passage to distal bowel, especially in the case of impacted stones. Percutaneous laser lithotripsy or Holmium: YAG laser via a flexible optic fiber through the working-channel of the endoscope, as recently reported by Alsolaiman *et al.*^[5], do not always result in success. In addition, the non-availability of these expensive equipments in most centers restricts their wide-spread use.

Many cases have been reported with migration of the stone

after unsuccessful attempts of endoscopic stone extraction or alternative lithotripsy methods. When un-fragmented stone migrates into the small bowel, its removal by a simple enterotomy is easily done. Enterotomy carries less morbidity rate when compared to duodenotomy particularly in patients with duodenal ulcer due to the erosion of duodenal wall by an impacted large stone. When the stone is broken down into several pieces by non-surgical methods and pieces are removed endoscopically, larger fragments which migrate distally can cause obstruction and require surgery. Intraoperative endoscopy may facilitate recognition and removal of remaining stones in the proximal gastrointestinal lumen. However, the presence of any remaining stone fragments in the gallbladder may critically raise the question whether the cholecystectomy is necessary or not. In the present case, the large piece of the gallstone was removed by enterotomy, but the presence of a remaining fragment, which was 2.5 cm in diameter in the gallbladder, necessitated cholecystectomy and cholecystoduodenal fistula breakdown in order to avoid any further attack as it has been reported in similar cases in the literature.

Intraoperative ultrasound is advised in cases where the surgeon is unable to localize exactly the site of the remaining stone fragments. In our case, although radiologists preoperatively reported the second stone fragment as situated in the duodenum causing closed-loop syndrome with a larger one located more distally, intraoperative ultrasound showed the remaining fragment still in the gallbladder. This finding changed our operative strategy from a simple enterotomy and stone extraction to a more complicated procedure such as cholecystectomy and duodenal wall repair.

In summary, endoscopic lithotripsy and stone extraction should be performed as a first-step treatment in patients with Bouveret's syndrome. When it fails, surgical lithotomy consisting of simple enterotomy may solve the problem. Although cholecystectomy and cholecystoduodenal fistula breakdown is not recommended routinely, especially when the patient's age and clinical status limit a more aggressive approach, they can be performed successfully when conditions force the surgeon to undertake such a decision.

REFERENCES

- 1 **Haris HW.** Biliary system. In: Norton JA, Bollinger RR, Chang AE, Lowry SF, Mulvihill SJ, Pass HI, Thompson RW, eds. *Surgery Basic Science and Clinical Evidence*. New York: Springer-Verlag 2001: 553-584
- 2 **Ahrendt SA, Pitt HA.** Biliary tract. In: Townsend CM Jr, Editor-in-Chief. *Sabiston Textbook of Surgery, The Biological Basis of Modern Surgical Practice*. Section X. Abdomen. 16th ed. Philadelphia: W.B. Saunders Company 2001: 1076-1111
- 3 **Salah-Eldin AA, Ibrahim MA, Alapati R, Muslah S, Schubert TT, Schuman BM.** The Bouveret syndrome: an unusual cause of hematemesis. *Henry Ford Hosp Med J* 1990; **38**: 52-54
- 4 **Nielsen SM, Nielsen PT.** Gastric retention caused by gallstones (Bouveret's syndrome). *Acta Chirurgica Scandinavica* 1983; **149**: 207-208
- 5 **Alsolaiman MM, Reitz C, Nawras AT, Rodgers JB, Maliakkal BJ.** Bouveret's syndrome complicated by distal gallstone ileus after laser lithotripsy using Holmium: YAG laser. *BMC Gastroenterol* 2002; **2**: 15
- 6 **Ondrejka P.** Bouveret's syndrome treated by a combination of extracorporeal shock-wave lithotripsy (ESWL) and surgical intervention. *Endoscopy* 1999; **31**: 834
- 7 **Maiss J, Hochberger J, Muehldorfer S, Keymling J, Hahn EG, Schneider HT.** Successful treatment of Bouveret's syndrome by endoscopic laser lithotripsy. *Endoscopy* 1999; **31**: S4-S5
- 8 **Malvaux P, Degolla R, De Saint-Hubert M, Farchakh E, Hauters P.** Laparoscopic treatment of a gastric outlet obstruction caused by a gallstone (Bouveret's syndrome). *Surg Endosc* 2002; **16**: 1108-1109

Icteric flare of chronic hepatitis B in a 95-year old patient

WS Wong, Wai Keung Leung, Henry L Y Chan

WS Wong, Wai Keung Leung, Henry L Y Chan, Department of Medicine and Therapeutics, the Prince of Wales Hospital, Hong Kong SAR, The Chinese University of Hong Kong

Correspondence to: Dr W K Leung, Department of Medicine and Therapeutics, 9/F, the Prince of Wales Hospital, 30-32 Ngan Shing Road, Shatin, N.T., Hong Kong. wkleung@cuhk.edu.hk

Telephone: +852-2632-3140 **Fax:** +852-2637-3852

Received: 2003-08-28 **Accepted:** 2003-10-23

Abstract

A 95-year old gentleman developed fatal icteric flare of chronic hepatitis B despite lamivudine treatment. This article highlights the atypical presentations of chronic hepatitis B in elderly patient and the need to consider this possibility for acute fulminant hepatitis in endemic areas.

Wong WS, Leung WK, Chan HLY. Icteric flare of chronic hepatitis B in a 95-year old patient. *World J Gastroenterol* 2003; 9(12): 2876-2877

<http://www.wjgnet.com/1007-9327/9/2876.asp>

CASE REPORT

A 95-year old gentleman was admitted in July 2003 for decreased appetite and reduced mobility. He enjoyed good past health and had no history of hepatitis or jaundice. Two weeks prior to admission, family members noted that he became drowsier and refused food. He was living at home with family and had no history of percutaneous exposure before admission. He had never had tattooing, blood transfusion, casual sex or illicit drug use. There was no traveling history for more than twenty years. The patient was not on any medication or herbs.

On admission, the patient was barely arousable. He could only answer simple questions. He was in deep jaundice and dehydrated. There was no stigma of chronic liver disease. Abdominal examination did not reveal any tenderness, organomegaly or ascites. Flapping tremor could not be demonstrated because the patient was in grade 3 hepatic encephalopathy.

Blood test results were compatible with the picture of severe hepatitis. The serum bilirubin level was 188 $\mu\text{mol/l}$, alkaline phosphatase was 76 IU/l (normal 40-100 IU/l), and alanine aminotransferase was 825 IU/l (normal <58 IU/l). The prothrombin time was prolonged at 18.1 seconds. Platelet count was $86 \times 10^9/\text{l}$. Renal function was normal. Urgent ultrasound scan showed normal liver echotexture and normal size spleen. The biliary trees were normal. There was no gallstone.

His hepatitis B surface antigen (HBsAg) was positive, IgM anti-hepatitis B core antigen (anti-HBc) was equivocal, hepatitis B e-antigen was negative, and antibodies to hepatitis B e-antigen (anti-HBe) was positive. Hepatitis B virus DNA was 97.9×10^6 copies/ml by TaqMan real-time polymerase chain reaction^[1]. The serology tests for hepatitis A, C, D and E viruses were negative.

Lamivudine 100 mg daily was commenced on the fourth day of admission, and supportive treatment with vitamin K, lactulose and intravenous fluids replacement were prescribed.

While the level of alanine aminotransferase was on decreasing trend, serum bilirubin and prothrombin time gradually increased (Figure 1). He developed progressive liver failure with worsening hepatic encephalopathy and eventually succumbed sixteen days after admission.

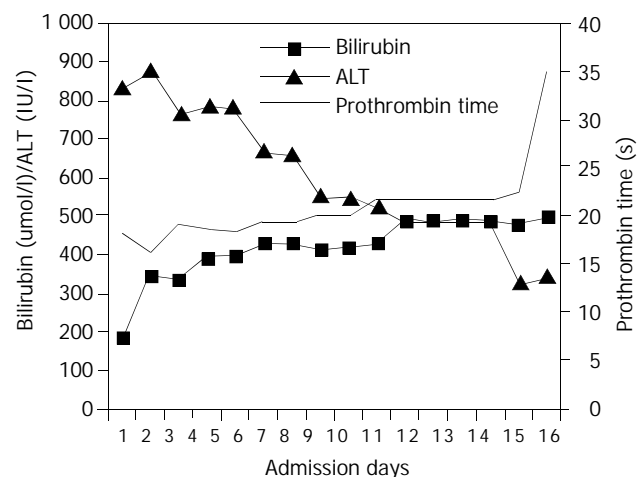


Figure 1 Serial blood results of the patient with acute flare of chronic hepatitis B. The serum bilirubin, alanine aminotransferase and prothrombin time are shown.

DISCUSSION

This case illustrates an unusual presentation of severe hepatitis B virus infection at an advanced age. Although liver biopsy has not been performed, other causes of acute hepatitis have been excluded by negative drug history and negative serology tests for other hepatitis viruses. The absence of risky percutaneous exposure renders the possibility of acute hepatitis B very unlikely. As a majority of chronic hepatitis B patients are asymptomatic and most people in Hong Kong do not have regular health check-up, it is most likely that this patient was suffering from chronic hepatitis B with HBsAg first discovered to be positive at this presentation. Equivocal IgM anti-HBc test is not diagnostic of acute hepatitis B but could also be detected in severe reactivation of chronic hepatitis B^[2].

According to most prospective series, reactivation of chronic hepatitis B typically occurred at around the second and third decades^[3-5]. Once a patient develops HBeAg seroconversion to anti-HBe, the durability reaches eighty percent. Patients often have quiescent disease afterwards, and the risks of complications, such as hepatocellular carcinoma and liver cirrhosis, are considerably reduced. Our patient probably has achieved sustained HBeAg seroconversion and disease remission several decades before this admission as he had negative HBeAg and no sign of liver cirrhosis at the age of 95. Reactivation of chronic hepatitis B causing jaundice and liver failure at this advanced age is uncommon. This case illustrates the importance to consider chronic hepatitis B as a cause of liver function derangement in endemic areas such as Asia.

Icteric reactivation of chronic hepatitis B carries a poor prognosis even with lamivudine treatment. In a series of 46

patients with severe reactivation of chronic hepatitis B with jaundice a quarter of patients died or required liver transplantation^[6]. When both independent predictors of liver-related mortality including thrombocytopenia (platelet count below $143 \times 10^9/l$) and hyperbilirubinemia (serum bilirubin greater than $172 \mu\text{mol/l}$) are present, as in our case, the mortality rate is up to 69.2 %.

In conclusion, despite atypical presentation and atypical age group, chronic hepatitis B should be considered in cases of acute fulminant hepatitis in endemic areas.

REFERENCES

- 1 **Chan HLY**, Chui AKK, Lau WY, Chan FKL, Wong ML, Tse CH, Rao ARN, Wong J, Sung JY. Factors associated with viral breakthrough in lamivudine monophylaxis of hepatitis B virus recurrence after liver transplantation. *J Med Virol* 2002; **68**: 182-187
- 2 **Maruyama T**, Schodel F, Iino S. Distinguishing between acute and symptomatic chronic hepatitis B virus infection. *Gastroenterology* 1994; **106**: 1006-1015
- 3 **McMahon BJ**, Holck P, Bulkow L, Snowball M. Serologic and clinical outcomes of 1536 Alaska natives chronically infected with hepatitis B virus. *Ann Intern Med* 2001; **135**: 759-768
- 4 **Lok AS**, Lai CL, Wu PC, Leung EK, Lam TS. Spontaneous hepatitis B e antigen to antibody seroconversion and reversion in Chinese patients with chronic hepatitis B virus infection. *Gastroenterology* 1987; **92**: 1839-1843
- 5 **Liaw YF**, Chu CM, Lin DY, Sheen IS, Yang CY, Huang MJ. Age-specific prevalence and significance of hepatitis B e antigen and antibody in chronic hepatitis B virus infection in Taiwan: a comparison among asymptomatic carriers, chronic hepatitis, liver cirrhosis, and hepatocellular carcinoma. *J Med Virol* 1984; **13**: 385-391
- 6 **Chan HL**, Tsang SW, Hui Y, Leung NW, Chan FK, Sung JJ. The role of lamivudine and predictors of mortality in severe flare-up of chronic hepatitis B with jaundice. *J Viral Hepat* 2002; **9**: 424-428

Edited by Wang XL

• CASE REPORT •

Pseudoaneurysm of gastroduodenal artery following radical gastrectomy for gastric carcinoma patients

Dong Yi Kim, Jae Kyoong Joo, Seong Yeob Ryu, Young Jin Kim, Shin Kon Kim, Yong Yeon Jung

Dong Yi Kim, Jae Kyoong Joo, Seong Yeob Ryu, Young Jin Kim, Shin Kon Kim, Division of Gastroenterologic Surgery, Department of Surgery, Chonnam National University Medical School, Gwangju, Korea

Yong Yeon Jung, Department of Radiology, Chonnam National University Medical School, Gwangju, Korea

Correspondence to: Dong Yi Kim, M.D. Division of Gastroenterologic Surgery, Department of Surgery, Chonnam National University Medical School, 8 Hakdong, Dongku, Gwangju 501-757, Korea. dockim@chonnam.ac.kr

Telephone: +82-62-220-6450 **Fax:** +82-62-227-1635

Received: 2003-08-28 **Accepted:** 2003-10-07

Abstract

We report a rare case of a postoperative pseudoaneurysm of the gastroduodenal artery following radical gastrectomy. Surgical trauma to the gastroduodenal artery during regional lymphadenectomy was considered the cause of the postoperative pseudoaneurysm. The pseudoaneurysm was successfully managed by ligating the bleeding vessel. We should consider the possibility of pseudoaneurysm formation in a patient with gastrointestinal bleeding in the postoperative period following radical gastrectomy with regional lymph node and perivascular lymphatic dissection.

Kim DY, Joo JK, Ryu SY, Kim YJ, Kim SK, Jung YY. Pseudoaneurysm of gastroduodenal artery following radical gastrectomy for gastric carcinoma patients. *World J Gastroenterol* 2003; 9(12): 2878-2879

<http://www.wjgnet.com/1007-9327/9/2878.asp>

INTRODUCTION

The causes of pseudoaneurysms include infection, trauma, and surgical procedures^[1]. The development of pseudoaneurysms after upper abdominal surgery is rare, and most occur after biliary and pancreatic surgery^[2-5]. There have been only a few reported cases of postoperative pseudoaneurysm of an artery following abdominal surgery. We recently encountered a patient with a ruptured pseudoaneurysm of the gastroduodenal artery following radical gastrectomy for gastric carcinoma.

CASE REPORT

A 73-year-old male was admitted with a two-month history of epigastric discomfort and weight loss. An upper gastrointestinal series, endoscopy, and abdominal CT scan suggested gastric carcinoma. The preoperative laboratory work-up was normal.

Laparotomy revealed an advanced gastric carcinoma involving the adjacent lymph nodes. No peritoneal dissemination or hepatic metastasis was found. The patient underwent a successful radical gastrectomy and the regional lymph nodes, and perivascular lymphatics surrounding the gastroduodenal artery were dissected.

Macroscopically, a curative resection was performed.

Postoperative microscopic examination revealed poorly differentiated adenocarcinoma involving the serosal layer of the stomach, and metastasis in one of the twenty-eight lymph nodes dissected.

On postoperative day eight, a wound infection with moderate fever developed, and examination of the anastomotic site revealed no leakage. Twenty-five days after the operation, he suddenly developed abdominal distention with hypovolemic shock. A tentative diagnosis of hemoperitoneum was made and an emergency angiography was performed. An emergency celiac trunk arteriogram revealed a pseudoaneurysmal sac originating from the gastroduodenal artery (Figure 1). To obliterate the pseudoaneurysm transcatheter embolization with steel coils was attempted (Figure 2), but failed. We performed an emergent laparotomy. There was a large hematoma around the gastroduodenal artery. The gastroduodenal artery was allegedly ligated. The patient recovered and was discharged from the hospital two weeks later. He had no subsequent bleeding episodes and was doing well two months following discharge.

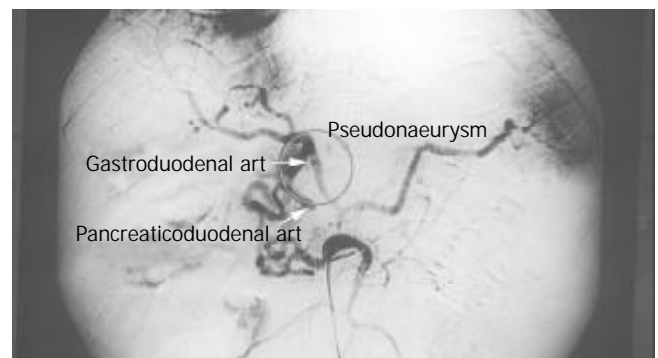


Figure 1 Anterior-posterior view of the superior mesenteric arteriogram showing a pseudoaneurysmal sac originating from the gastroduodenal artery.

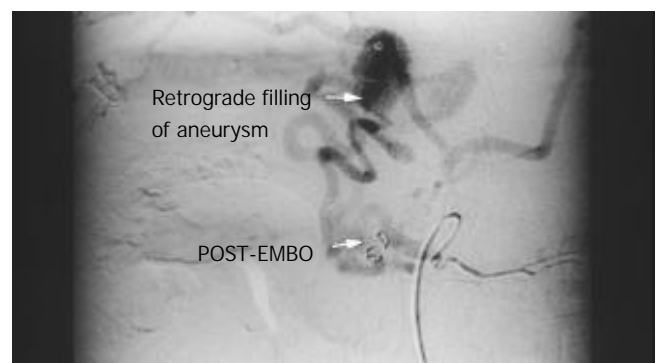


Figure 2 Superior mesenteric arteriogram after embolization shows the pseudoaneurysmal sac by retrograde filling.

DISCUSSION

Pseudoaneurysms result from a variety of mechanisms,

including infection, trauma, and surgical procedures^[1]. All have in common disruption of arterial continuity with extravasation of blood into the surrounding tissues. This ultimately results in the formation of a fibrous tissue capsule that progressively enlarges due to the unrelenting arterial pressure^[1]. Gastroduodenal artery aneurysms account for 1.5 % of all splanchnic artery aneurysms, but the true incidence of postoperative pseudoaneurysm of the gastroduodenal artery is unknown^[6]. Postoperative pseudoaneurysm formation is uncommon, but can follow surgical trauma during gastrointestinal surgery or perioperative local infection^[2,7,8]. There is usually a history of massive bleeding and perioperative local infection when the pseudoaneurysm develops^[2]. Our patient had a local wound infection and massive intra-abdominal bleeding.

Our review of the literature revealed no reported cases of postoperative pseudoaneurysm of the gastroduodenal artery following radical gastrectomy. We assumed that the pseudoaneurysm formation had been caused by a weakness in the arterial wall according to skeletonization resulting from lymphadenectomy.

When an intra-abdominal pseudoaneurysm is suspected, angiography is useful for determining the exact location of the pseudoaneurysm. In addition, it can save time and prevent the danger of an emergency laparotomy to locate the source of bleeding without angiography^[9]. In our case, emergent angiography was performed after the episode of massive intra-abdominal bleeding and demonstrated a pseudoaneurysm arising from the gastroduodenal artery. Many authors^[4,6,9-11] have recommended transcatheter occlusion or selective embolization as a useful method in high-risk patients. Basile *et al.*^[12], Bulut *et al.*^[13] and Furukawa *et al.*^[14], reported successful transcatheter arterial embolization in a patient who developed pseudoaneurysm after abdominal surgery. We tried transcatheter arterial embolization, but failed to control the bleeding.

Although it is impossible to know the true incidence of postoperative pseudoaneurysm of the gastroduodenal artery, it may develop due to iatrogenic injury during surgery^[4,15].

We should consider the possibility of pseudoaneurysm formation in a patient with intra-abdominal bleeding during the postoperative period following radical gastrectomy with regional lymph nodes and perivascular lymphatic dissection.

This report describes the successful management of a pseudoaneurysm of the gastroduodenal artery following radical gastrectomy, by ligation of the bleeding vessel.

REFERENCES

- 1 **Clark ET**, Gewertz BL. Pseudoaneurysms. In: Rutherford RB(ed): Vascular Surgery. 4th ed. Philadelphia: *W B Saunders* 1995: 1153-1161
- 2 **Iseki M**, Tada Y, Wada T, Nobori M. Hepatic artery aneurysm. Report of a case and review of the literature. *Jpn J Gastroenterol* 1983; **18**: 84-92
- 3 **Tan M**, Di Carlo A, Stein LA, Cantarovich M, Tchervenkov JI, Metrakos P. Pseudoaneurysm of the superior mesenteric artery after pancreas transplantation treated by endovascular stenting. *Transplantation* 2001; **72**: 336-338
- 4 **Sugimoto H**, Kaneko T, Ishiguchi T, Takai K, Ohta T, Yagi Y, Inoue S, Takeda S, Nakao A. Delayed rupture of a pseudoaneurysm following pancreaticoduodenectomy: Report of a case. *Surg Today* 2001; **31**: 932-935
- 5 **Almogy G**, Bloom A, Verstandig A, Eid A. Hepatic artery pseudoaneurysm after liver transplantation. *Transpl Int* 2002; **15**: 53-55
- 6 **Eckhauser FE**, Stanley JC, Zelenock GB, Borlaza GS, Freier DT, Lindenauer SM. Gastroduodenal and pancreaticoduodenal artery aneurysms: A complication of pancreatitis causing spontaneous gastrointestinal hemorrhage. *Surgery* 1980; **88**: 335-344
- 7 **Kelley CJ**, Hemingway AP, McPherson GA, Allison DJ, Blumgart LH. Non-surgical management of post-cholecystectomy haemobilia. *Br J Surg* 1983; **70**: 502-504
- 8 **Aranha GV**, O'Neil S, Borge MA. Successful nonoperative management of bleeding hepatic artery pseudoaneurysm following pancreaticoduodenectomy. *Dig Surg* 1999; **16**: 528-530
- 9 **Stabile BE**, Wilson SE, Debas HT. Reduced mortality from bleeding pseudocysts and pseudoaneurysm caused by pancreatitis. *Arch Surg* 1983; **118**: 45-51
- 10 **Kuno RC**, Althaus SJ, Glickerman DJ. Direct percutaneous coil and ethanol embolization of a celiac artery pseudoaneurysm. *J Vasc Interv Radiol* 1995; **6**: 357-360
- 11 **Kitagawa T**, Iriyama K, Azuma T, Yamakado K. Nonoperative treatment for a ruptured pseudoaneurysm of the celiac trunk: report of a case. *Surg Today* 1997; **27**: 1069-1073
- 12 **Basile A**, Boullosa-Seoane E, Dominguez-Viguera L, Certo A, Casal-Rivas M. Percutaneous embolization of a gastroduodenal artery aneurysm secondary to antrectomy and Roux en Y reconstruction. *Radiol Med* 2002; **104**: 374-377
- 13 **Bulut T**, Yamaner S, Bugra D, Akyuz A, Acarli K, Poyanli A. False aneurysm of the hepatic artery after laparoscopic cholecystectomy. *Acta Chir Belg* 2002; **102**: 459-463
- 14 **Furukawa H**, Kosuge T, Shimada K, Yamamoto J, Ushino K. Helical CT of the abdomen after pancreaticoduodenectomy: Usefulness for detecting postoperative complications. *Hepatogastroenterology* 1997; **44**: 849-855
- 15 **Satoh H**, Morisaki T, Kishikawa H. A case of a postoperative aneurysm of the common hepatic artery which ruptured into the remnant stomach after a radical gastrectomy. *Jpn J Surg* 1989; **19**: 241-245

Edited by Zhu LH

Surgical resection of duodenal lymphangiectasia: A case report

Chih-Ping Chen, Yee Chao, Chung-Pin Li, Wen-Ching Lo, Chew-Wun Wu, Shyh-Haw Tsay, Rheun-Chuan Lee, Full-Young Chang

Chih-Ping Chen, Chung-Pin Li, Wen-Ching Lo, Full-Young Chang, Division of Gastroenterology, Department of Medicine, Taipei Veterans General Hospital and Institute of Clinical Medicine, National Yang-Ming University School of Medicine, Taipei, Taiwan, China

Yee Chao, Cancer Center, Taipei Veterans General Hospital and National Yang-Ming University School of Medicine, Taipei, Taiwan, China

Chew-Wun Wu, Division of General Surgery, Department of Surgery, Taipei Veterans General Hospital and National Yang-Ming University School of Medicine, Taipei, Taiwan, China

Shyh-Haw Tsay, Department of Pathology, Taipei Veterans General Hospital and National Yang-Ming University School of Medicine, Taipei, Taiwan, China

Rheun-Chuan Lee, Department of Radiology, Taipei Veterans General Hospital and National Yang-Ming University School of Medicine, Taipei, Taiwan, China

Correspondence to: Chung-Pin Li, Division of Gastroenterology, Department of Medicine, Taipei Veterans General Hospital, No. 201, Sec. 2, Shih-Pai Road, Taipei, 11217, Taiwan, China. cpli@vghtpe.gov.tw

Telephone: +86-2-28757308 **Fax:** +86-2-28739318

Received: 2003-08-26 **Accepted:** 2003-10-12

Abstract

Intestinal lymphangiectasia, characterized by dilatation of intestinal lacteals, is rare. The major treatment for primary intestinal lymphangiectasia is dietary modification. Surgery to relieve symptoms and to clarify the etiology should be considered when medical treatment failed. This article reports a 49-year-old woman of solitary duodenal lymphangiectasia, who presented with epigastralgia and anemia. Her symptoms persisted with medical treatment. Surgery was finally performed to relieve the symptoms and to exclude the existence of underlying etiologies, with satisfactory effect. In conclusion, duodenal lymphangiectasia can present clinically as epigastralgia and chronic blood loss. Surgical resection may be resorted to relieve pain, control bleeding, and exclude underlying diseases in some patients.

Chen CP, Chao Y, Li CP, Lo WC, Wu CW, Tsay SH, Lee RC, Chang FY. Surgical resection of duodenal lymphangiectasia: A case report. *World J Gastroenterol* 2003; 9(12): 2880-2882
<http://www.wjgnet.com/1007-9327/9/2880.asp>

INTRODUCTION

Intestinal lymphangiectasia (IL) is a rare condition with widely variable symptoms and signs. Patients may be asymptomatic or present as vague abdominal pain, chronic diarrhea, steatorrhea, edema, chylous pleural effusion, ascites, hypoproteinemia, lymphocytopenia or protein-losing enteropathy^[1,2]. IL usually occurs in children or young adults, and is suspected to be caused by a congenital abnormality in the lymphatic system^[1-3]. Occasionally, IL can be seen in the aged people, which may be secondary to disorders causing

lymphatic obstruction, such as lymphoma, carcinoma, tuberculosis, constrictive pericarditis, retroperitoneal fibrosis, post-radiation effects, and repeated parasite infestation^[1,4-6]. Diagnosis depends on characteristic endoscopic findings and pathological features^[7-9]. However, it is sometimes difficult to differentiate primary from secondary IL. Surgical intervention may be a final resort to make a definite diagnosis and to relieve symptoms. Herein, we present a case with a solitary duodenal lymphangiectasia presenting as epigastralgia and chronic blood loss. The patient finally received surgical intervention and the symptoms resolved.

CASE REPORT

A 49-year-old woman was admitted to our hospital in February 1999 with progressive epigastralgia and malaise for 2 months. She had been well in the past and denied family history of systemic disorders. Physical examination showed mild anemic conjunctivae and tarry stool. There was no evidence of significant enteric protein loss.

Complete blood count revealed mild normocytic normochromic anemia (hemoglobin 10.5 g/dL). Stool examination disclosed positive occult blood (+++). Serum biochemistries as well as serum concentrations of immunoglobulins and tumor markers, including α -fetoprotein, carcinoembryonic antigen, carbohydrate antigen 19-9, and carbohydrate antigen-125, were all within normal limits. Urinary excretion of 5-hydroxyindoleacetic acid (5-HIAA) was normal. Upper gastrointestinal endoscopy showed a 3 cm irregular elevation with bulging border, superficial whitish spots, as well as hemorrhagic and friable mucosa in the second portion of duodenum (Figure 1a). Histological examination showed prominent, dilated lymphatic vessels in the mucosal and submucosal layers (Figure 1b). Upper gastrointestinal barium radiography demonstrated a cluster of polypoid filling defects, 3×3 cm in size, in the second portion of duodenum (Figure 1c). Abdominal sonography and computerized tomography (CT) showed no obvious abnormalities. Small intestine series and barium enema did not disclose any lesion. Antacids and a low-fat, high-protein diet supplemented with medium-chain triglycerides were prescribed for one month with no obvious improvement.

For treating refractory epigastralgia and chronic bleeding and excluding underlying diseases, the modified Whipple's operation with pylorus preservation was carried out in March 1999. A polypoid lesion in the second portion of the duodenum, 3×3 cm in size, was found 1 cm lateral to the papilla of Vater (Figure 1d). Pathological examination confirmed it to be an idiopathic lymphangiectasia. No underlying etiologies could be identified. After operation, the patient recovered well. Epigastralgia resolved and the blood hemoglobin returned to normal after surgery and during the later four-years' follow-up.

DISCUSSION

Intestinal lymphangiectasia has been well recognized as a disorder characterized by dilated lymphatic vessels of the gastrointestinal tract, especially the small intestine^[1-3]. It is a

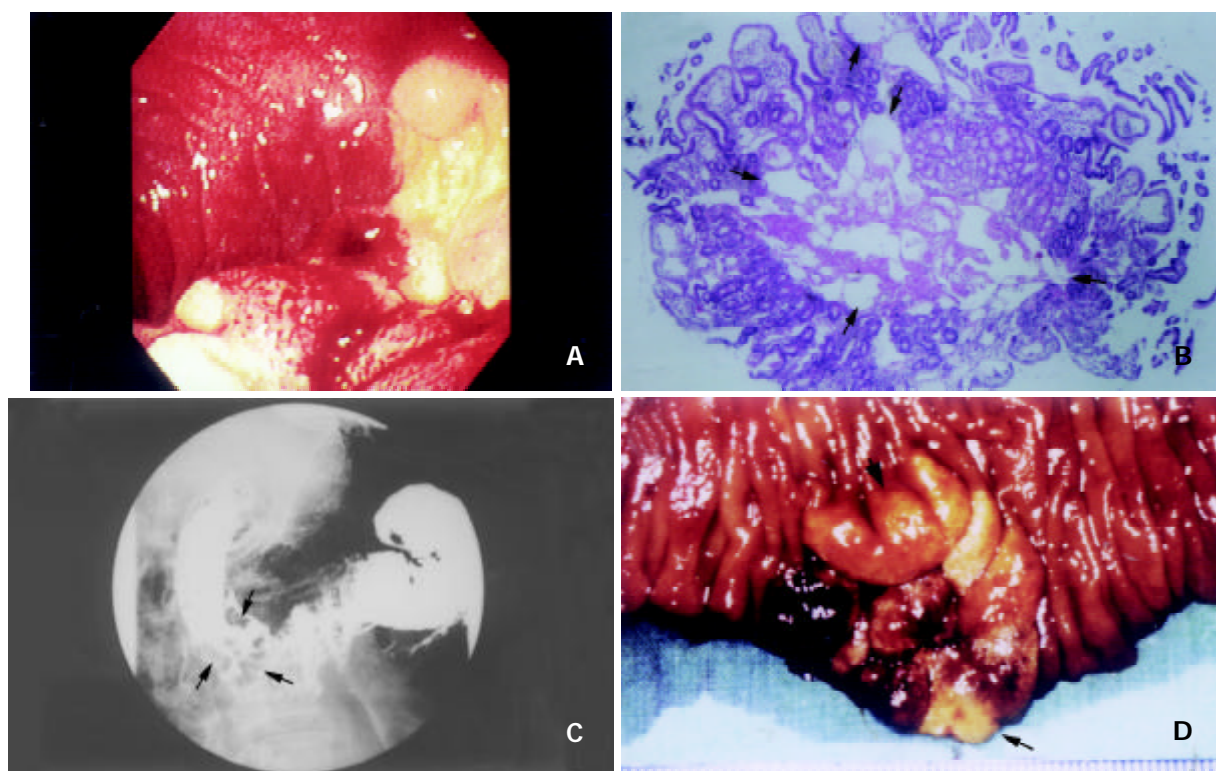


Figure 1 (a) Panendoscopy revealed a 3 cm irregular elevated lesion with whitish spots on the surface and a central crater with blood-coating in the second portion of duodenum. (b) Histology of the endoscopic biopsy showed prominent dilatation of intramucosal and submucosal lymphatic ducts (arrows), a picture of intestinal lymphangiectasia (Hematoxylin and eosin, $\times 40$). (c) Upper gastrointestinal series demonstrated a cluster of polypoid filling defects, 3 \times 3 cm in size, in the second portion of the duodenum (arrows). (d) Gross appearance of the surgical specimen revealed a sessile polypoid lesion, 3 cm in diameter, in the second portion of the duodenum (arrows).

rare condition related to fat malabsorption and protein-losing enteropathy. Distribution of IL can be segmented, multifocal or diffuse. The pathogenesis is believed to be due to obstruction of lymphatic drainage^[1-3]. According to the etiologies, IL can be classified into primary and secondary forms^[1,2]. Primary IL is usually associated with many genetic syndromes, such as Turner's syndrome^[2,10]. On the contrary, secondary IL is acquired, due to several kinds of gastrointestinal diseases and intra-abdominal or retroperitoneal pathologies, such as carcinoma, lymphoma, tuberculosis or constrictive pericarditis^[1,4-6].

Clinical manifestations are similar in both forms of IL, but with variable severity according to the extent of involvement. Some patients can be completely asymptomatic, while at the other extreme, some may be associated with protein-losing enteropathy, growth retardation, or recurrent gastrointestinal tract bleeding^[1,2,11]. The protein loss is suspected to be due to rupture of the dilated intramucosal or submucosal lacteals, or exudation from the epithelium^[3]. The hemorrhage may be due to rupture of the dilated lacteals, which have potential communications with blood vessels^[11].

Diagnosis depends on clinical suspicion. Specific endoscopic findings, accompanied by typical histological pictures can draw into the diagnosis^[7]. These endoscopic findings include white-tipped villi, scattered white spots, white nodules, and submucosal elevations^[7-9]. Typical histological pictures consist of dilated intramucosal and submucosal lacteals^[7-9]. CT scan can help to find the underlying causes of secondary IL^[12].

Treatment of IL depends on the severity and extent of involvement. For most patients with primary IL, due to generalized abnormalities and diffuse distribution, dietary modification with a low-fat, high-protein diet and supplementation of medium-chain triglycerides (MCT) is the mainstay of treatment^[1,2]. As MCT is absorbed from the

portal venous system directly rather than via lymphatics, it may avoid engorgement of the lymphatics, and thus reduce the opportunity for rupture^[2]. On the other hand, for patients with secondary IL, the underlying diseases should be treated. Surgical resection can be chosen when IL is confined to a segment of the intestine and has successfully treated protein-losing enteropathy, anemia or abdominal pain in intestine lymphangiectasia^[2,13-15].

In this case, an irregularly elevated lesion in the second portion of the duodenum combined with epigastralgia and chronic blood loss was found. Biopsies showed a picture of IL, however, secondary IL could not be excluded. Due to segmental involvement and to rule out underlying causes, surgical resection was performed. The symptoms were relieved and a definite diagnosis of idiopathic duodenal IL was made. In conclusion, surgical resection may be chosen to relieve symptoms and exclude underlying diseases in patients with solitary duodenal IL.

REFERENCES

- 1 **Rubin DC**. Small intestine: anatomy and structural anomalies In: Yamada T, ed. Textbook of gastroenterology. 3rd ed. Philadelphia: Lippincott Williams Wilkins 1999: 1578-1579
- 2 **Vardy PA**, Lebenthal E, Shwachman H. Intestinal lymphangiectasia: a reappraisal. *Pediatrics* 1975; **55**: 842-851
- 3 **Waldmann TA**, Steinfeld JL, Dutcher TF, Davidson JD, Gordon RS Jr. The role of the gastrointestinal system in "idiopathic hypoproteinemia." *Gastroenterology* 1961; **41**: 197-207
- 4 **Nelson DL**, Blaese RM, Strober W, Bruce R, Waldmann TA. Constrictive pericarditis, intestinal lymphangiectasia, and reversible immunologic deficiency. *J Pediatr* 1975; **86**: 548-554
- 5 **Rao SS**, Dundas S, Holdsworth CD. Intestinal lymphangiectasia secondary to radiotherapy and chemotherapy. *Dig Dis Sci* 1987;

- 32:** 939-942
- 6 **Oksuzoglu G**, Aygencel SG, Haznedaroglu IC, Arslan M, Bayraktar Y. Intestinal lymphangiectasia due to recurrent giardiasis. *Am J Gastroenterol* 1996; **91**: 409-410
- 7 **Abramowsky C**, Hupertz V, Kilbridge P, Czinn S. Intestinal lymphangiectasia in children: a study of upper gastrointestinal endoscopic biopsies. *Pediatr Pathol* 1989; **9**: 289-297
- 8 **Riemann JF**, Schmidt H. Synopsis of endoscopic and other morphological findings in intestinal lymphangiectasia. *Endoscopy* 1981; **13**: 60-63
- 9 **Aoyagi K**, Iida M, Yao T, Matsui T, Okada M, Oh K, Fujishima M. Characteristic endoscopic features of intestinal lymphangiectasia: correlation with histological findings. *Hepatogastroenterology* 1997; **44**: 133-138
- 10 **Rutlin E**, Wisloff F, Myren J, Serck-Hanssen A. Intestinal telangiectasia in Turner's syndrome. *Endoscopy* 1981; **13**: 86-87
- 11 **Perisic VN**, Kokai G. Bleeding from duodenal lymphangiectasia. *Arch Dis Child* 1991; **66**: 153-154
- 12 **Fakhri A**, Fishman EK, Jones B, Kuhajda F, Siegelman SS. Primary intestinal lymphangiectasia: clinical and CT findings. *J Comput Assist Tomogr* 1985; **9**: 767-770
- 13 **Kingham JG**, Moriarty KJ, Furness M, Levison DA. Lymphangiectasia of the colon and small intestine. *Br J Radiol* 1982; **55**: 774-777
- 14 **Jameson JS**, Boyle JR, Jones L, Rees Y, Kelly MJ. An unusual presentation of intestinal lymphangiectasia. *Int J Colorect Dis* 1996; **11**: 198-199
- 15 **Persic M**, Browse NL, Prpic I. Intestinal lymphangiectasia and protein losing enteropathy responding to small bowel resection. *Arch Dis Child* 1998; **78**: 194

Edited by Zhu LH

• CASE REPORT •

Life-threatening hemobilia caused by hepatic artery pseudoaneurysm: A rare complication of chronic cholangitis

Tsu-Te Liu, Ming-Chih Hou, Han-Chieh Lin, Full-Young Chang, Shou-Dong Lee

Tsu-Te Liu, Ming-Chih Hou, Han-Chieh Lin, Full-Young Chang, Shou-Dong Lee, Division of Gastroenterology, Department of Medicine, Taipei-Veterans General Hospital, and School of Medicine, National Yang Ming University, Taipei, Taiwan

Supported by in part, grant VGH-91-A-17 from the Taipei-Veterans General Hospital

Correspondence to: Ming-Chih Hou, M.D., Division of Gastroenterology, Department of Medicine, Veterans General Hospital, No 201, Sec 2, Shih-Pai Road, Taipei 11217, Taiwan. mchou@vghtpe.gov.tw

Telephone: +86-2-2875-7308 **Fax:** +86-2-2873-9318

Received: 2003-06-04 **Accepted:** 2003-08-19

Abstract

Hemobilia is one of the causes of obscure gastrointestinal haemorrhage. Most cases of hemobilia are of iatrogenic or traumatic origin. Hemobilia caused by a hepatic artery pseudoaneurysm due to ascending cholangitis is very rare and its mechanism is unclear. We report a 74-year-old woman with a history of surgery for choledocholithiasis 30 years ago, suffering from a protracted course of life-threatening gastrointestinal bleeding. A small intestines series and endoscopic retrograde cholangiopancreatography revealed a chronic cholangitis with marked contrast reflux into the biliary tree. Angiography confirmed the bleeding from a pseudoaneurysm of the middle hepatic artery. Coil embolization achieved successful hemostasis. We discussed the mechanism and reviewed the literature.

Liu TT, Hou MC, Lin HC, Chang FY, Lee SD. Life-threatening hemobilia caused by hepatic artery pseudoaneurysm: A rare complication of chronic cholangitis. *World J Gastroenterol* 2003; 9(12): 2883-2884

<http://www.wjgnet.com/1007-9327/9/2883.asp>

INTRODUCTION

Hemobilia, a phenomenon of bleeding into the biliary tree, is an unusual cause of obscure upper gastrointestinal bleeding. Most of the etiologies of hemobilia are iatrogenic or traumatic in origin^[1]. An hepatic artery aneurysm is a rare vascular lesion that accounts for nearly 10 % of hemobilia cases^[2], and is mostly due to atherosclerosis or trauma^[3,4]. A hepatic artery aneurysm due to biliary inflammation is less frequent and usually attributed to parasites or stone obstruction in the biliary tract^[5]. Inflammatory causes of hemobilia in the Far East are mainly due to parasitic infections, such as ascariasis or clonorchiasis, which have the tendency to invade the bile ducts and induce bleeding. Impacted stones may also erode the biliary mucosa and lead to bleeding. Severe hemobilia is rare, but can occur when a large stone erodes vessels of the hepatoduodenal ligament or the cystic artery^[6]. In contrast, hemobilia caused by reflux cholangitis without stones or parasitic infection, has not yet been reported and its mechanism is unclear. We present a case of life-threatening hemobilia from an hepatic pseudoaneurysm, complicated by reflux cholangitis due to previous biliary surgery.

CASE REPORT

A 74-year-old woman had a history of biliary stones and received a cholecystectomy, hepatic lateral segmentectomy and sphincterotomy over 30 years ago. In March 2001, she developed intermittent tarry stools and dizziness for one week and came to our hospital. At the emergency room, her blood pressure was 99/35 mmHg and her pulse rate was 93/minute. Physical examination showed a pale conjunctiva and mild epigastric tenderness. A hemogram showed microcytic hypochromic anemia with a hemoglobin level of 7.6 g/dl. An emergent gastro-duodenal endoscopy disclosed gastric ulcers near the angularis. Proton pump inhibitor therapy was started. On the third hospital day, massive hematemesis with hypovolemic shock occurred. An emergent endoscopy did not disclose any evidence of recent bleeding from the gastric ulcers, but a lot of fresh blood in the duodenal bulb and beyond was observed. An immediate angiography, Tc-99m-RBC scan, and colonoscopy all returned negative findings. An abdominal CT did not display any abnormal lesions. A small intestines series did not disclose any abnormal lesions, except an obvious contrast medium reflux from the duodenum into biliary tree (Figure 1).



Figure 1 Small intestines series show chronic cholangitis with obvious contrast medium reflux into the biliary tree (arrow).

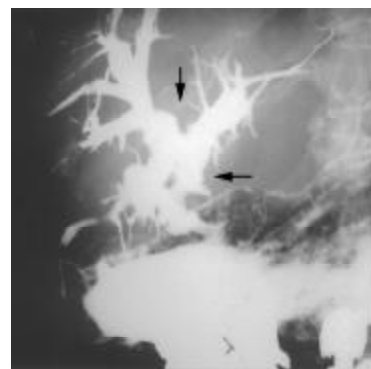


Figure 2 Angiography shows a small pseudoaneurysm (arrow) over the middle hepatic artery. Injecting the contrast medium into the middle hepatic artery opacified the intrahepatic biliary duct (arrowheads).

In the following days, intermittent tarry stools continued to pass. She suffered from upper abdominal pain before every bleeding episode. On the 16th day of admission, she had another massive hematochezia with hypovolemic shock. This time, the emergent endoscopy showed fresh blood flowing from the orifice of the ampulla of Vater. Endoscopic retrograde cholangiopancreatography found widening of the papillary orifice and amorphous filling defects of blood clots retained in the irregular and dilated biliary trees. An angiography showed a small pseudoaneurysm over the middle hepatic artery. Injection of a contrast medium into the middle hepatic artery also opacified the intrahepatic biliary ducts (Figure 2). A coil embolization was performed smoothly and no more event of hemobilia has been reported after this procedure.

DISCUSSION

There were many etiologies for hemobilia such as iatrogenic and accidental trauma, gallstones, inflammation, vascular malformations and tumours^[1]. Because interventional procedures and laparoscopic cholecystectomy were used more to manage hepatobiliary disorders, iatrogenic origins were the more frequent etiology for hemobilia^[1].

Hemobilia due to a hepatic artery aneurysm only accounted for 10 % of cases^[2], and was mostly due to atherosclerosis or trauma^[3,4]. Hepatic artery aneurysms due to biliary inflammation were usually attributed to parasites or stone obstruction in the biliary tract^[5], and rarely due to non-obstructive inflammations, as in this case. After sphincterotomy, biliary reflux of the duodenal chyme was observed in most patients, aerobilia in half and bactibilia in all^[7,8]. Infected bile may lead to cholangitis in more than 1 % of them^[9]. Although such a reflux might not always produce clinical symptoms, the biochemical changes suggested that there might be some degree of continuing low-grade damage within the liver parenchyma. Twenty percent of asymptomatic patients undergoing an endoscopic sphincterotomy for biliary stones still had persistent subclinical injury to the biliary tract^[10]. Liver biopsy showed periportal fibrosis and inflammation^[10]. The bile ducts were richly supplied by the hepatic artery, which forms a peri-biliary vascular plexus^[11]. As the inflammation proceeds and involves the collateral hepatic artery, a pseudoaneurysm forms and raises the risk of hemobilia.

The most common symptoms of hemobilia are upper gastrointestinal haemorrhage, upper abdominal pain, and jaundice. These occurred in 73 %, 52 %, and 30 % of cases, respectively, although the complete triad occurred in only 22 % of the them^[1]. For patients with upper gastrointestinal bleeding, an endoscopy is the first step. If blood or clotting is seen at the ampulla of Vater, hemobilia is the likely cause of the haemorrhage. However, only 12 % of these endoscopies might be diagnostic^[12]. The choice of subsequent investigations depends on the history and the level of suspicion. Abdominal sonography or computed tomography can detect common bile duct obstruction and identify intrahepatic lesions, such as stones or tumors. Endoscopic retrograde cholangiopancreatography may be helpful. Blood may be seen at the ampulla of Vater and contrast studies may show filling defects in the biliary

tree. Angiography could detect significant hemobilia in over 90 % of patients^[13], and allow the localization of vascular lesions and therapeutic embolization.

The management of hemobilia is aimed at stopping the bleeding and relieving biliary obstruction. Transarterial embolization is now the first line of intervention to stop the bleeding of hemobilia, which returned a high success rate of around 80 % to 100 %^[1], and lower morbidity or mortality rates than surgery^[14]. Surgical interventions, such as ligation of the bleeding vessel or excision of the aneurysm, should be considered if embolization fails or is contraindicated.

In conclusion, hemobilia is one of the causes of obscure gastrointestinal hemorrhage. Although iatrogenic cases have replaced traumatic ones as the major type of hemobilia, one should keep in mind that ascending cholangitis is a possibility and may sometimes be complicated by life-threatening hemobilia. In particular, the rupture of a hepatic artery aneurysm should be taken into consideration in patients with a remote history of endoscopic or surgical sphincterotomy.

REFERENCES

- 1 **Green MH**, Duell RM, Johnson CD, Jamieson NV. Haemobilia. *Brit J Surg* 2001; **88**: 773-786
- 2 **Harlaftis NN**, Akin JT. Hemobilia from ruptured hepatic artery aneurysm. Report of a case and review of the literature. *Am J Surg* 1977; **133**: 229-232
- 3 **Stauffer JT**, Weinman MD, Bynum TE. Hemobilia in a patient with multiple hepatic artery aneurysms: a case report and review of the literature. *Am J Gastroenterol* 1989; **84**: 59-62
- 4 **Baartz T**, Koveker G, Hehrmann R, Becker HD. Recurrent hematemesis and hemobilia in ruptured hepatic artery aneurysm - differential diagnostic aspects of acute, upper gastrointestinal hemorrhage. *Leber Magen Darm* 1996; **26**: 42-46
- 5 **Bloechle C**, Izbicki JR, Rashed MY, El-Sefi T, Hosch SB, Knoefel WT, Rogiers X, Broelsch CE. Hemobilia: presentation, diagnosis and management. *Am J Gastroenterol* 1994; **89**: 1537-1540
- 6 **Sandblom P**, Saegesser F, Mirkovitch V. Hepatic hemobilia: hemorrhage from the intrahepatic biliary tract, a review. *World J Surg* 1984; **8**: 41-50
- 7 **Seifert E**. Long-term follow-up after endoscopic sphincterotomy (EST). *Endoscopy* 1988; **20**(Suppl 1): 232-235
- 8 **Gregg JA**, De Girolami P, Carr-Locke DL. Effects of sphincteroplasty and endoscopic sphincterotomy on the bacteriologic characteristics of the common bile duct. *Am J Surg* 1985; **149**: 668-671
- 9 **Prat F**, Malak NA, Pelletier G, Buffet C, Fritsch J, Choury AD, Altman C, Liguory C, Etienne JP. Biliary symptoms and complications more than 8 years after endoscopic sphincterotomy for choledocholithiasis. *Gastroenterology* 1996; **110**: 894-899
- 10 **Greenfield C**, Cleland P, Dick R, Masters S, Summerfield JA, Sherlock S. Biliary sequelae of endoscopic sphincterotomy. *Postgrad Med J* 1985; **61**: 213-215
- 11 **Sherlock S**, Dooley K. Diseases of the liver and biliary system, 11th ed. London, Blackwell Science 2002: 255-265
- 12 **Yoshida J**, Donahue PE, Nyhus LM. Hemobilia: review of recent experience with a worldwide problem. *Am J Gastroenterol* 1987; **82**: 448-453
- 13 **Merrell SW**, Schneider PD. Hemobilia - evolution of current diagnosis and treatment. *West J Med* 1991; **155**: 621-625
- 14 **Lygidakis NJ**, Okazaki M, Damsios G. Iatrogenic hemobilia: how to approach it. *Hepatogastroenterol* 1991; **38**: 454-457

Edited by Wang XL